The Role of Tumour Microenvironmental Signals in TP53-dependent Therapeutic Strategies for Chronic Lymphocytic Leukaemia (CLL)

Author

Mohammed Howladar

Supervisors

Prof John Lunec
Dr Elaine Willmore

This Thesis submitted to the Faculty of Medical Sciences,
Newcastle University
In partial fulfilment of the requirements for the degree of Doctor of Philosophy

Biosciences Institute

Newcastle University Cancer Centre

Faculty of Medical Sciences

April, 2025

Abstract

Chronic lymphocytic leukaemia (CLL) is a haematologic malignancy of B cells that shows a highly heterogeneous clinical course, with approximately 90% of patient CLL samples being wild type for the *TP53* tumour suppressor gene at diagnosis. CLL accounts for approximately 1000 deaths annually in the United Kingdom alone, highlighting the need to unravel the molecular mechanisms that could be used to produce more effective treatment options. Since *TP53* disruption by either mutation and/or deletion occurs in only 10-15% of CLL cases, targeting MDM2 to activate TP53 in a non-genotoxic manner is a potential treatment strategy for wild type *TP53* CLL. In this study, the combination of WIP1 inhibitor (GSK2830371) with RG7388 was investigated to potentiate the stabilization and pro-apoptotic effects of wild type TP53 at lower concentrations. The potential effect of the microenvironment on the response to MDM2 and WIP1 inhibitors was modelled *ex-vivo*, including the stimulation of CLL cells with CD40 ligand (CD40L), IL-4 and B cell receptor (BCR) signalling with anti-IgM treatment. The results identified that WIP1 inhibitor potentiated the effect of the MDM2-p53 binding antagonist (RG7388) in wild type *TP53* haematological cell lines and non-proliferative CLL cells. The stabilization activity of TP53 was confirmed by the induction of downstream target genes. Furthermore, *ex-vivo* combined CD40L/IL-4 stimulation showed the proliferative CLL cells became more sensitive to RG7388 as a single agent treatment. The WIP1 inhibitor potentiated the effect of RG7388 and increased the expression of *TP53* dependent pro-apoptotic genes.

Both immobilized anti-IgM antibody and IL-4 signalling induced proliferation and cell survival signals, which was associated with the *ex-vivo* primary CLL cells becoming less sensitive to RG7388, and under these conditions the combination with WIP1 inhibitor also did not significantly potentiate the TP53 stabilization by RG7388. However, in the presence of IL-4 the expression of *TP53* downstream target genes showed a transcriptional induction of the *TP53*-dependent pro-apoptotic gene (*PUMA*) and negative regulator of TP53 (*MDM2*).

In summary, the WIP1 inhibitor (GSK2830371) significantly potentiated the effect of non-genotoxic small molecule MDM2 inhibitor (RG7388) in functional *TP53* CLL cells. Modelling the *ex-vivo* microenvironment with CD40L, IL-4 and BCR activation with anti-IgM antibody was found to reduce the sensitivity of the CLL cells to both single agent RG7388 and when in combination with GSK2830371. This highlighting the importance of the *in-vivo* microenvironment and the need to develop combination strategies that overcome its limiting effect on the response to p53-dependent therapies.

Dedicated to the memory of my father Talat Howladar, a great man whom I still miss every day

Declaration

I hereby declare that the work presented in this Ph.D. thesis entitled **"The Role of Tumour Microenvironmental Signals in TP53-dependent Therapeutic Strategies for Chronic Lymphocytic Leukaemia (CLL)"** has been performed entirely by me and has not been submitted for any other degree or academic institution.

Signed: *Mohammed Howladar*

Date: 30/03/2025

Acknowledgements

Thanks God, for this achievement and may I ask you to guide me to help the society and the universe.

I would most like to thank my supervisors Professor John Lunec and Dr Elaine Willmore for all of their support, encouragement and guidance over the last 5 years.

I would like to thank my annual progress panels Prof Julie Irving and Dr Gordon Strathdee for academic support and advice.

I would like to thank my colleagues for their contribution to the work: Dr Ahmad Mahdi, Dr Erhan Aptullahoğlu, Dr Victoria Chamberlain, Dr Emre Ozturk, Dr Abdullah Althuwaybi, Ahmet Yagbasan and all other members of the clinical and translational oncology research group for their help and technical support throughout the project. It has been a pleasure to work with you all and you made the last few years unforgettable.

I must also express huge thank you to my friends who support me during my journey.

Thanks to my sponsor, Shaqra University for providing me the opportunity to do my PhD at Newcastle University to support the vision of our leadership Prince Mohammed Bin Salman Al Saud.

I would also like to acknowledge and thank all CLL patients and their families for donating valuable samples to potentially lifesaving research.

Finally, and most importantly, ultimate gratitude to my mother Sadiqah Bashawri, grandmother and my Consultant brothers and sisters whom without their unconditional support I wouldn't have been able to achieve any success.

Contents

List of Figures

List of Table

List of Abbreviations

ALL	Acute lymphoblastic leukaemia
AML	Acute myeloid leukaemia
APCs	Antigen-presenting cells
ATM	Ataxia Telangiectasia Mutated (gene)
ATM	Ataxia telangiectasia mutated
ATP	Adenosine triphosphate
ATR	Ataxia telangiectasia and Rad3-related
BAFF	B-cell activating factor
BAX	BCL-2 associated X protein
BAX	BCL-2 Associated X Protein (gene)
BCA	Bicinchoninic acid assay
BCL2	B-cell CLL/lymphoma 2
BCL-2	B cell leukaemia/lymphoma 2
Bcl6	B-cell lymphoma 6
BCR	B cell receptor
BLK	B-lymphoid tyrosine kinase
BLNK	B cell linker protein
BM	Bone marrow
B-NHL	B-cell non-Hodgkin lymphoma
BRCA1	Breast Cancer Type 1 Susceptibility Protein (gene)
BSA	Bovine serum albumin
BTK	Bruton's tyrosine kinase
$CaCl_2$	Calcium chloride
CAP regimen	Cyclophosphamide, doxorubicin plus prednisone
CARMA1	Which phosphorylates caspase recruitment domain-containing membrane-associated guanylate kinase protein-1
CD40L	CD40 ligand
CDKN1A	Cyclin-dependent Kinase Inhibitor 1A (gene)
CDKs	Cyclin-dependent kinases
cDNA	Complementary deoxyribonucleic acid
CHK1,2, etc.	Checkpoint kinase
ChOP	Cyclophosphamide, doxorubicin, vincristine, and prednisone
CI	Confidence interval / combination index
CK1	Casein kinase 1
CLL	Chronic lymphocytic leukaemia
CLL-IPI	Chronic lymphocytic leukaemia international prognostic index
CO2	Carbon dioxide
cPARP	Cleaved poly (ADP-ribose) polymerase
DAG	Diacylglycerol
DBD	DNA-binding domain
DDR	DNA damage response
Del	Deletion (del(17p), del(13q) etc.)
dH_2O	Distilled water

DLBCL	Diffused large B-cell lymphoma
DMSO	Dimethyl sulfoxide
DNA	Deoxyribonucleic acid
DNAse	Deoxyribonuclease
dNTPs	Deoxynucleotide triphosphates
dUB	Deubiquitylase
DUSP4	Dual-specificity phosphatase
ECL	Enhanced chemiluminescence
EDTA	Ethylenediamine tetra acetic acid
EGR3	Early growth response 3
ERIC	European Research Initiative on CLL
ERK1/2	Extracellular signal-regulated kinase 1/2
FACS	Fluorescence activated cell sorting / flow cytometry
FBS	Foetal bovine serum
FC	Fludarabine and cyclophosphamide
FcR	Fc receptors
FCR	Fludarabine, cyclophosphamide and rituximab chemoimmunotherapy
FCS	Foetal calf serum
FDA	Food and Drug Administration
FISH	Fluorescence in situ hybridisation
FSC	Forward light scatter light
G0	Gap 0
G1	Gap 1
G2	Gap 2
GAPDH	Glyceraldehyde 3-phosphate dehydrogenase
GAPs	Gtpase-activating proteins
GDP	Guanosine diphosphate
GEF	Guanine nucleotide exchange factor
GEF	Guanine nucleotide exchange factor
GEFs	Guanine nucleotide exchange factors
GI_{50}	Growth inhibition of 50%
GRB2	Adaptor protein growth factor receptor-bound protein 2
GRB2	Growth factor receptor-bound protein 2
GSK3	Glycogen synthase kinase 3
GTP	Guanosine triphosphate
Gy	Gray
HCl	Hydrochloric acid
HRP	Horseradish peroxidase
IFN-γ	Interferon gamma
IgE	Immunoglobulin E
IgH	Immunoglobulin heavy chains
IGHV	Immunoglobulin heavy chain variable region
IgL	Immunoglobulin light chains
IL (-2,-4 etc)	Interleukin

IL-4R	Interleukin-4 receptor
IL-4Rα	Interleukin-4 receptor (alpha) polypeptide
IP3	Inositol-1, 4,5-triposphate
IRS	Insulin receptor substrate proteins
ITAMs	Immune-receptor tyrosine–based activation motifs
iwCLL	International Workshop on Chronic Lymphocytic Leukaemia
JAK	Janus kinase
JNK	C-Jun N-terminal kinases
LC_{50}	Lethal inhibition of 50%
LDH	Lactate dehydrogenase level
LNs	Lymph nodes
LRMP	Lymphoid-restricted membrane protein
LYN	Tyrosine-protein kinase
MALT1	Mucosa-associated lymphoid tissue lymphoma translocation 1
MAP	Mitogen-activated protein
MAPK	Mitogen-activated protein kinase
MBL	Monoclonal B lymphocytosis
MCL1	Myeloid cell leukemia-1
M-CLL	Mutant chronic lymphocytic leukaemia
MDM2	Mouse double minute 2
MDMX (MDM4)	Murine double minute X (murine double minute 4)
MEK	Mitogen-activated protein kinase
MRD	Minimal residual disease
mRNA	Messenger ribonucleic acid
mTORC2	Mammalian target of rapamycin complex 2
MUT	Mutated
MYC	Master Regulator of Cell Cycle Entry and Proliferative Metabolism
NAADP	Nicotinic acid adenine dinucleotide phosphate
NaCl	Sodium chloride
NADH	Nicotinamide adenine dinucleotide
NaOH	Sodium hydroxide
NFAT	Nuclear factor of activated T
NFKB (NF-κB)	Nuclear factor kappa-light-chain-enhancer of activated B cells
NKT	Natural killer cells
NPC	Nuclear pore complex
NR4A1	Nuclear receptor subfamily 4 group A member 1
O.D	Optical density
ORR	Overall response rate
OS	Overall survival
p-	Phosphorylated
PAMPs	Pathogen-associated molecular patterns
PARP	Poly ADP-ribose polymerases
PBS	Phosphate-buffered saline
PCR	Polymerase chain reaction
PCs	Proliferation centres

PDK1	Phosphoinositide dependent protein kinase1
PET-CT	Positron emission tomography-CT
PFS	Progression-free survival
PI3K (δ or γ)	Phosphoinositide 3-kinases
PIP2	Phosphatidylinositol-4,5-bisphosphate
PKCβ	Protein kinase Cβ
PLCγ2	Phospholipase Cγ2
PLK1	Polo-like kinase 1
PP2C	Type 2C protein phosphatases
PPM1D	Protein phosphatase 1D magnesium-dependent
PRR	Proline-rich region
PS	Phosphatidylserine
PTBs	Protein-binding domains
PUMA	P53 upregulated modulator of apoptosis
qRT-PCR	Quantitative real-time polymerase chain reaction
RAS/RAF1	Rapidly accelerated fibrosarcoma
RasGRP	Ras guanine-nucleotide releasing proteins
Rb	Retinoblastoma protein
RBC	Red blood cell
RE	Response elements
RNase	Ribonuclease
RPMI	Roswell park memorial institute
RT	Room temperature / reverse transcription
S6	Ribosomal S6 kinase
SAPK	Stress-activated protein kinases
SD	Standard deviation
SDS	Sodium dodecyl sulphate
SDS-PAGE	SDS-polyacrylamide gel electrophoresis
SEM	Standard error mean
SFKs	SRC-family kinases
sIgG	Surface immunoglobulin G
sIgM	Surface immunoglobulin M
SLL	Small lymphocytic lymphoma
SOCE	Store-operated Ca2+ entry
SRB	Sulforhodamine B
SRC	Kinases like
SSC	Side light scatter light
STAT	Signal transducer and activator of transcription
STIM	Stromal interaction molecule
STR	Short tandem repeat
SYK	Spleen tyrosine kinase
sβ2M	High serum β-2 microglobulin
T PLL	T cell prolymphocytic leukaemia
TAD	Transactivation domain
TAK1	Transforming growth factor α-activated kinase 1

TBS	Tris buffered saline
TBS-T	Tris buffered saline -tween
Tfh	T Follicular helper cells
TH	T helper cell
TH2	T helper cells type 2
TLRs	Toll-like receptors
T_m	Melting temperature
TNF	Tumour necrosis factor
TNFAIP3	A gene involved in the negative regulation of the NFKB pathway)
TNF-α	Tumour necrosis factor-α
TP53	Tumour protein p53
TP53INP1	Tumour protein 53-induced nuclear protein 1
TRAF	Tumour necrosis factor receptor-associated factor
Ub	Ubiquitin
U-CLL	Un-mutant Chronic Lymphocytic Leukaemia
uLMS	Uterine Leiomyosarcoma
UVR	Ultraviolet radiation
V	Volt
v/v	volume / volume
vs.	Versus
WB	Western blot
WBC	White blood cell
WIP1	Wild-type p53-induced phosphatase 1
WM	Waldenström's macroglobulinaemia
WT	Wild-type
XTT	Sodium 3′-[1-[(phenylamino)-carbony]-3,4-tetrazolium]-bis(4-methoxy-6-nitro) benzene-sulfonic acid hydrate
ZAP-70	Zeta-chain-associated protein kinase 70
ZIP	Zero interaction potency

Chapter 1: Introduction

1.1 Chronic Lymphocytic Leukaemia

1.1.1 Definition and epidemiology

Chronic lymphocytic leukaemia (CLL) is the most common type of lymphoid cancer in Western countries, comprising 25% of all leukaemia cases. The incidence of CLL is 4.2 cases per 100,000 people per year, and it is more common in men than in women (Stevenson & Caligaris-Cappio, 2004), with a male to female ratio of 1.3:1 to 1.7:1. CLL is typically diagnosed in adults, with a median age at diagnosis of 72 years (Siegel et al., 2023). The incidence of the disease is increased by more than 30 cases in 100,000 individuals per year in those aged over 80 years old. However, CLL can be diagnosed in rare cases among children and younger generation (Smith et al., 2011; Hernández et al., 1995). CLL patients may express an inherited genetic susceptibility, with family members of CLL patients having 6 to 9 fold increased risk of developing the disease (Eichhorst et al., 2015). To understand the genetic basis of susceptibility for CLL, genome-wide association studies have been conducted, revealing the presence of independent single-nucleotide polymorphisms (SNPs) located in various genomic loci. Notably, these SNPs have been identified in 2q21.2 (*CXCR4)* (Sellick et al., 2007). 10q23.31 (*ACTA2, FAS*), 18q21.33 (*BCL2*), 11p15.5 (*C11orf21*), 4q25 (*LEF1*), 2q33.1 (*CASP10, CASP8*), 9p21.3 (*CDKN2B-AS1*), 18q21.32 (*PMAIP1*), 15q15.1 (*BMF*), and 2p22.2 (*QPCT*) (Berndt et al., 2013).

1.1.2 Staging

Two widely accepted staging methods are available to predict the median survival rate to diagnose the CLL patients, as proposed by Rai and Binet classifications. (Rai et al., 1975; Binet et al., 1981). The original Rai classification has since been modified to reduce the number of prognostic groups from five to three. Both the Binet and Rai staging systems categorize patients into three major groups based on discrete clinical outcomes (Hallek et al., 2008). While the Binet staging system is more widely used in Europe, the Rai system is more commonly applied in the United States (Eichhorst et al., 2015). Importantly, these staging systems rely on a physical examination and standard laboratory tests and do not require the use of ultrasound, computed tomography (CT), or magnetic resonance imaging (MRI) (Hallek, Shanafelt, et al., 2018).

The modified Rai staging system divides CLL into three categories based on the level of risk: low, intermediate, and high. These categories correspond to stages 0, I and II, and III and IV,

respectively (Rai et al., 1975). Low-risk disease is characterized by lymphocytosis with leukaemia cells in the blood and/or bone marrow, where lymphoid cells make up more than 30% of the total cells (previously known as Rai stage 0) (lymphocytosis >15×10^9/L). Intermediate-risk disease is defined by the presence of lymphocytosis, lymphadenopathy in any location, and splenomegaly and/or hepatomegaly with or without palpable lymph nodes (previously known as Rai stage I or stage II). High-risk disease includes patients with CLL-related anaemia (haemoglobin <11 g/dL; previously known as stage III) or thrombocytopenia (platelet count <100 × 109/L; formerly known as stage IV) (Hallek et al., 2008).

The median survival times for the three categories are as follows: 10 years for low-risk (Rai 0), 8 years for intermediate-risk (Rai I and II), and 6.5 years for high-risk (Rai III and IV) (Pflug et al., 2014).

The Binet staging system classified the CLL based on the number of areas involved, which are determined by the presence of enlarged lymph nodes with a diameter of greater than 1 cm, as well as the presence of organomegaly, anaemia, or thrombocytopenia. The areas of involvement considered include the head and neck, axillae, groins, palpable spleen, and palpable liver. This system recommends three stages as follows (Binet et al., 1981).

Stage A:

- No anaemia: haemoglobin ≥10 g/dl
- No thrombocytopenia: platelets ≥100 × 10^9/L
- Less than three areas of lymphoid tissue enlargement involvement

Stage B: three or more areas of involvement

- No anaemia: haemoglobin ≥10 g/dl
- No thrombocytopenia: platelets ≥100 × 10^9/L
- Three or more areas of lymphoid tissue enlargement involvement at which should be greater than arras defined for stage A (Organomegaly)

Stage C:

- Anaemia: haemoglobin <10 g/dl, and/or
- Thrombocytopenia: platelets <100 × 10^9/L

- Any number of areas of lymphoid tissue enlargement with or without lymphadenopathy or organomegaly

The Binet staging system is commonly used in Europe and provides useful prognostic information, with stage C having the worst prognosis, followed by stage B and then stage A (Hallek et al., 2008).

Prior to the development of the Rai/Binet staging systems in the mid-1970s, there were no reliable criteria that could prospectively identify and diagnose CLL patients with poor prognosis and shorter survival from those with excellent overall prognose. The classification of Rai/Binet staging systems resolved this complexity and established the fundamental cornerstone in diagnosis and management of CLL for almost four decades. However, identifying mutations and abnormal cytogenetic patterns in CLL patients has revealed the limitations in the precision of Rai/Binet classification. Several studies were conducted on large-scale of CLL patients to identify the mutations and abnormal cytogenetic patterns and revealed that the Rai/Binet staging systems may not accurately distinguish between prognostic subgroups of CLL patients, and their capacity to predict outcomes for individual patients is limited (Bazargan et al., 2012; Sellner et al., 2012; Rossi et al., 2013). Furthermore, numerous novel genetic drivers have been identified in CLL through mutational and aberrant chromosomal studies (Landau et al., 2013; Rossi et al., 2014; Y. Wan & Wu, 2013). These genetic aberrations are now recognized as being crucial to the diverse biological and clinical phenotypes observed in CLL (Döhner et al., 2000).
As a result of lack of precision of Rai and Binet staging systems to distinguish between subgroups of CLL cells, various potential biomarkers have been developed to improve the accuracy of diagnosis, predict outcomes and guide therapeutic strategies (Pflug et al., 2014; Cramer & Hallek, 2011).

These independent prognostic factors include cytogenetic abnormalities such as 17p deletion, 11q deletion, 13q deletion and trisomy 12, as well as mutations in genes such as *TP53*, *NOTCH1*, *SF3B1*, and *BIRC3*. Other factors that have been associated with poorer prognosis include unmutated immunoglobulin heavy chain variable (*IGHV*) genes, high serum beta-2 microglobulin (sβ2M) levels, elevated lactate dehydrogenase (LDH) levels, and the presence of certain cell surface markers such as CD38 and ZAP-70 (Cortese et al., 2013; Pflug et al., 2014; Wierda et al., 2007).

1.1.3 Diagnosis

The initial step in diagnosing CLL involves a thorough medical history review and physical examination, followed by a complete blood count and differential white blood cell count (Verghese et al., 2011). To confirm the diagnosis of CLL, the presence of at least $5X10^9$/L CD5+/CD23+ monoclonal B lymphocytes (5000 cells/μl) in peripheral blood for more than three months is required (Hallek, Cheson, et al., 2018). Additionally, the clonality of circulating B lymphocytes should be assessed by analysing the *IGHV* gene somatic hypermutation status, as CLL patients with unmutated *IGHV* have a more aggressive form of the disease (Hamblin et al., 1999).

Characteristic features of CLL include the appearance of fragile lymphocytes, also known as "smudge cells," on a peripheral-blood smear (Figure 1.1). The percentage of these cells is an independent predictor of overall survival, with virtually all patients demonstrating some proportion of fragile lymphocytes ranging from 4 to 72% nuclei (Nowakowski et al., 2007). A higher percentage of smudge cells would favour the diagnosis of CLL. Morphological evaluation of a blood smear should show small mature lymphocytes with a narrow cytoplasm, a dense nucleus with partially aggregated chromatin, and the absence of visible nucleoli (Hallek et al., 2008; Hallek & Al-Sawaf, 2021). Overall, the diagnosis of CLL requires the combination of clinical, laboratory, and morphological criteria to confirm the presence of the disease.

Following the identification of lymphocytosis from a complete blood count, the subsequent step is to determine the composition of the cells in the blood through immunophenotyping. The lymphocytes associated with CLL exhibit a characteristic profile that includes CD5+, CD19+, CD20+ low, CD23+, CD22+ low/negative, CD79b+ low/negative, CD43+ low, sIgκ+ or sIgλ+ low, sIgM+ low, CD11c+ low/negative, FMC7 negative, CD10 negative, and CD103 negative (Abdel-Ghafar et al., 2012; Rodrigues et al., 2016).

The routine diagnosis of CLL does not involve bone marrow biopsy and aspiration. However, this procedure may be considered for patients who are undergoing clinical trials or those who have persistent cytopenia after treatment, to distinguish between leukemic infiltration and therapy-related toxicity. Imaging techniques such as ultrasound, computed tomography, magnetic resonance imaging, and positron emission tomography-CT (PET-CT) scanning are not typically recommended for routine CLL diagnosis or staging (Rodrigues et al., 2016).

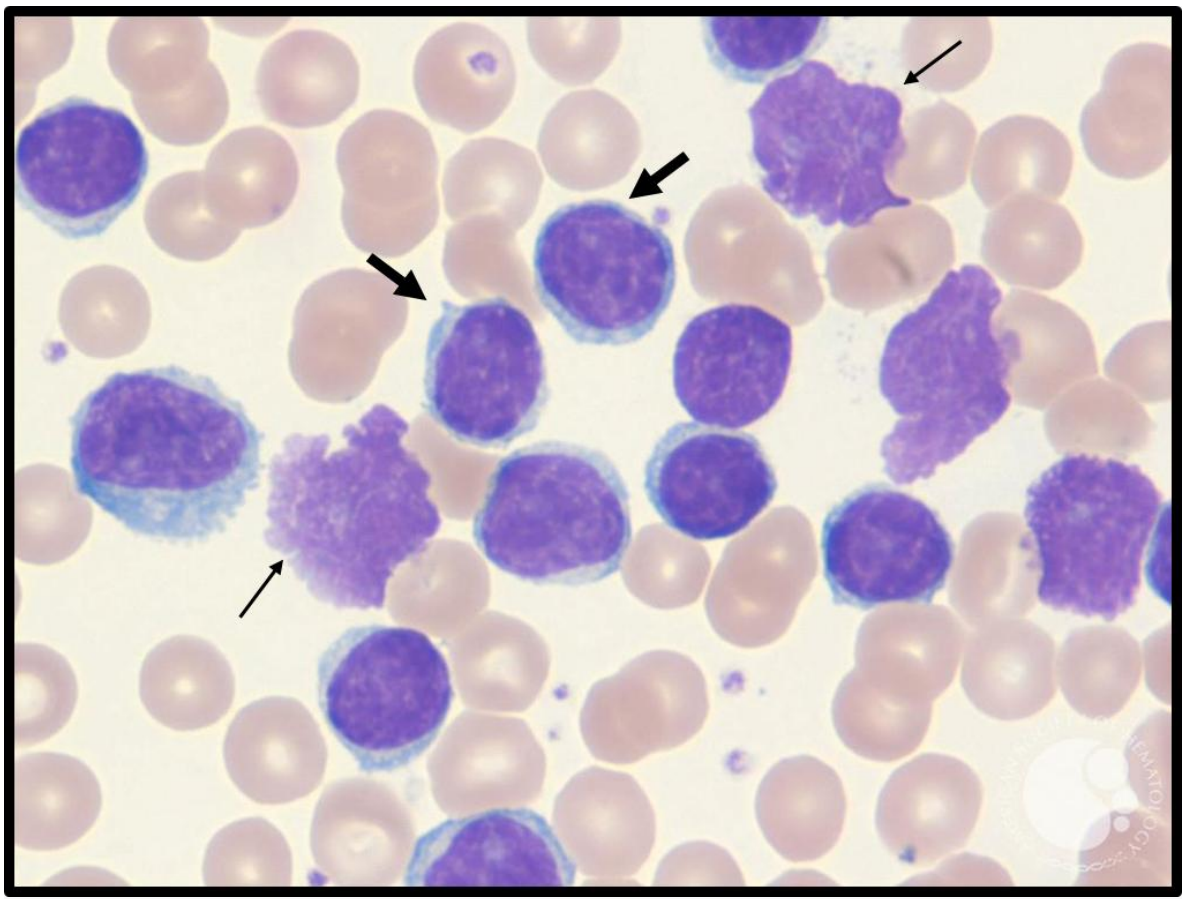

Figure 1.1 Blood smears of CLL patient. A microscopic evaluation of a peripheral blood smear, stained with Wright-Giemsa, may reveal the presence of "smudge cells", which are fragile lymphocytes with poorly defined, "crushed" cytoplasm and no distinguishable nuclei. An example of a smudge cell is indicated by a thin arrow. Typical CLL cells showed less than 10% prolymphocytes (wide arrows). (American Society of Hematology, 2023).

The most recent version of the International Workshop on Chronic Lymphocytic Leukaemia (iwCLL) guidelines (Hallek, Cheson, et al., 2018) provides clear recommendations on CLL diagnosis. The diagnosis of CLL is typically made through analysing blood counts, differential counts, a blood smear, and immunophenotyping. The World Health Organization's classification of hematopoietic neoplasia distinguishes CLL from small lymphocytic lymphoma (SLL) based on its leukemic appearance (Hallek et al., 2008). CLL is a disease that involves neoplastic B-cells, whereas T cell prolymphocytic leukaemia (T PLL) describes the entity formerly known as T CLL.

Monoclonal B lymphocytosis (MBL) (Hallek, Cheson, et al., 2018) is diagnosed whenever the B lymphocytes count is less than 5,000 cells/μL of total blood cells, and there is an absence of lymphadenopathy or organomegaly as defined by physical examination or CT scans, cytopenia or disease-related symptoms. However, the presence of a cytopenia caused by a typical marrow infiltrate is diagnostic of CLL, regardless of the number of peripheral blood B lymphocytes or lymph node involvement. MBL is known to progress to CLL at a rate of 1-2%

per year. It is important to distinguish MBL from CLL as the latter may require active treatment, whereas MBL may be monitored without intervention (Rawstron et al., 2008).

In SLL, the number of B lymphocytes should not exceed 5000 cells/μL of the total peripheral blood cell count in addition to the presence of lymphadenopathy and the absence of cytopenia caused by a clonal marrow infiltrate. Furthermore, histopathological examination of a lymph node biopsy should be performed the confirm the diagnosis of SLL.

1.1.4 Clinical prognostic markers

1.1.4.1 *IGHV* status

The determination of the mutational status of the immunoglobulin heavy chain variable region (*IGHV*) gene is a reliable prognostic factor in CLL (Damle et al., 1999). A DNA sequence that displays 98% or more homology to the germline *IGVH* sequence is considered unmutated. Unmutated *IGHV* is identified in approximately one-third of CLL cases and is linked with atypical morphology, aggressive disease, and significantly shorter survival rates than those with mutated *IGHV* (Figure 1.2) (Rai et al., 2001; Hamblin et al., 1999). However, the *VH3-21* gene segment is an exception to this rule, as it is associated with high-risk disease and poorer survival rates regardless of the mutational status (Thorsélius et al., 2006). The frequency of driver mutations in unmutated *IGHV* CLL is increased compared to mutated *IGHV* CLL (Landau et al., 2015). Despite that, the *IGVH* mutation analysis is not commonly performed in most of clinical laboratories because of its inherent limitations, which include the requirement for high-quality RNA for RT-PCR, a sufficient amount of CLL cells for accurate analysis, and its high cost. In addition to that *IGVH* mutation analysis is not recommended on the guide treatment decisions, especially for BTKi and venetoclax (Mato et al., 2016; Crombie & Davids, 2017; Stamatopoulos et al., 2017).

The B-cell response to an antigen is controlled by the B cell receptor (BCR) in both normal and malignant B-cells. The B-cells exhibit unique BCRs based on a variable combination of V, D, and J gene segments for the heavy chain, and V and J gene segments for the light chain. This repertoire is significantly increased through the introduction of somatic hypermutation during the germinal centre reaction, or T cell-independent hypermutation outside of the germinal centre.

In CLL cases, patients can be categorized based on the degree of somatic hypermutation, specifically those with mutated and unmutated *IGHVs*. This separation is based on an

arbitrary cut-off value that distinguishes sequence identities of 98% or greater from those that are less than 98%. Despite its arbitrary nature, these two groups have significantly different clinical courses. The *IGHV* mutation status is clinically relevant, as it predicts the risk of disease progression and outcome in untreated CLL patients. CLL patients with unmutated *IGHV* experience a rapid progression of the disease and early death, while those with mutated *IGHV* often have a slower progression and longer survival. The *IGHV* mutation status is of prognostic importance in all patient cohorts, including unselected patient cohorts, after treatment, and in early stage patients (Binet A). Clinical trial data confirms the impact of *IGHV* mutation on outcome. Although the *IGHV* status predicts the overall response rate and duration in CLL patients expressing this marker, there is little evidence for its use as a predictive marker in standard treatment regimens.

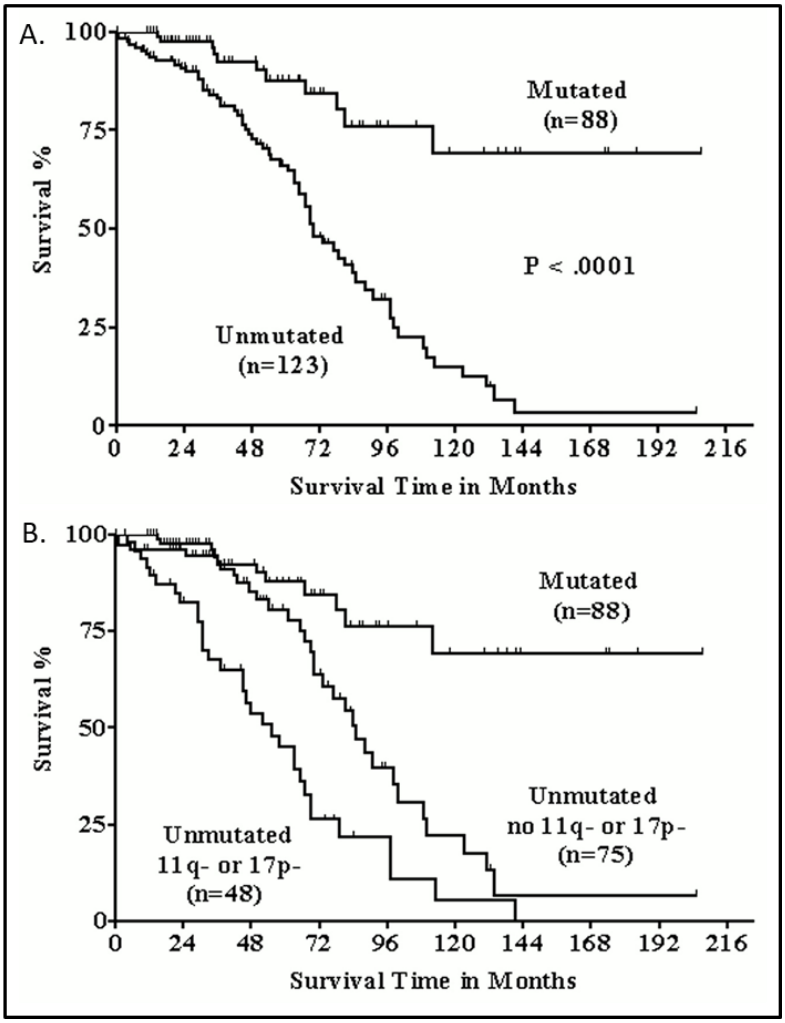

Figure 1.2 (A) **The prognostic significance of the *IGHV* mutation status in chronic lymphocytic leukaemia (CLL) patients.** (B) genomic aberrations of 11q and 17p deletion in CLL. In a total of 123 CLL patients who expressed unmutated *IGHV* genes, those who had high-risk genomic aberrations (48 patients) had a considerably lower survival rate compared to the patients who didn't have deletion in del11q or del17p (75 patients) (Rai et al., 2001).

1.1.4.2 CD38 expression

CD38 (cluster of differentiation 38) is a type II transmembrane glycoprotein that is present on the surface of various immune cells, including CD4+, CD8+, B lymphocytes, and natural killer cells (Hamblin, 2003). This protein serves as a multifunctional ecto-enzyme that is responsible for the synthesis and hydrolysis of cyclic ADP-ribose and the synthesis of Nicotinic acid adenine dinucleotide phosphate (NAADP). These reaction products play an important role in regulating intracellular calcium Ca^{2+} levels (Chini et al., 2002). CD38 is expressed on cells in a significant number of patients with CLL. Higher levels of CD38 expression in CLL cells are associated with aggressive clinical behaviour (Dürig et al., 2002). Patients with a high percentage of CD38-expressing CLL cells have a less favourable clinical course, with more advanced disease stage and shorter survival times compared to patients who do not express CD38 (Ibrahim et al., 2001; Matrai, 2013).

1.1.4.3 ZAP-70 expression

Zeta-chain-associated protein kinase 70 (ZAP-70) expression was demonstrated to be an effective tool for identifying patients with CLL who have a more severe disease course. Consequently, it was a valuable molecular marker for clinical use in patients with CLL (Dürig et al., 2003). Given that the mutation analysis of (*IGHV*) status is often impractical for clinical laboratories, ZAP-70 mRNA expression can be utilized as a predictive marker for *IGHV* status. By determining an optimal threshold for ZAP-70 expression, the majority of *IGHV*-unmutated CLL samples can be distinguished from *IGHV* -mutated CLL samples (Wiestner et al., 2003). However, ZAP70 is not widely used as a prognostic marker due to technical challenges including standardisation of flow cytometry quantification (Wang et al., 2012).

1.1.4.4 Cytogenetic abnormalities

CLL is a heterogeneous disease and cytogenetic abnormalities are known to play a significant role in its pathogenesis and progression. In fact, chromosomal abnormalities can be detected in up to 80% of CLL cases using interphase fluorescence in situ hybridization (FISH) analysis.

Interphase FISH is a technique that uses fluorescent probes to detect specific DNA sequences in cells undergoing interphase (the stage between mitotic divisions). By analysing the pattern of fluorescence signals, researchers can identify chromosomal abnormalities, such as deletions, duplications, and translocations, which are common in CLL (Döhner et al., 2000).

Some of the most common cytogenetic abnormalities found in CLL include deletion of the long arm of chromosome 13 (del[13q]), deletion of the short arm of chromosome 17 (del[17p]), and deletion of the long arm of chromosome 11 (del[11q]). These abnormalities are associated with different prognostic outcomes, with del(17p) being associated with a significantly poorer prognosis compared to del(13q) or normal cytogenetics (Juliusson et al., 1990; Shanafelt, Hanson, et al., 2008).

1.1.4.4.1 11q23 deletion

The deletion of the long arm of chromosome 11 (11q) is a chromosomal abnormality that is detected in 5-20% of patients diagnosed with CLL (Marasca et al., 2013; Döhner et al., 2000) and CLL patients who exhibit deletions in the 11q23 region tend to experience a more rapid disease progression and extensive lymphadenopathy (Grever et al., 2007). It is important to consider the presence of 11q deletions in the diagnosis and treatment of CLL, as it has significant implications for disease prognosis and management.

The ATM (ataxia-telangiectasia mutated) gene is located on 11q22-q23 within the minimal region of loss. The main function of *ATM* is to manage the maintenance of DNA repair and recombination, as well as to control the progress of the cell cycle (Negrini et al., 2010). Cells with *ATM* deficiency are unable to identify and repair DNA damage, which can lead to a higher risk of lymphoid cancers (Lavin, 2008).

One of the main functions of ATM in cells is to phosphorylate the serine-15 residue on p53 in response to DNA damage (Banin et al., 1998). The *ATM* gene mutations are detected in less than third of CLL patients with deletion 11q, suggesting that other genes may be involved in the pathogenesis of CLL in patients with 11q deletions (Austen et al., 2005).

1.1.4.4.2 17p13 deletion

Upon initial diagnosis, approximately 3–8% of CLL patients are diagnosed with a deletion in the short arm of chromosome 17 (del 17p) (Delgado et al., 2012). However, the prevalence of the del(17p) chromosomal abnormality among CLL patients was increased to 30% with relapsed or refractory disease (Stilgenbauer & Zenz, 2010; Campo et al., 2018). CLL patients with a 17p deletion express very poor prognosis due to their refractoriness to conventional therapy (Greipp et al., 2013; Buccheri et al., 2018).

CLL patients with del(17p) are classified at the highest risk prognostic group due to their shortest overall survival (OS) and progression-free survival (PFS). The, *TP53* gene is located on band 13 of the short arm of chromosome 17 (17p13), while *TP53* mutations can arise in 5-10% of cases even in the absence of (del[17p]) (Zenz et al., 2008; Puente et al., 2015; Nadeu et al., 2016) and more than 80% of CLL cases express (del[17p]) in combination with *TP53* mutation on the other allele (Figure 1.3) (Zenz et al., 2008).

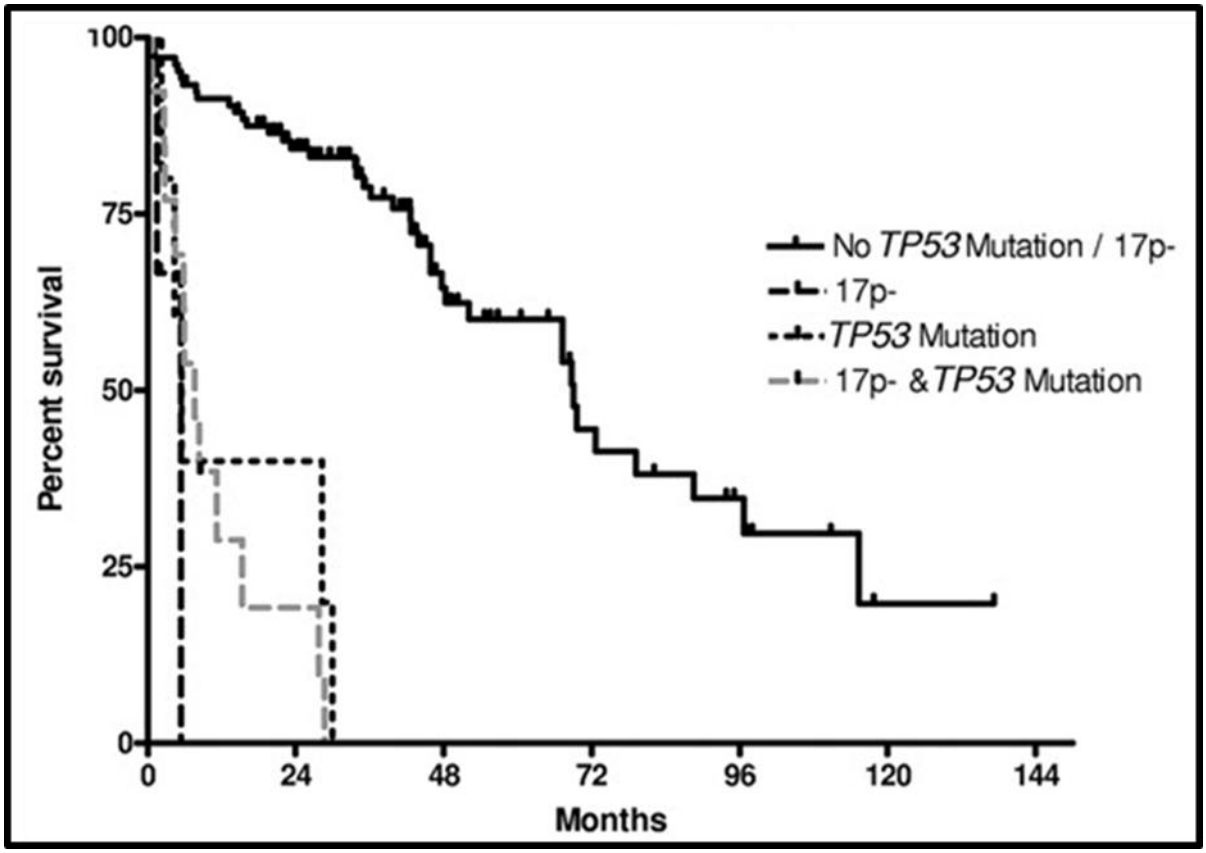

Figure 1.3 Prognostic significance of *TP53* mutations and/or del(17p) in CLL. The plot comparing CLL patients with mutated and unmutated *TP53*(-/+) gene del(17p). The presence of a *TP53* mutation and loss of the other *TP53* allele via del(17p) predicts the worst prognosis (Zenz et al., 2008).

1.1.4.4.3 13q14 deletion

Deletion of the long arm of chromosome 13 at cytoband 13q14 is most common genetic abnormality in CLL patients (Ouillette et al., 2008; Parker et al., 2011). Identification of deletion 13q14 subtype aberrations play a prognostic role the CLL management. Approximately 20% of CLL patients were found to exhibit large deletions (type II) of the 13q14 region that encompass the *RB1* gene, which were linked to reduced survival rates (Ouillette et al., 2011). The microRNAs miR-15a and miR-16-1 were considered as potential genes that may be involved in CLL, as they located on the region lost by 13q14 deletions.

These microRNAs, miR-15a and miR-16-1, have the ability to decrease the levels of the anti-apoptotic proteins BCL-2 and MCL-1, thereby promoting cell death. A decrease or loss of these microRNAs may contribute to the development of CLL (Cimmino et al., 2005; U. Klein et al., 2010).

1.1.5 Treatment of CLL

The requirement for treatment in CLL is determined by the stage of the disease and the prognosis. In the early stages (Binet A-B, Rai 0-II), patients are generally monitored without intervention until treatment becomes necessary. Although there have been significant advances in long-term survival through CLL treatment with combination chemotherapy and chemo-immunotherapy, standard therapy is not currently regarded as curative, and allogeneic stem cell transplantation (allo-SCT) is the only potential cure. However, the interesting role of SCT is linked with high morbidity and mortality rates and is therefore only recommended for younger patients with high-risk CLL. Thus, examining further biomarkers such as *IGHV* mutational status and other cytogenetic abnormalities to identify patients suitable for allo-SCT to achieve complete remission (CR). Currently, treatments with novel agents are being more frequently used in combination and at earlier stages of the disease. Although, it is uncertain yet whether these agents could substitute the allo-SCT or they are postponing the need for allo-SCT until the disease has progressed further. Unless new agents are introduced, it's probable that allo-SCT will remain relevant for patients who do not respond to treatment, experience intolerance to treatment, or lack the opportunity to use these novel agents (Gribben, 2018). There are a variety of treatment options available, including the following.

1.1.5.1 Chemotherapy

Chlorambucil, also known by its generic name Leukeran or Chlorbutin, is an alkylating agent that has been used since the 1950s in the treatment of CLL. Chlorambucil achieves its therapeutic effect by interfering with DNA replication (due to the formation of interstrand cross links) and transcription of RNA, leading to a disruption of nucleic acid function. This damage to DNA triggers cell cycle arrest and cellular apoptosis via the accumulation of p53 and MDM2, ultimately resulting in the activation of BCL-2-associated X protein (BAX), which promotes apoptosis. In patients with wild type *TP53*, chlorambucil-induced cell death occurs through a p53-dependent pathway (Begleiter et al., 1996).

A large randomized phase III trial compared the efficacy of chlorambucil alone versus chlorambucil in combination with the monoclonal antibody obinutuzumab among naïve untreated CLL patients with other comorbidities. The combination therapy showed a significant improvement in progression-free survival and overall survival compared to chlorambucil alone (Goede et al., 2014).

As a first-line treatment, chlorambucil has been shown to achieve an overall response rate of 60–90%, with a complete response rate of up to 20% in all patients (Eichhorst et al., 2009; Jaksic et al., 1997; Vidal et al., 2016). However, chlorambucil is now mostly used for patients with comorbidities who cannot tolerate chem-immunotherapy and targeted agents.

Fludarabine, also known by its commercial name Fludara, is a purine nucleoside analogue whose mechanism of action involves inhibition of DNA synthesis by interfering with ribonucleotide reductase and DNA polymerase, resulting in apoptotic death in patients with CLL (Pettitt, 2003; Robertson et al., 1993). Fludarabine demonstrated superior efficacy in response rates and longer progression-free survival compared to chlorambucil in CLL patients who have not received prior treatment (Rai et al., 2000; Catovsky et al., 2007).

Fludarabine is most often used in combination with cyclophosphamide and rituximab (FCR) as a first-line treatment option for young and fit CLL patients (Fischer et al., 2016; Kutsch et al., 2017). The FCR regimen showed superior efficacy compared to fludarabine alone, with higher overall response rates and longer progression-free and overall survival (Hallek et al., 2010). However, the FCR regimen is associated with higher rates of myelosuppression and infectious complications (Hallek & Al-Sawaf, 2021). In addition, this treatment option is limited by its side effects and reduced activity in patients with certain genetic risk factors such as *TP53* mutation, del(17p), del(11q), *NOTCH1* mutation, and unmutated *IGHV* status (Stilgenbauer et al., 2014).

1.1.5.2 Immunotherapy

CD20 is a cell surface molecule expressed exclusively on B cells, and it is thought to play a key role in regulating the activation, proliferation, differentiation, and function of these cells (Tedder & Engel, 1994). Targeting CD20 with rituximab is an important therapeutic approach in the treatment of CLL. While standard-dose rituximab has shown moderate clinical activity

in CLL (Schulz et al., 2002) its effectiveness is limited by the low expression of CD20 on leukemic cells (Almasri et al., 1992). However, higher doses of rituximab alone have been shown to improve the response rate (O'Brien et al., 2001). Its most important use is in combination with fludarabine and cyclophosphamide (FCR) as described above (Schulz et al., 2002; Tam et al., 2008).

1.1.5.3 Novel antibodies

Ofatumumab, commercially known as arzerra, a fully humanised monoclonal antibody to CD20, was granted approval for the treatment of CLL in 2010. It targets a unique epitope on the CD20 molecule, which is composed of both the large and small loops (Teeling et al., 2006).

A Phase II trial demonstrated significant activity and a favourable safety profile for ofatumumab as a single agent, providing clinical improvements in poor-risk patients with heavily pre-treated fludarabine- and alemtuzumab-refractory CLL (Wierda et al., 2010). In another Phase II study, ofatumumab was confirmed as a well-tolerated and effective therapeutic approach for treating previously untreated older patients with CLL (Vitale et al., 2020). However, a recent Phase II trial of idelalisib, a phosphatidylinositol-3-kinase δ (PI3Kδ) inhibitor, plus ofatumumab in CLL showed an unacceptable safety profile in the first-line setting, resulting in a short PFS despite a high overall response rate (ORR) (Lampson et al., 2019).

A phase III study compared ofatumumab with chlorambucil among untreated CLL patients who were not candidates for fludarabine-based therapy. The study showed that ofatumumab significantly improved progression free survival compared to chlorambucil alone (median PFS of 22.4 months vs. 13.1 months, HR 0.57 respectively) (Hillmen et al., 2015). The most common adverse events associated with the combination therapy were infusion-related reactions, neutropenia, and thrombocytopenia. Several Phase II and III clinical trials are currently evaluating ofatumumab for CLL.

Obinutuzumab (known by its commercial name as Gazyva/Gazyvaro) is a type II humanized monoclonal antibody targeting CD20, which has been approved for the treatment of CLL either in combination with chemotherapy or chemotherapy-free treatment. In comparison to

the other two anti-CD20 monoclonal antibodies rituximab and ofatumumab, obinutuzumab induces significantly larger amounts of cell death both *ex-vivo* by binding to CD20 on B cells and causing lysosomal-mediated cell death. Obinutuzumab has an increased antibody-dependent cellular cytotoxicity and direct-cell death, but no complement dependent cytotoxicity compared to rituximab (Davies et al., 2022; Gagez & Cartron, 2014).

A phase III study compared obinutuzumab plus chlorambucil to chlorambucil alone among untreated CLL patients with comorbidities. The obinutuzumab combination demonstrated a longer progression-free survival, higher overall response rate, and higher complete response rate. Adverse events were more common in the obinutuzumab group, including infusion-related reactions, neutropenia, and thrombocytopenia (Goede et al., 2014).

Obinutuzumab has also been evaluated in combination with other agents in CLL. In a phase Ib/II study, obinutuzumab was combined with venetoclax in CLL patients who had received at least one prior therapy. The combination therapy demonstrated an overall response rate of 77%, with a complete response rate of 21%. The most common adverse events were neutropenia and infusion-related reactions (Cramer et al., 2022; Fischer et al., 2019; Tausch et al., 2020).

In a large-scale phase III study conducted in previously untreated CLL patients, obinutuzumab combined with chlorambucil was superior to rituximab combined with chlorambucil in terms of complete response rates and PFS, with a median PFS of 26.7 months for obinutuzumab-chlorambucil and 16.3 months for rituximab-chlorambucil (HR 0.39) (Goede et al., 2014). Obinutuzumab in combination with chlorambucil has been approved for the first-line treatment of CLL patients with comorbidities making them unsuitable for full-dose fludarabine-based therapy in the US since 2013 and in Europe since July 2014 (Goede et al., 2015).

In January 2019, the US FDA approved ibrutinib (Imbruvica), a Bruton's tyrosine kinase (BTK) inhibitor, in combination with obinutuzumab for the treatment of previously untreated adult CLL patients, including those with high-risk disease. Ibrutinib plus obinutuzumab is the first chemotherapy-free, anti-CD20 combination regimen approved for CLL. At a median follow-up of 31.3 months, ibrutinib plus obinutuzumab significantly prolonged PFS compared to chlorambucil plus obinutuzumab, with a 77% reduction in risk of progression or death (iLLUMINATE clinical trial) (Moreno et al., 2019).

Alemtuzumab, also known by its generic name Campath, is a monoclonal antibody that targets the CD52 antigen, a protein present on the surface of mature lymphocytes, but not on their stem cells (Alinari et al., 2007; Faderl et al., 2005; Frampton & Wagstaff, 2003; Tembhare et al., 2013). It was used as second line therapy for CLL. A combination of fludarabine and alemtuzumab has been shown to provide better progression-free survival (median PFS, 23.7 months vs. 16.5 months, HR 0.61) and overall survival (median not reached vs. 52.9 months) in relapsed or refractory CLL patients compared to fludarabine monotherapy (Elter et al., 2011). Although, initial studies did not demonstrate improved survival in high-risk CLL patients treated with alemtuzumab (Jones et al., 2013). Subsequent studies found that the combination of alemtuzumab and fludarabine had a manageable safety profile and provided benefits to patients with an adverse biological profile (Mauro et al., 2014).

1.1.5.4 BCR signalling inhibitors

Ibrutinib (originally known as PCI-32765 and commercially as Imbruvica) is a highly potent and specific small molecule inhibitor that binds irreversibly to Bruton's tyrosine kinase (BTK), which is essential for BCR signalling (Satterthwaite & Witte, 2000). BTK is critical for the survival of leukemic cells in various B-cell malignancies, including CLL (Tsukada et al., 1993; Craxton et al., 1999). Both *in-vitro* and *in-vivo* assays showed that PCI-32765 induced cytotoxicity (Pan et al., 2007). Preclinical studies demonstrated that targeting BTK with PCI-32765 inhibited the proliferation of CLL cells *in-vitro* and *in-vivo* and effectively blocks survival signals provided externally to CLL cells (Herman et al., 2011; Ponader et al., 2012).

In February 2014, the FDA granted accelerated approval for ibrutinib as a breakthrough therapy for patients with CLL who had undergone at least one prior therapy, based on the positive results from the phase II trial (Byrd et al., 2013). The subsequent phase III trial, RESONATE, showed that ibrutinib was significantly more effective than ofatumumab in improving overall response rates (ORR) in patients with relapsed/refractory CLL, including those with high risk chromosome (del[17p]) 13.1 deletion and resistance to chemoimmunotherapy (Byrd et al., 2014). Additionally, ibrutinib as a single agent demonstrated superiority over chlorambucil in initial therapy for patients with CLL or SLL in the RESONATE-2 trial (Burger et al., 2015). Further studies provided additional evidence

and updated long-term safety and efficacy results for the use of ibrutinib in difficult subsets of CLL and SLL patients (O'Brien et al., 2016; Byrd et al., 2019).

Due to its significant efficacy, ibrutinib has become a preferred treatment option (Byrd et al., 2021; Y. Khan & O'Brien, 2019) over others like FCR, idelalisib plus rituximab or bendamustine plus rituximab for relapsed/refractory CLL (Wendtner, 2019). However, despite its effectiveness, there is still a need for alternative treatment options for the small proportion of patients who relapse during ibrutinib therapy due to mutations in BTK (Woyach et al., 2014). As a result, ongoing clinical trials are evaluating ibrutinib in patients with CLL and ibrutinib resistance mutations. Although, ibrutinib and recently acalabrutinib and zanubrutinib are the FDA approved BTK inhibitors for CLL treatment (Brown et al., 2023; Byrd, Hillmen, et al., 2021), other BTK inhibitors, such as tirabrutinib (ONO- 4059) and CC-292 are currently being developed and are expected to become available for clinical use in the near future (Brown et al., 2016; Wu et al., 2017; Tam et al., 2015).

Acalabrutinib (ACP-196, marketed as Calquence) is a potent selective second-generation BTK inhibitor that irreversibly binds to the protein. Compared to ibrutinib, acalabrutinib has shown higher selectivity and inhibition of BTK activity, making it a promising compound in this class of inhibitors (Harrington et al., 2015; Wu et al., 2017). Preclinical studies in mouse models of CLL demonstrated significant reduction in tumour burden and increased survival, indicating its potent on-target effects and efficacy (Herman et al., 2017). In a phase I/II study, acalabrutinib demonstrated impressive clinical activity in relapsed CLL patients, including those with del(17p), with an ORR of 95% at a median follow-up of 14.3 months, while the ORR was 100% among patients with del(17p) (Byrd, Woyach, et al., 2021).

In a Phase II study, acalabrutinib was combined with obinutuzumab, in patients with previously untreated CLL. The combination therapy demonstrated an overall response rate of 93%, with 87% of patients achieving a partial response and 6% achieving a complete response. The most common adverse events were infusion-related reactions, headache, and diarrhoea.(Sharman et al., 2020).

Another Phase II study evaluated the combination of acalabrutinib with venetoclax, a BCL2 inhibitor, in patients with relapsed/refractory CLL. The combination therapy demonstrated an overall response rate of 95%, with 79% of patients achieving a complete response. The most common adverse events were neutropenia, diarrhoea, and upper respiratory tract infection (Byrd et al., 2013). Currently, a phase III trial is underway to compare acalabrutinib (ACP-

196) and ibrutinib in high-risk CLL patients who have been previously treated (NCT 02477696).

Idelalisib, previously known as GS-1101 and CAL-101, and currently marketed as Zydelig, is a small molecule inhibitor of phosphatidylinositol 3-kinase-δ (PI3Kδ), an enzyme presents in normal lymphoid cells (Lucas et al., 2014; Okkenhaug & Vanhaesebroeck, 2003) as well as in malignant B cells, including CLL (Brown et al., 2016) . Among different PI3K isoforms, the delta isoform of the p110 catalytic subunit of (PI3Kδ) acts as predominant mediator for PI3K highly expressed in white blood cells (WBC) for B cell function signals (Takeda et al., 2019; Thian et al., 2020). Idelalisib induces caspase-dependent cytotoxicity in primary CLL cells, irrespective of the commonly used prognostic markers, such as del(17p) and *IGVH* status. It also impedes various signals that activate B cells, such as CD40 ligand (CD40L), TNF-α, and fibronectin (Brown et al., 2016). In addition, idelalisib has been demonstrated to enhance the sensitivity of CLL cells towards bendamustine, fludarabine, and dexamethasone in stromal cocultures (Hoellenriegel et al., 2011).

After ibrutinib was approved, the use of idelalisib ± rituximab was included in the European Society for Medical Oncology (ESMO) clinical practice guidelines for CLL in 2015 (Furman et al., 2014; Jones et al., 2017) Idelalisib, in combination with rituximab exhibited an ORR of 76.5% in patients with high-risk CLL carrying both del(17p) and $TP53^{MUT}$ mutations, whereas patients receiving placebo and rituximab had an ORR of 0% (Coutre et al., 2018; Furman et al., 2014).

In another phase II study, idelalisib was evaluated as a single agent in patients with relapsed CLL who were not candidates for chemotherapy due to advanced age or comorbidities. The study showed an overall response rate of 57% and a median progression-free survival of 11 months. The most common adverse events were diarrhoea, fatigue, and nausea. (O'Brien et al., 2015).

Idelalisib has also been evaluated in combination with other agents in CLL. In a phase III study, idelalisib was combined with bendamustine and rituximab, a monoclonal antibody commonly used in patients with relapsed or refractory CLL. The combination therapy demonstrated a significantly higher overall response rate (84% vs. 68%) and longer progression-free survival (median of 20.8 months vs. 11.1 months) compared to bendamustine and rituximab alone. The most common adverse events were neutropenia, pyrexia, and diarrhoea (Zelenetz et al., 2017).

After conducting a large-scale phase III trial, the FDA approved idelalisib in July 2014 for the treatment of several hematologic malignancies, including relapsed CLL when used in combination with rituximab (Furman et al., 2014). In the European Union, idelalisib has been authorized for use in combination with rituximab in patients with relapsed CLL, or as a first-line treatment in patients with *TP53* abnormalities that are not suitable for chemoimmunotherapy.

Despite its efficacy, idelalisib has been associated with some adverse events, including autoimmune toxicities, hepatotoxicity, and pneumonitis. These side effects led to the discontinuation of idelalisib in some patients and the implementation of risk mitigation strategies, such as close monitoring and prophylactic treatment (Coutré et al., 2015).

In conclusion, idelalisib has emerged as a promising therapeutic option for high-risk CLL patients, including those with del(17p) and other adverse prognostic factors. As a targeted therapy, idelalisib holds the potential for prolonged efficacy and reduced toxicity compared to conventional chemoimmunotherapy regimens. However, it is important to note that serious adverse events have been observed in patients treated with idelalisib and rituximab, leading to treatment discontinuation in some cases. Grade ≥3 adverse events, such as pneumonia, diarrhoea, and neutropenic fever, have been reported in 6-20% of patients (Brown et al., 2014; O'Brien et al., 2013).

Duvelisib, also known as IPI-145 and marketed as Copiktra, is a small dual molecule inhibitor of two different isoforms of phosphoinositide 3-kinase, PI3Kδ and PI3Kγ developed for treating haematological malignancies. It is approved by the US Food and Drug Administration (FDA) for the treatment of relapsed or refractory CLL and SLL (D. A. Rodrigues et al., 2018; Tangudu et al., 2019).

Consequently, in September 2018, the FDA approved duvelisib as a new drug for the treatment of relapsed/refractory CLL after at least two prior therapies (Flinn et al., 2018). Currently, duvelisib is under further investigation in several clinical trials because it increases the risk of infections and autoimmune complications, such as pneumonitis and colitis.

1.1.5.5 BCL-2 inhibitors

The B cell leukaemia/lymphoma 2 (BCL-2) protein family is known to play a crucial role in the survival of CLL cells, as indicated by previous studies (Cory & Adams, 2002; Moore et al., 2007). These proteins are responsible for regulating apoptosis primarily through the intrinsic apoptotic pathway (Letai, 2008). In CLL, the anti-apoptotic proteins BCL-2, BCL-xL, and MCL-1 are frequently overexpressed, leading to poor prognosis and shorter survival (Robertson et al., 1996; Pepper et al., 1997).

Navitoclax (also known as ABT-263) is an orally available small-molecule inhibitor that selectively targets BCL-2/BCL-xL protein interactions, contributing to the survival of CLL cells. Navitoclax has been found to significantly enhance the antitumor activity of relevant therapeutic regimens, including R-CHOP, rituximab, bortezomib, and rapamycin, both *in-vitro* and *in-vivo* models of B cell lymphoma.

In a Phase I study, navitoclax was administered orally to relapsed or refractory CLL patients. The study demonstrated that more than 50% of the patients showed a reduction in the lymphocytosis and 35% showed a partial response rate. The most common adverse events were thrombocytopenia, anaemia, and neutropenia (Roberts et al., 2012).

Despite its promising results, navitoclax has some limitations, including dose-limiting thrombocytopenia and neutropenia. To overcome these limitations, a second-generation BCL-2 inhibitor, venetoclax, was developed, which has shown superior efficacy and tolerability compared to navitoclax (Roberts et al., 2016).

Venetoclax, also known as ABT-199 or venclexta, was derived from navitoclax and exhibits enhanced bioavailability and a greater affinity for BCL-2 compared to BCL-xL (Souers et al., 2013). Venetoclax's ability to induce apoptosis in CLL cells is ten times more potent than navitoclax while avoiding detrimental effects on platelets (Seymour et al., 2018).

A phase I dose-escalation study involving 56 patients with relapsed or refractory CLL assessed the safety and efficacy of venetoclax (Roberts et al., 2016). The ORR across all patients was 79%, with a complete remission rate of 20% and a progression-free survival (PFS) rate of 69% after 15 months. Patients in subgroups with adverse prognostic factors, such as fludarabine resistance, del(17p), and unmutated *IGHV*, had an ORR ranging from 71

to 79%. The findings of the phase I study justified the need for further evaluation in larger randomized trials (Anderson et al., 2016).

A subsequent phase II trial involving 107 patients with relapsed or refractory CLL and del(17p) demonstrated the safety and efficacy of venetoclax observed in the phase I trial. Venetoclax monotherapy elicited a response in 85 out of 107 patients, with 18 achieving minimal residual disease (MRD) negativity in the peripheral blood and six attaining MRD negativity in the bone marrow (Stilgenbauer et al., 2016).

In 2016, the FDA approved venetoclax for use in relapsed or refectory CLL patients with del(17p) alteration who were previously treated. Ongoing clinical trials are investigating the use of venetoclax in combination with other drugs such as duvelisib (NCT 03534323), and ibrutinib (NCT 03513562).

1.2 B-cell receptor (BCR) signalling

One of the main aims of this PhD project was to investigate potential effects of the CLL cell microenvironment on the response of CLL cells to MDM2 and WIP1 inhibitors, particularly factors involved in B-cell receptor signalling. This was modelled with primary CLL cells *ex-vivo* and included the influence of stimulation with CD40L, IL-4 and anti-IgM. The following provides background information on BCR signalling.

1.2.1 BCR signalling in normal B-cells

In normal B-cells, the initial engagement of the antigen to BCR through surface immunoglobulin (sIg) leads to formation of the signalosome, which is a complex of kinases and scaffold proteins, tethered at sIg activation sites of the plasma membrane (Pierce & Liu, 2010). The formation of the signalosome complex induces membrane movement and aggregation of BCR components that leads to phosphorylation of immune-receptor tyrosine–based activation motifs (ITAMs) in the cytoplasmic C-terminal tail of BCR-associated Igα (CD79A) and Igβ (CD79B) by the SRC-family kinase LYN. Then, the phosphorylated ITAMs recruits the spleen tyrosine kinase (SYK) to the receptor through its tandem SH2 domain, leading to SYK activation via SRC-family kinase-dependent phosphorylation. The BCR signal is further propagated by SYK via association with the adaptor protein, B cell linker protein (BLNK), and activated its downstream signalling components Bruton Tyrosine Kinase

(BTK) and phospholipase Cγ2 (PLCγ2), phosphatidylinositol 3-kinase (PI3K), and VAV. The Vav family proteins (Vav1, Vav2, Vav3) are cytoplasmic guanine nucleotide exchange factors (GEFs) for Rho-family GTPases. Then, further distal BCR signals of PLCγ2 and /Rapidly Accelerated Fibrosarcoma (RAS/RAF1) signalling cascade are involved in the activation of mitogen-activated protein kinase (MEK) pathways, including the extracellular signal-regulated kinase 1/2 (ERK1/2) (Hashimoto et al., 1998; Stevenson et al., 2011). Signals produced from those signalosomes initiate and regulate downstream signalling cascade including RAS/RAF/MEK/ERK pathway, which are significant for B-cell fate decisions such as proliferation, survival, migration, differentiation and cell death.

1.2.2 BCR-mediated signalling in CLL cells

CLL is classified into two subsets based on the somatic hypermutation changes of tumour *IGHV* genes. CLL with unmutated *IGHV* genes U-CLL which derive from naïve $CD5^+$ $CD27^-$ B cells of the healthy normal antibody types and CLL with mutated *IGHV* genes M-CLL derive from post-germinal centre $CD5^+$ $CD27^+$ cells (Forconi et al., 2010; Seifert et al., 2012). Clinically, both U-CLL and M-CLL have distinct response against therapy, with U-CLL having more aggressive disease (BCR signalling due to engagement of antigen with sIgM can be ongoing in both groups). The presence or absence of signalling is dependent on the distinct responses between subtypes to determine clinical behaviour (Stevenson et al., 2011). Anergy, a state of cellular lethargy, which is induced following positive antigen signalling engagement in the absence of T-helper cell, is observed in all CLL cells but (Cambier et al., 2007) prominently in M-CLL and is associated with indolent disease (Stevenson et al., 2011). In contest, antigen engagement signalling induce cells proliferation and survival appears more in U-CLL cells (Byrd et al., 2013).

In-vivo in CLL patients, antigen signalling engagement with sIgM of BCR is thought to occur within proliferation centres (PCs) which are predominantly found in the lymph nodes (LNs) of CLL patient organs. Following BCR stimulation, CLL cells migrate to blood circulation, carrying temporary “imprint” parts/residue from the prior tissue-based stimulation (Coelho et al., 2013; Calissano et al., 2011). Patients with M-CLL blood cells possess CLL with anergy markers which is includes strong down-modulation of sIgM expression and signalling stimulation of (ERK1/2) phosphorylation and NFAT cells expression (Mockridge et al., 2007; Apollonio et al., 2013). In contrast, patients with U-CLL cells are able to maintain the antigen signalling and sIgM expression responsiveness and express higher positive marker of BCR signalling levels, including the proliferation and survival promoting proteins including MYC

and MCL-1 (Pepper et al., 2008; W. Zhang et al., 2010). The positive signalling of U-CLL is associated with more progressive disease.

Positive antigen signalling can be mimicked in *ex-vitro* microenvironment by stimulating the CLL cells with immobilised anti-IgM antibodies, which increases expression of BCR signalling markers in CLL samples U-CLL that retain sIgM responsiveness (Petlickovski et al., 2005; Krysov et al., 2012). Even though, the clinical response behaviour of M-CLL cells are distinct from U-CLL cells, there is heterogeneity within these subsets, particularly within M-CLL more than U-CLL cells (Mockridge et al., 2007).

1.2.3 BCR signalling in CLL cells

BCR signalling plays a crucial role in the pathogenesis of CLL. CLL cells express a BCR that is typically composed of sIg molecule and a dimer of the CD79a/CD79b proteins. The sIg molecule recognizes antigens, and its engagement by antigen leads to the activation of downstream signalling pathways that promote cell survival, proliferation, and resistance to apoptosis (Herman et al., 2011).

The activation of BCR signalling in CLL is facilitated by the microenvironment in which CLL cells reside, which provides co-stimulatory signals that enhance BCR-mediated signalling. In addition, CLL cells undergo a process of antigenic selection that leads to the enrichment of cells with BCRs that exhibit increased signalling capacity (Burger & Wiestner, 2018).

Shortly after its discovery, BTK was identified as a downstream component of BCR signalling following the antigen receptor (Figure 1.4) (Du & Lovly, 2018). BTK is associated with cellular membrane complex of B-cells. BTK is attached to the cytoplasm of cells in an inactive form. Upon activation of the BCR by an antigen, BTK is recruited to the cell membrane, where it becomes phosphorylated and triggers a signalling cascade that leads to various cellular responses.

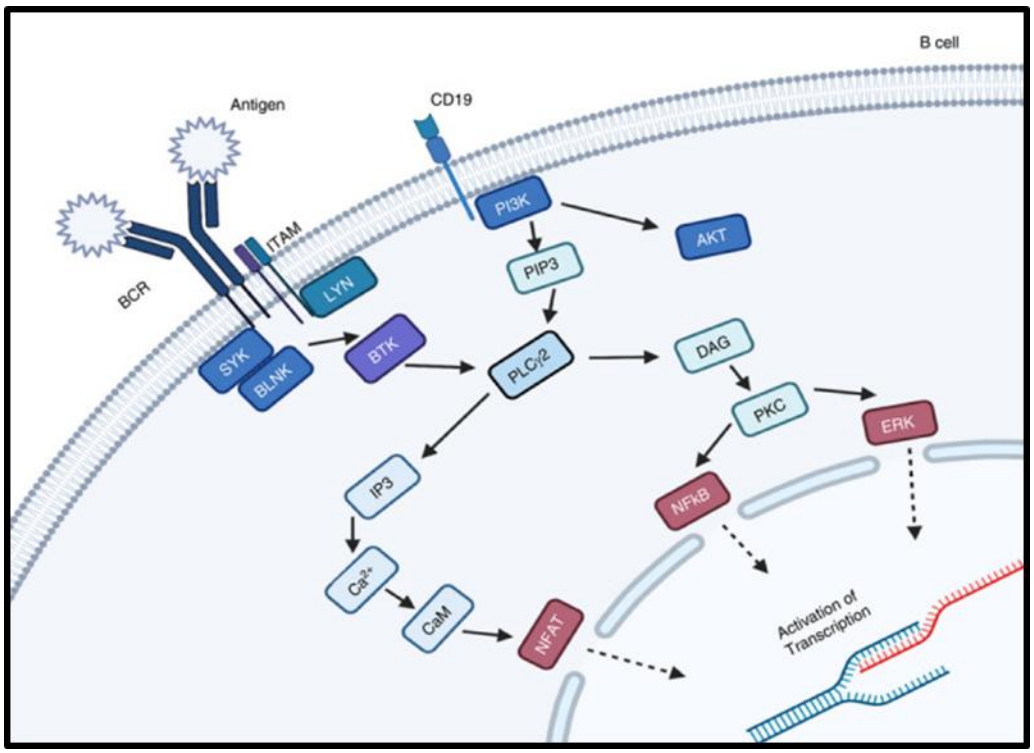

Figure 1.4 Structural overview of BTK and its position within the B-cell receptor signalling pathway (McDonald et al., 2021)**.**

1.2.4 Proximal B Cell Receptor Signalling Events

The process of BCR signalling is initiated when an antigen is recognized and subsequently leads to the phosphorylation of CD79 molecules that are associated with the BCR. This event activates the proximal signalling molecules, which ultimately results in the formation of a central signalling complex, referred to as the signalosome (Figure 1.5). The activation of the signalosome leads to the downstream activation of various signalling cascades, including the NFAT, nuclear factor κB (NF-κB), and Ras-extracellular-signal-regulated kinase (ERK) pathways. Additionally, the co-receptor CD19 is essential for the activation of the PI3K–AKT pathway.

The BCR is composed of a pair of identical immunoglobulin heavy (IgH) and light (IgL) chains, each possessing a distinctive variable region that enables the recognition of diverse antigens present in the surrounding environment. The extracellular segment of the BCR is non-covalently linked to a disulfide-linked heterodimer comprised of CD79A and CD79B. This association allows the BCR to be expressed on the plasma membrane and enables the internalization of the BCR after antigen recognition (Gazumyan et al., 2006; Hou et al., 2006).

The intracellular segment of the CD79 molecules comprises ITAMs, which serve as binding sites for SRC kinases like LYN, FYN, and B-lymphoid tyrosine kinase (BLK). Upon

crosslinking of the BCR by specific antigens, these SRC kinases phosphorylate the ITAM tyrosine (Saijo et al., 2003).

During the early stages of B-cell development, the ITAM in CD79 contains two tyrosine residues separated by 11 amino acids, followed by either leucine or isoleucine (Sanchez et al., 1993; Flaswinkel & Reth, 1994). Phosphorylation of these tyrosine residues by kinases such as SRC-family kinases (SFKs) trigger the activation of spleen tyrosine kinase (SYK), which plays a crucial role in signalosome formation with other kinases and adaptor proteins (Figure 1.5). SYK is recruited to the phosphorylated CD79-ITAM, thereby promoting the formation of B cell linker protein (BLNK) complexes that activate downstream signalling pathways, including BTK, PLCγ2, VAV, and growth factor receptor-bound protein 2 (GRB2), (Holroyd & Michie, 2018).

BLNK is an essential protein that acts as a scaffold to recruit SYK, BTK, and PLCγ2 in close proximity. When these proteins are deficient, it results in attenuated cytosolic Ca2+ response upon BCR stimulation (Ishiai et al., 1999). It is widely recognized that the BCR-driven constitutive but low-level "tonic" signalling and BAFFR signalling are critical for B-cell survival (Lam et al., 1997; Thompson et al., 2001; Gross et al., 2001; Miller & Hayes, 1991; MacKay et al., 2010). In the majority of follicular B-cells, this signalling is propagated through the activation of SYK (Schweighoffer et al., 2013). Surprisingly, the engagement of BAFF and its receptor leads to the direct phosphorylation of both CD79A and SYK, resulting in the activation of the PI3K and ERK signalling pathways. This suggests a cross-communication between two different receptors for B-cell survival (Schweighoffer et al., 2013).

1.2.4.1 IKK/NFκB Pathway

In response to BCR stimulation, the phosphorylated adaptor protein BLNK binds to PLCγ2 and BTK, which then activates PLCγ2 to produce the second messenger, DAG and inositol-1, 4,5-triposphate (IP3), resulting in the activation of downstream signalling events including NF-κB, activator protein 1(AP-1), cAMP response element-binding protein (CREB) and Bcl2 family genes. (Hikida & Kurosaki, 2005; Kurosaki et al., 2010).

Subsequently, DAG generated by PLCγ2 activates protein kinase Cβ (PKCβ), which phosphorylates caspase recruitment domain-containing membrane-associated guanylate kinase protein-1 (CARMA1). The phosphorylated CARMA1 recruits another kinase, TGFα-

activated kinase 1 (TAK1), which associates with the inhibitor of κB (IκB) kinase (IKK) complex (IKKα, IKKβ and IKKγ), letting TAK1 phosphorylate IKKβ (Shinohara et al., 2005). This leads to the formation of a complex between CARMA1, mucosa-associated lymphoid tissue lymphoma translocation protein 1 (MALT1), and B cell lymphoma 10 (BCL10), known as the CBM complex, which functions as a scaffold to facilitate IKK activation. The activated IKK phosphorylates IκB, leading to its ubiquitin-mediated degradation. Once IκB is degraded, NFκB translocates to the nucleus for gene regulation. The activity of NFκB is further reinforced by positive feedback regulation, as the activated IKKβ phosphorylates CARMA1 on Ser578, which contributes to the interaction of CARMA1 with MALT1 and BCL10, enhancing IKK activation (Shinohara et al., 2007).

1.2.4.2 Ras/ERK Pathway

The activation of the ERK mitogen-activated protein (MAP) kinase pathway is a consequence of BCR stimulation (Nagaoka et al., 2000; Yasuda et al., 2008; Rowland et al., 2010). This pathway is regulated by a family of RAS small GTP-binding proteins, which can be activated by the guanine nucleotide exchange factor (GEF) that replaces Ras-bound GDP for GTP and is inactivated by GTPase-activating proteins (GAPs), which set Ras proteins back to its GDP-bound inactive state. In particular, the Ras guanine-nucleotide releasing proteins (RasGRP) family members, such as RasGRP1 and RasGRP3, act as major GEFs in this process. The C1 subdomain of RasGRP3 binds to DAG, a product of PLCγ2 activation, thereby controlling Ras activation and the ERK-MAP signalling pathway (Oh-Hora et al., 2003; Coughlin et al., 2005). Once GTP-bound, Ras activates the Raf-1/BRaf complex, which subsequently phosphorylates MEK1 and MEK2, leading to the activation of ERK. In addition, GRB2 can also activate Ras by associating with the cytoplasmic tail of the BCR heavy chains (Engels et al., 2009). The dimerization of ERK, which is phosphorylated by MEKs, allows it to translocate to the nucleus where it activates downstream transcription factors such as *Fos*, *Jun*, and *Ets* family proteins for transcriptional regulation of genes involved in proliferation (Dong et al., 2002; Hollenhorst, 2012).

1.2.4.3 PI3K Pathway

The activation of PI3K is initiated by CD19, a B cell-specific membrane protein that contains multiple tyrosine residues on its cytoplasmic tail. Upon activation of the BCR, the tail of CD19 is phosphorylated by LYN, which creates a binding site for the PI3K subunit, p85α. The association of LYN with tyrosine-phosphorylated CD19 releases the auto-inhibitory function of LYN, leading to amplification of its activity (Fujimoto et al., 2000). The adaptor protein, NCK (NCK1 and NCK2), is required to initiate the PI3K pathway, which directly binds to phosphorylated Tyr204 on CD79A, dependent on LYN, and phosphorylates BCAP for its recruitment to the signalosome (Castello et al., 2013). Activated PI3K converts PIP2 to PIP3, a secondary lipid messenger by phosphorylation. PIP3 recruits AKT and phosphoinositide dependent protein kinase1 (PDK1) to the plasma membrane, enabling PDK1 and the mammalian target of rapamycin complex 2 (mTORC2) to phosphorylate AKT at both serine 473 (Ser^{473}) and threonine residue (Limon & Fruman, 2012).

Phosphorylated AKT inhibits the mTOR signalling by phosphorylating TSC complex (Amin & Schlissel, 2008; Dengler et al., 2008; Dominguez-Sola et al., 2015; Holroyd & Michie, 2018; Lin et al., 2010; Mansson et al., 2012; Sander et al., 2015; Srinivasan et al., 2009). AKT also phosphorylates glycogen synthase kinase 3 (GSK3), which contributes to activation of multiple molecules regulating cell growth, such as c-Myc and cyclin D3 (Gregory et al., 2003; Cato et al., 2011). Furthermore, AKT inhibits the mTOR signalling via TSC complex phosphorylation (Inoki et al., 2002).

Upon antigen recognition by the BCR, CD19 and other adaptor protooncogenic proteins VAV interact with tyrosine residue at position Y391EEP (Y^{391}EEP) in the cytoplasmic tail of CD19, which is presumably phosphorylated by SYK (O'Rourke et al., 1998), facilitating localization of LYN and SYK in close proximity. VAV is then phosphorylated by SYK (Chen et al., 2011) and functions as a GEF for Rho GTPases such as Rac2 (Arana et al., 2008).

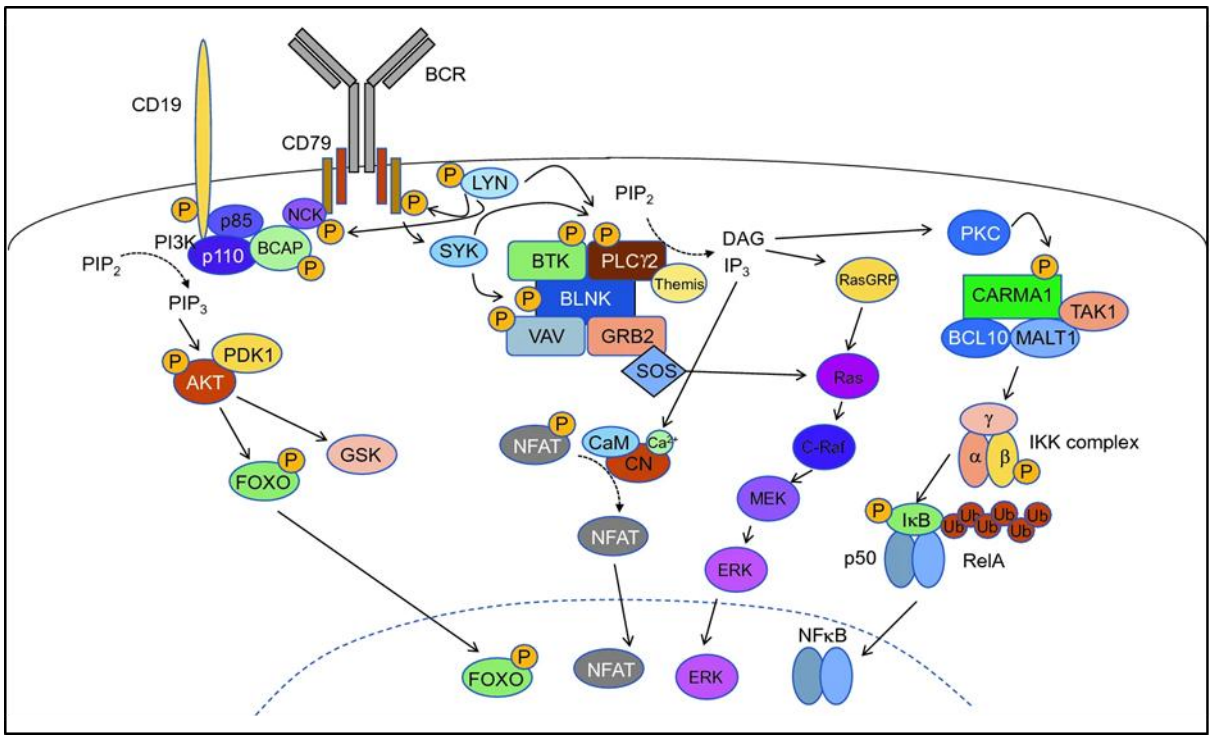

Figure 1.5 B cell signalling pathway. BCR signals cascade initiated through phosphorylation of CD79, resulting in SRC and non-SRC kinase activation. The kinases phosphorylate other co-effector signal molecules such as BTK, PCLγ2 and BLNK, which form signalosome. PCLγ2 activates Ras-ERK, IP3 and IKK–NFκB pathways. IP3 further activates calcium–NFAT pathway. CD19 activates PI3K–AKT pathway (Tanaka & Baba, 2020).

1.3 Tumour Suppressor Protein, p53

1.3.1 A brief history

Initially in 1979, multiple studies identified p53 as the cellular protein of the host that was targeted by the Large Tumour Antigen of SV40 DNA tumour virus, which is an oncoprotein carried by this virus (Met al., 1979; Lane & Crawford, 1979; Linzer & Levine, 1979; Smith et al., 1979). Up until the mid-1980s, the *TP53* gene was commonly believed to be an oncogene, as inferred from the use of p53 cDNA clones and the assumption that an increase in p53 expression led to tumorigenesis based on evaluations of the outcomes of such expression in various experimental model systems (Eliyahu et al., 1984; Jenkins et al., 1984; Parada et al., 1984).

Subsequently, it was discovered that additional p53 cDNA clones were unable to replicate the transforming effects observed with earlier clones. Further analysis of these p53 cDNA clones through sequencing showed that the ones that behaved as oncogenes contained mutations that differed from the sequence of murine wild type p53 obtained from normal tissues (Eliyahu et al., 1984; Finlay et al., 2023).

It was established that mutations in p53 were frequently observed in cell lines derived from tumours (Eliyahu et al., 1984), and it was observed that mutant cDNA of p53 derived from mouse tumours could indeed stimulate cell transformation, whereas the wild type p53 could not. Subsequent investigations and observations validated that p53 functions as a tumour suppressor, as indicated by the frequent loss of wild type p53 alleles in colorectal cancer (Baker et al., 1989) along with the mutation of the remaining allele. Additionally, it was observed that overexpression of wild type p53 could suppress transformation of cultured cells (Finlay et al., 1989).

Additional indications of p53 role as a tumour suppressor have been identified. For instance, germline *TP53* mutations are mainly responsible for the severe hereditary condition called Li Fraumeni syndrome, which is characterized by the early onset of several types of cancer (Malkin et al., 1990; Srivastava et al., 1990). Moreover, p53 knock-out mice, demonstrated a very high incidence of cancer (mostly lymphomas) (Donehower et al., 1992).

In the 1990s, it was discovered that p53 functions as a transcription factor. Multiple investigations uncovered that p53 features a functional transcriptional transactivation domain (Fields & Jang, 1990) and can bind strongly to specific DNA sequences (Bargonetti et al., 1991). This capacity to bind and transactivate genes distinguishes wild type *TP53* from practically all cancer associated *TP53* mutants. These research studies revealed the p53 binding consensus sequence, which eventually allowed for genome-wide computational searches to identify possible p53 binding sites. Subsequently, it was found that p53 transactivates *CDKN1A*, which encodes the cyclin-dependent kinase inhibitor $p21^{WAF1}$ (El-Deiry et al., 1993), and the proapoptotic *BAX* gene (Toshiyuki & Reed, 1995). Numerous *TP53* transcriptional target genes have since been identified, which p53 transactivates by binding to p53 response elements (RE) located upstream or within these genes. Many of these genes encode proteins that are closely linked to apoptosis or cell cycle control. In addition, p53 was subsequently found to possess non-transcriptional biochemical activities (Vaseva & Moll, 2009).

In 1992, researchers discovered the MDM2 protein, which is a crucial negative regulator that interacts with p53. MDM2 is an E3 ubiquitin ligase that is specific to p53, and it was shown to bind to p53 tightly and inhibit its biochemical activity, as well as target p53 for degradation (Momand et al., 1992). This occurs through the ubiquitylation and subsequent proteasomal degradation of p53 (Oliner et al., 1993). MDMX, which was identified in 1996 as a paralogue of MDM2, enhances MDM2 activity and contributes to the degradation of p53, but on its own it does not have any measurable E3 ligase activity (Shvarts et al., 1996; Linares et al., 2003).

1.3.2 The structure and function of p53

1.3.2.1 The structure of p53

The *TP53* gene is situated on the short arm of chromosome 17 and was cloned and sequenced in 1983. The human p53 protein is comprised of 393 amino acids and has distinct domains and regions that are natively unfolded, as well as in a reversible equilibrium with tetramer formation when it binds to a DNA p53-binding consensus sequence. The protein was given the name "p53" due to its migration at around 53kDa in SDS-polyacrylamide gel electrophoresis. Figure 1.6 shows the domain structure of the p53 protein along with the location of mutations frequently found in p53.

The N-terminal region of the p53 protein contains two important domains, namely the transactivation domain (TAD) spanning residues 1-62, and the proline-rich region (PRR) spanning residues 63-94. The TAD can interact with various regulatory proteins, including MDM2 and CBP/p300, which play crucial roles in regulating the stability and transcriptional activity of p53 (Chi et al., 2005).

The DNA-binding domain (DBD) of p53, consisting of residues 94–312 out of the total 393 amino acids, plays a crucial role in both cytosolic and nuclear functions of the protein (Joerger & Fersht, 2008). Majority of p53 mutations found in cancer are in the DBD (Joerger & Fersht, 2007; Green & Kroemer, 2009) and almost all of them occur at so-called mutation hot spots, which are clustered within the DBD as shown in the *IARC TP53* Mutation Database (Olivier et al., 2002). These oncogenic mutations, including *R175H*, *R282W*, *R248Q*, *R273H/L* and *R249S*, further destabilize the DBD, which is already thermodynamically and kinetically unstable, and weaken its binding to promoters of downstream target genes (Ang et al., 2006).

The TP53 protein exists as an active tetramer consisting of four identical, which associate via their tetramerization domains at the C-terminus (TDs; residues 325-355) (Iwabuchi et al., 1993). In response to cellular damage, p53 activates the expression of genes that play a vital role in DNA repair, apoptosis, cell cycle arrest, and senescence. This activation occurs through the binding of p53 to its specific DNA response elements located near the promoters of *TP53* target genes. The DBD of p53 binds to double-stranded target DNA containing two decamer motifs, RRRCWWGYYY, separated by a spacer of 0-13 base pairs. Here, W is either A or T, R is either C or G, and Y is either C or T (Vogelstein et al., 2000; Wang et al., 2009; El-Deiry et al., 1992).

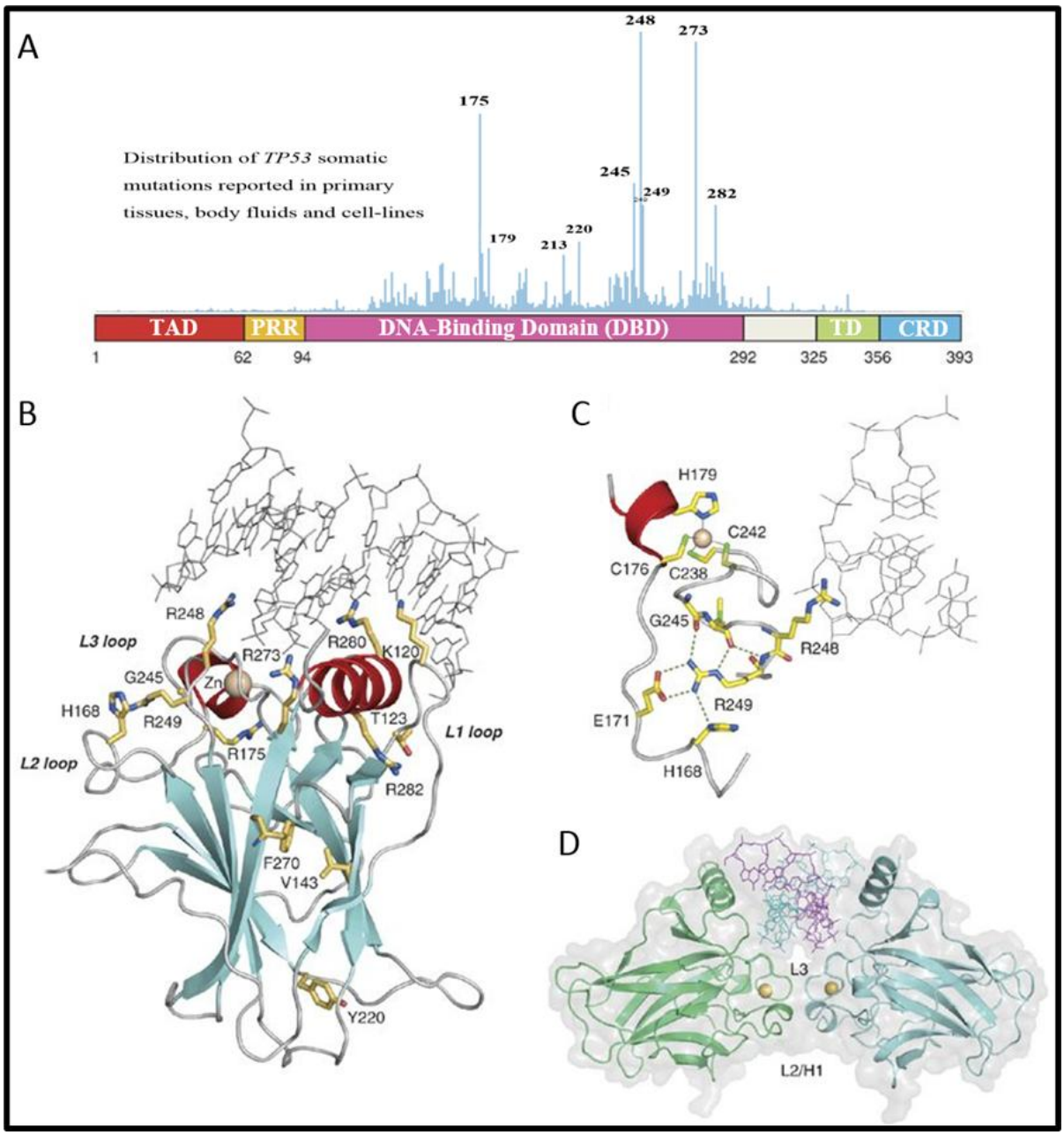

Figure 1.6 Domain structure of p53. (A) The 393-amino acid protein includes a transactivation domain (TAD) located at the N-terminus, followed by a proline-rich region (PRR), a central DNA-binding core domain (DBD), a tetramerization domain (TD), and a C-terminal regulatory domain (CRD). The frequency of TP53 somatic mutations observed in primary tissues, body fluids, and cell lines are represented by vertical bars, which are based on data obtained from the TP53 mutation database of the International Agency for Research on Cancer (IARC), (version R19, www-p53.iarc.fr) (B) Ribbon diagram of the structure of the DNA-bound p53 core domain (PDB ID code 2AHI) (Kitayner et al., 2006; Joerger & Fersht, 2007).(C) Close-up view of the L2/L3 region, including the zinc-binding site, in the structure of DNA-bound wild-type. (D) DBD dimer bound to a DNA half-site (PDB ID code 2AC0) (Joerger & Fersht, 2007).

1.3.2.2 The functions of p53

The p53 tumour suppressor is a transcription factor that regulates several genes with diverse functions such as DNA repair, metabolism, cell cycle arrest, apoptosis, and senescence (Levine & Oren, 2009; Wade et al., 2010). The protein's stability and level are increased, and

its transcription factor function is activated, by upstream signalling in response to various stressors, while downstream components execute the appropriate cellular response (Brown et al., 2009). The *TP53* gene and encoded p53 protein have been found to be mutated or functionally inactivated to varying extents in most human cancers (Hollstein et al., 1991; Wade et al., 2013). It is one of the most frequently mutated genes in human cancer (Olivier et al., 2010). Mutation of *TP53* results in loss of wild type p53 tumour suppressor function and can also have dominant oncogenic functions (gain-of-function mutations) that are entirely independent of wild type p53, causing cancer cell development, survival, and proliferation (Muller & Vousden, 2013).

1.3.3 Cell cycle checkpoints and regulation by p53

1.3.3.1 Cell cycle and p53

Cell division is a complex process that involves the duplication of genetic material and precise regulation of the cell cycle. Signals from growth regulatory proteins and genetic integrity monitors ensure that the genetic material is undamaged before the cell divides. The cell cycle consists of four distinct phases, including G1, S, G2, and M phases, through which progression is regulated by cyclin-dependent kinases (CDKs) that form active heterodimeric kinase complexes when bound with their cyclin partners. CDKs are a type of protein kinase that phosphorylate serine and threonine residues.

Specific cyclin/cdk heterodimers are formed during each phase of the cell cycle. However, before proceeding to the next phase, signalling pathways monitor the successful completion of previous events to ensure successful cell cycle progression (Malumbres & Barbacid, 2001).

The process of cell division initiated with the gap 1 (G1) phase, followed by DNA synthesis (S) phase in which DNA replication occurs, and then another gap phase (G2). In the G2 phase, the cell grows, produces organelles and proteins, and rearranges its contents to prepare for the next phase, mitosis (M). The phases G1, S, and G2 together are referred to as interphase. There is also a resting phase called G0, where cells exit the cell division cycle and stop growing and dividing (Vermeulen et al., 2003).

Mitogenic signals initiate the formation of complexes of cyclin D and CDK4/6, which activate the transition from the G1 phase to the S phase by phosphorylating various cellular targets such as the retinoblastoma (Rb) protein. Hyperphosphorylation of Rb attenuates its growth inhibitory functions and promotes transcriptional activation via the E2F family. The

E2F proteins activate the transcription of *CCNE*, which encodes cyclin E that then interacts with CDK2, resulting in increased Rb phosphorylation and passage through the restriction point. When Rb is hyper-phosphorylated, it no longer binds to E2F transcriptional factor, and instead, E2F is released to stimulate the expression of genes that drive cells from G1 phase to S phase. Cyclin A and CDK2 are necessary for S phase progression, and cyclin A-CDK1 is required to transition from G2 to M phase, which is regulated by the cyclin B-CDK1 complex. Other proteins, such as Polo-like kinase 1 (PLK1) and Aurora kinases (Aurora A and Aurora B), are necessary for regulation of cell cycle progression (Figure 1.7) (Otto & Sicinski, 2017).

Signals that inhibit growth counteract the progression from G1 to S phase by increasing the expression of proteins that inhibit CDK activity. These include the INK4 family (p16INK4A, p15INKB, p18INK4C and p19INK4D), which bind to CDK4/6 and prevent their association with cyclin D, resulting in inhibition of CDK4/6 kinase activity and arrest at the G1 phase. Additionally, the CIP/KIP family (p21CIP1, p27KIP1, and p57KIP2) can bind to all cyclin-CDK complexes and predominantly inhibit the kinase activity of CDK2 and CDK1, leading to arrest at both G1 and G2 phases.

After DNA damage occurs, the cell activates various mechanisms to either remove or manage the damage or trigger apoptosis to eliminate the cell. A DNA damage checkpoint is one such mechanism that arrests the cell cycle from progressing, giving time for the repair and protection of damaged or unfinished chromosomes to prevent their transfer. This DNA damage response reaction is essential for cellular survival and genomic stability (Sancar et al., 2004).

Moreover, specialized proteins detect DNA damage and initiate cell cycle arrest through checkpoint kinase 2 (CHK2) and p53 in the G1 phase or through CHK1 in the S or G2 phase. This process is depicted in (Figure 1.7) (Otto & Sicinski, 2017).

CDK inhibitors play a crucial role in cell cycle arrest when exposed to different stimuli such as cellular stress (Sherr & Roberts, 1995). The cyclin-dependent kinase inhibitor known as p21, or $p21^{WAF1/Cip1}$, is encoded by the *CDKN1A* gene, which is a primary transcriptional target of p53 and has been extensively researched (Figure 1.8) (Dotto, 2000). The crucial function of $p21^{WAF1/Cip1}$ in suppressing tumours has been demonstrated through studies on $Cdkn1a^{-/-}$ mice, which developed various types of tumours, including hematopoietic, endothelial, and epithelial tumours, accounting for approximately 65% of all tumours (Martín-Caballero et al., 2001). Upon sensing DNA damage, p53 initiates the expression of *CDKN1A*,

which is responsible for inhibiting the progression of cell cycle both at the G1/S 2 (Brugarolas et al., 1995) and G2/M phases (Waldman et al., 1996; Bunz et al., 1998). During G1 phase arrest, p21WAF1 modulates the activity of E2F by inhibiting the recruitment of co-activators to the E2F transcriptional complex through disrupt the interaction between cyclin E/CDK2 and Rb (Delavaine & La Thangue, 1999). In addition, $p21^{WAF1}$ inhibits the kinase activity of CDK1 leading to cell-cycle arrest in the G2/M phase (Chan et al., 2000).Meanwhile, GADD45, for which the gene is also a downstream target of p53, prevents the progression of G2/M by inhibiting the cyclin B-CDK1 complex, eventually leading to G2 arrest (Zhang et al., 1994).

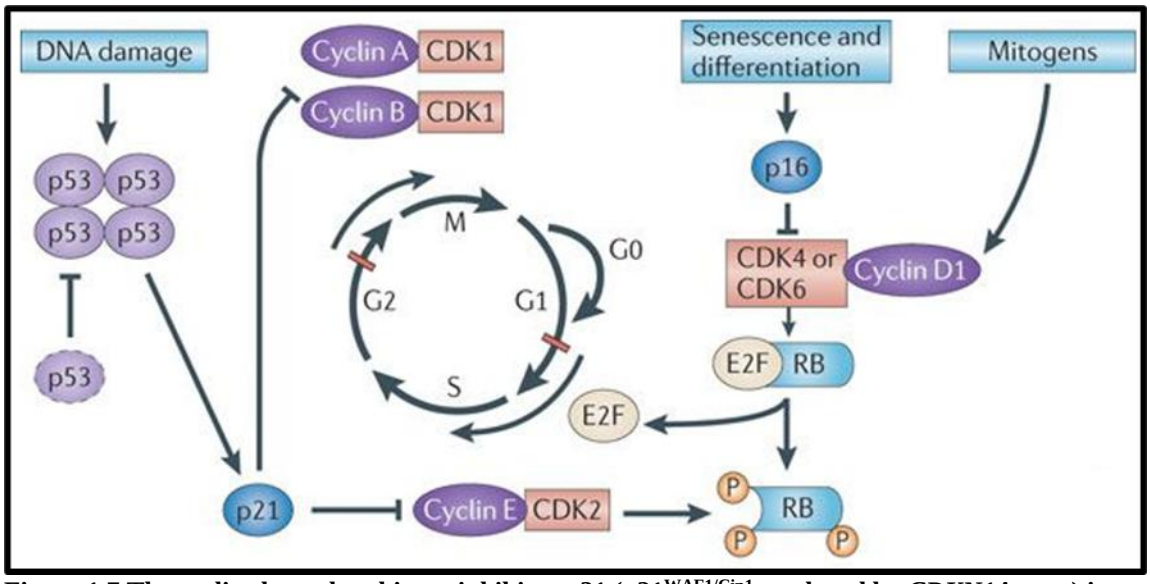

Figure 1.7 The cyclin-dependent kinase inhibitor p21 ($p21^{WAF1/Cip1}$ produced by *CDKN1A* gene) is a crucial target of p53 that inhibits various cyclin-CDK complexes and arrests the cell cycle. The activation of $p21^{WAF1}$ prevents the phosphorylation of RB by cyclin-CDK complexes. The RB protein in a hypo-phosphorylated state binds to the E2F transcription factor, thus preventing the progression of the cell cycle from G1 to S phase. (Leemans et al., 2011).

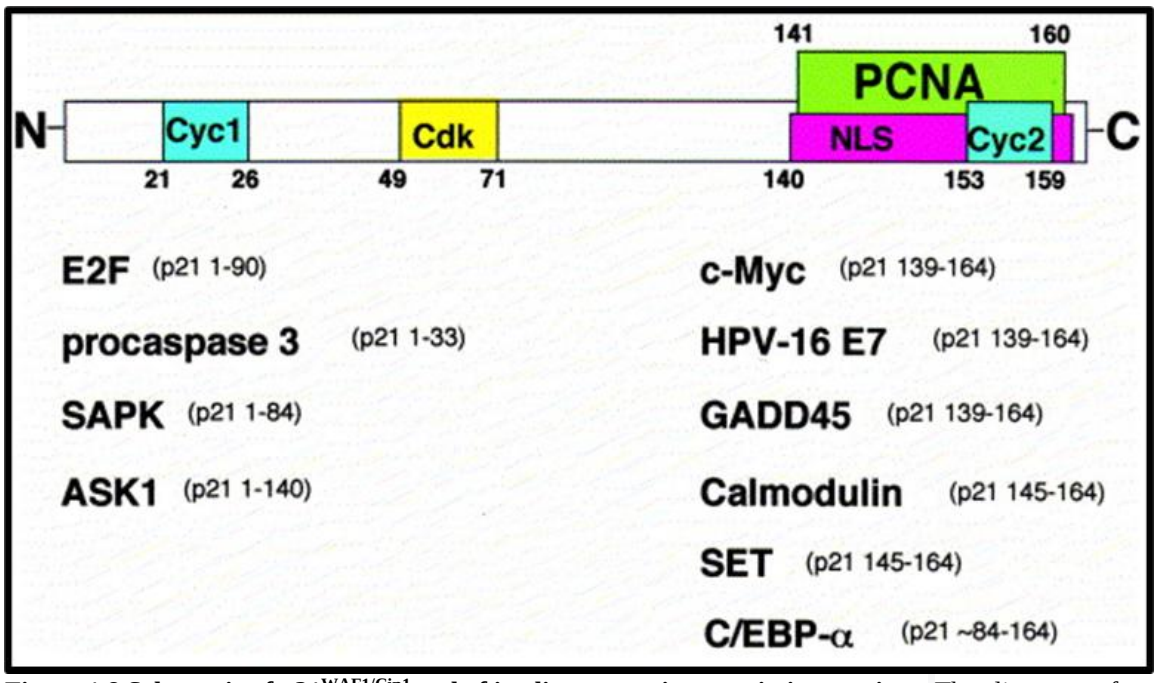

Figure 1.8 Schematic of p21$^{WAF1/Cip1}$ and of its direct protein–protein interactions. The alignment of proteins to the N- or C-terminus domains of p21 is expressed by the terms left and right, respectively. Cyc1 and Cyc2: cyclin binding sites. CDK: kinase-binding site. NLS: nuclear localization signal. PCNA: proliferating cell nuclear antigen binding site. The p21 binding domains for the listed proteins are indicated as amino acid residues between brackets (Dotto, 2000).

1.3.3.2 Phosphorylation of p53

The initiation of p53 activation in response to DNA damage or replication stress is mediated by the protein kinases ATM and ATR, which are activated by double-strand breaks and single-strand breaks, respectively. Phosphorylation of p53 at the N-terminus hinders MDM2 binding and promotes interaction with other transcription factors. Among the various phosphorylation sites, Ser15 phosphorylation is considered a pivotal event in p53 activation. Following this modification, casein kinase 1 (CK1) can sequentially phosphorylate threonine 18 (Thr18) through the phosphorylated Ser15 as a recognition determinant. Previous studies indicate that phosphorylated Thr18 inhibits the p53/MDM2 association, thereby uncoupling p53 from degradation. Although phosphorylation of residues other than Thr18 in the TAD does not significantly affect the interaction of p53 with MDM2, it stimulates interaction with CBP/p300, a transcriptional cofactor of p53. Two essential principles regulate p53 induction and activation: phosphorylation of N-terminal sites acts as a switch, allowing for quick uncoupling of MDM2 and recruitment of key transcription factors, while the cooperation between different phosphorylation sites permits fine-tuning of the association between p53 and p300/CBP, which acetylates the lysine of the C-terminus of p53 (J. T. Lee & Gu, 2010; Loughery & Meek, 2013).

1.3.4 TP53 abnormalities in CLL

TP53 aberrations constitute a potent prognostic and predictive indicator in CLL, guiding clinical decisions regarding treatment. These aberrations are closely linked to significantly reduced survival rates and suboptimal responses to chemoimmunotherapy (Zenz et al., 2010). *TP53* aberrations can be developed through a variety of genetic alterations, including deletion of the short arm of chromosome 17 (del[17p]), as well as mutations such as missense mutations (accounting for 75% of *TP53* mutations detected), insertions or deletions (indels), nonsense mutations or splice-site mutations (Leroy et al., 2014). *TP53* gene mutations primarily affect the DNA-binding domain, which is composed of exons 4-8 of the *TP53* gene. However, mutations may also occur in the oligomerization domain or C-terminal domain. In CLL, there are five frequently altered codons (codons 175, 179, 209, 248, and 273), which are considered 'hotspot' codons (Zenz et al., 2010).

Deletion of the short arm of chromosome 17 (del[17p]) is observed in around 4-9% of CLL patients at the time of diagnosis (Döhner et al., 2000; Delgado et al., 2012; Zenz et al., 2010). These patients have a very poor prognosis, primarily due to their unresponsiveness to standard therapies (Greipp et al., 2013; Buccheri et al., 2018). In numerous clinical trials, patients with del(17p) exhibited the shortest overall and progression-free survival, indicating an unfavourable prognosis (Catovsky et al., 2007; Grever et al., 2007; Hallek et al., 2008). The loss of *TP53* is thought to be responsible for the dismal prognosis associated with del(17p). Although del(17p) is rare at the time of diagnosis, the frequency of its occurrence significantly increases up to 30% in patients with relapsed or treatment-resistant disease (Stilgenbauer et al., 2009).

The *TP53* gene is located on band 13 of the short arm of chromosome 17, specifically at 17p13. In around 5-10% of CLL patients which show no deletion of 17p, *TP53* is disrupted by mutations (Zenz et al., 2008; Puente et al., 2011; Nadeu et al., 2016). Around 80% of CLL patients with del(17p) also exhibit *TP53* mutations on the remaining allele, while some patients possess *TP53* mutations without del(17p) (Zenz et al., 2008; Rossi et al., 2009).

The most common technique used for evaluating *TP53* status in CLL is fluorescence in situ hybridization (FISH) to detect del(17p), sanger sequencing, and next generation sequencing to identify *TP53* mutations. The results of clinical studies highlight the significance of examining *TP53* aberrations, encompassing both del(17p) and *TP53* mutations, prior to each therapy course to facilitate informed therapeutic decisions and enhance patient outcomes (Malcikova et al., 2018).

The impairment of the P53 pathway can also result from alternative mechanisms, including the deactivation of the *ATM* (ataxia-telangiectasia mutated) gene, which is a plausible cause of P53 dysfunction in CLL 1(Pettitt et al., 2001). The *ATM* gene encodes a protein kinase that has a significant role in inducing cellular responses to DNA double-strand breaks, by phosphorylating important players in DNA damage-response pathways, such as p53, breast cancer susceptibility gene 1 (*BRCA1*), and checkpoint kinase 2 (*Chk2*) (Shiloh, 2003). Moreover, *ATM* can directly bind to p53, and is responsible for the activation of p53 through the phosphorylation of serine-15 (Ser15) (Khanna et al., 1998).

1.3.5 Role of p53 in chronic lymphocytic leukaemia

One of the factors that contribute to CLL pathogenesis and resistance to therapy is the dysfunction of the tumour suppressor protein p53. In response to genotoxic stress, p53 activates the expression of downstream target genes such as $p21^{WAF1/Cip1}$ and *BAX*, which induce cell cycle arrest and apoptosis, respectively. Conversely, loss or mutation of p53 can lead to genomic instability, cell survival, and tumorigenesis. *TP53* mutations are found in up to 10-20% of CLL cases, and their presence is associated with poor prognosis, treatment resistance, and transformation to aggressive lymphoma (Stilgenbauer & Zenz, 2010; Zenz et al., 2010).

In addition to *TP53* mutations, other factors that affect p53 activity in CLL include aberrant expression or activation of *MDM2*, a negative regulator of p53, or alterations in downstream p53 targets such as $p21^{WAF1/Cip1}$ and *BAX*. For example, overexpression of *MDM2* can lead to p53 degradation and inhibition of apoptosis in CLL cells, whereas low levels of $p21^{WAF1/Cip1}$ or *BAX* can impair p53-mediated cell cycle arrest and apoptosis (Zenz et al., 2010; Stilgenbauer & Zenz, 2010).

The consequences of p53 dysfunction in CLL are manifold and include increased genomic instability, immune evasion, and therapy resistance. For instance, p53 deficient CLL cells may accumulate DNA damage and chromosomal abnormalities that promote clonal evolution and disease progression. Moreover, p53 dysfunction can impair the immunogenicity of CLL cells by reducing their expression of surface antigens and promoting immune escape, as well as by altering the cytokine and chemokine profiles of the microenvironment. Finally, p53 dysfunction can affect the response to standard and novel therapies for CLL, such as chemotherapy, immunotherapy, and targeted agents 5(Stilgenbauer & Zenz, 2010).

Given the crucial role of p53 in CLL pathogenesis and therapy response, several research efforts are focused on understanding its mechanisms and developing new therapeutic strategies. For example, several drugs that target p53 or its regulatory pathways are being investigated, such as MDM2 inhibitors and PRIMA-1, which can restore p53 activity or induce p53-independent apoptosis (Stilgenbauer & Zenz, 2010). Moreover, combinations of p53-targeting agents with other drugs such as venetoclax, a BCL-2 inhibitor, or lenalidomide, an immunomodulatory agent, are being explored in preclinical and clinical studies. Finally, biomarkers that predict p53 dysfunction or response to therapy in CLL are being developed, such as functional assays of p53 activity, gene expression profiling, and imaging techniques (Stilgenbauer & Zenz, 2010).

In summary, p53 plays a critical role in regulating apoptosis and DNA damage response pathways in CLL, and its dysfunction contributes to disease progression and therapy resistance. Further research into the mechanisms and clinical implications of p53 dysfunction in CLL may lead to new therapeutic strategies and biomarkers for this challenging disease. Also, in the majority of cases p53 is wild-type and functional and this can potentially be exploited using non-genotoxic MDM2 inhibitors to activate p53.

1.3.6 MDM2 gene and protein

The *MDM2* gene, which encodes the murine double-minute type 2 (MDM2) protein, is located on chromosome 12 (12q14.3-q15). The *MDM2* gene was initially identified as an amplified sequence present in the form of double minutes from the transformed mouse cell line 3T3-DM (Fakharzadeh et al., 1991). The MDM2 protein was subsequently found to form a tight complex with both mutant and wild type p53 protein in rat cells transfected with *Trp53* genes (Momand et al., 1992). The human analogue, *HDM2* gene, codes for a 90kDa nuclear phosphoprotein that has been found overexpressed in various human tumours such as soft tissue sarcoma, glioma, and breast cancer (Bond et al., 2006; Araki et al., 2010).

The gene consists of 11 exons with over 40 splice variants identified in normal and tumour tissues (Bartel et al., 2002). The full-length transcript of MDM2 encodes for a protein of 497 amino acids, with a predicted molecular weight of 56kDa, but the full-length protein migrates at around 90kDa in SDS-PAGE due to post-translational modifications and amino acid composition of the protein (Saucedo et al., 1999; Sawai & Domae, 2011). The functional domains of MDM2 include the p53 binding domain (residues 19–108), an acidic domain

(residues 237–300), a central zinc-finger (residues 301–332), and a RING-finger domain at its C-terminal end (residues 433–488) (Kussie et al., 1996).

1.4 An overview of MDM2

1.4.1 MDM2 regulates p53 stability and function

In wild type p53 cancers, MDM2 and MDMX act as negative regulators for p53 stability. MDM2, which is itself transcriptionally driven by p53, is a crucial factor in the downregulation of p53 (Figure 1.9). It can attach to p53, inhibiting its transcriptional activity and leading to its degradation through ubiquitination. As a result, the growth-inhibitory and pro-apoptotic activities of p53 are inhibited, thus promoting the survival and growth of cancer cells (Brown et al., 2009). MDM2 can also join forces with MDMX, a closely related paralogue, to form a heterodimeric complex which facilitates p53 degradation (Linares et al., 2003). MDM2 also ubiquitinates MDMX and promotes the degradation of the MDM2-MDMX heterodimer complex when subjected to ionizing radiation. The activity of MDM2 is negatively regulated by p14ARF (Robertson & Jones, 1998; Zhang & Xiong, 2001).

MDM2 is a crucial E3 ubiquitin ligase that plays a dual role in regulating p53 function, by inhibiting p53 transcriptional activity and promoting its proteasomal degradation (Momand et al., 1992; Kubbutat et al., 1997; Chao, 2015). Under normal conditions, MDM2 ubiquitinates p53, marking it for proteasomal degradation and preventing its transcriptional transactivation domain from functioning. MDM2 has also been shown to localize p53 in the cytoplasm (Shvarts et al., 1996). The interaction between MDM2 and p53 is mediated by specific amino acid residues in the N-terminal hydrophobic cleft of MDM2, which are also important for p53 binding to the transcriptional machinery (Haines et al., 1994). This interaction is highly regulated by different post-translational modifications (Kussie et al., 1996).

Ubiquitination and proteasomal regulation play a crucial mechanism within cells for maintaining protein homeostasis, regulating cell cycle progression, and controlling various cellular stress processes. Ubiquitination is a post-translational modification process in which ubiquitin molecules are covalently attached to a lysine residue target protein through iso peptide pound. Ubiquitin is a small protein consisting of 76 amino acids, and it plays a crucial role in regulating various cellular processes, including protein degradation, DNA repair, signal transduction, and cell cycle progression. Ubiquitination is a reversible process which is

mainly regulated by sequential series of enzymatic reactions involving ubiquitin-activating enzymes (E1), ubiquitin-conjugating enzymes (E2) and ubiquitin ligases (E3) (Clague et al., 2019). E1 enzymes activate ubiquitin molecule by forming a thioester bond between the C-terminal glycine residue of ubiquitin and a cysteine residue on the E1 enzyme in an ATP-dependent manner. E2 enzyme transferred the activated ubiquitin molecule from E1 enzyme to a cysteine residue on an E2 enzyme, forming a thioester bond. Then, E3 ligases facilitate the transfer of ubiquitin molecule from the E2 enzyme to a lysine residue on the target protein, resulting in the formation of an isopeptide bond between the C-terminal glycine of ubiquitin molecule and the ε-amino group of the lysine residue on the target protein (Damgaard, 2021). Once the protein is tagged with ubiquitin molecule, it will be recognized by 19s proteins which is a cap of the proteasome. Then, the target protein will be converted into small peptides by proteases which subsequently released and degraded into amino acids by cytosolic and nuclear peptidases (Glickman & Ciechanover, 2002).

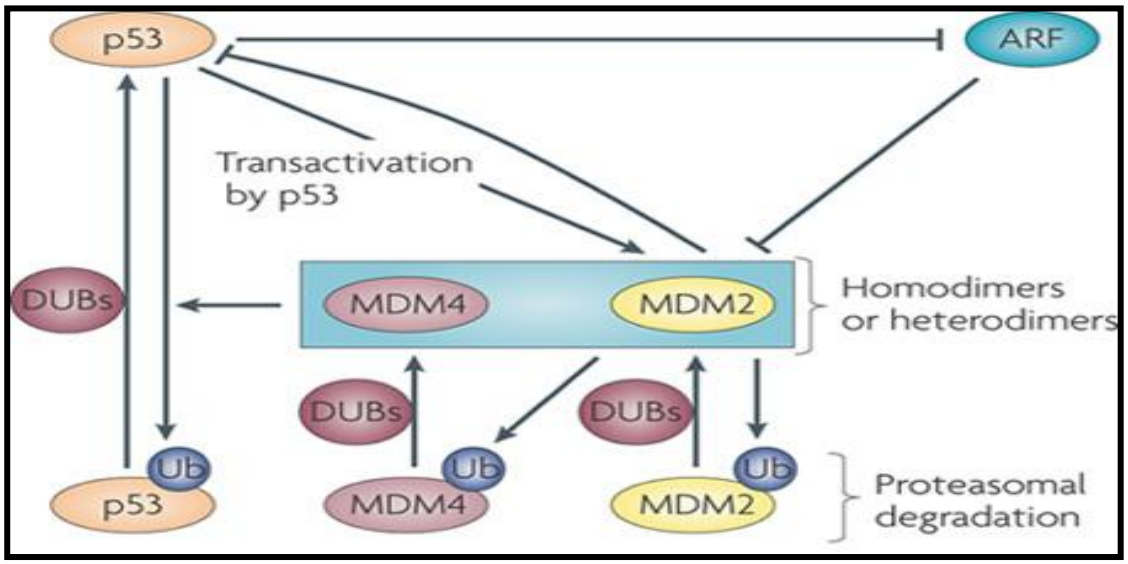

Figure 1.9 The negative feedback loop control of cellular p53 by MDM2 and MDM4. Ub, ubiquitin; dUB, deubiquityla**se** (Brown et al., 2009).

1.4.2 MDM2 as a therapeutic target

Several studies have shown that the *TP53* tumour-suppressor gene is mutated in almost 50% of human cancers (Vogelstein, 1990; Soussi et al., 2006). However, the prevalence of *TP53* mutations varies significantly depending on the type of cancer, ranging from 38%-50% in ovarian, oesophageal, colorectal, head and neck, larynx, and lung cancers to about 5% in paediatric malignancies and some adult cancers such as CLL, sarcoma, and melanoma (Olivier et al., 2010). In some tumours, the protein expression or function of *TP53* is suppressed and reduced, rather than mutated. Targeting the p53 pathway in these cases could

provide a useful strategy for cancer therapy. The MDM2 protein is an essential negative regulator of p53 and is physically linked to it (Figure 1.10). Overexpression of MDM2 can result in inactivation of wild type p53 protein function by forming a negative auto-regulatory loop with p53, thus inhibiting its activity through complex formation (Momand et al., 1992; Picksley & Lane, 1993). It has also been shown that mice lacking MDM2 die early in development but develop normally if they are co-deficient for *Trp53*, indicating that the critical role of MDM2 in development is also the physiological regulation of p53 function. Mice lacking MDM4 do not have the same phenotype, but they are also rescued by *Trp53* knockout (Berndt et al., 2013; Luna et al., 1995). Some tumours overexpress MDM2 and MDMX, which suggests that they inhibit p53 activity and behave as oncogenes (Marine et al., 2006). Therefore, targeting MDM2 to release p53 from its inhibitory action has been explored for cancer treatment (Burgess et al., 2016; Lane & Crawford, 1979).

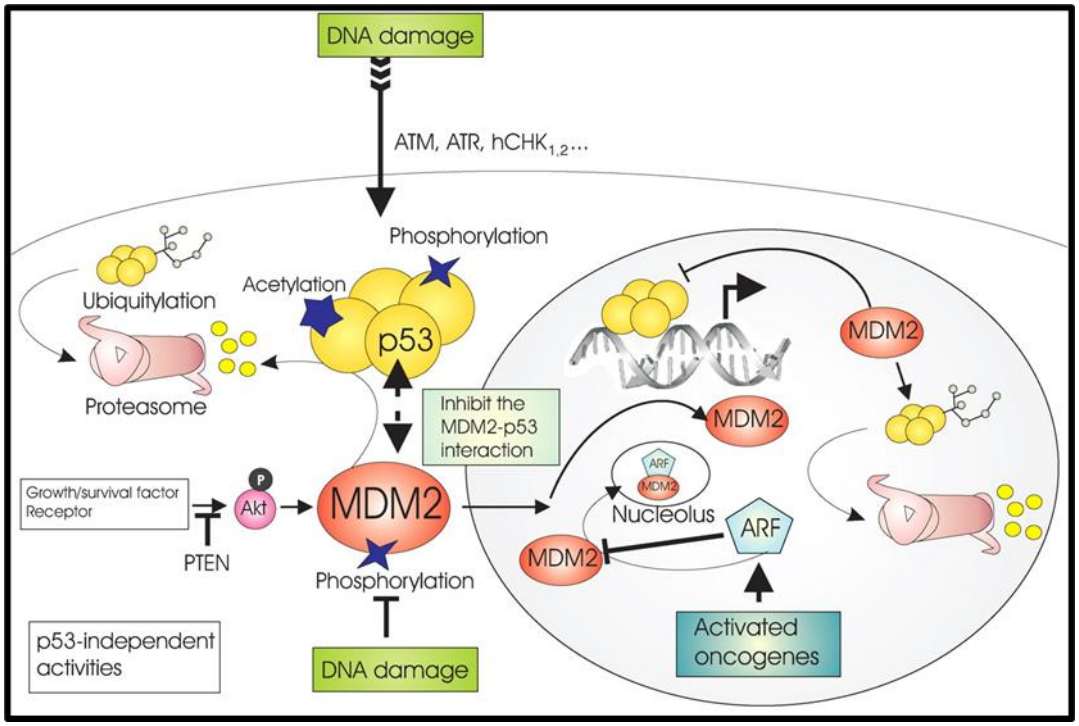

Figure 1.10 Regulation of p53 by MDM2. MDM2 and p53 are linked to each other through an autoregulatory negative feedback loop aimed at maintaining low cellular p53 levels in the absence of stress. p53 stimulates the expression of MDM2, in turn, inhibits p53 activity by promoting its degradation through a ubiquitin-dependent pathway on nuclear and cytoplasmic 26S proteasome (Moll & Petrenko, 2003).

1.4.2.1 Development of small molecule MDM2 inhibitors

The principle of MDM2-p53 binding antagonists is to stabilise p53 protein levels and activity by preventing the binding to MDM2 and preventing the degradation of p53 by MDM2 (Brown et al., 2009). These non-genotoxic compounds act as MDM2 inhibitors by binding to the N-terminal p53-binding pocket of MDM2 leading to accumulation of the p53 protein. The free p53 protein activates downstream transcriptional targets to initiate growth inhibitory and pro-apoptotic cascade pathways (Ding et al., 2013; Vu et al., 2013).

Using high throughput screening of synthetic chemicals, Vassilev and colleagues identified a group of cis-imidazoline compounds, which they named nutlins, that bind to and mask the p53 binding pocket on MDM2 (Vassilev et al., 2004). Nutlin-3 was the first generation MDM2 inhibitor which demonstrated the effect of p53 stabilisation on *in-vitro* cancer cells and *in-vivo* human tumour xenografts in nude mice (Vassilev et al., 2004; Polański et al., 2014). In cell free assays, nutlins were found to be capable of inhibiting the MDM2-p53 interaction with IC_{50} values ranging from 100-300nM. After isolating both enantiomers of a nutlin-3 racemic mixture, it was determined that nutlin-3a was 150-fold more potent than the in-active enantiomer at inhibiting the MDM2-p53 interaction *in-vitro* (nutlin-3a IC_{50}=0.09μM and nutlin-3b IC_{50}=13.6μM). The atomic resolution X-Ray diffraction crystal structure of nutlin-2 bound to MDM2 confirmed that nutlins mimic the three main amino acid residues on p53 that are involved in its interaction with MDM2 (Shangary & Wang, 2009).

Treatment of various cell lines with nutlin resulted in a dose-dependent increase in downstream transcriptional targets of p53, such as $p21^{WAF1/Cip}$ and *MDM2*, if *TP53* status was wild type. This led to cell cycle arrest, apoptosis, and growth inhibition of the *MDM2* amplified SJSA1 osteosarcoma cell line *in-vitro*. Treatment of SJSA-1 tumour xenografts in nude mice with 200 mg/kg twice daily over a 20-day period resulted in the inhibition of tumour growth with no apparent systemic toxicity. These findings provided proof of concept that selective small molecule inhibitors of the MDM2-p53 interaction could offer non-genotoxic therapeutic options for activating p53. Since then, the inhibitory activity of MDM2 inhibitors and their biochemical effect on p53 signalling has been extensively investigated with nutlin-3 and other novel MDM2 inhibitors, and studies have consistently shown that *TP53* wild type cell lines respond with growth inhibition following treatment with MDM2 inhibitors and canonical p53 transcriptional targets are induced in a class-independent manner (Zhao et al., 2015).

1.4.2.2 Further developments: second-generation MDM2 inhibitors

Since the discovery of nutlins, a variety of chemical classes of MDM2 antagonists, including more potent orally bioavailable compounds suitable for *in-vivo* use, have been identified and progressed through preclinical and early phase clinical studies (Zhao et al., 2015). Currently, at least seven compounds have advanced to clinical trials, namely RG7112/RO5045337, RG7388/RO5503781, MI77301/SAR405838, AMG232, CGM097, DS-3032b, ALRN-6924, KRT-232, APG-115 and MK8242. The first MDM2 antagonist to reach phase 1 clinical trials was RG7112 (IC_{50}=18nM), which is derived from nutlin-3a (Ray-Coquard et al., 2012; Yujun Zhao et al., 2014). This compound was administered orally to patients with advanced well-differentiated/poorly differentiated liposarcomas and haematological malignancies, with patients receiving three cycles of 20 -1920mg/m2/day over a 10-day period with 18 days rest between each cycle. RG7112 was generally well tolerated, with the most significant adverse effects being neutropenia and thrombocytopenia, which is consistent with the mechanism of action of MDM2 antagonists and is considered an on-target effect, although this has not been definitively established. Analysis of tumour samples obtained from patients after 8 days of treatment showed signs of activation of p53 downstream targets and inhibition of proliferation. Plasma levels of macrophage inhibitory cytokine-1 (MIC-1/GDF15) correlated with RG7112 plasma measurements, suggesting that MIC-1 could serve as a surrogate pharmacodynamics marker for activation of p53. Overall, 14/20 patients showed stable disease for the duration of the treatment, and one had confirmed partial response, which was considered promising. Nevertheless, it was commented that future trials need to carefully consider the potential for haematological toxicities (Ray-Coquard et al., 2012a).

Second generation MDM2-p53 binding antagonists, including RG7388 (idasanutlin) (Ding et al., 2013) and HDM201 (siremadlin) (Hyman et al., 2016), were demonstrated to efficiently suppress tumour growth *in-vivo* and have progressed to clinical trials. In late 2011, RG7338 (IC_{50}=6nM), which was designed based on the structure of RG7112 and MI-219 (an MDM2 inhibitor of the spiro-oxindole family), entered phase I clinical trials in patients with solid tumours. In addition to mimicking the structure of the three key amino acids at the N terminus of p53 (F19, W23, and L26), the 2-Chlorophenyl group also makes π-π interactions with p53 H96 (Figure 1.11) (Zhao et al., 2015). Maximum tolerated doses of RG7388 were dependent on scheduling, and this compound had similar dose-limiting haematological toxicities as observed with RG7112 (Johnson-Farley et al., 2015). This compound was taken forward to phase II trials under the name idasanutlin with a dose of 500mg/m2 with daily, 5-day

scheduling. An extensive review of the list of reported MDM2 inhibitors at different stages of development was reported by (Zhao et al., 2015). Since then, a Newcastle University/Astex alliance in-house iso-indolinone series derived compound is also now in phase 1&2 clinical trial as ASTX295.

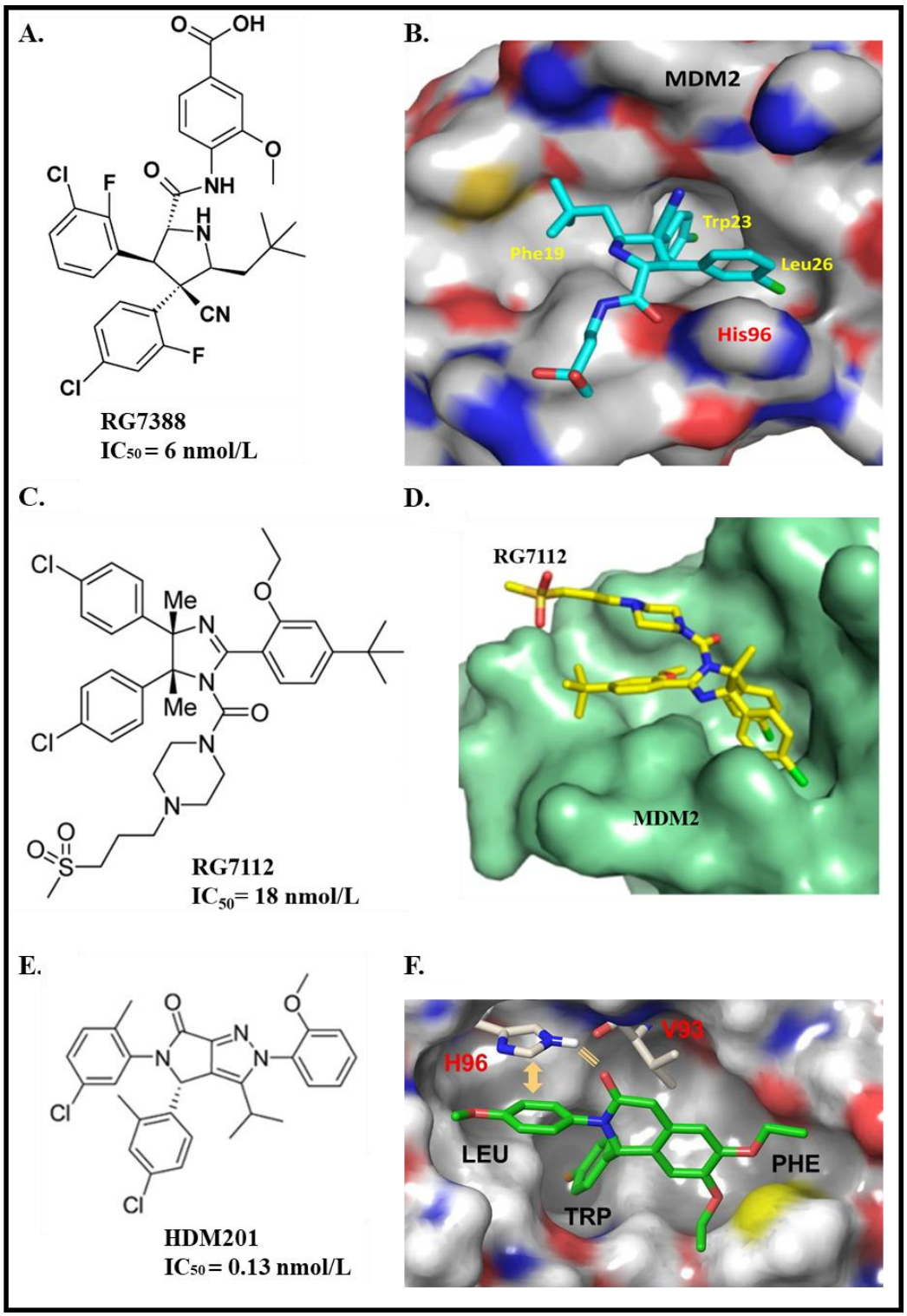

Figure 1.11 RG7388, RG7112 and HDM201. Chemical structure of (A) RG7388 (C) RG7112 (E) HDM201. Crystal structure of MDM2 bound to (B) RG7388 (D) RG7112. (D) HDM201 The three MDM2 sub-pockets are labelled PHE (Phe[19]), TRP (Trp[23]) and LEU (Leu[26]). (Furet et al., 2016; Zhao et al., 2015).

1.4.2.3 The potential for clinical use of MDM2 inhibitors in CLL

Current treatment options for CLL include chemoimmunotherapy, BTK inhibitors (such as ibrutinib and acalabrutinib), and BCL2 inhibitors such as venetoclax, however, these therapies are not curative and often result in the development of drug resistance.(Hallek, 2019; Jain et al., 2019). Therefore, there is a need for alternative targeted treatment strategies for CLL particularly for patients who have relapsed or are refractory to standard treatments.

One promising approach is the use of MDM2 inhibitors, which have shown efficacy in preclinical studies in CLL.(Kojima et al., 2005). MDM2 is an E3 ubiquitin ligase that plays a critical role in the regulation of the tumour suppressor protein p53 (Wade et al., 2013). In CLL, MDM2 is overexpressed, leading to the degradation of p53 and the inhibition of its tumour suppressor function (LeBlanc et al., 2002). By inhibiting MDM2, the levels of p53 can be restored, leading to apoptosis of CLL cells. In wild-type *TP53* CLL MDM2 inhibitors can activate p53 by blocking its interaction with MDM2, leading to apoptosis of cancer cells (Ciardullo et al., 2019).

While clinical data specifically for CLL is limited, preclinical studies have shown that MDM2 inhibitors can induce apoptosis in CLL cells and enhance the effects of standard therapies (Stilgenbauer et al., 2016) (Clinical trials.gov).

Another preclinical study has demonstrated that nutlin-3a induces apoptosis in primary CLL cells by activating p53 and downregulating the anti-apoptotic protein MCL-1 (Kojima et al., 2006; Drakos et al., 2011; Pan et al., 2017). In further study, a combination of the MDM2 inhibitor RG7112 and ibrutinib showed synergistic activity against CLL cells *in-vitro* and *in-vivo* (Yee et al., 2013; Jain et al., 2019; Andreeff et al., 2016). Furthermore, another preclinical study demonstrated that nutlin-3a sensitizes the CLL cells to the cytotoxic effects of fludarabine and rituximab (Kojima et al., 2006; Shangary & Wang, 2009).

RG7388 (idasanutlin) also showed promising results in phase I clinical trials with relapsed or refractory CLL patients (Ding et al., 2013). In a study of 54 patients, idasanutlin produced an overall response rate of 72%, with a complete response rate of 18%. In addition, the phase I/II clinical trial of idasanutlin for AML patients is currently ongoing (NCT00710528 and NCT01090414 (Konopleva et al., 2022; Yee et al., 2021; Brown et al., 2014). Currently, the phase I/II clinical trial of KRT-232, novel small molecule of MDM2 inhibitor in a combination with acalabrutinib is investigated for treatment of CLL and Diffuse Large B-Cell

Lymphoma (DLBCL) patients (NCT04502394) (ClinicalTrials.gov). The most common adverse events were gastrointestinal and hematologic, which were generally manageable.

A different MDM2 inhibitor, DS-3032b, has shown potent activity against AML cells in preclinical studies phase I/II clinical trials in patients with advanced solid tumours and lymphomas (Ishizawa et al., 2018). In preclinical studies, DS-3032b has been shown to induce apoptosis of AML and Multiple Myeloma cells in a p53-dependent manner, suggesting that it may be effective in CLL patients with wild type p53 (NCT02579824). MDM2 inhibitors have the potential to be effective therapies for AML, particularly in patients with functional p53 (Konopleva et al., 2020). Ongoing clinical trials will further evaluate the safety and efficacy of these agents in CLL and to identify biomarkers that may predict response to treatment.

1.5 An overview of PPM1D/WIP1

1.5.1 PPM1D/WIP1 gene and proteins

The *PPM1D* gene is located on the long arm of chromosome 17 (17q23.2), with base co-ordinates chr17: 60590183-60676280 (UCSC genome browser). Alternative splicing of the mRNA of this gene results in two transcripts that encode two different sized proteins, both of which retain their phosphatase activities (Chuman et al., 2009). The shorter transcript produces a 605 amino acid long WIP1 protein (PPM1D605), while the longer transcript, which includes an additional exon with a premature stop codon, results in a 430 amino acid long WIP1 protein (PPM1D430) (Figure 1.12). While, the PPM1D605 protein is found ubiquitously across human tissue types, the WIP1 protein isoform encoded by PPM1D430 is exclusive to testes and leukocytes.

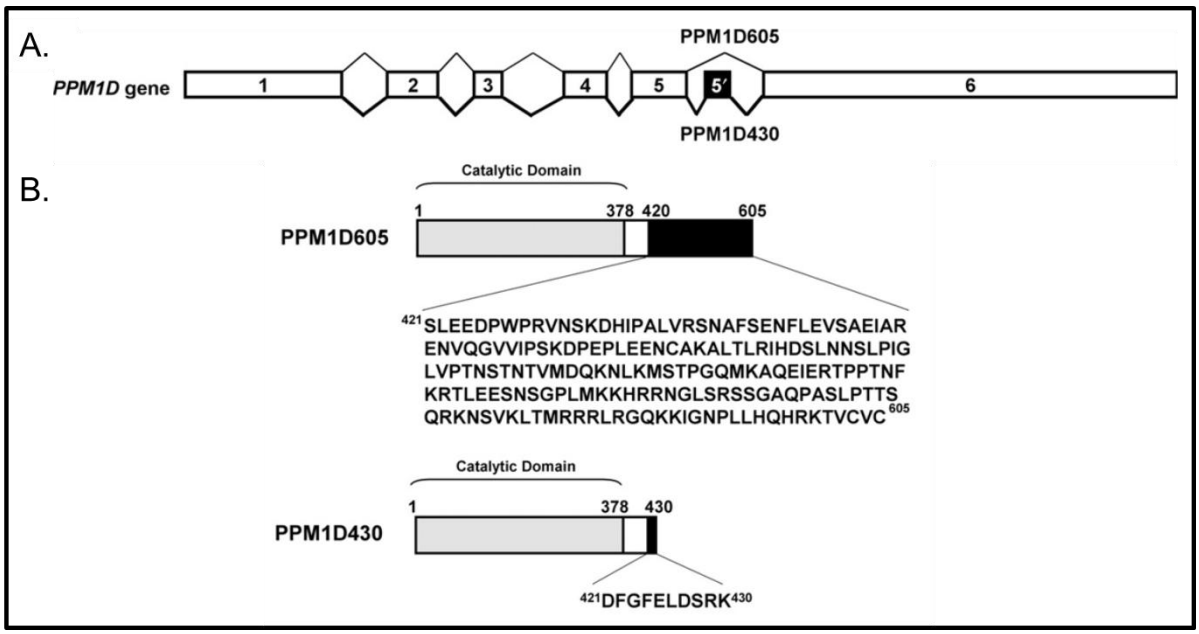

Figure 1.12 The diagram shows the location of PPM1D and the transcription of stop codon PPM1D605 and PPMD430 with respect to the WIP1 catalytic site (Chuman et al., 2009).

1.5.2 PPM1D/WIP1 in cancer

The viability of PPM1D-null transgenic mice suggests that the WIP1 protein is not required for embryonic development. However, male mice with the PPM1D-null genotype exhibited sporadic growth retardation, atrophy of reproductive organs, decreased fertility, reduced lifespan, and compromised immune function, whereas the female mice were less cancer prone and did not show such symptoms. These results suggest that WIP1 plays an important role in spermatogenesis, lymphoid cell function, and cell cycle regulation (J. Choi et al., 2002).

The defect in male infertility issues in response to Wip1 deficient mice are likely due to a result of the combined impacts on both the cells involved in spermatogenesis and the epididymis. Similar situation seen in the estrogen receptor alpha knockout mouse, which the mutation influenced both the testicular somatic cells and the epididymis (Hess et al., 1997).

1.5.3 Targeting WIP1 with the WIP1 phosphatase inhibitor, GSK2830371

GSK2830371, a small molecule allosteric inhibitor, can inhibit the enzymatic activity of WIP1 protein by binding to the flap subdomain of WIP1 and promotes ubiquitin-mediated degradation of WIP1 (Figure 1.13) (Gilmartin et al., 2014). PPM1D (Protein Phosphatase, Mg2+/Mn2+ Dependent 1D), also known as WIP1 (Wild-type p53-induced phosphatase 1), is an oncogenic protein phosphatase that regulates a variety of cellular processes, including

DNA damage response and cell cycle checkpoint control. PPM1D plays a critical role in negatively regulating the activity of the p53 tumour suppressor protein.

Interestingly, PPM1D is also a transcriptional target of p53, which means that PPM1D forms a negative autoregulatory feedback loop to ensure homeostatic regulation of wild-type p53. When cells are exposed to various forms of stress, such as DNA damage, p53 is activated and upregulates the expression of PPM1D. Once produced, PPM1D helps to restore normal cellular functions by dephosphorylating p53 and other signalling molecules involved in p53 regulation (Lu et al., 2008).

This negative feedback loop helps to maintain the proper balance of p53 activity, preventing excessive p53-mediated cell death or senescence. However, dysregulation of this loop can also contribute to the development of cancer including gene amplification and mutations in PPM1D. Hyperactivity or overexpression of WIP1 protein have been frequently found in various human cancer types including neuroblastoma, medulloblastoma, leukaemia, lymphoma, colon, lung, breast and ovarian cancers. The inhibition of WIP1 activity has been demonstrated to sensitize cancer cells to DNA-damaging agents and increase the efficacy of chemotherapy (Zhang et al., 2006; Kleiblova et al., 2013).

In summary, PPM1D/WIP1 is a transcriptional target of p53 and plays an important role in the regulation of p53 activity and other cellular processes. Dysregulation of PPM1D expression or activity can contribute to the development of cancer, making it a potential therapeutic target for cancer treatment.

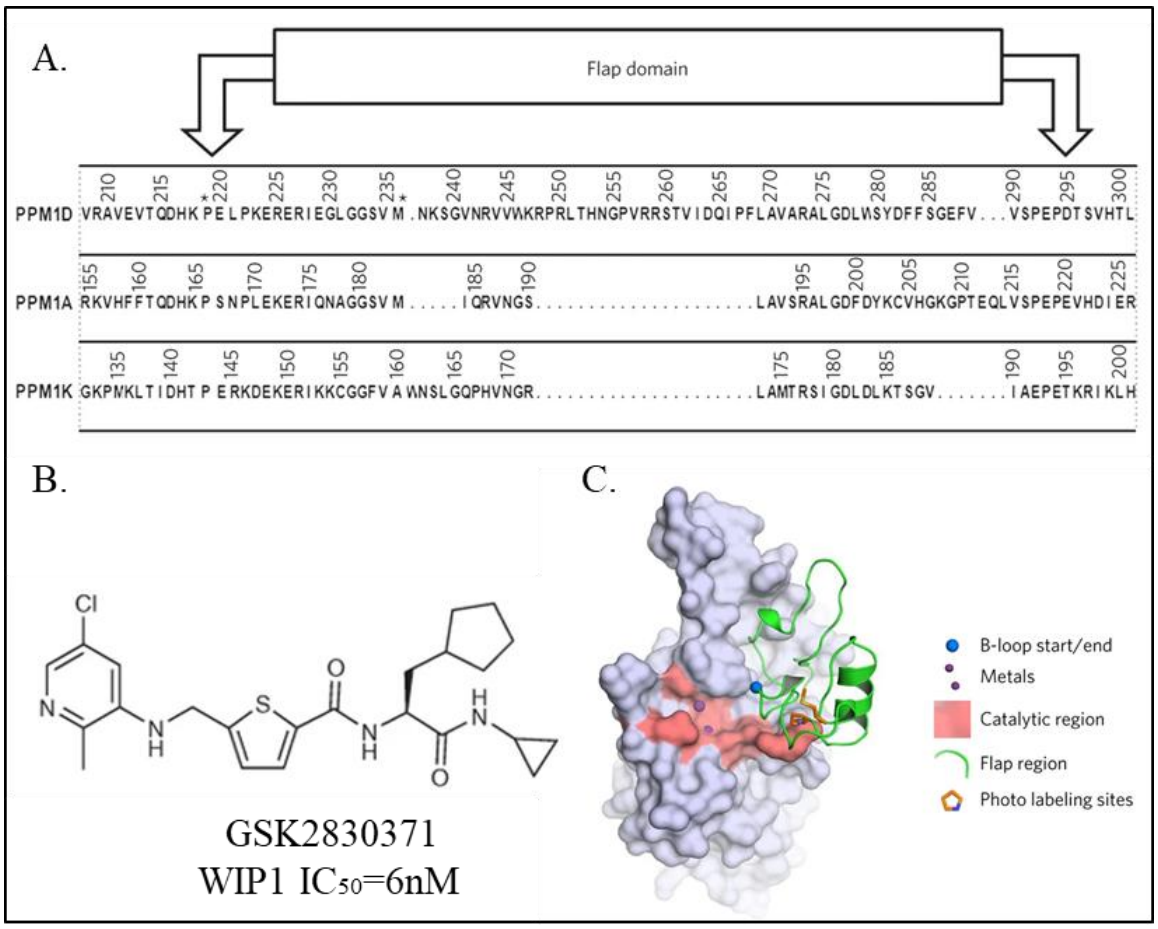

Figure 1.13 WIP1 inhibitor (GSK2830371) binding to flap subdomain domain of WIP1 specifically (A) Structure of GSK2830371. (B) Structure of WIP1 inhibitor (GSK2830371) (C) WIP1 model based on the PPM1A crystal structure (Gilmartin et al., 2014)

1.5.4 WIP1 phosphatase and homeostasis of p53 in response to stress and DNA damage

Multiple p53 negative autoregulatory mechanisms allow for reversible p53-induced cell cycle arrest in response to sub-lethal damage (Harris & Levine, 2005). While the p53-MDM2 negative autoregulatory feedback loop is the most crucial in maintaining p53 stability and function, there exist other subtle feedback mechanisms that prevent the activation of p53 growth inhibitory and lethal functions. One of these mechanisms is p53-mediated induction of PPM1D/WIP1. *PPM1D* will be used to refer to the gene, while WIP1 will refer to the protein. WIP1 directly dephosphorylates phospho-p53^{Ser15}, which is the product of stress related kinases, and indirectly affects the phosphorylation of other residues (Thr18 & Ser20) that are important for the dissociation of p53 from MDM2. Additionally, WIP1 dephosphorylates various proteins, including ATM^{Ser1981}, CHEK1^{Ser345} & CHEK2^{Thr68}, γH2AX, p38α^{Thr180} (MAPK pathway), nuclear factor kappa B^{Ser536} (NF-κB^{Ser536}), UNG2^{Thr6}, XPC^{Ser196} and XPA^{Ser892}, which leads to the dampening down of DNA damage response and stress signalling to p53. WIP1 also increases the stability of MDM2^{Ser395} and MDMX^{Ser403}, negatively regulating p53 (Figure 1.14) (Lowe et al., 2012; Lu et al., 2007).

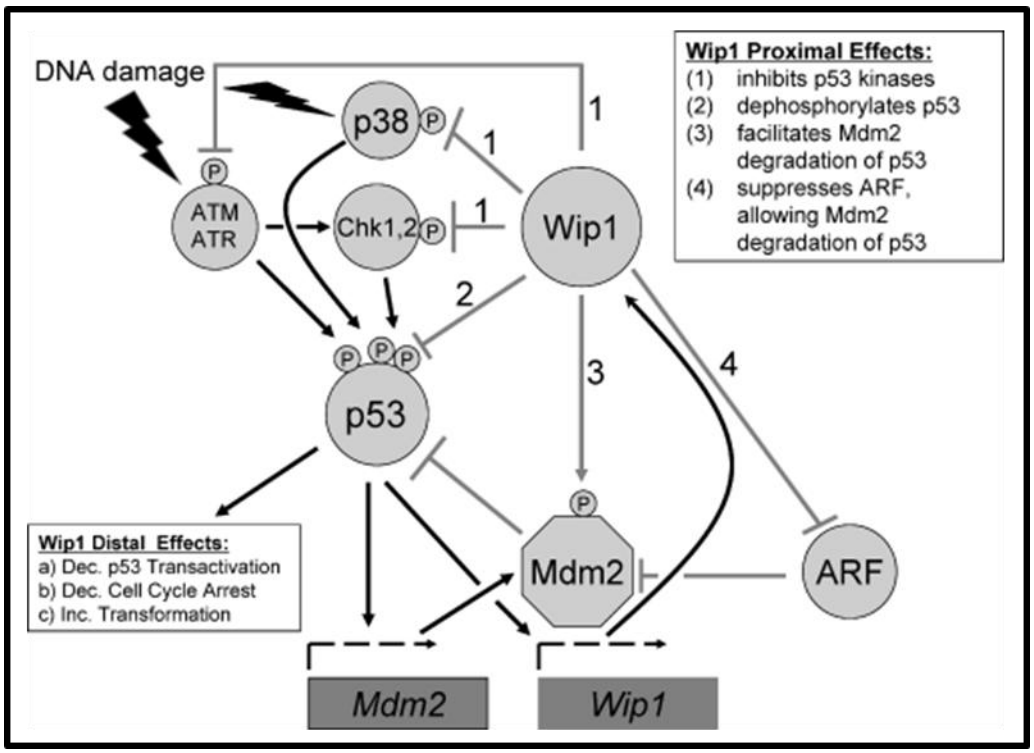

Figure 1.14 WIP1 inhibits p53 activity by multiple mechanisms (Lu et al., 2008)

1.5.5 Pre-clinical studies with GSK2830371

Pre-clinical studies with GSK2830371 demonstrated the potential for WIP1 inhibition as a cancer therapeutic strategy for increasing the efficacy of p53 dependent therapies, including non-genotoxic activation of p53 by MDM2 inhibitors.

GSK2830371 can enhance the antitumor effect of DNA-damaging agents, such as ionizing radiation and cisplatin, in various cancer types, including leukaemia, lymphoma, breast, and ovarian cancers (Pecháčková et al., 2017; Uyanik et al., 2021).

The pre-clinical studies have demonstrated that GSK2830371 can enhance p53-mediated tumour suppression in combination with MDM2 inhibitors such as nutlin-3, nutlin-3a, RG7388, or chemotherapy. GSK2830371 as a single agent has selective inhibitory effects on the growth of MCF-7 and MX-1 cells, PPM1D amplified breast cancer cells, and a specific subset of wild type p53 haematological cancer cell lines (Gilmartin et al., 2014). Notably, in a previous study of our group, cells with various PPM1D gene alterations (gain-of-function mutations, amplification, or copy number gain) were found to be resistant to GSK2830371 as a single agent, except for MCF-7 cells (Esfandiari et al., 2016).

1.6 Hypothesis and Aims

In previous investigations, researchers have explored the therapeutic potential of synthetic small molecules that inhibit the interaction of p53-MDM2, aiming to activate wild-type p53 (Brown et al., 2009). Among these compounds, RG7388 (idasanutlin), a second-generation MDM2-p53 binding antagonist, has been developed and demonstrated enhanced potency (IC_{50}=6nM), selectivity, and bioavailability (Ding et al., 2013). RG7388 has been found to activate wild type p53, leading to p53 stabilization, induction of p21 and MDM2 expression, and the promotion of p53-dependent apoptosis in various cell types, including primary CLL cells (Wu et al., 2018; Chamberlain et al., 2021; Chen et al., 2015; Ciardullo et al., 2019; Zanjirband et al., 2016). Interestingly, RG7388 has progressed through phase II clinical trials and has subsequently entered phase III clinical trials (ClinicalTrials.gov Identifier: NCT02545283), marking it as the first MDM2-p53 binding antagonist to reach this advanced stage. Current published early clinical trial data revealed that idasanutlin is a promising target therapy agent for wild type p53 CLL as a single agent and in combination treatments (Daver et al., 2023; Italiano et al., 2021; Yee et al., 2021).

1.6.1 Hypothesis

The purpose of this study is to evaluate the effect of WIP1 inhibition to potentiate the activity of MDM2-p53 binding antagonists as potential therapeutic agents in CLL. In addition, to evaluate the effect of the WIP inhibitor in response to MDM2-p53 binding antagonists in the presence of different microenvironmental stimulation signals including CD40L, IL-4 and anti-IgM stimulation of the BCR.

1.6.2 Aims

1. Use the MDM2-p53 binding antagonist RG7388 (idasanutlin) to probe the functional status of the MDM2-p53 network in CLL and test the therapeutic potential of MDM2 inhibition, alone and in combination with a WIP1 inhibitor (GSK2830371) in the evolving treatment landscape for CLL.
2. Carrying out further primary CLL sample experiments with combination treatment of WIP1 phosphatase inhibitor and RG7388 in the presence and absence of IL-4 signals.

3. Identifying the combination effect of RG7388 with WIP1 phosphatase inhibitor on proliferating CLL cells when co-cultured on CD40L expressing fibroblast feeder layers.
4. Using Anti-IgM to stimulate CLL cell BCR signalling and evaluate the effect on response to RG7388 in combination with WIP1 phosphatase inhibitor.
5. Mechanistic studies investigating protein changes by western immunoblotting and gene expression profiles at the mRNA level by qRT-PCR for primary CLL samples to define transcriptional gene changes activated by RG7388 in combination with WIP1 inhibitor for both non-dividing CLL cells and in the presence of microenvironment signals which stimulate cell survival and proliferation.

Chapter 2: Material and Method

2.1 Culture of established cell lines

In the study, a total of six different cell lines were used, including two isogenic NALM-6, parental NALM-6, CD40L and NTL (Table 2.1). The parental NALM-6 cell line is wild type *TP53*^{WT} and the two isogenic lines included, heterozygous knockout *TP53*$^{+/-}$ and homozygous knockout *TP53*$^{-/-}$ were purchased from Horizon Discovery and were collaboratively shared by Professor Julie Irving (Faculty of Medical Sciences-Newcastle University). The NALM-6 cell line is derived from B-cells of acute lymphoblastic leukaemia (ALL). The genetic status of *TP53*^{WT} NALM-6 cell line was obtained from IARC TP53 (International Agency on Research on Cancer) database and COSMIC (Catalogue of Somatic Mutations in Cancer) database.

OCI-Ly3 is B-cell non-Hodgkin's lymphoma cell line extracted from the bone marrow of 52 years old man diagnosed with B-cell non-Hodgkin lymphoma (B-NHL) at stage 4B of a relapsed condition. OCI-Ly3 is also described as DLBCL.

The CD40L and NTL were adherent cell lines used for co-culture with primary CLL cells. CD40L and NTL cell line, derived from mouse fibroblasts tissue, were gifted from Professor Chris Pepper (Brighton & Sussex Medical School). CD40L cells are mouse L cells which have been transfected with a CD40 ligand expression construct and express the ligand on their surface. NTL cells are the same mouse L cells but have been transfected with the corresponding empty plasmid vector and do not express the CD40 ligand. NTL is used as a control feeder layer that does not stimulate growth of CLL cells. All cell culture procedures and media preparation were carried out under aseptic techniques in a class II containment safety hood. (Biomat2, Medair Technologies, MA, USA). Mycoplasma infection of cell line cultures were regularly checked by using Mycoalert® Mycoplasma Detection Kit (LT07-118, Lonza, Switzerland).

The parental NALM-6, OCI-Ly3, CD40L and NTL cell lines were obtained from the NICR authenticated cell line resource and were authenticated by STR (short tandem repeat) profiling (NewGene, Newcastle, UK). All the cell lines were cultured no more than 30 passages from purchase before replacing them with another cell vail from the frozen stocks in liquid nitrogen.

Cell Line	Cell Type	Origin	*TP53* status
Nalm-6 (+/+)	B-cell precursor leukemia	Acute lymphoblastic leukemia (ALL)	**Wild type**
Nalm-6 (+/-)	B-cell precursor leukemia	Acute lymphoblastic leukemia (ALL)	**Heterozygous knockout TP53(+/-)**
Nalm-6 (-/-)	B-cell precursor leukemia	Acute lymphoblastic leukemia (ALL)	**Homozygous knockout TP53(-/-)**
OCI-Ly3	B-lymphocyte	B cell non-Hodgkin's lymphoma	**Wild-type**
CD40L	Transfected with CD40 ligand	Mouse L-fibroblast	**Mutant**
NTL	Transfected with empty vector	Mouse L-fibroblast	**Mutant**

Table 2.1 Genetic status of cell lines.

2.1.1 Cell line authentication

The characteristic features of a cell line are subject to changes over time as a result of its passage number. High passage number cells have been observed to exhibit alterations in morphology, response to stimuli, growth rates, and protein expression compared to cells at lower passage numbers. Additionally, chromosomal aberrations in cell lines have been found to have an increased likelihood of occurring over time, as documented in multiple studies (Chang-Liu & Woloschak, 1997). To ensure the reliability of experimental results, all investigations were conducted using cell lines that had undergone fewer than 30 passages since purchase or authentication. This was achieved by replacing cultures from frozen stocks kept in liquid nitrogen. The cell lines were obtained from the NICR authenticated cell line resource and subjected to authentication through the use of STR (short tandem repeat) profiling (NewGene, Newcastle, UK) (Nims et al., 2010; Reid et al., 2023).

2.1.2 Passaging and seeding

All cell lines were cultured in RPMI 1640 medium (R8758, Sigma, Dorset, UK) containing 2mM L-Glutamine and supplemented with 10% foetal calf serum (FCS), 1% penicillin/streptomycin of 100 U/mL Penicillin and 100 µg/mL Streptomycin. Cell lines were grown in humidified incubators (Incu Safe, Sanyo, IL, USA) at 37°C with 5% CO_2. Based on the number of the cells required for an experiment, the cell lines were grown in different flasks, 25cm^2, 75cm^2 or 175cm^2 (Corning, Amsterdam, Netherlands). The cell lines were passaged every three days or whenever the confluency of the cells reached 70% of the flask surface area.

For passaging the adherent cell lines, first, the cells were washed with 10ml of phosphate-buffered saline (PBS). Then, 1-2ml of 1x trypsin-EDTA (Sigma, Dorset, UK) was added to the cells after the PBS was aspirated. The cells were incubated with trypsin-EDTA at 37^{0}C until they detached. An equal volume of culture medium was added to the cells in order to stop the trypsin activity. The resulting cell suspension was collected in a sterile 20ml universal tube (Greiner, UK) and centrifuged at 250xg for 5 minutes to pellet the cells. The old culture medium (including trypsin-EDTA) was removed from the cells. The pellet was washed once more a by suspending the cells in 10ml of fresh medium prior to centrifugation as previously. The supernatant was aspirated, and the cell pellet was resuspended in a fresh pre-warmed full medium. The cells were then ready for experiments or further passaging.

For passaging the suspension cells, the cells were collected directly into a sterile 20ml universal tube (Greiner, UK) without adding trypsin-EDTA and washed once with fresh pre-warmed full medium. Then, the cells were treated in the same way previously mentioned.

2.2 Cell count

The density of the cells for each experiment was determined through one of two methods depending on the cell sample in the experiment. A Neubauer haemocytometer (manufactured by Hawksley, Sussex, UK) or a Coulter counter (manufactured by Beckman Coulter) was used. To ensure consistency across experiment repetitions, the same technique was always used.

2.2.1 Haemocytometer counting of cells

Several techniques can be used to estimate cell density. In this study, a Neubauer haemocytometer (Hawksley, Sussex, UK) was used to determine cell density. The haemocytometer was prepared as per the manufacturer's instructions. A 10µl sample of fresh cell suspension was applied on both grid sides of the haemocytometer. Microscopically, cells were counted manually in all four grid square corners of both sides of the haemocytometer. The area of each grid square corners is 1mm x 1mm = $1mm^2$ with 0.1mm in depth. The final volume of each square at that depth is 100 µl. Once the total cell count is obtained, the average cell count of the eight squares was calculated and multiplied by the dilution factor and then multiplied by 10^4 to estimate the suspension cell density. Having the approximate number of the cells per ml, cells were seeded in a new flask or plate with an appropriate volume of full medium for either passage or experiments.

Trypan blue (0.4% w/v) was used to determine the viability of the cells. The cells were diluted in 1:1 volume and counted under the microscope by haemocytometer. The dead cells were stained blue upon exposure to trypan blue while the viable cells with intact plasma membrane will remain clear.

2.2.2 Coulter counting of cells

The Coulter counter was used to count the CLL cells which were co-cultured on the irradiated feeder layer cells. The coulter counter was adjusted to count the cells whose size varies between (4-15 microns) in diameter. The CLL cells were diluted in 1:10 in BD FACSFlow™ Sheath Fluid. The diluted CLL cell suspension was subjected to analysis using a particle counter (Coulter). In this process, CLL cells were suspended in a conductive fluid, FACSFlow, and passed through the probe hole into a separate conductive fluid, thereby interrupting the electrical current across the channel. Since the impedance caused by the cell or particle is proportional to its volume, the counter can be adjusted to count only particles that falls within the average diameter (4-15 microns). The Coulter counter counts the number of particles per 0.5ml, and therefore the average count obtained from three measurements is multiplied by dilution factors to determine the number of cells/ml in the initial cell suspension.

2.3 Isolation and culture of primary CLL cells

Peripheral-blood samples were obtained from patients diagnosed with CLL, following the written informed consent according to institutional guidelines and the agreement protocol of the Declaration of Helsinki. Samples were collected from patients at various stages of disease, including at diagnosis, during 'watch and wait' or during relapse, aiming for a total white blood cell (WBC) count of at least $30x10^9$/L. All the blood samples were collected in sterile disposable EDTA tube and stored under the auspices of the Newcastle Academic Health Partners Biobank (http://www.ncl.ac.uk/biobanks/collections/nbrtb/). Furthermore, the CLL diagnosis was made according to the IWCLL-164 NCI 2008 criteria (Hallek & Al-Sawaf, 2021; Hallek et al., 2008).

2.3.1 Lymphoprep

CLL cells were isolated from EDTA blood samples by density gradient centrifugation (Lymphoprep, Axis-Shield) following the manufacturer's protocol. The freshly obtained CLL cells were resuspended in RPMI-1640 medium supplemented with 10% (v/v) foetal calf serum (FCS), 100U/mL Penicillin, 100µg/mL Streptomycin and 2mM L-Glutamine 10% (v/v) at a concentration of $5x10^6$ cells/ml which would then be seeded in a new flask/plate with an appropriate volume for further experiments. In addition, $5x10^6$ cells were suspended in RNA latter for future RNA isolation and a further $5x10^6$ cells were collected for future DNA extraction, both of which were stored at -80°C. The remaining CLL cells were resuspended in FCS with 10% DMSO and stored for future planned experiments. Prior to -80°C storage, the aliquots of CLL cells were placed in 'Mr Frosty' ™ (which provides 1°C/min cooling rate with isopropyl alcohol) for 24hr at -80°C for gradual cooling of the CLL cells.

2.4 Growth curves

Prior to performing growth inhibition assays, the optimum seeding density for each cell line needs to be determined by generating the growth curve analysis. Growth curves were initially obtained to determine the growth pattern, doubling time, optimum seeding densities and incubation time of the cell lines for different experiments. The cells were seeded in a volume of 100µl medium/well using six different cell densities of $0.1x10^5$, $0.2x10^5$, $0.4x10^5$, $0.8x10^5$,

$1.6x10^5$ and $3.2x10^5$cells/ml for each time point and then incubated at 37°C, 5% CO_2. Then, at the end of each time point, 50µl/well of the XTT reagent was added to each well in the plate (including the cells and the blank background control wells) for 4 hours to estimate cell number. The FLUOstar Omega plate reader (BMG Labtech) was used to measure the absorbance at 450nm wavelength of the wells containing cells and the blank background control wells. Growth curves of cell lines were created using GraphPad Prism Version 6.05 software (GraphPad Software Inc.).

2.4.1 XTT assay

In 1988, the XTT assay was developed by Scudiero et al to measure drug inhibitory effects on the metabolic activity and proliferation of tumour cell lines (Scudiere et al., 1988). The XTT assay is based on the reduction of XTT by NADH produced in the mitochondria via trans-plasma membrane electron transport and an electron mediator. Reduction of XTT occurs in metabolically active cells and produces a water soluble orange coloured formazan product in the culture medium, which can be detected using an absorbance-based microplate reader.

The measurement of cell proliferation in metabolically active cells was carried out using a soluble formazan orange dye called tetrazolium reagent, specifically 2,3-bis(2-methoxy-4-nitro-5-sulfophenyl)-5-[(phenylamino)carbonyl]-2H-tetrazolium hydroxide (XTT). The amount of formazan produced is directly proportional to the number of viable cells present. XTT, a second-generation tetrazolium dye, was initially identified as an effective method to measure cell growth and drug sensitivity in tumour cell lines (Scudiere et al., 1988). Since then, tetrazolium salts have become one of the most widely used tools in cell biology for measuring the metabolic activity of cells, including those of mammalian and microbial origin (Berridge et al., 2005).

Both the primary specimens and cell lines were subjected to an incubation process under optimized suitable culture conditions, supplied with requirements of the experimental parameters. Upon completion of the experiment, the XTT assay was conducted to measure the metabolic activity of the cells.

The cells were seeded in 96 well plates at six different densities in a total volume of 100µl per well for each time point and incubated at 37°C with 5% CO_2. At appropriate chosen time points, the cells were exposed to a mixture of XTT reagent (manufactured by Roche, USA) in an appropriate ratio of labelling reagent to electron coupling reagent (1:50) and maintained at a

temperature of 37°C in an environment containing 5% CO_2. The length of the incubation period was determined upon the density of primary CLL cells, and the cell line employed in the experiment. Through pre-optimization efforts, the optimal incubation period was found to be 4 hours for B-cell lines and 8 hours for primary CLL cells. Upon completion of the incubation period, a spectrophotometric analysis was undertaken to determine the alteration in colour density, with absorbance measurements taken at a wavelength of 450nm using a FLUOstar Omega plate reader produced by BMG Labtech.

2.4.2 Sulforhodamine B (SRB) assay

In 1990, the SRB assay was developed by Skehan SRB is a water-soluble dye used to identify cell density by binding to the amino acid residues of the cell proteins (Skehan et al., 1990). The cells were seeded in 96 wells plate at five different densities in a total volume of 100µl per well. On the next day, the cells were fixed using Carnoy's reagent, a mixture of acetic acid and methanol in 3:1 proportion, at 4°C for one hour. After that, the cells were washed five times with distilled water and then, dried at room temperature. Then, the cells were stained with 100µl of 0.4% SRB (diluted in 1% acetic acid) for 30 minutes. The cells were washed 5 times with 1% acetic acid to remove excess SRB day and then dried at 60°C. After that, 100µl of 10mM Tris-HCl was added to each well and the plate was placed on a shaker for 20 minute to dissolve the SRB. The absorbance was measured at 570nm using a 96 well plate spectrophotometer.

2.5 Viability and Growth inhibition assay and cell treatment

For the Growth inhibition assay, XTT reagent is used to determine the GI_{50} values of the chemical compounds against the cell lines by constructing a concentration-response curve: this gives the concentration of a compound at which inhibits the growth of the cell population by 50% compared to untreated control cell growth. For primary cell studies such as CLL cells *ex-vivo,* the cytotoxicity of the cells can be expressed as LC_{50} value (lethal concentration required to decrease 50% of viability). The LC_{50} value is a measure of the viable inhibitory potency of a compound on CLL cells.

2.5.1 Established cell lines

The growth inhibition assays were performed by seeding the cells in 96 well plates (Corning) at densities according to the growth curves and doubling time data which were previously generated. The cells were treated with a range of concentrations, above and below the GI_{50} value. For adherent cell lines (mouse fibroblast CD40L and NTL), the cells were incubated for 24 hours after seeding in order to allow them to attach to the surface but not for the suspension OCI-Ly3 cell line and primary CLL cells. Following the treatment, the cells were incubated at 37°C with 5% CO_2 for 72 hours, which allows at least two doubling times for the untreated controls. By the end of the incubation time, the activated XTT reagent was added to all wells as mentioned previously and re-incubated again in at 37°C with 5% CO_2 for 6 hours. The XTT assay was used to measure cell growth inhibition compared to solvent DMSO control. The absorbance was measured using the plate spectrophotometer at 450nm wavelength. The background subtracted absorbance values were normalized to the control (DMSO/solvent) and expressed as percentage of relative growth. GraphPad Prism Version 6.05 software (GraphPad Software, Inc.) was used to plot the growth inhibition curves. The experiment was repeated three times independently. Standard deviation (SD) and the mean ± standard error of the mean (SEM) of the GI_{50} were calculated from each independent experiments.

2.5.2 Primary CLL cells

Serial dilutions in 100% DMSO were prepared from the 10mM stock to allow dosing of cells at a final concentration of 0.5% DMSO which on its own had been established to produce minimal cytotoxic effects on cells. The primary cells including normal donors and CLL patient cells can tolerate up to 0.6% (v/v) of the DMSO concentration with no effect on their cellular viability.

The primary CLL cells were seeded at 100µL/well in 96-well plates (Corning) and treated with different drug concentrations immediately after they were isolated. A broad-spectrum range of concentrations were selected to determine LC_{50} of the CLL cells. Each drug concentration and DMSO control were carried out in three replicate wells. Treated CLL cells were incubated for 48 hours with a final DMSO concentration of 0.5% (v/v). After the incubation, the XTT assay was performed to measure the *ex-vivo* cytotoxicity of the CLL cells. The optimal incubation time for the CLL cells with the XTT reagent was determined to be 8 hours from the pre-optimization procedure. The absorbance was measured using the plate spectrophotometer at

450nm wavelength. The values were normalised to DMSO controls and expressed as percentage (%) of cell viability. GraphPad Prism Version 6.05 software (GraphPad Software, Inc.) was used to plot the concentration-response curves.

2.5.3 Matrix experiment

For the dose–response matrix experiment, either cell lines or primary CLL cells were seeded in 96 wells plate as previously described. The cell line were seeded in concentration of 1.6 x 10^5 cell/ml and the primary CLL cells were seeded in $5x10^6$ cells/ml in a total volume of 100µL/well Range of drug concentrations were used to treat the cells with single agent and in combinations with a final DMSO concentration of 0.5% (v/v).The vertical wells were treated with range of GSK2830371 concentrations and the horizontal wells were treated with RG7388 concentrations The cell lines were exposed to the treatment for 72 hours while, the primary CLL cells were exposed to the treatment for 48 hours. The drug inhibition effect on cell number was determined as described above using XTT assay. The synergistic or antagonistic effect of the combination treatment was assessed by the SynergyFinder interactive web application. The synergy score was identified through the Zero interaction potency (ZIP) model (Ianevski et al., 2017). The percentage of cell inhibition in response to drug combination treatments is visualised as a synergy landscape map over the dose matrix. The intensity of the colour indicates dose regions that show strong synergy or antagonism.

2.6 Compounds

All compounds were supplied in a powder form and had to be dissolved in DMSO (Sigma-Aldrich) according to the standard operating procedure for weighing out potent carcinogens. The compounds were aliquoted in 10mM stock concentration and stored at -20°C for further use. Different concentrations were prepared with a final concentration of 0.5% DMSO which alone had minimal cytotoxic effects on cell growth.

2.6.1 MDM2 inhibitors

MDM2-p53 binding antagonists are a class of compounds that prevent the interaction between MDM2 and p53 by binding to the p53-binding pocket of MDM2. This leads to the stabilization of p53, as MDM2-mediated ubiquitylation and degradation are inhibited. This activation of the p53 pathway induces cell cycle arrest, apoptosis, and growth inhibition of cancer cells that have a wild type p53 status.

RG7388 and HDM201 are two different MDM2 inhibitors which were kindly supplied by Astex Pharmaceuticals. The compounds were weighed and carefully transferred to clean containers following established protocols for weighing potent carcinogens. RG7388 (Idasanutlin) (Figure 2.1 A), is a second generation MDM2-p53 binding antagonist that has been shown to efficiently suppress tumour growth *in-vivo*. clinical trial is investigating the efficacy of RG7388 for patients with relapsed multiple myeloma (NCT02633059), relapsed or refractory acute myeloid leukaemia respectively (NCT02670044, NCT02545283), phase I/II acute leukaemia or solid tumours in a combination with either chemotherapy or venetoclax (NCT04029688) and relapsed or refractory follicular lymphoma or DLBCL (NCT03135262, NCT02624986) (https://clinicaltrials.gov).

HDM201 (Figure 2.1 B), a new generation MDM2-p53 binding antagonist with highly selective binding bucket affinity, is also under investigation in early clinical trials (Hyman et al., 2016).

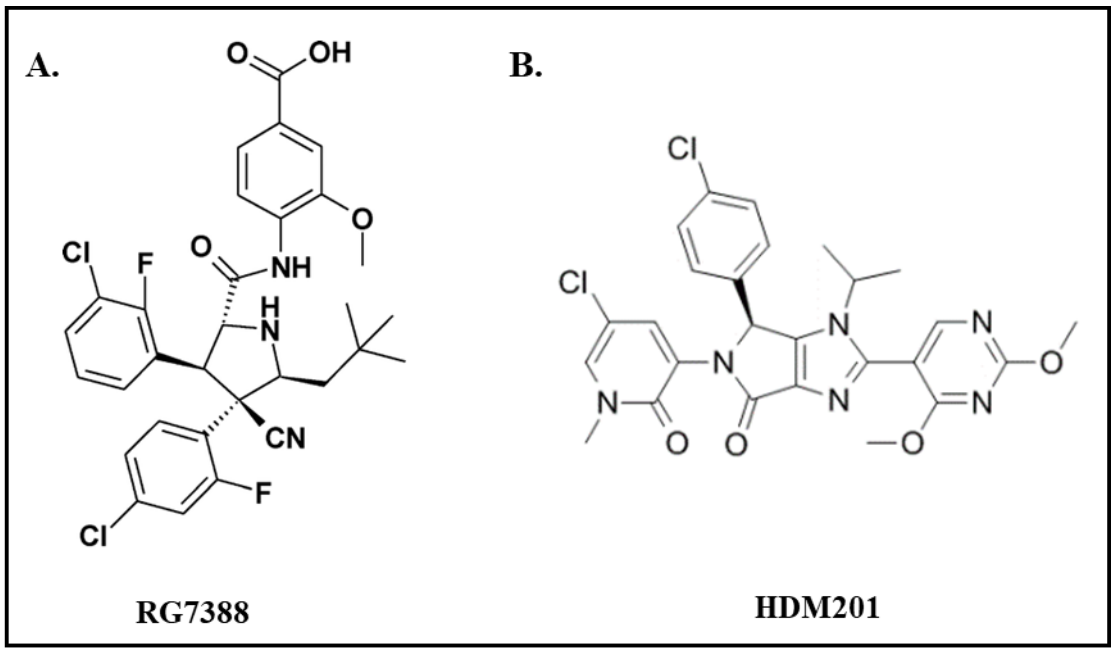

Figure 2.1 Structure of MDM2 inhibitors (A) RG7388 and (B) HDM201.

2.6.2 PPM1D/WIP1 inhibitor, GSK2830371

GSK2830371 allosterically inhibits the enzymatic activity of WIP1 protein and also enhances ubiquitin-mediated degradation of WIP1 (Gilmartin et al., 2014). GSK2830371 was purchased from Sigma-Aldrich.

GSK2830371 is a selective specific inhibitor inhibits the catalytic activity of WIP1 protein by binding to the flap subdomain and disrupting the stability at the proximal allosteric site known to be the WIP1 ubiquitination site (K238).

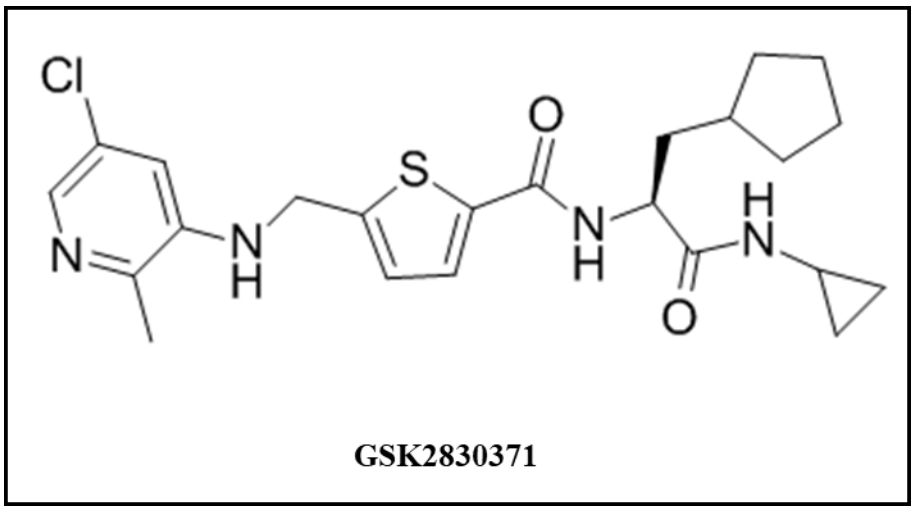

Figure 2.2 Structure of WIP1 inhibitor (GSK283031) (Gilmartin et al., 2014).

2.7 Western blotting

Western blot analysis is performed to identify the changes in protein expression of cells in response to treatment by using specific antibodies which bind to target proteins. In the western blot technique, the samples were run vertically from the positive toward the negative charge electrode at adjusted voltage and time. The proteins were separated according to charge and molecular weight.

The term "Western blotting" was introduced by Neil Burnette in 1981 (Burnette, 1981). This technique has been widely used to detect and semi-quantitatively analyse specific proteins and their post-translational modifications in complex protein mixtures, using specific antibodies. The process involves initially separating proteins in a mixture based on their mass (kDa) through SDS-polyacrylamide gel electrophoresis (SDS-PAGE), followed by transferring them

onto a nitrocellulose membrane across an electric field. The proteins are then adsorbed and immobilized onto the membrane, likely through electrostatic and hydrophobic interactions. Specific antibodies linked to horseradish peroxidase (HRP) are then used to detect proteins of interest and visualize them through detection of chemiluminescence.

2.7.1 Preparation of cell lysates

In western blotting analysis, cells were cultured in 6-well plates (Corning) at density of $1x10^6$ cells/ml for cell lines and $5x10^6$ cells/ml for CLL cells. Then, cells were treated with compound(s) of interest at specific concentrations for different time points. By the end of each time point, the suspension of cells were collected into microcentrifuge tubes and spun down at 2000g for 3 minutes. The cell pellet was washed by suspended in 1ml PBS and spun down again. After that, 40µl of SDS lysis buffer (a mixture of 0.0625M Tris-HCl pH 6.8, 10% (v/v) glycerol (Sigma) and 2% (w/v) SDS (Sigma) was added to lyse the cell lines. For primary CLL cells, 30µl of SDS lysis buffer was added to harvest the cell pellet because the CLL cells are very small compared to the suspension cell lines. After harvesting the cells, the cell lysate was heated at 100°C for 10 min. Then, the cell lysates were sonicated at an amplitude 6 for 5 seconds 3 times (Soniprep 150, MSE, UK) to break up DNA and reduce the viscosity of the sample. After this step the protein estimation assay can be performed or the cell lysates could be stored in -20°C freezer.

2.7.2 Protein estimation assay

In protein estimation assay, the Pierce® BCA (Bicinchoninic acid) Protein Assay kit (Pierce, Rockford, IL, USA), was used to determine the total protein concentration in cell lysates by converting the Cu^{+2} to Cu^{+1} in alkaline solution and producing bicinchoninic acid which is purple in colour. The BCA assay is based on the reaction between the sodium salt of bicinchoninic acid and the cuprous ion of biuret. A set of protein standards were prepared from a stock of bovine serum albumin (BSA) at 2mg/ml, which was diluted into 0.2, 0.4, 0.6, 0.8, 1.0 and 1.2 mg/ml to prepare the standard curve. The cell lysate of each sample was diluted in water with a ratio of 1:10 (5µl sample and 45µl water).

In a 96-well plate (Corning), 10µl of distilled water was add into the blank wells as a negative control followed by BSA standards and diluted lysate samples to each corresponding wells (10µl /well). Each BSA standard concentration and sample lysates were loaded in four

repeated wells. Then, a mixture of reagent A and B of the Pierce BCA protein assay kit were prepared with a proportion of 50:1 respectively, based on the total number of wells which need to be tested, followed by transferring 190µl of the mixture to all wells containing samples. After the plate was incubated at 37 °C for 30 minutes, the optical densities were measured at 562nm absorption wavelength using a FLUOstar Omega plate reader (BMG Labtech). The protein concentration in each diluted lysate sample was calculated and multiplied by the dilution factor (x10) to determine the actual value of undiluted protein concentration. A standard curve was generated using known BSA standard concentrations and the assay measurement (absorbance at 562nm) of protein concentrations in diluted lysate samples.

2.7.3 SDS-PAGE and transferring proteins to nitrocellulose membrane

Equal quantities of protein (20-25µg) from each lysate was mixed with loading buffer (a mixture of 2.5ml 0.5M Tris/HCl pH6.8, 0.4g SDS, 1ml βeta-mercaptoethanol, 2ml glycerol, 1ml 0.1% bromophenol blue, 13.5ml distilled water) to achieve final volume of 15µl. After 10 min heating at 100°C, the samples were loaded into the wells of the gel and separated according to molecular weight by electrophoresis through SDS-polyacrylamide gels (4-20% Mini-PROTEAN® TGX™ Gel, BioRad). The first and the last wells of the gel were loaded with known molecular weight standards (SeeBlue™ Pre-stained Protein Standard, Invitrogen). The samples were run in a vertical electrophoretic separation technique at 180 V for 45 minutes until the sample loading dye reached the bottom of the gel. After PAGE separation, the proteins were transferred horizontally and immobilized onto Hybond™ C nitrocellulose membranes (Amersham Buckinghamshire, UK) at 100 V for 30 minutes.

2.7.4 Blocking and antibody labelling

Before probing the immobilized target proteins with specific antibodies, the membrane was blocked with 5% non-fat milk in 1x TBS/Tween for 45 minutes to prevent non-specific binding of the antibodies. After that, the membranes were probed with specific primary antibodies targeting the protein of interest either at room temperature (RT) for 1-1.5 hours or 4°C overnight. Table (2.2) lists all the primary antibodies used with their species and optimal incubation time. HRP conjugated polyclonal goat anti-mouse immunoglobulins (P 0447, Dako) or polyclonal goat anti-rabbit immunoglobulins (P 0448, Dako) were used as the secondary antibodies directed against the specific species of the primary antibody at a dilution of 1:1000 at room temperature for 45-60 minutes. After the secondary antibody incubation, a mixture of an equal volume 1:1 of enhanced chemiluminescence (ECL) reagents 1 and 2 (BIO-RAD) were added to the membrane for 1 min at RT. The ECL reagent reacts with the (HRP) conjugated secondary antibodies complex on the membrane and generates light signals which were captured either by a camera in the G-Box machine or X-ray film (Super RX, Fujifilm) developed using a Mediphot 937 (Colenta, Austria) automated film processor.

Protein	Product	Source	Company	Dilution	Blocking/ Incubation
PARP	Anti-PARP antibody, C2-10	Monoclonal mouse	Trevigen	1:1000	5% milk/ 12-18 hrs
MDM2	Anti-MDM2(IF-2), OP46	Monoclonal mouse	Calbiochem	1:300	5% milk/ 12-18 hrs
p53	Anti-Human p53 protein, M7001	Monoclonal mouse	Dako	1:500	5% milk/ 12-18 hrs
p-p53(S15)	Anti-Human Phosphop-53 protein	Monoclonal rabbit	Abcam	1:10.000	5% BSA/ 12-18 hrs
$p21^{WAF1}$	Anti-p21WAF1 (EA10), OP64	Monoclonal mouse	Calbiochem	1:100	5% milk/ 12-18 hrs
Actin	Anti-Actin antibody: A4700	Monoclonal mouse	Sigma	1:3000	5% milk/ 12-18 hrs
GAPDH	GAPDH (14C10), #2118	Monoclonal rabbit	Cell Signaling	1:3000	5% milk/ 12-18 hrs
WIP (F-10)	sc-376257	Monoclonal mouse	Santa Cruz	1:3000	5% milk/ 12-18 hrs
MCL1	Anti-MCL-1 antibody, #4572	Polyclonal rabbit	Cell Signaling	1:1000	5% BSA/ 12-18 hrs
BCL-2	Sc-509	Monoclonal mouse	Santa Cruz	1:500	5% milk/ 12-18 hrs
BCL-XL	Anti-Bxl-xL antibody, #2762	Polyclonal rabbit	Santa Cruz	1:1000	5% BSA/ 12-18 hrs
PUMA	PC686 (Calbiochem)	Polyclonal rabbit	Calbiochem	1:500	5% milk/ 12-18 hrs
ERK	ERK 1/2 (K-23): sc-94	Polyclonal rabbit	Santa Cruz	1:1000	5% BSA/ 12-18 hrs
p-ERK	p-ERK (E-4): sc-7383	Monoclonal mouse	Santa Cruz	1:1000	5% BSA/ 12-18 hrs
p70 S6 Kinase	p70 S6 Kinase #9202	Monoclonal rabbit	Cell Signaling	1:1000	5% BSA/ 12-18 hrs
Phospho-p70 S6 Kinase	Phospho-p70 S6 Kinase (Thr389) (108D2)	Monoclonal rabbit	Cell Signaling	1:1000	5% BSA/ 12-18 hrs
2º goat anti mouse HRP	PO447 (Dako)	Goat	Dako	1:1000	similar to 1º antibody
2º goat anti rabbit HRP	PO448 (Dako)	Goat	Dako	1:1000	similar to 1º antibody

Table 2.2 Primary antibodies used in western blotting.

2.8 Flow cytometry cell sorting

Fluorescence activated cell sorting (FACS) is a technique used to isolate and analyse the properties of each individual single cells from sample of mixed population. Cells were labelled with specific fluorescent dyes that binds to protein of targeted cells. The Flow cytometer machine measures the fluorescence of the cells as they were passed through a laser beam and the cells were sorted according to the fluorescence intensity. FACS is common technique used in cell separation, cell labelling, and cell analysis. Cells are analysed based on a variety of parameters, including cell size, shape, surface markers, fluorescence intensity, and other parameters.

A FACSCalibur™ flow cytometer (Becton Dickinson, BD Biosciences) was used to detect the expression of proteins of interest on cell surface. FACS analysis was performed by using a fluorescence-conjugated antibodies which bind to CD40L (also known as CD154) protein on the mouse fibroblasts L cells. The CD154 antibody is associated with a fluorescent dye molecule then coupled to target protein on cell surface. The cell will be detected by fluorescence light when it passes through the laser beam. A beam of single light wavelength is directed to mixture of suspension cells based upon light scattering and fluorescent properties of each cell. Multiple detectors were used to conduct the light beam: forward light scatter (FSC) is the light that is refracted by a cell in the forward direction, side light scatter (SSC) is the light that is refracted by a cell in a different direction from its original path and the fluorescence emission signals is light generated from molecules excited by laser light at specific wavelengths different from the forward and side light scatter.

2.8.1 Sample preparation and FACS protocol

For CD40L surface antigen detection experiment, direct conjugated monoclonal mouse anti-human antibodies were obtained from BD Bioscience, containing BD Pharmingen™ stain buffer with FBS. The fluorescein isothiocyanate (FITC) conjugated anti-CD154 (anti-CD40L) and IgG FITC isotype-matched control were used to stain both cell lines, CD40L and NTL. FITC is a green fluorescent dye that is excited by blue light.

For cell line immunostaining, mouse fibroblast cells expressing CD40L and NTL control, were seeded at concentration of $1x10^6$ cells/ml into three different microcentrifuge tubes, labelled CD154, IgG and unlabelled cells. The cells were washed twice with cold PBS buffer

by centrifugation at 300xg for 3 minutes and the cell pellet was resuspended in 100µL of PBS buffer. Each tube of the cell line was incubated with a saturating concentration of FBS stain buffer containing the corresponding antibody (anti-CD154 or IgG) for 20 minutes on ice, and protected from light. The corresponding antibody directly bound to the specific target antigen on the cell surface membrane. After incubation, cells were washed twice with 1ml of PBS buffer to remove unbound dye by centrifugation at 300xg for 5 minutes. The supernatant was discarded and the cells were resuspended in 0.5ml of PBS buffer. The FBS stained cells with corresponding antibodies were measured by flow cytometry FACSAttune™ (Becton Dickinson, BD Pharmingen™) after sampling and analysing by CellQuest™ software (Becton Dickinson). Each single labelled cell passes through a column. The lasers beam excited the fluorescent dyes and detectors measure the fluorescence intensity of the dyes. The cells are sorted into different groups based on the fluorescence intensity, cell size and shape. The FSC channel sorts cells based on their size. Cells with large size is sorted by high FSC channel and smaller cells are sorted by low FSC channel. In addition, SSC channel sorts cells based on their granularity. Cell population with high granularity is sorted into the high SSC channel and less granular cells are sorted into the low SSC channel.

The machine fluorescence calibration was checked using calibration beads (Calibrite beads, Becton-Dickinson). The antigens expression was determined as the net mean fluorescence intensity (MFI), calculated by comparing the peak fluorescence distribution of the isotypic control-stained population with that of the positively stained sample for each cell line. The cell line expressing CD40L was identified by gating on anti-CD154 positivity, which showed a different scale and cell scatter area compared to anti-IgG antibody. The gate area should include the majority of the cell distribution scatter while excluding debris and dead cells which typically appear in the bottom left corner.

For unstained cell line evaluation, both CD40L and NTL cells were treated in exact the same way of antibody signals with substitute the antibody with PBS. Unstained cell lines were performed to evaluate the differences in cells distribution in the absence of the antibody signals as negative control. The number of events were set to 30,000 per sample.

2.8.2 FACSCalibur instrument setting and gating

Samples were processed using a FACSCalibur™ (Becton Dickinson, BD Biosciences), CellQuest™ software was used to optimise the instrument settings based on FSC and SSC dot

plots of untreated control samples of each cell line. On the histogram plot, the Y-axis shows the number of events or cells that express fluorescence light and the X-axis shows the relative fluorescence intensity detected from each cell. A large number of events detected at one particular intensity will be represented as a peak on the histogram can be interpreted as a positive control.

2.8.3 Data analysis

In order to calculate the proportion of cells (events) that expressed the antibodies, CD154 or IgG on their surface, Cyflogic Software Version 1.2.1 (CyFlo Ltd) was used to manually gate the single-cells on the SSC-A *vs.* FSC-A scatter plot. Each cell line had its own gate which showing the spread of cell population expressing the antibody. Based on peaks corresponding to CD154 and IgG antibodies, the percentage of events were calculated.

2.9 Molecular biology

2.9.1 DNA extraction and quantification

The extraction of DNA is a crucial step in molecular biology, because it is one of the techniques have been shown to produce high-quality DNA rapidly. For this study, DNA was extracted using the QIAamp DNA Mini Kit (QIAGEN, 51306) according to the manufacturer's protocol. This kit is designed to purify total DNA quickly and easily, and it uses QIAamp Mini columns coated with a unique silica membrane that binds to 20µg of the DNA in the presence of a high concentration of chaotropic salt, allowing for elution in a small volume of low-salt buffer. Lysate samples were washed twice with buffer to release DNA bound to silica membrane. After purification, the DNA was released from the silica membrane and eluted in 200µl of elution buffer (10mM Tris-Cl; 0.5mM EDTA; pH 9.0) provided by the kit. The eluted DNA samples were stored at +4°C until further use.

2.9.2 RNA extraction and quantification

For RNA extraction, cells were cultured in 6-well plate (Corning) at a density of $1x10^6$ cells/ml for cell line and $5x10^6$ cells/ml for primary CLL cells. Then, cells were treated with compound of interest at the specified concentration for desired time points. At time of harvest,

whole cell suspensions were collected into microcentrifuge tubes. The wells were washed with phosphate buffer saline (PBS) to be sure that all cells were collected into the microcentrifuge tubes. The cells were spun down at 2000g for 3min. The medium was removed and cell pellets was washed once with PBS. Then, the cell pellets were stored in freezer at -80°C. Total RNA was extracted from the cell pellet using RNeasy Mini Kit (Qiagen, Germany) following the manufacturer's protocol. A DNase treatment step with on-column digestion was carried out using the RNase-free DNase kit (Qiagen). The RNA purity and concentration was identified by measuring the O.D at 260nm with an ND-1000 spectrophotometer (NanoDrop Technologies, ThermoScientific, UK). The absorbance ratio of A260/A280 is commonly used to evaluate RNA purity. The high-quality of RNA purification is considered at A260/A280 ratio in range of (1.8-2.1).

2.9.3 Estimation of nucleic acid concentration

The Nucleic acids purity and concentration was identified by measuring the optical density (O.D) at 260nm and 280nm with an ND-1000 spectrophotometer (NanoDrop Technologies, ThermoScientific, UK). The Nanodrop machine has a sample loading platform that includes a receiving fibre optic, onto which one microliter of the sample was loaded. The sample loading platform needs to be cleaned after each use and deionized distilled water is used as a blank control. Nucleic acids absorb light at 260nm, while proteins and phenol contaminants absorb at 280nm. Thus, the ratio of these absorbances is used to evaluate the purity of the samples. The ratio of A260/A280 was used to identify nucleic acids purity and to calculate the appropriate RNA volume required for qRT-PCR reactions. The ratio of A260/A280 value of nucleic acids with a good purity range between 1.7 to 2.0. The A260/A280 ratio of approximately 1.8 indicates pure DNA, while a ratio of around 2.0 indicates pure RNA. Furthermore, absorbance of A260/A230 ratio is another possible used as a secondary indicator to measure the nucleic acid purity with expected values usually higher than the A260/A280 ratio for a given sample, typically ranging from 2.0 to 2.2. low value of A260/A230 ratio indicates contamination by carbohydrates or solvents, as both of these absorb strongly at 230nm.

2.9.4 Complementary DNA (cDNA) synthesis

Complementary DNA (cDNA) is a form of DNA that is synthesized from a single-stranded RNA template by the action of reverse transcriptase (RNA dependent DNA polymerase). The reverse transcriptase is an enzyme which uses the RNA template and a primer complementary to the RNA in order to synthesis cDNA strand which can be used as a template for the PCR. The cDNA was produced using the High-Capacity cDNA Reverse Transcription Kit (Applied Biosystems by Thermo Fisher Scientific, 4368814) as described by the manufacturer. A master mix of the kit's reagents was prepared in volumes specified in (Table 2.5), and this was multiplied by the number of RNA samples to be reverse-transcribed. Then, 14.2µl of RNA (0.5 µg) plus 5.8µl of the master mix were added to each of the labelled 0.2ml PCR tubes (STARLAB, UK). The samples were then incubated in a GeneAmp PCR System 9700 thermal cycler (Applied Biosystems) under the following conditions: 10 minutes at 25°C, 2 hours at 37°C, 5 minutes at 85°C and stored at -20°C until further use.

Reagent	Volume (per sample)
10X RT buffer	2 µl
100 mM dNTP	0.8 µl
Oligo$(dT)_{15}$ Primer	2 µl
50 U/µl Reverse Transcriptase	1 µl
RNA (0.5 µg)	14.2 µl

Table 2.3 Reaction components for reverse transcription.

2.9.5 Primer-directed polymerase chain reaction (PCR)

The primers used in this study were designed with the aid of the Primer BLAST tool available through the National Centre for Biotechnology Information (NCBI) and were custom synthesized by Eurogentec Ltd. (Southampton, UK). The sequences of all sense and antisense primers used in the study are provided in (Table 2.4).

Genes	Primer Forward (5'-3')	Primer Reverse (5'-3')
GAPDH	CGACCACTTTGTCAAGCTCA (Ex.8)	GGGTCTTACTCCTTGGAGGC (Ex.9)
CDKN1A	CTGGAGACTCTCAGGGTCGA (Ex.2)	CTCTTGGAGAAGATCAGCCG (Ex.3)
MDM2	AGTAGCAGTGAATCTACAGGGA (Ex.8)	CTGATCCAACCAATCACCTGAAT (Ex.9)
BBC3(PUMA)	ACCTCAACGCACAGTACGA (Ex.3)	CTGGGTAAGGGCAGGAGTC (Ex.4)
BAX	CCCGAGAGGTCTTTTTCCGAG (Ex.4)	CCAGCCCATGATGGTTCTGAT (Ex.5)
FAS	AGATTGTGTGATGAAGGACATGG (Ex.3)	TGTTGCTGGTGAGTGTGCATT (Ex.4)
NOXA1 (NADPH oxidase activator 1)	TGCTACACAATGTGGCGTC (Ex.2)	ACTTGGACAATGGCCTCCCTTA (Ex.4)
TP53INP1	TCTTGAGTGCTTGGCTGATACA (Ex.3)	GGTGGGGTGATAAACCAGCTC (Ex.3)
PPM1D (WIP1)	TTTCTCGCTTGTCACCTTGC (Ex.1)	TTCCAAGAACCACCCCTGAG (Ex.2)
MCL1	GTGCCTTTGTGGCTAAACACT (Ex.4)	AGTCCCGTTTTGTCCTTACGA (Ex.5)
BCL2	GGTGGGGTCATGTGTGTGG (Ex.2/3)	CGGTTCAGGTACTCAGTCATCC (Ex.3/4)
TP53	CAGCACATGACGGAGGTTGT (Ex.7)	TCATCCAAATACTCCACACGC (Ex.8)

Table 2.4 PCR primers. NOXA1 primer represents NADPH oxidase activator 1**.**

2.9.6 Polymerase chain reaction (PCR)

The Polymerase Chain Reaction (PCR) is a highly efficient *in-vitro* biochemical technique commonly applied in molecular biology to rapidly and precisely amplify low copies of a specific DNA segment of interest. PCR was first developed by Kary Mullis in 1983 and later improved in its current form by Saiki et al. (Mullis, 1990; Saiki et al., 1988).

PCR amplification requires a pair of oligonucleotide primers, which are around 20 bp in length, for successful delivery into nucleus and target specific sequences. Each primer binds to its template on the DNA strand and starts to amplify through repeated cycles of DNA denaturation, annealing and extension by DNA polymerase with deoxyribonucleic acids (dNTPs) (dATP, dTTP, dCTP and dGTP) and appropriate co-factors.

Each PCR reaction includes pair sets of an appropriate primer desired to target the DNA segment which needs to be amplified, a DNA template, Platinum™ Taq Green Hot Start DNA Polymerase (Invitrogen, 11966026), deoxyribonucleic acids (dNTPs), $MgCl_2$, proprietary buffer solution and sterile water (Table 2.5). PCR runs were carried out by using GeneAmp PCR System 9700 thermal cycler (Applied Biosystems) through the standard optimised cycling parameters recommended for the specified *DNA polymerase* (initial denaturation phase: 94˚C for 2 min; 35 PCR cycles: denaturation of 30 sec at 94°C, annealing of 30 sec at ~55°C (depending on primer melting temperature-T_m) and extending of 1min/kb at 72°C; hold at 4°C). The primer melting temperature (T_m) is the temperature at which one-half of the DNA duplex will dissociate into single stranded and indicates the duplex stability.

Component	50 µl reaction	Final concentration in 50 µl reaction
Water, nuclease-free	to 50 µl	-
10X Green PCR Buffer, -Mg	5 µl	1X
50 mM $MgCl_2$	1.5 µl	1.5 mM
10 mM dNTP mix	1 µl	0.2 mM each
10 µM forward primer	1 µl	0.2 µM
10 µM reverse primer	1 µl	0.2 µM
Platinum *Taq* DNA polymerase	0.2 µl	2U/rxn
Template DNA	varies	<500ng/reaction

Table 2.5 Components of PCR reaction.

2.9.7 Quantitative real-time PCR (qRT-PCR)

Quantitative real-time PCR (qRT-PCR) is a technique used for amplification and simultaneous quantification of nucleic acids on the basis of PCR. The qRT-PCR was carried out to detect and measure the difference in genes expression after treatment. The total RNA or messenger RNA (mRNA) were extracted and then transcribed into cDNA using a reverse transcriptase enzyme, following the manufacturer's protocol with the Promega Reverse Transcription System (A3500, Promega). The qRT-PCR runs were performed by using SYBR green RT-PCR master mix (Life Technologies) following the manufacturer's guidelines using the gene specific cDNA primers shown in (Table 2.4).

The specific primers were designed to target regions of the gene's mRNA, including all known splice variants, to measure the transcription quantity of the gene of interest. SYBR Green is a fluorescent dye that binds specifically to double-stranded DNA (dsDNA), with an excitation wavelength of approximately 485nm and an emission wavelength of around 524nm. The fluorescent signal emitted from SYBR Green is directly proportional to the amount of dsDNA, allowing for real-time measurement of PCR dsDNA quantity after each elongation step.

For qRT-PCR reaction, a total of 20ng/µL from each cDNA sample was diluted in 10µL of final reaction volume. Standard optimised cycling parameters were used and products detected in real time on an ABI 7900HT system (Stage 1: 50˚C for 2 minutes, Stage 2: 95˚C

for 10 minutes then 40 cycles of 95˚C for 15 second and 60˚C for 1 minute). GAPDH was used as endogenous control. The DMSO solvent control samples were used as the calibrator for each independent repeat. Data were presented as the mean ± SEM relative quantities (RQ) of three well repeats of intra-experiment.

2.10 Statistical analysis

The statistical analyses were conducted using the GraphPad Prism Version 6.05 software, developed by GraphPad Software. Inc. The primary endpoint examined in the clinical cases under study was overall survival (OS), which was recorded in months from the time of diagnosis to the cut-off date for follow up or censoring date. The Kaplan-Meier method and Log-Rank test were utilized to determine the differences in cumulative survival, and the hazard ratios were also calculated, representing the relative rate of death in each group based on the slopes of the survival curves. Additionally, treatment-free survival was defined as the time duration between diagnosis and the first treatment (TTFT: Time to First Treatment).

For statistical comparisons, appropriate paired or unpaired t-tests and one-way ANOVA with correction for multiple hypothesis testing were used as appropriate for statistical comparisons unless other specific test was applied and stated in the corresponding figure legends. The results were presented as either the mean ± SEM or mean ± SD, unless additional details were mentioned. The *p*-values were less than 0.05 considered statistically significant at the 95% confidence level (ns: not significant, $p > 0.05$; *, $p < 0.05$; **, $p < 0.01$; ***, $p < 0.001$; ****, $p < 0.0001$).

2.11 Primary CLL cell stimulation

2.11.1 Interleukin-4 (IL-4) stimulation

Interleukin-4 (IL-4) can be used to stimulate the primary CLL cells (Hewamana et al., 2008; Kay & Pittner, 2003). In this study, the CLL cells were directly treated with IL-4 at a concentration of 10ng/ml prior seeding the CLL cells in the 96 wells plate (Corning). Each 10ml of suspension CLL cells at $5x10^6$ cells/ml were treated with 1µL of IL-4 (10ng/ml). In addition, IL-4 was added on both CD40L and NTL fibroblast cells to enhance the CLL cell proliferation signals *ex-vivo* microenvironment.

2.11.2 CD40L stimulation

CD40L is expressed on activated CD4+ T lymphocytes. CD40 receptors are normally present on leukemic B-cells. The activation of T helper cell triggers the proliferation of B-cells through binding of CD40L to CD40 receptors. Mouse fibroblast L-cell were transfected with CD40L in order to mimic the *ex-vivo* environment that CLL cells are exposed to within the lymph nodes. The CD40L stimulation is one of the most efficient ways to stimulate CLL cell proliferation (Burley et al., 2022; Hewamana et al., 2008; Pepper et al., 2011). The same mouse fibroblast L-cell had been transfected with empty plasmid vector to for feeder layer that do not express the CD40L on their surface (known as NTL or control feeder layer cells). The NTL cells used as a negative control condition which not expressing the CD40L on their surface.

2.11.2.1 Irradiation of feeder layer cells

The reason for irradiation of the feeder layer cells was to stop cell division and proliferation, meanwhile maintaining the cell viability and metabolic activity. Both CD40L and NTL adherent cells, were seeded in 24 wells plate at a concentration of $5x10^7$ cells/ml in a total volume of 0.5ml per well. Then, cells were incubated at 37°C with 5% CO_2 for 2 hours to allow them to settle down and attach in the well. After that, the monolayer cells were irradiated by X-ray system with 15Gy (320kV and 10mA) for 12 minutes (D3300 X-ray system).

2.11.2.2 Co-culture of primary CLL cells

Following irradiation, the monolayer cells were incubated at 37°C with 5% CO_2 overnight. The next day, both irradiated feeder layer cells, CD40L and NTL, were washed with PBS once prior adding the CLL cells. The primary CLL cells were added to each well at a concentration of $1x10^6$ cell/ml in a total volume of 1ml in full fresh medium including IL-4 at a concentration of 10ng/ml. Both CLL and monolayer cells were incubated at 37°C with 5% CO_2 for 72 hours. After that, CLL cells were counted every four days using the coulter counter, to monitor the proliferation rate in order to determine when to start the treatment (once proliferation was confirmed). The feeder layer cells were replaced every four days. The effect of treatment on the CLL proliferation rate was monitored every 4 days by counting the CLL cell number whenever they the CLL cells were transferred into a new irradiated monolayer.

2.11.3 Anti-IgM immobilization or BCR signal

2.11.3.1 Coupling of the antibody with magnetic beads

All of the antibody coupling procedure was performed in a tissue culture hood at room temperature using Dynabead Antibody coupling kit (life technologies 14311D) as described by the manufacturer. The kit contents and volumes are outlined in (Table 2.6) Dynabeads® M-270 Epoxy beads which were supplied in the kit, which covalently bind to primary amino and sulfhydryl groups of the target antibody.

The beads were resuspended in 1ml of C1 reagent and washed gently by pipetting up and down. Then, the beads were transferred into new 5ml plastic vessel and attached to magnet for 1min. After that, the supernatant was removed while the plastic vessel (beads) was attached against to magnet. Then, the beads were gently washed with 1ml of C1 reagent by pipetting up and down. There were 60mg of beads in total. The kit was divided into half to prepare beads coupled with F(ab')2-IgM and F(ab')2-IC (Southern Biotechnologies), giving 30mg of beads for each antibody. 500µl of the beads were transferred to another 5ml plastic vessel. Both plastic vessels were attached against to magnet for 1min and the supernatant were removed. After that, in a new tube, C1 reagent was mixed to each antibody individually without the beads. For Anti-Human IgM-F(ab')2, 600µl of the antibodies were mixed with 900µl of C1. For a control, 60µl of IgG-F(ab')2 were mixed with 1440µl C1. Then, each antibody mixture was transferred to the beads in the plastic vessel separately. 1.5ml of C2 reagent was added to both antibodies and mixed. The plastic vessels including the antibodies

and the beads were sealed with Nesco™ film and were placed into falcon tube for overnight incubation on a roller at 37°C.

The next day, the plastic vessels were attached to the magnet for 1 min and the supernatant was removed. The beads were washed with three different buffers and the supernatant gently was removed each time by attaching the beads against the magnet. Starting with 1.6ml of HB buffer, LB buffer and SB buffer consequently. Two more washes were applied with 1.6ml of SB buffer. Then, the beads were incubated on a roller at room temperature (RT) for 15 minutes with the 1.6ml of SB buffer remaining from the last wash. After the incubation, the supernatant was removed and the beads were resuspended in 3ml of SB buffer (100µl SB per mg beads; 10mg/ml AB coupled beads). Sodium azide was added at volume of 10µl per 1ml of beads. Aliquots of 1ml were stored at 4°C.

Component	Amount
Dynabeads® M-270 Epoxy	>60 mg
C1	20 ml
C2	8 ml
HB	15 ml
LB	15 ml
SB	40 ml

Table 2.6 Components of Dynabead antibody coupling kit.

2.11.3.2 Stimulation of CLL cells

Before incubating the primary CLL with immobilization anti-IgM antibody, the beads were washed three times repeatedly with 1ml of full fresh RPMI-1640 medium (R8758, Sigma Aldrich, Dorset, UK) to remove the sodium azide particles and each time the supernatant was removed gently by attaching the beads against the magnet for 1 min. After the third washing, the immobilised anti-IgM beads were resuspended in a fresh medium with their original volume and were placed in ice.

Then, the primary CLL cells were added to the immobilization anti-IgM beads in a ratio of (2:1). For primary CLL stimulation, two beads were used to stimulate one CLL cells. Based on this ratio, 3µl of immobilized anti-IgM beads were incubated with 100µl of primary CLL cells for 1-hour.

After immobilised anti-IgM stimulation, the CLL cells were washed three times with full fresh RPMI-1640 medium by adjusting the beads against the magnet and the supernatant were collected into a new microcentrifuge tube. Then, the anti-IgM stimulated CLL cells were treated with different drug concentrations and incubated for a specific period of time. Then, at the end of the treatment the CLL cells were harvest and collected to identify the changes in the downstream proteins.

Chapter 3: The Effect of MDM2 and WIP1 Inhibitors on Cell Lines Derived from Haematological Malignancies

3.1 Introduction

Several studies have investigated different inhibitors to eliminate the abnormal proliferation of cancer cells. Targeting negative regulators of p53 with specific small molecules (MDM2i and WIP1i) to inhibit the activity of MDM2 and WIP1 proteins, leading to activation of the p53 cascade is one of the novel therapeutic strategies being explored in cancer treatment, particularly in p53 functional cancers (Wu et al., 2018; Deng et al., 2020; Wu et al., 2021).

RG7388 (idasanutlin), a second generation MDM2-p53 binding antagonist, has been investigated across multiple cancers, including B-cells (NALM-6, OCI-Ly3, HAL01) and haematological malignancies disorder patients such as AML and polycythemia vera (Corbali & Eskazan, 2020; Mascarenhas et al., 2022; Aptullahoglu, Wallis, et al., 2023). The WIP1 inhibitor (GSK2830371) was developed to explore inhibition of the phosphatase negative feedback loop regulation of p53, which leads to increased phosphorylation and stabilisation of p53 (Gilmartin et al., 2014).

p53 plays an essential role in preventing aberrant cell proliferation and maintaining genomic integrity. Therefore, several pharmaceutical strategies have been manipulating p53 to develop a non-genotoxic compound to maximize the specificity and sensitivity of its ability to eradicate malignant cells (Brown et al., 2009; Chène, 2003). The activity of functional p53 is mainly regulated through direct interaction with the MDM2 protein (Haupt et al., 1997; Moll & Petrenko, 2003).

Several *in-vitro* studies have been published on the strategy of using MDM2 inhibitors in combination with the GSK2830371, WIP1 inhibitor and reported synergistic effects against a range of cancer cell types, biliary tract cancer (BTC) cell lines (Deng et al., 2020).

Another *in-vivo* study has confirmed that the combination of WIP1 inhibitor (GSK2830371) potentiates the activity of RG7388 by increasing the phosphorylation of p53 which leads to increase the growth inhibition of liver adenocarcinoma cells, uterine Leiomyosarcoma (uLMS), and cutaneous melanoma in a p53 dependent manner (Chamberlain et al., 2021; Esfandiari et al., 2016; Wu et al., 2018, 2022).

Although the combination of WIP1 and MDM2 inhibitors (RG7388) has been investigated in a range of different cancers, however there is no data for haematological cells. Therefore, this study has sought to investigate the effect of RG7388 in a combination with GSK2830371 on

cell line models derived from B-cell haematological malignancies before progressing to explore the effect of this combination against primary CLL cells *ex-vivo*.

It was reported from our group and other studies that the effectiveness of MDM2 inhibitor mainly depends on the stabilization of functional p53 activity. Thus, wild type p53 cells respond well to the inhibitor compared to the mutant p53 cells. The potentiation effect of the WIP1 inhibitor on the response to MDM2-p53 binding antagonists has also been found to be dependent on p53 status (Wu et al., 2018, 2021; Esfandiari et al., 2016).

3.2 Hypothesis and Aims

The aim of the work presented in the current chapter was to examine the effect of the WIP1 inhibitor in combination with an MDM2 inhibitor on a panel of NALM-6 haematological cell lines with three different isogenic p53 backgrounds: wild type *TP53*, heterozygous *TP53* and mutant *TP53* (null). In addition, OCI-Ly3 cells were used in the study as another example of a haematological B-lymphoma cell line. In addition, the effect of MDM2 inhibitors (RG7388 and HDM201) as single agents had already been investigated previously by our group (Aptullahoglu, Ciardullo, et al., 2023; Ciardullo et al., 2019).

3.3 Results

3.3.1 The growth inhibition effect of WIP1 inhibitor on isogeneic p53 NALM-6 cells

The aim of this section was to determine the cytotoxic effect of WIP1 inhibitor (GSK2830371) on the proliferation of isogenic *TP53* NALM-6 cells. A wide range of WIP1 inhibitor concentrations was used to determine the inhibitory effect on both functional and non-functional *TP53* NALM-6 cells. In addition, to measure the effect of the GSK2830371 inhibitor on *TP53* functional NALM-6 cells, whether in the heterozygous or wild type *TP53* form.

(Figure 3.1) shows the results for independent repeat experiments measuring the cell proliferation of isogenic NALM-6 cell lines treated with the WIP1 inhibitor for 72 hours. Following the treatment, the XTT assay was used to measure the relative proliferation of the cells compared to DMSO solvent only treated controls. All the three isogonics p53 NALM-6 cells were treated with a wide range of WIP1 inhibitor concentrations, from 0.01 to 10μM. In conclusion, over this concentration range, the GSK2830371 WIP1 inhibitor had little effect on the NALM-6 cell line proliferation, whether it possessed functional or non-functional *TP53* genetic background.

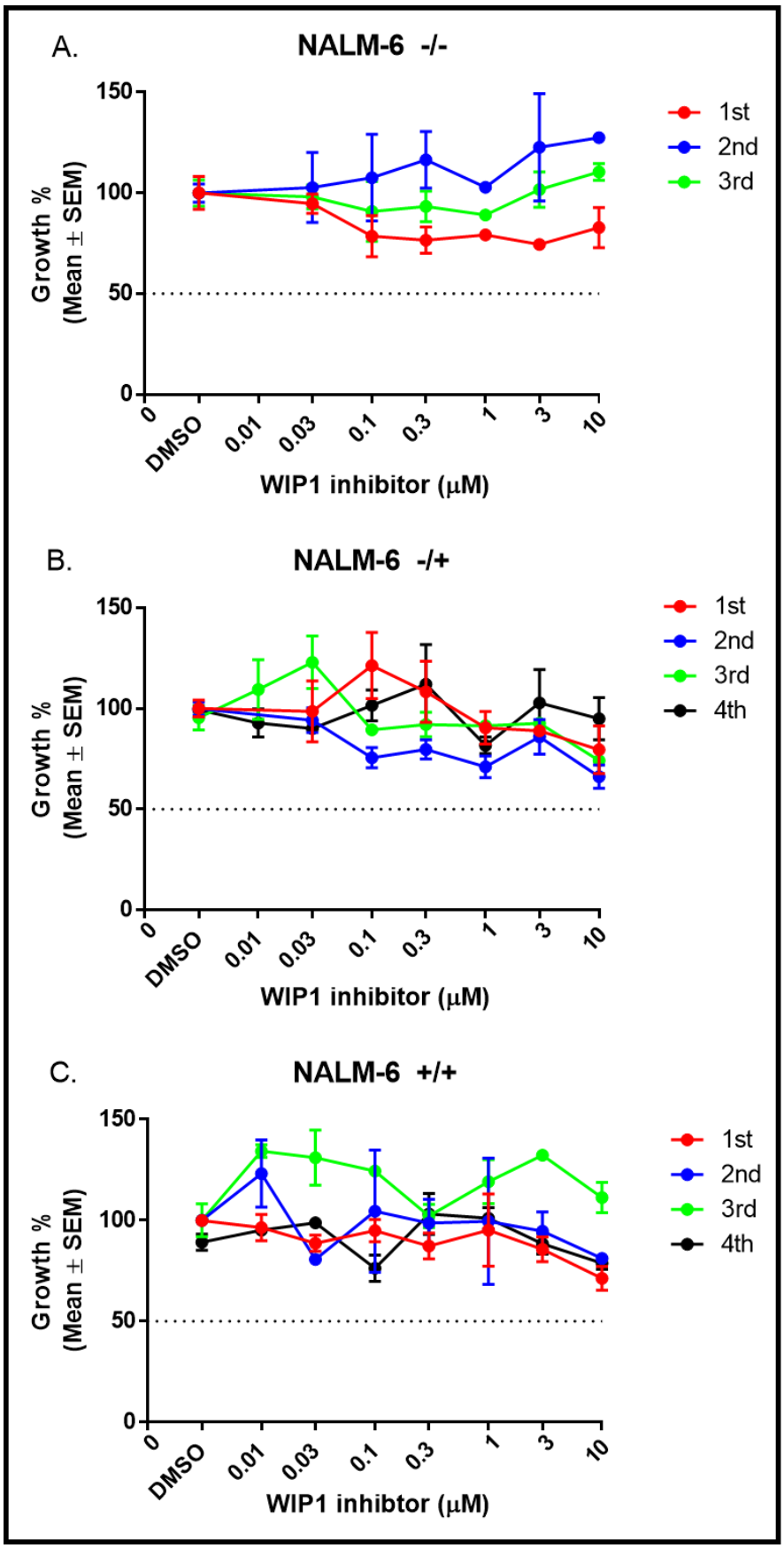

Figure 3.1 The effect of WIP1 inhibitor on isogenic TP53 NALM-6 cells. (A) Mutant p53 NALM-6(-/-) (n=3). (B) Heterozygous p53 NALM-6(-/+) (n=4). (C) Wild type p53 NALM-6(+/+) (n=4). The growth inhibition measured by XTT assay for isogenic TP53 NALM-6 cell line treated with different concentrations of GSK2830371 for 72hrs. Each line shows an independent repeat (e.g. 1st: red, 2nd: blue, 3rd: green and 4th: black). Bars show the mean ± SEM. All % of growth was normalized to DMSO treatment for individual experiment. (SEM, standard error of the mean).

3.3.2 The growth inhibition effect of MDM2 inhibitors (RG7388/HDM201) on otherwise isogeneic TP53 wild type and mutant NALM-6 cells

The aim of this section is to determine the effect of MDM2 inhibitors (RG7388 and HDM201) on the proliferation of isogenic *TP53* wild-type and mutant NALM-6 cells. The same method was used as described in the previous section (3.3.1). A range of both RG7388 and HDM201 concentrations was used to determine the effect on the proliferation of both *TP53* functional and non-functional NALM-6 cells. In addition, to compare the effect of the MDM2 inhibitors on both $TP53^{(+/+)}$ homozygous and $TP53^{(+/-)}$ monoallelic NALM-6 cells.

NALM-6 cells with different isogenic *TP53* background were treated with wide ranges (0.01, 0.03, 0.1, 0.3, 1 and 3μM) of the MDM2 inhibitors, RG7388 and HDM201 (Figure 3.2). Following the 72 hours of treatment, cell proliferation was determined by XTT assays. The effect of various concentrations was normalized to the effect of DMSO which was included as a control for untreated cells.

Mutant p53 NALM-6(-/-) cells did not show a concentration dependent inhibition effect on the cell proliferation, either with RG7388 nor HDM201 (Figure 3.2 A&D). In contrast, both the heterozygous $TP53^{(+/-)}$ NALM-6 cells and $TP53^{(+/+)}$ wild type NALM-6 cells showed a concentration dependent inhibition of cell proliferation (Figure 3.2 B, C, E, F) in response to both MDM2 inhibitors, RG7388 and HDM201. Interestingly, one functional *TP53* allele was sufficient to show a dose dependent inhibitory response of the cells to both MDM2 inhibitors (RG7388/HDM201).

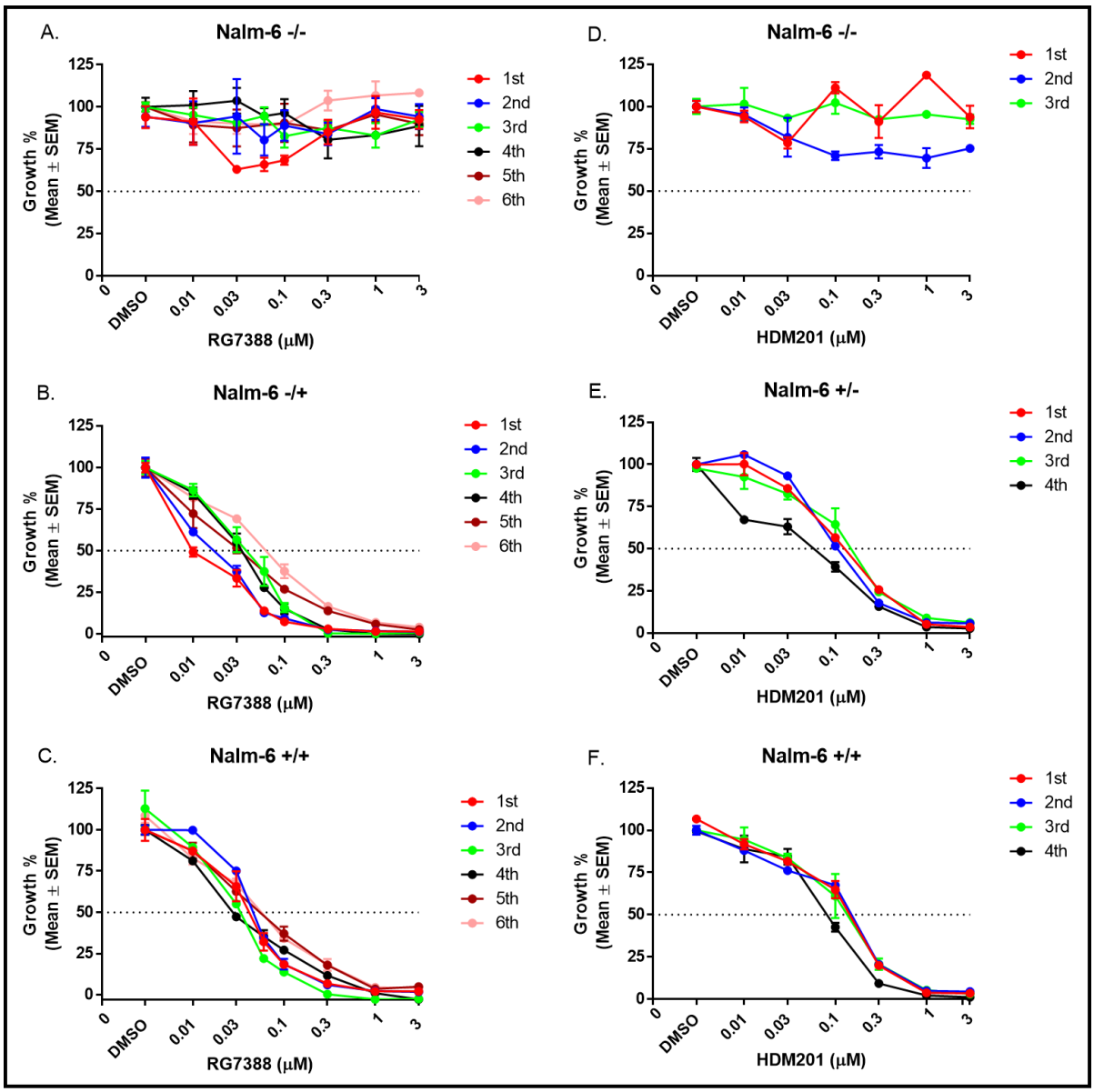

Figure 3.2 The concentration dependent effect of MDM2 inhibitors (RG7388/HDM201) on the proliferation of isogenic TP53 NALM-6 cell line. (A) NALM-6 (-/-) with RG7388. (B) NALM-6 (-/+) with RG7388. (C) NALM-6 (+/+) with RG7388. (D) NALM-6 (-/-) with HDM201. (E) NALM-6 (-/+) with HDM201. (F) NALM-6 (+/+) with HDM201. The effect of RG7388 was repeated (n=6) consecutive times on all isogenic p53 NALM-6 cells, while the effect of HDM201 was repeated (n=4) times on both heterozygous p53(-/+) and wild type p53(+/+) and (n=3) times on mutant p53(-/-) NALM-6 cells. The growth inhibition measured by XTT assay for after 27hrs of the treatment. Each line shows an independent repeat (e.g. 1st: red, 2nd: blue, 3rd: green, 4th: black, 5th: purple and 6th: pink). Bars show the mean ± SEM. Each independent repeat of experiment was normalized to DMSO treatment for individual experiment.

3.3.3 The potentiation of RG7388 growth inhibition by the WIP1 inhibitor is dependent on p53 status

In this section, the ability of WIP1 inhibitor to potentiate activity of MDM2 inhibitor was tested. GSK2830371 at 2.5μM was initially used in a combination with a wide range of RG7388 concentrations (0.01, 0.03, 0.1, 0.3, 1 and 3μM). The following data are the summary of isogenic p53 NALM-6 cell response to treatment with the MDM2 and WIP1 inhibitors for 72 hours. (Figure 3.3) illustrates the effect of RG7388 and GSK2830371 (2.5μM) inhibitors as single agents and in combination on the isogenic p53 NALM-6 cells.

For mutant p53 NALM-6(-/-) cells (Figure 3.3 A), neither single treatment nor the combination inhibited cell proliferation. With heterozygous and wild type p53 NALM-6 (Figure 3.3 B&C), WIP1 (2.5μM) inhibitor alone does not have much of an inhibition effect on the growth activity of either of the NALM-6 cell lines with a functional *TP53* allele. However, RG7388 by itself was able to inhibit the growth activity of NALM-6 cells with at least one functional *TP53* allele in a concentration dependent manner. Furthermore, despite having little effect on its own, 2.5μM WIP1 inhibitor markedly potentiated the anti-proliferative effect of RG7388 with both NALM-6 *TP53*(+/+) and NALM-6 *TP53*(+/-) cell lines. It was seen that the combination of WIP1 (2.5μM) inhibitor with RG7388 (0.01μM) inhibits more than 50% of heterozygous and wild type p53 NALM-6 cell proliferation.

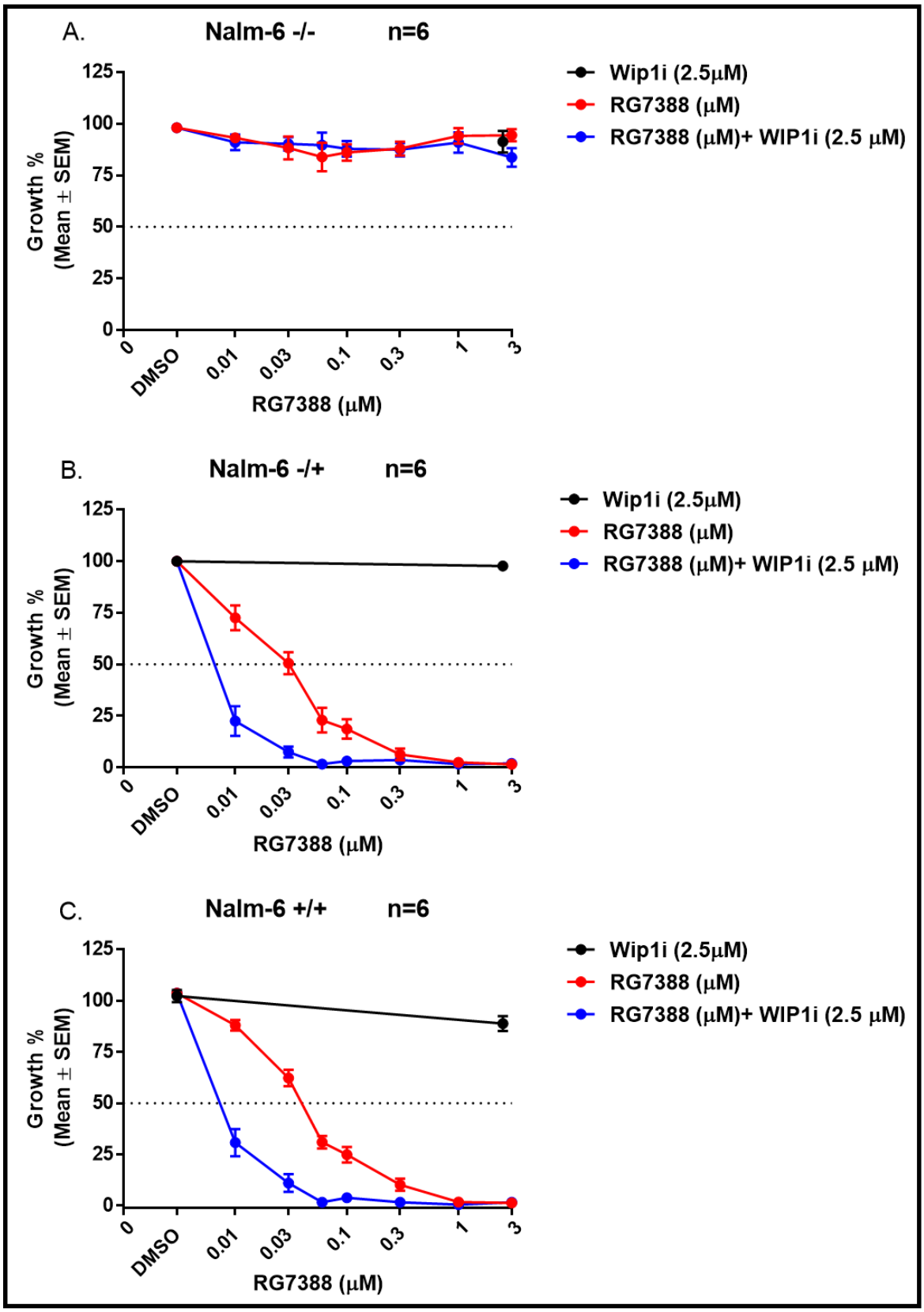

Figure 3.3 WIP1 inhibitor potentiated the growth inhibitory effect of MDM2 antagonist (RG7388) in a p53 dependent manner with functional TP53 alleles. (A) Mutant TP53(-/-) (B) monoallelic TP53(-/+) (C) wild type TP53(+/+). The growth inhibition was measured by XTT assay for isogenic TP53 NALM-6 cell line treated with different concentrations of RG7388 in combined with or without GSK2830371 (2.5μM) for 72 hours. The effect of each drug compound was repeated on consecutive different cell passages. Each line shows an independent repeat (n=6) of experiment averaged by itself. All % of growth was normalized to DMSO treatment for individual experiment. Bars show the mean ± SEM.

3.3.4 The potentiation of HDM201 growth inhibition by the WIP1 inhibitor is dependent on p53 status

In this section, we determined the ability of WIP1 inhibitor to potentiate the activity of another MDM2-p53 binding antagonist, HDM201. GSK2830371, at (2.5μM) was again used in combination with a wide range of HDM201 concentrations (0.01, 0.03, 0.1, 0.3, 1 and 3μM) for 72 hours of treatment exposure. (Figure 3.4) shows the effect of HDM201 and GSK2830371 (2.5μM) inhibitor as single agents and in combination treatment on the proliferation of the isogenic p53 NALM-6 cell line panel.

(Figure 3.4) demonstrates the effect of MDM2 (HDM201) and WIP1 (2.5μM) inhibitors single agents and in combination treatment on the proliferation of the NALM-6 TP53 knockout cell line panel. The HDM201 results mirrored what was seen for RG7388, consistent with the p53 dependence and potentiation by the WIP1 inhibitor being an MDM2-p53 binding antagonist drug class effect.

Thus, non-functional p53 knockout NALM-6 (-/-) cells, did not response to either the MDM2 or the WIP1 (2.5μM) inhibitors as single agents or in combination (Figure 3.4 A). In parallel experiments, with functional p53 isogenic NALM-6 cells (Figure 3.4 B&C), WIP1 (2.5μM) inhibitor as a single agent showed little inhibitory effect on the proliferation of *TP53* monoallelic (-/+) and wild type (+/+) NALM-6 cells. In contrast, HDM201 by itself inhibited the proliferation of both NALM-6 cell lines with a functional p53 allele in a concentration dependent manner. Furthermore, combination with the WIP1 (2.5μM) inhibitor potentiated the effect of HDM201, with inhibition of proliferation much greater than the effect of HDM201 alone. The combination of WIP1 (2.5μM) with MDM2 inhibitor (HDM201) at (0.01μM) concentration inhibited proliferation of the p53 functional cell lines by approximately 50%, whereas the HDM201 alone required at least ten times that dose (0.1μM to achieve the same level of growth inhibition. Interestingly, the potentiation effect of the GSK2830371, WIP1 inhibitor appeared to be greater for combination with HDM201 that with RG7388. However, the average GI_{50} ratio of RG7388 and HDM201 in the presence or absence of WIP1 inhibitor looked similar for the *TP53* wild type (+/+) and *TP53* monoallelic (-/+) NALM-6 cells.

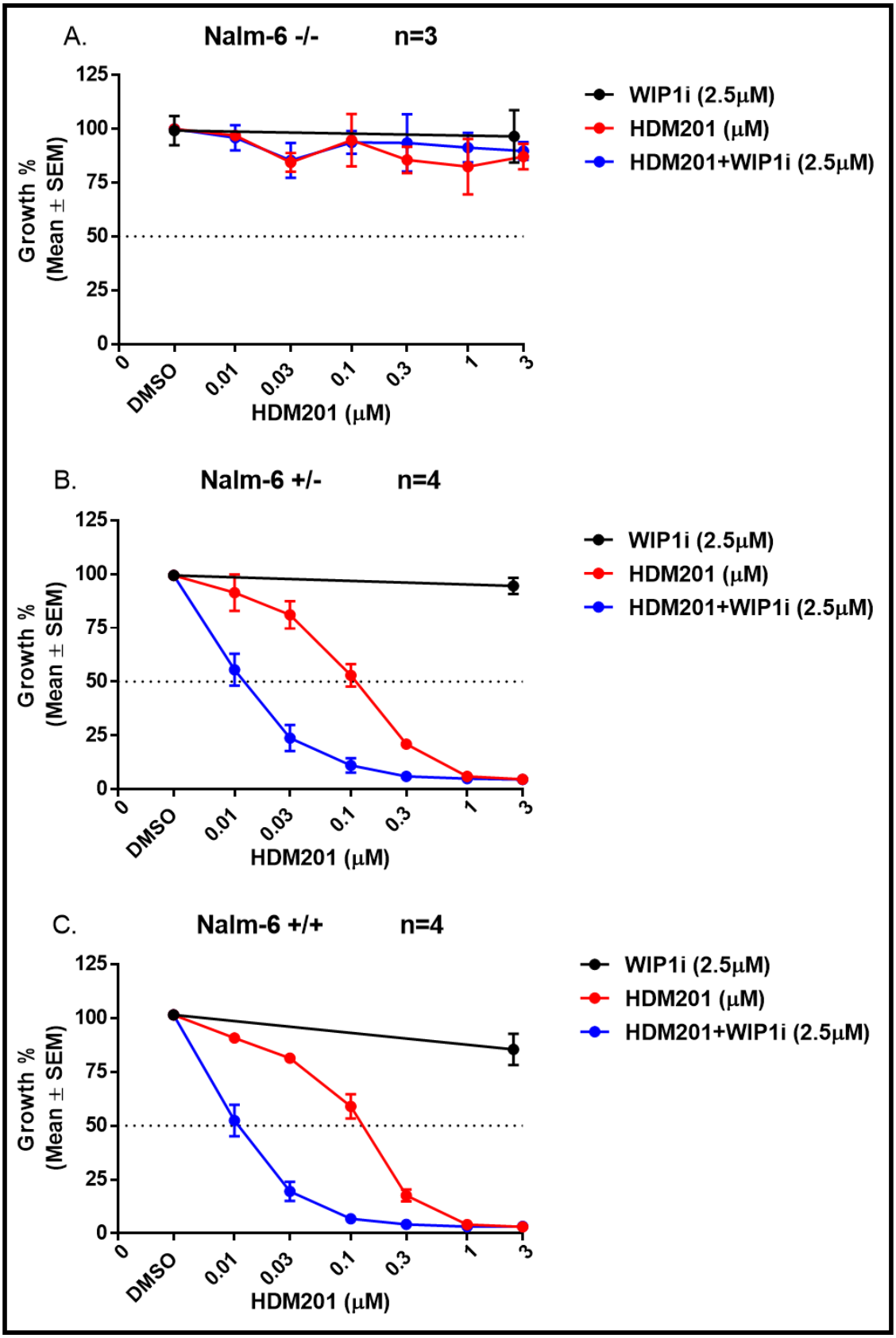

Figure 3.4 The combination with WIP1 inhibitor (2.5μM) potentiates the effect of HDM201 on the proliferation of functional TP53 NALM-6 cell lines in a concentration dependent manner. (A) Mutant TP53(-/-) (n=3) (B) monoallelic TP53(-/+) (n=4) (C) wild type TP53(+/+) (n=4). The growth inhibition was measured by XTT assay for isogenic TP53 NALM-6 cell line treated with different concentrations of RG7388 in combined with or without GSK2830371 (2.5μM) for 72 hours. Each line shows an independent repeat of experiment (n=4) averaged within itself. All % of growth was normalized to DMSO treatment for individual experiment. Bars show the mean ± SEM.

3.3.5 The WIP1 inhibitor GSK2830371 potentiates the p53-dependent anti-proliferative effect of MDM2 inhibitors (RG7388/HDM201)

This section summarizes and compares the effect of the GSK2830371 WIP1 inhibitor when combined with either RG7388 or HDM201 for both monoallelic *TP53* (-/+) and wild type (+/+) NALM-6 cells (Figure 3.5). Each point in the plot shows the GI_{50} for 50% inhibition of cell proliferation, as measured by XTT assay, following 72 hours exposure to the corresponding agent, for each individual experiment.

For monoallelic *TP53* NALM-6(-/+) cells (Figure 3.5 A), combination with the WIP1 inhibitor significantly potentiated the anti-proliferative effect of both RG7388 and HDM201 (p=0.014) and (p=0.007). The average GI_{50} of RG7388 was 0.031μM ±0.008 and of HDM201 was 0.119μM ±0.02 for the response of the p53 monoallelic NALM-6 (-/+) cells (Table 3.1). Furthermore, the combination treatment of WIP1 inhibitor (2.5μM) with either RG7388 or HDM201 significantly reduced the GI_{50} values of the MDM2 inhibitors, to 0.012μM ±0.0006 and 0.016μM ±0.002, respectively (p>0.05) (Table 3.1).

For wild type *TP53* NALM-6(+/+) cells (Figure 3.5 B), the average GI_{50} of RG7388 was 0.042μM ±0.006 and for HDM201 was 0.114μM ±0.019 (Table 3.2). Additionally, the combination treatment of WIP1 (2.5μM) with either RG7388 or HDM201 significantly potentiated the effect of the MDM2 inhibitors, GI_{50} values reduced to 0.013μM ±0.0008 and FF0.015μM ±0.0016, respectively (p>0.005) (Table 3.1 and Table 3.2).

Considering both plots in (Figure 3.5), it can be concluded that one functional p53 allele is sufficient for MDM2 inhibitors to stabilise the activity of p53 and inhibit the cell growth activity. Interestingly, there was a significant difference in response to the two MDM2 inhibitors (RG7388 and HDM201) whether on monoallelic *TP53* NALM-6(-/+) or wild type p53 cells. Monoallelic *TP53* NALM-6(-/+) cells were significantly sensitive to RG7388 than HDM201 (p=0.0014). Moreover, wild type *TP53* NALM-6(+/+) cells were significantly sensitive to RG7388 than HDM201 (p=0.003). In addition, the combination of WIP1 inhibitor (2.5μM) has more significant potentiation effect of the MDM2 inhibitors (RG7388 and HDM201) on both monoallelic *TP53*(-/+) and wild type *TP53*(+/+) NALM-6 cells.

Looking to the fold change differences in response to MDM2 inhibitors in the presence and absence of WIP1 inhibitors, there was differences in the average fold change of both RG7388 and HDM201 with or without WIP1 inhibitor combination in response to either monoallelic *TP53*(-/+) or wild type *TP53*(+/+) NALM-6 cells. In monoallelic *TP53* NALM-6(-/+) cells, the average fold change differences between the RG7388 ± WIP1 inhibitor was 0.024 and

between the HDM201 ± WIP1 inhibitor was 0.011. There was a factor of 2-fold change in the combination response of WIP1 inhibitor with RG7388 than HMD201 (Table 3.1). In contrast, wild type *TP53* NALM-6(+/+) cells, the average fold change differences between the RG7388 ± WIP1i was 0.035 and between the HDM201 ± WIP1i was 0.013 which showed a factor of 4-fold change in the combination response of WIP1 inhibitor with RG7388 than HMD201 (Table 3.2).

Figure 3.6, comparing between the efficacy of MDM2 inhibitors (RG7388 and HDM201) either on monoallelic *TP53*(-/+) or wild type *TP53*(+/+) NALM-6 cells. MDM2 inhibitors (RG7388 and HDM201) as a single agent had no significant GI_{50} inhibition differences in response neither on monoallelic *TP53*(-/+) nor wild type *TP53*(+/+) NALM-6 cells (Figure 3.6 A&C). On the other hand, the combination of RG7388 with GSK2830371 significantly inhibited the growth activity of monoallelic *TP53*(-/+) compared to wild type *TP53*(+/+) NALM-6 cells. Monoallelic *TP53*(-/+) NALM-6 cells become significantly sensitive to the combination treatment of RG7388 with GSK2830371 compared to wild type *TP53*(+/+) NALM-6 cells (Figure 3.6 B). However, the combination of HDM201 with GSK2830371 had no significant difference in the GI_{50} inhibition effect on neither monoallelic *TP53*(-/+) nor wild type *TP53*(+/+) NALM-6 cells (Figure 3.6 C).

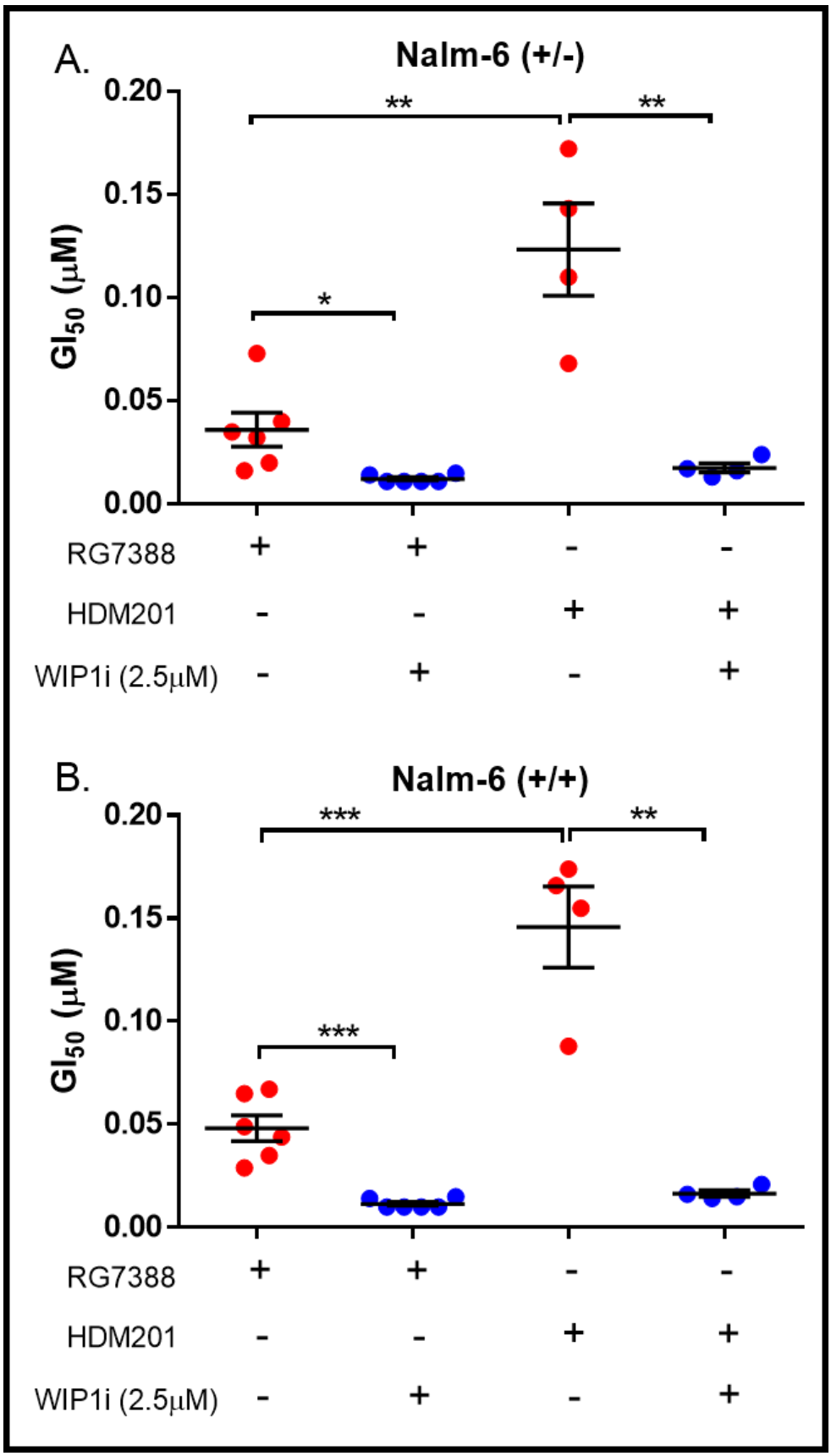

Figure 3.5 Summary of GI_{50} values for each individual experiment for p53 functional NALM-6 cell lines treated with MDM2 and WIP1 inhibitors. (A) heterozygous TP53(-/+) (B) wild type TP53(+/+). XTT assay determined the GI_{50} of RG7388 (n=6) and HDM201(n=4) in combination with or without GSK2830371 (2.5μM) for 72hrs. The response for MDM2 inhibitor (RG7388/HDM201) alone and in combination with WIP1i are shown in red and blue colours respectively. Each dot shows an independent repeat. Bars show the mean ± SEM. Statistical significance is identified by one tail paired t-test. (**, p <0.005; ***, p <0.0005).

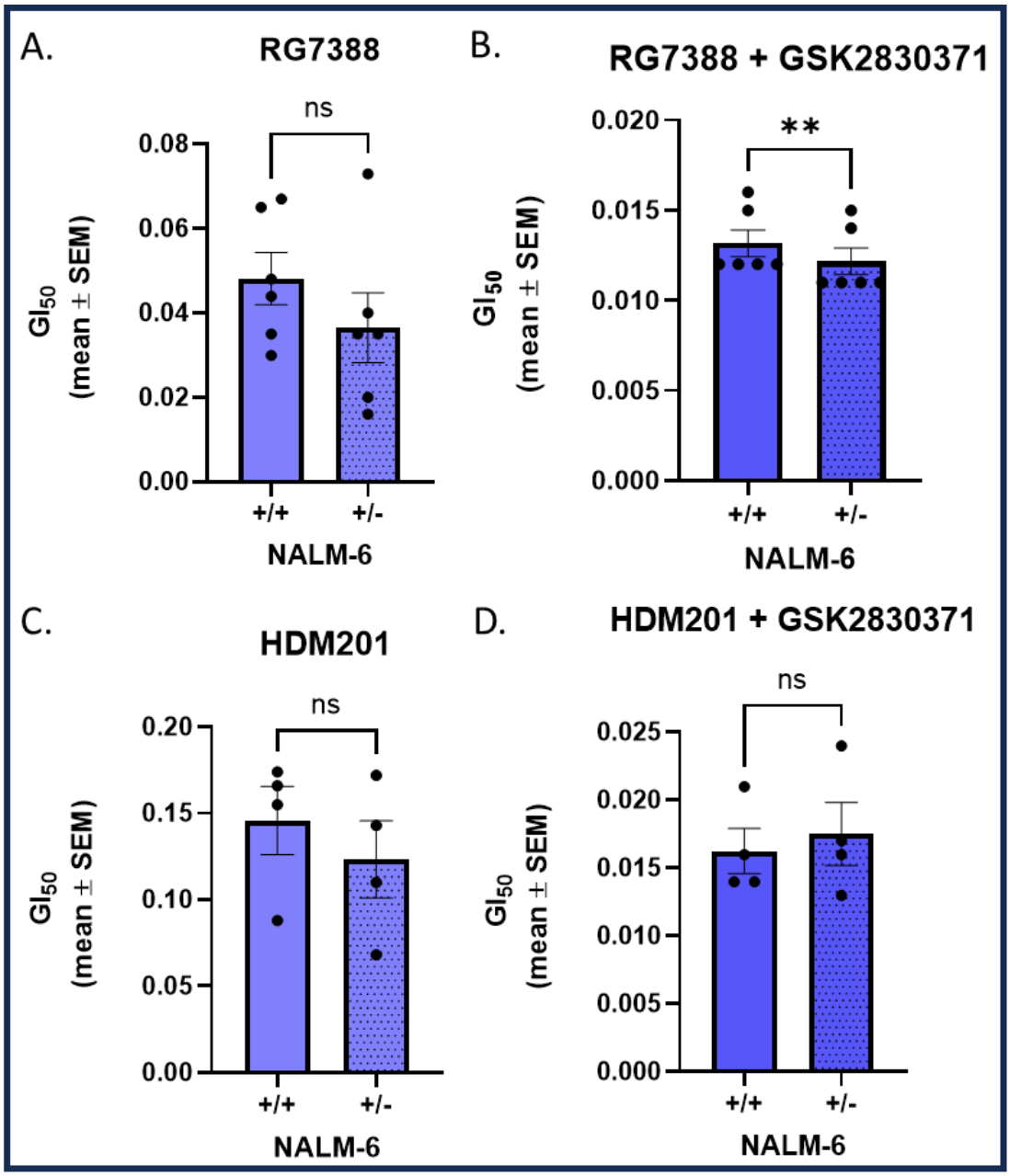

Figure 3.6 Comparison between heterozygous and wild type TP53 NALM-6 cells in response to MDM2 and WIP1 inhibitor. Heterozygous TP53(-/+) and wild type TP53(+/+) NALM-6 cells treated with wide ranges of RG7388 and HDM201 alone and in combination with GSK2830371 for 72hrs. XTT assay determined the GI_{50} in response to the treatment, RG7388 (n=6) and HDM201(n=4) in combination with GSK2830371. Each dot represents an independent experiment. Bars show the mean ± SEM. Statistical significance is identified by one tail paired t-test. (**, p <0.005; ***, p <0.0005).

GI_{50} (µM)	NALM-6 (-/+)					
	RG7388	RG7388+ WIP1i	Fold changes	HDM201	HDM201 +WIP1i	Fold changes
1st	0.016	0.011	0.691	0.143	0.024	0.167
2nd	0.020	0.011	0.565	0.110	0.017	0.156
3rd	0.040	0.011	0.281	0.172	0.016	0.093
4th	0.035	0.011	0.316	0.068	0.013	0.192
5th	0.035	0.015	0.426	-	-	-
6th	0.073	0.014	0.191	-	-	-
Average	**0.031 (±0.008)**	**0.012 (±0.0006)**	**0.389 (±0.081)**	**0.119 (±0.02)**	**0.016 (±0.002)**	**0.136 (±0.102)**
p-value	**0.014**			**0.007**		

Table 3.1 The GI_{50} of MDM2 inhibitor (RG7388/HDM201) as a single agent and in combination with WIP1 inhibitor (2.5µM) on heterozygous TP53(-/+) NALM-6 cells. The fold changes represent the ratio of GI_{50} inhibition values for RG7388/HDM201 ± WIP1i. The GI_{50} values represent the average independent repeats ±SEM. One tail t-test determine the p-value.

GI_{50} (µM)	NALM-6 (+/+)					
	RG7388	RG7388 +WIP1i	Fold changes	HDM201	HDM201 +WIP1i	Fold changes
1st	0.044	0.012	0.272	0.166	0.016	0.097
2nd	0.048	0.012	0.250	0.174	0.021	0.119
3rd	0.035	0.012	0.355	0.155	0.014	0.090
4th	0.030	0.012	0.380	0.088	0.014	0.155
5th	0.065	0.015	0.239	-	-	-
6th	0.067	0.016	0.240	-	-	-
Average	**0.042 (±0.006)**	**0.013 (±0.0008)**	**0.311 (±0.131)**	**0.144 (±0.019)**	**0.015 (±0.002)**	**0.108 (±0.084)**
p-value	**0.0006**			**0.003**		

Table 3.2 The GI_{50} of MDM2 inhibitors (RG7388/HDM201) as a single agent and in combination with WIP1 inhibitor (2.5µM) on the wild type TP53 NALM-6(+/+) cells. The fold changes represent the ratio of GI_{50} inhibition values for RG7388/HDM201 ± WIP1i. The GI_{50} values shown represent the mean of independent repeats ±SEM. One tail t-test determine the p-value.

3.3.6 Diffuse large B-cell lymphoma OCI-Ly3 cells were more sensitive to HDM201 in the presence of the GSK2830371 WIP1 inhibitor

OCI-Ly3 was included as another example of haematological B-cell linage to investigate the effect of the HDM201 and WIP1 (2.5μM) inhibitors (Figure 3.7). The OCI-Ly3 cells were treated with a range of HDM201 concentrations as a single agent and in a combination with WIP1 (2.5μM) inhibitors in three consecutive individual experiments. Following 72 hours treatment, the effects on cell growth were measured by XTT assay.

(Figure 3.6 A) HDM201 as a single agent inhibits the OCI-Ly3 growth activity in a concentration dependent inhibition manner. The combination of WIP1 inhibitor with HDM201 induces the inhibition effect of the OCI-Ly3 growth activity in a concentration dependent inhibition manner. The combination of HDM201 with the WIP1 inhibitor, gives a HDM201 GI_{50} of 0.242μM ±0.02 in the presence of WIP1 inhibitor compared to HDM201 alone which was 1.47μM ±0.06 (Figure 3.7) (Table 3.3). The graph shows the difference in OCI-Ly3 cells inhibition in response to HDM201 and in a combination with the WIP1 inhibitor. It can be seen that WIP1 inhibitor alone does not have much inhibition of cell growth activity. However, there is a concentration-dependent decrease of OCI-Ly3 growth with HDM201. Furthermore, the combination of WIP1 inhibitor potentiates the effect of HDM201. The GI_{50} summary plots represents the concentration that inhibits 50% of OCI-Ly3 growth activity and shows that the WIP1 inhibitor with HDM201 significantly inhibited the growth activity of OCI-Ly3 ($p<0.005$). The OCI-Ly3 cells become significantly more sensitive to MDM2 inhibitor (HDM201) in the presence of the WIP1 inhibitor (Figure 3.6 B).

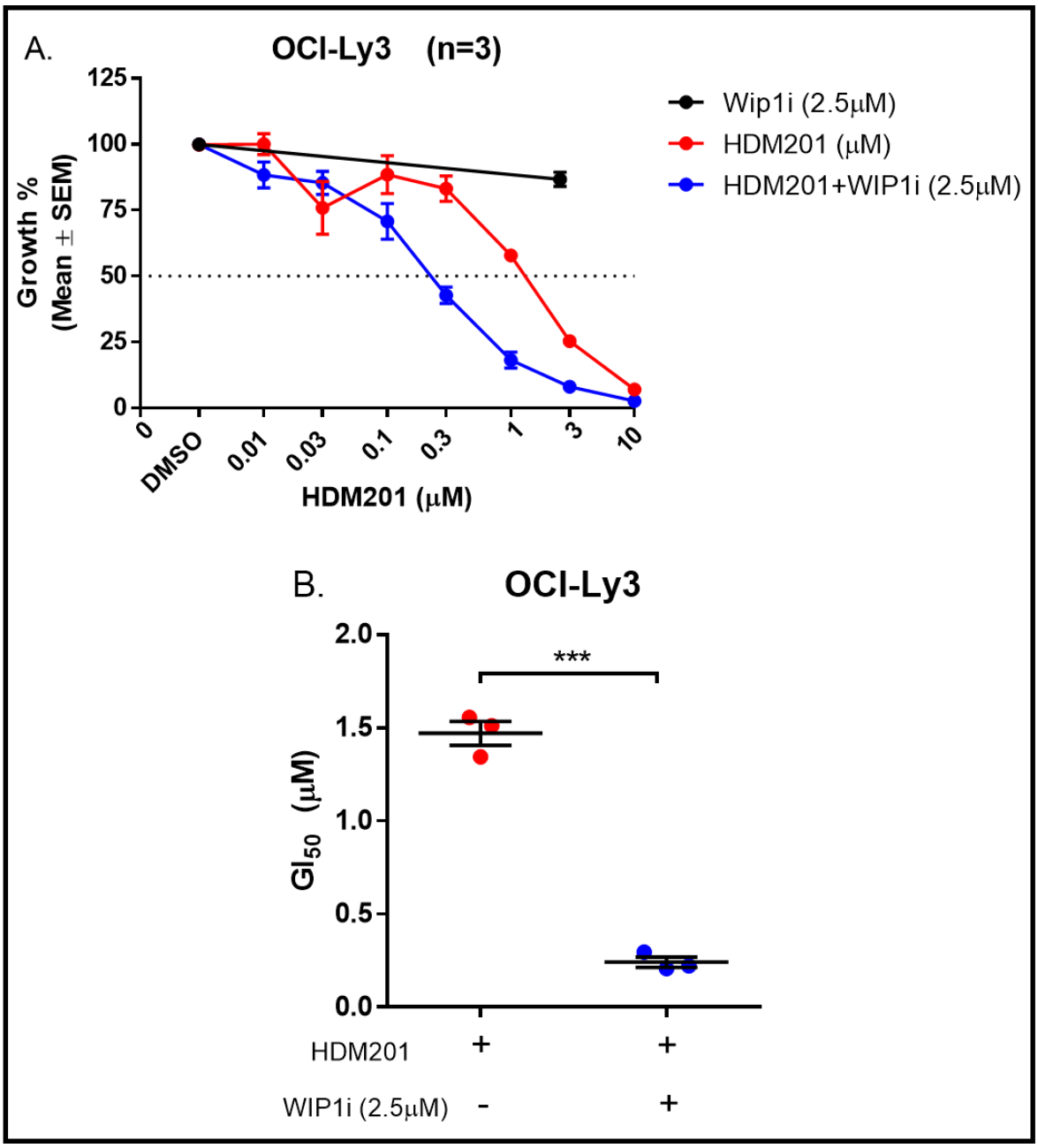

Figure 3.7 The inhibition effect of HDM201 alone and in combination with GSK2830371 on the proliferation of the OCI-Ly3 cell line. (A) The growth inhibition measured by XTT assay for OCI-Ly3 cell line treated with different concentrations of HDM201 combined with or without WIP1i (2.5μM) for 72hrs. Each line shows an independent repeat of experiment (n=3) was averaged within itself. All % of growth was normalized to DMSO treatment for individual experiment and the error bars show the mean ±SEM of each concentration. (B) Summary of GI_{50} values for HDM201 with or without WIP1i of independent repeats (n=3). The error bar represents the overall mean ±SEM for the independent experiments. There was a significant difference between the mean values for HDM201 treatment with or without WIP1i (one tailed paired t-test p=0.007).

GI_{50} (µM)	OCI-Ly3		
	HDM201	HDM201+ WIP1i	Fold changes
1st	1.556	0.296	0.190
2nd	1.344	0.208	0.155
3rd	1.511	0.222	0.147
Average	**1.470 (±0.06)**	**0.242 (±0.02)**	**0.165 (±0.43)**
p-value	**0.0007**		

Table 3.3 The GI_{50} of HDM201 as a single agent and in combination with WIP1 inhibitor (2.5µM) on OCI-Ly3 cells. The fold changes represent the ratio of GI_{50} inhibition values for HDM201 ± WIP1i.

3.3.7 Synergy Finder matrix combination studies for MDM2 and WIP1 inhibitors

To extend the studies on the combination, matrix experiments were performed on a wide range of MDM2 (RG7388) and WIP1 inhibitor concentrations to determine whether there was any dose dependent synergistic effect of the combination treatment on the isogenic p53 NALM-6 cells, mutant, heterozygous and wild type. Following 72 hours of treatment, the percentage inhibition of the cell culture proliferation was assessed using the XTT assay. The percentage inhibition results were averaged and normalized to the DMSO vehicle control. The experiment was repeated on three different consecutive cell passages, with intra-experimental triplicates for each single agent and combination concentrations. The WIP1 inhibitor concentrations used were 100, 300, 1000, 3000 and 10.000nM, and for RG7388 they were 10, 30, 100, 300, 1000, 3000 and 10.000nM. The graphs and the ZIP (Zero Interaction Potential) synergy scores were generated using the synergyfinder.org online analysis tool. (Figure 3.8) shows the effect of the WIP1 and RG7388 inhibitor concentrations on the *TP53* double knockout NALM-6(-/-) cells. Both MDM2 and WIP1 inhibitors as a single agent had very little inhibitory effect on the cell proliferation. The squares in the heat map diagram are designed to illustrate the percentage inhibition effect for the various concentration

combination treatments. There was some inhibition of cell growth activity at high concentrations. In general, the results were consistent with the anticipated lack of effect with non-functional p53 NALM-6(-/-) cells. The mean inhibition effect of RG7388 and WIP1 inhibitor treatment across the concentration range was 4.89% (p=1.33e-14). (Figure 3.8 B) The heat map and the 3-D plots represent the ZIP synergy scores of the combination treatment, for which the average was -2.74 (p=4.71e-02), indicating a small degree of antagonism, mainly driven by the high dose effects.

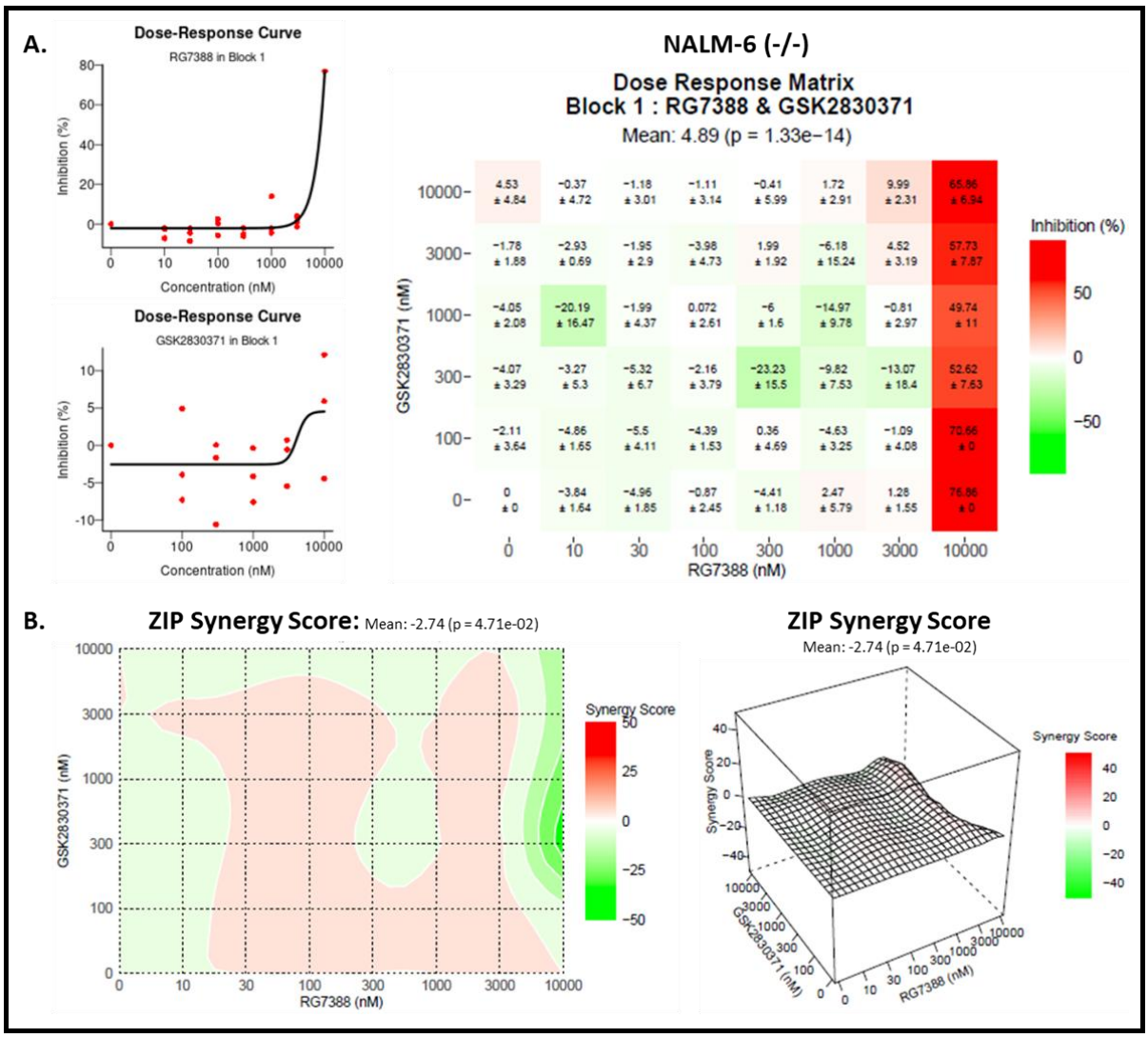

Figure 3.8 The synergistic effect of RG7388 in combination with the WIP1 inhibitor on the NALM-6(-/-) cell line. The Matrix experiment designed to find the synergistic effect and the optimum highest concentration to obtain the greatest combination effect. The NALM-6(-/-) cell line, with mutant background on both p53 alleles, was treated with RG7388 and the WIP1 inhibitor for 72 hours. After the treatment incubation, the XTT assay was used to determine the cell viability. (A) The scatter plot graph shows the response of RG7388 and WIP1 inhibitors as a single agent treatment (n=3). The matrix plot shows % inhibition of cell viability in response to the treatment ±SEM of three independent repeats. (B) The Zero Interaction Potency (ZIP) score with heat map and 3-D plot. The red colour shows the inhibition effect while the green colour shows the antagonism effect. The experiment was performed on independent consecutive cell passages with average ± SEM and the data was analysed through the Synergyfinder.org website.

3.3.8 One functional allele of TP53 is sufficient for the inhibition of cell growth, and positive peak synergy scores at low doses, in response to MDM2 (RG7388) and WIP1 inhibitors

(Figure 3.9) shows matrix experiment result of monoallelic *TP53* NALM-6(-/+) cells, using a wide range of MDM2 (RG7388) and WIP1 inhibitor concentrations to determine the synergetic effect of the combination treatment.

Treatment with RG7388 on its own showed a concentration-dependent inhibition of the cell proliferation, with a GI_{50} value of 46nM in comparison to the WIP1 inhibitor which showed a much higher GI_{50} value of >10μM (Figure 3.9 A). The mean inhibition effect of the concentration response matrix on the monoallelic *TP53*(-/+) NALM-6 cells was 80.72 ($p<2e-234$) (Figure 3.9 B). The heat map model and the 3-D plots show the ZIP synergy score distribution of the combination treatments for which the average value was 6.57 (p=3.70e-04). The area with intensive red colour indicates the highest synergy score concentration combination, while the area with lighter colour indicates a lower synergy score. Green regions indicate additive to inhibitory combination concentrations. The peak ZIP synergy score occurred within 10-30nM of RG7388 in combination with a WIP1 inhibitor concentration between 1000-3000nM. The peak ZIP synergy score was 26.48 ±1.25.

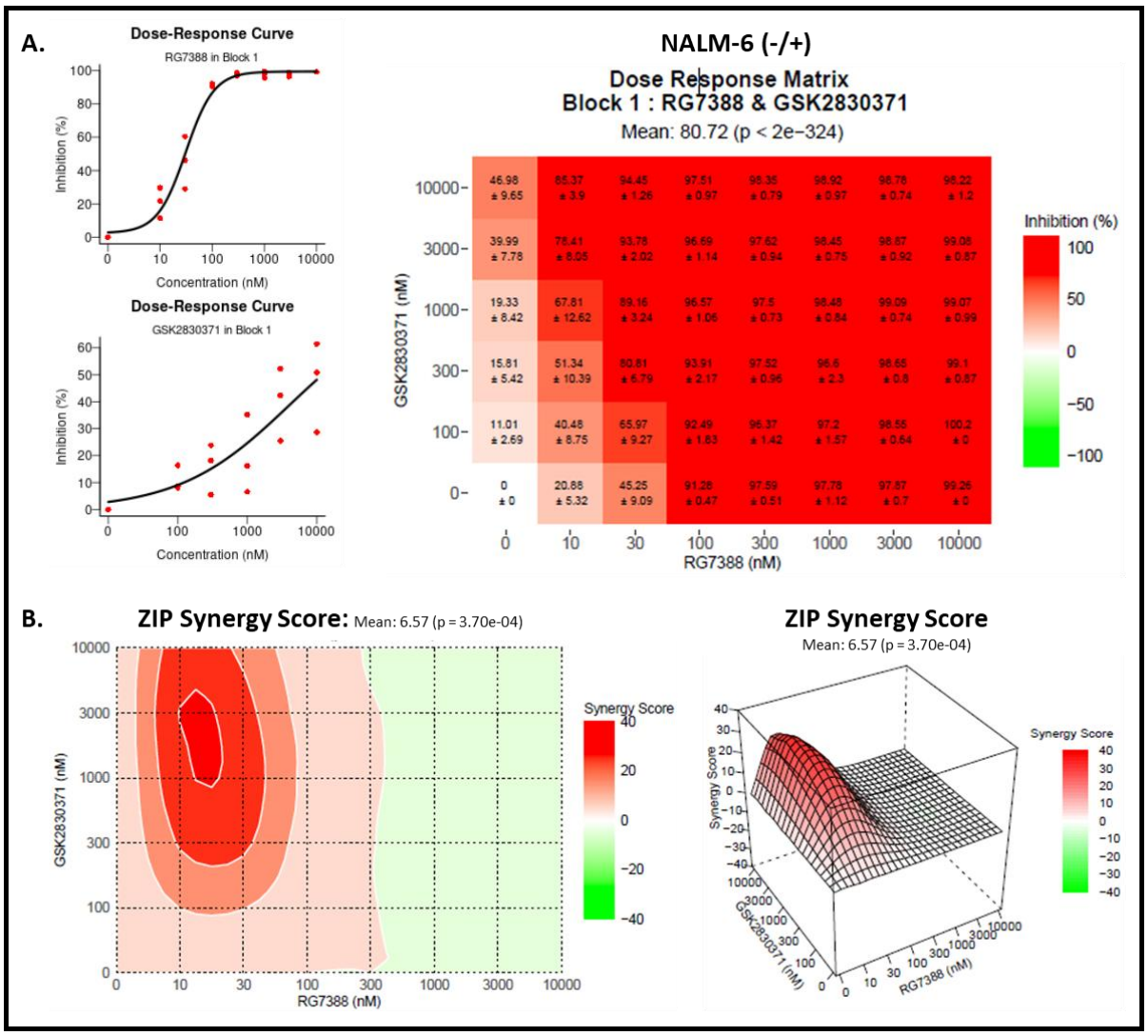

Figure 3.9 The synergy effect of WIP1 and MDM2 inhibitors for growth inhibition of the monoallelic TP53 NALM-6(-/+) cells. (A) The scatter plot shows concentration response curve of single agent, RG7388 and GSK2830371. Representative dose response matrix analysis shows % inhibition of cell growth across range of RG7388 and GSK830371alone and in combination with average ± SEM (B) The synergistic landscape showed the ZIP synergy score in response to the treatment. The dark intensive red colour represents the highest synergy. The 3-D plot shows the peak ZIP synergy score in greater interpolated detail. Matrix experiment designed to find the synergistic effect and the optimum highest concentration to obtain the greatest combination effect. Monoallelic TP53 NALM-6(-/+) cell line treated with RG7388 and the WIP1 inhibitor for 72 hours and XTT assay determined growth inhibition. ZIP synergy score was determined at each dose combination and quantified by most synergistic area score. The experiment was performed on independent consecutive cell passages (n=3) and the data was analysed through the Synergyfinder.org website.

3.3.9 The synergistic effect of the WIP1 inhibitor GSK2830371 on RG7388 is dependent upon wild type p53

The similar matrix design experiment which was described in (3.3.8) for monoallelic *TP53*(-/+) NALM-6 cells were also performed here to identify the effect of WIP1 and MDM2 inhibitors in combination on the proliferation of homozygous (biallelic) *TP53*(+/+) wild type NALM-6. In particular, to determine optimal concentration ranges for any synergistic effect of the combination treatment on the wild type *TP53*(+/+) NALM-6 cells, and to compare the results found on the monoallelic *TP53*(-/+) NALM-6 knockout cells.

The matrix result for wild type p53 NALM-6(+/+) cells (Figure 3.10 A) show that RG7388 as a single agent produced a concentration dependent inhibition of cell proliferation with a GI_{50} value of 47nM. The GSK2830371 alone produced a maximum mean percentage inhibition value of 27.86% at the highest tested concentration (10μM). For concentrations of RG7388 between (0-100nM) dose range, the combination of WIP1 inhibitor showed a concentration-dependent synergistic effect. At higher doses of RG7388 the percentage inhibition is already maximal and there is no scope for further potentiation with the WIP1 inhibitor. The mean ZIP synergy score for the combination treatment on wild type p53 NALM-6(+/+) cells was 10.11 (p=2.11e-07). The highest ZIP synergy scores occurred within the 10-30nM dose range of RG7388 in a combination with a WIP1 inhibitor concentration between 1,000-10,000nM. The mean ZIP score was 10.11, with a peak value of 33.93 ±1.74.

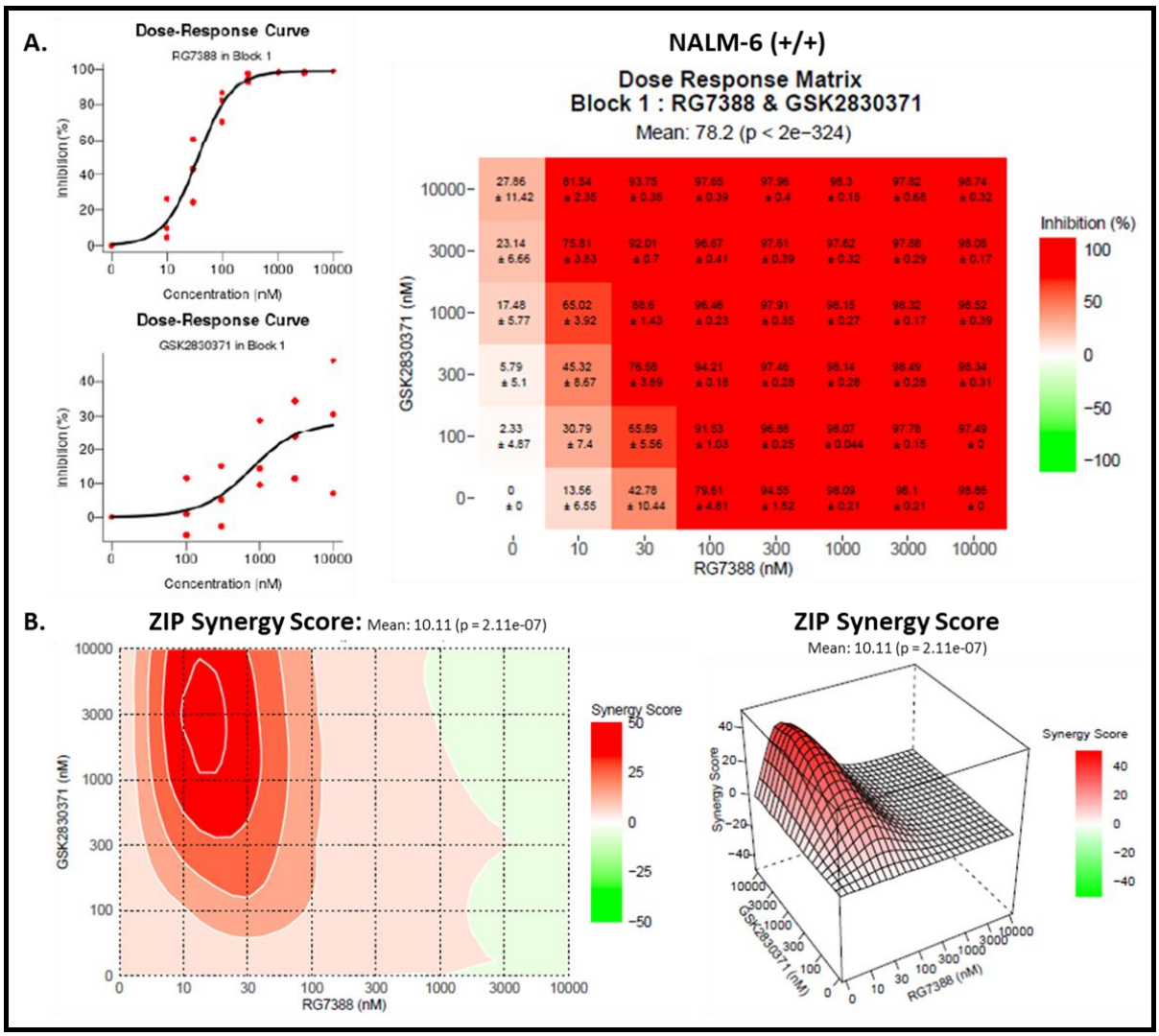

Figure 3.10 The inhibition effect of RG7388 in combination with GSK2830371 on the wild type TP53(+/+) NALM-6 cell line. A range of concentrations was used to find any synergistic combinations and to determine the highest concentration at which the greatest combination effect may occur. The cells were treated with RG7388 and the WIP1 inhibitor for 72 hours, following which cell viability reflective of cell culture proliferation was measured by XTT assay. (A)The scatter plot graph shows percentage inhibition effect of single agent treatment for RG7388 and WIP1 inhibitor (n=3). The matrix table shows the individual % inhibition effect for each combination treatment ±SEM. (B) The ZIP score on heat map and 3-D plot. The ZIP score provides a measure of the synergistic effect of combination treatment. On the heat map diagram, the intensity of the red colour represents the highest synergistic effect of the combination treatment.

The following (Figure 3.11) showed a summary of the ZIP synergy score of the isogenic NALM-6 cells in response to RG7388 in a combination with WIP1 inhibitor. The ZIP synergy score of a combination treatment in response to wild type *TP53*(+/+) NALM-6 cells was 10.11, while for the monoallelic *TP53*(-/+) NALM-6 cells was 6.57. In comparison, the double knockout *TP53*(-/-) NALM-6 cells showed a ZIP synergy score of (-2.74) in response to WIP1 inhibitor and RG7388 combination (Figure 3.11 A).

The *TP53* double knockout NALM-6(-/-) cells showed very low inhibition effect in response to the combination treatment due to missing of functional *TP53* alleles. In contrast, both the monoallelic *TP53*(-/+) and wild type *TP53* (+/+) NALM-6 cells showed smaller inhibition

(%) effect in response to the combination treatment (80.72 and 78.2%) (Figure 3.11 B). Interestingly, wild type *TP53*(+/+) NALM-6 cells showed significantly higher peak synergy score compared to both the monoallelic *TP53*(-/+) and *TP53*(-/-) double knockout NALM-6 cells (p>0.005) and (p>0.0005). Moreover, monoallelic *TP53*(-/+) NALM-6 cells showed significant high peak synergy score compared to *TP53*(-/-) double knockout NALM-6 cells (p>0.0005) (Figure 3.11 C).

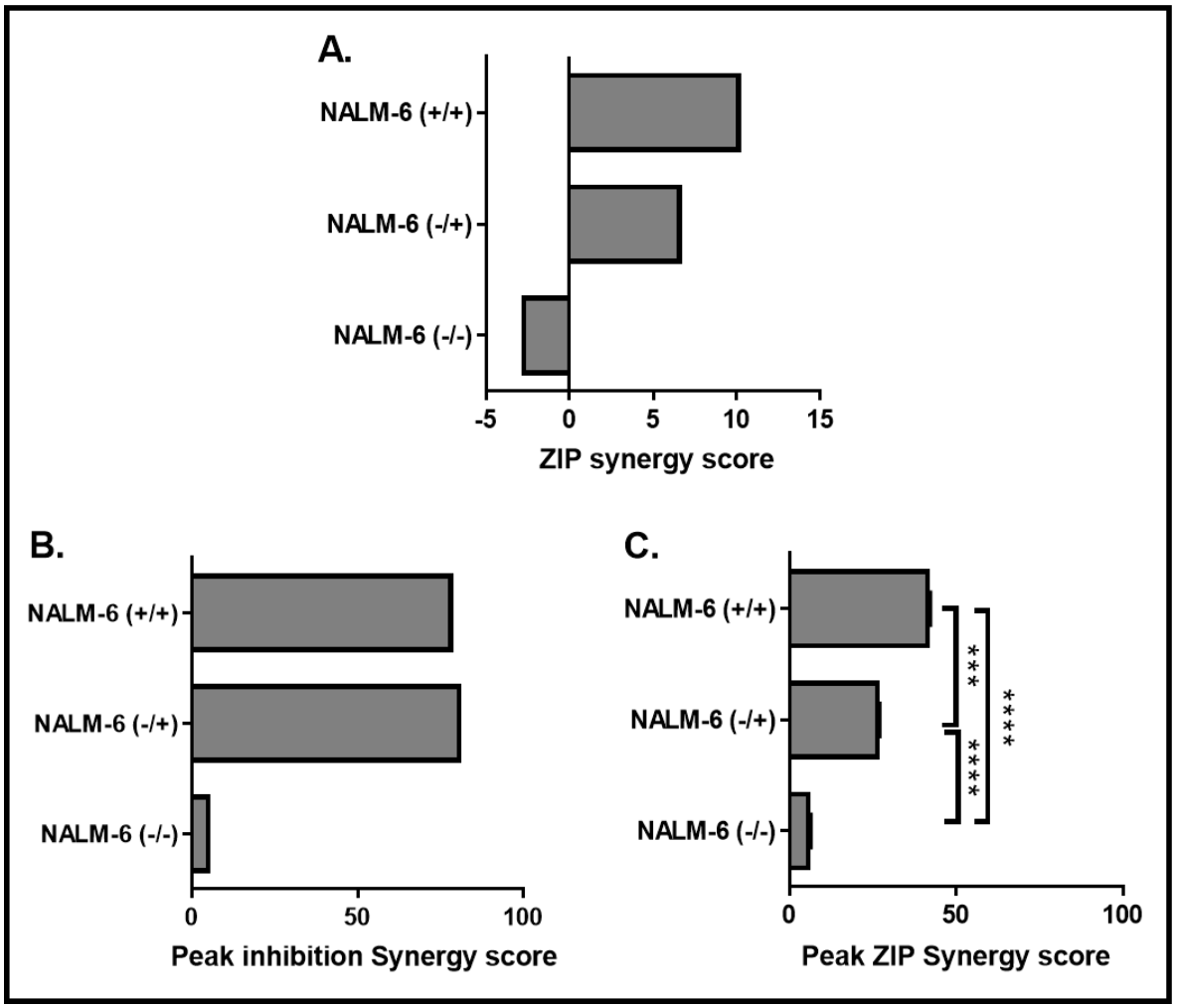

Figure 3.11 Summary plot displaying the synergy score for RG7388 in combination with WIP1 inhibitor determined by zero interaction potency (ZIP) model. The isogenic TP53 NALM-6 cells treated with wide range concentrations of GSK2830371 in combination with RG7388 for 72hr. The cell viability was determined by XTT assay. The experiment repeated on three different passage cell line (n=3)**.** (A) Average ZIP synergy score. (B) Peak inhibition synergy score. (C) Peak ZIP synergy scores**.** The error bar represents the ±SEM of repeated independent experiments. The ZIP score analysed using Synergyfinder.com.

3.3.10 GSK2830371 WIP1 inhibitor increases the stabilisation effect of RG7388 on p53 in both monoallelic TP53 (+/-) knockout and wild type TP53 (+/+) bi-allelic NALM-6 cells

Western immunoblots were performed to determine the changes in the levels of p53 and expression of specific p53 transcriptional target proteins in both the monoallelic *TP53*$^{(-/+)}$ NALM-6 and *TP53*$^{(+/+)}$ biallelic parental cells after treatment with MDM2 and WIP1 inhibitors. The cells were exposed to different concentrations of RG7388 (0.1 and 0.5μM) with and without 2.5μM WIP1 inhibitor for two different time points, 6 and 24 hours. The densitometry analysis represents the change in the protein in response to the treatment relative to DMSO for 6 and 24 hours (Figure 3.11 B&C).

In (Figure 3.12), western blotting showed a concentration-dependent increase in the total p53 protein level and its transcriptional targets, WIP1, MDM2 and p21, in response to RG7388 relative to DMSO for both 6 and 24 hours. Moreover, loss of WIP1 protein with GSK2830371 (2.5μM). In addition, combination with WIP1 inhibitor increased the expression of p53, MDM2 and p21 following 6 hours treatment compared to treatment with RG7388 (0.1μM) alone. In contrast, total p53 protein level and its transcriptional targets did not show much change with combination of WIP1 inhibitor and RG7388 (0.5μM). The WIP inhibitor at (2.5μM) has a dual action of both induces the degradation of WIP1 protein and inhibits its phosphatase activity. The combination treatment shows evidence of p53 stabilisation and increase in the level of the p53 transcriptional target gene proteins, p21 and MDM2, at 6 and 24 hours. The densitometry analysis showed concertation dependent increase in p53 and MDM2 in response to RG7388 alone and in combination of WIP1 inhibitor at 6 and 24 hours (Figure 3.12 B&C).

The phosphorylation activity of p53 is not detected with either RG7388 treatment alone or in combination with WIP1 inhibitor relative to the DMSO at 6 and 24 hours (Figure 3.12 B&C). However, at 24 hours treatment, the appearance of cleaved PARP (cPARP) indicates that the cells are undergoing apoptosis. Interestingly, the cPARP signal relative to full-length PARP is stronger following combination treatment with (0.5μM) RG7388 and (2.5μM) GSK2830371 compared with the effect of (0.5μM) RG7388 alone, showing potentiation of RG7388 induced cytotoxicity by the WIP1 inhibitor.

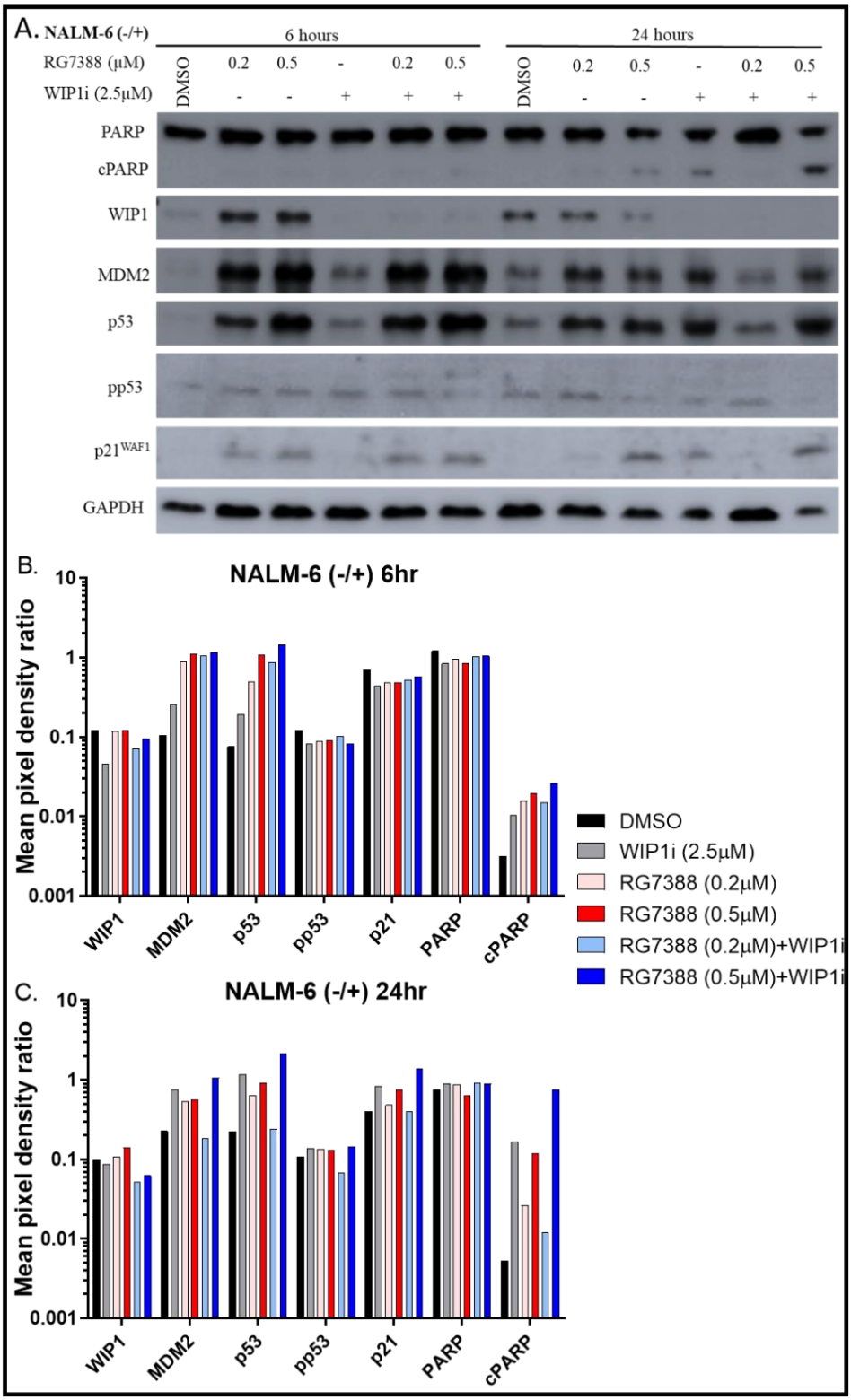

Figure 3.12 Western immunoblots of heterozygous TP53(-/+) NALM-6 cells treated with MDM2 and WIP1 inhibitors for 6 and 24 hours. Heterozygous TP53(+/+) NALM-6 cells treated with RG7388 (0.2, 0.5μM) alone and in combination with GSK2830371 (2.5μM). (A) RG7388 stabilises the activity of p53 target protein and the combination of GSK2830371 showed further stabilisation. GAPDH was used as the loading control. Doses of RG7388 represent 5× and 10× the GI_{50} concentrations. All strips were from the same membrane which was cut into three. The top strip was probed for WIP1, MDM2 and PARP; the middle for pp53, p53 and GAPDH; and the third with p21 antibody. (B) Densitometry analysis of protein expression at 6 and (C) 24 hours. There was a concentration dependent increases in the TP53 target proteins in response to RG7388 and RG7388 with WIP1 inhibitor. The cell lysate was collected from n=1 independent experiment. The mean pixel density ratio for all proteins was background corrected and the values were normalized relative to GAPDH, except cPARP for which the ratio was calculated relative to full length PARP.

The western immunoblots of a wild type *TP53*(+/+) NALM-6 cells were performed to investigate the changes in the p53 target protein levels (Figure 3.13). The cells were treated with both WIP inhibitor at (2.5μM) and RG7388 at 0.2μM and 0.5μM. The concentrations were selected based on 5x and 10x including the GI_{50} value of single and combination effect for 6 and 24 hours. Densitometry analysis represents the change in the protein in response to the treatment relative to DMSO for 6 and 24 hours (Figure 3.13 B&C).

The western blot showed that RG7388 stabilises the activity of p53 protein and its targets including WIP1, MDM2 and p21 in a concentration dependent induction manner with an increase in treatment response at 6 and 24 hours. Moreover, phosphorylation activity of p53 is induced with the increases in response to the treatment.

In the combination treatment, the additional of the WIP1 inhibitor (2.5μM) potentiated the stability of the total p53 protein which also increase the expression of its target proteins such as MDM2 and p21, compared to the treatment with RG7388 treatment alone. Furthermore, (2.5μM) of WIP1 inhibitor was sufficient to degrade the WIP1protein synthesis expression and induces the activity of RG7388. The densitometry analysis showed concentration dependent increase in MDM2, p53, Pp53 and p21 protein levels in response to RG7388 alone and further with combination of WIP1 inhibitor at 6 hours (Figure 3.13 B). Total p53 was increased with RG7388 and WIP1 inhibitor combination treatment at 24 hours (Figure 3.13 C).

Phosphorylated p53 was induced with a combination of WIP1 inhibitor with RG7388 in a concentration dependent manner at 6 hours but could not be detected at 24 hours. Moreover, total PARP was detected at 6 hours with no expression of cPARP in response to the treatment. However, by 24 hours treatment, the expression of total PARP expression was decreased and the cPARP was induced which indicates the cells are undergoing apoptosis. Interestingly, the cPARP signal relative to full-length PARP is stronger following combination treatment with RG7388 (0.5μM) and GSK2830371 (2.5μM) compared with the effect of RG7388 (0.5μM) alone, showing potentiation of RG7388 induced cytotoxicity by the WIP1 inhibitor.

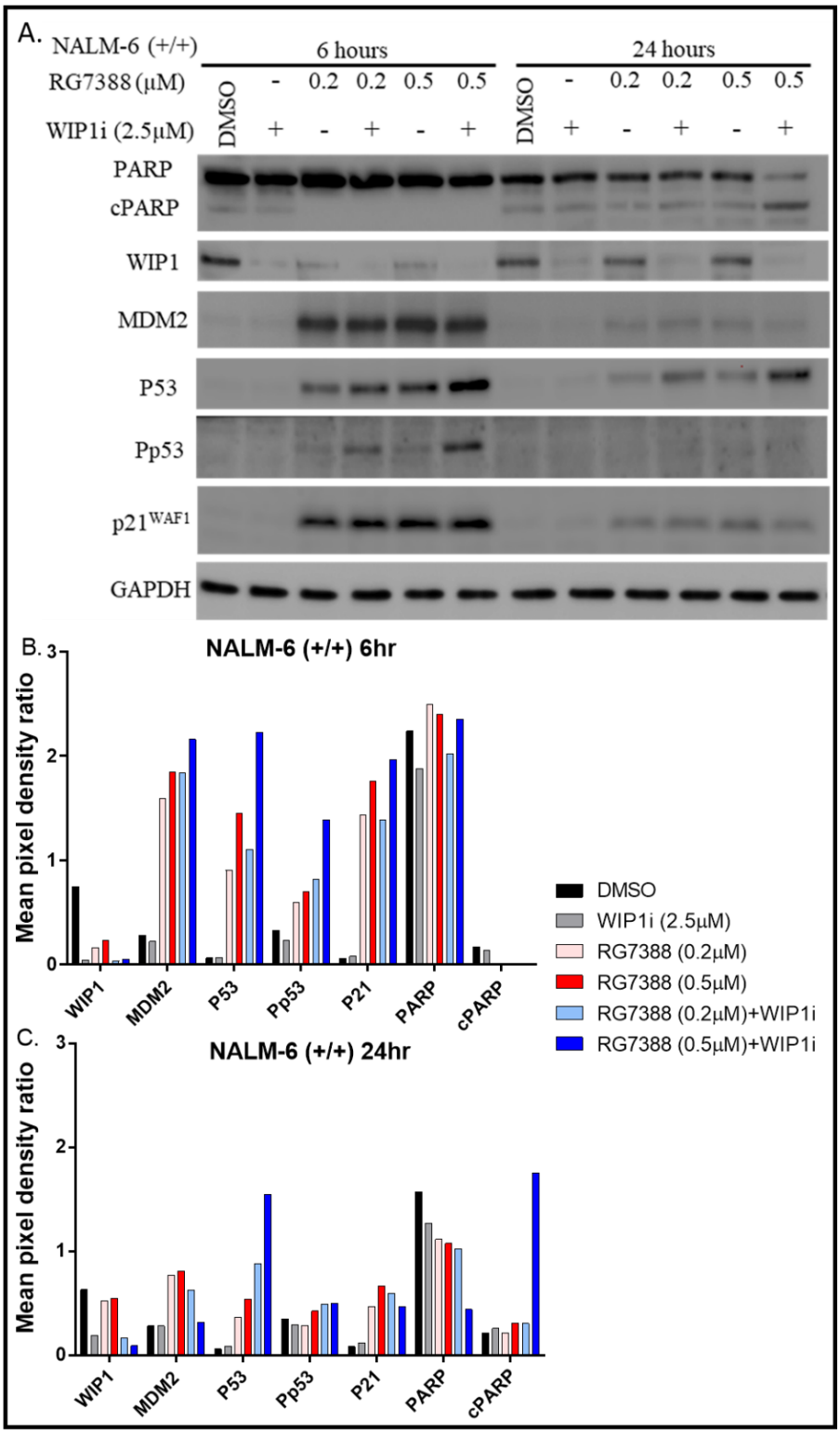

Figure 3.13 Western immunoblots of wild type TP53(+/+) NALM-6 cells in response to MDM2 and WIP1 inhibitors. Wild type TP53(+/+) NALM-6 cells treated withRG7388 (0.2, 0.5μM) alone and in combination with GSK2830371 (2.5μM) for 6 and 24 hours. (A) RG7388 stabilises the activity of p53 target protein in concentration dependent manner and the combination of WIP1 inhibitor further stabilises their activity. GAPDH was used as the loading control. Doses of RG7388 represent 5× and 10× the GI_{50} concentrations. All strips were from the same membrane which was cut into three. The top strip was probed for WIP1, MDM2 and PARP; the middle for pp53, p53 and GAPDH; and the third with p21 antibody. (B) Densitometry analysis of protein expression at 6 and (C) 24 hours. There was a concentration dependent increases in the TP53 target proteins in response to RG7388 and RG7388 with WIP1 inhibitor. Western blot and densitometry analysis performed for n=1 independent experiment. The mean pixel density ratio for all proteins was background corrected and the values were normalized relative to GAPDH, except cPARP for which the ratio was calculated relative to full length PARP.

3.3.11 The combination of WIP1 inhibitor with RG7388 increased the transcription of p53 target genes

To further investigate the mechanism and transcriptional consequences of increased p53 stabilisation and phosphorylation due to WIP1 phosphatase inhibition, quantitative reverse transcriptase PCR (qRT-PCR) was used to measure mRNA changes in the expression of the *TP53* target genes. A selected panel of gene transcripts was tested to identify the effect of MDM2 and WIP1 inhibitors on wild type *TP53*$^{(+/+)}$ NALM-6 cells after 6 hours of treatment. The wild type *TP53* cells were treated with WIP1 inhibitor at 2.5μM in combination with RG7388 at (0.2μM) and (0.4μM). The fold change in gene expression was calculated by normalization to DMSO and Actin. The set of genes in the panel was categorized based on their functions into TP53 negative regulator feedback (*PPM1D*, *MDM2*, *TP53*, *TP53INP1*), cell cycle arrest (*CDKN1A*), pro-apoptotic (*PUMA*, *NOXA*, *BAX*) and anti-apoptotic (*MCL1*, *BCL2*) genes.

The mRNA expression of *TP53* target genes, *PPM1D*, *MDM2*, *TP53*, *TP53INP* and *CDKN1A*, was increased with RG7388 treatment as a single agent in a concentration dependent manner (Figure 3.14 B-C). Moreover, the combination treatment of WIP1 inhibitor (2.5μM) with RG7388 also showed an induction in the fold change expression of TP53 target genes with a concentration dependent increase in response to RG7388 (0.2μM). In contrast, the expression of *TP53* target genes, *MDM2*, *TP53*, *TP53INP1* and *CDKN1A* are reduced in response to WIP1 inhibitor in combination with RG7388 (0.4μM) relative to RG7388 (0.4μM) alone. Moreover, the RQ value at the higher concentration of RG7388 (0.4μM) is reduced by the WIP1 inhibition.

Interestingly, the mRNA expression of the *PPM1D* gene was reduced in the presence of the WIP1 inhibitor (2.5μM) for both single and combination treatment with RG7388 (Figure 3.14 B). In contrast, the presence of WIP1 inhibitor (2.5μM) significantly increased the mRNA expression of the other p53 target genes (*PPM1D*, *MDM2*, *TP53*, *TP53INP* and *CDKN1A*) compared to (0.2μM) RG7388 treatment alone (Figure 3.14 B&C). However, the combination treatment of WIP1 inhibitor (2.5μM) with at the higher dose of RG7388 (0.4μM) slightly reduced the mRNA expression of *MDM2*, *TP53INP1* and *CDKN1A*.

For the pro-apoptotic genes, the *PUMA* (*BBC3*) gene showed the highest fold change in mRNA expression with RG7388 treatment, compared to *NOXA* (*PMAIP1*) and *BAX* (Figure 3.14 D). Moreover, RG7388 as a single agent treatment induced the mRNA expression of *PUMA* and *BAX* in a concentration dependent manner, but not for *NOXA*.

In addition, the combination treatment of WIP1 inhibitor (2.5μM) and RG7388 induced the fold change expression of *PUMA* and *BAX* genes in relative to DMSO. In contrast, the *NOXA* gene showed a reduction in the mRNA expression with a combination of WIP1 inhibitor and RG7388 relative to DMSO. Generally, with the doses used combination treatment with WIP1 inhibitor with RG7388 reduces the mRNA expression of pro-apoptotic genes, *PUMA*, *NOXA* and *BAX*, compared to RG7388 treatment alone.

For the anti-apoptotic genes, the *MCL1* mRNA was significantly increased with RG7388 alone and in a combination of WIP1 inhibitor with RG7388 relative to DMSO (Figure 3.14 E). The addition of WIP1 inhibitor reduced the fold change expression of RG7388 alone at (0.4μM), and there was no significant change in combination with (0.2μM) RG7388. In contrast, *BCL2* mRNA expression showed little change with either RG7388 alone or in combination with WIP1 inhibitor. However, RG7388 (0.4μM) produced a slight increase in mRNA expression and the combination of WIP1 inhibitor reduced that expression.

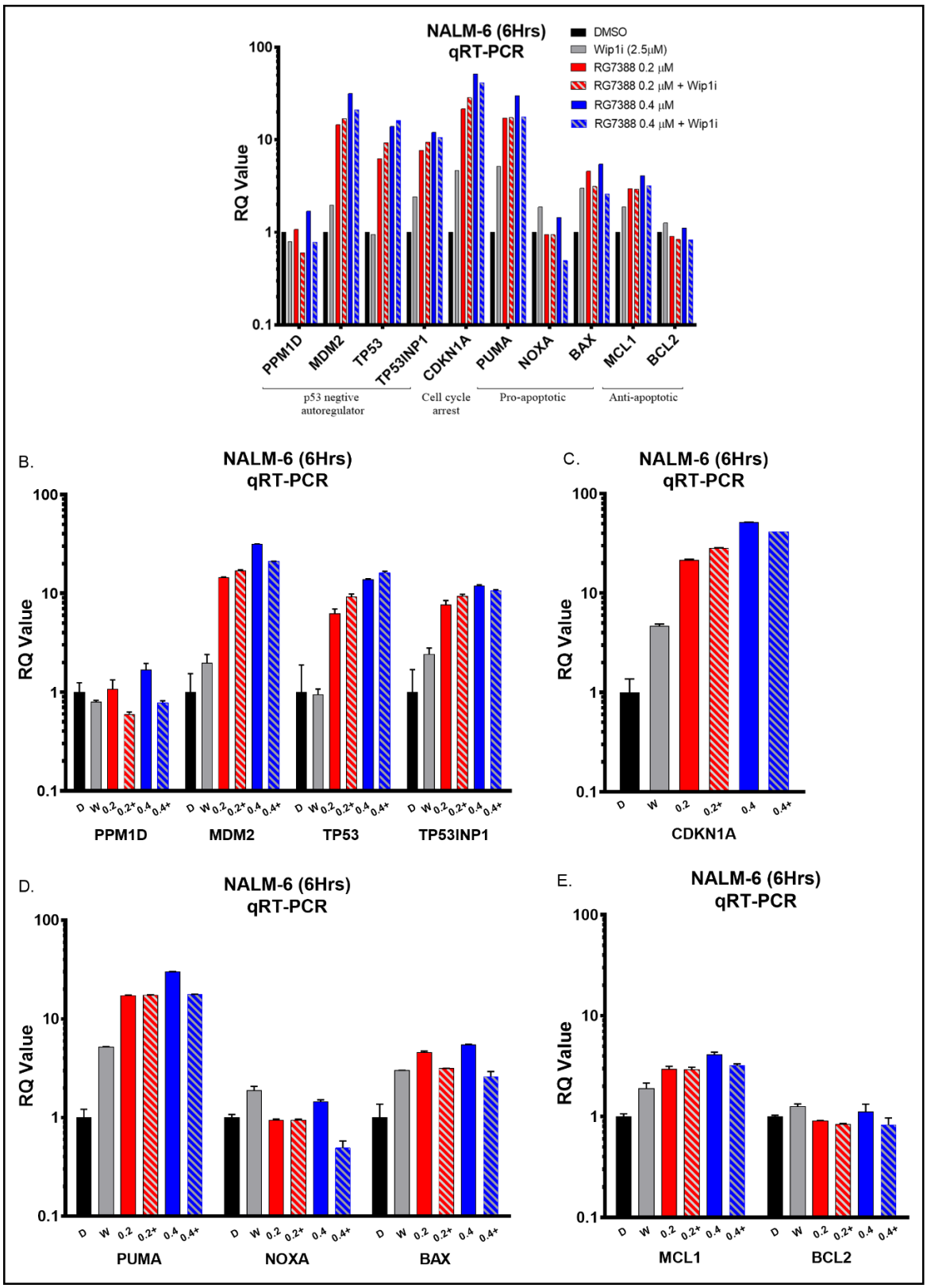

Figure 3.14 The mRNA expression of p53 transcriptional target genes of wild type TP53(+/+) by qRT-PCR. (A) Fold changes in mRNA expression of selected p53 transcriptional target genes in response to either RG7388 (0.2-0.4μM) as a single agent and in a combination with (2.5μM) WIP1i (GSK2830371) for 6 hours relative to DMSO solvent and GAPDH. (B) Fold change in mRNA expression of p53 dependent targe genes (C) pro-apoptotic (D) cell cycle arrest and (E) anti-apoptotic genes. The cell lysate was collected from (n=1) experiment. Statistical significance was determined by t-test one tail between with and without WIP1i treatments. Only the statistical significance differences for treatment with or without WIP1i are indicated above the bars (****, $p < 0.00005$). GAPDH was used as endogenous control and DMSO treated cells were used as the calibrator between three replicated intra-experimental wells, showing the error bar of ± standard error of mean (SEM). RQ values were calculated based on the formula $2^{-\Delta\Delta Ct}$.

3.4 Discussion

Considering the crucial function of p53 in preventing aberrant cell proliferation, maintaining genomic integrity and influencing the response to chemotherapy (Brown et al., 2009; Chène, 2003; Vu et al., 2013; Ding et al., 2013) this will rise an interest of using WIP1 inhibitor in a combination with MDM2 inhibitor to develop a new pharmacological strategy aimed at increasing the activity of functional p53. In this Chapter, haematological B-cell lines (NALM-6 and OCI-Ly3) were evaluated in response to MDM2 and WIP1 inhibitors. In addition, the p53-transcriptional activity, including pro-apoptotic gene expression specific to p53-targeted was identified.

The WIP1 inhibitor up to 10μM had little effect on the growth of isogenic p53 NALM-6 cells. The genetic *TP53* background of NALM-6 cells did not make any difference to the lack of response to the WIP1 inhibitor alone. The principal mechanism of the WIP1 inhibitor depends upon the increased phosphorylation and stabilisation of p53 compared with the effect of the MDM2 inhibitor alone. For initial combination experiments WIP1 inhibitor at (2.5μM) was chosen as the highest concentration that alone does not have an effect on cell growth, based on experiments here as well as has been found from our group with different cancer cell line models (Chamberlain et al., 2021; Wu et al., 2018, 2021, 2022).

Esfandiari, A. and his colleagues investigated a panel of *TP53* wild-type and mutant/null cell line pairs differing in their *PPM1D* genetic status and found them to be generally in-sensitive to growth inhibition by single agent GSK2830371. However, combination with MDM2 inhibitors (nutlin-3/RG7388) in *TP53* wild-type cell lines induce cell death by decreasing WIP1 expression leading to increased p53 Ser15 phosphorylation, which was known to increase p53 transcriptional activity (Esfandiari et al., 2016).

The treatment of $p53^{wt}$ cancer cells with MDM2 antagonists has been clearly demonstrated to disrupt the MDM2-p53 binding interaction and activate p53, leading to cell cycle arrest both *in-vitro* and *in-vivo*. Furthermore, second generation of MDM2 inhibitors such as idasanutlin (RG7388), HDM201 (siremadlin) or AMG232, reduce off-target effects and show little or no effect in p53 non-functional cells at doses which strongly inhibit the growth and proliferation of wild-type p53 cells (Ding et al., 2013; Sun et al., 2014).

Several reports indicated a lack of induction of apoptosis in multiple $p53^{wt}$ cells treated with MDM2 antagonists. Some studies also suggested that treatment of $p53^{wt}$ cells with MDM2 antagonists reduced cell apoptosis. Tovar and Paris in their study reported that nutlin-3a

strongly induced cell cycle arrest in 10 different $p53^{wt}$ cell lines at doses which, in most of these cell lines, barely induced apoptosis (Tovar et al., 2006; París et al., 2008). Similarly, Paris and Huang et al, reported that nutlin-3a induced cell cycle arrest and a senescence-like state in several cell lines, however in most of these cell lines proliferation resumed once the drug was removed (Huang et al., 2009; París et al., 2008).

The effect of MDM2 inhibitors (RG7388/HDM201) is dependent on the stabilisation of p53 proteins and the function of *TP53* transcriptional target genes. In the current study the MDM2 inhibitor as a single agent treatment showed a concentration dependent inhibition of cell growth with a concentration dependent induction of p53 activity.

Various small-molecule inhibitors of MDM2-p53 interaction, including SAR405838, MK-8242, DS-3032b, NVP-CGM097, RG7112, HDM201, RG7388, ALRN-6924 and AMG 232, are undergoing assessment at different clinical trial phases for cancer therapy (ClinicalTrials.gov). However, challenges still exist and the development of resistance to these MDM2 inhibitors has been observed after prolonged treatment. Therefore, combining MDM2 inhibitors with other agents might be effective and promising strategies against the acquired resistance (Liao et al., 2018).

The p53 protein in both monoallelic and wild type NALM-6 cells was able to be stabilised by the MDM2 inhibitor in a concentration dependent manner to increase p53 activity. There was 2-fold differences in the RG7388 response between the p53 heterozygous (mono-allelic) and wild type (bi-allelic) NALM-6 cells (Table 3.1 and Table 3.2). Furthermore, the combination of WIP1 inhibitor at (2.5µM) potentiated the concentration dependent effect of RG7388 in both p53 heterozygous and wild type NALM-6 cells. The potentiation by WIP1 inhibitor was dependent on the stabilisation effect of RG7388 on wild type p53 rather than the effect of WIP1 inhibitor by itself. The potentiation by the WIP1 inhibitor was seen in both the heterozygous and wild type p53 NALM-6 cells (Figure 3.5). Indeed, the WIP1 inhibitor showed similar potentiation of RG7388 activity in p53 wild type $TP53^{(+/+)}$ and monoallelic $TP53^{(+/-)}$ NALM-6 cells (Table 3.1 and Table 3.2). Interestingly, one functional *TP53* allele is sufficient to stabilises p53 protein activity on both wild-type $TP53^{(+/+)}$ and monoallelic $TP53^{(+/-)}$ NALM-6 cells in response to RG7388. In addition, monoallelic $TP53^{(+/-)}$ NALM-6 cells were more sensitive to the RG7388 than wild-type NAML-6 cells have two functional $TP53^{(+/+)}$ alleles (Figure 3.5).

OCI-Ly3 was also investigated as a B-cell line of lymphoid lineage. The cells were treated with 2.5µM of WIP1 inhibitor and in a combination with HDM201 (siremadlin), a second-

generation MDM2 inhibitor. OCI-Ly3 cells are wild type for *TP53*. The WIP1 inhibitor (2.5μM) as a single agent again did not have any inhibitory effect on cell growth. By contrast, HDM201 as a single agent showed a concentration dependent inhibition of the cell growth. Furthermore, combination with the WIP1 inhibitor (2.5μM) significantly potentiated the inhibition effect of HDM201 inhibitor (Figure 3.7) ($p<0.005$). Interestingly, OCI-Ly3 cells are less sensitive to the HDM201 treatment than both monoallelic $TP53^{(-/+)}$ and wild type (bi-allelic) $TP53^{(+/+)}$ NALM-6 cells. The average GI_{50} of HDM201 on OCI-Ly3 is 1.47μM ±0.06, (Figure 3.3) while on monoallelic $TP53^{(-/+)}$ is 0.11μM ±0.02 and 0.14μM ±0.01 on (bi-allelic) $TP53^{(+/+)}$ NALM-6 cells (Table 3.1 and Table 3.2).

Similar with my finding, novel potent MDM2-p53 antagonist, ASTX295, was founded to be more selective in response to panel of cell lines derived from haematological malignancies with wild type p53. It was reported that NALM-6 cells were more sensitive in response to MDM2-p53 antagonist than OCI-Ly3 cells. In addition, the OCI-Ly3 cells were the lowest sensitive cells in response to ASTX295 compared to the panel of the haematological malignancies cells which were included in the study (Willmore et al., 2020; Aptullahoglu, Wallis, et al., 2023).

In the literature, NVP-CGM097, p53-HDM2 inhibitor selective for MDM2 antagonist, was tested on a panel of 113 $p53^{wt}$ and 243 $p53^{mut}$ cell lines (Jeay et al., 2015). Interestingly, Jeay and his colleagues reported that even though, most of the $p53^{mut}$ cancer cell lines were exclusively resistant to MDM2 antagonists, however 70 out of 113 $p53^{wt}$ cells were non-responsive to the NVP-CGM097 (Jeay et al., 2015). In these insensitive cases, wild type p53 status alone was not sufficient to provide a response to MDM2 antagonists and the additional of other factors were required to modulate the p53 pathway and induce apoptosis (Jeay et al., 2015).

Suggested examples of factors which could influence response include some MDM4 regulator molecules such as exportin (XPO1) (Yoshimura et al., 2014), or nucleophosmin could block the activation of p53 in some $p53^{wt}$ cells (Colombo et al., 2002). Moreover, $p53^{wt}$ cells with low MDM2 levels are assumed to be poor targets for MDM2 antagonist therapy due to the lack of molecular targets and absence of *MDM2* gene amplification (Skalniak et al., 2018).

Interestingly, $p53^{wt}$ cell lines that express strong evidence of p53 activation through induction of p21 expression level in western blot results showed an ability of stop the cell cycle in response to idasanutlin treatment although, the degree of apoptosis was variously induced in

response to the drug. Thus, the downstream target factor molecules of p53 regulators need to be investigated in the presences of idasanutlin treatment (Skalniak et al., 2018).

Caspase 3 activation was reported to induce apoptosis of $p53^{wt}$ cell lines in response to the nutlin-3 treatment (Saha et al., 2010). However, low apoptotic induction in MCF-7 cells was attributed to lack of caspase 3 activity (Jänicke, 2009; Jänicke et al., 1998). On the other hand, both U-2 OS and SJSA-1 cells carry MDM2 gene amplifications (Drummond et al., 2016; Flørenes et al., 1994) and show high basal expression of MDM2 proteins. Both U-2 OS and SJSA-1 cells showed an increase in p53 induction in a concentration dependent manner with MDM2 antagonists idasanutlin treatment and a negative feedback loop for p53 activity (Wu et al., 1993). Although, MDM2 protein expression in both SJSA-1 and U-2 OS cells was increased in response to idasanutlin, SJSA-1 cells showed stronger and more rapid MDM2 protein induction than U-2 OS cells (Kojima et al., 2006a; Skalniak et al., 2018).

Consequently, the inability of MDM2 antagonist to induce apoptosis in some cancer cells has been suggested to allow time for them to gain additional mutations that confer resistance to the MDM2 inhibitors. Initially, this was reported in response to the first generation MDM2 antagonist, Nutlin-3a, (Michaelis et al., 2011; Aziz et al., 2011; Wei et al., 2013), and then followed later with the further generation compounds, i.e., SAR405838 (Jung et al., 2016; Gianna Hoffman-Luca et al., 2015), MI-63 (Drummond et al., 2016), and HDM201 (Chapeau et al., 2017).

Combination treatment has been explored as a strategy to obviate the potential problem of the development of resistance to MDM2 inhibitors. In the current study, matrix experiments were designed to examine whether the exposure of a wide range of WIP1 and MDM2 inhibitor concentrations identified synergistic concentration ranges. Mutant p53 NALM-6(-/-) showed very little inhibition of cell proliferation or viability up to high concentrations (10μM) of RG7388 and GSK2830371 (Figure 3.8). In contrast, both the p53 heterozygous (Figure 3.9) and wild type NALM-6 cells (Figure 3.10), which express functional *TP53* genes, showed a concentration dependent inhibition in response to RG7388 treatment. In addition, the combination of WIP1 inhibitor showed a potentiation effect of the p53 activity in a concentration dependent manner. Further to that, the combination treatment of WIP1 with MDM2 inhibitors generated a synergetic effect on functional p53 NALM-6 cells, however the bi-allelic wild type p53 NALM-6 cells showed a greater synergistic effect than the monoallelic heterozygous NALM-6 cells (Figure 3.11).

Western blot results showed stabilisation of p53 protein in both p53 heterozygous (Figure 3.12) and wild type NALM-6 cells (Figure 3.13) with RG7388 in a concentration dependent manner. In addition, the combination of WIP1 inhibitor (2.5µM) induced greater stabilisation of p53 compared to RG7388 alone for both 6 and 24 hours timepoints. Furthermore, the transcriptional expression of p21 and MDM2, the p53 transcriptional target proteins, were induced more with combination of WIP1 inhibitor treatment compared to RG7388 single treatment. Moreover, cPARP protein was detected at 24 hours and was induced to a greater extent with WIP1 inhibitor combination compared to RG7388 alone.

Looking at the changes in the mRNA level, *CDKN1A*, a cell growth arrest gene showed the highest fold change in expression across all the genes in the panel with a concentration dependent increase with the concentration of either RG7388 (0.2µM) alone or in a combination with WIP1 inhibitor (2.5µM) (Figure 3.14 C). Moreover, higher concentration of RG7388 at (0.4µM) showed an increased in the fold change expression of *CDKN1A* however, the combination of WIP1 inhibitor reduced the expression due to concentration and the CLL cells might dead.

Furthermore, p53 negative regulatory genes, *MDM2, TP53 and TP53INP1* showed concentration dependent increase in their fold change expression with RG7388 and WIP1 inhibitor combination treatment relative to the DMSO (Figure 3.14 B). Furthermore, WIP1 inhibitor combination with RG7388 induced the fold change expression of *TP53* target genes in a concentration dependent manner with RG7388. Although, the RG7388 concentrations, which were chosen for the qRT-PCR experiments, were high compared with the (10-30nM) dose range of maximum synergy seen in your matrix combination experiments. Thus, the RQ value at the combination of WIP1 inhibitor potentiates the effect of RG7388 at (0.2µM) and induces the expression of TP53 target genes. In comparison, combination of WIP1 inhibitor with RG7388 at (0.4µM) reduces TP53 target genes expression.

Interestingly, the mRNA expression of the *PPM1D* gene was reduced in the presence of the WIP1 inhibitor (2.5µM) for both single and combination treatment with RG7388 (Figure 3.14 B). In contrast, the presence of WIP1 inhibitor (2.5µM) significantly increased the mRNA expression of the other p53 target genes (*PPM1D*, *MDM2*, *TP53*, *TP53INP* and *CDKN1A*) compared to (0.2µM) RG7388 treatment alone (Figure 3.14 B&C). However, the combination treatment of WIP1 inhibitor (2.5µM) with at the higher dose of RG7388 (0.4µM) slightly reduced the mRNA expression of *MDM2*, *TP53INP1* and *CDKN1A*. These results are consistent with previous studies showing an induction of p53 negative regulatory genes following treatment with MDM2 inhibitors in combination with WIP1inhibitor in response to

a panel of Uterine Leiomyosarcoma, ovarian, liver adenocarcinoma and cutaneous melanoma cell lines, respectively (Wu et al., 2018, 2022; Chamberlain et al., 2021; Zanjirband et al., 2016).

For the pro-apoptotic genes, *PUMA* showed the highest fold changes expression compared to *NOXA* and *BAX*. Moreover, RG7388 induced the fold change expression of the pro-apoptotic genes, *PUMA, NOXA* and *BAX* in a concentration dependent manner however, the combination of WIP1 inhibitor reduced their expression (Figure 3.14 D). In similar concept, Ciardullo et al. was reported an induction in the expression of the pro-apoptotic *PUMA* gene was dominant response in CLL cells after RG7388 treatment (Ciardullo et al., 2019).

On the other hand, the anti-apoptotic genes, *MCL1* showed a concentration dependent induction in their fold change mRNA expression with both RG7388 and combination of WIP1 inhibitor. However, *BCL-2* showed little change in expression with treatment relative to DMSO (Figure 3.14 E).

In the study by Skalniak, L and co-workers, found that cancer cells could be resistant to idasanutlin not only due to the de novo appearance of DNA mutations but also with pre-existing cells. Specially, since the monoclonal $p53^{wt}$ U-2 OS cells were carry the resistant cell clones in their population in response to idasanutlin (Skalniak et al., 2018).

In conclusion, the current study demonstrated that GSK2830371, a WIP1 inhibitor, alone up to 10μM showed no growth-inhibitory activity. Conversely, MDM2 inhibitor, RG7388 and HMD201, showed a dose dependent inhibition on cell growth activity. Moreover, the combination of GSK2830371 further potentiated the growth-inhibitory and activity of MDM2 inhibitors by increasing phosphorylation and stabilisation of p53 in functional p53-dependent manner.

Chapter 4: The Cytotoxic Effect of MDM2 and WIP1 Inhibitors on Primary CLL Samples

4.1 Introduction

Several studies have investigated the effect of combining GSK2830371, with RG7388, on various types of cancer cells. Pechackova suggested that WIP1 phosphatase inhibition might be a promising therapeutic strategy for breast cancer treatment, particularly in combination with MDM2 antagonists (Pechackova et al., 2016). The Genomic alterations of *PPM1D* can be massively identified as amplifications of chromosome 17q, frequently observed in ovarian and breast cancer (Bulavin et al., 2002; Li et al., 2002; Lambros et al., 2010; Rauta et al., 2006; Tan et al., 2009). The combination of GSK2830371 and nutlin-3 had a synergistic effect on p53 activation and increased the expression of p53-target genes, reducing cell viability and inducing apoptosis (Pechackova et al., 2016).

In this chapter a panel of 11 freshly isolated primary CLL samples was used to assess the efficacy of RG7388 as a single agent and in combination with the GSK2830371. The MDM2-p53 binding antagonist RG7388 (idasanutlin) is one of a novel class of anti-cancer therapy, which acts by disrupting the interaction between p53 and MDM2 to non-genotoxically activate p53 wild type. The overall aim of the study was to provide pre-clinical investigations to support the clinical evaluation of RG7388 alone and/or in combination with a WIP1 inhibitor for CLL patients, to improve outcome and reduce drug toxicity.

4.2 Hypothesis and Aims

In the current chapter, results are described for experiments to determine whether this synergy extended to *ex-vivo* tested primary CLL cells.

All CLL cell samples were obtained with appropriate consent from the peripheral blood of patients who had been diagnosed with CLL disease. Following informed consent, the CLL samples were collected and stored under the auspices of the Newcastle Biobank, according to the institutional guidelines and the Declaration of Helsinki (http://www.ncl.ac.uk/biobanks/). CLL diagnosis was identified according to the IwCLL-164 NCI 2008 criteria (Hallek, Cheson, et al., 2018; Hallek, Shanafelt, et al., 2018).

4.3 Evaluating *ex-vivo* effects of MDM2/p53 antagonists as single agents in patient derived CLL cells

4.3.1 Characterisation of the CLL cohort

Eleven primary CLL samples were included in this study. Some characteristics of the CLL patients, including *TP53* status, are summarised in (Table 4.1). Clinical information, including disease stage and treatment, were provided by the attending physician.

Tumour ID	Age	Sex	Binet stage	Treatment	Cytogenetic abnormalities	[1]*TP53* status (W/B)	RG7388 LC_{50} (µM)
299	71	F		none	none	WT	6
302	73	M	C	FCR, Ibrutinib		WT	0.56
303	64	F	C	none	del(13q)	WT	0.26
304	88	F	A	none		WT	0.26
305	81	M		none	none	WT	0.31
306	77	F	C	C, F, FCR		WT	0.75
307	78	M	C	none	del(13q)	WT	0.49
308	74	M	A	none		WT	0.15
309	61	M	A	none	del(13q)	WT	2.68
310	74	F		none		WT	0.57
311	54	M		none	del(11q)	WT	0.26
312	83	F	A	none		WT	0.12
313	80	F	A	none		WT	0.17
314	68	M	C	C (2017) Ven (11/2019)		WT	0.23
315	70	F	C	none		WT	0.86
316	79	M		none		WT	1.46
317	75	M	B	none		WT	0.90

[1]*TP53* status was determined by the stabilization of p53 protein by western blot after treatment with MDM2 inhibitors.
Blank boxes indicate that there was no data available.
C: Chlorambucil, F: Fludarabine, FCR: Fludarabine + Cyclophosphamide + Rituximab, Ven: Venetoclax.

Table 4.1 Characteristics of the CLL cohort patient samples tested *ex-vivo* with MDM2 inhibitors.

4.4 Results

4.4.1 The cytotoxic effect of GSK2830371 WIP1 inhibitor on primary CLL cells

To evaluate the effect of WIP inhibition, 11 different primary CLL samples were treated with GSK2830371 (2.5μM) for 48 hours. DMSO was used as vehicle control. Following the treatment time, primary CLL cells viability was measured by XTT assay. The inhibitory effect was normalized to the effect of DMSO solvent alone to determine the percentage CLL cell viability. The WIP1 inhibitor at 2.5μM was identified to be the highest concentration that did not cause much inhibition in the cells viability based on NALM-6 cells result in the Chapter 3.

Prior results had shown that 2.5μM of the GSK2830371 WIP1 inhibitor, while reducing WIP1 catalytic activity and protein levels, alone does not have significant inhibitory effect on the viability of a wide range of cell lines (Wu et al., 2021; Esfandiari et al., 2016; Wu et al., 2022). This was also observed in the experiments described in the previous Chapter 3 for isogenic *p53*(-/+) knockout NALM-6 cells, in which (2.5μM) GSK2830371 showed little inhibitory effect on cell viability. In the present Chapter 4:, results are described first for the effect of 2.5μM GSK2830371 on the viability of primary CLL cells (Figure 4.1).

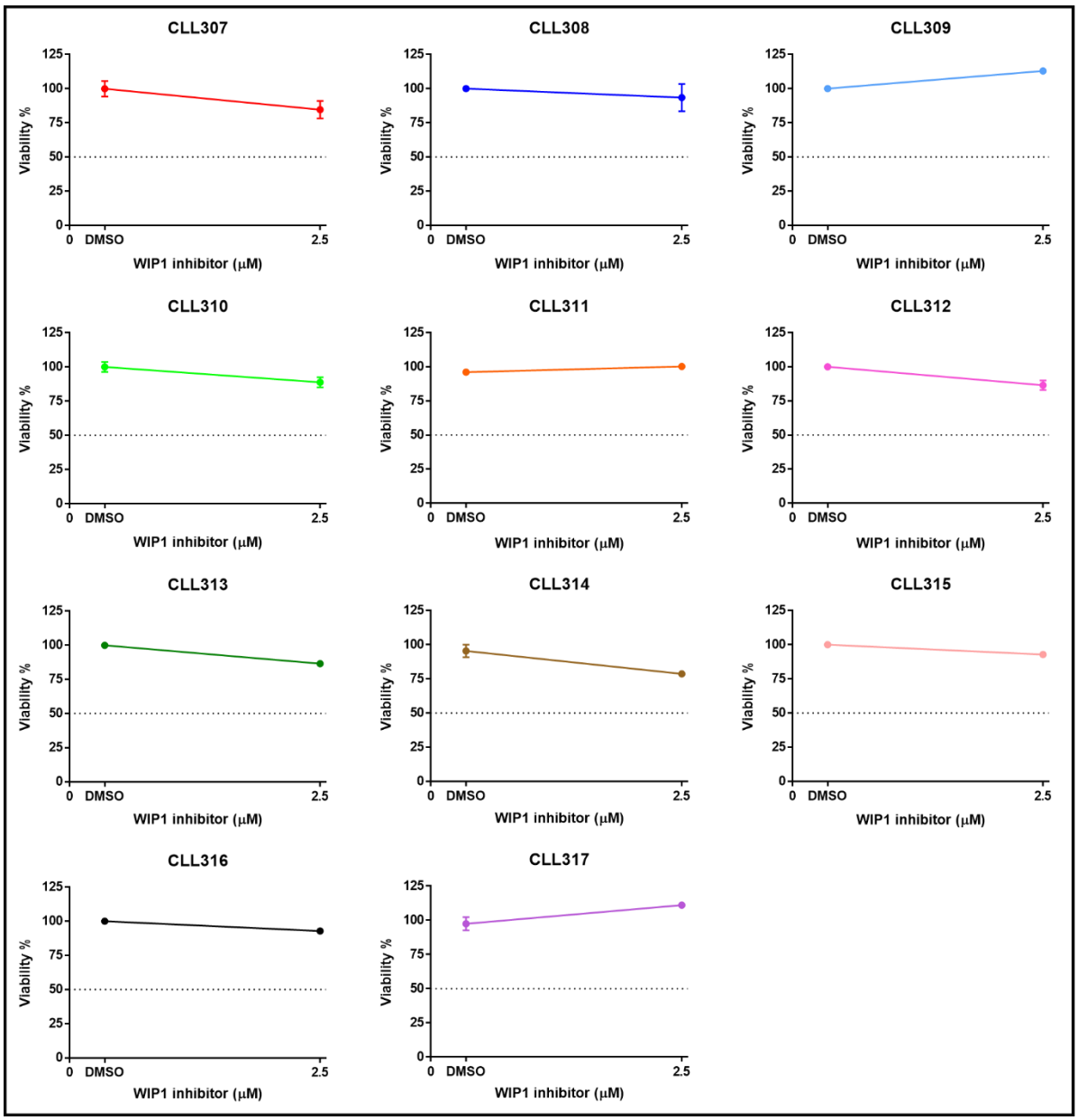

Figure 4.1 The *ex-vivo* effect of WIP1 inhibitor on the viability of primary CLL cell. Different primary CLL samples (n=11) treated with GSK2830371 (2.5μM) for 48hors. XTT was used to assessed cell viability. Each experiment was performed once on the primary CLL cells with three intra-replicates for each concentration. Bars show the mean ± SEM of intra-replicate within the experiment. All % of cell viability was normalized to DMSO treatment for individual experiment. (SEM, standard error of the mean).

Figure 4.2 illustrates the effect of WIP inhibitor (2.5μM) on viability across the panel of primary CLL samples. (Figure 4.2 A) shows the absolute XTT absorbance values and (Figure 4.2 B) shows the inhibitory effect of WIP1 inhibitor normalised to DMSO only control values. Despite considerable variation in the basal metabolic activity XTT readings between the CLL samples, the GSK2830371 WIP inhibitor (2.5μM) did not had much inhibition effect on the basal CLL sample cell viability in the majority of the CLL cell cohort (Figure 4.2 B). Although, some of primary CLL cell samples showed very low cell metabolic activity level compared to the others. However, regardless of this, the effect of GSK2830371 did not change

the metabolic activity of the CLL cells (Figure 4.2 A). CLL309 showed the lowest cell metabolic activity compared to the other CLL cells in the cohort. Although, WIP inhibitor (2.5µM) did not show inhibition effect on the CLL cells metabolic activity.

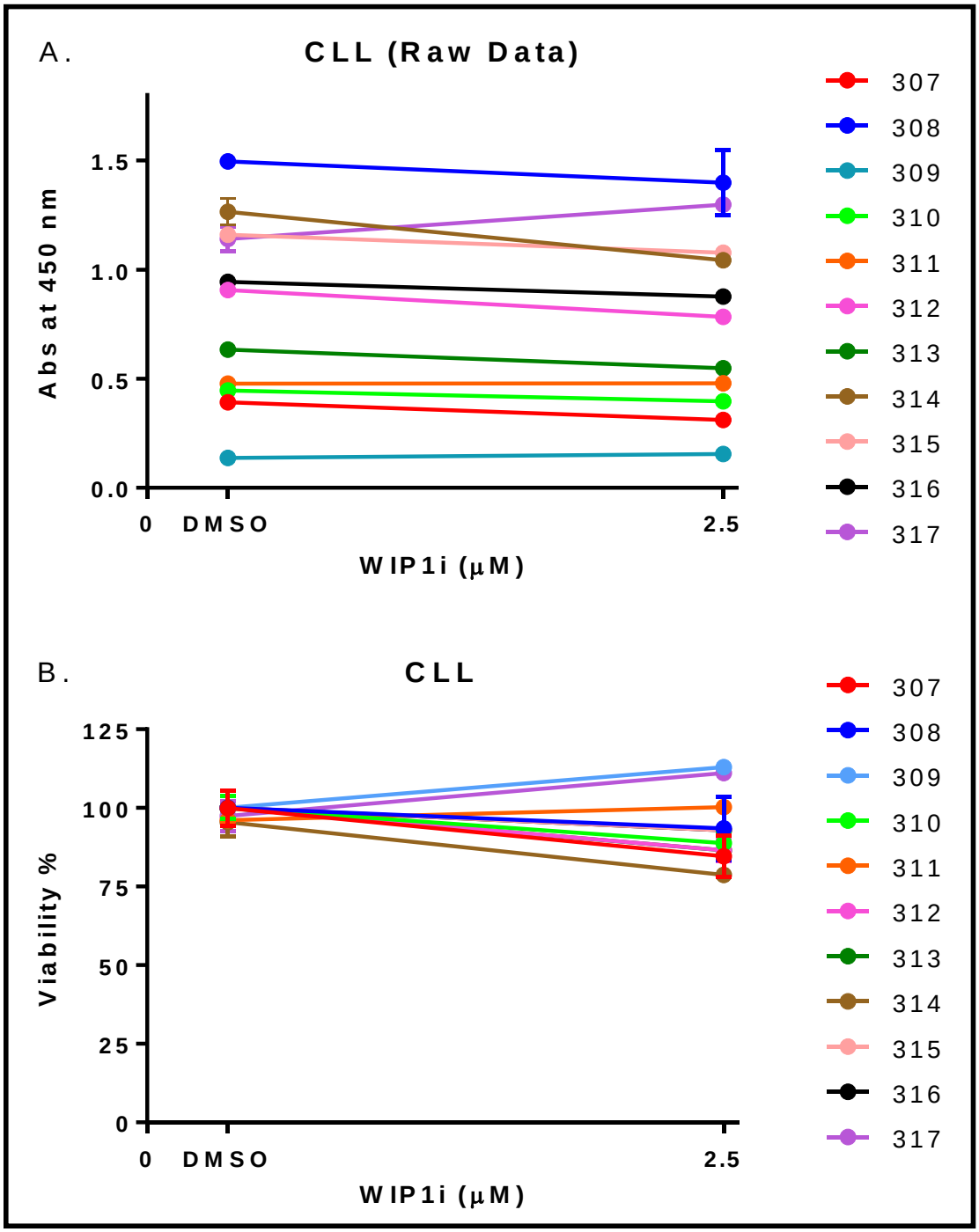

Figure 4.2 Summary of the viability of primary CLL patient samples in response to WIP1 inhibitor (2.5µM). (A) The XTT assay raw data absorbance values at 450nm. (B) The viability of the CLL cells with DMSO normalization for each corresponding sample. CLL samples (n=11) treated with GSK2830371 (2.5µM) for 48 hours and the CLL cell viability was determined by XTT assay. The bars represent the intra-replicates for each concentration. Each line represents different CLL sample.

4.4.2 The cytotoxic effect of MDM2 inhibitor (RG7388) on primary CLL cells

This section describes the *ex-vivo* dose-dependent effect of RG7388 (idasanutlin) on the primary CLL cell samples. (Figure 4.3) shows the effect of RG7388 on 11 primary CLL patient samples. The CLL cells were treated with a wide range of RG7388 concentrations. Following the 48 hours of treatment, the CLL cell metabolic activity was measured using an XTT assay. The inhibition effect of each concentration was normalized to the effect of DMSO solvent alone as a control for un-treated cells. DMSO levels were matched to that used in treated samples and maintained at a concentration of 0.5% (v/v) which had minimal effect on cell metabolic activity. RG7388 showed a concentration dependent inhibition effect on the viability of the primary CLL cells in a concentration-dependent manner.

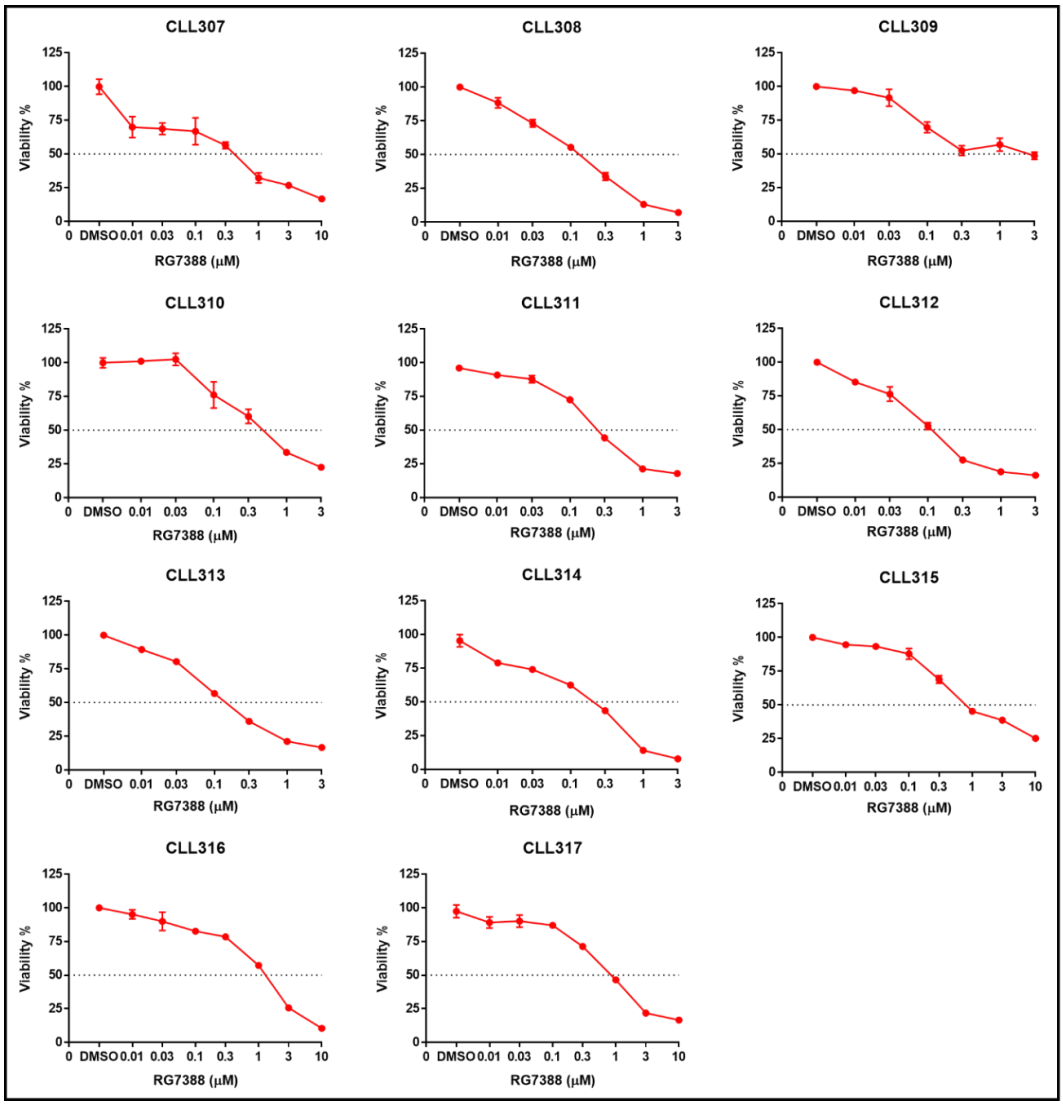

Figure 4.3 Effect of the *ex-vivo* treatment with MDM2 inhibitor on the primary CLL cell viability. Concentration dependent cytotoxicity of RG7388 on CLL cell. A cohort set of CLL samples (n=11) was treated *ex-vivo* with a wide concentration range of MDM2 inhibitor (RG7388) for 48 hours and viability measured by XTT assay. CLL cell viability was normalized to DMSO treatment for individual experiment. Each experiment was performed once on the primary CLL cells. Bars show the mean ± SEM of intra-replicate of concentrations within the experiment.

Most of the primary CLL samples had an LC_{50} inhibition value for RG7388 within (0.1-1µM) except sample CLL309, whose LC_{50} of RG7388 was 2.6µM (Table 4.2 A). Figure 4.4 summarizes the actual XTT assay OD value absorbance at 450nm for CLL samples in response to RG7388. The CLL cells showed varying 450nm absorbance for the DMSO only controls. CLL309 cells had the lowest basal cell metabolic activity compared to other CLL samples in the cohort. However, CLL309 did still show a concentration-dependent further inhibition of viability with RG7388 doses below 0.3µM. Interestingly, CLL309 showed that 50% of the cells are unresponsive to RG7388, even at 3µM (Figure 4.2).

Considering the behaviour of CLL samples in response to MDM2 inhibitor (RG7388), with the exception of sample 309, it can be inferred from the sub-micromolar LC_{50} values that the cohort of CLL samples responded as functional *TP53*(+/+) wild type cells. The (Figure 4.4 A) shows a summary plot and (Figure 4.2 A) LC_{50} values show that RG7388 produced a concentration dependent inhibition on the CLL cell metabolic activity. Furthermore, Figure 4.4 B) represents the inhibition effect of RG7388 normalized to the DMSO and shows the variation in response between CLL samples, reflecting the molecular heterogeneity of CLL. The mean LC_{50} values for all the 11 primary CLL samples showed that the majority were sensitive to RG7388, with the majority of the primary CLL cells in the cohort achieving an LC_{50} with RG7388 less than 1µM (Table 4.2 A) except the CLL309 and CLL316. The CLL309 cell expressed low metabolic activity compared to the other CLL cells in the cohort. In addition, the CLL316 sample had an RG7388 LC_{50} value of 1.46µM, with no indication of a resistant sub-population.

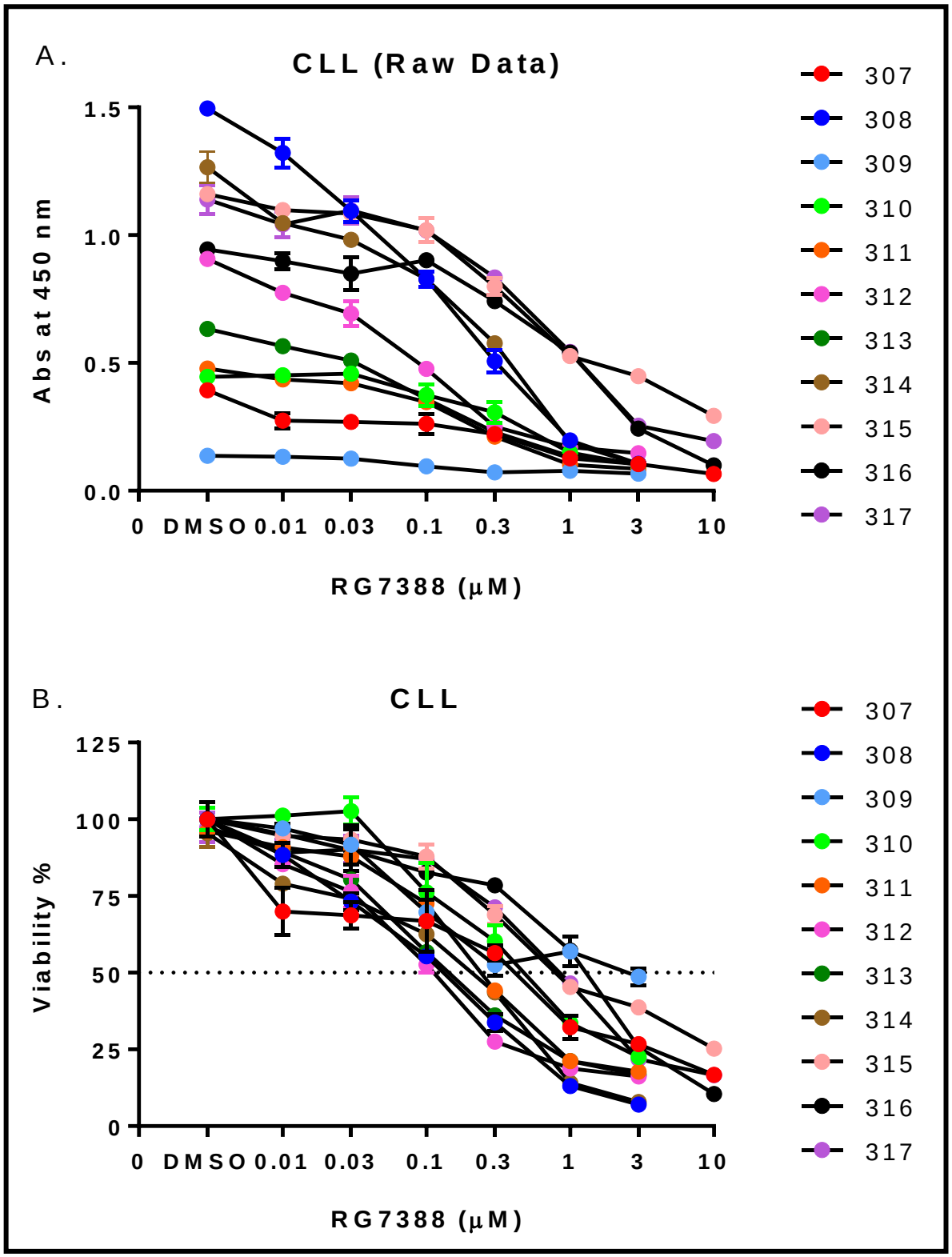

Figure 4.4 Summary of primary CLL sample responses to RG7388 (n=11). (A) The raw data XTT assay absorbance at 450nm following RG7388 treatment. (B) The dose-dependent inhibitory effect of RG7388 on the CLL viability with normalization to DMSO control. Different primary CLL samples was treated with wide range of RG7388 for 48 hours and the XTT assay was used to assessed the cell viability. The error bar represents three intra-replicates of concentrations within the experiment ± SEM. Each colour shows individual primary CLL samples which treated once.

4.4.3 The cytotoxic effect of WIP1 inhibitor in a combination with MDM2 inhibitor (RG7388) on primary CLL cells

To determine the inhibition effect of RG7388 in combination with WIP1 (2.5µM) inhibitor, primary CLL samples were treated with a wide concentration range of RG7388 in a combination with WIP1 (2.5µM) inhibitor. Following the 48 hours of the treatment, the viability of the CLL cells was measured by XTT assay.

As a single agent treatment effect, the WIP1 (2.5µM) inhibitor showed a minimum inhibition effect of the primary CLL cells viability (Figure 4.1). In contrast, RG7388 showed a concentration-dependent inhibition of viability of CLL cells (Figure 4.3). Furthermore, the combination of WIP1 (2.5µM) inhibitor potentiated the inhibitory effect of RG7388 in a concentration dependent manner in comparison to the effect of RG7388 concentrations (Figure 4.5). The combination treatment of WIP1 (2.5µM) inhibitor with RG7388 inhibited the viability of the primary CLL cells in a concentration dependent manner. The potentiation effect of WIP1 (2.5µM) inhibitor with RG7388 varied between the CLL cells however, all the CLL cells in the cohort showed an additional decrease in viability due to the potentiation effect (Figure 4.6). The LC_{50} inhibition of RG7388 and RG7388 in combination with the WIP1 inhibitor is shown (Table 4.2 A).

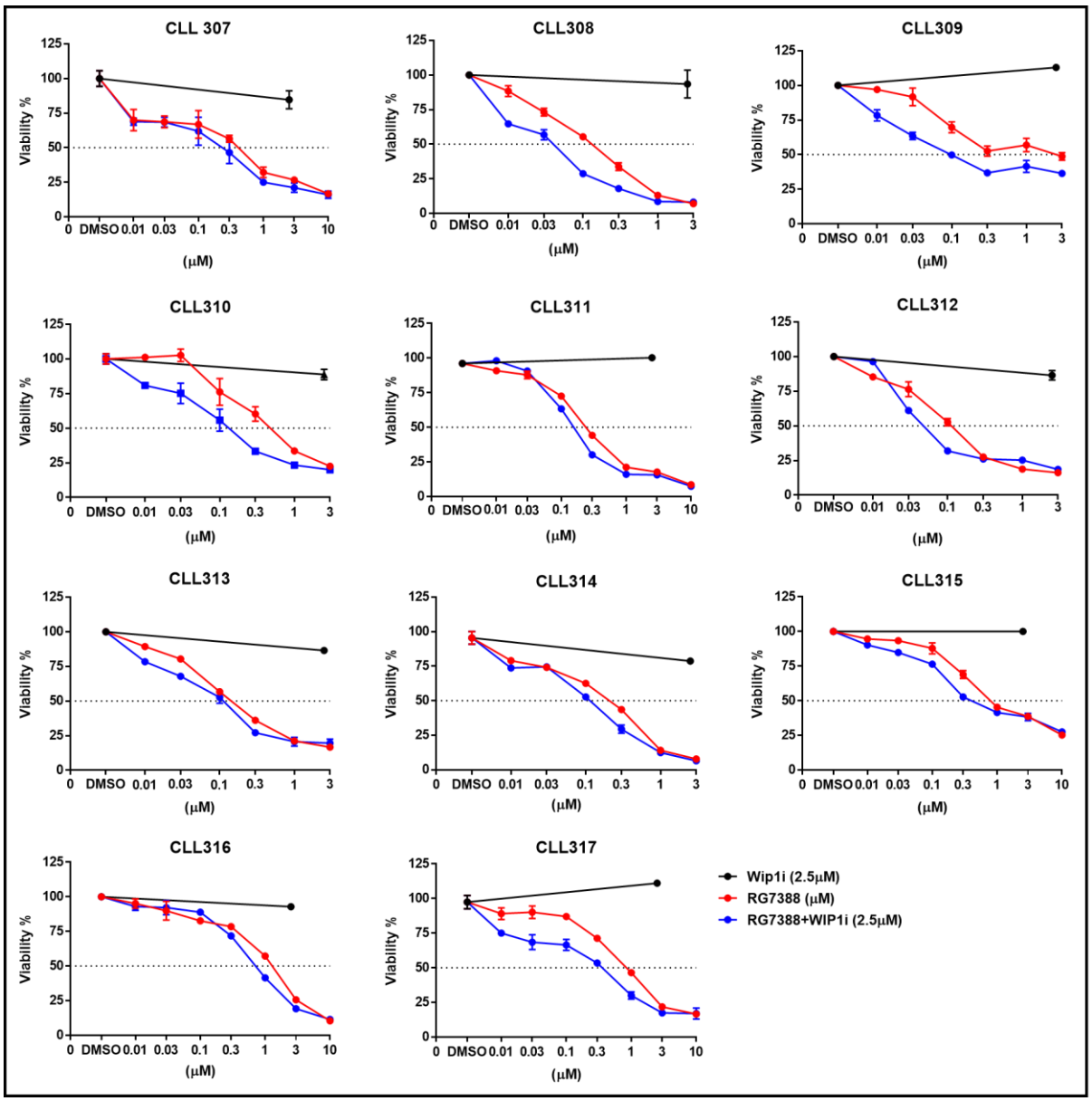

Figure 4.5 WIP1 inhibitor (2.5μM) potentiates the activity of RG7388 in a concentration dependent manner. A cohort of CLL samples (n=11) treated with GSK2830371 (2.5μM) in a combination with a range of RG7388 concentrations for 48 hours. XTT assay was used to determine cell viability. Each primary CLL sample exposed to different treatments in the same experiment. Each experiment performed once with three intra-replicates. All % of cell viability was normalized to DMSO treatment for individual experiment. Bars show the mean ±SEM.

4.4.4 Summary of percentage inhibition of the viability of primary CLL samples following treatment with WIP1 and MDM2 (RG7388) inhibitors

There was a statistically significant additional reduction in the metabolic activity of the CLL cells in response to different concentrations of RG7388 with a combination of WIP1 inhibitor (2.5μM) in a concentration dependent manner (Figure 4.6). Looking at the cohort of 11 CLL samples, there was an inhibition of CLL cell viability in a concentration dependent manner. In

addition, the combination of WIP1 inhibitor (2.5µM) significantly potentiated the effect of RG7388 across a range of RG7388 doses (Figure 4.6).

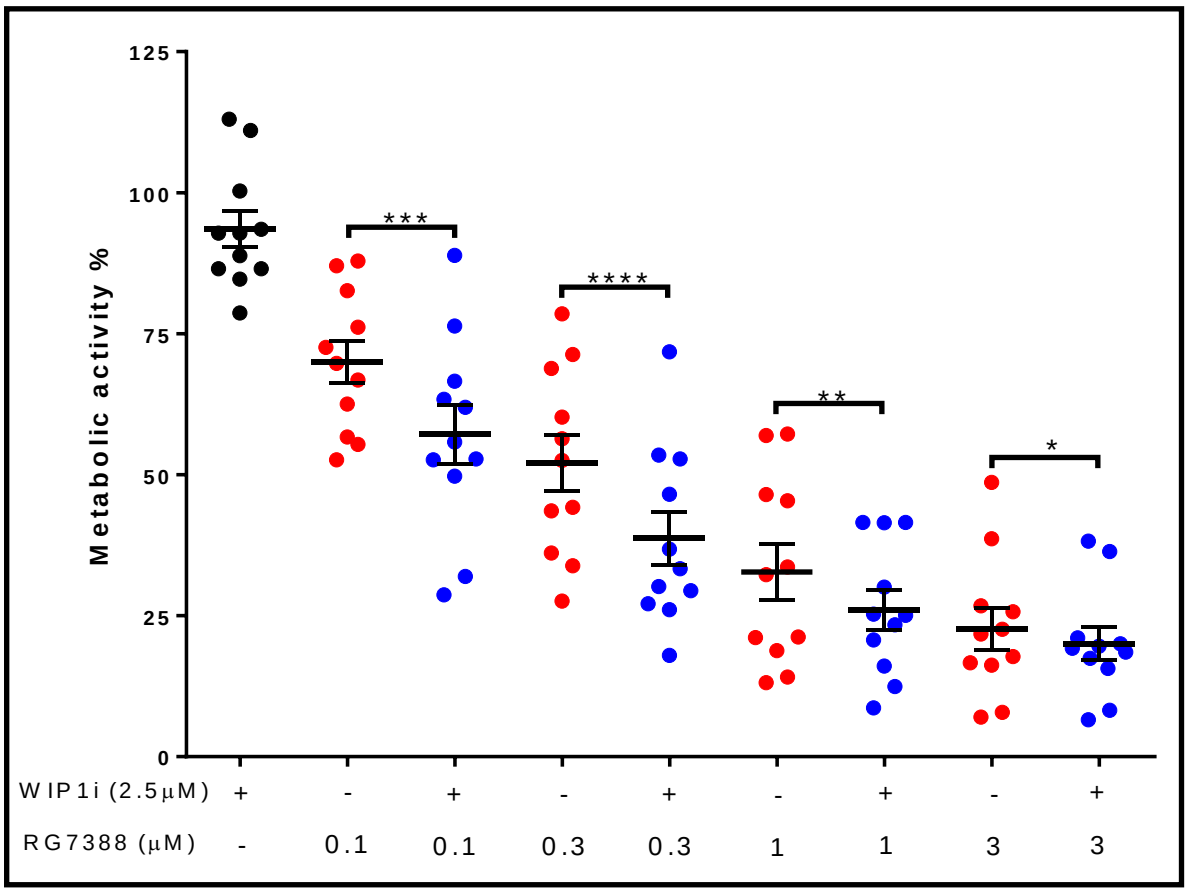

Figure 4.6 The inhibition effect in the metabolic activity of the CLL samples in response to RG7388 and in a combination to WIP1 inhibitor. Cohort of primary CLL samples (n=11) treated with range of RG7388 concentrations in combination with GSK2830371 (2.5µM) for 48hrs followed by XTT assay to determine CLL cell metabolic activity. All metabolic activity % was normalized to DMSO treatment for individual experiment. Each experiment was performed once on the primary CLL cells. The black colour shows the effect of GSK2830371, red shows RG7388 alone and blue shows the combination treatment. Data are presented as an average mean ± SEM of intra-replicate of concentrations within the experiment. Statistical significant p-values is indicated by paired t-test one tail (*, $p < 0.05$, **, $p < 0.01$, ***, $p < 0.001$).

4.4.5 The LC_{50} and LC_{70} values of WIP1 and MDM2 inhibitors (RG7388) on primary CLL samples

To investigate the effect of RG7388 and WIP1 inhibitor on primary CLL cell viability, the LC_{50} and LC_{70} values were calculated. The LC_{70} was calculated to determine whether the potentiation by WIP1 inhibitor could show more significant effect with lower concentration effect level of RG7388.

Figure 4.7 shows the LC_{50} or LC_{70} values for either RG7388 or the combination of RG7388 with WIP1 inhibitor (2.5µM). These were calculated by determining the concentration needed to reduce the viability to 50% or 30% compared to untreated cells. The combination of WIP1 inhibitor (2.5µM) with RG7388 significantly decreased the average LC_{50} from 0.72 ± 0.23µM to 0.25 ± 0.06µM (p=0.02) (Table 4.2 A) and decreased the average LC_{70} from 169nM ± 0.51 to 0.084nM ± 0.02 (p=0.008) (Table 4.2 B). The primary CLL cells became significantly more sensitive to RG7388 when combined with the GSK2830371 WIP1 inhibitor. Furthermore, the potentiation by WIP1 inhibitor showed more significant effect with lower concentration of RG7388 at LC_{70} compared to LC_{50}.

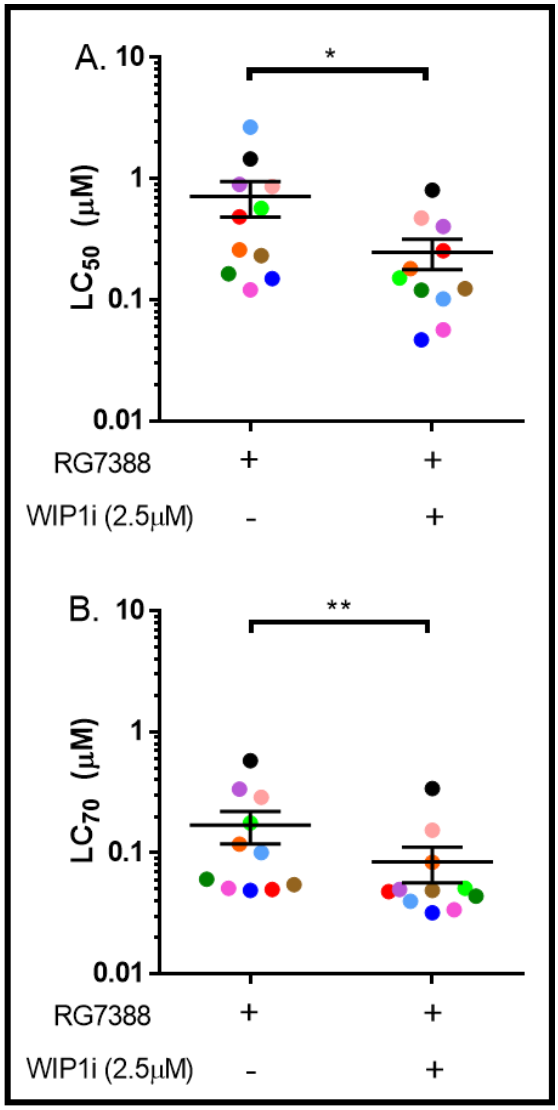

Figure 4.7 The LC_{50} (A) and LC_{70} (B) values showing the range of responses to RG7388 alone and in combination with WIP1 inhibitor (2.5µM) in a cohort of different CLL samples (n=11). Each individual CLL sample is marked with specific colour code. (A) The LC_{50} value of a combination treatment with GSK2830371 and RG7388 was significantly lower compared to the effect of RG7388 alone (p = 0.02). (B) The LC_{70} value of WIP1 inhibitor in combination with RG7388 was significantly lower compared to RG7388 alone (p = 0.08). Data are presented as an average mean ± SEM. Statistical significant p-values (*, $p < 0.05$, **, $p < 0.05$) are indicated by paired t-test one tail.

A.

LC_{50} (µM)	RG7388	RG7388+WIP1i (2.5µM)	Fold Changes
CLL 307	0.485	0.255	0.526
CLL 308	0.150	0.051	0.340
CLL 309	2.676	0.101	0.038
CLL 310	0.569	0.152	0.267
CLL 311	0.260	0.181	0.696
CLL 312	0.121	0.057	0.471
CLL 313	0.165	0.121	0.733
CLL 314	0.232	0.124	0.534
CLL 315	0.862	0.474	0.550
CLL 316	1.457	0.804	0.552
CLL 317	0.900	0.404	0.449
Average	**0.716 (±0.23)**	**0.248 (±0.06)**	-

B.

LC_{70} (µM)	RG7388	RG7388+WIP1i (2.5µM)	Fold Changes
CLL 307	0.050	0.048	0.960
CLL 308	0.049	0.032	0.653
CLL 309	0.101	0.040	0.396
CLL 310	0.177	0.051	0.288
CLL 311	0.118	0.084	0.712
CLL 312	0.051	0.034	0.667
CLL 313	0.061	0.044	0.721
CLL 314	0.055	0.049	0.891
CLL 315	0.290	0.154	0.531
CLL 316	0.050	0.048	0.588
CLL 317	0.049	0.032	0.148
Average	**0.169 (±0.51)**	**0.084 (±0.02)**	-

Table 4.2 The LC_{50} and LC_{70} values of primary CLL samples (n=11) in response to RG7388 and in combination with WIP1 inhibitor (2.5µM). (A) LC_{50} (B) LC_{70}. The fold changes represent the ratio of GI_{50} inhibition values for RG7388 ± WIP1 inhibitor.

4.4.6 The synergistic effect of WIP1 (GSK2830371) and MDM2 inhibitor (RG7388) combination on primary CLL samples

All the matrix figures, 3-D graphs and ZIP synergy scores were generated from https://synergyfinder.org. For the matrix designed experiments, (section A) show the inhibition effect of single agent concentrations (either RG7388 or WIP1 inhibitor) on the viability of primary CLL samples. The matrix diagram shows the colour coded percentage inhibition for each single agent and combination treatment represented in small squares. This generates a broad view of the inhibition effect of the RG7388 and WIP1 inhibitor for a wide range of concentration combinations on the viability of the primary CLL cells.

In (section B), the matrix diagram and the three-dimension (3-D) diagram represent the zero-interaction potential (ZIP) scores for the combination treatments. The colour coded illustrated the degree of synergy (red) or antagonism (green) across the range of treatment combinations tested. In addition, the dose combination generating a peak or minimum ZIP synergy score is identified. The ZIP score helps to determine whether the combination treatment produces an antagonistic or synergistic effect.

The matrix model experiment was performed on eight freshly isolated CLL patient samples (CLL307, CLL310, CLL311, CLL312, CLL313, CLL314, CLL315, CLL316) and one cryopreserved CLL sample (CLL311 TH), which were exposed to a wide range of RG7388 and WIP1 inhibitor concentrations. Following 48 hours of treatment, the CLL cell viability was measured by XTT assay. The average ZIP synergy score of the combination treatment is summarized in (Figure 4.10 A). Example individual synergy plots are shown for one fresh sample (Figure 4.8) and one cryopreserved sample (Figure 4.9).

4.4.6.1 CLL311

(Figure 4.8 A) shows an example of the inhibition effect on CLL cell viability in response to RG7388 and WIP1 inhibitors. Freshly isolated CLL311 cells showed a dose dependent inhibition of cell viability with RG7388 treatment. RG7388 (less than 300nM) were able to inhibit the cells viability by 50% of viable CLL311 cells. However, up to 10,000nM of WIP1 inhibitor as a single agent did not inhibit the CLL311 cell viability. The combination with WIP1 inhibitor potentiated the effect of RG7388 in a concentration dependent manner.

(Figure 4.8 B) shows the ZIP synergy score for CLL311 in response to RG7388 in combination with WIP1 inhibitor. Most of the combination synergy effect on CLL311 was found with (10-300nM) RG7388 in combination with (100-1000nM) WIP1 inhibitor. The mean ZIP synergy score of WIP1 inhibitor in combination with RG7388 for CLL311 cells was 9.27, with a peak synergy score of 29.07 which indicates a significant synergistic effect of the combination treatment.

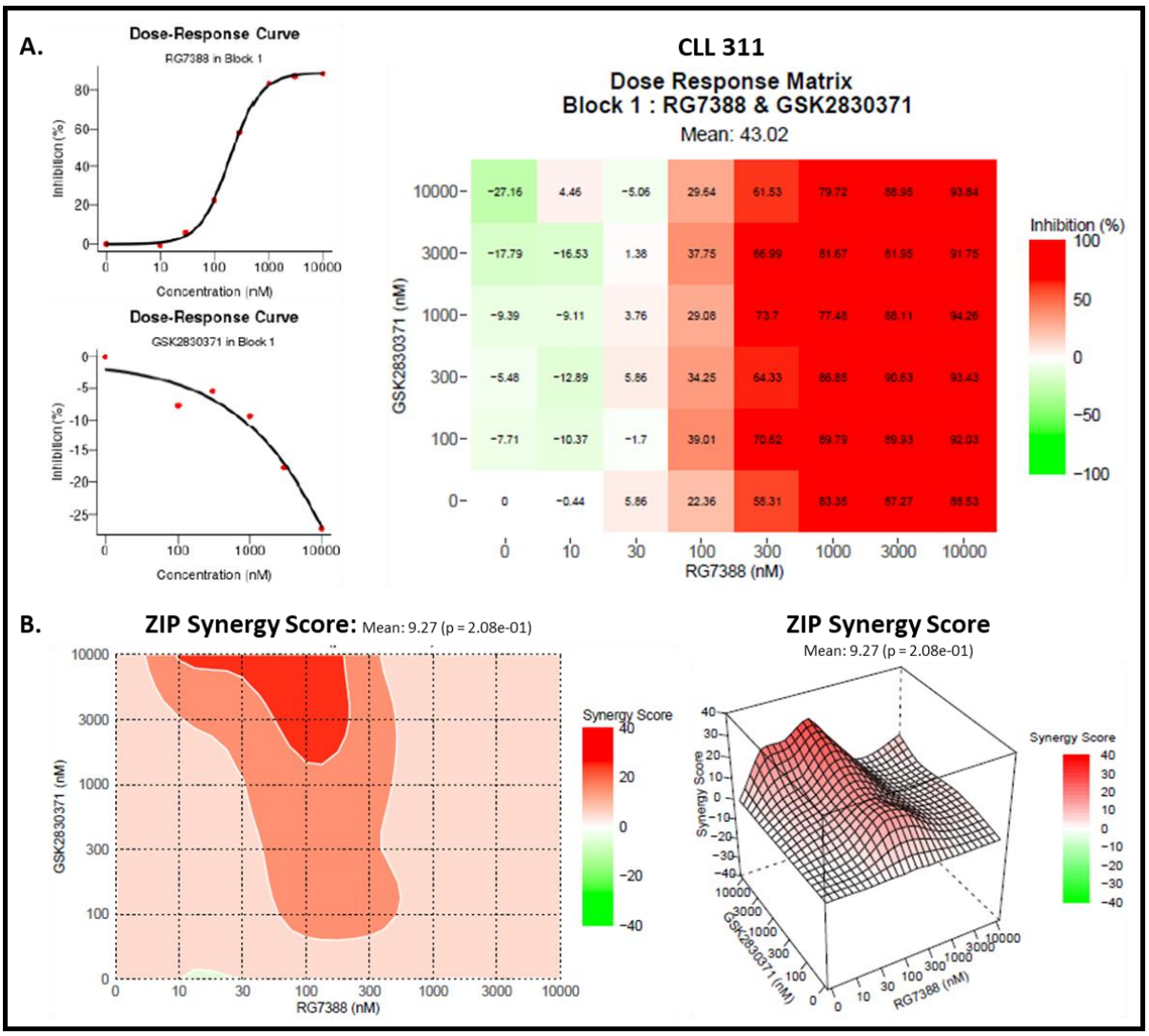

Figure 4.8 The synergistic effect of RG7388 in combination with WIP1 inhibitors on freshly isolated primary CLL311 cells. The matrix model designed to find the synergistic effect and the optimum highest concentration to obtain the greatest combination effect. The primary CLL cells treated with wide range of RG7388 and GSK2830371 concentrations for 48 hours. The CLL cell viability assessed by XTT assay. (A) The graph shows single dose response inhibition effect in response to RG7388 and WIP1 inhibitor. The representative dose response analysis showing the % inhibition of cell viability in response to wide range of the treatment (B) The synergistic landscape shows synergy ZIP score in response to combination treatment of RG7388 and WIP1 inhibitor. The intensive red colour represents the highest synergy area. The 3-D plot shows the peak ZIP synergy score in greater interpolated detail. The experiment was performed once on each CLL sample in a total of (n=8) different samples. The data was analysed by the Synergyfinder.org website.

4.4.6.2 CLL311 (cryopreserve)

To compare with the response of freshly isolated cells, (Figure 4.9) shows the results of combination treatment for a thawed cryopreserved sample of CLL311. RG7388 showed a concentration dependent inhibition effect on the viability of cryopreserved CLL311. RG7388 (1000nM) inhibited the cell viability by an average of 50%. This contrasted with the fresh CLL311 cells for which 1000nM RG7388 had shown 88.5% inhibition.

The combination of WIP1 inhibitor still potentiated the effect of RG7388 to inhibit the viability of the thawed cryopreserved CLL311 cells in a concentration dependent manner. Most of the inhibition effect on cryopreserved CLL311 was produced with (30-100nM) RG7388 in a combination with (1000-10,000nM) WIP1 inhibitor. The average mean inhibition effect of WIP1 inhibitor with RG7388 on the thawed cryopreserved CLL311 cells was 24.51 which was 50% (2x) lower than for the freshly isolated CLL311.

The mean ZIP synergy score for WIP1 inhibitor in combination with RG7388 for cryopreserved CLL311 cells was 9.58, which is close to the mean ZIP score for freshly isolated CLL311 cells 9.27. The peak synergy scores were also similar, 29.61 and 29.07 respectively for thawed cryopreserved and freshly isolated CLL311 cells respectively. It was concluded that the combination of WIP1 inhibitor with RG7388 produced similar average and peak synergistic effect for the same dose range on the viability of both freshly isolated and thawed cryopreserved CLL311 cells.

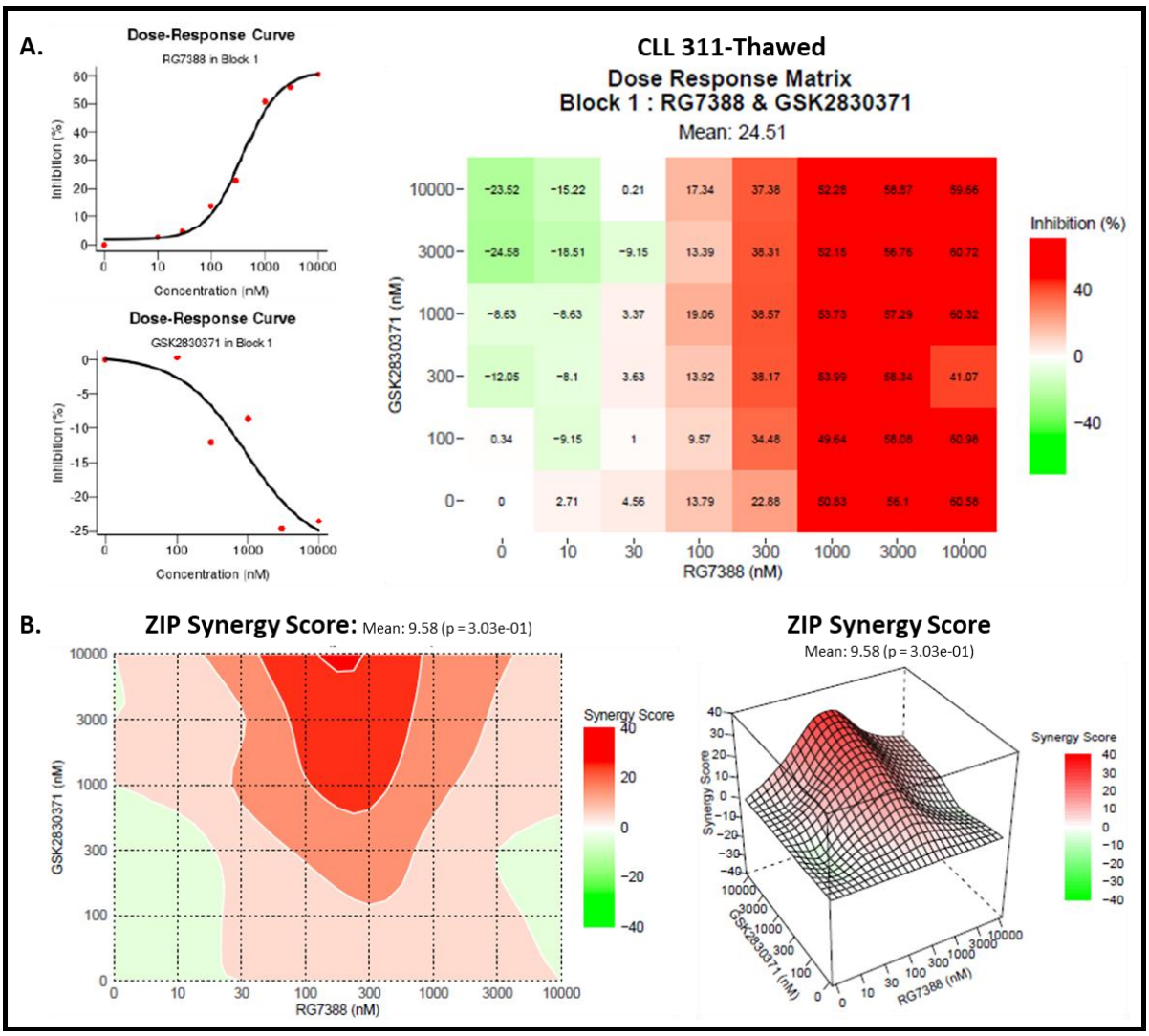

Figure 4.9 The inhibition effect of RG7388 in combination with WIP1 inhibitors on cryopreserved isolated primary CLL311 cells. The cryopreserved CLL311 cells were thawed and treated with wide range of MDM2 and WIP1 inhibitors for 48 hours to compare the treatment responses with freshly isolated CLL cells. The cell viability determined by XTT assay. (A) Dose response inhibition effect in response to RG7388 and GSK2830371. The matrix model shows the individual % inhibition effect for each combination treatment. (B) Synergy ZIP score in response to combination treatment of RG7388 and WIP1 inhibitor. The red colour represents the synergistic effect while the green colour represents the antagonistic effect. The 3-D plot shows the peak ZIP synergy score in greater interpolated detail. The Synergyfinder.org website identifies the range of ZIP scores for a synergistic effect to be greater than 10 and any score less than 10 is defined as an antagonistic effect.

The majority of the CLL samples in the cohort did not show an inhibition of cell viability in response to a single treatment of WIP1 inhibitor for doses up to 10µM, however, some of the CLL cell samples showed approximately 40% inhibition of cell viability. By contrast, RG7388 showed an inhibition of CLL cell viability in a concentration dependent manner. For the combination treatment, WIP1 inhibitor was able to potentiate the effect of RG7388 on all of the CLL samples with a variety of potentiation extend from CLL cell to another based on the activity of RG7388. Furthermore, the majority of the CLL cohort samples showed a synergistic effect with a combination of WIP1 inhibitor and RG7388 treatment except for

CLL307, which showed an overall additive to antagonistic effect with the combination treatment (-2.17) (Figure 4.10 A).

Table 4.3 summarises the mean ZIP score for each individual primary CLL sample in the cohort. The ZIP score determines whether the combination of WIP inhibitor with RG7388 had a synergistic or antagonistic effect. According to the ZIP synergy score results, the majority of the primary CLL samples showed a peak synergy range effect with combination of WIP1 inhibitor with RG7388 apart from CLL307. In contrast, looking to the peak ZIP synergy score, all of the CLL samples in the cohort showed a synergistic inhibition of the viability of the CLL cells with combination treatment of RG7388 and WIP1 inhibitor (Figure 4.10 B). Some of the CLL cells showed higher peak ZIP synergy score compared to the others (Table 4.3 B).

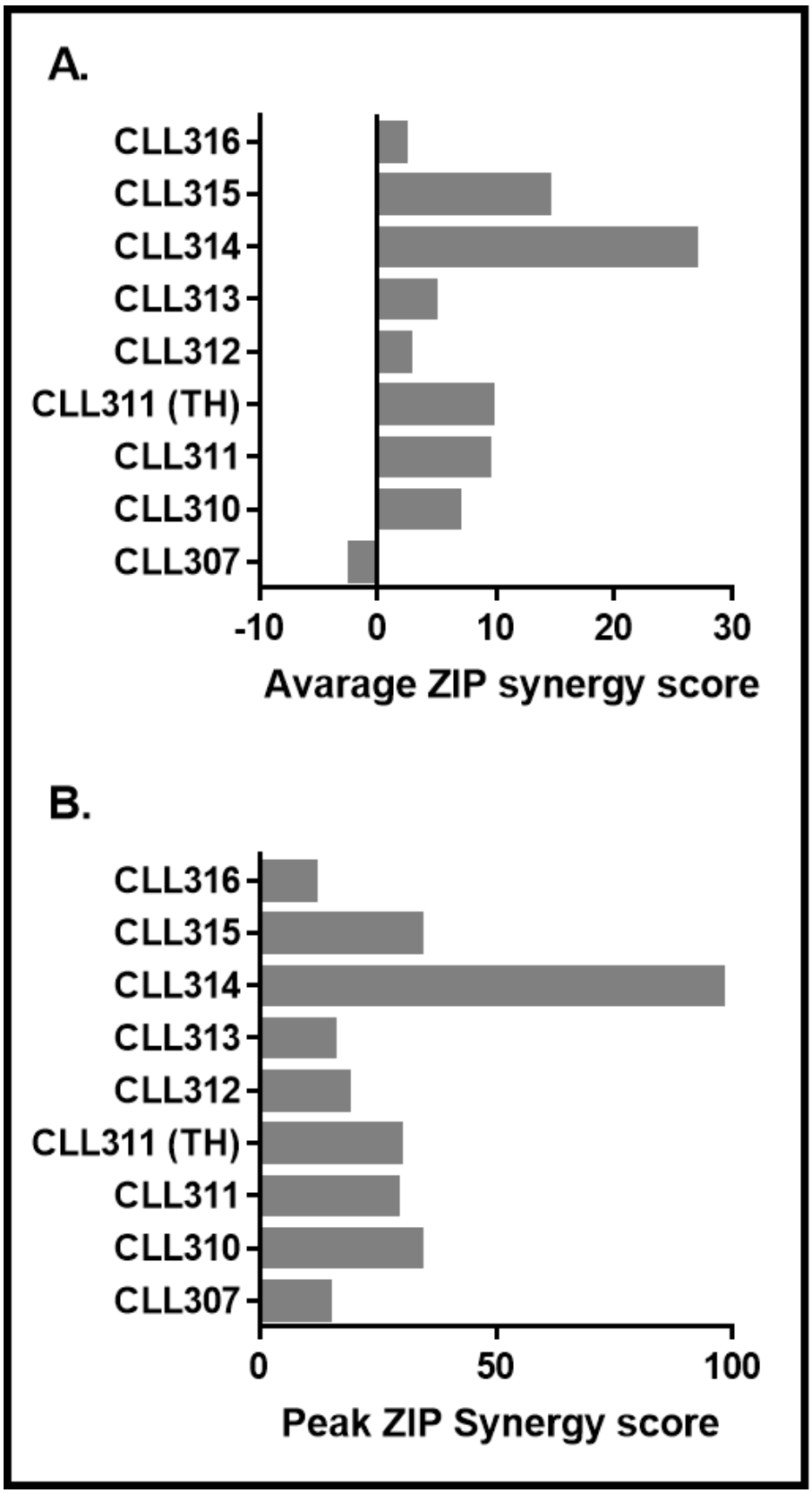

Figure 4.10 Summary of synergy score for RG7388 in combination with WIP1 inhibitor determined by zero interaction potency (ZIP) model. (A) ZIP synergy score of 11 primary CLL samples treated with ranges of concentrations of RG7388 and GSK2830371. Cohort of (n=11) CLL samples ($5x10^6$ cells/ml) treated with RG7388 and WIP1i in combination up to (10μM) for 48hours. The cell viability was determined by XTT assay. All the primary CLL samples were freshly isolated except for CLL311 sample, for which the experiment was performed on both fresh and thawed cryopreserved cells. (B) The peak ZIP synergy score of the same cohort of 11 primary CLL samples to determine the highest concentration at which the synergistic effect was generated with combination treatment. (TH) Thawed sample.

A.

Average ZIP score	RG7388+WIP1i
CLL 307	-2.17
CLL 310	6.75
CLL 311	9.27
CLL 311 (TH)	9.58
CLL 312	2.71
CLL 313	4.84
CLL 314	26.86
CLL 315	14.34
CLL 316	2.31

B.

Peak ZIP synergy score	RG7388+WIP1i
CLL 307	14.40
CLL 310	34.04
CLL 311	29.07
CLL 311 (TH)	29.61
CLL 312	18.49
CLL 313	15.45
CLL 314	97.54
CLL 315	34.04
CLL 316	11.51

Table 4.3 (A) **The average zero interaction potential (ZIP) score of CLL samples from combination treatment of MDM2 inhibitors (RG7388) with WIP1 inhibitor.** (B) The peak ZIP synergy score of WIP1 inhibitor with RG7388. (TH) Thawed sample.

4.4.7 MDM2 inhibitor (RG7388) induces p53 protein and its downstream targets in a concentration dependent manner in p53WT primary CLL samples

After identifying the cytotoxicity responses of CLL cells to combination treatment with RG7388 and WIP1 inhibitors, mechanistic studies were conducted by western immunoblotting to test for cellular changes in protein levels downstream of p53 under the same treatment conditions. The primary CLL cells were treated with both RG7388 and WIP1 inhibitor for 6 and 24 hours. The CLL cell lysates were collected following treatment with a range of RG7388 concentrations at the indicated time points. The changes in expression of p53 and its primary negative regulator MDM2, were compared relative to DMSO, together with the negative cell cycle regulator $p21^{WAF1}$. CLL apoptosis was assessed by the relative protein expression levels of full-length PARP and cPARP.

Figure 4.11 illustrates an example of a western immunoblot for primary CLL sample, CLL299 cells exposed to a range of RG7388 concentrations. Dose-dependent stabilisation of functional p53 was clearly evident, associated with an increase in the downstream transcriptional targets MDM2 and $p21^{WAF1}$ after 6 and 24 hours. Full-length PARP protein level was reduced with increased dose of RG7388 at 6 hours and further reduction was detected at 24 hours. In contrast, a gradual increase in the 85kDa cPARP protein level was detected at 6 and 24 hours of RG7388 treatment. The induction of 85kDa PARP cleavage product in a concentration-dependent manner with RG7388 indicates that the RG7388 treatment drives the CLL299 to cell death in a dose-dependent manner. The CLL299 cells expressed high basal cPARP level in the DMSO solvent controls thus, might be because the CLL299 is cryopreserved sample. This indicated the CLL cells might also be responding to a different background signalling mechanism to initiate the apoptosis. In addition, the CLL cell viability is limited in the absence of microenvironmental survival signals. Although, cPARP was detected in the CLL299 DMSO controls, the RG7388 treatment reduced the levels of full-length PARP protein in a concentration dependent manner. This likely reflects the RG7388 dependent induction of apoptosis in the viable cell sub-population. The β-Actin signal showed that there was equal total protein loading in all conditions.

The western immunoblot results of other four different primary CLL samples (CLL308, CLL309, CLL310, CLL311, CLL312, CLL313) treated with wide range of RG7388 for 6 and 24 hours are summarised in Figure 4.13.

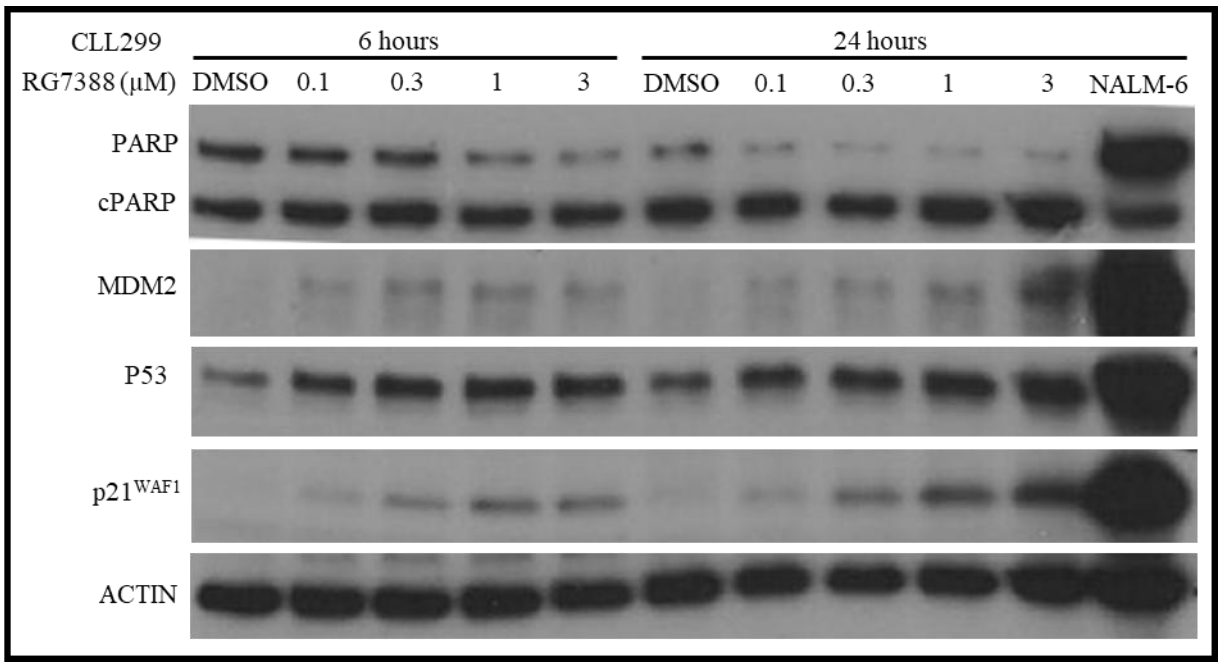

Figure 4.11 Western immunoblot of p53 and its transcriptional targets in response to MDM2 inhibitor (RG7388). Cryopreserved CLL299 cells were treated with a wide range of RG7388 for 6 or 24 hours. Wide range of RG7388, including the IC_{50} concentrations, used to determine the change in the TP53 protein and its target proteins. All strips were from the same membrane which was cut into three. The top strip was probed for WIP1, MDM2 and PARP; the middle for p53 and β-Actin; and the third with p21 antibody. β-ACTIN used as the loading control. The cell lysate was collected from (n=1) experiment. Nalm-6 ($TP53^{WT}$) cells treated with RG7388 for 6 hours were used as a positive control for molecular weight protein expression.

4.4.8 Changes in the anti-apoptotic proteins with stabilization of p53

A western immunoblot was performed on CLL308 primary cells to determine the downstream p53 target protein expression changes in response to RG7388. Moreover, this experiment included the detection of anti-apoptotic proteins MCL-1, BCL-2 and BCL-xL to assess whether these were altered in response to RG7388 treatment and might have an impact on cell survival.

Figure 4.12 shows primary CLL308 cells treated with wide ranges of RG7388 for 6 and 24 hours. RG7388 stabilised p53 protein and its transcriptional downstream target protein, MDM2 in a concentration-dependent manner. Although, the RG7388 treatment resulted with p53 stabilisation followed by MDM2 expression, the $p21^{WAF1}$ could not be detected in CLL308. Furthermore, the PARP cleaved protein was detected with high concentration of RG7388 at both 6 and 24 hours. Since the signal for the cPARP protein was very faint in CLL308, we decided to investigate the level of anti-apoptotic proteins.

Looking to the anti-apoptotic proteins MCL-1, BCL-2 and BCL-xL, the primary CLL308 cells did not show any obvious changes in the MCL-1 protein levels with different treatment conditions. However, BCL-2 level increased with RG7388 treatment at 6 and 24hr time points

relative to DMSO (Figure 4.12 A). CLL303, included as a control for molecular weight location, showed changes in the protein level of BCL-xL in response to RG7388 (3μM) compared to the DMSO (Figure 4.12 A).

The densitometry analysis of MCL-1 showed no change in response to RG7388 relative to DMSO at 6 hours treatment. In comparison at 24 hours, MCL-1 showed increase in the protein expression in response to range of RG7388 concentrations relative to DMSO (Figure 4.12 C). The densitometry analysis of BCL-2 showed increase in the protein expression in response to range of RG7388 concentrations relative to DMSO at 6 and 24-hours (Figure 4.12 C). Moreover, BCL-xL protein level showed no change in response to RG7388 at both 6 and 24-hours treatment. The densitometry analysis of BCL-xL protein showed no change in response to RG7388 (1-3μM) at both 6 and 24-hours relative to DMSO treatment (Figure 4.12 B-D).

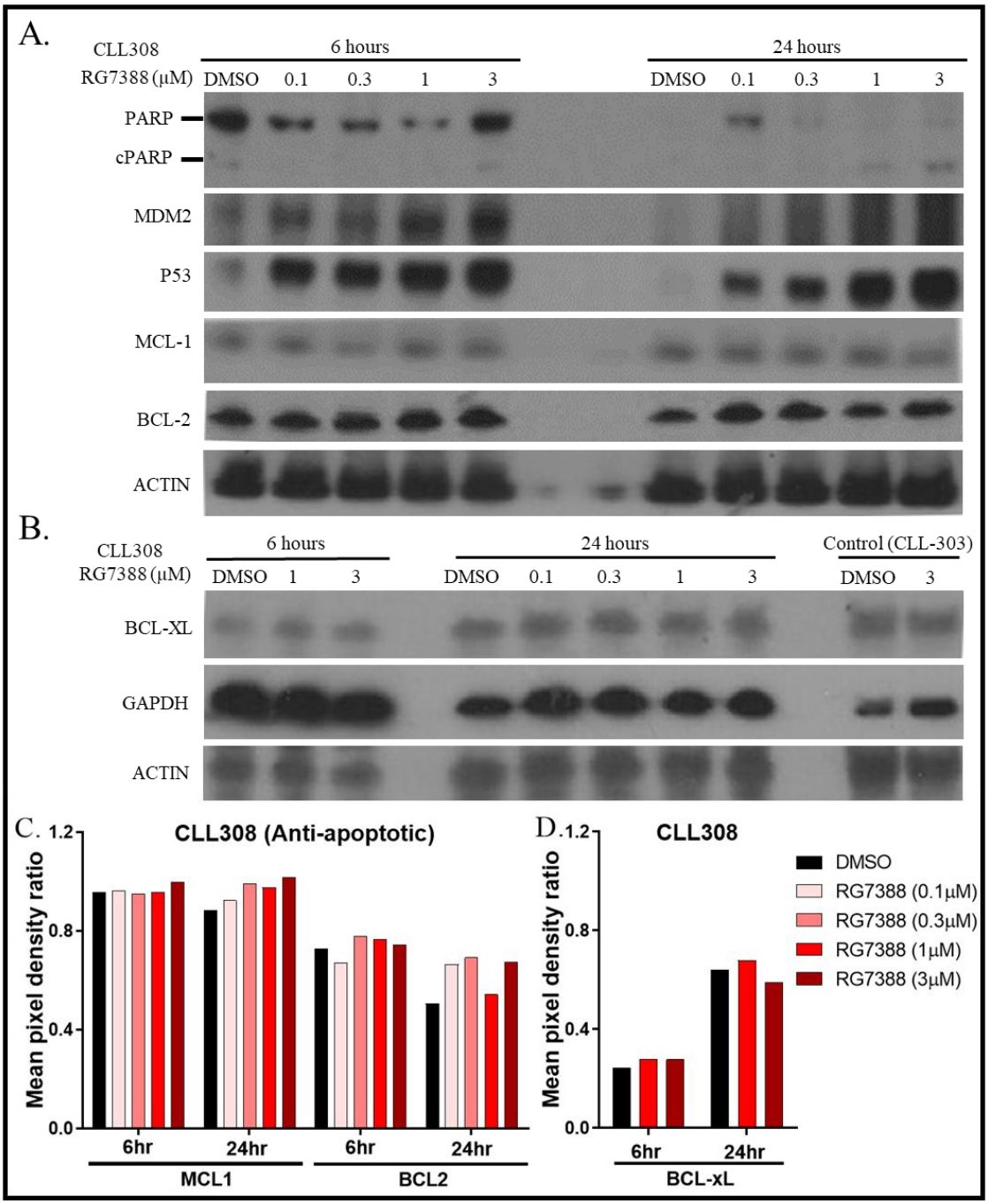

Figure 4.12 Western immunoblot of CLL308 cells treated with RG7388. (A) Stabilization of p53 and its transcriptional target MDM2, and Anti-apoptotic (MCL1, BCL1) at 6 and 24 hours. Range of RG7388, including the IC_{50} concentration, was used to determine the change in the target proteins. (B) The expression of BCLxL protein level in response to the RG7388 at 6 and 24 hours. CLL303 used as control for antibody marker. All antibodies were probed on the same membrane except for BCL-xL was detected on new membrane from the same lysate. GAPDH and β-Actin used as the loading control. (C) Densitometry of MCL1 and BCL2 proteins corresponding to the expression level in response to RG7388 concentrations. (D) Densitometry of BCL-xL protein level at 24hr compared to 6hr in response to RG7388. The mean pixel density ratio for all proteins was background corrected and the values were normalized relative to β-Actin. The cell lysate was collected from freshly isolated CLL308 (n=1) experiment.

4.4.9 The stabilization of p53 activity by the MDM2 inhibitor (RG7388) induces the apoptotic protein marker (cPARP) in p53WT primary CLL samples

Western immunoblotting was routinely performed on primary CLL samples to investigate the changes in p53 protein levels and that of p53 transcriptional target genes in response to RG7388 treatment. The densitometry provided a summary measurement of the p53 functional status of the patient CLL samples. In addition, to the ability of RG7388 to activate p53, the ability to induce apoptosis with an MDM2 inhibitor in the primary CLL cells was determined. Freshly isolated CLL cells were treated with a range of RG7388 concentrations for 6 and 24 hours. The CLL cells were harvested immediately with SDS lysis buffer at the end of the time point.

Figure 4.13 summarises the western immunoblotting results for seven different primary CLL samples (n=7) were treated with a range of RG7388 concentrations for 6 or 24 hours. In addition, DMSO solvent vehicle treatment alone was included as a control. Extracts from NALM-6 (*TP53*^{WT}) cells treated with RG7388 for 6 hours were also included as a positive control to check that the antibodies were working and the correct position of signals

It can be seen that RG7388 results in stabilisation of p53 protein expression and induction of MDM2 in a concentration-dependent manner at 6 and 24 hours. p21^{WAF1} protein level showed an increase in response to RG7388 concentrations relative to DMSO treatment control. The expression of full-length PARP was reduced with RG7388 treatment over time while, the cPARP was increased. The increase of cPARP in a concentration dependent manner indicated that apoptosis occurred in the CLL cells in response to p53 stabilisation and activation by RG7388.

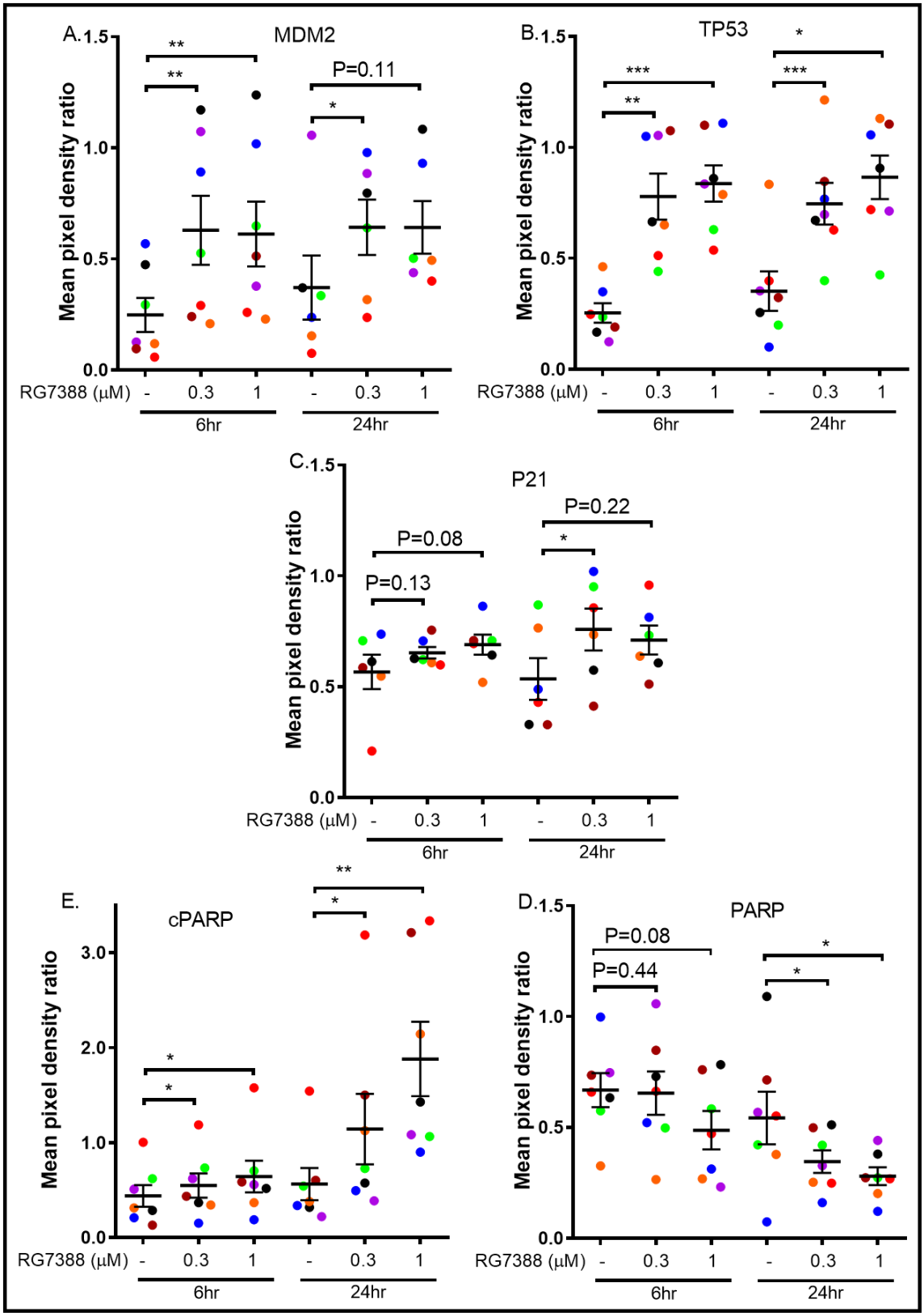

Figure 4.13 Summary of western immunoblot densitometry changes for TP53 and it's target proteins of CLL cells in response to RG7388. Different primary CLL samples (n=7) treated with RG7388 (0.3 and 1μM) for 6 and 24 hours. The immunoblot for each sample was performed on lysate (n=1) times. (A) MDM2 (B) TP53 (C) P21 (D) PARP full-length (E) cPARP. The mean pixel density ratio for all proteins was background corrected and the values were normalized relative to GAPDH, except cPARP for which the ratio was calculated relative to full-length PARP. Each colour represents primary CLL sample. The error bar represents the average mean ±SEM for all CLL samples. Statistical significance of differences (*, $p < 0.05$, ** $p < 0.005$, ***, $p < 0.0005$) is shown above each bar for each treatment compared with DMSO control. Only the p-values less than 0.05 are shown by paired t-test one tail.

4.4.10 WIP1 inhibitor induces the stabilization of MDM2 inhibitor (RG7388) in p53-dependent manner through phosphorylation of p53WT of CLL samples

In Figure 4.14, the western blot was performed on primary CLL313 cells to determine the effect of RG7388 in combination with GSK2830371 WIP1 inhibitor on p53 and p53-target gene protein expression. The CLL313 cells were incubated with range of RG7388 concentrations in combination with WIP1 inhibitor (2.5μM) for 6 and 24 hours. The changes in the protein levels in response to RG7388 and WIP1 inhibitor treatment were examined relative to the signals in DMSO control. The densitometry analysis illustrated the change in the protein expression in response to the treatment at 6 and 24 hours (Figure 4.14 B&C).

The RG7388 treatment for 6 and 24 hours stabilised and activated p53 in a concentration dependent manner. In addition, combination with the WIP1 inhibitor further increased the stabilization of p53, particularly at lower doses of RG7388. Combination of WIP1 inhibitor with the lower concentration of RG7388 (0.1μM) increased the level of total p53 protein. However, the combination of WIP1 inhibitor with higher RG7388 concentrations, (0.3, 1μM) showed a slight reduction in p53 expression, this is likely to be due to the CLL cell death at the higher doses.

There was an increase in the phosphorylation of p53 in parallel to total p53. Firstly, with a single effect of RG7388, there was a concentration dependent induction of p53 phosphorylation. In addition, on combination with WIP1 inhibitor, a concentration dependent increase in p53 phosphorylation with RG7388 was seen. The densitometry analysis showed concentration dependent increase in phosph-p53 protein expression with combination of RG7388 with WIP1 inhibitor (Figure 4.14 B&C). The increase in phosph-p53 was again more evident in combination of with the lowest dose of RG7388 (0.1μM) compared to higher concentrations.

MDM2 protein was induced with the RG7388 and WIP1 inhibitor at 6 hours but surprisingly not at 24 hours. $P21^{WAF1}$ was very faint to detect at both time points. WIP1 protein levels were reduced by the WIP1 inhibitor treatment at 6 and 24 hrs exposure. Moreover, WIP1 inhibitor (2.5μM) was sufficient to degrade the WIP1 protein and prevents its catalytic activity, resulting in increased levels of p53 phosphorylation.

PARP cleavage was induced with RG7388 as a single agent and in a combination with WIP1 inhibitor in a concentration dependent manner. In addition, the combination of RG7388 (0.1μM) with WIP1 inhibitor produced a greater increase in PARP cleavage than at the higher

concentrations. GAPDH was used as endogenous loading control for protein concentrations across the wells of different conditions which were equally loaded.

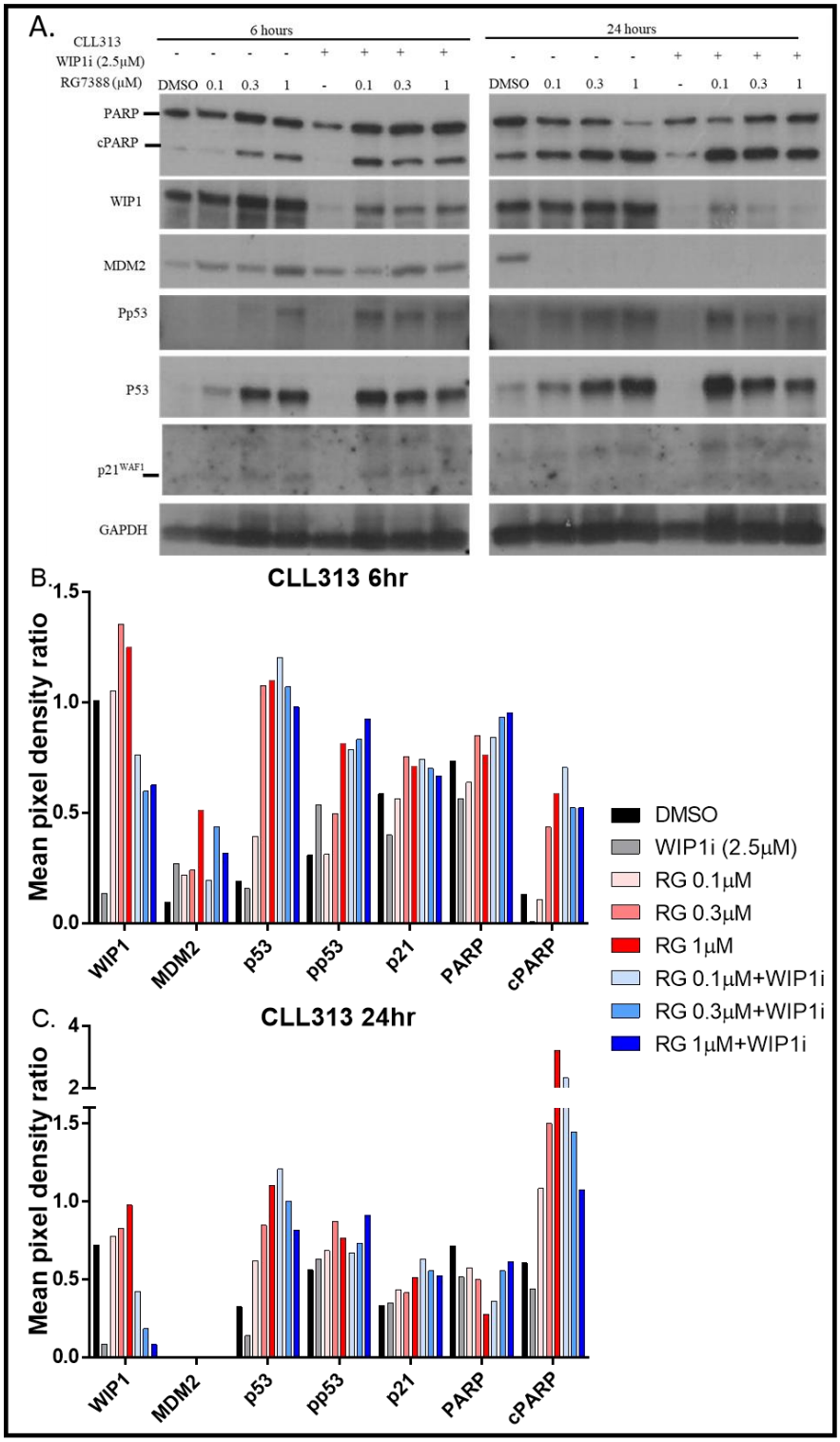

Figure 4.14 Western immunoblotting of primary CLL313 treated with RG7388 and WIP1 inhibitors at 6 and 24 hours. (A) The expression of p53 and it's target proteins in response to range of RG7388 alone and in combination with GSK2830371 (2.5μM). Doses of RG7388 includes the LC_{50} concentration. (B) Densitometry measure of TP53 and it's transcription target protein in response to treatment at 6 and (C) 24 hours. The experiment performed on fresh extracted lysate (n=1). Both time point treatments were performed in the same condition next to each other on separate membranes. GAPDH used as an endogenous control. The mean pixel density ratio for all proteins was background corrected and the values were normalized relative to GAPDH, except cPARP for which the ratio was calculated relative to full-length PARP. Gradual red colour represents the RG7388 alone and the gradual blue ones represents the combination of WIP1i.

4.4.11 Transcriptional changes in response to RG7388

To investigate the potential changes in the mRNA expression of p53 target genes, pro-apoptotic and anti-apoptotic genes for primary CLL cells in response to MDM2 inhibitor using the qRT-PCR technique. The extracted mRNA samples were collected from the CLL308 primary sample after 6 and 24 hours of RG7388 treatment. The change in the transcript levels of the p53 target genes for RG7388 treatment was calculated by the ΔΔCt method relative to DMSO control and the β-Actin reference gene Ct values for each corresponding treatment condition.

Following 6 hours treatment (Figure 4.15 A) with RG7388, the mRNA expression of the pro-apoptotic genes, *PUMA*, *BAX* and *FAS* was increased. Interestingly, the fold change expression of *PUMA* is already maximal at the lowest dose of RG7388, with a very high level of induction. In addition, *MDM2*, the p53 negative regulatory gene, showed a concentration dependent high fold increase in mRNA expression. In contrast, the anti-apoptotic genes, *MCL1* and *BCL2*, did not show a significant change in their mRNA expression with RG7388 treatment at 6 hours.

(Figure 4.15 B) shows that exposing CLL308 to RG7388 for 24 hours increases the fold change mRNA expression of *MDM2* and *TP53INP1* in a concentration dependent manner. Moreover, mRNA expression of the pro-apoptotic genes also increased with RG7388 concentration. For the anti-apoptotic gene levels, *MCL1* and *BCL2*, there was a reduction in the mRNA level with RG7388 treatment for (0.1-1μM) doses, however, there was slight increase in the mRNA expression with RG7388 (3μM). Although, the Ct value of the *BCL2* expression in response to RG7388 (3μM) did not show much differences from the Ct value of the DMSO, the RQ calculation identified the fold change differences relative to β-Actin normalization.

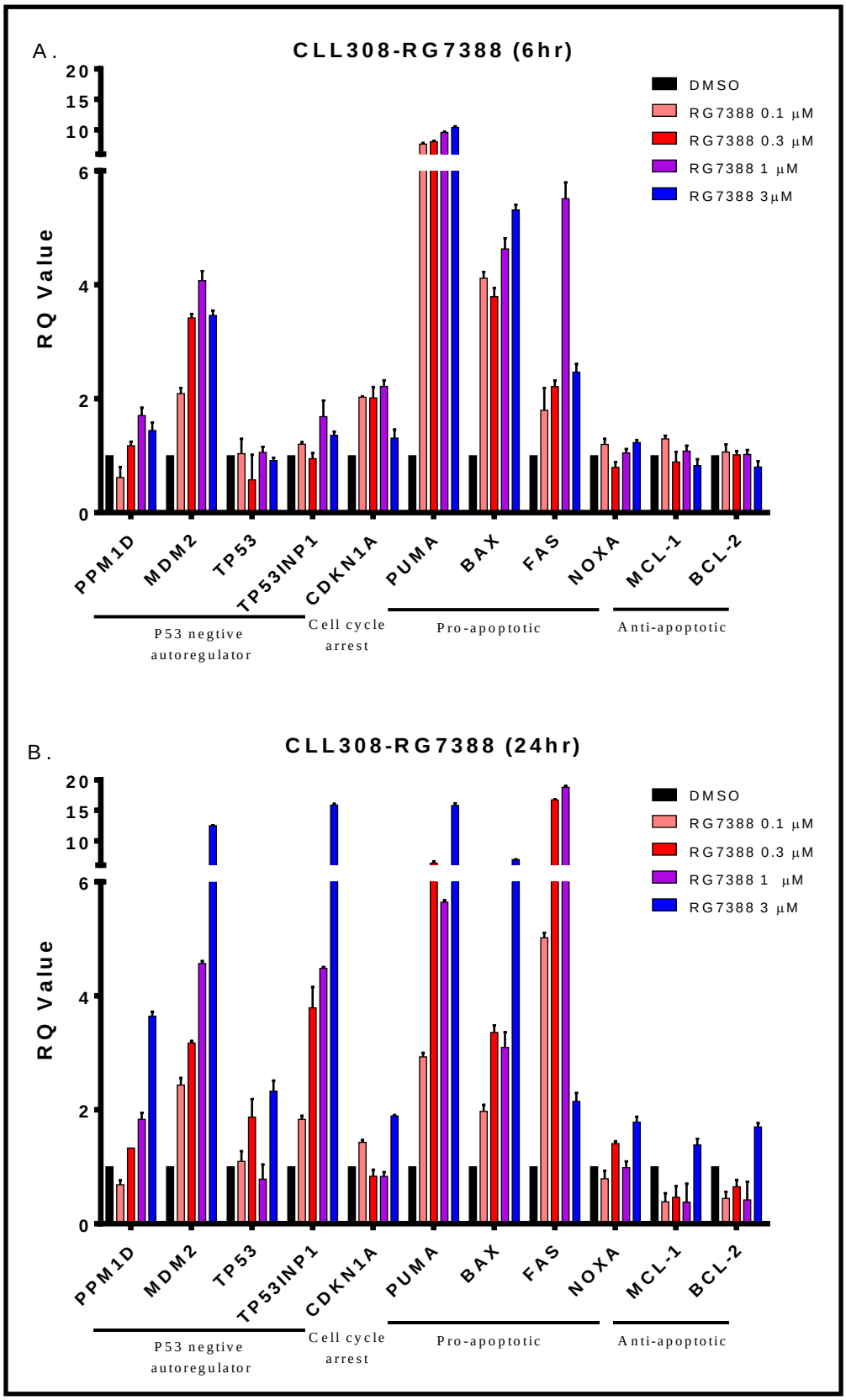

Figure 4.15 Fold change in mRNA expression of selected p53 transcriptional target genes of primary CLL308 sample with *ex-vivo* treatment of RG7388 by qRT-PCR. (A) 6 hours (B) 24 hours. Freshly isolated CLL cells treated with wide range of RG7388 concentrations. *β-ACTIN* was used as the endogenous control and DMSO-treated cells were used as the calibrator between three repeated wells of each concentration. Error bars represent the mean ± SEM of intra-replicate wells of the experiment (n=1). RQ values were calculated using the formula 2ΔΔCt.

Figure 4.16 shows a summary comparison of the transcriptional changes in CLL308 with RG7388 at 6 and 24 hours alongside each other in more detail for each group of genes. Upon RG7388 treatment, the mRNA expression of p53-dependent target genes, *MDM2* and *TP53INP1* showed a concentration dependent increase with RG7388 treatment. At 6-hour treatment, the mRNA expression of the p53 negative regulators, *PPM1D*, *MDM2* and *TP53INP1* showed fold change increases and further induction was detected at 24 hours. (C&D) *CDKN1A* surprisingly did not show much change in expression at either 6 or 24 hours. (E&F) Furthermore, the pro-apoptotic genes, *PUMA*, *BAX* and *FAS* all showed increases in mRNA expression at 6 hours and further increases in expression at 24 hours, however the mRNA levels of *NOXA* did not change appreciably. *PUMA* showed the highest fold change in expression at 6 hours and *FAS* showed the highest fold change in expression with RG7388 treatment for 24 hours. (G&H) For the anti-apoptotic genes, the mRNA expression of *MCL1* and *BCL2* showed no change in response to RG7388 at both 6 and 24 hours.

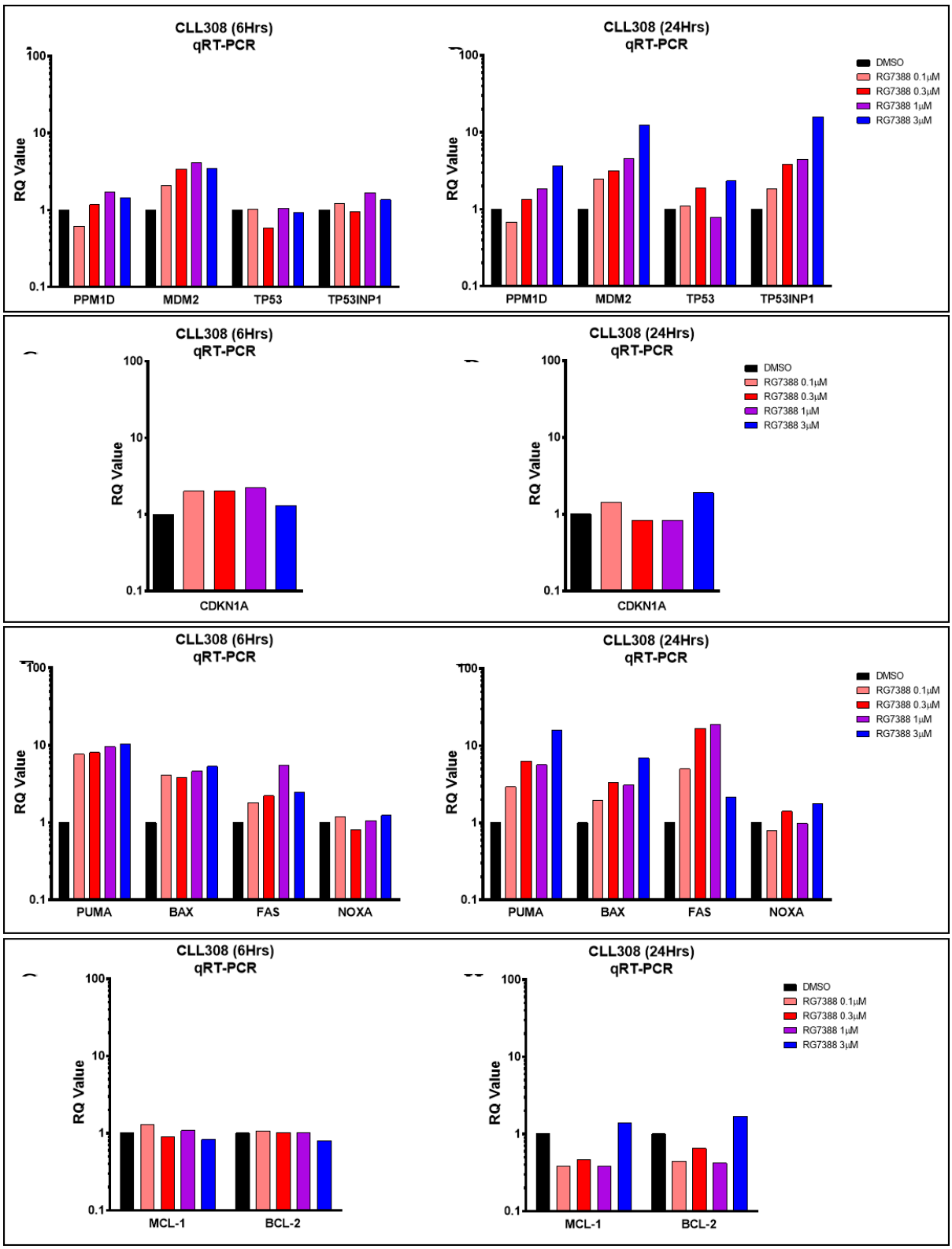

Figure 4.16 Summary of fold changes in the mRNA expression of CLL308 after exposure to RG7388 for 6 or 24 hours. (A-B) Negative regulator p53 genes, *PPM1D*, *MDM2*, *TP53* and *TP53INP1*. (C-D) *CDKN1A* (E-F) Proapoptotic genes, *PUMA*, *BAX*, *FAS* and *NOXA*. (G-H) Anti-apoptotic genes, *MCL1* and *BCL2*. Freshly isolated CLL cells treated with range of RG7388 concentrations for indicated time point followed by qRT-PCR analysis. *β-ACTIN* was used as the endogenous control and DMSO-treated cells were used as the calibrator between three repeats of each concentration. Error bars represent the mean ± SEM of three intra-replicate wells of the experiment (n=1). RQ values were calculated using the formula 2ΔΔCt.

4.4.12 Transcriptional changes in response to RG7388 in combination with WIP1 inhibitor

To investigate the potential changes of p53 target genes in response to the MDM2 inhibitor with a combination of WIP1 inhibitor in functional *TP53* CLL samples, the chosen gene panel was assessed using the qRT-PCR technique. The extracted mRNA was collected from the primary CLL313 after 6 and 24 hours of RG7388 with a combination of WIP1 inhibitor (2.5μM). The fold changes (RQ) in the mRNA levels of the p53 target genes was calculated using the ΔΔCt method relative to DMSO only treatment with normalisation to β-Actin expression for each corresponding condition. The Ct value of DMSO and β-Actin did not change significantly with any of the conditions.

(Figure 4.17 A) shows the mRNA expression of gene panel for CLL313 treated with RG7388 in combination with WIP1 inhibitor for 6 hours. The mRNA expression of the pro-apoptotic genes, *PUMA*, *BAX* and *FAS* were increased by combination treatment of WIP1 inhibitor with RG7388 compared to single agent treatment with RG7388. Furthermore, the expression of p53 negative regulator genes, *MDM2*, *TP53INP1* and *CDKN1A* were all increased by combination treatment of WIP1 inhibitor with RG7388 relative to RG7388 alone. In contrast, the anti-apoptotic genes, *MCL1* and *BCL2* did not show much difference in expression either with single or combination treatment.

After 24 hours of treatment (Figure 4.17 B), the pro-apoptotic genes, *PUMA*, *BAX* and *FAS* showed the highest increases in expression among the gene panel. Interestingly, the combination treatment of WIP1 inhibitor with RG7388 (0.1μM) increased expression of *PUMA*, *BAX* and *FAS* relative to treatment with RG7388 (0.1μM) alone. In contrast, the combination of WIP1 inhibitor with RG7388 at the higher doses (0.3 and 1μM) inhibited the induction of *PUMA*, *BAX* and *FAS* mRNA expression.

Similarly, the expression of *MDM2*, *TP53INP1* and *CDKN1A* was increased by combination treatment of WIP1 inhibitor with RG7388 (0.1μM) relative to RG7388 (0.1μM) alone. However, again the combination of WIP1 inhibitor with higher concentrations of RG7388 (0.3 and 1μM) reduced *MDM2*, *TP53INP1* and *CDKN1A* mRNA expression. This might be because the strong efficiency of WIP1 inhibitor to potentiate the activity of RG7388 at low concentration. Thus, the combination with high concentration of RG7388 with WIP1 inhibitor might be toxic and killing all cells. It can be obviously seen from (Figure 4.6) that the combination of WIP1 inhibitor significantly potentiated the effect of RG7388 in a concentration dependent manner.

Looking to the anti-apoptotic genes, *MCL1* and *BCL2*, they did not show much difference in their expression either with single or combination treatment for 24 hours.

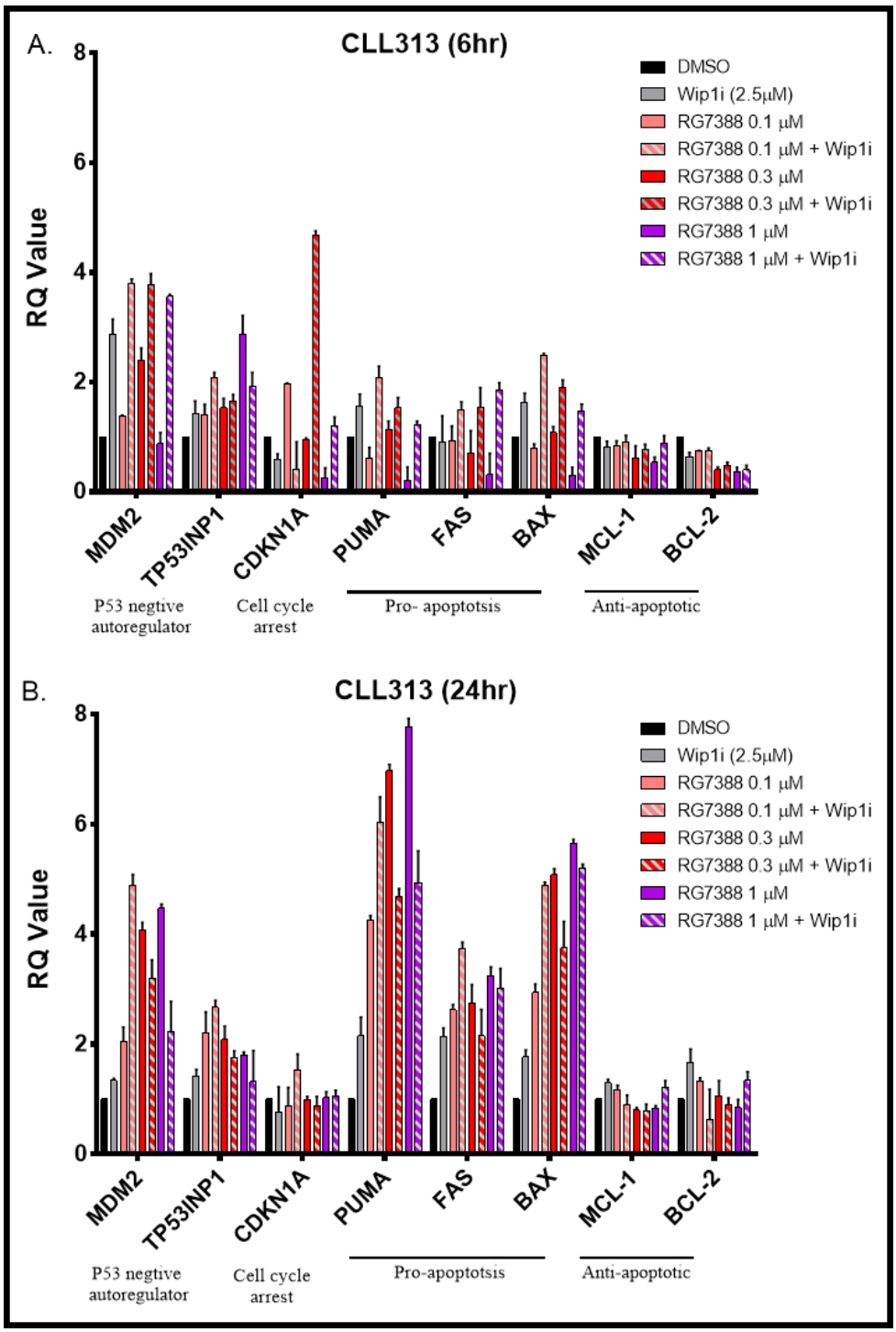

Figure 4.17 Fold changes in the expression of gene panel for primary CLL313 was exposed *ex-vivo* to RG7388 and WIP1 inhibitor. (A) CLL cells treated for 6 hours and (B) 24 hours. qRT-PCR measures the mRNA expression of genes panel was measured in response to RG7388 (0.1, 0.3, 1 and 3μM) and in a combination with GSK2830371 at (2.5 μM) relative to DMSO solvent control (untreated condition). The striped columns represent the combination treatment while the solid columns represent the single treatment. *β-ACTIN* was used as the endogenous control and DMSO-treated cells were used as the calibrator between three repeats of each concentration. Error bars represent the mean ± SEM of three intra-replicate wells of the experiment (n=1). The RQ value represents the fold change expression of the p53 target genes relative to the ΔΔCt for DMSO treatment and *β-ACTIN*.

Figure 4.18 shows the transcriptional changes in CLL313 induced by RG7388 in combination with WIP1 inhibitor at 6 and 24 hours alongside each other in more detail for each group of genes. (Figure 4.18 A&B) showed the fold changes in the transcriptional level of p53 negative regulator genes, *MDM2* and *TP53INP1*. *MDM2* showed a concentration-dependent increase in mRNA expression in response to RG7388 in combination with WIP1 inhibitor at 6 hours. On further extension of the treatment to 24 hours, the combination of WIP1 inhibitor with RG7388 (0.1μM) potentiated the increased expression of *MDM2*. However, the combination of WIP1 inhibitor with RG7388 (0.3 and 1μM) reduced expression. *TP53INP1* showed little change in expression with the combination of WIP1 inhibitor and RG7388 (0.1 and 0.3μM), however, with higher concentration of RG7388 (1μM) and WIP1 inhibitor the *TP53INP1* there was a reduction in the mRNA relative to RG7388 (1μM) alone.

Looking to the cell cycle arrest gene (Figure 4.18 C&D), *CDKN1A* showed a high increase in mRNA expression with combination treatment of WIP1 inhibitor with RG7388 at 6 hours compared to 24 hours. In addition, CLL313 expressed more *CDKN1A* with combination treatment of WIP1 inhibitor with RG7388 compared to RG7388 alone. The combination of WIP1 inhibitor potentiated the expression of RG7388 at 6 and 24 hours.

The pro-apoptotic genes (Figure 4.18 E&F), *PUMA*, *BAX* and *FAS* showed expression increases in response to RG7388 in combination to WIP1 inhibitor at 6 hours and further induction at 24 hours.

For the anti-apoptotic genes (Figure 4.18 G&H), the mRNA expression of *MCL1* and *BCL2* showed no changes in response to the combination of WIP1 inhibitor with RG7388 at 6 and 24 hours. This is consistent with *MCL1* and *BCL2* not being directly transcriptionally regulated by p53.

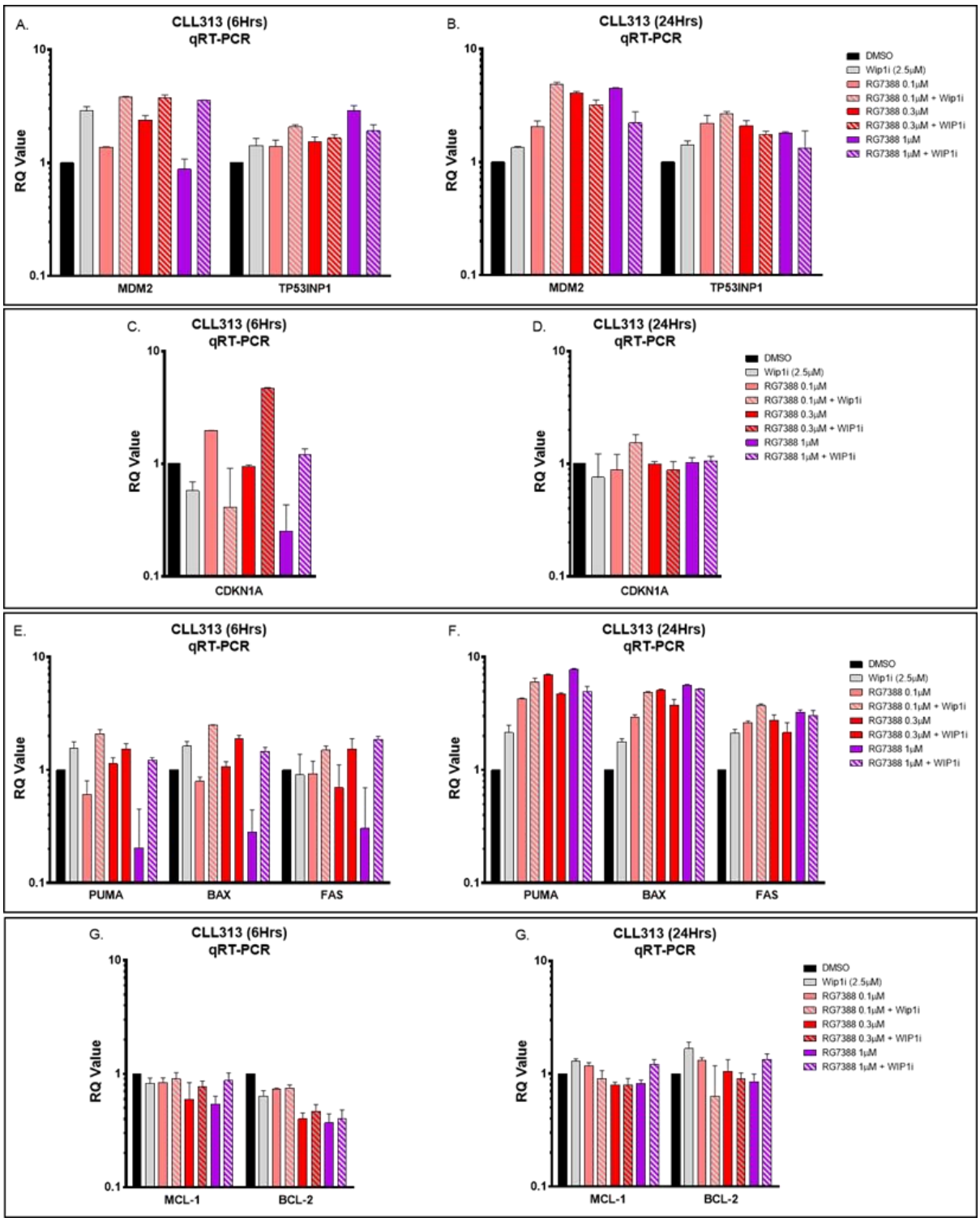

Figure 4.18 Summary of the fold changes in the mRNA expression of selected p53 transcriptional target genes of CLL313 in response to a combination of RG7388 with WIP1 inhibitor by qRT-PCR. (A-B) Negative regulator p53 genes, *PPM1D*, *MDM2*, *TP53* and *TP53INP1*. (C-D) Cell cycle arrest, *CDKN1A* (E-F) Pro-apoptotic genes, *PUMA*, *BAX*, *FAS* and *NOXA*. (G-H) Anti-apoptotic genes, *MCL1* and *BCL2***.** mRNA expression of p53 transcriptionally regulated genes were determined in response to range of RG7388 (0.1, 0.3, 1μM) with and without GSK2830371 (2.5 μM) 6 and 24 hours relative to DMSO solvent control (untreated condition) and *β-ACTIN* control. Each concentration repeated in three wells intra-excrement. Error bars represent the mean ± SEM of three intra-replicate wells of the experiment (n=1). The striped columns represent the combination treatment while the solid columns represent the single treatment.

4.5 Discussion

The survival outcome of CLL cells in response to p53 stimulation signals depends upon the strength of upstream cellular receptors and auto-regulatory signals in the upstream p53 pathway network and the balance of pro-apoptotic and anti-apoptotic proteins in the downstream pathway.

In this chapter, a cohort of 11 primary CLL samples were exposed to the MDM2 (RG7388) and WIP1 (GSK2830371) inhibitors as a single agent and in combination to determine the effect on CLL cell viability. A wide range of GSK2830371 and RG7388 concentrations were used to investigate the inhibitory effect of the treatment on the viability of primary CLL cells. Up to 10μM of WIP1 inhibitor alone showed around 40% inhibition effect on the viability of primary CLL cells. However, concentrations up to 3μM of WIP1 inhibitor alone showed no inhibitory effect on CLL cell viability (data not shown). Therefore, WIP1 inhibitor at (2.5μM) was chosen as the highest concentration that alone does not have any effect on the cell viability (Figure 4.2). A similar response effect for GSK2830371 as a single agent for doses up to (2.5μM) have been found by our group on a wide variety of cancer cell lines irrespective of p53 status, as long as they are not mutated or amplified for *PPM1D* (Chamberlain et al., 2021; Esfandiari et al., 2016; Wu et al., 2018, 2021). However, GSK2830371 suppresses cell growth in cells with increased PPM1D expression or mutations, with IC_{50} values below (4μM). This effect was not observed in p53 mutant cells (such as BT474) that nevertheless had amplified WIP1 (Esfandiari et al., 2016; Gilmartin et al., 2014). Several studies have shown that GSK2830371 can enhance the effectiveness of MDM2 inhibitors in $p53^{WT}$ cell lines (Esfandiari et al., 2016; Wu et al., 2018, 2021). As a result, it was speculated that GSK2830371 might have a similar effect on CLL cells when combined with MDM2 inhibitors. The results presented in this Chapter are in line with previous finding studies, which had demonstrated that at a concentration of (2.5μM), GSK2830371 can significantly boost the inhibitory effects of RG7388 and other MDM2 inhibitors to increase the mRNA expression of genes that are targets of p53 driven transcription (Wu et al., 2018; Esfandiari et al., 2016; Chamberlain et al., 2021).

The novelty of this study is the investigation of the combination effect of WIP1 and MDM2 inhibitors has not been previously reported for CLL. In the studies, we reported RG7388 as a single agent showed a concentration dependent inhibition of the viability of CLL cells, as previously described (Ciardullo et al., 2019). The combination effect of WIP1 inhibitor and

RG7388 potentiated the concentration dependent ability of RG7388 to reduce CLL cell viability.

Results from the matrix design experiments showing the synergistic effect for the majority of the CLL samples with the combination treatment (Figure 4.10). A decrease in viability of the primary CLL cells was seen with the combination treatment. In addition, the average ZIP synergy score indicating positive synergy was observed in all the primary CLL samples of the cohort (>10) apart from CLL307, for which there appeared to be an antagonistic effect (-2.17) (Figure 4.10 A) (Table 4.3).

The western immunoblot results showed that RG7388 stabilises the activity of p53 protein and increases the protein levels of its known transcriptional target genes, MDM2 and WIP1 in a concentration dependent manner at 6 and 24 hours. The expression level of $p21^{WAF1}$ protein was very faint to be detected in the cohort of CLL samples (Figure 4.13). Jihyun Lee found that $p21^{WAF1/CIP1}$ is involved in a negative regulation of p53 protein stability in several types of cancer cells by forming a complex with p53, leading to an increase in p53 degradation (J. Lee et al., 2021).

cPARP was induced and the total PARP was decreased with RG7388 in a concentration-dependent manner for both 6 and 24 hour time points, showing evidence of apoptosis (Figure 4.13). Furthermore, the anti-apoptotic protein level showed no change in MCL-1 in response to RG7388 at 6 and 24 hours. However, the level of BCL-2 increased in response to RG7388 for 6 hours and decreased with 24 hours treatment. Moreover, BCL-xL protein level increased in response to RG7388 for 24 hours (Figure 4.12).

Interestingly, the expression of the anti-apoptotic genes, *MCL1* and *BCL2* did not change with 6 hours treatment of RG7388, showing these genes not to be regulated by p53 activation in primary CLL cells (Figure 4.16 G). In contrast, both *MCL1* and *BCL2* genes showed decrease in their expression with RG7388 treatment except with RG7388 (3μM) which showed a 2-fold change in response to at 24 hours (Figure 4.16H).

Following treatment with MDM2 inhibitor in combination with GSK2830371, cPARP protein level was increased relative to single agent treatment with RG7388, indicating that at low doses there is insufficient activation of p53 and/or suppression of its negative regulators resulting from MDM2 inhibitor treatment alone and that this can be further enhanced by combination with WIP1 inhibition to increase the induction of apoptosis in CLL cells (Figure 4.14).

For the mRNA transcriptional messages, MDM2 inhibitor (RG7388) alone showed concentration dependent increases in mRNA expression for the p53 negative feedback regulator genes, *PPM1D*, *MDM2*, *TP53INP1* at both 6 and 24 hours (Figure 4.15 A&B). The mRNA expression of *MDM2* was increased up to 4-fold in response to RG7388 at 6 hours and furthermore with longer treatment for 24 hours, *MDM2* and *TP53INP* showed 15-fold increases in mRNA expression in a concentration dependent manner. Moreover, the pro-apoptotic genes, *PUMA*, *BAX* and *FAS* genes showed fold change increases in a concentration dependent manner with RG7388 alone and in combination of WIP1 inhibitor at both 6 and 24 hours, providing evidence for their mechanistic involvement in the increased cytotoxicity (Figure 4.18 E&F).

Interestingly, following the combination treatment of RG7388 with GSK2830371, the expressions of some of the negative regulator p53 transcriptional target genes; *MDM2*, *TP53INP1* and *CDKN1A***;** were also further induced in comparison to the single agent treatment of RG7388. All of the increases in expression were by more than 2-folds (Figure 4.18 A&C). However, the negative feedback of MDM2 and WIP1 induction is futile in the presence of the continued presence of the RG7388 and WIP1 inhibitors, thus, tipping the balance of transcriptional changes in favour of increased pro-apoptotic gene expression.

Chamberlain et al reported in her study of $p53^{WT}$ uLMS cells that the transcript levels of *CDKN1A* were significantly increased with increased p53 activation following the combination treatment. In addition, the mRNA expression of coupled pro-apoptotic genes, *PUMA*, *FAS* and *NOXA* were increased consistent, with the increased p53 transcriptional activity pushing the cells into apoptosis (Chamberlain et al., 2021). Similar findings were reported by Wu et al. for the combination treatment of cutaneous melanoma cell lines with RG7388 and GSK2830371 (Wu et al., 2018).

The results presented in this chapter show that MDM2 inhibitors stabilise and increase the activity of p53, and that inhibiting WIP1 phosphatase amplifies the p53 activation signals. Thus, the effect of the MDM2 and WIP1 inhibitors on the induction of pro-apoptotic genes is concluded to be the key regulator for driving the CLL cells into apoptosis, out-competing the anti-apoptotic proteins BCL-2 and MCL-1, which act downstream of p53. As a single agent treatment, MDM2 inhibitor (RG7388) reduced CLL cell viability in a concentration dependent manner and this was shown to be potentiated by inhibition of WIP1 by GSK2830371, even though alone GSK2830371 show little or no effect on the CLL cell viability. In addition, reduction in total PARP along with an increase in the expression of the cleaved-PARP apoptotic marker, was observed with RG7388 as a single agent and this was

further increased with the combination treatment. Moreover, the significant increase in the mRNA expression of pro-apoptotic genes, *PUMA*, *FAS* and *NOXA* indicated a sustained increase in the activation of p53 transcriptional activity driving the CLL cells into apoptosis.

On combination treatment, there was a induction in the transcriptional level of *CDKN1A*, indicative of increased p53 activation (Figure 4.18 C&D), however in the context of the experiments described in this chapter, the antiproliferative $p21^{WAF1}$ protein encoded by *CDKN1A* had no obvious role for *ex-vivo* non-proliferating CLL cells. The *ex-vivo* modelling of proliferative *in-vivo* micro-environmental signals and their potential effect on the response to MDM2 inhibitor treatment is addressed in subsequent chapters.

In conclusion, GSK2830371, as a single agent treatment had no or little inhibitory effect on the viability of the primary CLL cells. In contrast, MDM2 inhibitor, RG7388 showed concentration dependent inhibition effect on the functional p53 CLL cells. Furthermore, in the combination treatment, WIP1 inhibitor potentiated the activity of RG7388 to stabilises the cytotoxic activity, protein expression and selected p53 target genes of p53-functional CLL cells.

Chapter 5: CLL Co-cultured with Fibroblast Cells Expressing CD40L

5.1 Introduction

CLL patients have very variable clinical outcomes due to the heterogenous nature of the disease (Messmer et al., 2005). Primary CLL cells are non-proliferative cells *in-vitro* unless they are activated by the presence of microenvironmental stimulation factors. Thus, several drug testing and therapeutic studies use different *in-vivo* signals to enhance the CLL cells survival and proliferation in culture (Buggins et al., 2010; Ferretti et al., 2011; Herishanu, Pérez-Galán, et al., 2011; Patten et al., 2008). Recently, a variety of co-culture model systems have been developed to mimic the *in-vivo* CLL microenvironment toward the survival and proliferation of the CLL cells (Coscia et al., 2011; Ferretti et al., 2011; Pepper et al., 2011).

Mainly, the survival, proliferation, and antigen-presenting activity of normal B-cells is initiated due to the signals transduced through the surface immunoglobulin (sIg) receptors for antigen binding and through the CD40 receptors for CD40L. Thus, the biological behaviour of the B-CLL cells could be altered by either pharmacological agents or biological response modifiers that influence pathways initiated by these molecules.

Lymph node biopsies from CLL patients with aggressive disease contain activated T lymphocytes. In the lymph nodes *in-vivo*, the CLL cells interact with activated $CD4^+$ T cells (Hamilton et al., 2012). In addition, the CD40 receptors on the surface of the CLL cells interact with its ligand CD40L on activated T lymphocytes. The interaction between CD40-CD40L induces the upregulation responses of surface markers and chemokines (Scielzo et al., 2011; Hamilton et al., 2012).

Tumour proliferation mainly occurs in the lymph nodes, bone marrow and spleen where the pseudofollicles are developed (Patten et al., 2008). The interaction of CLL cells with stimulation factors such as T lymphocytes, the microvasculature, soluble factors and other stromal elements trigger the survival and proliferation of the tumour cells. Moreover, the lymph nodes of CLL patients with aggressive disease could also contain a substantial population of $CD31^+$ vessels (Patten et al., 2008) and $CD31^+$ nurse like cells (Deaglio et al., 2005).

Furthermore, interactions between the CLL cells and endothelial cells enhance the survival of CLL cells (Buggins et al., 2010; Hamilton et al., 2012) and induce the expression of CD38 and integrin subunit alpha 4 (ITGA4) (CD49d) on the tumour cells, which are associated with aggressive disease and worse clinical outcome prognosis. (Majid et al., 2011; Shanafelt, Geyer, et al., 2008).

Various soluble proteins and membrane bound interaction factors could interact with CLL B-cell surface receptors causing drug resistance and preventing CLL cells from undergoing apoptosis. Stromal cell derived factor-1 (also known as C-X-C motif chemokine 12 (CXCL12), B-cell activating factor, A PRoliferation Inducing Ligand (APRIL) (T. Endo et al., 2007; Nishio et al., 2005) vascular endothelial growth factor, and CD40L are all examples of microenvironmental stimulation factors that lead to progression of CLL, resistance to treatment and prevention of apoptosis.

CD40 ligation signals are believed to have a central upregulation role in CLL by promoting cell proliferation, survival, and regulating migration to lymph node tissue (Caligaris-Cappio, 2003). It has been suggested that, in an appropriate microenvironment, the ligation between the CD40 receptor and CD40L $CD4^+$ T cells, engaged by autologous activated $CD4^+$ T helper cells along with other costimulatory signals, IL-4, IL-21 and, IL-7, play a key role in CLL expansion in a recently developed adoptive transfer mouse model of CLL cells (Bagnara et al., 2011).

In the proliferation centre, CLL cells come into close contact with activated CD40L on $CD4^+$ T helper cells (Ghia et al., 2002). Even though CD40L stimulation itself increases the CLL cell proliferation cascade (Tromp et al., 2010), it also induces resistance to apoptosis by altering the apoptotic profile of CLL cells (Kater et al., 2004). CD40 stimulation signals enhance the anti-apoptotic profile of B-CLL cells by upregulation of BCL-xL and Bfl-1 expression and downregulation of the BH3-only protein Harakiri (Grumont et al., 1999; H. H. Lee et al., 1999). It was revealed that CD40 stimulation causes significant changes in four apoptotic regulators, including a substantial increase in the Bid protein Despite being resistant to apoptosis induced by death-receptors and chemotherapy, B-CLL cells stimulated by CD40 became highly susceptible to being targeted and killed by autologous cytotoxic T-cells (Kater et al., 2004). There might be other stimulation factors and cytokines secreted by activated $CD4^+$ T cells that contribute to the CLL cell proliferation.

In CLL patients, the $CD4^+$ T cells stimulate the proliferation and the survival activity of the CLL cells by secreting cytokines, such as IL4 (Stevenson & Caligaris-Cappio, 2004). Predominantly, These T cells are present in the bone marrow and around the proliferation centres, called “pseudofollicles” in lymph nodes of CLL patients (Pizzolo et al., 1983).

B CLL cells generate and exhibit on their cell surface both ligands and receptors of pro-survival cytokines such as IL-2, IL4, IL-8 and TNFa, which influence survival. Nevertheless, it remains uncertain whether an enhanced microenvironment is the exclusive reason for

extended CLL cell survival, or if the CLL cells are inherently more receptive to microenvironmental signals.

IL-4 is one of the critical cytokines that has a direct stimulation effect on B-cell activation signals. The stimulation signals of IL-4 upregulate B-cell proliferation and survival through different pathways such as BCR, IgM and CD40L of B-cells (Banchereau et al., 1993; Durie et al., 1994). Although, both the CD40L and the IL-4 signals stimulated the B CLL cells through different pathways, this co-stimulation could have a synergistic effect.

5.2 CD40L on model CLL cells

The CLL microenvironment plays a critical role in modulating NF-κB activity through different B-cell signals, such as BCR, TLRs and CD40. Furthermore, stimulation signals via various CLL cell receptors and cytokines creates a niche that promotes B-cell survival and proliferation, characterized by NF-κB activation. The activation of the NF-κB pathway is linked to resistance against conventional chemotherapies and targeted inhibitors such as ibrutinib and venetoclax. Signalling through NF-κB stimulation enhances the expression of anti-apoptotic proteins MCL-1, BCL-xL and surviving (Jayappa et al., 2017; Souers et al., 2013).

Similarly, the *ex-vivo* CD40L-expressing fibroblast microenvironment promotes B-cells (CLL) interaction with accessory cells such as those expressed on the T cells. The interactions between malignant B-cells (CLL) and T cells within the lymph nodes microenvironment activate NF-κB signalling pathways, leading to the secretion of tumour-promoting cytokines and growth factors that support CLL cell proliferation, survival, and drug resistance (Kawano et al., 2015; Podar et al., 2009).

5.3 The CD40-CD40L interaction

When the CLL B-cells migrate to the lymph nodes (Figure 5.1), the CD40L comes into contact with the CD40 receptors, which lacks intrinsic catalytic activity. and establishes sending signals by recruitment of TNF receptor associated factors 1, 2, 3, 5, and 6 (TRAF) (Grammer & Lipsky, 2000; Hostager et al., 2000). These TRAF molecules initiate the downstream signalling which activates phosphoinositide 3 kinase (PI3K), phospholipase Cγ,

mitogen-activated protein kinases (MAPKs), JAK3 and NF-κB (Hömig-Hölzel et al., 2008; Grammer & Lipsky, 2000). Then, the JAK3, which is associated with the cytoplasmic tail of CD40, becomes phosphorylated, resulting in the activation of STAT3 (signal transducer and activator of transcription 3) (Hanissian & Geha, 1997).

Upon the CD40-CD40L interaction, the following three subfamilies of MAPKs are activated the extracellular signal-regulated kinase 1 (Erk1) and (Erk2), the c-jun kinases (Jnk1) and (Jnk2), and the kinase p38/MAPK (Craxton et al., 1998; Sutherland et al., 1996).

MAPKs which are serine/threonine protein kinases, are activated by dual phosphorylation on a specific tyrosine and threonine residue, respectively. After that, activated MAPKs phosphorylate other nuclear substrates such as the transcription factors c-Jun, Elk-1, Egr-1, and Atf-2, which allows them to bind with specific DNA promoter sequences and modulate the transcription of specific target genes (Hömig-Hölzel et al., 2008; Van Kooten & Banchereau, 2000).

This co-culture system has demonstrated that the CD40L signals have ability to inhibit the spontaneous apoptosis in CLL cells. The same co-culture system was used to determine the effect of the aspirin analogue 4HBZ on CLL cells. Pepper et al., found that 4HBZ inhibited the pro-survival effect of CD40L microenvironment. Although, the CD40L co-culture system selectively increased COX-2 mRNA transcription and protein levels however, the additional of 4HBZ under these conditions inhibited COX-2 expression levels (Pepper et al., 2011).

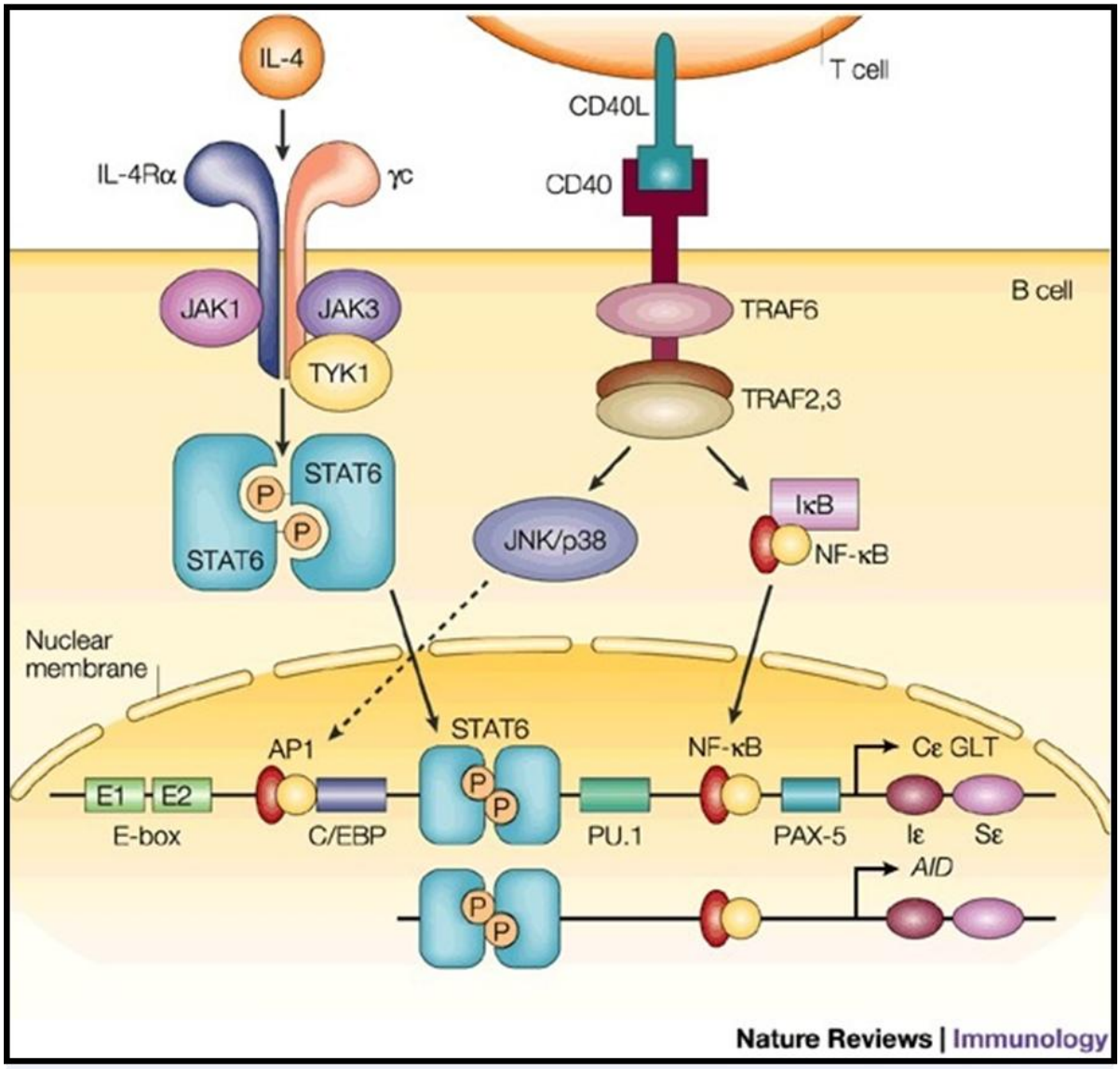

Figure 5.1 The interaction between interleukin-4 (IL-4) and its receptor (IL-4R) triggers the recruitment and stimulation of Janus-activated kinase 1 (JAK1), JAK3, and TYK1, which are tyrosine kinases. These kinases, in turn, initiate the activation of signal transducer and activator of transcription 6 (STAT6). The interaction between CD40 receptor expressed on B-cells and CD40 ligand (CD40L) expressed on T cells recruits and activate the tumour necrosis factor receptor-associated factors (TRAFs). Activation of TRAFs leads to activate the translocation of nuclear factor-κB (NF-κB) and activator protein 1 (AP1), which are transcription factors into the cell nucleus. Stimulation signals of both IL-4R and CD40 interactions enhance the transcription activity of activation-induced cytidine deaminase (AID) and Cε germ-line transcripts (Cε GLTs) through NF-κB and STAT6 transcription (Geha et al., 2003).

5.4 Hypothesis and Aims

CLL cells behave differently when they are stimulated to proliferate in bone marrow and lymph nodes compare with their non-proliferative state in the peripheral circulation. Therefore, it is also important to evaluate the effect of RG7388 on proliferating CLL cells.

In this chapter, the transfected mouse fibroblast cells, expressing either CD40L or NTL were used as a monolayer cell to mimic the *ex-vivo* microenvironment of the CLL cells in the human body. In addition, IL-4 was added to enhance the proliferation signals.

The aims of the work presented in this chapter were.

- Optimising the fibroblast tissue culture systems for co-culturing the primary CLL cells on CD40 ligand expressing irradiated feeder layers.
- Measuring the expression of the CD40L on the surface of the CD40L mouse fibroblast cells.
- Measuring the stability of the RG7388 (idasanutlin) MDM2 inhibitor in the co-culture system.
- Test the antiproliferative and cytotoxic effect of RG7388 MDM2-p53 binding antagonist on the proliferating CLL cells.
- Determine the effect of CD40L and Il-4 stimulation on the response of the MDM2-p53 signalling network to RG7388 treatment alone and in combination with a WIP1 inhibitor.
- Determine the transcriptional and translational changes in the proliferating CD40L CLL cells in response to the combination treatment of MDM2 and WIP1 inhibitor.

5.5 Results

5.5.1 The cytotoxic effect of fresh and incubated RG7388 on the growth of wild type NALM-6 cells.

Before commencing co-culture experiments, the stability of the MDM2 inhibitor (RG7388) was determined by measuring the efficiency of the drug for growth inhibition of NALM-6 B-cells. The wild type (+/+) and heterozygous (-/+) *TP53* NALM-6 cells were exposed to two different RG7388 stocks, one which was freshly prepared prior the experiment and the other which was prepared before the experiment and pre-incubated in full medium for 48 hours in a 37°C CO_2 incubator.

Figure 5.2 shows the effect of RG7388 on wild type NALM-6, for either freshly prepared drug or prepared and incubated at 37°C for 48 hours before exposed to heterozygous *TP53*(-/+) and wild type *TP53*(+/+) NALM-6 cells. The heterozygous *TP53*(-/+*)* NALM-6 cells were used to identify whether the freshly prepared or 48 hours pre-incubated RG7388 had different

effectiveness to stabilises the *TP53* activity with one functional allele. Under both conditions, RG7388 showed a concentration dependent inhibition effect.

The GI_{50} inhibition effect of heterozygous *TP53*(-/+) NALM-6 cells in response to the freshly prepared RG7388 was (0.069µM ± 0.003SEM) and with 48 hours incubated RG7388 was (0.064µM ± 0.003SEM) (Figure 5.2 A). The GI_{50} for wild type *TP53*(+/+) NALM-6 cells in response to the freshly prepared RG7388 was (0.071µM ± 0.003SEM) and that for 48 hours incubated RG7388 was (0.069µM ± 0.007SEM) (Figure 5.2 B) (Table 5.1).

There was no significant difference between the effect of the RG7388 which were freshly prepared immediately before the experiment compared to the RG7388 which was pre-incubated at 37°C for 48 hours prior the exposed to both heterozygous *TP53*(-/+) (p=0.38) and wild type *TP53*(+/+) NALM-6 cells (p=0.30) (Figure 5.3) (Table 5.1).

The summary Figure 5.3 shows the individual and mean GI_{50} values for experiments which tested the response to either RG7388 which was freshly prepared or pre-incubated for 48 hours prior the treatment.

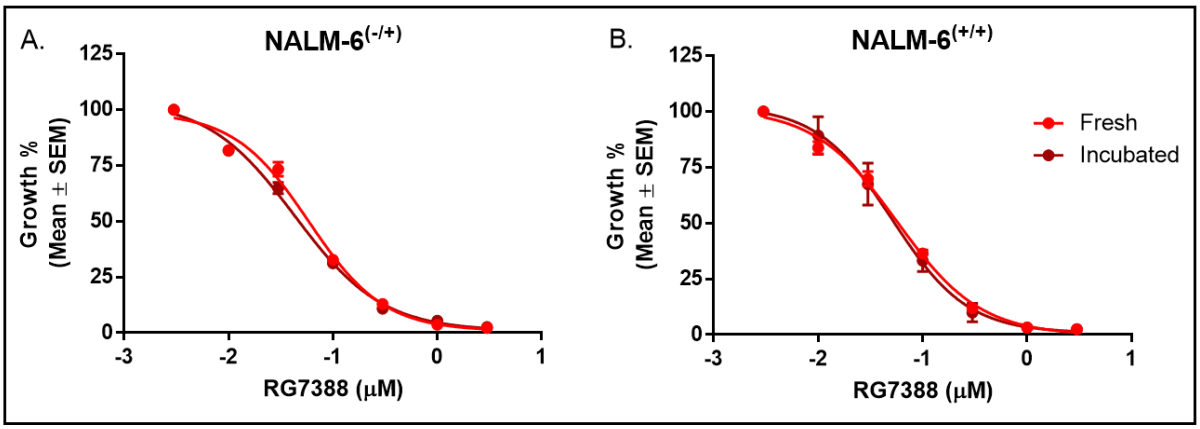

Figure 5.2 The growth inhibition effect of preincubated or freshly prepared RG7388 on (A) heterozygous and (B) wild type *TP53* NALM-6 cells. To determine the stability of RG7388 in *ex-vivo* microenviroment experiment, freshly prepared (red line) and 48hr pre-incubated at 37°C in CO_2 perior the experiment (dark red line) was used to treat the iso-geneic TP53 NALM-6 cell. The growth inhibition determined by XTT assay after 72 hours after the treatment. The error bar shows an average of minimum (n=4) repeats from independent cell passage. The bars show the average mean ± SEM. Each % growth inhibition of independent repeats was normalized to it's own DMSO treatment for individual experiment.

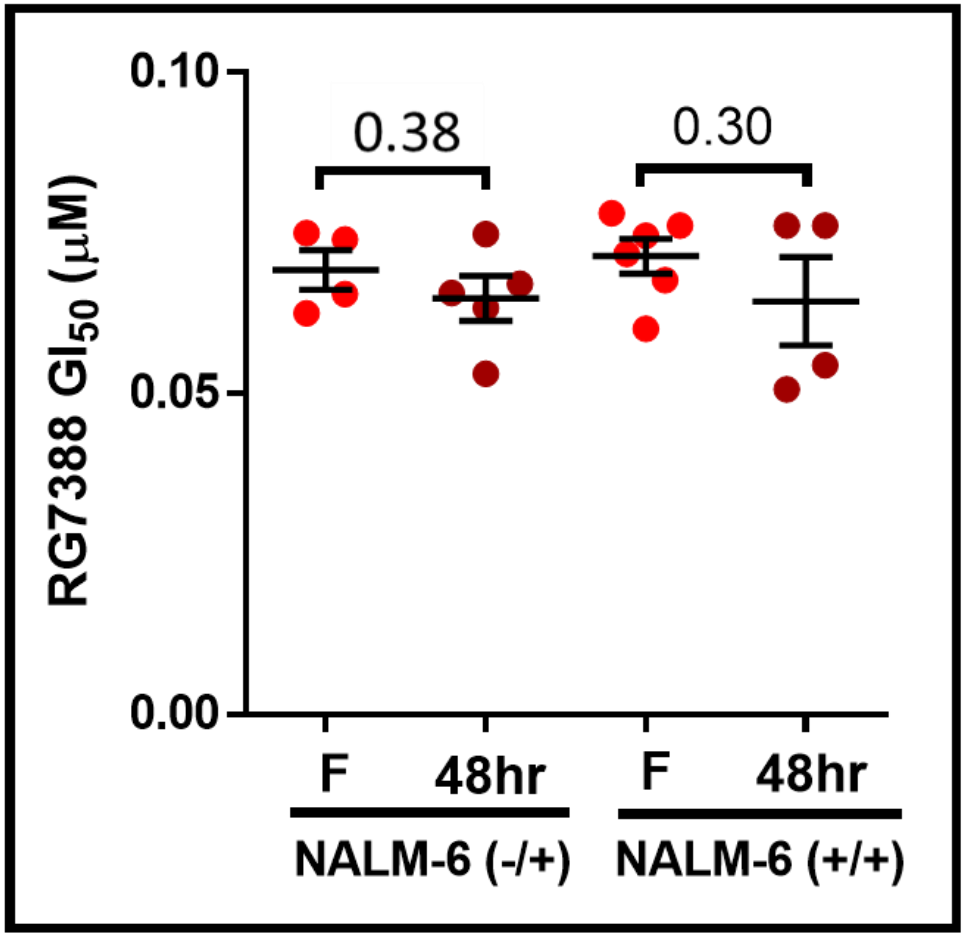

Figure 5.3 Summary of The GI_{50} values for RG7388, either freshly prepared or pre-incubated at 37^0C for 48 hours prior the treatment on iso-geneic TP53 NALM-6 cell. XTT assay assessed the GI_{50} of RG7388 after 72 hours. The response of MDM2 inhibitor freshly prepared (F) or pre-incubated (48hr) are shown in red and dark red colours respectively. Each dots represents an independent repeat of experiment. Error bar indicates average mean ± SEM of independent minimum repeats (n=4). RG73888 prepared prior the experiment NALM-6(-/+) (n=4), NALM-6(+/+) (n=6), RG73888 pre-incubated NALM-6(-/+) (n=5), NALM-6(+/+) (n=4). Statistical significance was determined by ANOVA test for multiple comparisons, significance taken at $p < 0.05$. There is no significant differences between freshly and pre-incubated RG7388 conditions on either cell lines. Only the p-value between (F) and (48hr) of RG7388 treatment for both cell lines are displayed on the graphs.

GI_{50} (µM)	RG7388		
	Freshly prepared	48hr pre-incubated	p-value
NALM-6 (-/+)	0.069 (±0.003)	0.064 (±0.003)	0.38
NALM-6 (+/+)	0.071 (±0.003)	0.069 (±0.007)	0.30

Table 5.1 GI_{50} of RG7388 freshly prepared (F) or pre-incubated in a full medium for 48 hours at 37°C prior the treatment to heterozygous and wild type TP53 NALM-6 cells. The average mean ± SEM values were calculated for experiments repeated on consecutive cell passages. RG73888 freshly prepared prior the experiment NALM-6(-/+) (n=4), NALM-6(+/+) (n=6), RG73888 pre-incubated NALM-6(-/+) (n=5), NALM-6(+/+) (n=4). Multiple comparisons ANOVA test was applied to compare between diffrernt RG7388 treatment conditions.

5.5.2 The stability of pre-incubated RG7388 in full medium with CD40L expressing monolayer cells, tested by the effect on the growth of wild type and heterozygous NALM-6 cells

Here we investigated the stability of pre-incubated MDM2 inhibitor (RG7388) with CD40L fibroblast cells for 48 hours prior to testing on NALM-6 cells. Both wild type and heterozygous *TP53*(-/+) NALM-6 cells were used to test against the RG7388 which was either freshly prepared or pre-incubated with CD40L fibroblast cells for 48 hours.

(Figure 5.4) shows the inhibition effect of RG7388 which were pre-incubated with CD40L fibroblast cells and IL-4 at 37°C for 48 hours prior to testing on NALM-6 cells. For the pre-incubated RG7388 with the CD40L fibroblast and IL-4 prior exposed to the NALM-6 cells, there was a concentration-dependent effect of the treatment on both wild type and heterozygous *TP53* cells. The experiment was repeated on six different cell passages.

The GI_{50} inhibition effect of pre-incubated RG7388 with CD40L fibroblast and IL-4 was (0.045µM ± 0.004SEM) in wild type *TP53*(+/+) NALM-6 and (0.043µM ± 0.007SEM) in heterozygous *TP53*(-/+) NALM-6 cells. There was no significant difference between the effect of pre-incubated RG7388 with CD40L on wild type NALM-6 and heterozygous *TP53*(-/+) NALM-6 cells (Figure 5.5). In contrast, the efficacy of RG7388 for growth inhibition of NALM-6 cells appeared to be more potent after pre-incubation with the CD40L monolayer cells and IL-4 compared with freshly prepared RG7388. Both heterozygous and wild type *TP53* NALM-6 cells become significantly sensitive to the pre-incubated RG7388 with CD40L and IL-4 compared to the absence of CD40L and IL-4 pre-incubation in full medium treatment (*TP53*(-/+) p=0.02) (*TP53*(+/+) p=0.007) (Table 5.2).

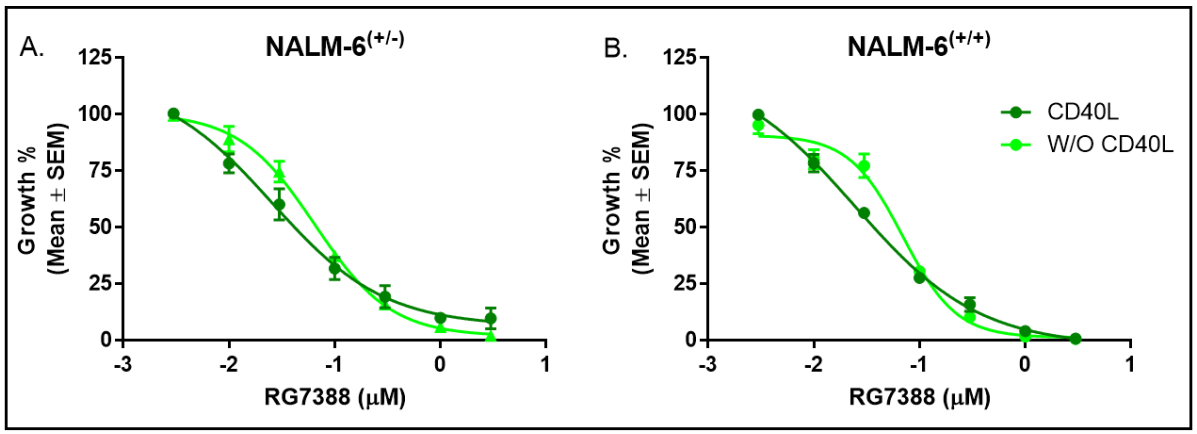

Figure 5.4 The growth inhibition effect of (A) heterozygous and (B) wild type TP53 NALM-6 in response to RG7388 which was pre-incubated at 37°C with CD40L fibroblast cells for 48 hours. The stability of RG7388 in *ex-vivo* microenviroment CD40L/IL-4 co-culture experiment, RG7388 pre-incubated at 37°C in CO_2 with CD40L/IL-4 (dark green line) and without CD40L/IL-4 (green line) monolayer, freshly prepared perior treatment of iso-geneic TP53 NALM-6 cell. XTT assay used to assessed cell growth % inhibition after 72 hours of treatment. Each independent repeat of experiment was averaged within itself and normalized to DMSO treatment. Bars represent the average of minimum (n=3) mean ± SEM of repeats from independent cell passage. RG73888 freshly prepared prior the experiment (n=3), RG73888 pre-incubated with CD40/IL-4 (n=6).

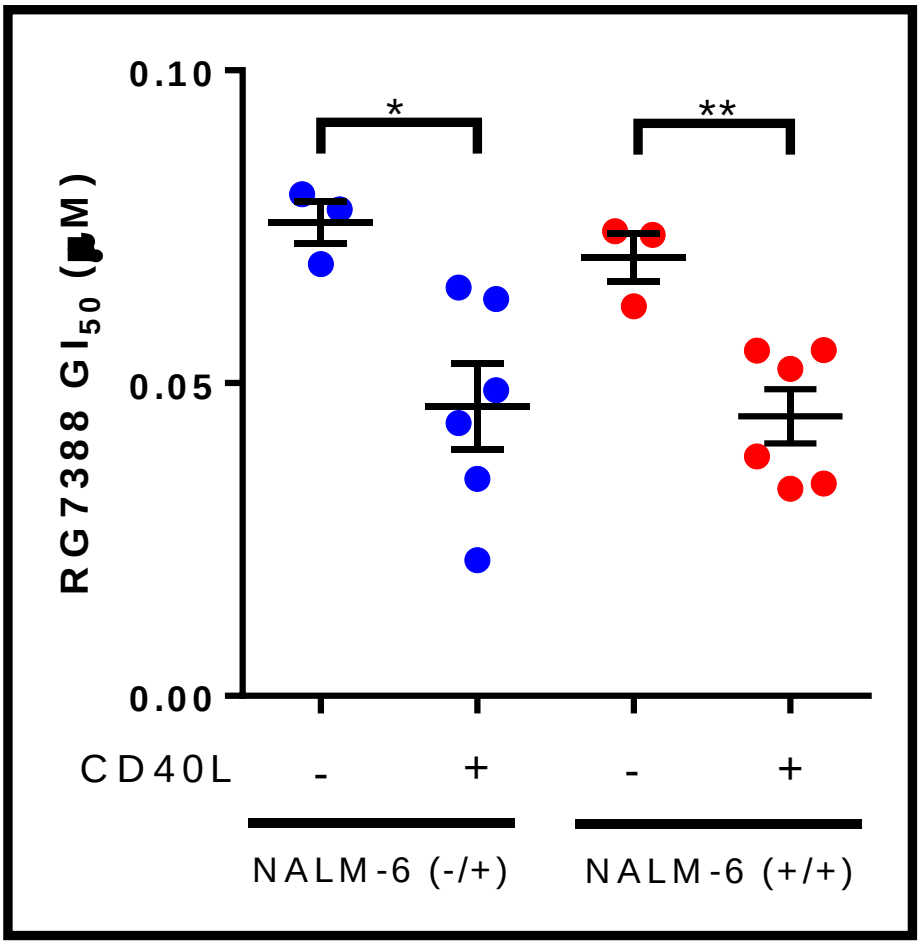

Figure 5.5 The effect of RG7388 pre-incubation with CD40L cells and IL-4 for 48 hours prior to testing on either *TP53* heterozygous or wild type NALM-6 cells. Isogeneic TP53 NALM-6 cells treated either with RG7388 pre-incubated with CD40L/IL-4 for (48hr) (dark green line) or freshly prepared (green line) prior the experiment. XTT assay was used to assess the GI_{50} values of treatment after 72 hours. Each dots represents an independent repeat of experiment. Bar indicates average mean ± SEM of independent repeats (n=4 with absence of CD40/IL-4 and n=6 with CD40/IL-4 pre-incubation). Statistical significance was determined by ANOVA test for multiple comparisons, significance taken at $p < 0.05$. (*, $p < 0.05$; **, $p < 0.001$).

GI_{50} (μM)	RG7388		
	CD40L(-)/IL-4	CD40L(+)/IL-4	p-value
NALM-6 (-/+)	0.076 (±0.003)	0.043 (±0.007)	0.02
NALM-6 (+/+)	0.071 (±0.004)	0.045 (±0.004)	0.007

Table 5.2 The GI_{50} of RG7388 exposed to CD40L fibroblast cells and IL-4 for 48 hours prior treatment to heterozygous and wild type TP53 NALM-6 cells for an additional 48 hours. The average mean and ± SEM were calculated for all repeated experiments on consecutive cell passage. RG73888 with absence of CD40/IL-4 (n=4) and with CD40/IL-4 pre-incubation (n=6). Statistical significance was determined by ANOVA test for multiple comparisons, significance taken at $p < 0.05$.

5.5.3 Optimization of the irradiation conditions for preparation of CD40L monolayer cells

This section describes experiments to investigate the optimum irradiation doses that can be used to stop the proliferation of the CD40L expressing fibroblast cells without affecting the subsequent CLL cell metabolic activity and proliferation. The original protocol (Pepper et al., 2011) suggested 75Gy, however it was hypothesised that a lower dose would be sufficient to halt proliferation without having an adverse effect on the ability of the CD40L fibroblasts to promote the survival and proliferation of primary CLL cells, as well as being more cost-effective. Therefore, a range of irradiation doses including 3.75, 7.5, 15 and 30Gy, were used to determine the effect of the irradiation on the proliferation activity of the fibroblast CD40L cells. Then, the number of the CD40L cells were counted daily for 72 hours. The aim of this experiment was to identify the irradiation dose that can maintain the number of the fibroblast cells constant without any proliferation or apoptosis/decreases for the duration of the *ex-vivo* experiments with CLL cells supported on the CD40L fibroblast monolayer.

Figure 5.6 shows how the different irradiation doses (Gy) affected cell proliferation. CD40L cells were seeded in four different plates of 24 wells at concentration of $0.6x10^6$ cells/ml for 0.5ml per well. Each plate was irradiated with different irradiation dose. After that, the feeder cells were counted and the microscopic images were taken at the same time for visual inspection. Each time point was counted from three different wells. The non-irradiated cells were used as a control (0Gy). Cells which were irradiated with either 3.75Gy or 7.5Gy were still able to proliferate, as judged by the increased cell number at 48 hours. Even though, at high irradiation dose, the monolayer cells appear confluent because, the cells get larger, extended

and more flattened. In contrast, at lower irradiation doses, the number of cells per unit area were less and the cell counts drop (Figure 5.7).

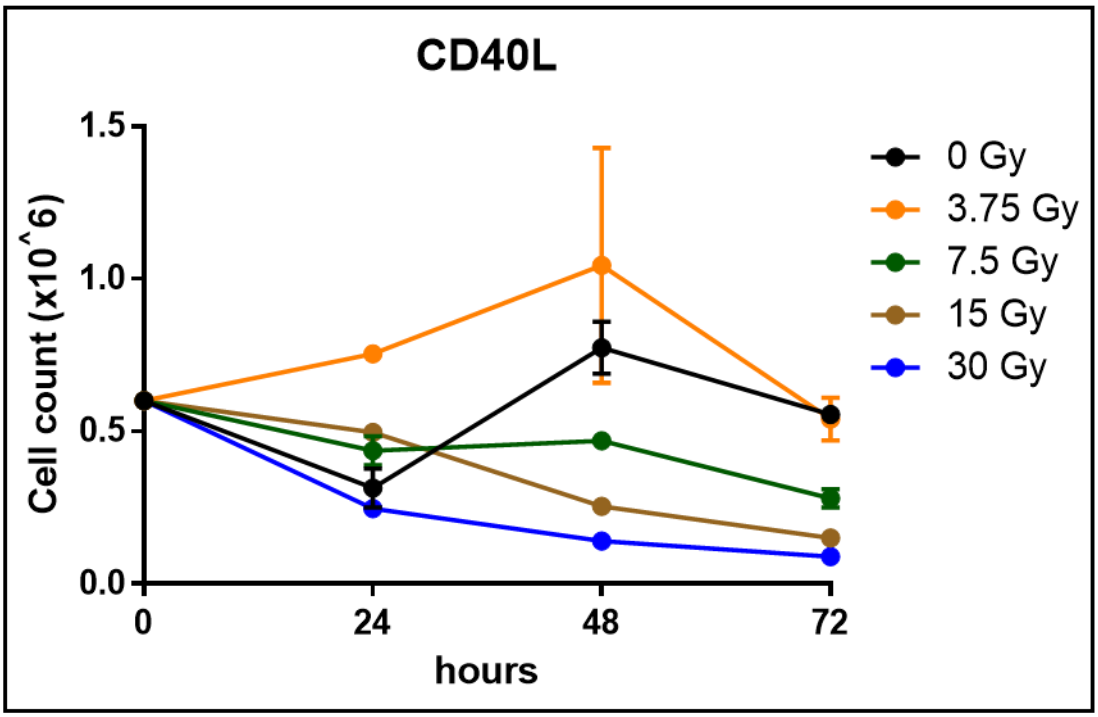

Figure 5.6 Cell count reduction of CD40L fibroblast cell in response to different irradiation doses. CD40L cells seededed in 0.6x10^6 cells/ml in a total volume of 0.5ml/well in four different 24 wells plate. Each plate was irradiated with different range of irradiation dose. The cell growth was monitored by counting the number of cells every 24 hours for 72 hours in total. Each time point was counted from three different wells and bars show the mean ± SEM of intra-experimental repeats. The experiment performed on (n=1) CD40L cells. (Gy=Gray).

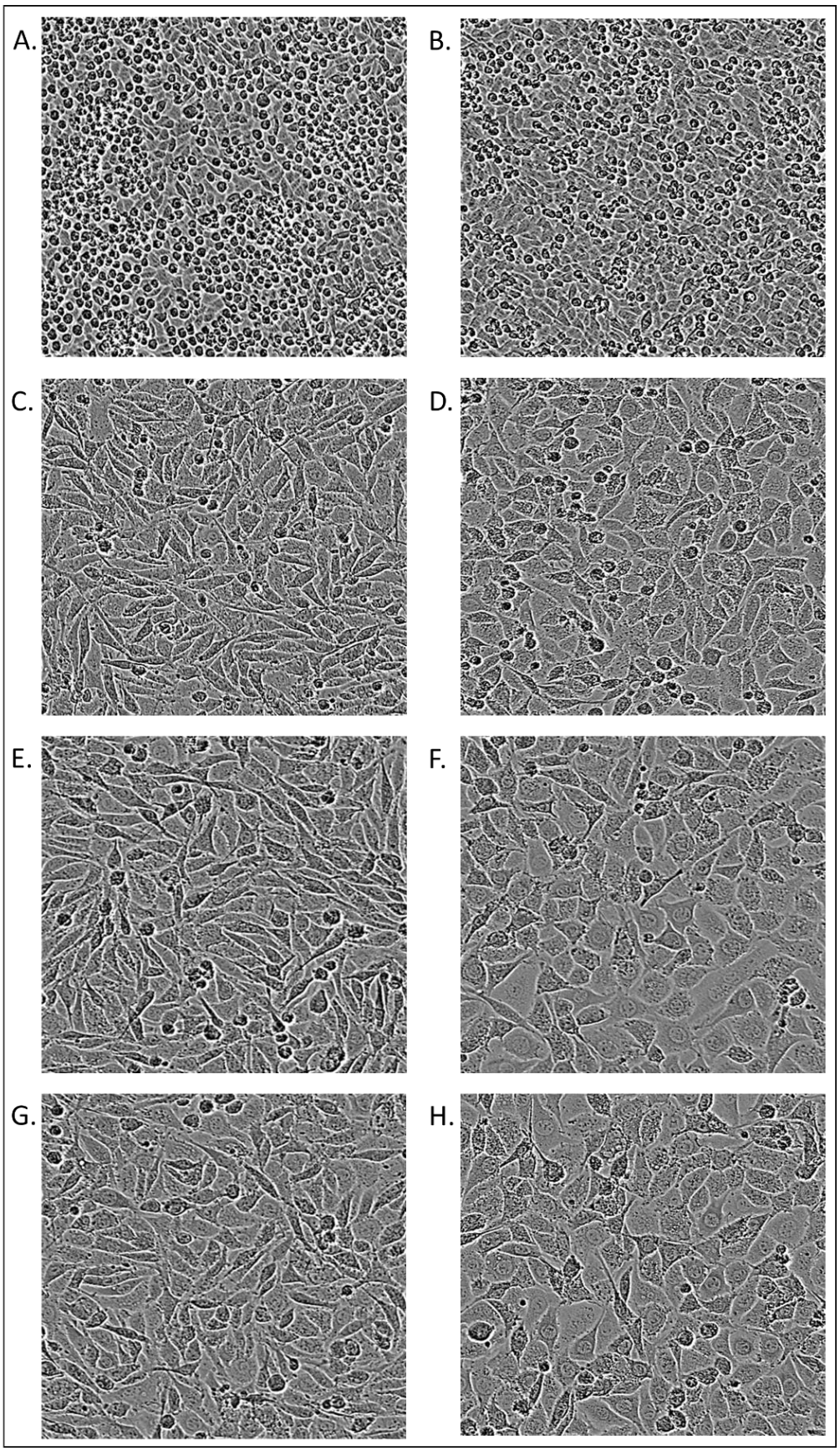

Figure 5.7 IncuCyte images of mouse fibroblast cells, NTL (the left panel) and CD40L (the right panel) irradiated with a range of X-ray doses after 4 days. (A) NTL, no irradiation, (B) CD40L, no irradiation, (C) NTL-15 Gray, (D) CD40L-15 Gray, (E) NTL-30 Gray, (F) CD40L-30 Gray, (G) NTL-75 Gray, (H) CD40L-75 Gy. Cells seededed in $0.6x10^6$ cells/ml in four different 24 wells plate. Each plate was irradiated with different range of irradiation dose. Images were taken by the machine on selected time points. (Gy=Gray)

5.5.4 Growth inhibition curves of CD40L and NTL cell line treated by RG7388

The main aim of the work described in this chapter was to mimic the *ex-vivo* environment of CLL cells by co-culturing the primary CLL cells on a CD40L expressing fibroblast monolayer, followed by treatment of the CLL cells with the MDM2 inhibitor to understand the effect of the CD40L interaction on the sensitivity of the CLL cells. Thus, further experiments were performed to investigate whether the RG7388 had an indirect effect on the growth and CD40L expression of the irradiated mouse fibroblast CD40L/NTL cells.

The fibroblast CD40L and NTL cells were seeded in 96 wells at a concentration of $1x10^6$ cells per well in a final volume of 100µl. Then, the cells were treated with different concentrations of MDM2 inhibitor (RG7388) in 0.5% DMSO for 4 days. At that end of the exposure, their proliferation was measured using an SRB assay (2.4.2).

Figure 5.8 shows the dose-dependent effect of RG7388 on both CD40L and NTL cells. The proliferation of the CD40L and NTL cell monolayers showed minimal reduction and did not reach the GI_{50} value even with a high concentration of RG7388 (3µM).

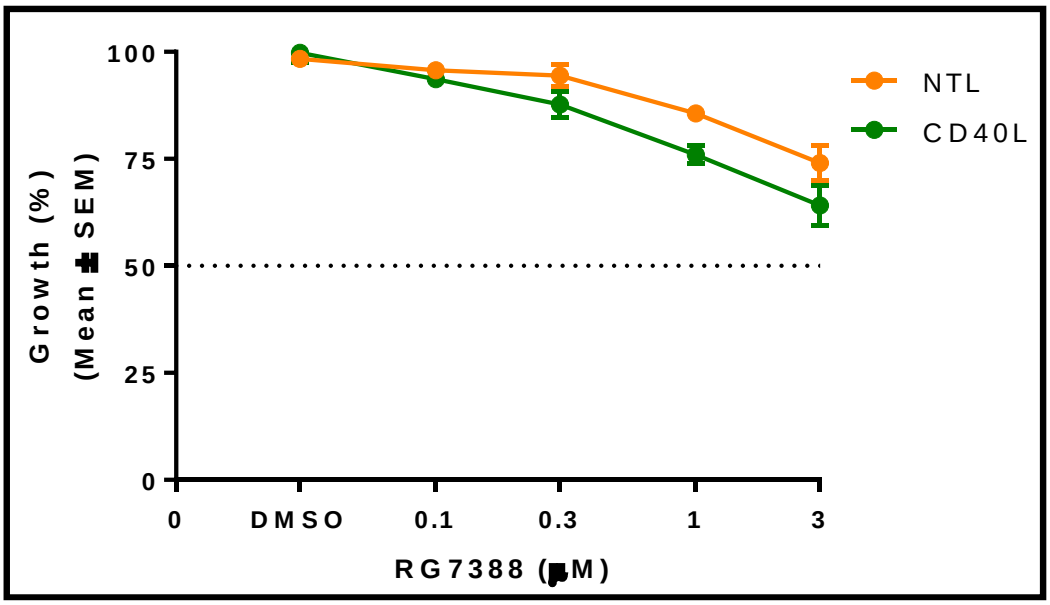

Figure 5.8 The viability of irradiated CD40L and NTL cell treated with MDM2 inhibitor for 96 hours. Cells were seeded in $1x10^6$ cells/well in in a final volume of 100µl. The growth inhibition effect of RG7388 treatment were determined after 72 by SRB analysis. All % of growth was normalized to DMSO treatment for individual cell line. Each concentration repeated in three different wells and bars show the mean ± SEM of intra-experimental repeats. The experiment performed on (n=1) cells.

5.5.5 Checking the expression of CD40L on the surface of fibroblast cells by FACS Analysis

The experiment was performed to confirm the presence of CD40L receptor expression on the CD40L fibroblast cells and its absence on NTL cells. The CD40L cells are expected to express ligand for CD40 however, the NTL cells should not express CD40 ligand as they are an empty vector transfected control cell line.

FACS analysis results confirmed that positive expression of CD40 ligand was only detected on CD40L cells (Figure 5.10) and not on NTL cells (Figure 5.9). Furthermore, the cells, gated out in the bottom left corner represent cell debris. The overlays show that NTL cells did not exhibit any immunoreactivity for the anti-CD-154 (CD40L) antibody whereas the CD40L cells were confirmed to show clear positive staining and hence surface expression of CD-154.

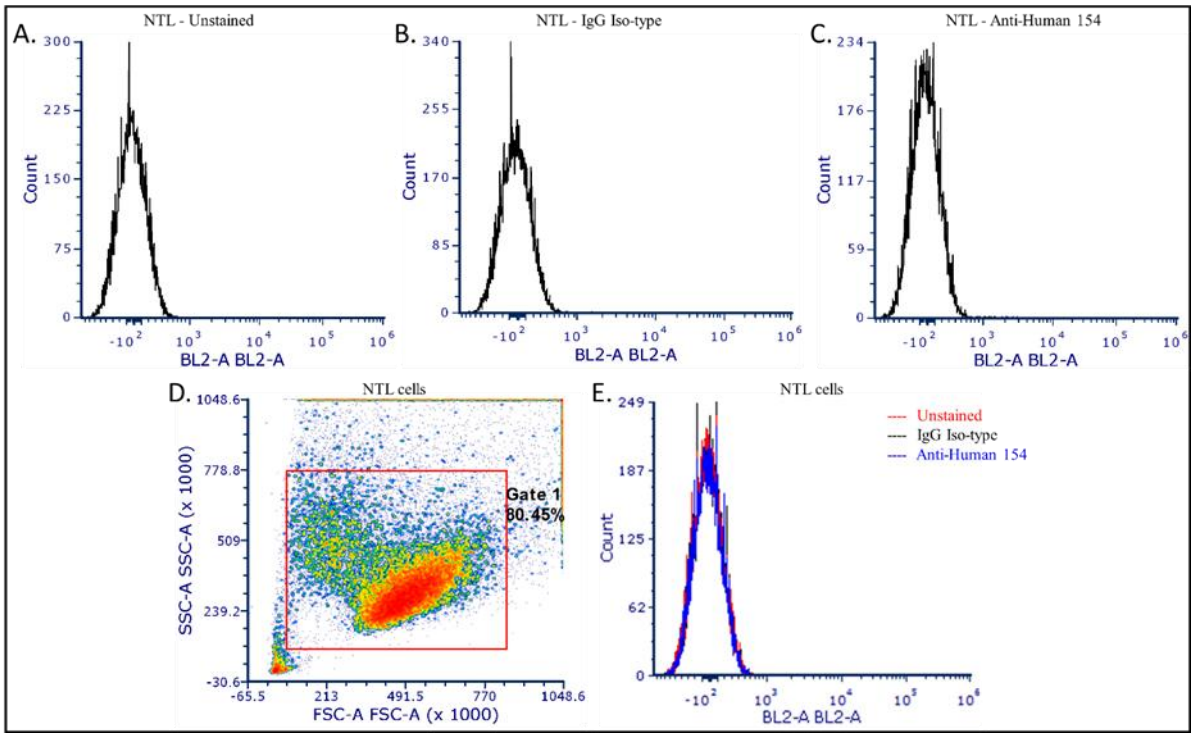

Figure 5.9 The NTL cells stained with different antibodies to detect the CD40 antigen on their surface. (A) Unstained, (B) IgG Iso-type antibody (C) CD-154 antibody, (D) cells gating, (E) all antibodies overlayed with background signals from unstained cells. NTL mouse fibroblast cells seeded in concentration of $1x10^6$ cells/ml and incubated with CD154 and IgG antibodies in separate tubes for 20min. FACSCalibaur used to detect the expression of the fluorescence emission. The experiment performed in (n=1) repeat to determine the expression of CD40L on cell surface.

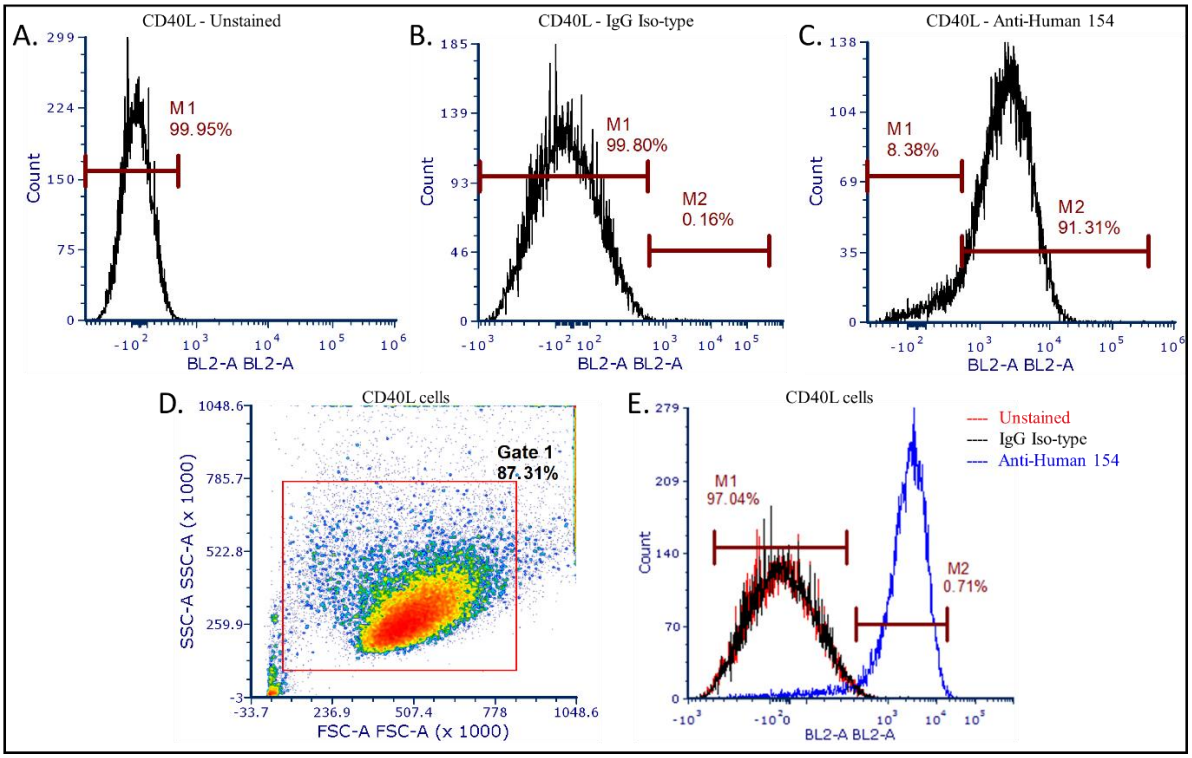

Figure 5.10 CD40L cells stained with different antibodies to detect the CD40 antigen on their surface. (A) Unstained, (B) IgG Iso-type, (C) CD-154, (D) cells gating, (E) receptors expression overlayed with background signals from unstained cells. CD40L mouse fibroblast cells seeded in concentration of $1x10^6$ cells/ml and incubated with CD154 and IgG antibodies in separate tubes for 20min. FACSCalibaur used to detect the expression of the fluorescence emission. The experiment performed in (n=1) repeat to determine the expression of CD40L on cell surface.

5.5.6 RG7388 stabilised TP53 expression and activity in primary CLL cells co-cultured with CD40L fibroblast cells

A western immunoblot was performed to determine the change in the expression of TP53 and downstream target proteins MDM2 and $p21^{WAF1}$ for the primary CLL cells after co-culturing with CD40L/IL-4 and treatment with RG7388. In addition, the ability of RG7388 to drive the proliferative CLL cells which were stimulated with CD40L to apoptosis was examined by detection of PARP cleavage.

The fibroblasts cells were seeded in 24 wells plate at a concentration of $0.6x10^6$ cells/ml and then irradiated with 30Gy. On the next day, the primary CLL cells were added in a concentration of $1x10^6$ cells/ml including the IL-4 (10ng/mL). Following co-incubation for 6 hours, the cells were treated with a range of RG7338 concentrations for another 6 hours. Then, the CLL cells were collected gently and processed for the western immunoblotting.

Figure 5.11 shows the protein expression in primary CLL309 cell sample co-cultured with CD40L fibroblast cells and IL-4 in response to RG7388 for 6 hours. In addition, RG7388 treated NALM-6 cells were included as a positive control. RG7388 increased TP53 protein

levels in a concentration dependent manner. Moreover, MDM2 and $p21^{WAF}$ were weakly induced with RG7388 (3µM) treatment relative to the DMSO control. Total PARP and cPARP showed no obvious changes with RG7388 treatment at this early time point.

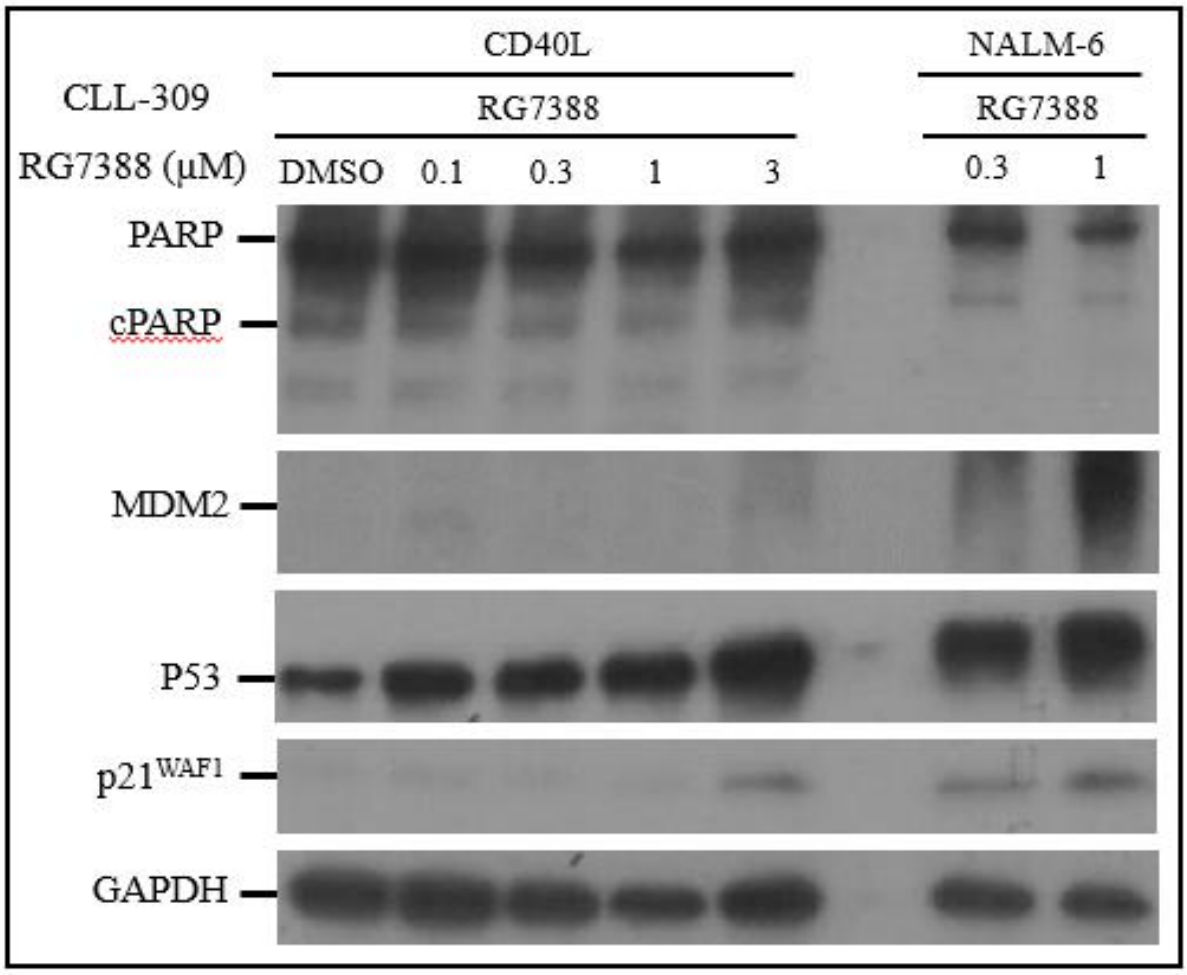

Figure 5.11 Western immunoblot p53 and downstream target proteins in primary CLL309 cells co-cultured on irradiated CD40L fibroblast cells with IL-4 in response to RG7388. Mouse fibroblast cells expressing CD40L was irradiated (30GY). CLL309 cultured on irradiated CD40L/IL4 for 6hrs followed by treatment with increasing concentrations of RG7388, including the LC_{50} concentrations for an additional 6hrs. The cell lysate was collected from (n=1) experiment. All strips were from the same membrane which was cut into three. The top strip was probed for MDM2 and PARP; the middle for p53 and GAPDH; and the third with p21 antibody. GAPDH used as the loading control. Nalm-6 ($TP53^{WT}$) cells treated with RG7388 for 6hrs used as a positive control for molecular weight protein expression.

5.5.7 CLL cell count increased with CD40L/IL-4 co-culture and was inhibited in a dose dependent manner by RG7388

After the CD40L co-culture was optimised, primary CLL cell experiments were performed to determine the effect of RG7338 treatment on CLL cells when they were stimulated to proliferate on the CD40L monolayer feeder cells.

Initially, the primary CLL cells including IL-4 were co-cultured on the top of the irradiated CD40L and NTL fibroblasts monolayer cells. The proliferation rate of CLL cells were varies from sample to another. Most likely, CLL cells start to proliferate on the fifth day after CD40L stimulation signals. The proliferation of CLL cells were determined by counting the actual CLL cells using the cell coulter count and the haemocytometer. Following the CLL cells proliferation commenced, different concentrations of RG7388 were exposed to the CLL cells microenvironment.

The monolayer cells were replaced and not become exhausted to keep the CD40L signals continually in contact and active with CLL cells. The protocol in details mentioned in (section 2.11.2).

CLL284 cells showed a reduction in the CLL count with the DMSO control on the 3rd day of CD40L and NTL monolayer co-cultured including IL-4 from the initial seeding time point (Figure 5.12). However, the CLL cells initiated to proliferate commonly after the 5th day of NTL and CD40L co-culture. Thus, determined the heterogeneity of CLL cells to respond to the CD40L/IL-4 signals. Although, RG7388 showed concentration dependent inhibition in the proliferation rate, even at the treatment time the CLL cell count was reduced from the seeding point. It seems the IL-4 had some signals on proliferation effect on NTL/IL-4 co-culture that did not express on the other samples.

Apart from CLL284, both freshly isolated and cryopreserved CLL samples which were co-cultured with irradiated CD40L/IL-4 fibroblast cells showed increases in the number of untreated (DMSO) cells in a time-dependent manner (right side panel of Figure 5.12 and Figure 5.13). Moreover, RG7388 treatment reduces the number of the CLL cells relative to the DMSO control at each time point. Interestingly, RG7388 treatment prevented the proliferation of the CLL cells which were co-cultured with irradiated CD40L cells. CLL cells proliferation was inhibited by more than 50% of cell viability even at the lowest dose of RG7388 (0.03μM).

For the CLL cells which were co-cultured with irradiated NTL/IL-4 fibroblast cells (left side panel of (Figure 5.12 and Figure 5.13), the number of the CLL cells decreased whether in the presence or absence of the RG7388 treatment. It was clear that CLL cells could not proliferate on the irradiated NTL fibroblast cells in the absence of CD40Ligand. However, even in the absence of proliferation, the CLL cells number was further decreased in response to the RG7388 in a dose dependent concentration manner relative to DMSO control.

For further investigation, the p53 pathway activation by RG7388 in CLL cells co-cultured with CD40L expressing feeder cells needs to be determined. In addition, since the RG7388 at (>1μM) concentration was toxic and able to inhibit the viability of CLL cells in the absence of CD40L stimulation, it may prevent the proliferation and survival signal cascades such as phosphorylation of ERK and p70 S6 kinase.

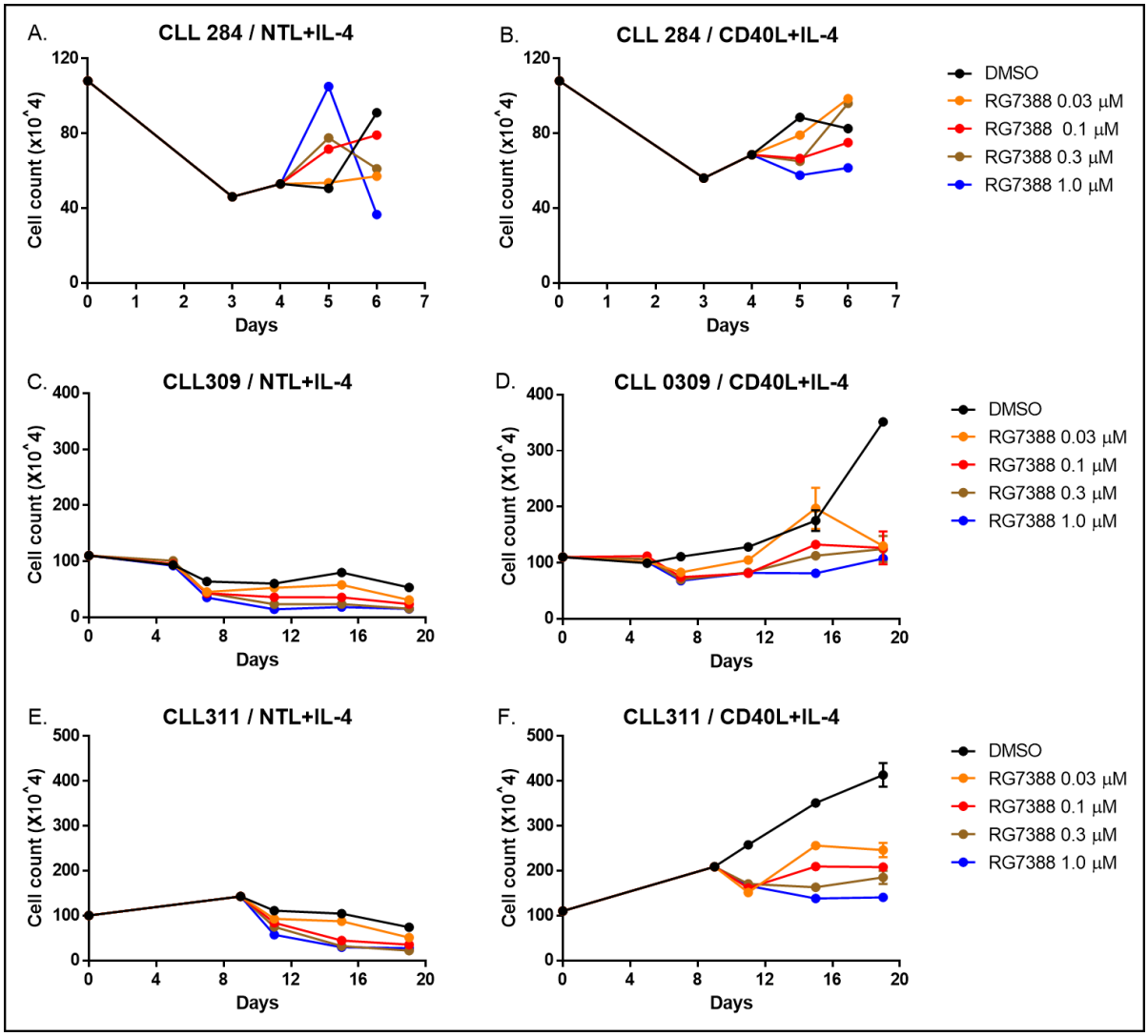

Figure 5.12 The *ex-vivo* effect of RG7366 on primary CLL cells co-cultured with NTL/IL-4 (left panel) and CD40L/IL-4 (right panel) fibroblast cells. Freshly isolated primary CLL cells ($1x10^6$ cell/well) co-cultured with irradiated (30Gy) NTL/IL-4 and CD40L/IL-4 fibroblast cells for indicative time points. RG7388 treatment was started when the CLL cells showed evidnce of proliferation. Each concentration repeated in three wells and bars show the mean ± SEM of intra-experimental repeats. Each line shows an independent cell effect in response to the treatment relative to cell number on start treatment. CLL cell count were monitored every 96hrs after treatment. The *ex-vivo* experiment performed on (n=1) for each individual CLL sample. Coulter counter was used to count CLL cells.

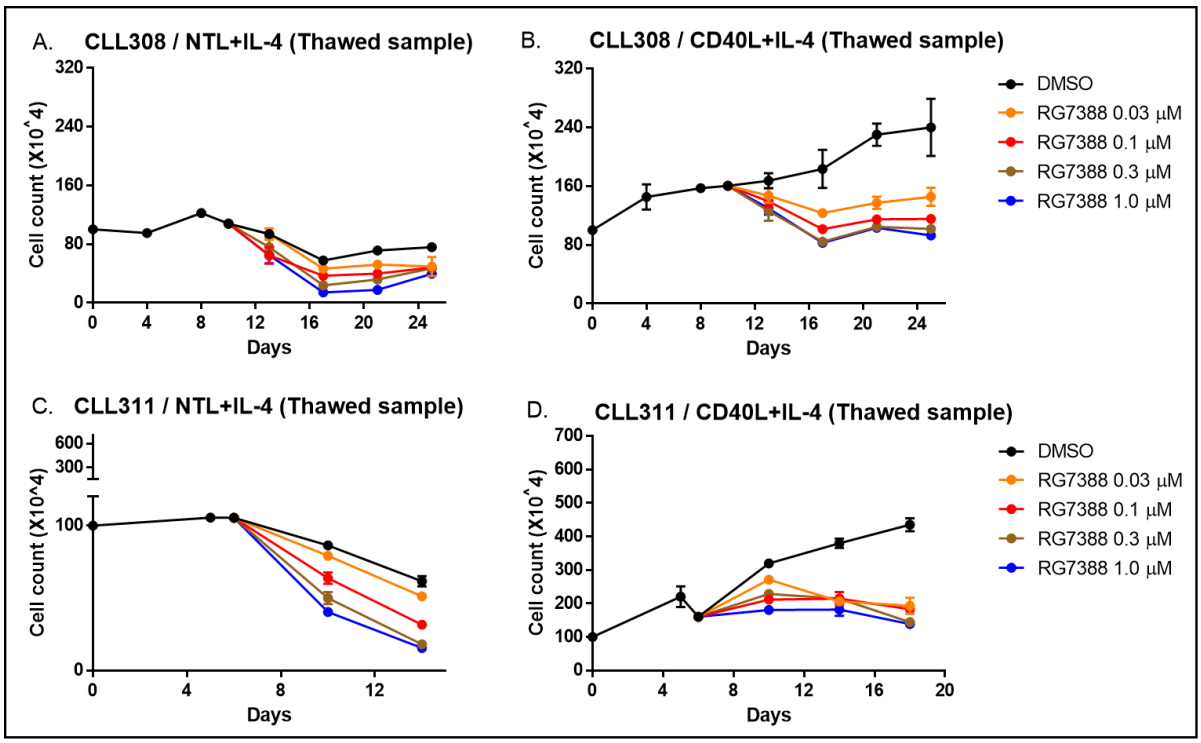

Figure 5.13 The *ex-vivo* effect of RG7366 on cryopreseved primary CLL cells co-cultured with NTL/IL-4 (left panel) and CD40L/IL-4 (right panel) mouse fibroblast cells. Immediately after thawed, cryopreseved CLL cells (1x10^6 cell/well) co-cultured with irradiated (30Gy) NTL/IL-4 and CD40L/IL-4 fibroblast cells for indicative time points. RG7388 treatment was started when the CLL cells showed evidence of proliferation. Each concentration repeated in three wells and bars show the mean ± SEM of intra-experimental repeats. Each line shows an independent cell effect in response to the treatment relative to cell number on start treatment. CLL cell count were monitored every 96hrs after treatment. The *ex-vivo* experiment performed on (n=1) for each individual CLL sample. Coulter counter was used to count CLL cells.

5.5.8 Estimated IC_{50} values for RG7388 inhibition of CLL proliferation induced by CD40L/IL-4 stimulation

In the following section, the IC_{50} of RG7388 on co-cultured CLL cell by CD40L/IL-4 and NTL/IL-4 microenvironment was calculated (Figure 5.14 and Figure 5.15). Regarding to the results described above (section 5.5.7), the difference in CLL cell count determine the inhibition effect of RG7388 over the stimulation signals. The inhibition activity was illustrated in Log. inhibition vs. response non-linear fitting format.

CLL cells signals potentiated the activity of RG7388. CLL cells co-cultured with CD40L/IL-4 cells become significantly sensitive to RG7388 treatment compared to NTL/IL-4 co-cultured CLL cells (p=0.009) (Figure 5.16).

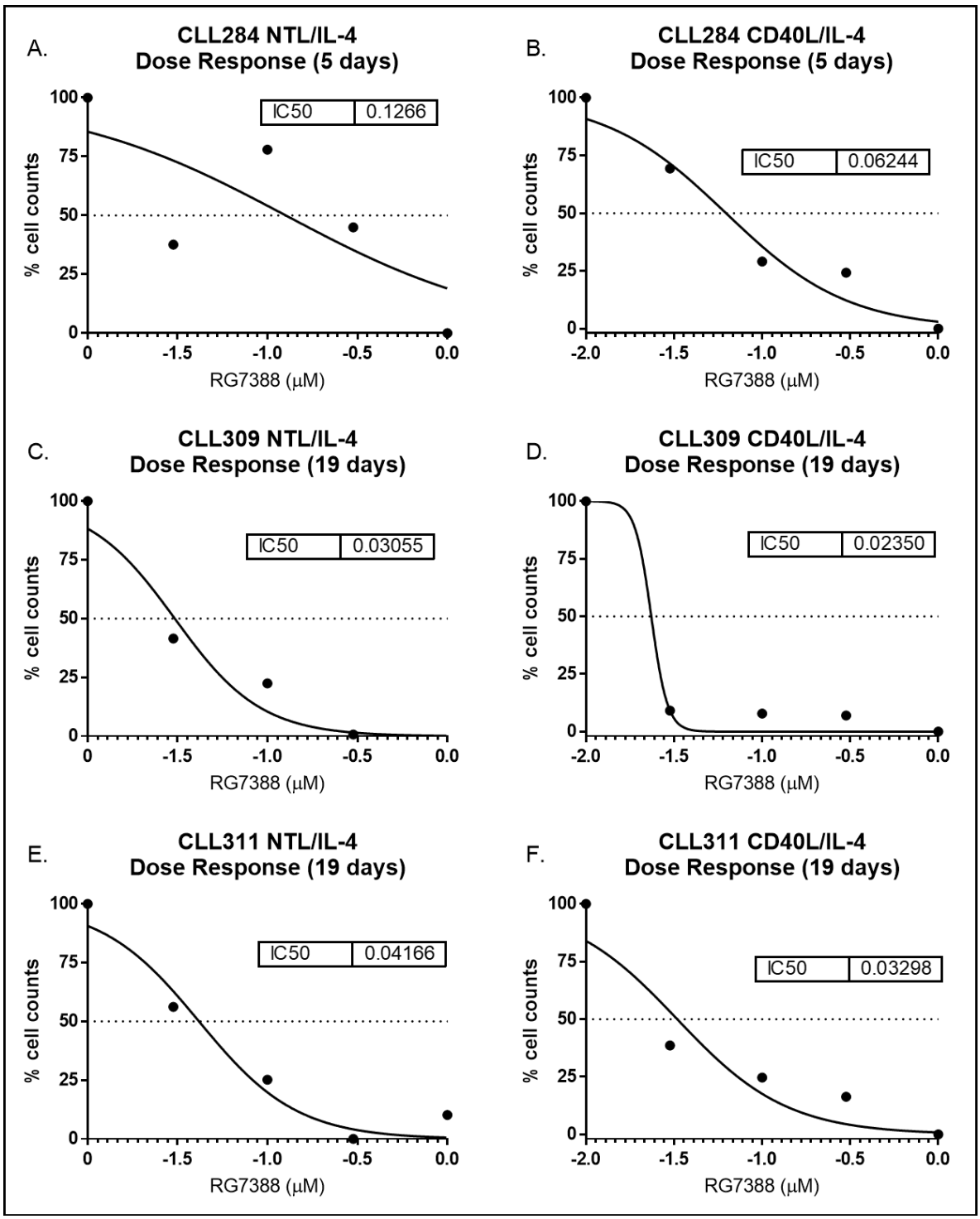

Figure 5.14 Effect of RG7388 in response to CLL cells proliferation induced by microenvironment stimuli. (A-B) CLL284, (C-D) CLL309, (E-F) CLL311. Freshly isolated CLL cells were *ex-vivo* co-cultured with either NTL or CD40L expressing feeder cells in the presence of IL-4 for indicative time point. CLL cells were treated with range of RG7388 at the start of proliferation. CLL cells were counted monitoring change in CLL cell number in response to the treatment every 96hrs. Concentration-dependent reduction in CLL cell count in response to RG7388 exposure compared with untreated controls condition. Change in % cell count was illustrated in Log. inhibition vs. response non-linear fitting format. The IC_{50} of RG7388 indicated. The *ex-vivo* experiment performed on (n=1) for each individual CLL sample.

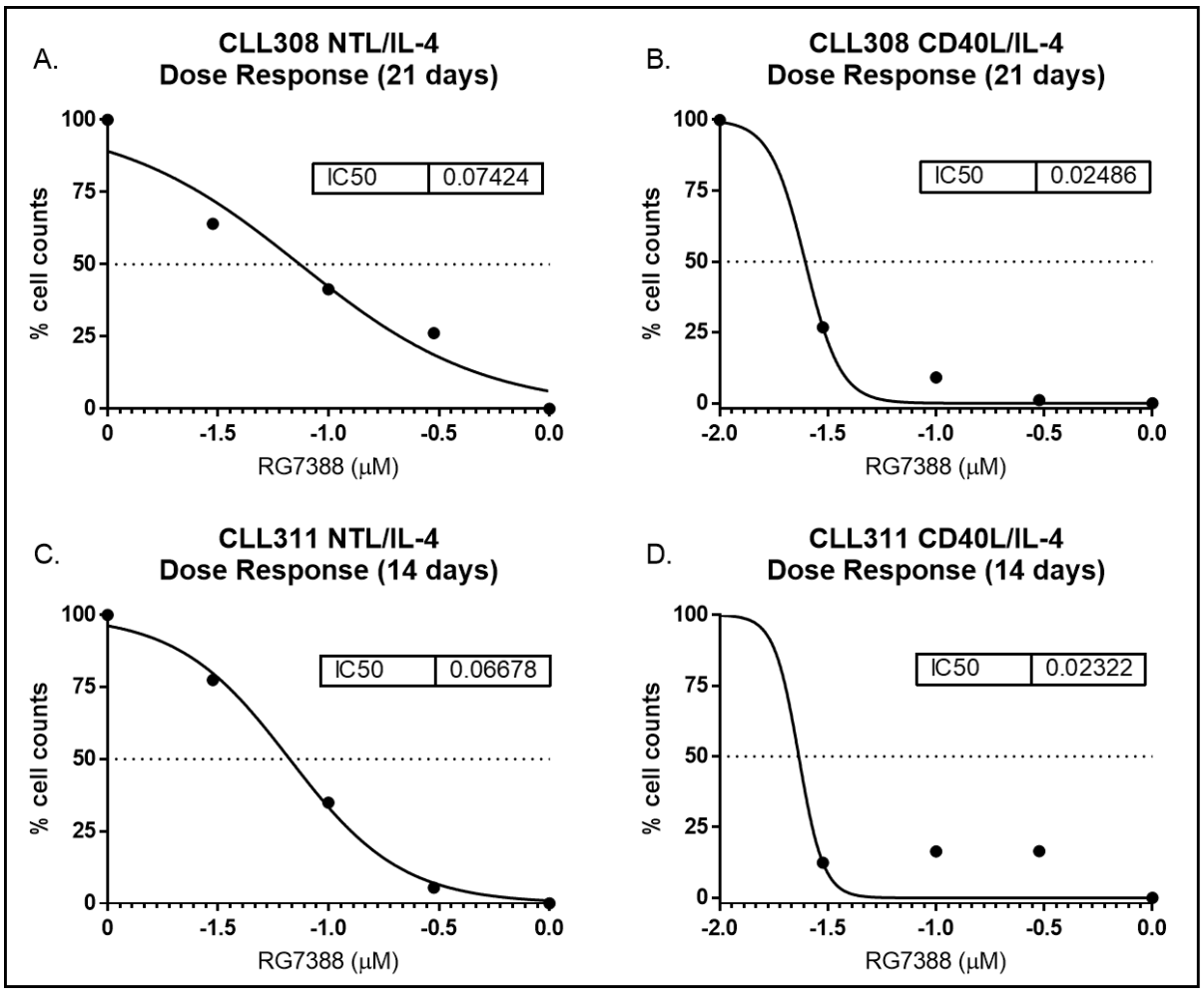

Figure 5.15 Effect of RG7388 on cryopreserved CLL cells proliferation induced by microenvironment stimuli. (A-B) CLL308, (C-D) CLL311. Thawed cryopreserved CLL cells were *ex-vivo* co-cultured with either NTL or CD40L expressing feeder cells in the presence of IL-4 for indicative time point. CLL cells were treated with range of RG7388 at the start of proliferation. CLL cells were counted monitoring change in CLL cell number in response to the treatment every 96hrs. Concentration-dependent reduction in CLL cell count in response to RG7388 exposure compared with untreated controls condition. Change in % cell count was illustrated in Log. inhibition vs. response non-linear fitting format. The IC_{50} of RG7388 indicated. The *ex-vivo* experiment performed on (n=1) for each individual CLL sample.

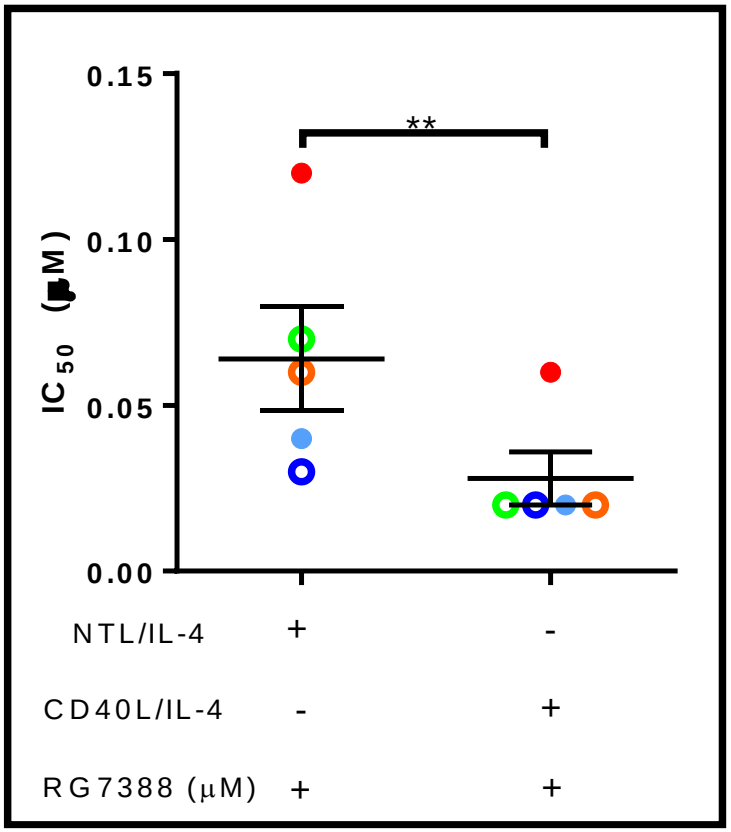

Figure 5.16 The IC_{50} of RG7388 on CLL cells co-cultured with CD40L and NTL in the presence of IL-4. Each colour code represents individual primary CLL sample. The empty circle showed the effect of freshly isolated CLL sample and the solid circle showed the effect of cryopreserved. The experiment performed on (n=5) different primary CLL samples and data are presented as an average mean ± SEM. Statistically significant p-values are indicated by paired t-test one tail. (**, $p < 0.005$)

IC_{50} (μM)	RG7388	
	NTL/IL-4	CD40L/IL-4
CLL 309	0.12	0.06
CLL 310	0.03	0.02
CLL 311	0.04	0.02
CLL 312	0.07	0.02
CLL 313	0.06	0.02
Average	0.064 ± 0.015	0.03 ± 0.01
P value	0.009	

Table 5.3 The IC_{50} values for RG7388 in response to the CLL counts relative to DMSO control for samples (n=5) co-cultured with either NTL/IL-4 or CD40L/IL-4. Data are presented as an average mean ± SEM. Statistically significant p-values are indicated by paired t-test one tail. (**, $p < 0.005$)

5.5.9 The downstream target protein level of CLL cells induced in response to CD40 signalling throw the CD40 ligand

After co-culturing the primary CLL cells with irradiated fibroblast CD40L and NTL including IL-4 cells, the change in the downstream protein level in response to the CD40-CD40L signals need to determine the proliferation activity. The western blot was performed to identify the change in the basal proteins level of proliferation cascade through phosphorylation of ERK and p70 S6 kinase activity of primary CLL cells (n=6) in response to the stimulation signals of CD40L/IL-4 co-cultured cells. The lysate of the primary CLL cells were collected after the CLL cells were co-cultured with CD40L and NTL cells including IL-4 at 12 hours (Figure 5.17).

Slightly increases in the phosphorylation activity of ERK in CLL cell co-cultured with CD40L/IL-4 monolayer cells compared to NTL/IL-4 controls. This was particularly evident with CLL309, which interestingly also showed a strong increase in proliferation when grown on the CD40L/IL-4 monolayer.

Two different isoforms of total ERK (ERK1/2) protein were detected at 44/42 kDa. In the CD40L/IL-4 co-cultured, the CLL cells showed increased detection of both isoforms compared to the corresponding NTL/IL-4 co-cultured samples. Phosphorylated p70 S6 kinase protein was induced with CD40L/IL-4 co-culture compared to the NTL/IL-4 negative control. The immunoblots were also probed for MCL-1 and BCL-2 anti-apoptotic proteins to check for any CD40L/IL-4 changes in expression, but none were found.

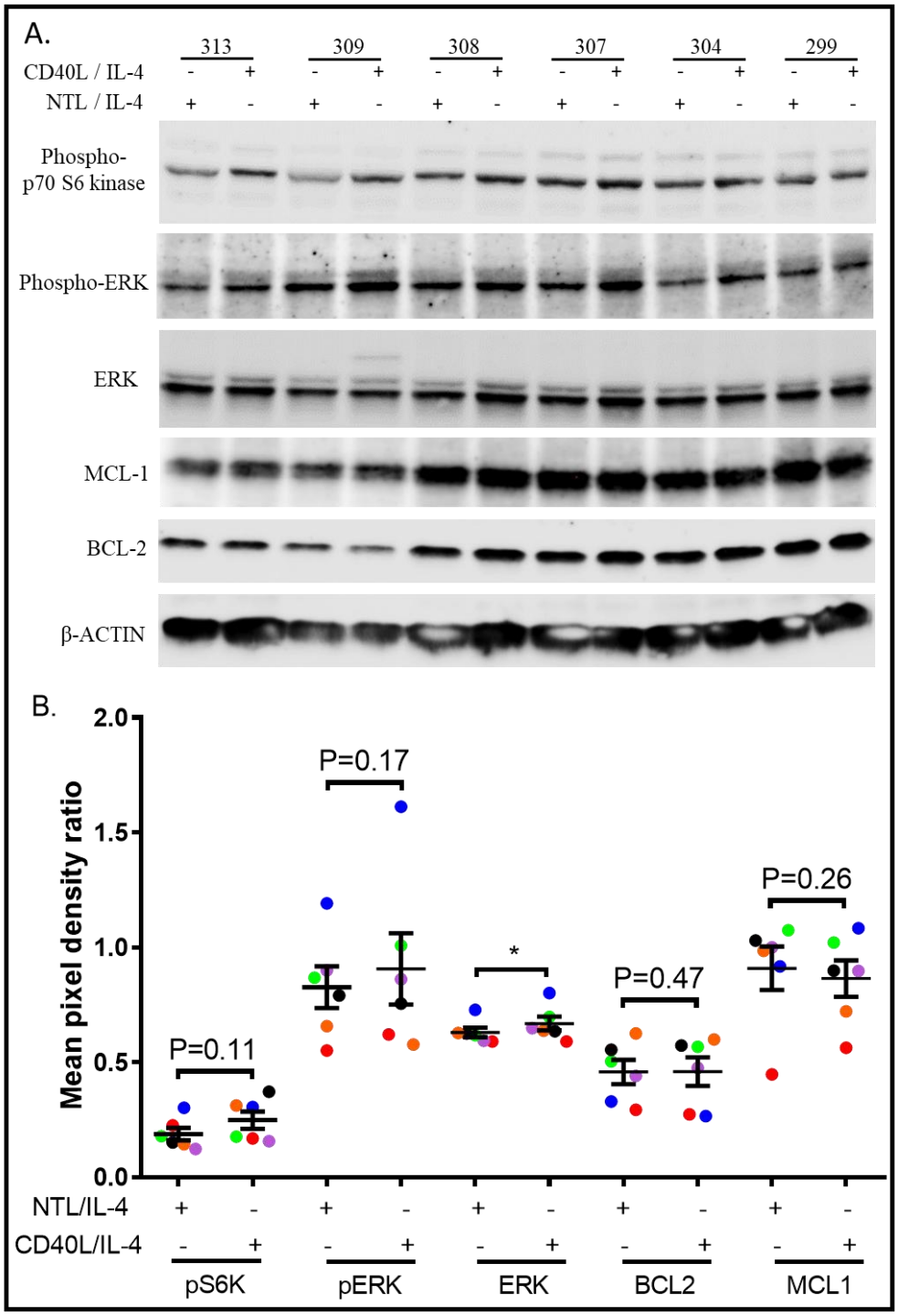

Figure 5.17 Western immunoblot of CLL cells *ex-vivo* co-cultured with microenvironment stimuli. (A) Primary CLL samples (n=6) co-cultured with irradiated (30Gy) either NTL or CD40L expressing feeder cells in the presence of IL-4 for 12hrs. Phosphorylation activity of pERK and p70 S6 kinase are evidence for proliferation signals. MCL1 and BCL2 determine the anti-apoptotic change. β-actin was used as the loading control. All strips were from the same membrane. (B) Densitometry analysis determines the change in the protein level with NTL/IL-4 and CD40L/IL-4 co-cultured CLL cells. The mean pixel density ratio for all proteins was background corrected and the values were normalized relative to β-actin, except pERK and p70 S6 kinase for which the ratio was calculated relative to ERK and S6 kinase. Western blot and densitometry analysis performed for n=1 experiment. Only significant changes between NTL/IL-4 and CD40L/IL-4 stimulation are displayed on the graphs by paired t-test one tail. The p-values less than 0.05 are shown (*, $p < 0.05$). Data are presented as mean ± SEM for all CLL samples.

5.5.10 The basal expression of a p53 pathway gene panel for CLL cells co-cultured with CD40L/IL-4

After looking to the changes at the protein expression level, the changes in the mRNA transcript levels were investigated for primary CLL cells (n=6) co-cultured with irradiated fibroblast cells expressing either CD40L or NTL on their surface in the presence of IL-4 for 6 hours followed by mRNA extraction.

Prior to investigating the response to RG7388, an experiment was performed to identify the Ct levels as an inverse measure of the basal mRNA expression of a panel of p53 target genes in primary CLL cell samples co-cultured with CD40L/IL-4 or NTL/IL-4 monolayers (Figure 5.18).

The basal Ct level of *PPM1D* and *TP53INP1* were significantly increased with CD40L/IL-4 cells co-cultured relative to NTL/IL-4 cells. Moreover, the Ct value of *MDM2* showed a trend for increase with CD40L compared to NTL however, it was not significant (p=0.2). *CDKN1A* showed a reduction in Ct with CD40L stimulation compared to the NTL signals, indicating an increase in gene expression. *TP53* gene did not show clear change in the Ct basal level either with irradiated CD40L or NTL co-cultured cells (Figure 5.19 A).

On the pro-apoptotic genes, the basal Ct value of *PUMA* and *BAX* appeared to be increased with CD40L co-culture compared to NTL. The statistical t-test was applied to calculate the differences between the presence and absence of CD40L stimulation. Furthermore, the basal Ct expression level for *NOXA* and *FAS* showed a significant reduction in Ct values with CD40L stimulation compared to NTL, indicating increased expression. CD40L/IL-4 co-culture significantly induces the Ct level of *NOXA* (p=0.0017) and *FAS* (p=0.049) in comparison to NTL (Figure 5.19 B).

On the anti-apoptotic genes, *MCL1* and *BCL2*. There was no significant difference between the basal expression of the *MCL1* and *BCL2* genes with co-culture stimulation of neither CD40L versus NTL irradiated cells (Figure 5.19 C).

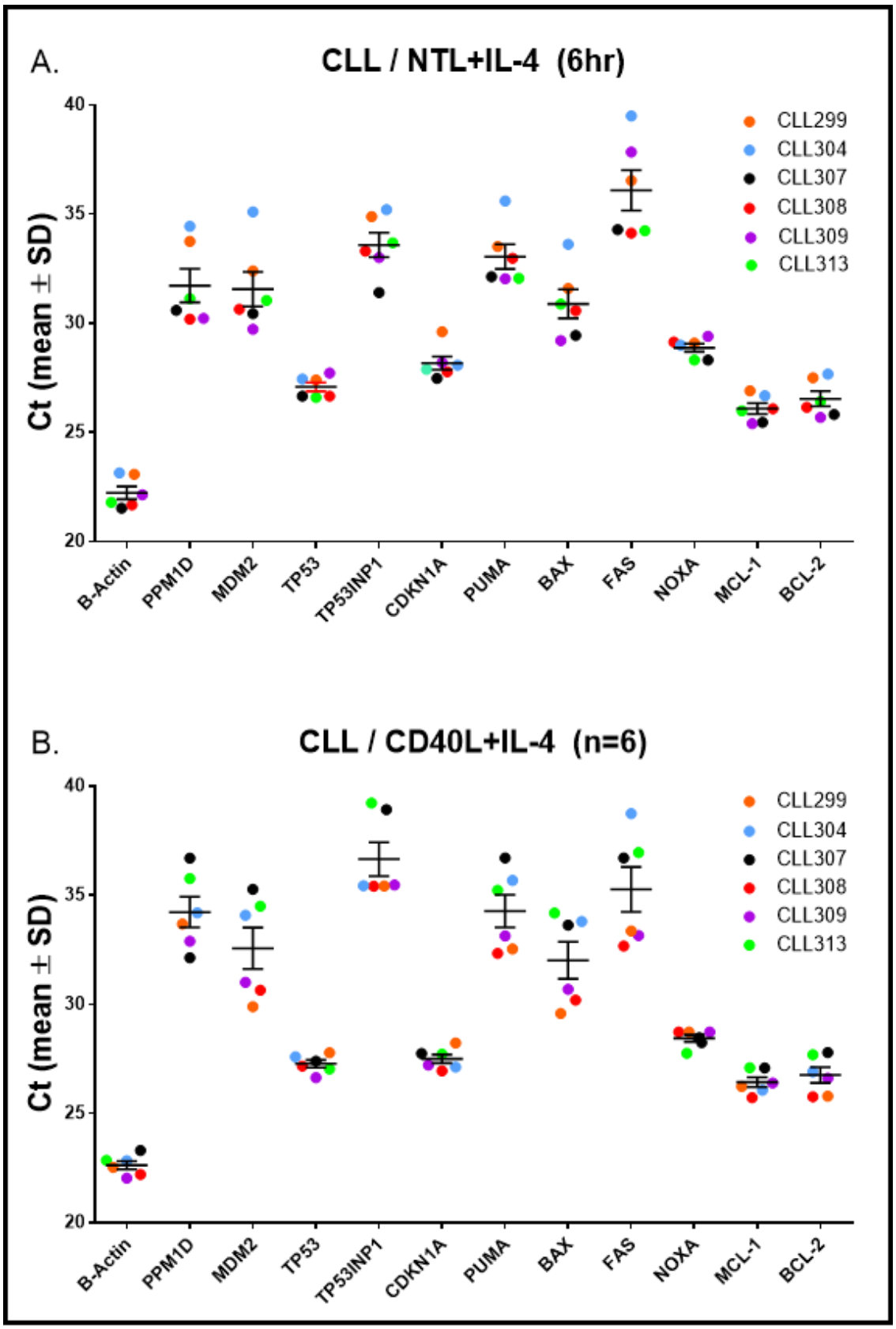

Figure 5.18 The basal mRNA expression of p53 transcriptional target genes of primary CLL cells *ex-vivo* co-cultured with microenvironment stimulation. (A) NTL and (B) CD40L fibroblast cells in the presence of IL-4 for 6 hours. Primary CLL samples (n=6) co-cultured with irradiated (35Gy) NTL and CD40L expressing feeder cells in the presence of IL-4 for 6hrs. qRT-PCR is used to measure the mRNA expression of p53 dependent targe genes. DMSO treated cells were used as the calibrator between three replicated intra-experimental wells. Error bars show the mean ± SEM of different CLL samples. Each colour represents individual CLL cell. The experiment performed in (n=1) repeat on each primary CLL sample.

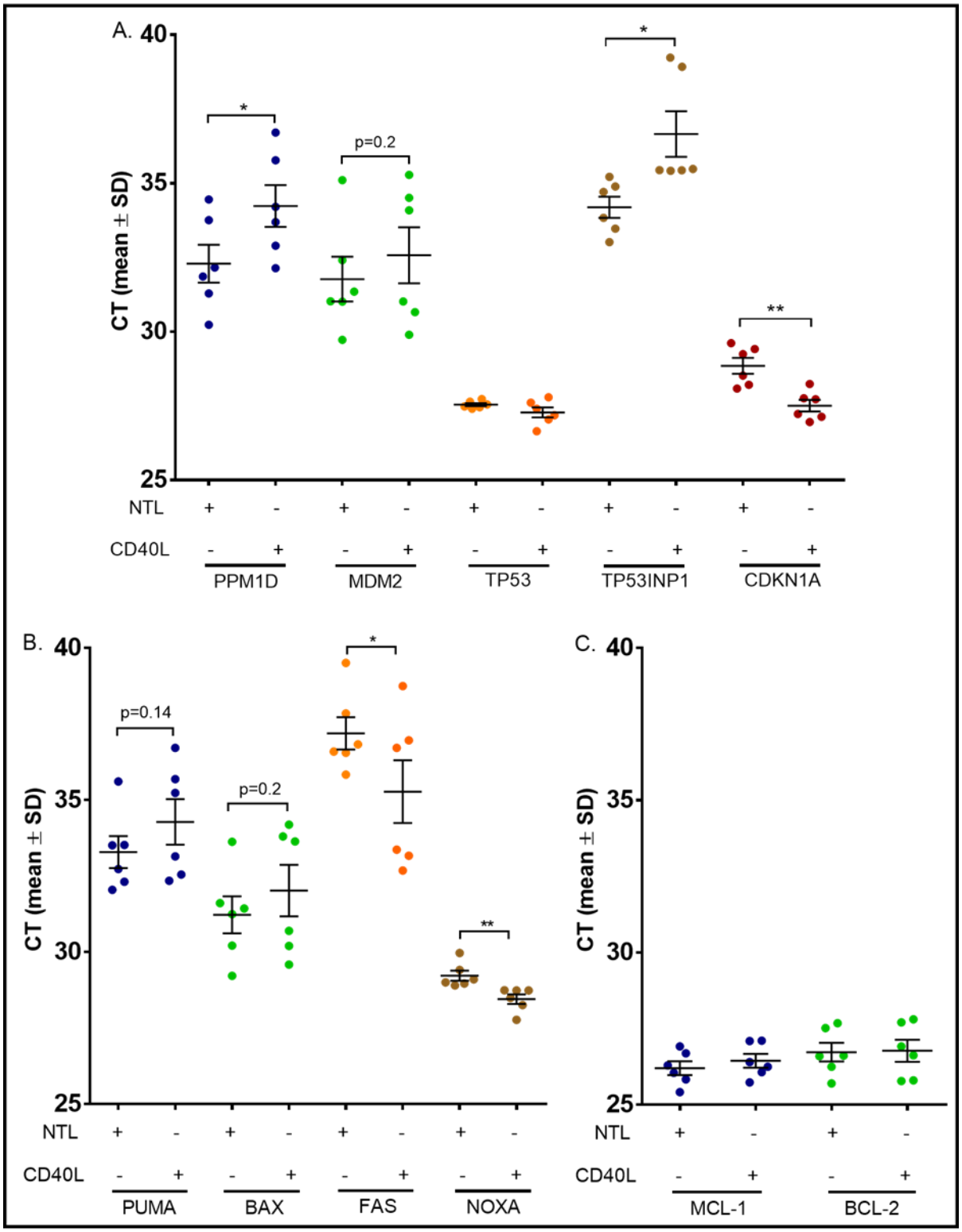

Figure 5.19 Summary of the changes in the Ct basal mRNA expression of CLL cells co-cultured with CD40L or NTL fibroblast cells for 6 hours (n=6). (A) TP53 negative regulator target genes, (B) pro-apoptotic genes, (C) Anti-apoptotic genes. Gene expression compared between CD40L stimulation and NTL negative control. The statistical paired t-test one tailed was applied to determine change expression (p-value). The error bar represent mean ± SEM. The significance differences between NTL and CD40L stimulation are indicated above the horizontal bars. Only the p-values less than 0.05 are shown in (* $p < 0.05$, ** $p < 0.005$).

5.5.11 The expression of gene panel for CLL cells co-cultured with CD40L/IL-4 in response to WIP1 inhibitor alone

The aim of the next experiment was to determine the transcriptional mRNA changes of CLL cells co-cultured with CD40L and NTL cells followed by WIP1 inhibitor treatment. The primary CLL cells co-cultured with irradiated CD40L or NTL fibroblasts in the presence of IL-4 for 6 hours prior exposed to GSK2830371 (2.5μM). Following the stimulation, the CLL cells were treated with WIP1 inhibitor at (2.5μM) for additional 6 hours. Then, the CLL cells were harvested to identifying the changes in the mRNA expression of target genes.

CD40L/IL-4 co-cultured cells showed that *CDKN1A*, *NOXA* and *PUMA* genes express the highest fold change differences in response to WIP1 inhibitor. In contrast, *MDM2*, *CDKN1A*, *PUMA, FAS* and *NOXA* showed the highest fold change expression in response to WIP1 inhibitor with irradiated NTL co-cultured cells (Figure 5.20).

The TP53 negative regulator genes showed an increase in the expression of *PPM1D*, *MDM2* and *TP53* with NTL co-culture cells relative to CD40L in response to WIP1 inhibitor. Furthermore, *TP53INP1* and *CDKN1A* showed no significant differences neither with NTL nor CD40L co-cultured in WIP1 inhibitor (Figure 5.21 A). In contrast, the expression of pro-apoptotic genes, *BAX* and *FAS* were decreased in CLL co-cultured with CD40L compared to NTL in the presences of WIP1 inhibitor. In addition, *PUMA* and *NOXA* did not show significant changes in their expression whether with CD40L nor NTL co-cultured in the presence of WIP1 inhibitor (Figure 5.21 B). The anti-apoptotic genes, *MCL2* and *BCL2* did not show much significant difference in response to WIP1 inhibitor with both CD40L and NTL co-cultured cells (Figure 5.21 C).

To sum up, we can determine that WIP1 inhibitor (2.5μM) does not have a significant change in the expression of the gene panel on both CD40L and NTL co-cultured cells.

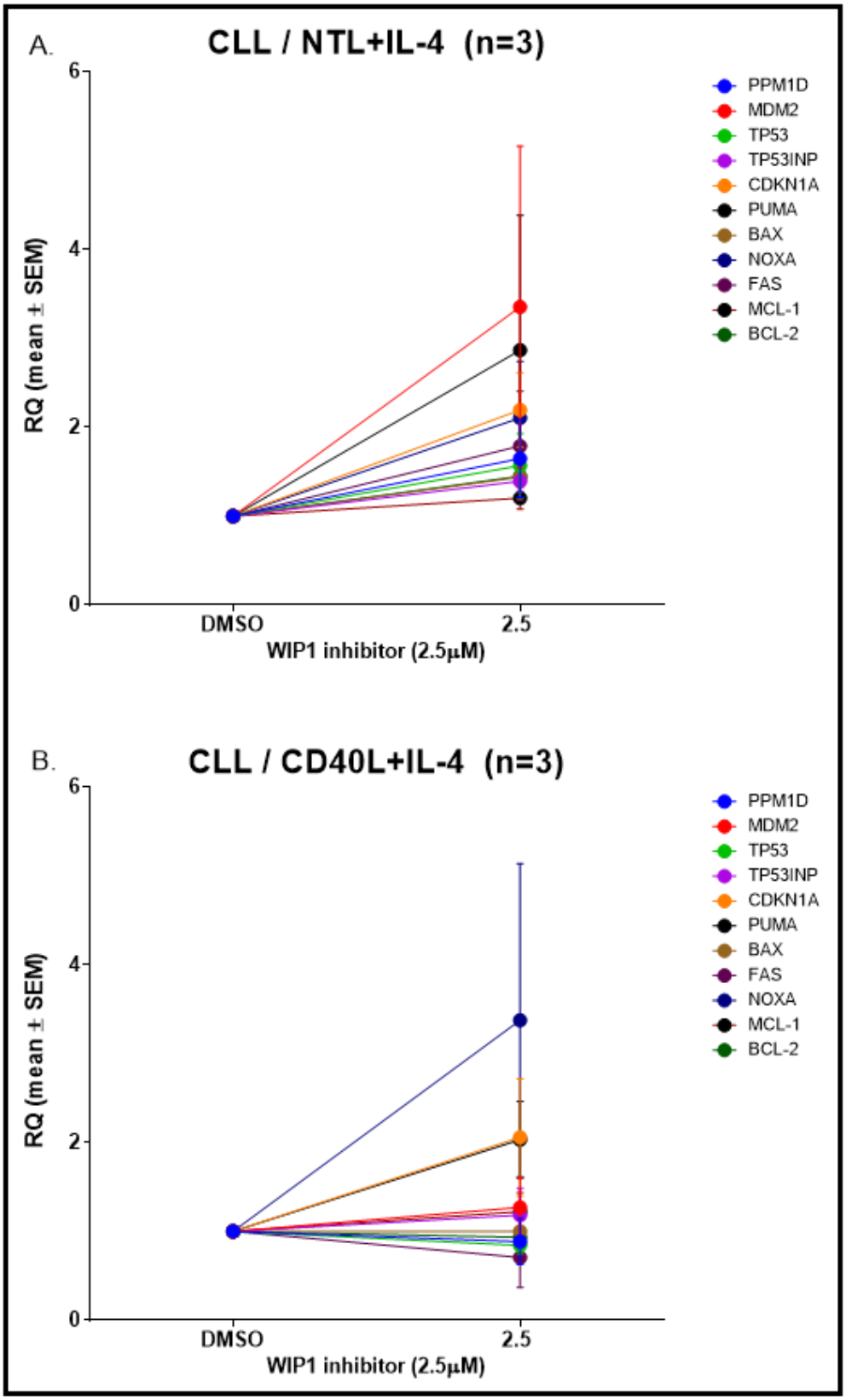

Figure 5.20 Fold changes in the mRNA expression of selected p53 transcriptional target genes of primary CLL cells co-cultured with *ex-vivo* microenvironment stimulation in response to WIP1 inhibitor. Primary CLL samples (n=3) co-cultured with irradiated (A) NTL and (B) CD40L fibroblast cells in the presence of IL-4 for 6 hours, followed by treatment of GSK2830371 (2.5µM) for 6hrs. qRT-PCR measured the mRNA gene expression. *β-ACTIN* was used as the endogenous control and DMSO-treated cells were used as the calibrator between three intra-replicate wells of the treatment concentration. Error bars represent the mean ± SEM of different CLL samples. The experiment performed in (n=1) repeat on each primary CLL sample. RQ values were calculated using the formula 2ΔΔCt.

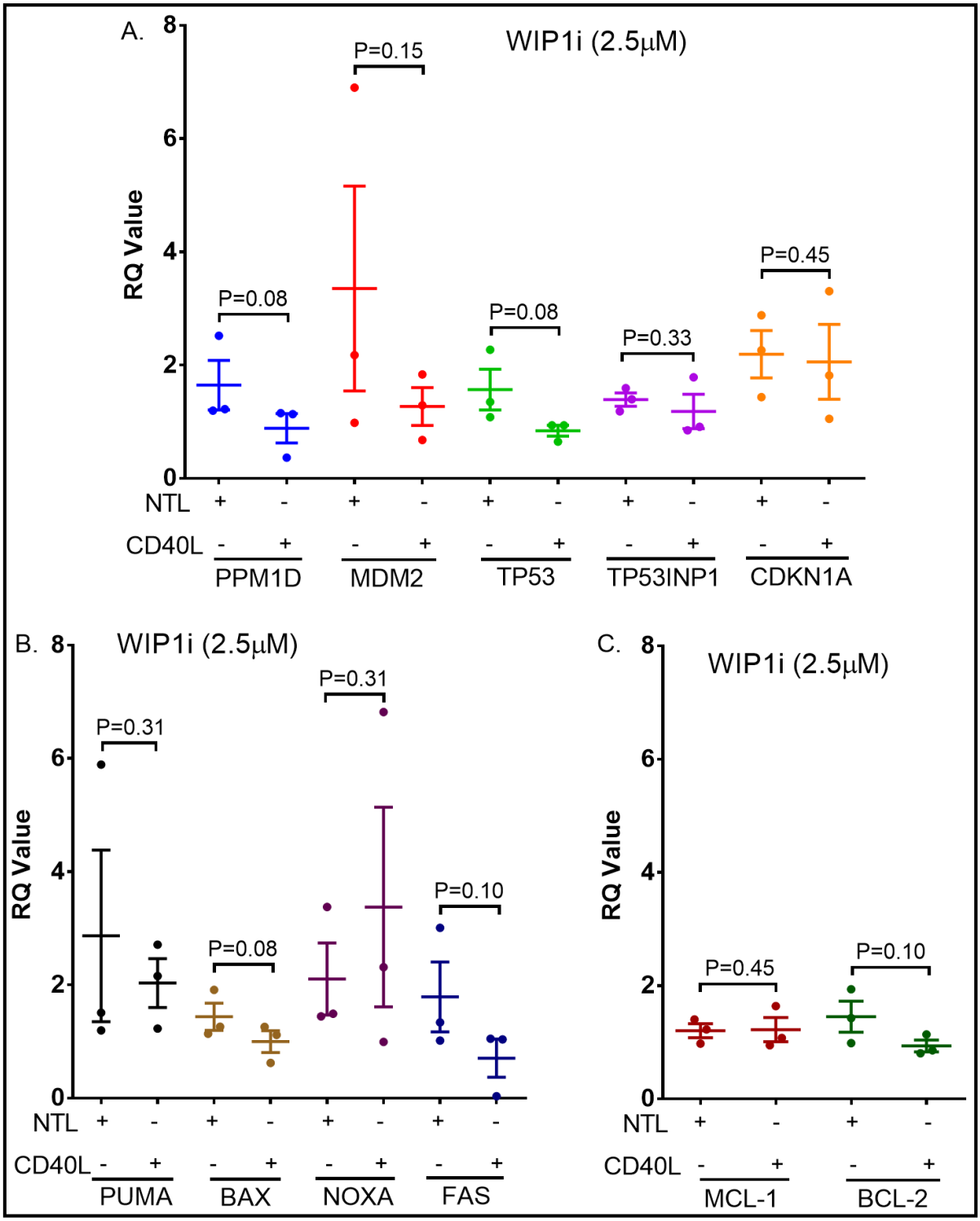

Figure 5.21 Summary of the differences in mRNA fold change expression of CLL cells *ex-vivo* co-cultured with either CD40L/IL-4 or NTL/IL-4 fibroblast cells in response to WIP1i (2.5µM) by qRT-PCR. (A) p53 negative regulator, (B) pro-apoptotic, (C) anti-apoptotic. Primary CLL samples (n=3) co-cultured with *ex-vivo* microenviroment stiulation for 6hrs and followed by GSK2830371 (2.5µM) treatment for additional 6hrs. The error bar represent mean ± SEM of different CLL samples. Each dots represent individual CLL sample. Each colour represents mRNA expression of certain gene in response to the treatment with NTL and CD40L stimulation. The significance differences between NTL and CD40L stimulation are indicated above the horizontal bars for each gene by one tail paired t-test, significance taken at $p < 0.05$.

5.5.12 The expression of the gene panel for CLL cells co-cultured with CD40L in response to RG7388

The purpose of this experiment was to determine the transcriptional change in gene expression level of CLL cell co-cultured with fibroblast CD40L or NTL in response to MDM2 inhibitor after 6 hours of treatment. In addition, examining the change in gene expression across range of RG7388 concentrations.

The primary CLL cells were co-cultured with irradiated fibroblast cells either CD40L or NTL for 6 hours prior exposed to RG7388. Following the stimulation, the CLL cells were treated with RG7388 (1μM and 3μM) for an additional 6 hours. Then, the CLL cells were harvested for identifying the changes in the expression of specific target genes. The fold changes were calculated relative to *Actin* and DMSO treatment.

In primary CLL cells, the fold change expression of *MDM2*, *CDKN1A, NOXA* and *PUMA* were obviously increased with both NTL and CD40L co-cultured cells in response to RG7388 treatment relative to DMSO untreated response (Figure 5.22).

The expression of *TP53* negative regulator gene in response to the RG7338 (1μM), *MDM2* and *CDKN1A* genes showed remarkable fold change expression with both CD40L and NTL co-cultured cells relative to the DMSO However, there is no differences in *MDM2* and *CDKN1A* expression neither with CD40L nor NTL co-cultured cells in response to RG7338 (1μM). Furthermore, the expression of *TP53* gene was decreased with CD40L signals relative to NTL co-cultured cells in response to RG7338 (1μM). In addition, *TP53INP1* gene did not show many changes in its expression with both CD40L and NTL co-cultured cells in response to RG7338 (1μM) (Figure 5.23 A).

In contrast, the pro-apoptotic genes, the expression of *PUMA* and *NOXA* were decreased with CD40L signals in response to RG7338 (1μM) relative to NTL co-cultured cells. In addition, *BAX* and *FAS* did not show significant changes in their expression with both CD40L and NTL co-cultured cells relative to RG7338 (1μM) (Figure 5.23 B). Moreover, *MCL1* and *BCL2* showed no differences in response to RG7338 (1μM) whether in the presence or absence of CD40L signals (Figure 5.23 C).

With RG7388 (3μM), the expression of *MDM2* was increased on both CD40L and NTL co-cultured cells. In contrast, the expression of *PPM1D*, *TP53*, *TP53INP1* and *CDKN1A* were decreased with CD40L co-cultured cells relative to NTL control (Figure 5.24 A).

The expression of pro-apoptotic genes, *PUMA*, *BAX*, *NOXA* and *FAS* were decreased with CD40L co-cultured cells compared to NTL in the presence of RG7388 (3µM) (Figure 5.24 B). The *MCL1* and *BCL2* did not show significant difference in their expression on both CD40L and NTL co-cultured cells with RG7388 (3µM) (Figure 5.24 C).

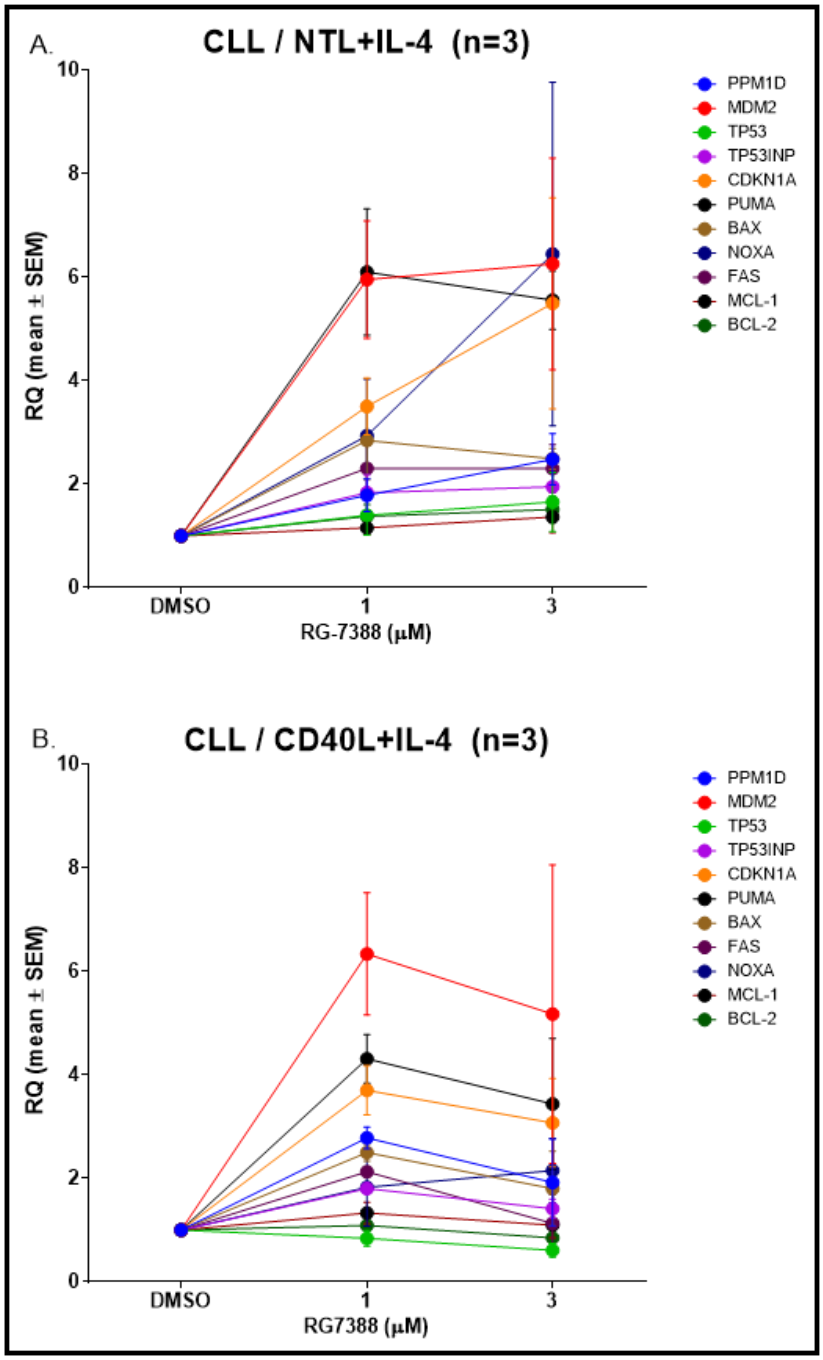

Figure 5.22 Fold changes in the mRNA expression of selected p53 transcriptional target genes of primary CLL cells co-cultured with *ex-vivo* microenvironment stimulation in response to RG7388 by qRT-PCR. Primary CLL samples (n=3) co-cultured with irradiated (A) NTL and (B) CD40L fibroblast cells in the presence of IL-4 for 6hrs, followed by RG7388 (1-3µM) treatment for 6hrs. *β-ACTIN* was used as the endogenous control and DMSO-treated cells were used as the calibrator between three intra-replicate wells of each concentration. The experiment performed in (n=1) repeat on each primary CLL sample and the error bars represent the mean ± SEM of CLL samples. RQ values were calculated using the formula 2ΔΔCt.

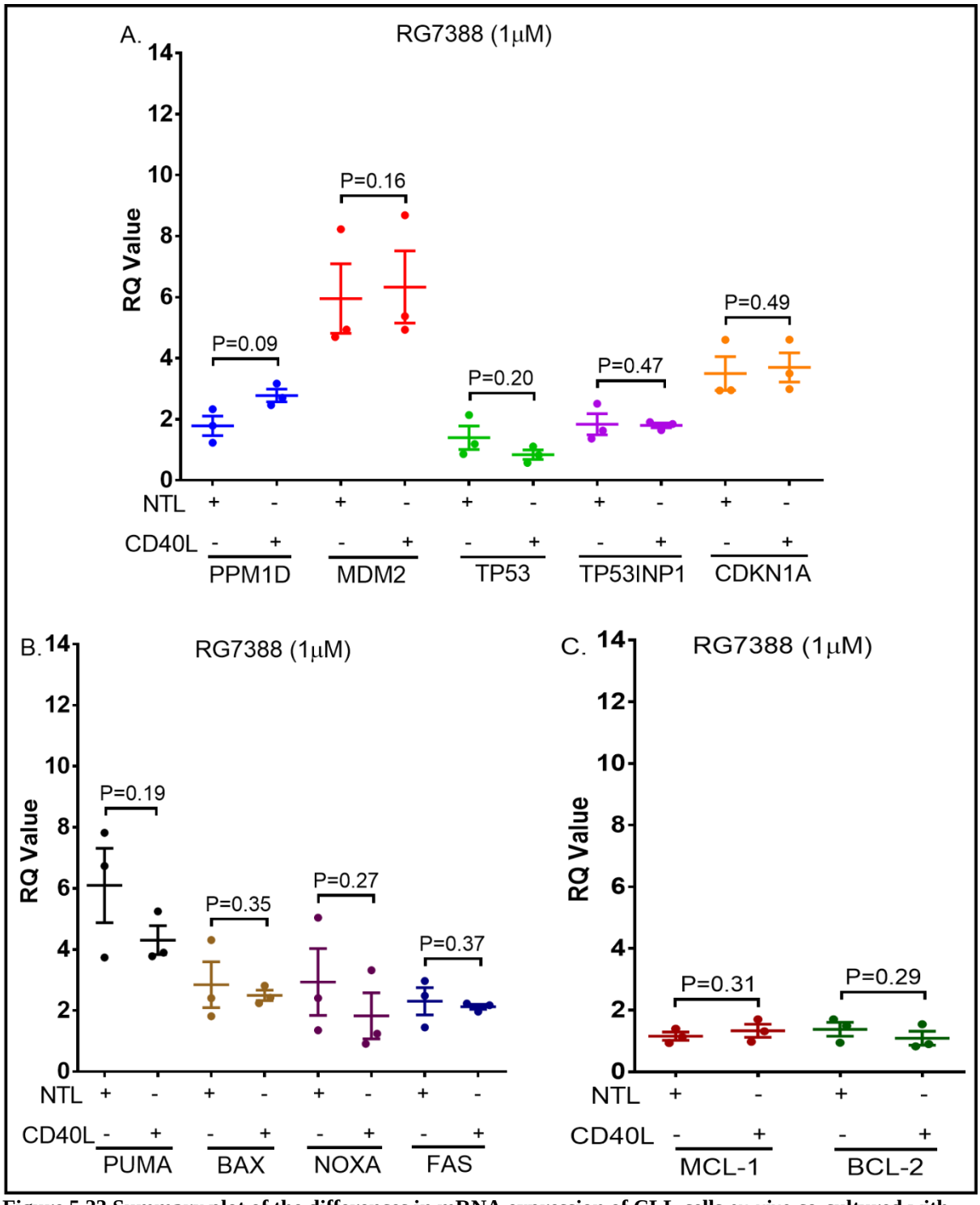

Figure 5.23 Summary plot of the differences in mRNA expression of CLL cells *ex-vivo* co-cultured with either NTL control or CD40L expressing fibroblast cells in the response to RG7388 (1μM) for 6 hours on separate samples taken from (n=3) patients. The genes are grouped as: (A) p53 negative regulator, (B) pro-apoptotic, (C) anti-apoptotic. Each point represents the mean value for an individual patient. The error bars in each case represent the mean ± SEM for the n=3 patient samples. Each colour represents mRNA expression of certain gene in response to the treatment with NTL and CD40L stimulation. One tailed paired t-test p-values are shown for the significance of differences between the mean values for NTL control and CD40L stimulated samples, significance taken at $p < 0.05$.

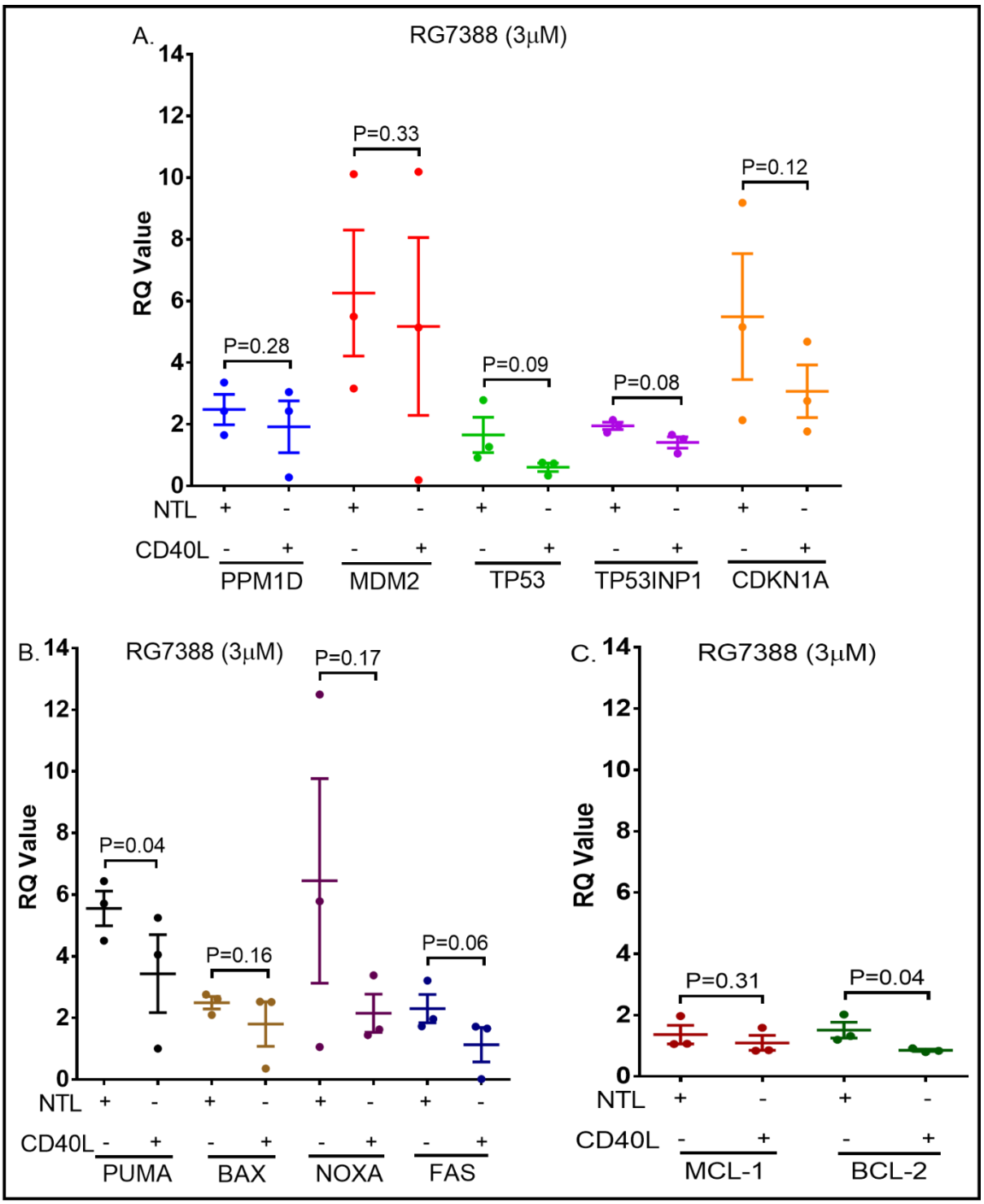

Figure 5.24 Summary plot of the differences in mRNA fold change expression of primary CLL cells *ex-vivo* co-cultured with either CD40L/IL-4 or NTL/IL-4 fibroblast cells in response to RG7388 (3μM) by qRT-PCR. (A) p53 negative regulator, (B) pro-apoptotic, (C) anti-apoptotic. Primary CLL samples (n=3) co-cultured with *ex-vivo* microenviroment stimulation for 6hrs and followed by RG7388 (3μM) treatment for additional 6hrs. The error bar represent mean ± SEM of different CLL samples. Each point represents the mean value for an individual patient. Each colour showed mRNA expression of certain gene in response to the treatment with NTL and CD40L stimulation. One tailed paired t-test p-values are shown for the significance of differences between the mean values for NTL control and CD40L stimulated samples, significance taken at $p < 0.05$.

5.5.13 The expression of the gene panel in CLL cells co-cultured with CD40L in response to RG7388 in a combination with WIP1 inhibitor

The aim of this experiment is to investigate whether the combination of WIP1 inhibitor increases the genetic transcriptional expression by potentiation the activity of RG7388 on CLL cells co-cultured with CD40L and NTL. Following the 6 hours co-culture stimulation, CLL cells were treated with WIP1 inhibitor in combination with RG7388 for additional 6 hours.

In primary CLL cells, the fold change expression of *MDM2*, *CDKN1A, NOXA* and *PUMA* were obviously increased with both NTL and CD40L co-cultured cells in response to a combination treatment of RG7388 with WIP1 inhibitor relative to DMSO untreated response (Figure 5.25 A). In contrast, in the CLL co-cultured with NTL fibroblast cells, the expression of *PUMA* was induced with combination of WIP1 inhibitor with RG7388 (1µM) but no much change with RG7388 (3µM) (Figure 5.25 B).

With RG7388, the expression of *MDM2* and *CDKN1A* were increased with WIP1 inhibitor combination treatment on both CD40L and NTL co-cultured cells. In contrast, *PPM1D*, *TP53* and *TP53INP1* did not show much change differences with a combination treatment with CD40L and NTL co-cultured cells (Figure 5.26 A and Figure 5.27 A).

Looking to the pro-apoptotic genes, the expression of *PUMA*, *BAX* and *NOXA* were increased with a combination of WIP1 inhibitor with RG7388 in the presence of CD40L co-cultured cell signalling however, *FAS* was decreased (Figure 5.26 B and Figure 5.27 B).

In comparison, the expression of *PUMA* and *NOXA* were increased in the CLL cells co-cultured with NTL whether in response to RG7388 or in combination to WIP1 inhibitor. In contrast, *BAX* and *FAS* did not show much increases in their expression relative to combination treatment with CLL cells co-cultured with NTL. Furthermore, in the CLL co-cultured with NTL fibroblast cells, the expression of *PUMA* showed little increases with combination of WIP1 inhibitor with RG7388 (1µM) but no much change with RG7388 (3µM) (Figure 5.26 B and Figure 5.27 B).

Looking to the anti-apoptotic genes, *MCL1* and *BCL2* did not show fold change differences in their expression relative to the RG7388 and WIP1 inhibitor either with CD40L or NTL co-cultured cells (Figure 5.26 C and Figure 5.27 C).

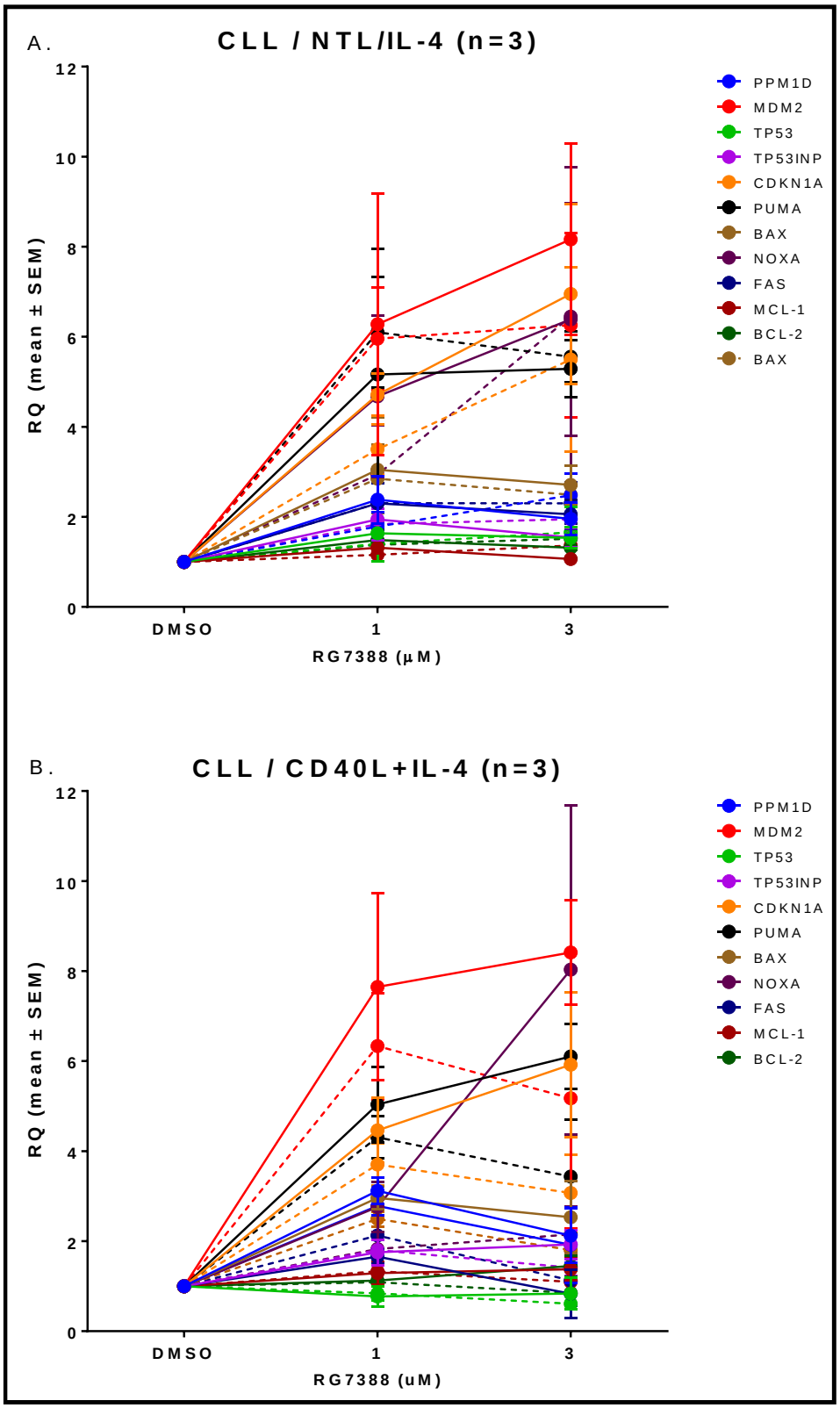

Figure 5.25 Fold change in mRNA ecpression of selected p53 transcriptional target genes of primary CLL cells co-cultured with *ex-vivo* microenvironment stimulation in response to RG7388 in combination with WIP1 inhibitor by qRT-PCR. Different primary CLL samples (n=3) co-cultured with irradiated (A) NTL control and (B) CD40L fibroblast cells in the presence of IL-4 for 6hrs, followed by RG7388 (1-3µM) treatment with and without GSK2830371 (2.5µM) for additional 6hrs. The effect of RG7388 alone represents in dash line, and the combination with WIP1i (2.5µM) is solid line. *β-ACTIN* was used as the endogenous control and DMSO-treated cells were used as the calibrator between three intra-replicate wells of each concentration for individual sample. The experiment performed in (n=1) repeat on each primary CLL sample and the error bars represent the average mean ± SEM of CLL samples. RQ values were calculated using the formula 2ΔΔCt.

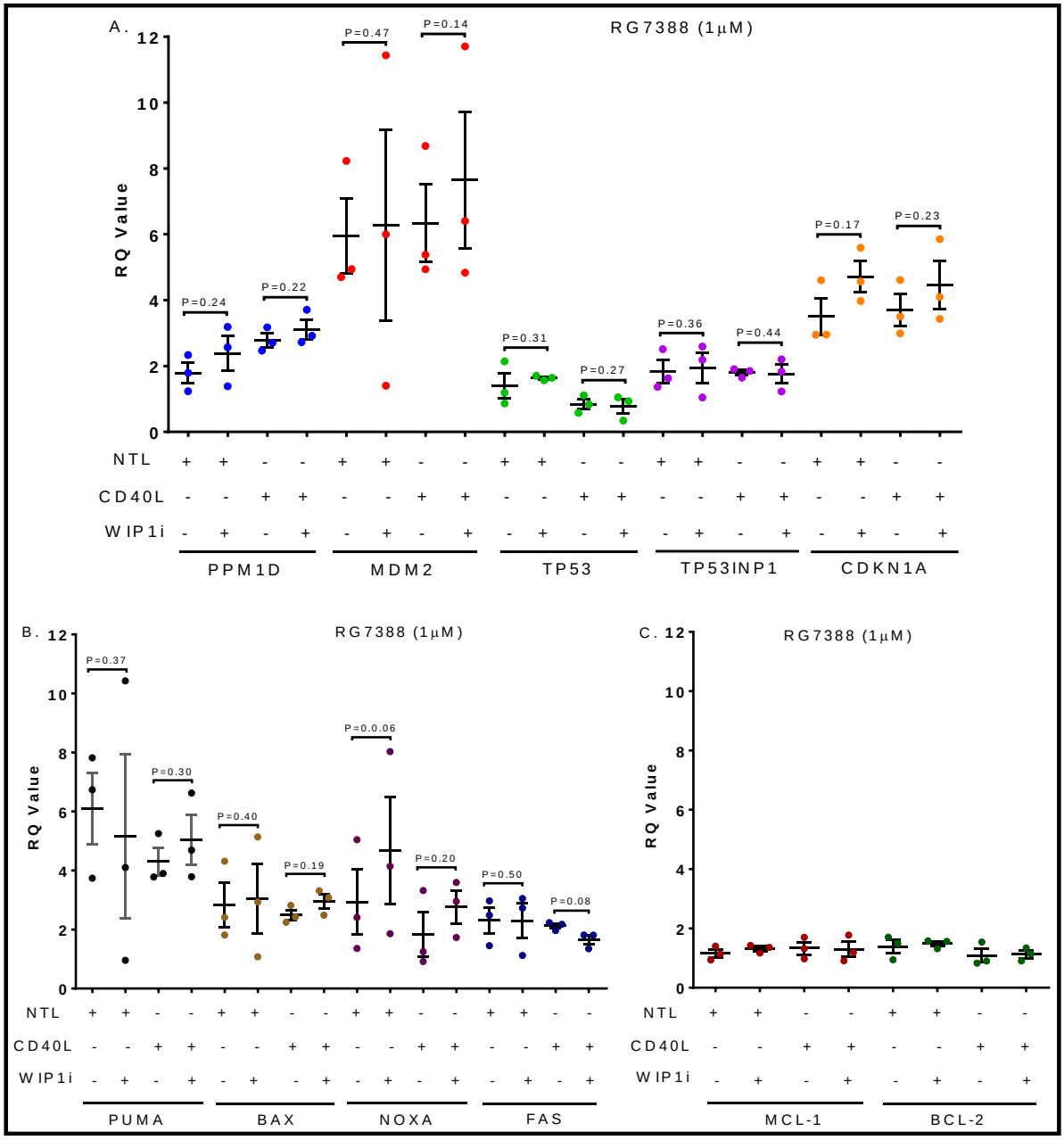

Figure 5.26 Summary plot comparing the fold changes of the mRNA expression of primary CLL cells *ex-vivo* co-cultured with NTL/IL-4 and CD40L/IL-4 fibroblast cells in response to RG7388 (1µM) in a combination with WIP1 inhibitor (2.5µM). The genes grouped as: (A) p53 negative regulator, (B) pro-apoptotic, (C) anti-apoptotic. Primary samples taken from (n=3) separate patient and co-cultured with *ex-vivo* microenvironment stimulation for 6hrs then, followed by RG7388 (1µM) with and without GSK2830371 (2.5µM) treatment for additional 6hrs. Each colour represents mRNA expression of certain gene in response to the treatment with NTL and CD40L stimulation. Each point represents the mean value for an individual patient and the error bars in each case represent the average mean ± SEM for the (n=3) patient samples. One tailed paired t-test p-values are shown for the significance differences between the mean values for RG7388 treatment with or without WIP1i are displayed above the horizontal bars, significance taken at $p < 0.05$.

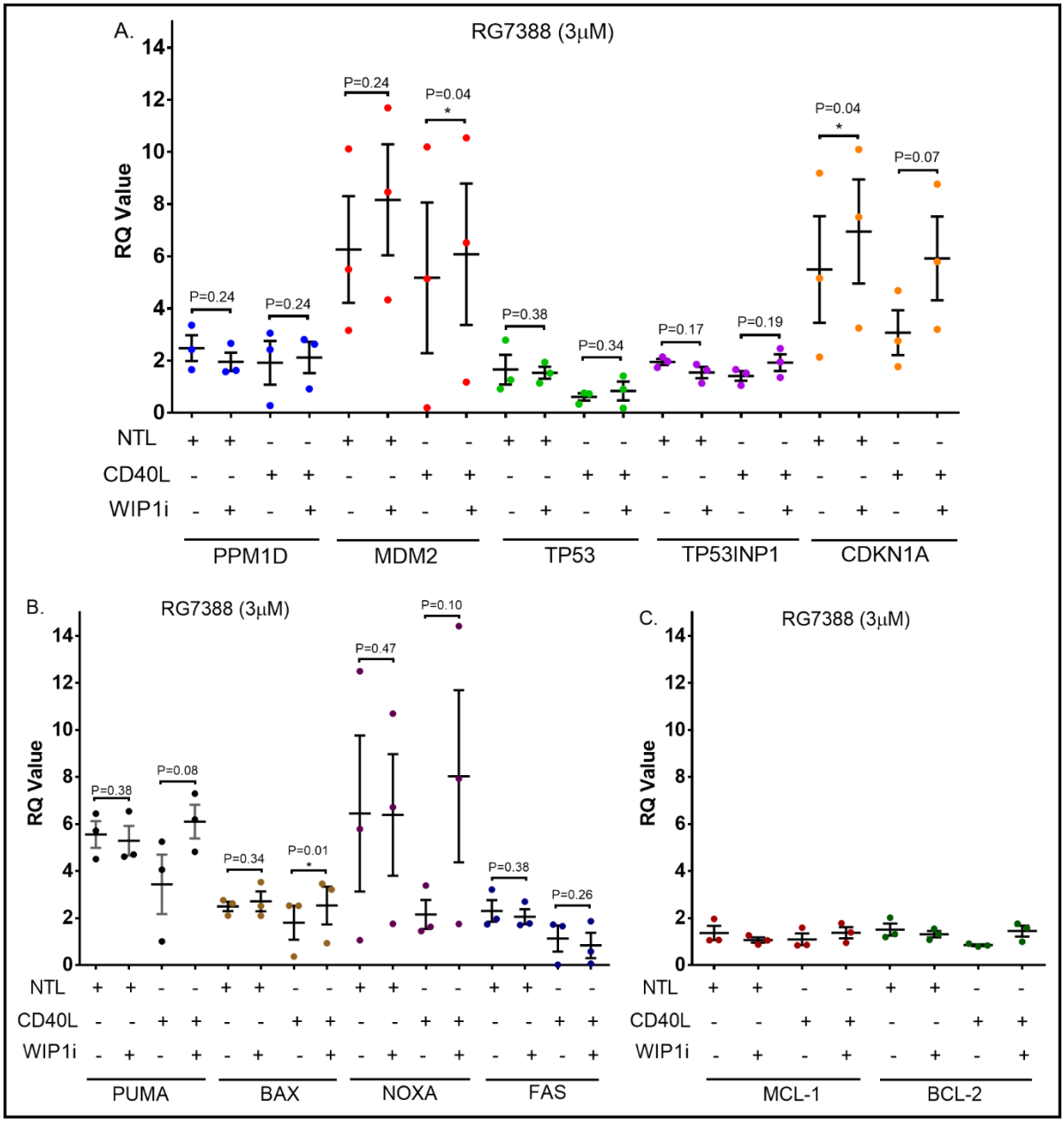

Figure 5.27 Summary plot comparing the fold changes in mRNA expression of primary CLL cells *ex-vivo* co-cultured with NTL/IL-4 and CD40L/IL-4 fibroblast cells in response to RG7388 (3μM) in combination with WIP1 inhibitor by qRT-PCR. (A) p53 negative regulator, (B) pro-apoptotic, (C) anti-apoptotic. Primary CLL samples (n=3) co-cultured with *ex-vivo* microenviroment stimulation for 6hrs and followed by RG7388 (3μM) with and without GSK2830371 (2.5μM) treatment for additional 6hrs. Each colour showed mRNA expression of certain gene in response to the treatment with NTL and CD40L stimulation. Each point represents the mean value for an individual patient and the error bars in each case represent the average mean ± SEM for the n=3 patient samples. One tailed paired t-test p-values are shown for the significance of differences between the mean values for RG7388 treatment with or without WIP1i are displayed above the horizontal bars, significance taken at $p < 0.05$.

5.6 Discussion

Primary CLL B-cells alone do not proliferate spontaneously *in-vitro*. Thus, several studies have investigated different stimulation factors to mimic the microenvironments to stimulate CLL cells proliferation. The ligation interaction of CD40/CD40L is one of the most effective modulators of CLL B-cell growth (Burley et al., 2022; Cantwell et al., 1996; Haselager et al., 2021).

Ranheim et al. reported that $CD4^+$ T cells provide cytokines and antigen-dependent co-stimulatory signals which mimic a dynamic aspect of microenvironment for the tumour *in-vivo* (Ranheim et al., 1995). Furthermore, the interaction of CD40L/CD40 induces the activity of NF-κB (Cheng & Baltimore, 1996) which effects on the growth, differentiation, and apoptosis of CLL cells (Rathmell et al., 1995).

The survival of the CLL cells in response to both IL-4 and CD40L stimulations was much better than the response of non-malignant B-cells. The interaction of IL-4 with its ligand on the surface of CLL cells showed an increase in the stimulation of downstream signalling cascade without changing in the affinity between ligand and receptor. In contrast, the interaction of IL-4 with its receptor on non-malignant B-cells relatively expressed with a very low affinity. Furthermore, the interaction of CD40L with its cellular ligand receptors on CLL cells showed 30-fold higher binding affinity than non-malignant B-cells. Although, the interaction of CD40L in non-malignant B-cells showed a sigmoidal shape response with does dependent (Bhattacharya et al., 2015). CLL cells express 3-fold more IL-4 receptor/ligand molecules on their surface cell membrane compared to non-malignant B-cells (Douglas et al., 1997). Thus, the binding interactions of the IL-4 with their receptors in CLL cells were showed much stronger responses than non-malignant B-cells (Bhattacharya et al., 2015).
CLL B-cells behave differently when they are stimulated to proliferate through different molecules and signals in bone marrow and lymph nodes compare with their non-proliferative state in the peripheral circulation. Therefore, it was also important to evaluate the effect of RG7388 on proliferating CLL cells.

Irradiated CD40L expressing mouse fibroblast monolayer feeder cells and IL-4 were used with primary CLL cells *ex-vivo* to model the effect of these *in-vivo* microenvironment proliferation signals. In addition, NTL mouse fibroblasts cells, which did not express the CD40 ligand on their surface, were included as a negative control. CLL cells were co-cultured by seeding onto

the irradiated feeder layer cells (NTL and CD40L) in order to stimulate the CLL cells to proliferate.

IL-4 and CD40L originating from T cells, was shown to be the most efficient ligand for the survival effect on CLL cells from spontaneous apoptosis *in-vitro*. This effect was independent of the *IGHV* status: patients with mutated or non-mutated *IGHV* status did not show a statistically different response to any ligand combination (Bhattacharya et al., 2015).
In *ex-vivo* microenvironment of CD40L/IL-4 stimulation, RG7388 as a single agent treatment stabilises the activity of *TP53* gene on CLL cell samples which have a functional *TP53* leading to inhibit the proliferation of the CLL cells in a concentration dependent manner in CLL cells over time. (Figure 5.12) shows the results for three freshly isolated primary CLL samples; and two cryopreserved samples (Figure 5.13). The CLL cells which were treated with high concentration of RG7388 (1μM) showed no CLL cells proliferation and cell count number remained similar to the seeding cell number. In comparison, there was a substantial increase in the number of CLL cells which were untreated (DMSO vehicle control).

On the NTL feeder layer, the CLL cells were not able to proliferate. Furthermore, there was a concentration-dependent decrease in CLL cell counts for the different concentrations of RG7388. Although, the inhibition effect of MDM2 inhibitor is differs from CLL cell to another thus, the proliferation signals and increasing in CLL cells number were varies from sample to another.

In *ex-vivo* microenvironment stimulation of CD40L/IL-4, the primary CLL cells became more sensitive to RG7388 treatment compared to the effect with NTL/IL-4 co-cultured in the absence of CD40L stimulation.

In this chapter, it was concluded that the MDM2 inhibitor was able to inhibit the proliferation of the primary CLL cells *ex-vivo* co-cultured with CD40L/IL-4. RG7388 limited the number of the CLL cells from increasing and proliferating following CD40L/IL-4 stimulation signals relative to DMSO.

On the other hand, the primary CLL cells could not proliferate on the NTL/IL-4 feeder co-culture which does not express CD40L on the surface even with the presence of IL-4 signals. Furthermore, RG7388 showed a concentration-dependent inhibitory effect on CLL cell count with IL-4 signals. The *ex-vivo* microenvironment of CD40L/IL-4 stimulation was able to stimulate both freshly isolated and cryopreserved CLL cells. Furthermore, the RG7388 was able inhibit proliferation activity in the presence of *ex-vivo* CD40L/IL-4 stimulation. Also, the IC_{50} of RG7388 on *ex-vivo* co-cultured CLL cells with CD40L/IL-4 is lower than the IC_{50} of

RG7388 with NTL/IL-4 co-culture (Table 5.3). Thus, *ex-vivo* CD40L/IL-4 co-cultured CLL cells are more sensitive to the RG7388 treatment than NTL/IL-4 co-cultured CLL cells. RG7388 was able to continue inhibiting the growth of CLL co-cultured with CD40L/IL-4 signal stimulation and prevent proliferation.

Another study reported that CDK inhibitor, CR8, induced the anti-proliferative effect on CLL co-cultured with CD154/IL-4 and causing apoptosis in proliferative CLL cells. Treated the CD154/IL-4 co-cultured CLL cells with CR8 inhabited the expression of NF-κB transcription factors in stimulated CLL cells and NF-κB–regulated genes associated with CLL cell survival (Cosimo et al., 2013).

The western blot (Figure 5.11) showed the changes in the downstream target proteins in response to MDM2 inhibitor. RG7388 stabilised the activity of negative regulator of TP53 target proteins including TP53, MDM2 and $p21^{WAF1}$. The expression of p53 protein in CLL cells co-cultured with CD40L/IL-4 was strongly induced in a concentration dependent manner in response to RGG7388 treatment. In addition, both MDM2 and $p21^{WAF1}$ were slightly induced in a concentration-dependent manner with RG7388. The induction of $p21^{WAF1}$ indicated the cell cycle growth arrest of CLL co-cultured CD40L/IL-4 within 6 hours of RG7388 treatment. The weak expression of these target proteins might indicate the CLL cells need longer time to initiate the proliferating signals and for the transcriptional protein to be produced and detected. Moreover, the expression of total and cleaved PARP proteins showed no obvious changes at this early time point in response to RG7388 treatment relative to DMSO.

In addition, the basal protein level of downstream proliferation and survival signals was investigated in 6 different CLL cells co-cultured either with CD40L or NTL in the presence of IL-4 for 12 hours (Figure 5.17). The phosphorylation activity of p70 S6 kinase protein was induced in the CLL cells co-cultured with CD40L/IL-4 compared to NTL/IL-4. Moreover, both the total ERK and its phosphorylation activity were induced in the CLL cells co-cultured with *ex-vivo* CD40L/IL-4 compared to NTL/IL-4.

The anti-apoptotic proteins, MCL-1 and BCL-2 did not show any difference in their transcriptional activity in CLL cells whether co-cultured with *ex-vivo* CD40L/IL-4 or NTL/IL-4 microenvironments.

Looking at the basal expression level of p53 negative regulator target genes of co-cultured CLL cells (Figure 5.19 A), the expression of *PPM1D*, *MDM2* and *TP53INP1* were induced

with CD40L/IL-4 than NTL/IL-4. Meanwhile, the expression of *CDKN1A* significantly reduced with CD40L/IL-4 co-cultured cells than NTL/IL-4 ($p>0.005$).

Consistent with our results, Jacob et al., reported that CD40L/IL-4 stimulation significantly induces the DNA synthesis of CLL B-cells (Jacob et al., 1998). Klein et al also illustrated the importance of the protein expression level to regulate the B-cells apoptosis, cell cycle and DNA repair (A. Klein et al., 2000). Grdisa et. al, also found that an induction in expression of the proteins which were related to cell proliferation especially occurred when cells were co-stimulated with both CD40L and IL-4 (Grdisa, 2003).

Furthermore, the basal expression level of *FAS* and *NOXA*, the pro-apoptotic genes were significantly reduced with CD40L/IL-4 than NTL/IL-4 stimulations (Figure 5.19 B). However, the basal expression level of *PUMA* and *BAX* were increased in CLL cells co-cultured with CD40L/IL-4 than NTL/IL-4 stimulation. The basal expression of anti-apoptotic genes, *MCL1* and *BCL2* did not show difference in the CLL cells expression level with neither CD40L/IL-4 nor NTL/IL-4 (Figure 5.19 C).

Although, the Fas antigen and its ligand have been identified as critical mediators of apoptotic deletion of peripheral, autoreactive B-cells (Rathmell et al., 1995). Rothstein et al. reported that CD40L stimulated B-cells induced to express the Fas antigen would be protected from Fas mediated deletion by cross-linking of the surface antigen receptor (Rothstein et al., 1995). Thus, failure to delete the auto-reactive B-cells in patients with CLL might be due to failed Fas mediated apoptosis in those non-malignant cells. Interestingly in our study, we found that *FAS* basal expression was significantly reduced in CLL co-cultured with CD40L/IL-4 compared to NTL/IL-4 *ex-vivo* microenvironments. This is due to the stimulation signals of CD40/CD40L interactions (Figure 5.19 B).

Similarly, it was reported that combination of both CD40L and IL-4 stimulation together increases the CLL B-cell viability in comparison to the stimulation of each signal alone. Furthermore, the overall protein synthesis was increased with CD40L and IL-4 stimulation together. A significant increase in the expression of cyclins D2 and D3, which are characteristic of late G1-phase, were detected with co-stimulation of CD40L and IL-4. Additional to that, cyclin E which is characteristic of the transition from G1 to S-phase was induced as well (Wagner et al., 1998).

Several studies reported that CD40 ligation could be used to upregulate the adhesion and co-stimulatory molecules in B CLL cells (Buhmann et al., 1999; Van Den Hove et al., 1997). In CLL B-cells stimulation, excessive signals of IL-4 further enhance the expression of both B7-

1 and B7-2 molecules. Although, additional expression of CD40 might provoke an acquired CD40L deficiency syndrome in B CLL cells (Cantwell et al., 1997).

Another study reported that CD154L/IL-4 co-cultured CLL cells were resistant to dasatinib in a combination with either chlorambucil or fludarabine. The optimal utilization of dasatinib could involve by combining it with agents like 17-DMAG, which reduced the pro-survival signalling triggered by stroma, CD154, and IL-4 (Mccaig et al., 2011). Although, CLL patients who expressing the greatest therapeutic resistant challenges are most likely to be chemo-refractory, thus novel combination treatment might be effective.

Looking at the treatment effect of WIP1 inhibitor (2.5μM) (Figure 5.21), GSK2830371 as a single agent did not show difference in the fold change expression of negative regulator *TP53* target genes (*PPM1D*, *TP53INP1*, *TP53*, *MDM2*, *CDKN1A*), proapoptotic (*PUMA*, *BAX*, *FAS*, *NOXA*) and anti-apoptotic (*MCL1*, *BCL2*) genes whether with *ex-vivo* co-cultured of CD40L and NTL in addition to IL-4. However, RG7388 treatment showed reduction in the fold change expression of *PUMA*, *NOXA* and *FAS*, the pro-apoptotic genes, of the CLL cell co-cultured with CD40L/IL-4 compared to NTL/IL-4 (Figure 5.23).

Similar finding was reported by Ciardullo et al, that RG7388 triggered the activity of functional p53 of CLL cells. As a result of restoring its p53-transcriptional activity, leading to induces the expression of pro-apoptotic genes. Furthermore, RG7388 initiated the apoptosis of CLL samples which possess a functional p53 status.(Ciardullo et al., 2019).

As a consequence of apoptotic activity and apoptotic genes upregulation, RG7388 significantly reduces the cell viability of p53-functional CLL samples (Figure 5.23 and Figure 5.24). This outcome is consistent with the findings of phase I clinical trial that assessed the impact of RG7112, an earlier generation of MDM2 inhibitor, on leukaemia (Rossi et al., 2012).

In addition, RG7388 upregulating the pro-apoptotic genes and the pro-apoptotic activation of functional-p53 CLL cells particularly *PUMA*, in response to RG7388. Although *BAX* expression changes little compared to the change in *PUMA* expression (Ciardullo et al., 2019).

Looking at the effect of RG7388 in a combination with WIP1 inhibitor, the fold change expression of *MDM2*, *CDKN1A*, *PUMA*, *BAX* and *NOXA* were induced in CLL cell co-cultured with both CD40L/IL-4 and NTL/IL-4 compared to the single treatment of RG7388 (Figure 5.26 and Figure 5.27). It is interestingly, the pro-apoptotic genes were increased with

the combination treatment of RG7388 and GSK2830371 in the CD40L/IL-4 co-cultured CLL cells. In addition, the induction of *CDKN1A* indicted that the co-cultured CD40L/IL-4 CLL cells were in arrest growth cell cycle status due to the effect of combination treatment of RG7388 and GSK2830371.

For the BCL family anti-apoptotic gene expression (Figure 5.26 and Figure 5.27), *MCL1* and *BCL2*, the absence of upregulation changes whether with RG7388 or in combination with WIP1 inhibitor in our study is in line with the results of Ciardullo study that showed (Ciardullo et al., 2019).

In response to treatment, Romano et al. reported that CD40/CD40L interaction stimulation alone decrease the spontaneous signalling and drug induced apoptosis with fludarabine treatment (Romano et al., 1998). However, both CD40/CD40L interaction and IL-4 signals had an influence on apoptosis. Stimulated CD40L and IL-4 signals induce the influence of apoptosis of CLL B-cells in response to fludarabine (Romano et al., 1998). Bryostatin, the protein kinase C modulator, induced similar effects in response to CLL B-cells stimulated by CD40L and IL-4 signals (Kitada et al., 1999). Both of these agents induced elevation of the anti-apoptotic *BCL2* family protein *MCL1* and *BCL2* in B CLL cells. In addition, the level of NF-κB/Rel nuclear protein was induced with CD40 antigen stimulation in response to fludarabine by decreasing the apoptosis in B CLL cells (Furman et al., 2000; Schattner, 2000; Hiromura et al., 1999).

For the first time, CLL cells co-cultured with CD40L/IL-4 was investigated in response to RG7388 in combination to WIP1 inhibitor. Taken all demonstrated result together, we identify that RG7388 as a single agent treatment effectively blocked the proliferation signals, provided to CLL cells through the *in-vitro* microenvironment model using CD40L and IL4.

RG7388 induces the expression of p53-target genes and selected pro-apoptotic gene, *PUMA*, of *in-vitro* CLL cells co-cultured with CD40L. In addition, the combination of WIP1 inhibitor further induces the expression of pro-apoptotic gene, *PUMA*.

Chapter 6: Stimulation of CLL Cells by IL-4

6.1 Introduction

IL-4 is a pleiotropic glycoprotein discovered in 1982 as a T cell-derived soluble growth factor that stimulates B-cell proliferation (Howard et al., 1982; Isakson et al., 1982). By 1986, it was identified that the human IL-4 cDNA encodes for 153 amino acid residues of the human sequences and the secreted protein produced consists of 129 amino acid residues (F. Lee et al., 1986; Noma et al., 1986). The secreted IL-4 is produced with various molecular weights of 15, 18, or 19 kDa, depending upon the N-linked oligosaccharides terminal (Carr et al., 1991).

IL-4 is a unique cytokine produced by TH2 cells. Following antigen interaction binding, naive CD4+ TH cells undergo differentiation into several distinct functional subsets based on the expression of its major transcription factor specific cytokine secretion (Schmitt & Ueno, 2015). For instant, Th1 cells express T-bet and produce IFN-γ; TH17 cells express RORγt and produce IL-17.

TH2 cells are one of the main major sources of IL-4 cytokine production, in addition to other cells. TH2 cells are characterized by expression of the transcription factor GATA3 and the production of IL-4, IL-5, and IL-13, which are collectively called type-2 cytokines.

Follicular helper Th (Tfh) cells, another type of CD4+ Th2 cell which are located in the B-cell follicles of lymph nodes, also produce IL-4, IL-10, IL-21 cytokines and CXCL13 (Crotty, 2014; Choi et al., 2024). Unlike TH2 cells, the Tfh cells are defined by the high expression of the transcription factor Bcl6 and a low expression of GATA3. Furthermore, Tfh cells produce a small quantity of IL-2 cytokines in addition to the high production of IL-4 (Johnston et al., 2009; Nurieva et al., 2009).

Natural killer (NKT) cells, a unique subset of T cells recognizing the lipid antigens presented by CD1d molecules, also produce IL-4 cytokines. Moreover, several other types of innate immune cells are capable of producing IL-4, including eosinophils, basophils and mast cells.

IL-4 is a cytokine that protects normal and malignant B cells from apoptosis and increases sIgM expression on mammalian murine splenic B cells. It is primarily produced by TH2 of the type 2 in response to engagement of the T cell receptor, and by mast cells and basophils upon cross-linking of the high-affinity receptor for immunoglobulin E (IgE) (Chomarat & Banchereau, 1998; Pernis & Rothman, 2002). IL-4 also can be produced by activated natural killer T cells and eosinophils (Gessner et al., 2005). In CLL patients, IL-4 target genes are

overexpressed by the cells purified from the lymph nodes, compared with cells derived from matched blood and bone marrow samples.

IL-4 interaction enhances the proliferation (Mainou-Fowler et al., 1995), and differentiation (Tony et al., 1991) of activated B-cells (CLL). In addition, on binding and stimulation of BCR, IL-4 promotes DNA synthesis in activated B-cells after stimulation with sIg and anti-CD40 antibody (Mainou-Fowler et al., 2001). Moreover, IL-4 enhances the expression of the adhesion molecule ICAM (Carlsson et al., 1993) and up-regulates the expression of HLA class II and CD23 antigens (Mainou-Fowler et al., 2001; Tony et al., 1991).
IL-4 signalling is involved in promoting the differentiation and proliferation of TH2 cells, IgE synthesis, and gene expression in alternatively activated macrophages through binding to its IL-4 receptor (IL-4R) type I (P. Choi & Reiser, 1998).

Predominantly, the IL-4 signalling pathway is initiated from the IL-4R through the IL-4Rα (alpha) polypeptide, which is a component of two types of IL-4Rs (Figure 6.1). The IL-4 type I receptor, composed of IL-4Rα and common gamma chain (γc), which is also a subunit of IL-2, IL-7, IL-9, IL-15, and IL-21 receptor complexes (Goenka & Kaplan, 2011).

The IL-4 type II receptor is composed of IL-4Rα and IL-13Rα1 subunits. Although, type I receptor binds exclusively to IL-4, the IL-4 signals can be stimulated through both IL-4R types I and II, whereas IL-13 can only stimulate the type II IL-4R.

Mainly IL-4 type I receptors are the only IL-4 receptors which are expressed in the hematopoietic cells, specifically in T cells, basophils, mast cells, and mouse B-cells. In contrast, IL-4 type II receptors are expressed in non-hematopoietic cells (Junttila et al., 2008).

Ligand binding of the IL-4 to its respective partner, IL-4R activates JAK tyrosine kinase motifs, which are associated with the cytoplasmic tails of the IL-4 receptors. IL-4R Type I activates JAK1 and JAK3, whereas IL-4R type II activates JAK1, JAK2, and Tyk2. Then, the tyrosine residues of the IL-4Rα chain become phosphorylated and act as docking sites for other adaptor or signalling molecules such as STAT family of proteins (STAT6) (Kelly-Welch et al., 2005).

The first tyrosine residue of IL-4Rα interacts with the protein-binding domains (PTBs) such as insulin receptor substrate (IRS) proteins. Phosphorylated IRS binds to the p85 subunit of PI3K to activate the PI3K/AKT cascade, and to the adaptor protein growth factor receptor–bound protein 2 (GRB2) to activate the Ras/Raf/MEK/ERK signalling cascade. The adaptor protein GRB2 binds the phosphorylated IRS receptor and recruit guanine nucleotide exchange

factor (GEF) into the complexes. GEF displaces the Guanosine diphosphate (GDP) on inactive Ras and replaces it with Guanosine-5'-triphosphate (GTP), which turns Ras into the active form. The activated Ras complex then phosphorylates Raf. The activated Raf then phosphorylates the downstream MAPK MEK1/2, which phosphorylates and activates the final MAPK in the cascade. This pathway is linked to the proliferation of CLL B-cells and other cell types such as TH2 and the induction of genes associated with alternatively activated macrophages in response to IL-4.

From the second to the fourth phosphorylated tyrosine residue of IL-4Rα interact with the SH2 domain of STAT6. Phosphorylated STAT6 dimerizes and then migrates to the nucleus where it binds to the promoters of IL-4 responsive genes, which are associated with IgE classes. STAT6 is dephosphorylated by various SH2 domain–containing phosphatases to negatively regulate the signalling (Kelly-Welch et al., 2005).

Hematopoietic cells such as T and B-cells including CLL cells express only the type I receptor, whereas cells of the myeloid lineage such as monocytes, macrophages, and fibroblasts express both type I and type II IL-4 receptors.

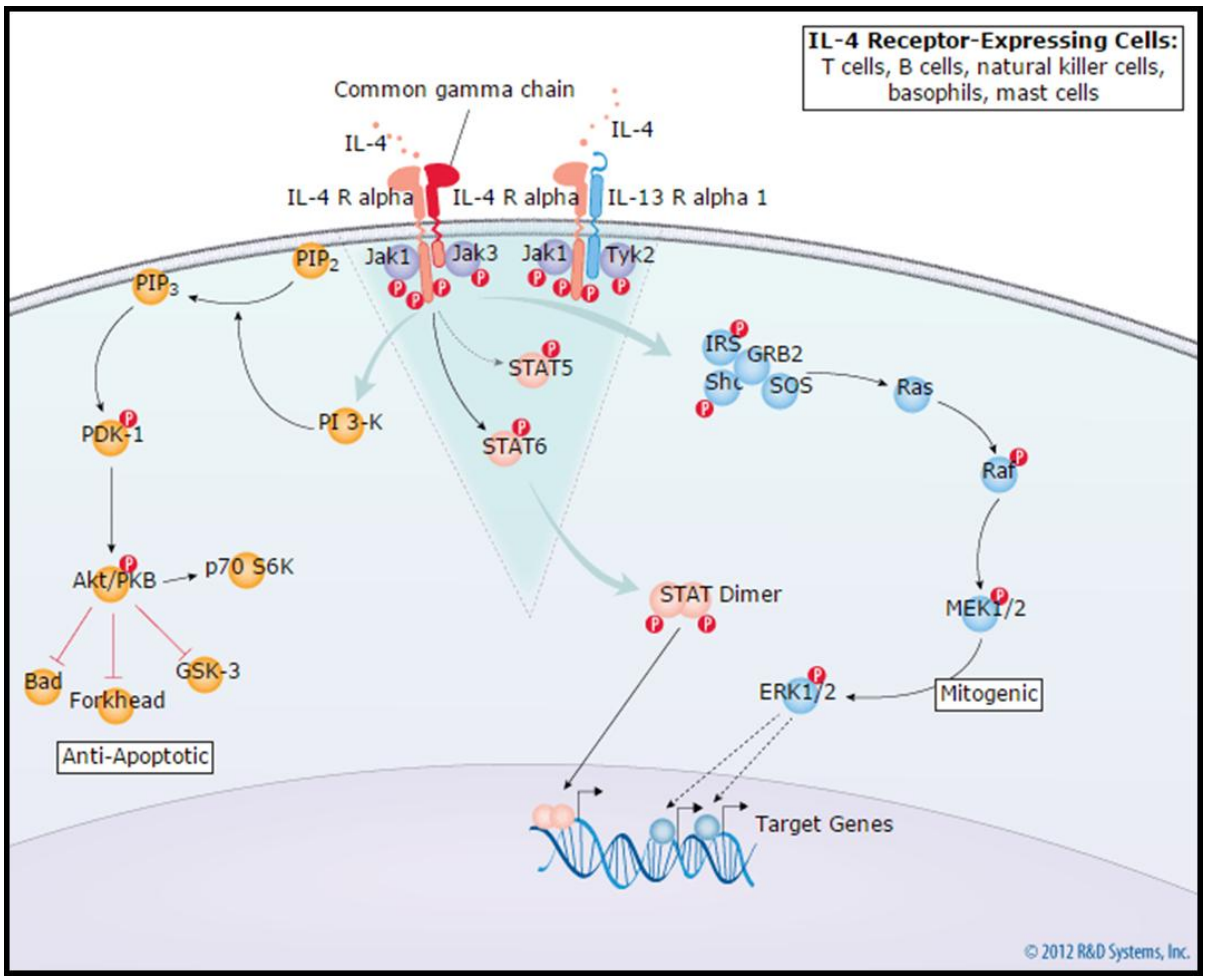

Figure 6.1 Interleukin-4 (IL-4) is a glycosylated cytokine that is secreted by T cells, natural killer T cells, eosinophils, and mast cells. The IL-4 signal transduction initiated through two different types of IL-4 receptors (IL-4Rs) polypeptide complex. IL-4 type I receptor, which is expressed on hematopoietic cells, and IL-4 type II receptor, which is expressed on non-hematopoietic cells. The type I receptor composed of the IL-4 receptor alpha (IL-4Rα) and common gamma-chain (IL-4Rγc). Type II receptor composed of the IL-4 receptor alpha (IL-4Rα) and IL-13 receptor alpha (IL-13Rα) which can be stimulated by either IL-4 or IL-13 molecules. IL-4 plays an essential role in the development of allergic inflammation and asthma by increasing the expression of Fc epsilon RI on the surface of B cells, basophils, and mast cells. In addition, IL-4 is promoting the survival and proliferation cascade of the mast cell, basophil, and eosinophil chemotaxis. (Reproduced from R&D systems website)

6.2 Hypothesis and Aims

CLL patients with progressive disease express a high number of T cells that secrete IL-4 compared to CLL patients with non-progressive disease or healthy individuals with normal B cells. Thus, CLL cells express significantly higher numbers of IL-4Rs compared to normal B cells.

When CLL cells migrate to either bone marrow or lymphoid organs, they are exposed to different extracellular signals, which promote their survival and proliferation. IL-4 is one of the signals that suppresses the basal apoptotic mechanism by inducing the expression of anti-

apoptotic proteins and is therefore potentially important in the response to therapeutic intervention.

In this study, I would like to investigate the influence of IL-4 on the *ex-vivo* response of CLL cells to TP53 activation by the MDM2 inhibitor idasanutlin (RG7388) and its combination with a WIP1/PPM1D phosphatase inhibitor (GSK280371). IL-4 may increase the metabolic activity of CLL cells.

- The XTT metabolic assay will be used to determine the effect of the compounds on the mitochondrial activity and viability of CLL cells in the presence or absence of IL-4.
- Western immunoblotting will be used to determine the effect IL-4 on protein expression responses to WIP1 and MDM2 inhibitors.
- qRT-PCR will be used to investigate the changes in gene transcriptional levels following treatment with MDM2 and WIP1 inhibitors in the presence and absence of IL-4.

6.3 Results

6.3.1 The effect of IL-4 on the response of CLL cells to the WIP1 inhibitor

The study was conducted to investigate the effect of WIP1 inhibitor on response to the primary CLL cells in the presence and absence of IL-4 cytokine.

6.3.1.1 IL-4 has minimal effect on the response of cryopreserved CLL cells to WIP1 inhibitor

Three cryopreserved CLL cells were treated with WIP1 inhibitor in the presence of IL-4 (Figure 6.2). It found that WIP1 inhibitor as a single agent treatment had no or little effect on the metabolic activity of the CLL cells either in the presence or absence of IL-4 in comparison to the DMSO control. However, in the presence of IL-4 CLL the cells had a higher metabolic activity compared to the absence of IL-4.

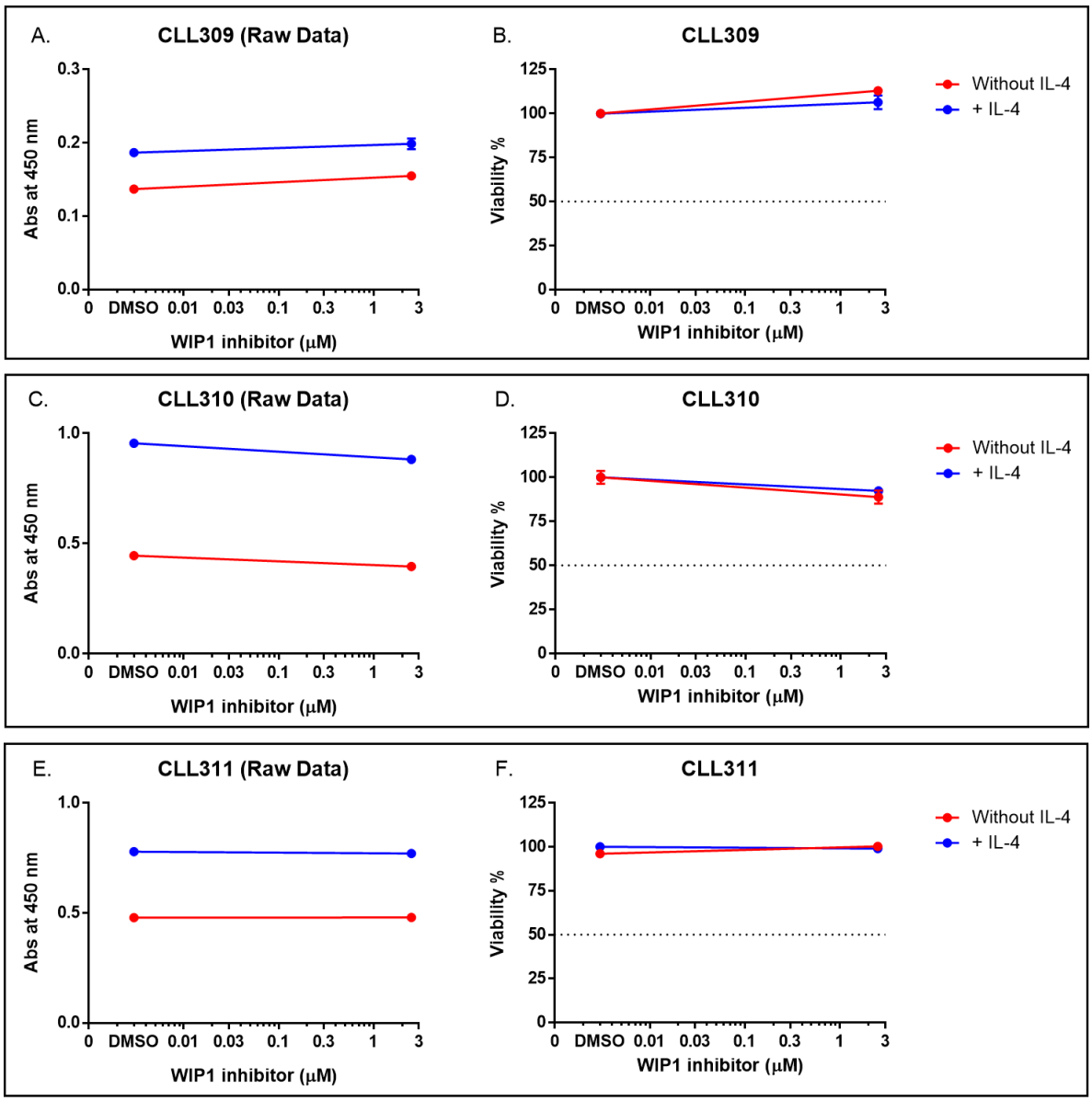

Figure 6.2 The *ex-vivo* effect of WIP1 inhibitor on viability of cryopreserved CLL cell in the presence of IL-4. The left graphs show cells absorbance data at 450nm and the right graphs show cells % viability relative to DMSO control normalization. (A-B) 309, (C-D) 310 and (E-F) 311. Different cryopreserved CLL cell samples (n=3) exposed to GSK2830371 (2.5μM) for 48 hours with and without IL-4 followed by XTT assay. Each experiment was performed once on the primary CLL cells with three intra-replicates. Bars show the mean ± SEM of intra-replicate within the experiment.

6.3.1.2 The WIP1 inhibitor has little effect on freshly isolated CLL cells either in the presence or in absence of IL-4

Four freshly isolated CLL cells express high metabolic activity compared to the cryopreserved CLL cells on both conditions, whether in the presence or in the absences of IL-4 (without IL-4 p=0.009 and with IL-4 p=0.0008) (Figure 6.3). In addition, the presence of IL-4 increases the basal CLL cell metabolic activity more than in the absence of IL-4 (p=0.0008) (Figure 6.4).

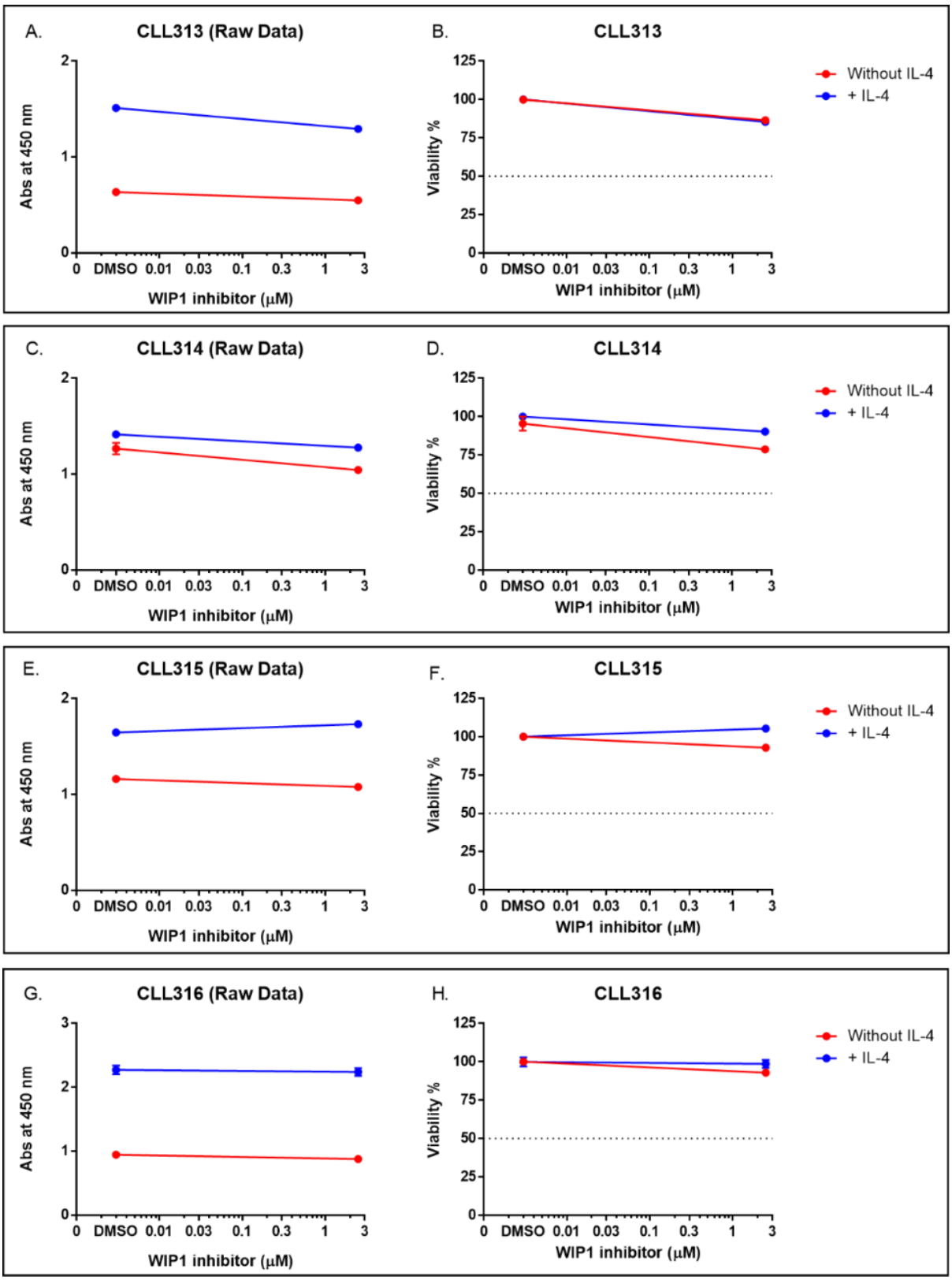

Figure 6.3 The *ex-vivo* effect of WIP1 inhibitor on primary CLL cell in the presence of IL-4. The left graphs show cells absorbance data at 450nm and the right graphs show cells % viability relative to DMSO control normalization. (A-B) 313, (C-D) 314, (E-F) 315 and (G-H) 316. Freshly isolated CLL cell samples (n=4) treated with GSK2830371 (2.5μM) for 48 hours with and without IL-4 followed by XTT assay. Each experiment was performed once on the primary CLL cells with three intra-replicates. Bars show the mean ± SEM of intra-replicate within the experiment.

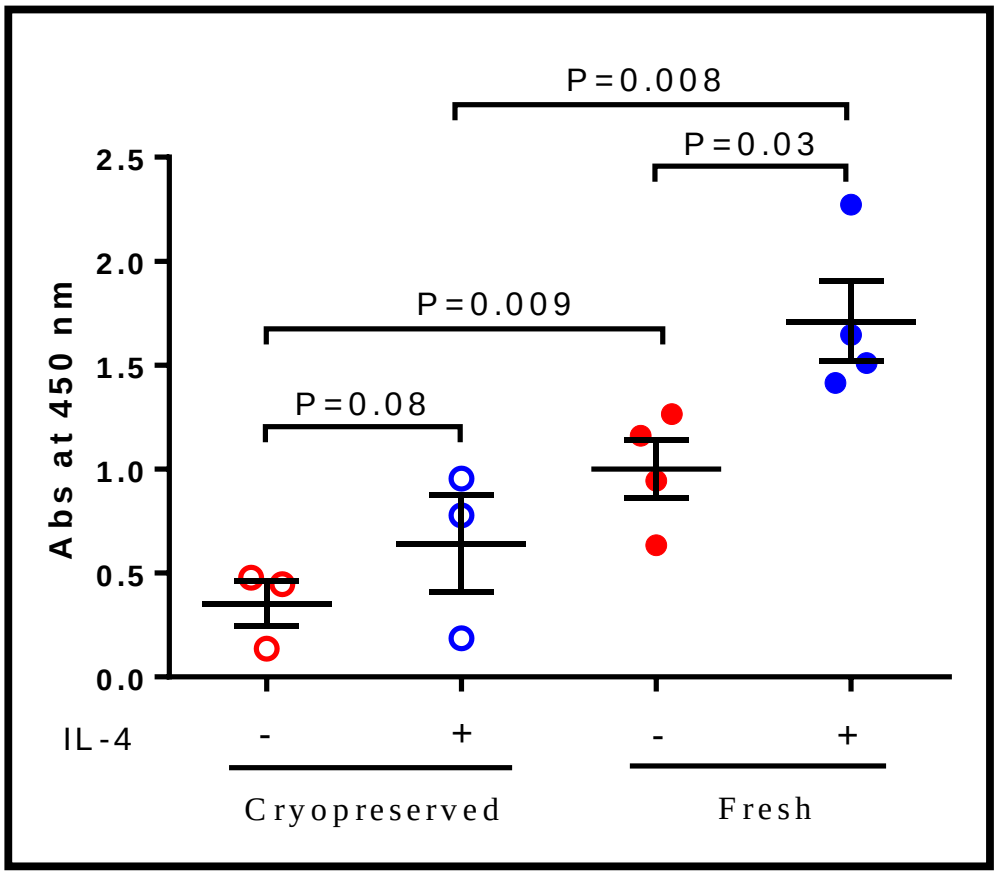

Figure 6.4 Basal metabolic activity of CLL samples cryopreserved and fresh with the presence of IL-4. The white circles represent the cryopreserved CLL samples (n=3) and the solid ones represent the fresh CLL samples (n=4). The red colour represents CLL cells absorbance in the absence of IL-4 and the blue colour show CLL cells absorbance with IL-4. XTT assay used to determine cells viability after 48hrs of IL-4 treatment. Error bars show the average mean ± SEM of different CLL samples. Statistical significance was determined by t-test one tail, significance taken at $p < 0.05$).

6.3.1.3 The presence of IL-4 has a significant protective effect on CLL cell viability against the inhibitory effect of WIP1 inhibitor

It is seen that in the absence of IL-4, CLL cells express lower metabolic activity compared to the presence of IL-4. In comparison, CLL cells which were treated with IL-4 showed a two-fold increase in their metabolic activity (Figure 6.5).

There was no significant difference in the primary CLL cells absorbance for WIP1 inhibitor-treated compared to the DMSO control, even though with IL-4 treatment, the CLL metabolic activity was increased significantly compared to the absence of IL-4. The basal absorbance activity level of CLL cells with IL-4 treatment is significantly increased compared to parallel CLL cells without IL-4 treatment ($p=0.016$). Furthermore, in the presence of WIP1 inhibitor the viability of CLL cells were significantly increased by IL-4 ($p<0.05$). The metabolic

activity of the CLL cells in response to the WIP1 inhibitor (2.5µM) (Figure 6.5 B) shows no significant difference with or without IL-4 treatment.

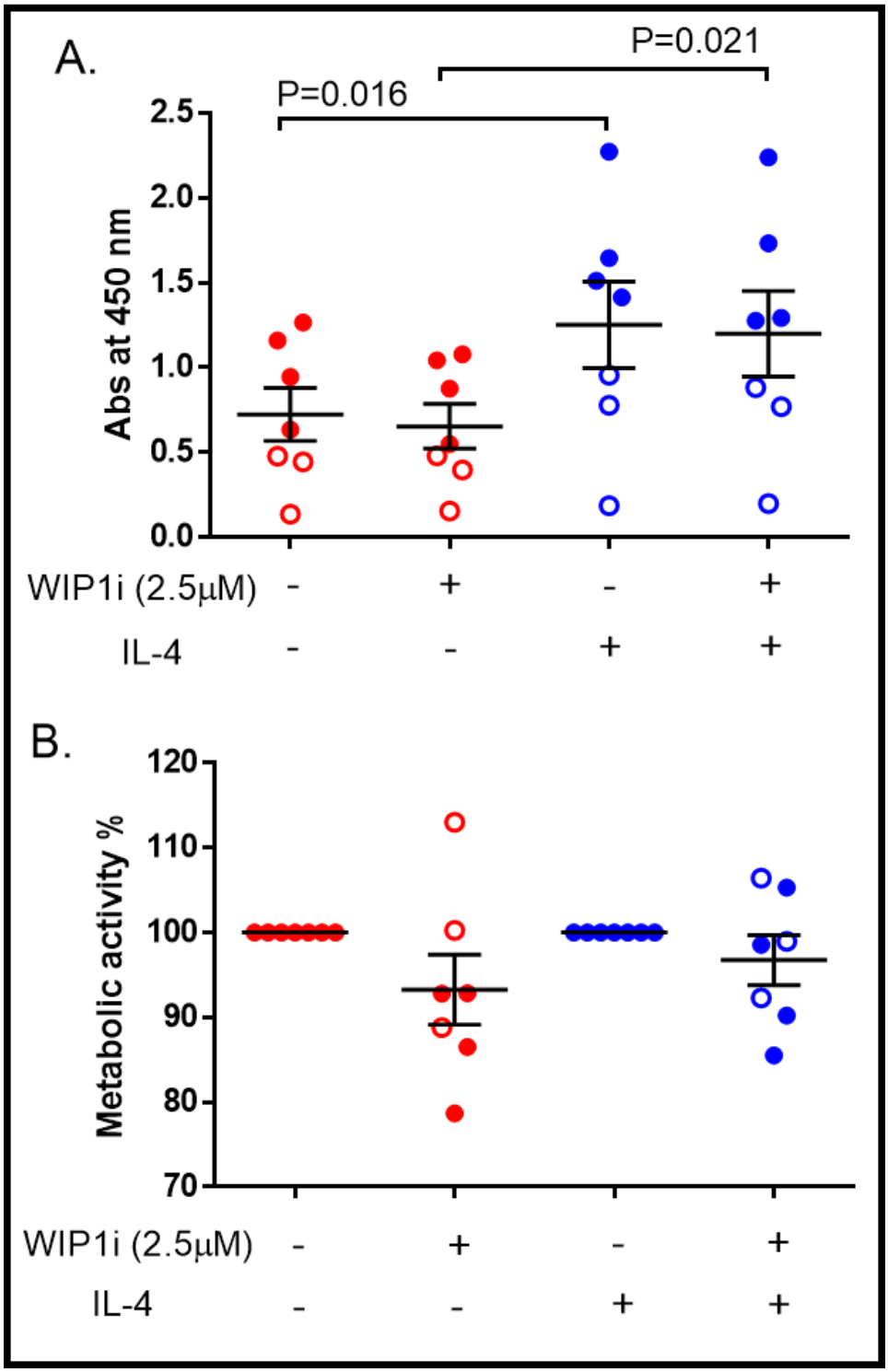

Figure 6.5 Summary of the results examining sensitivity of CLL cells to the WIP1 inhibitor. The solid circles represent the fresh primary CLL samples (n=4), and the empty circles represent (n=3) the cryopreserved ones. (A) The absorbance OD value at 450nm with the effect of WIP1 inhibitor in the presences and absences of IL-4. (B) The inhibition effect of GSK2830371 (2.5µM) on the metabolic activity of primary CLL cells normalized to DMSO control treatment. XTT assay used to determine cells % metabolic activity after 48hrs of treatment. Error bars show the average mean ± SEM of total CLL samples. Statistical significance was determined by t-test one tail, significance taken at $p < 0.05$.

6.3.2 Primary CLL samples shows a concentration dependent decrease in viability in response to RG7388 with and without IL-4

A study was conducted to investigate the effect of MDM2 inhibitor (RG7388) on primary CLL cells in the presence of IL-4. The experiments were performed on both the cryopreserved and freshly isolated CLL cells. The results for each set of CLL samples were initially represented in separate figures.

6.3.2.1 Presence of IL-4 has protective effect on cryopreserved CLL cells following treatment with RG7388

Although, cryopreserve CLL samples become more metabolically activate in the presence of IL-4, the RG7388 had a concentration dependent effect on the CLL cells viability. In addition, the presence of IL-4 increases CLL cells viability compared to absence of IL-4. RG7388 causes a reduction in the absorbance value in a concentration dependent manner either with or without IL-4.

Moreover, DMSO normalization shows that RG7388 had a concentration dependent decrease on CLL cell viability either with or without IL-4 treatment. Samples CLL310 and CLL311 showed a protective effect of IL-4 on the response to RG7388, however there was no apparent difference observed with sample CCL309, suggesting any protective effect may be sample-dependent (Figure 6.6). It is of note that for sample CLL309 the basal metabolic activity of the thawed CLL cells was particularly low and the result likely to be less reliable.

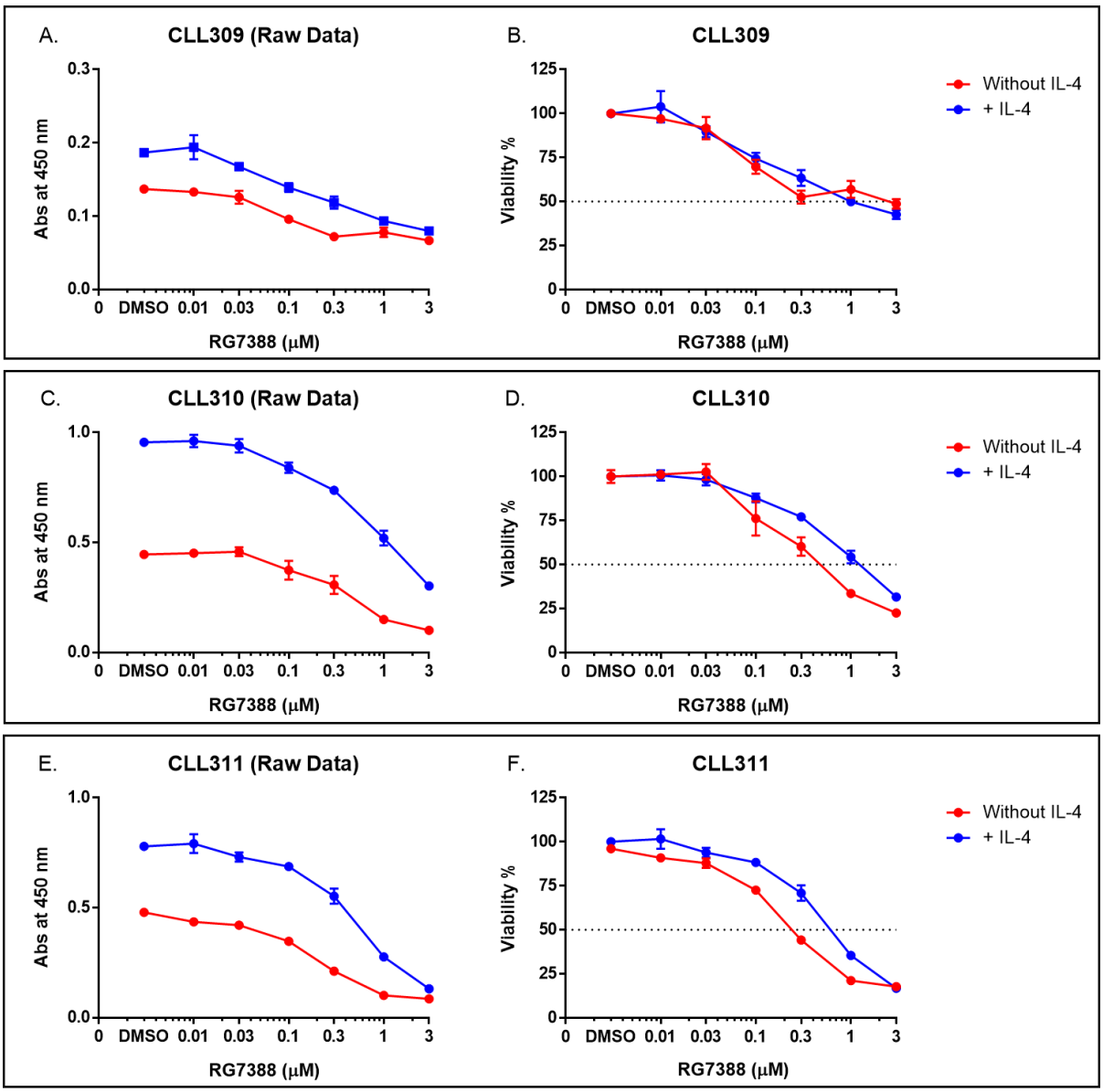

Figure 6.6 The effect of RG7388 on the viability of cryopreserved CLL cells in the presence of IL-4. The left graphs show cells absorbance data at 450nm and the right graphs show cells % viability relative to DMSO control normalization. (A-B) 309, (C-D) 310 and (E-F) 311. A cohort set of cryopreserved CLL samples (n=3) treated *ex-vivo* with a wide concentration range of MDM2 inhibitor (RG7388) with and without IL-4 for 48 hours and viability measured by XTT assay. CLL cell viability was normalized to DMSO treatment for individual experiment. Each experiment was performed once on the primary CLL cells. Bars show the mean ± SEM of three intra-replicate of concentrations within the experiment.

6.3.2.2 Freshly isolated CLL cells are less sensitive to RG7388 in the presence of IL-4

Here, we investigated the effect of RG7388 on freshly isolated CLL cells in the presence of IL-4 (Figure 6.7). RG7388 reduced the CLL cells viability (absorbance) in a concentration dependent manner. Treating fresh isolated CLL cells with IL-4 increased CLL cells metabolic activity compared to non-IL-4 treated cells. It was found that freshly isolated CLL cells become less sensitive to RG7388 treatment in the presence of IL-4 compared to parallel CLL

samples in the absence of IL-4. Although, RG7388 produced a dose dependent reduction in metabolic activity with and without the presence of IL-4, there was a clear large protective effect of IL-4 against the RG7388 cytotoxicity with all four samples tested.

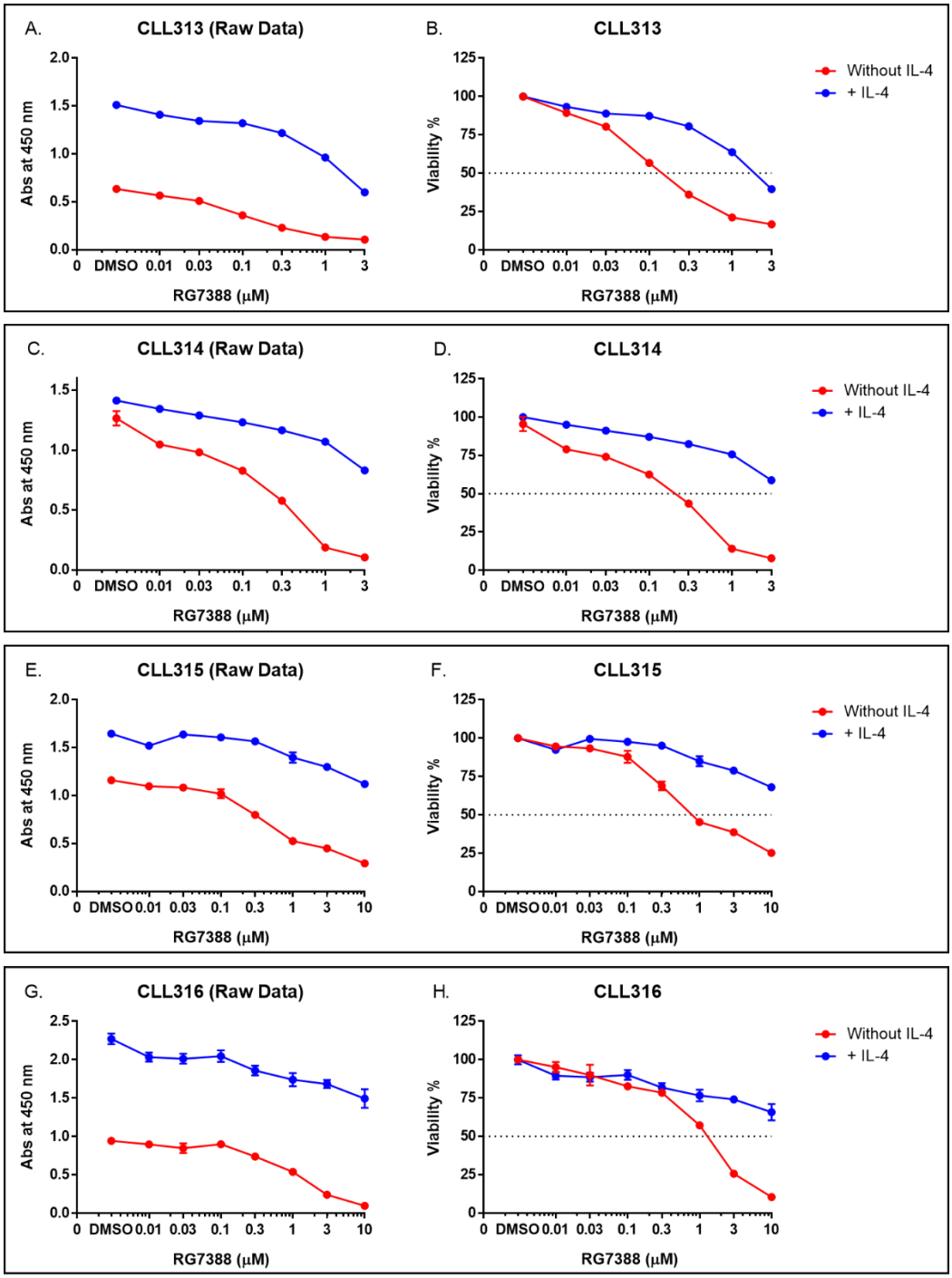

Figure 6.7 The effect of RG7388 on the viability of primary CLL cells in the presence of IL-4. The left graphs show cells absorbance data at 450nm and the right graphs show cells % viability relative to DMSO control normalization. (A-B) 313, (C-D) 314, (E-F) 315 and (G-H) 316. A cohort set of freshly isolated CLL samples (n=4) treated *ex-vivo* with a wide concentration range of MDM2 inhibitor with and without IL-4 for 48 hours and viability measured by XTT assay. CLL cell viability was normalized to DMSO treatment for individual experiment. Each experiment was performed once on the primary CLL cells. Bars show the mean ± SEM of three intra-replicate of concentrations within the experiment.

6.3.2.3 IL-4 protects against the inhibitory response of RG7388 on CLL sample viability

Figure 6.8 shows a summary of the effect of RG7388 on four freshly isolated CLL samples in the presence and absence of IL-4. The CLL cells treated with IL-4 show less sensitivity in response to RG7388 compared to treatment with RG7388 alone. Furthermore, there was a concentration dependent decrease in viability either with or without the presence of IL-4. Treating the CLL cells with IL-4 produced a protective effect against the cytotoxicity of RG7388 treatment.

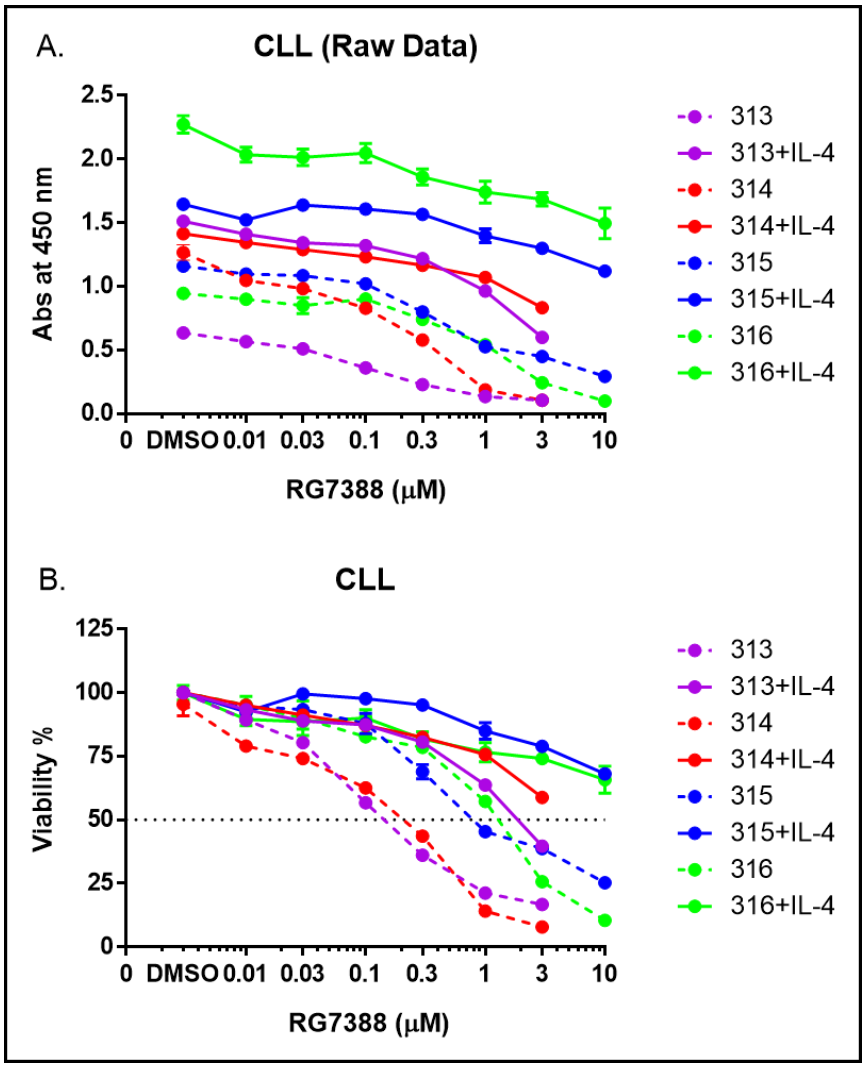

Figure 6.8 Summary of freshly isolated primary CLL samples in responses to RG7388 with IL-4. (A) The raw data absorbance at 450nm following RG7388 treatment. (B) The dose-dependent inhibitory effect of RG7388 on the CLL viability with normalization to DMSO control. The dash line represents the effect of RG7388 in the absence of IL-4 and the solid line shows the effect of RG7388 with IL-4. Each colour represents the treatment effect of individual CLL sample. Different freshly isolated primary CLL samples (n=4) treated with wide range of RG7388 with and without IL-4 for 48 hours and the XTT assay was used to assessed the cell viability. The error bar represents three intra-replicates of concentrations within the experiment ± SEM. Each colour shows individual primary CLL samples which treated once.

6.3.2.4 IL-4 significantly increases the CLL cells metabolic activity and reduces the sensitivity to RG7388

Figure 6.9 shows the effect of two different concentrations of RG7388 (1 and 3µM) on seven primary CLL samples. There is a significant difference in CLL cell sample response in the presence of IL-4 compared to absence of IL-4 treatment. (Figure 6.9 A) The basal expression level of CLL cells with DMSO (control) treatment showed a significant increase in the CLL sample metabolic activity with IL-4 treatment (p=0.020). (Figure 6.9 B and C) shows the effect of IL-4 on the XTT assay 450nm absorbance levels for CLL cell sample metabolic activity and its decrease with RG7388 (1µM) and (3µM) treatment. The normalised metabolic activity of the CLL samples was consistently significantly increased in the presence of IL-4, for both RG7388 (1µM) and (3µM) treatment (p=0.009 and p=0.032) (Figure 6.9 D and E).

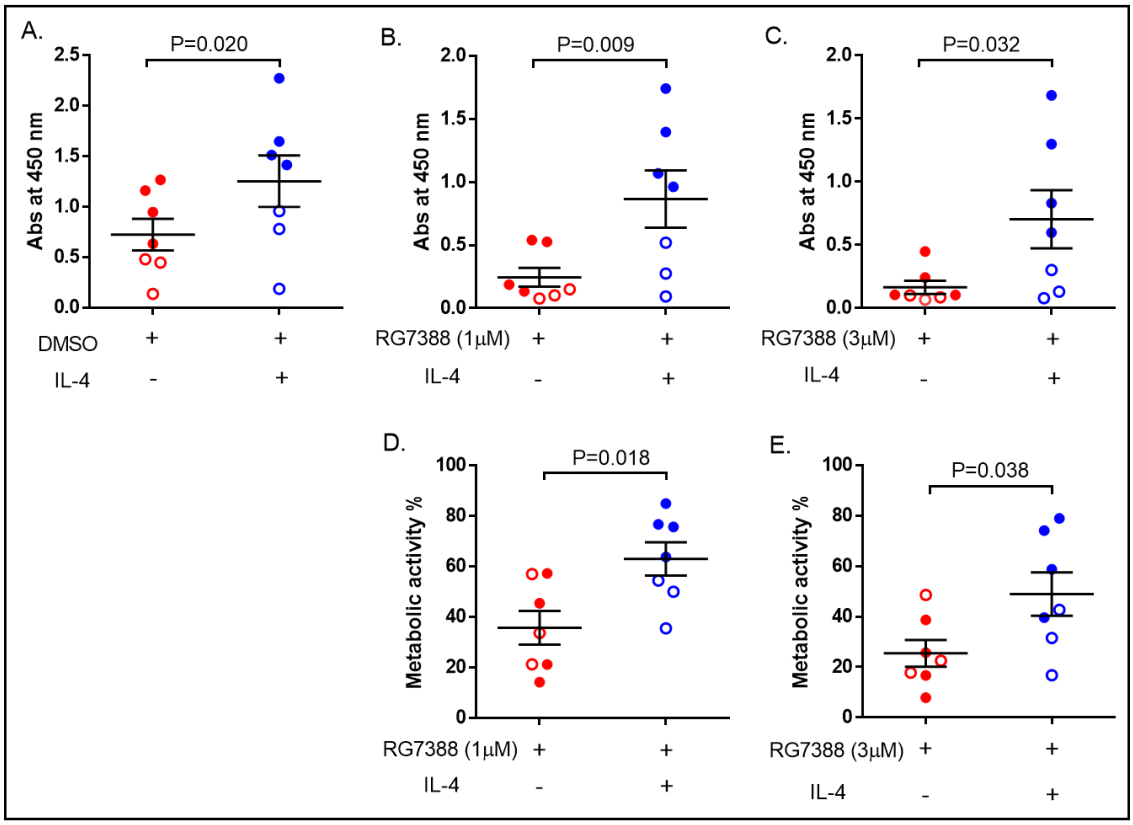

Figure 6.9 Summary plot comparing the *ex-vivo* effect of RG7388 on primary CLL cells in the presence of IL-4. A cohort of CLL samples (n=7) treated with RG7388 (1, 3µM) with and without IL-4 for 48hrs. The upper graphs show raw data absorbance at 450nm at (A) DMSO control. (B) RG7388 (1µM) (C) RG7388 (3µM). The lower graphs show the % metabolic activity of the CLL cells relative to DMSO normalization (D) RG7388 (1µM) (E) RG7388 (3µM). The solid colour circles represent the freshly isolated CLL cells (n=4) and the empty circles represent the cryopreserved CLL samples (n=3). The red colour shows the effect of RG7388 without IL-4 and the blue colour show the effect of RG7388 with IL-4. Error bar represents average mean ± SEM of total CLL samples. Paired t-test 2-tailed are shown for the significance differences between the mean values for RG7388 treatment with or without Il-4 are displayed above the horizontal bars, significance taken at $p < 0.05$.

6.3.2.5 The LC_{70} value for RG7388-treated primary CLL cells is significantly higher in the presence of IL-4

Figure 6.10 shows the LC_{70} values for seven primary CLL samples treated with RG7388 in the presence of IL-4. The summary scatter plot for CLL samples shows a consistent and significant increase in the mean LC_{70} in the presence of IL-4 compared to the absence of IL-4 ($p=0.042$) (Figure 6.10). The individual LC_{70} values for RG7388 were consistently higher in the IL-4 treated cells compared to the absence of IL-4 (Table 6.1).

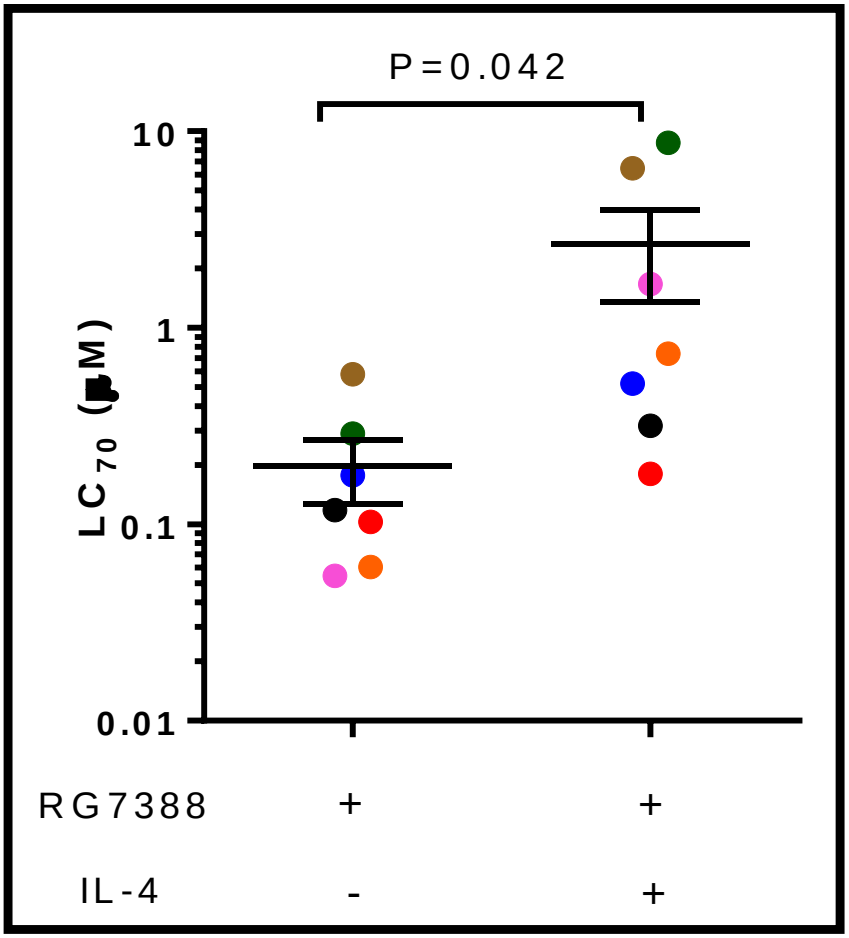

Figure 6.10 Summary comparing the LC_{70} values of RG7388 for CLL cells in the presences of IL-4. Each colour represents the effect of different CLL sample (n=7) treated with range of RG7388 ± IL-4 for 48hrs by XTT assay. The error bar represents the average mean ± SEM of CLL samples. Statistical significance was determined by paired t-test one tail between the presence and absence of IL-4 response to RG7388 ($p < 0.05$).

LC_{70} (µM)	RG7388		
	IL-4 (-)	IL-4 (+)	Fold change
CLL 309	0.10	0.18	1.8
CLL 310	0.18	0.52	2.9
CLL 311	0.12	0.32	2.7
CLL 313	0.06	0.74	12.3
CLL 314	0.05	1.67	33.4
CLL 315	0.29	8.75	30.2
CLL 316	0.58	6.47	11.2
Average	0.20 ± 0.07	2.66 ± 1.31	-
p-value	0.042		-

Table 6.1 The LC_{70} of CLL samples (n=7) in response to RG7388 in the presence and absence of IL-4. (mean ± SEM, paired t-test one tail).

6.3.3 The combination treatment of WIP1 inhibitor (2.5μM) and RG7388 reduced the CLL sample metabolic activity in a dose dependent manner in either the presence or absence of IL-4

The main aim of this study was to determine whether WIP1 inhibitor could potentiate the effect of RG7388 on the response of primary CLL samples in the presence and absence of IL-4. The experiments were performed on both the cryopreserved and freshly isolated CLL cells.

6.3.3.1 Cryopreserve CLL cells showed a small protective effect of IL-4 on the combination treatment response to WIP1 inhibitor and RG7388

Cryopreserved CLL samples (n=3) become less sensitive to the combination treatment of WIP1 inhibitor (2.5μM) with RG7388 in the presence of IL-4 compared to the absence of IL-4 (Figure 6.11). There is a dose dependent decrease in metabolic activity either in the presence or absence of IL-4. IL-4 substantially increased the basal metabolic activity of the thawed cryopreserved CLL samples. There was also some difference in the metabolic activity of cryopreserve CLL in response to the combination of WIP1 inhibitor (2.5μM) and RG7388 with the presence of IL-4.

Normalizing the combination effect of WIP1 inhibitor (2.5μM) and RG7388 relative to DMSO control, the response of the thawed cryopreserved CLL samples with or without IL-4 was similar. The viability of the cryopreserve CLL cells was reduced by the combination treatment in an RG7388 dose dependent manner, with a consistent small protective effect in the presence of IL-4.

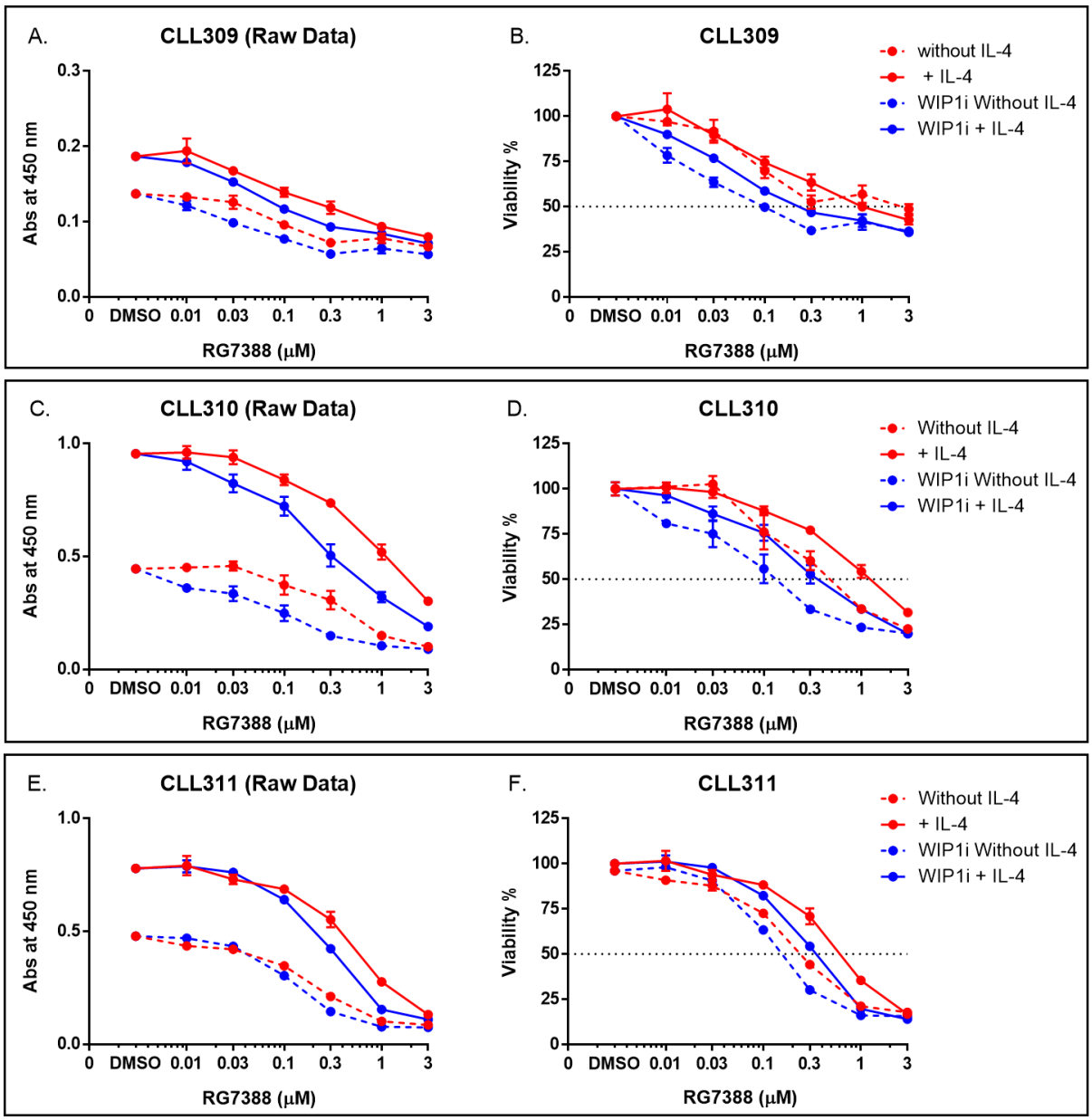

Figure 6.11 WIP1 inhibitor (2.5µM) potentiates the activity of RG7388 in a concentration dependent manner either in the presences or abcennce of IL-4. The left graphs show cells absorbance data at 450nm and the right graphs show cells % viability relative to DMSO control normalization. (A-B) 309, (C-D) 310 and (E-F) 311. A cohort of cryopreserve CLL samples (n=3) treated with GSK2830371 (2.5µM) in a combination with a range of RG7388 concentrations ± IL-4 for 48 hours. XTT assay used to determine cell viability. The red line colour represents the RG7388 treatment and the blue line colour represents the combination treatment effect. The dash line represents the treatment effect in the absence of IL-4 and the solid line shows the treatment effect with IL-4. Each CLL sample exposed to different treatments in the same experiment. Each experiment performed once with three intra-replicates. Concentration. All % of cell viability was normalized to DMSO treatment for individual experiment. Bars show the mean ± SEM.

6.3.3.2 Freshly isolated CLL cells are less sensitive to combination of WIP1 inhibitor and RG7388 in the presence of IL-4

Four freshly isolated CLL samples were treated with RG7388 in combination with WIP1 inhibitor (2.5μM) in the presence of IL-4 (Figure 6.12). Fresh isolated CLL samples express high basal metabolic activity. Addition of IL-4 increased the basal metabolic activity of the CLL cells. However, there was a dose dependent inhibition of the metabolic activity by the WIP1 inhibitor (2.5μM) in combination with RG7388, whether in the presence or absence of IL-4. This difference was maintained on normalization relative to the DMSO control. Furthermore, the freshly isolated CLL cells showed a larger protective effect of IL-4 against the combination treatment (Figure 6.12) compared to the thawed cryopreserved samples (Figure 6.11).

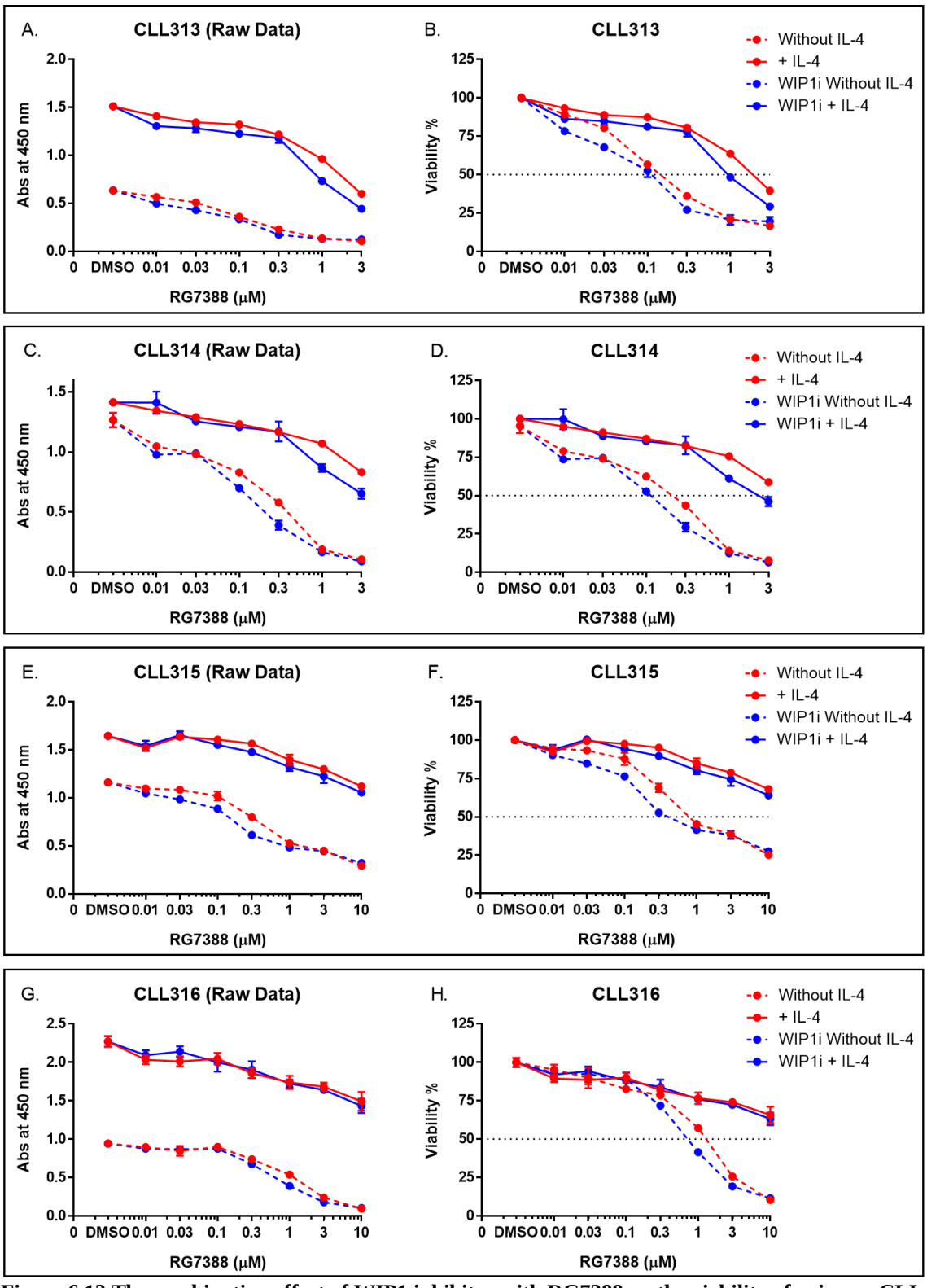

Figure 6.12 The combination effect of WIP1 inhibitor with RG7388 on the viability of primary CLL cells in the presence of IL-4. The left graphs show cells absorbance data at 450nm and the right graphs show cells % viability relative to DMSO control normalization. (A-B) 313, (C-D) 314, (E-F) 315 and (G-H) 316. A cohort of freshly isolated CLL samples (n=4) treated with GSK2830371 (2.5μM) in a combination with a range of RG7388 concentrations ± IL-4 for 48 hours. XTT assay used to determine cell viability. The red line colour represents the RG7388 treatment and the blue line colour represents the combination treatment effect. The dash line represents the treatment effect in the absence of IL-4 and the solid line shows the treatment effect with IL-4. Each CLL sample exposed to different treatments in the same experiment. Each experiment performed once with three intra-replicates. Concentration. All % of cell viability was normalized to DMSO treatment for individual experiment. Bars show the mean ± SEM.

6.3.3.3 Dose dependent inhibitory effect of RG7388 on freshly isolated CLL samples with and without IL-4

In Figure 6.13, CLL cells showed a decrease in their metabolic activity in a dose dependent manner whether in the presence or absence of IL-4. Furthermore, CLL cells become less sensitive to the effect of the combination treatment in the presence of IL-4 compared to the absence of IL-4. CLL315 and CLL316 did not reach the LC_{50} inhibition effect of the combination treatment up to 10µM.

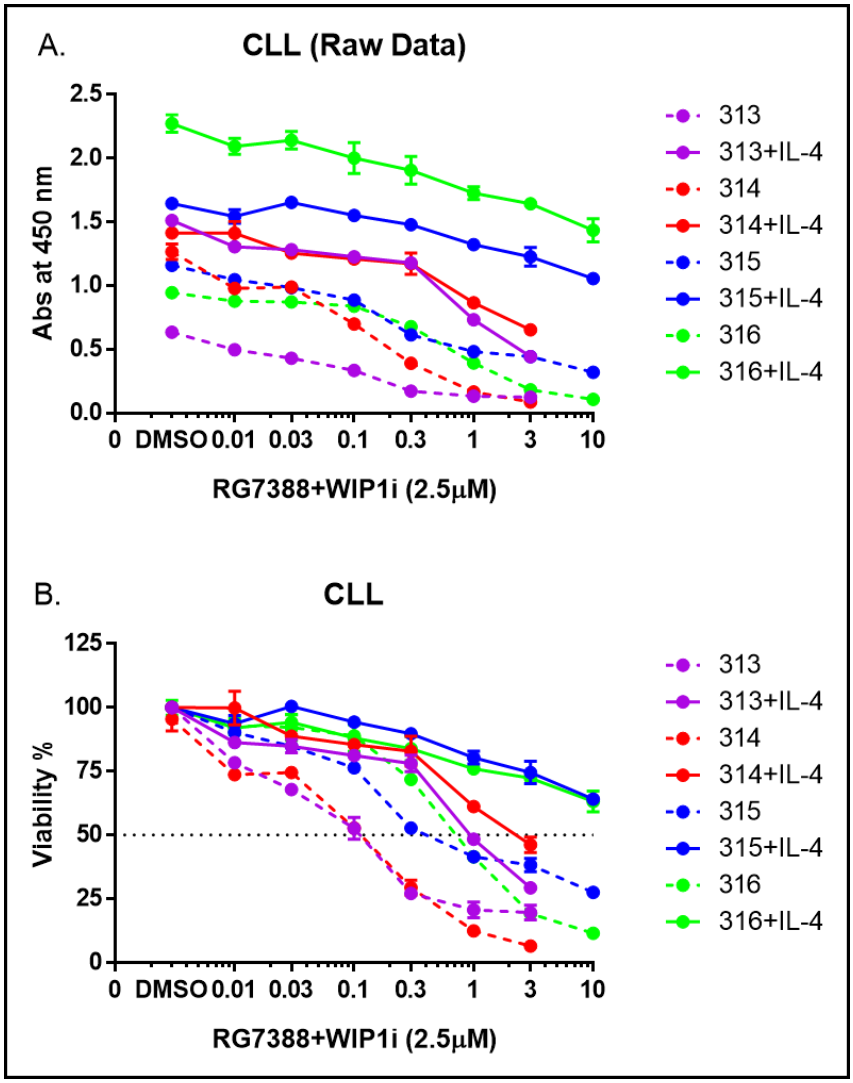

Figure 6.13 Summary of freshly isolated primary CLL samples in responses to RG7388 in combination with WIP1 inhibitor with IL-4. (A) The raw data absorbance at 450nm following the combination treatment. (B) The dose-dependent inhibitory effect of RG7388 and GSK2830371 (2.5µM) ± IL-4 on the CLL viability with normalization to DMSO control. The dash line represents the treatment effect in the absence of IL-4 and the solid line shows the treatment effect with IL-4. Each colour represents the treatment effect of individual CLL sample. Different freshly isolated primary CLL samples (n=4) treated with WIP1i (2.5µM) in combination with wide range of RG7388 ± IL-4 for 48 hours and the XTT assay was used to assessed the cell viability. The error bar represents three intra-replicates of concentrations within the experiment ± SEM. Each colour shows individual primary CLL samples which treated once.

6.3.3.4 IL-4 significantly increases the metabolic activity of CLL cells and reduces the sensitivity of CLL cells to RG7388

A group of seven CLL primary samples were treated with two different concentrations of RG7388 (1 or 3μM) in combination with WIP1 inhibitor (2.5μM) in the presence or absence of IL-4 for 48 hours (Figure 6.14). The combination treatment of RG7388 with WIP1 inhibitor (2.5μM) significantly reduced CLL cells metabolic activity, but to a lesser extent in the presence of IL-4. The IL-4 produced an increase in both the raw data mean absorbance at 450nm ($p=0.023$) and the normalized percentage metabolic activity in comparison to the absence of IL-4 ($p=0.016$) (Figure 6.14 A&B). Moreover, with the RG7388 (3μM) and WIP1 inhibitor (2.5μM) combination, both the mean absorbance level (raw data) for the CLL samples and the percentage metabolic activity normalised to DMSO control were significantly increased with IL-4 treatment ($p=0.032$ and $p=0.055$, respectively) (Figure 6.14 C&D).

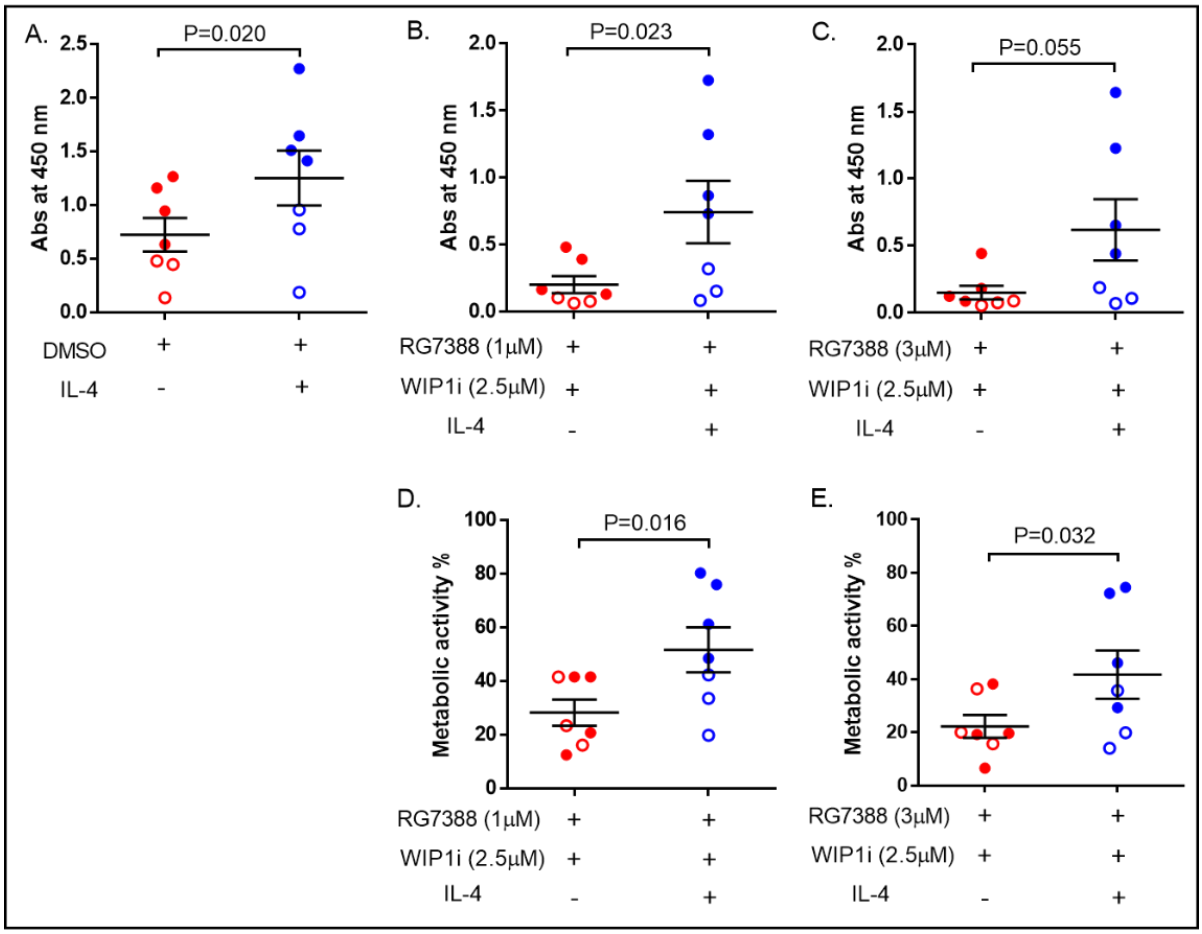

Figure 6.14 Summary plot comparing the *ex-vivo* effect of RG7388 in combination with WIP1 inhibitor on primary CLL cells in the presence of IL-4. A cohort of CLL samples (n=7) treated with RG7388 (1, 3μM) in combination with GSK2830371 (2.5μM) ± IL-4 for 48hrs. The upper graphs show raw data absorbance at 450nm at (A) DMSO control. (B) RG7388 (1μM)+WIP1i (C) RG7388 (3μM)+WIP1i. The lower graphs show the % metabolic activity of the CLL cells relative to DMSO normalization (D) RG7388 (1μM)+WIP1i (E) RG7388 (3μM)+WIP1i. The solid colour circles represent the freshly isolated CLL cells (n=4) and the empty circles represent the cryopreserved CLL samples (n=3). The red colour shows the combination treatment effect without IL-4 and the blue colour show the combination effect of with IL-4. Error bar represents average mean ± SEM of all CLL samples. Paired t-test 2-tailed are shown for the significance differences between the mean values for combination treatment ± IL-4 is displayed above the horizontal bars, significance taken at $p < 0.05$.

6.3.3.5 The RG7388 LC_{70} values are significantly increased in response to a combination of the WIP1 inhibitor in the presence of IL-4

Figure 6.15 shows the LC_{70} values of seven primary CLL samples treated with WIP1 inhibitor and RG7388 in the presence of IL-4. The summary plot of CLL samples shows a significant increase in LC_{70} in the presence of IL-4 (p=0.05) (Figure 6.15). CLL cells become more resistant to the combination effect of RG7388 and WIP1 inhibitor (2.5µM) with the presence of IL-4. IL-4 produced a protective effect against the combination of RG7388 and WIP1 inhibitor (2.5µM). The individual LC_{70} values for a combination of WIP1 inhibitor with RG7388 were higher for the IL-4 treated samples (Table 6.2).

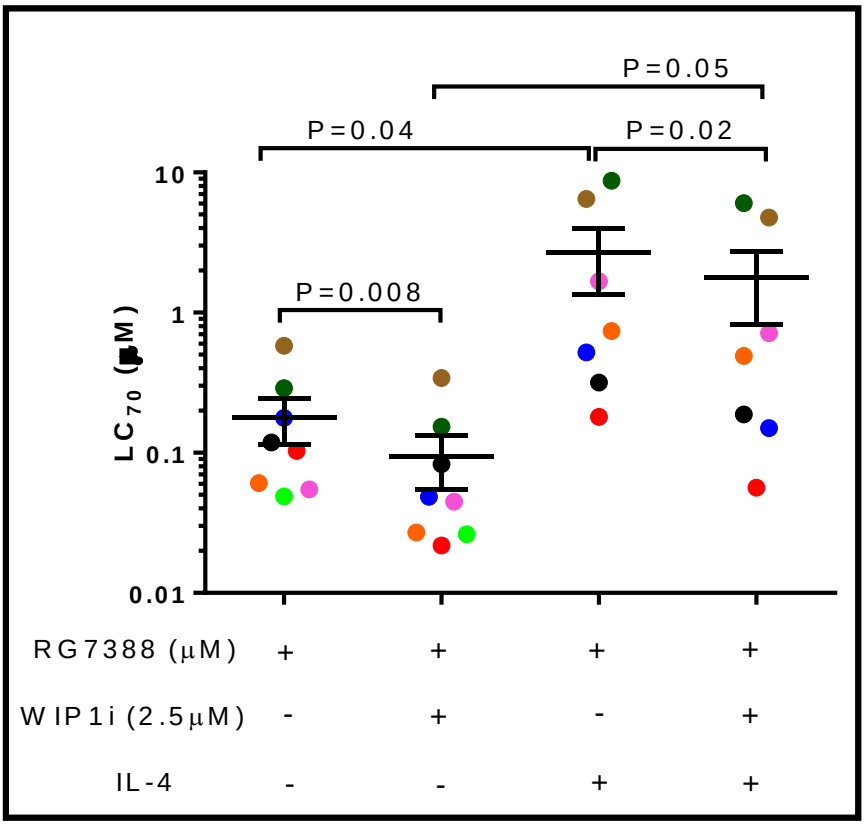

Figure 6.15 Summary plot comparing the LC_{70} values of WIP1 inhibitor in combination with RG7388 for primary CLL cells in the presences of IL-4. Each colour represents the effect of different primary CLL sample (n=7) in response to the GSK2830371 (2.5µM) and RG7388 treatment ± IL-4 for 48 hrs by XTT assay. The error bar represents average mean ± SEM of all CLL samples. Statistical significance was determined by paired t-test one tail between the presence and absence of IL-4 in response to the combination treatment ($p < 0.05$).

LC_{70} (µM)	RG7388			RG7388+WIP1i		
	IL-4 (-)	IL-4 (+)	Fold change	IL-4 (-)	IL-4 (+)	Fold change
CLL 309	0.10	0.18	1.8	0.02	0.06	3
CLL 310	0.18	0.52	2.89	0.05	0.15	3
CLL 311	0.12	0.32	2.67	0.08	0.19	2.38
CLL 313	0.06	0.74	12.33	0.03	0.49	16.33
CLL 314	0.05	1.67	33.40	0.04	0.72	18
CLL 315	0.29	8.75	30.17	0.15	6.06	40.4
CLL 316	0.58	6.47	11.16	0.34	4.77	14.03
Average	0.20 ± 0.07	2.66 ± 1.31	-	0.10 ± 0.07	1.77 ± 1.31	-
p-value	0.042		-	0.052		-

Table 6.2 The LC_{70} of CLL samples (n=7) in response to a combination of WIP1 inhibitor with RG7388 in the presence and absence of IL-4. The fold changes represent the ratio of GI_{50} inhibition values in the presence and absence in response to the treatment. (mean ± SEM, paired t-test one tail).

6.3.4 RG7388-induced (cPARP) protein is decreased in the presence of IL-4

To investigate potential mechanisms of the IL-4 protective effect, western immunoblotting was performed to investigate changes in p53 and its transcriptional target proteins, MDM2, $p21^{WAF1}$ and WIP1. The phosphorylation of p53 was detected to test whether this was increased in response to WIP1 phosphatase inhibition. In addition, PARP cleavage was looked at as a measure of apoptosis and BCL-2 as an indicator of any anti-apoptotic changes associated with the expression level of this protein.

6.3.4.1 IL-4 reduces the expression of cPARP and the stability of P53 of CLL

Sample CLL311 was treated with RG7388 (1µM) as a single agent and in a combination with WIP1 inhibitor (2.5µM) in the presence of IL-4 for 6 and 24 hours. The NALM-6 cell line was treated with RG7388 (3µM) and is used as a positive control for total p53 protein stability (Figure 6.16).

For this sample, both the total and cleaved PARP protein signals appeared to be reduced at 6 hours in the presence of IL-4. In addition, in the absence of IL-4 the cPARP protein level was induced by 6 hour and was further increased at 24hr with either RG7388 treatment alone or in combination with WIP1 inhibitor. The relative amount of cleaved PARP at 24 hours was reduced in the presence of IL-4. This identification is consistent with the protective effect of IL-4.

RG7388, either alone or in combination with WIP1i increased the level of total p53 protein, at 6 and 24 hours, but to a lesser extent in the presence of IL-4, particularly at 6 hours. MDM2 protein expression was also induced at 6 and 24 hours, and to a greater extent relative to p53 levels in the presence of IL-4, suggesting a more active MDM2 negative feedback on p53 in the presence of IL-4. The p53 phosphorylation signals were weak, but appeared to be higher in the absence of IL-4 and potentially suppressed when IL-4 was present. $p21^{WAF1}$ was not detected in sample CLL311, either in the presence or absence of IL-4.

In the absence of IL-4 the BCL2 signal was higher at 24 hours compared to 6 hours time point with either single agent RG7388 or in combination with WIP1i. This effect was not apparent with the IL-4 treated samples. The strongest effect evident was RG7388 treatment leading to the stabilisation of p53 protein in a time-dependent manner. The WIP1 signals were indistinct, but the intensity appeared to be diminished in the presence of the WIP1 inhibitor.

Figure 6.17 densitometry analysis summarises the western immunoblot results of three different CLL samples (CLL311, CLL315, CLL316) treated with RG7388 in a combination with WIP1 inhibitor (2.5μM) in the presence of IL-4 for 6 and 24 hours. RG7388 stabilises the activity of total p53 of CLL cells in the presence and absence of IL-4 and the combination of WIP1 inhibitor induces the stabilization further more (Figure 6.17 A&B). MDM2 is reduced in response to the combination treatment in the presence of IL-4 compared to absence of IL-4 at both 6 and 24 hours (Figure 6.17 C&D). WIP1 inhibitor (2.5μM) inhibited the activity of WIP1 protein with the presence and absence of IL-4 (Figure 6.17 E&F). cPARP was induced with combination treatment in the presence of IL-4 at 24 hours (Figure 6.17 H).

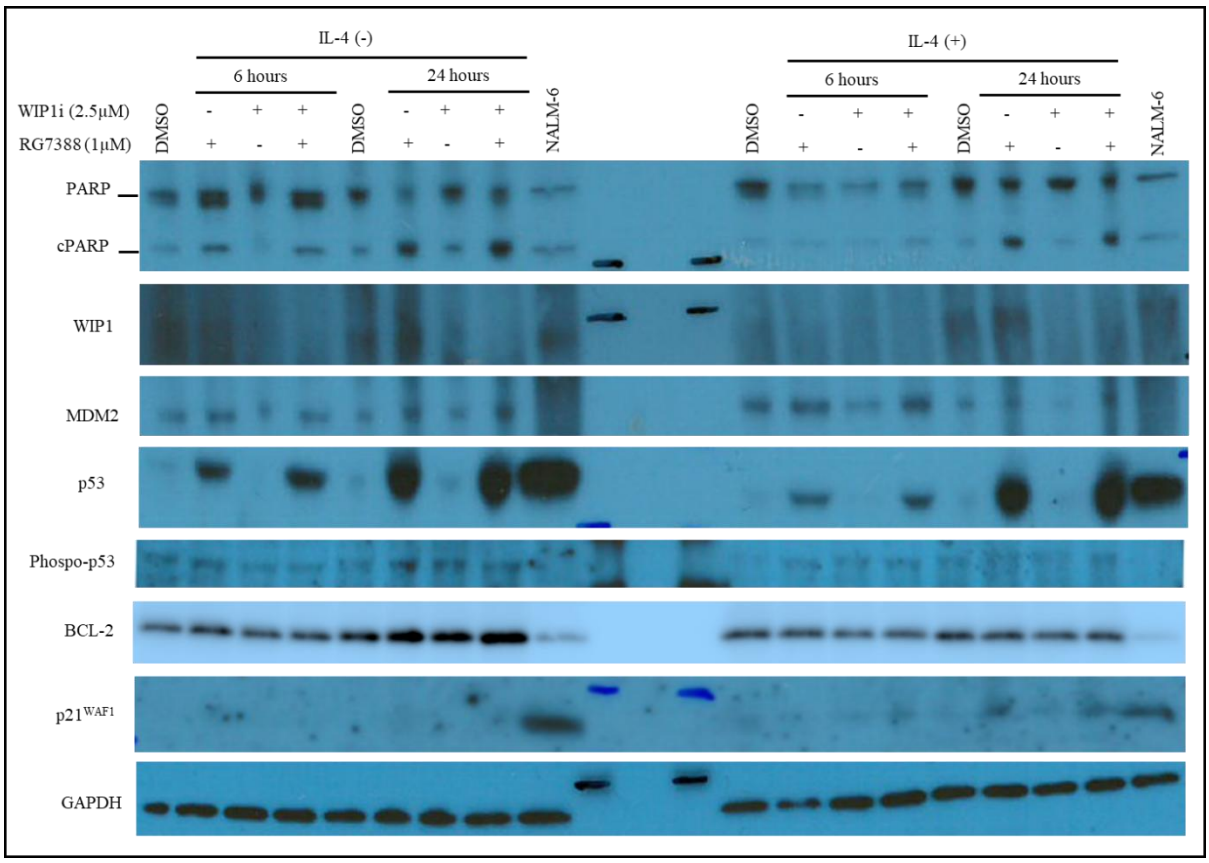

Figure 6.16 Western immunoblot of CLL311 sample treated with RG7388 and WIP1 inhibitor in the presence of IL-4. Primary CLL311 cells treated with GSK2830371 (2.5µM) in combination with RG7388 (1µM) for 6 and 24hrs ± IL-4. RG7388 (1µM) represent the LC_{50} concentration for CLL311 with WIP1i combination treatment in the presence of IL-4. The NALM-6 ($TP53^{WT}$) cell line treated with RG7388 (3µM) was used as a positive control for molecular weight protein expression. RG7388 stabilises the activity of p53 and its transcriptional target protein, and the combination of WIP1 inhibitor showed further stabilisation either with or without IL-4. The experiment performed on cell extracted lsysate (n=1). Both time point treatments were performed in the same condition next to each other on same membrane. The pen marker in the middle of the membrane represents the ladder marker protein. GAPDH used as an endogenous control. All strips were from the same membrane which was cut into three. The top strip was probed for WIP1, MDM2 and PARP; the middle for phospho-p53, p53, and GAPDH; and the third with p21 and BCL-2 antibody.

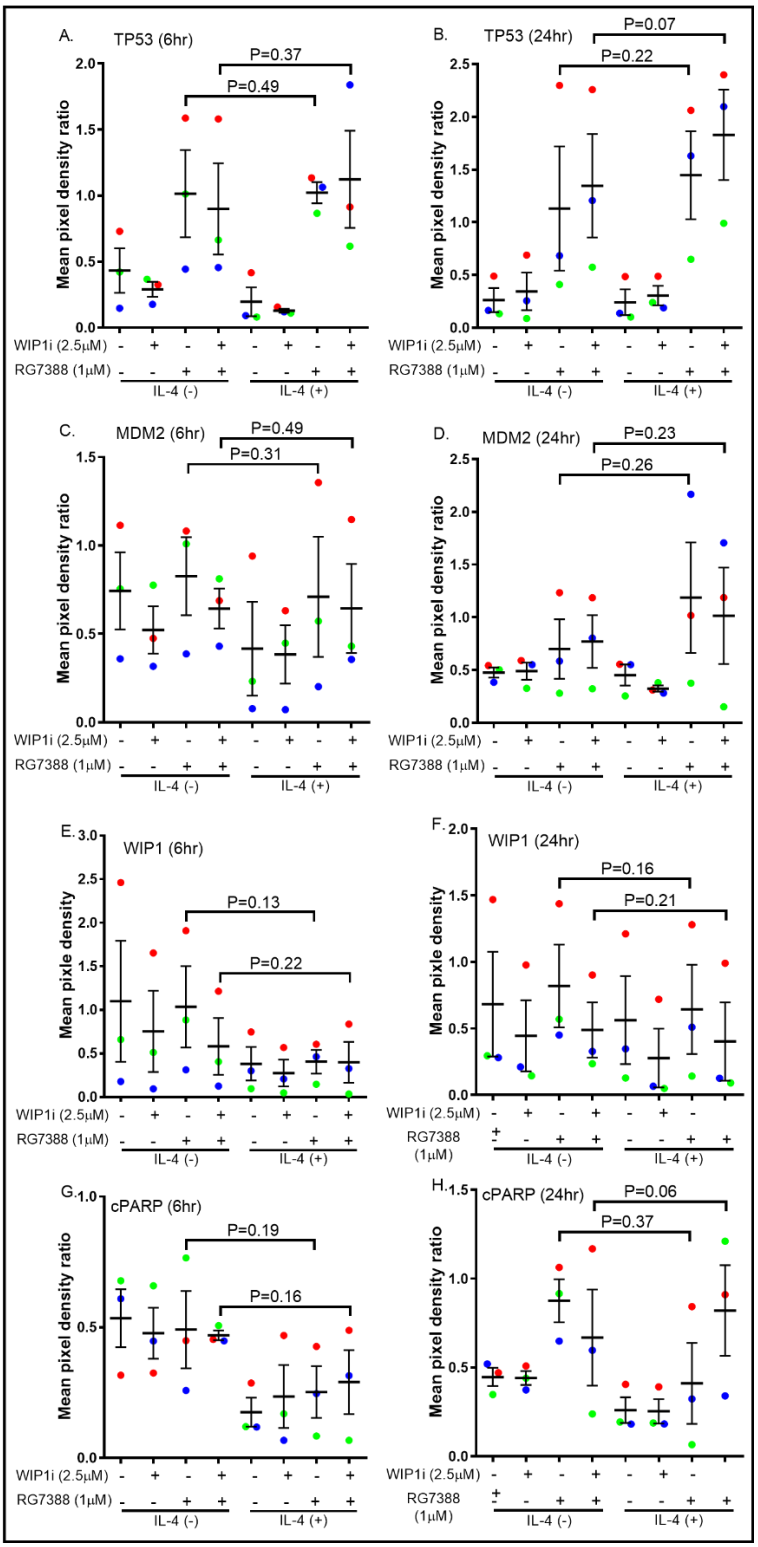

Figure 6.17 Summary of western immunoblot densitometry changes for TP53 and it's target proteins of CLL cells in response to combination of WIP1 ihhibitor with RG7388 in the presence of IL-4. Different primary CLL samples (CLL311, CLL315, CLL316) trated with GSK2830371 (2.5μM) in combination with RG7388 (1μM) ± IL-4 for 6 and 24hrs. The western immunobloting for each sample was performed on cell lysate (n=1) times. The left graphs represent the treatment effect at 6hrs and the right graphs represent the treatment effect at 24hrs. (A-B) TP53 (C-D) MDM2 (E-F) WIP1 (G-H) PARP full-length and cPARP. WIP1 inhibitor potentiates the activity of RG7388 to stabilises TP53 in the presence and absence of IL-4. The mean pixel density ratio for all proteins was background corrected and the values were normalized relative to GAPDH, except cPARP for which the ratio was calculated relative to full-length PARP. Each colour represents primary CLL sample (n=3). The error bar represents the average mean ±SEM for all CLL samples. Statistical significance of differences is shown above error bar for compared the effect of IL-4 on RG7388 treatment alone and in combination with WIP1i. Only the p-values less than 0.05 are shown by paired t-test one tail.

6.3.5 The synergistic effect of RG7388 with the combination of WIP1 inhibitors in the presence of IL-4 on cryopreserved CLL samples

A matrix combination design was used to test the combinations of an extended range of RG7388 and WIP1 inhibitor concentrations on CLL cells in the presence and absence of IL-4. Wide ranges of RG7388 concentrations were used in combination with WIP1 inhibitor concentrations. The experiment was performed to determine whether the combination of RG7388 with WIP1 inhibitor had either synergism or antagonism effect with and without IL-4, and for what dose combinations.

In the absence of IL-4 (Figure 6.18 A&B), CLL314 showed a concentration dependent inhibition effect of RG7388 as a single agent although, CLL cells showed a protective effect with concentrations lower than 100nM. Due to the heterogeneity of CLL cells, the inhibition effect of RG7388 is varies between samples. In contrast, WIP1 inhibitor up to 10,000nM had no inhibition effect on the viability of CLL314 in the absence of IL-4. However, the combination of WIP1 inhibitor potentiated the effect of RG7388. The LC_{50} of RG7388 alone was less than 300nM on CLL314 in the absence of IL-4.

In the presence of IL-4 (Figure 6.19 A&B), WIP1 inhibitor up to (10μM) alone had little (< 3%) inhibition effect on CLL314 viability while, RG7388 alone showed dose dependent inhibition effect. The combination of WIP1 inhibitor potentiated the effect of RG7388. The LC_{50} of RG7388 alone was around 10,000nM for CLL314 in the presence of IL-4. The presence of IL-4 produces a protective effect on CLL cells in response to the treatment and CLL cells become less sensitive to the treatment.

The average ZIP synergy score for CLL314 was (26.86) with the combination of RG7388 and WIP1 inhibitor in the absence of IL-4 (Figure 6.18 C), while it was (21.16) in the presence of IL-4 (Figure 6.19 C). Furthermore, the maximum synergistic effect of the combination treatment for CLL314 in the absence of IL-4 was with RG7388 at (30-100nM) and WIP1 inhibitor (3,000-10,000nM) with peak of 85.58. In comparison to the presence of IL-4, the maximum synergistic effect of the combination treatment for CLL314 was increased to (3,000-10,000nM) with both RG7388 and WIP1 inhibitor with peak of 42.65. The ZIP synergy score of each CLL samples in response to the treatment whether in the presence or absence of IL-4 were discussed in the next section.

The matrix model experiment was performed on three freshly isolated CLL patient samples (CLL314, 315, 316) and two cryopreserved CLL sample (CLL310, 311 TH), which were

exposed to a wide range of RG7388 and WIP1 inhibitor concentrations in the presence of IL-4. Following 48 hours of treatment, the CLL cell viability was measured by XTT assay. CLL314 illustrated an example of matrix model results and the ZIP synergy score of other CLL samples were summarized in the Figure 6.20.

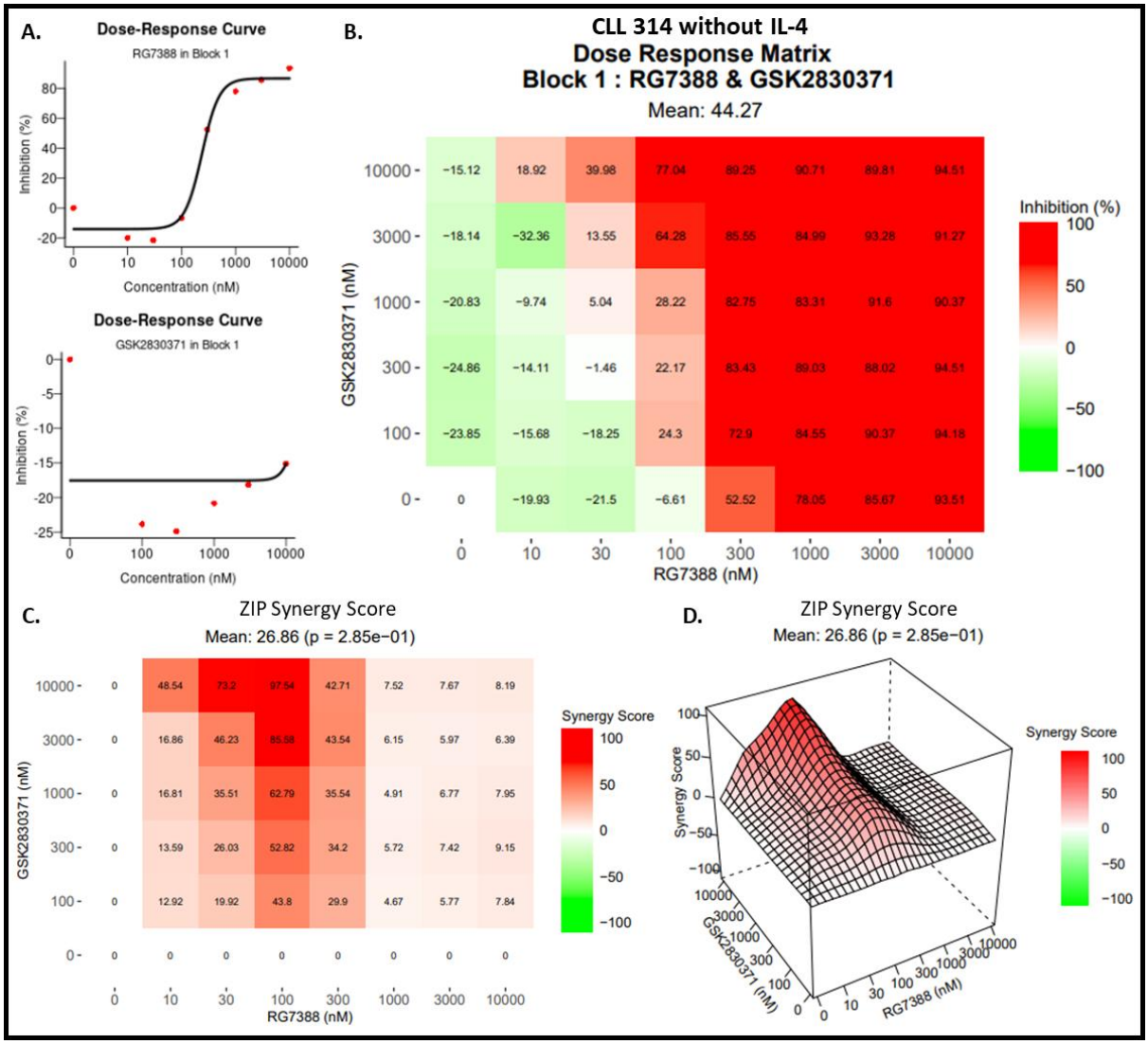

Figure 6.18 The synergistic effect of RG7388 in combination with WIP1 inhibitors in the absence of IL-4 on primary CLL314 cells. The matrix model designed to find the synergistic effect and the optimum highest concentration to obtain the greatest combination effect. Freshly isolated CLL cells treated with wide range of RG7388 and GSK2830371 concentrations (0.01-10µM) for 48hrs. The CLL cell viability assessed by XTT assay. DMSO is included as solvent vehicle (control). (A) The graph shows single dose response inhibition effect in response to RG7388 and WIP1 inhibitor. (B) The representive dose response analysis showing the % inhibition of cell viability in response to wide range of the treatment (C) Synergy map represent the area with the greatest synergy are marked with intense red colour and the square represent the Zero Interaction Potency (ZIP) synergy score of the combination treatment. (D) The 3-D diagram shows the peak ZIP synergy score in greater interpolated detail. The experiment was performed once on each individual CLL sample in a total of (n=8) different samples. The data was analysed by the Synergyfinder.org website.

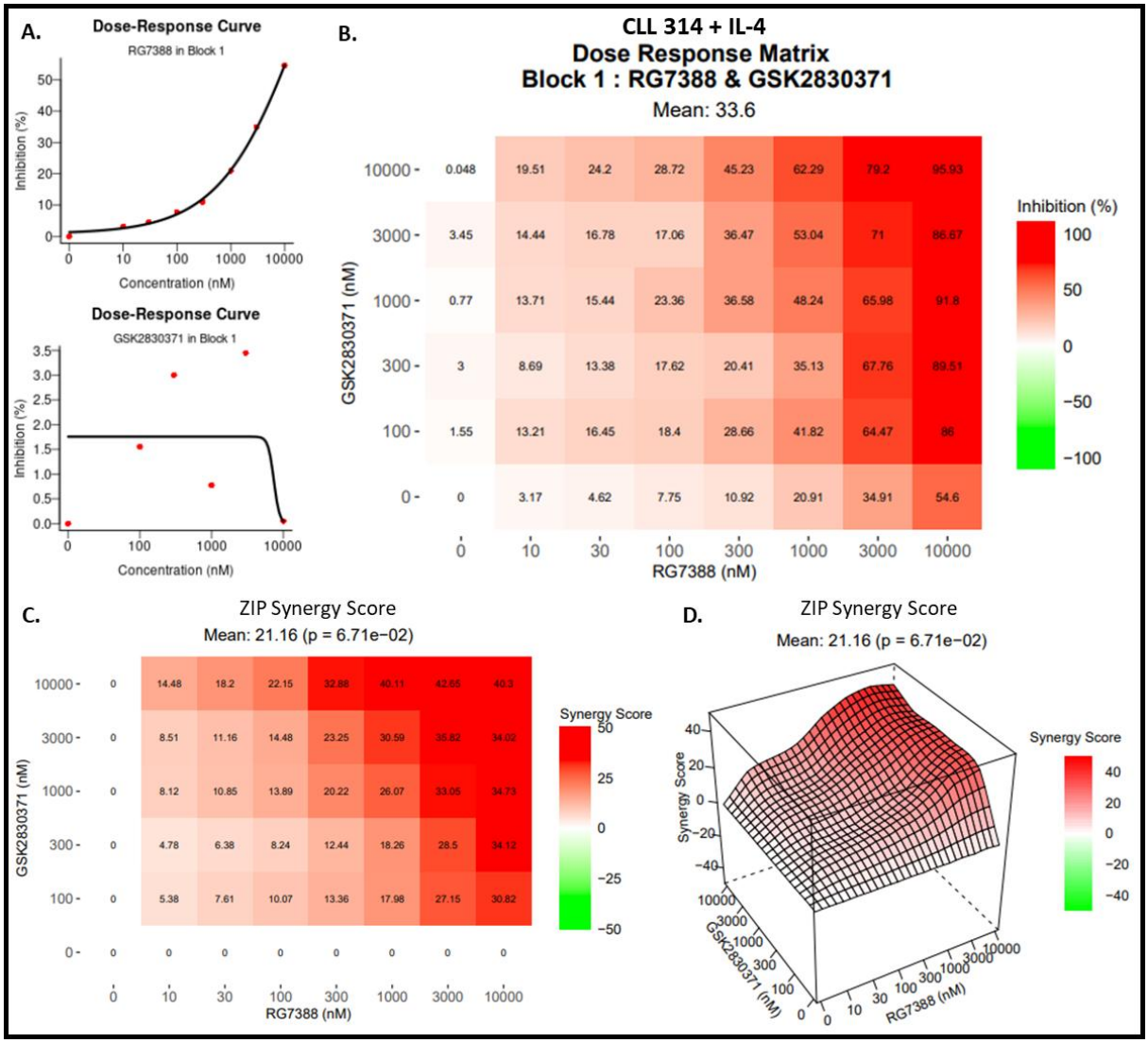

Figure 6.19 The inhibition effect of RG7388 in combination with WIP1 inhibitors in the presence of IL-4 on primary CLL314 cells. Freshly isolated CLL311 cells treated with wide range of RG7388 and GSK2830371 concentrations (0.01-10μM) in the presence of IL-4 for 48hrs and the CLL cell viability was determined by XTT assay. DMSO is included as solvent vehicle (control). A dose–response matrix design was used to assess synergy and determine doses at which the greatest synergy was observed, as determined by the Zero Interaction Potency (ZIP) Model. (A) The scatter plot curves shows the percentage inhibition effect of single agent treatment for RG7388 and GSK2830371. (B) Matrix table model shows the individual % inhibition effect for each combination treatment. (C) Synergy ZIP score in response to combination treatment of RG7388 and GSK2830371. The red colour represents the synergistic effect and the intensity of red colour represents the highest synergistic effect of the combination treatment. (D) The 3-D plot shows the peak ZIP synergy score in greater interpolated detail. The experiment performed once on each individual CLL sample (n=1). The Synergyfinder.org website identifies the range of ZIP scores for a synergistic effect to be greater than 10 and any score less than 10 is defined as an antagonistic effect.

6.3.5.1 The average synergy ZIP score of RG7388 and WIP1 inhibitor differs between fresh and cryopreserved CLL samples

Of the five primary CLL samples, two were thawed cryopreserved samples (TH) and three were freshly isolated, and these were treated with a range of combination concentrations of RG7388 and WIP1 inhibitor in the presence and absence of IL-4 for 48 hours (Figure 6.20).

Most of the CLL samples, except for CLL310, showed a reduction in the average ZIP synergy score to a varying extent for the combination effect of RG7388 and WIP1 inhibitor with IL-4 compared to the combination effect without IL-4. However, there was no significant difference in the average ZIP score across the set of CLL samples between the presence and the absence of IL-4 (Figure 6.20 B). Although, CLL cells which were treated with a combination without IL-4 show a scattered ZIP score distribution, the ZIP scores appeared to have a narrow distribution in the presence of IL-4 (Figure 6.20 B).

Regarding to the average ZIP score values (Figure 6.20 C&D), freshly isolated CLL cells showed a higher synergistic effect of combination treatment of RG7388 and WIP1 inhibitor without IL-4 compared to in the presence of IL-4. Freshly isolated CLL cells become less sensitive in response to RG7388 and WIP1 inhibitor in the presence of IL-4. The synergistic effect of the combination treatment cannot be evaluated separately for cryopreserved CLL samples due to fluctuating responses and limited number of samples.

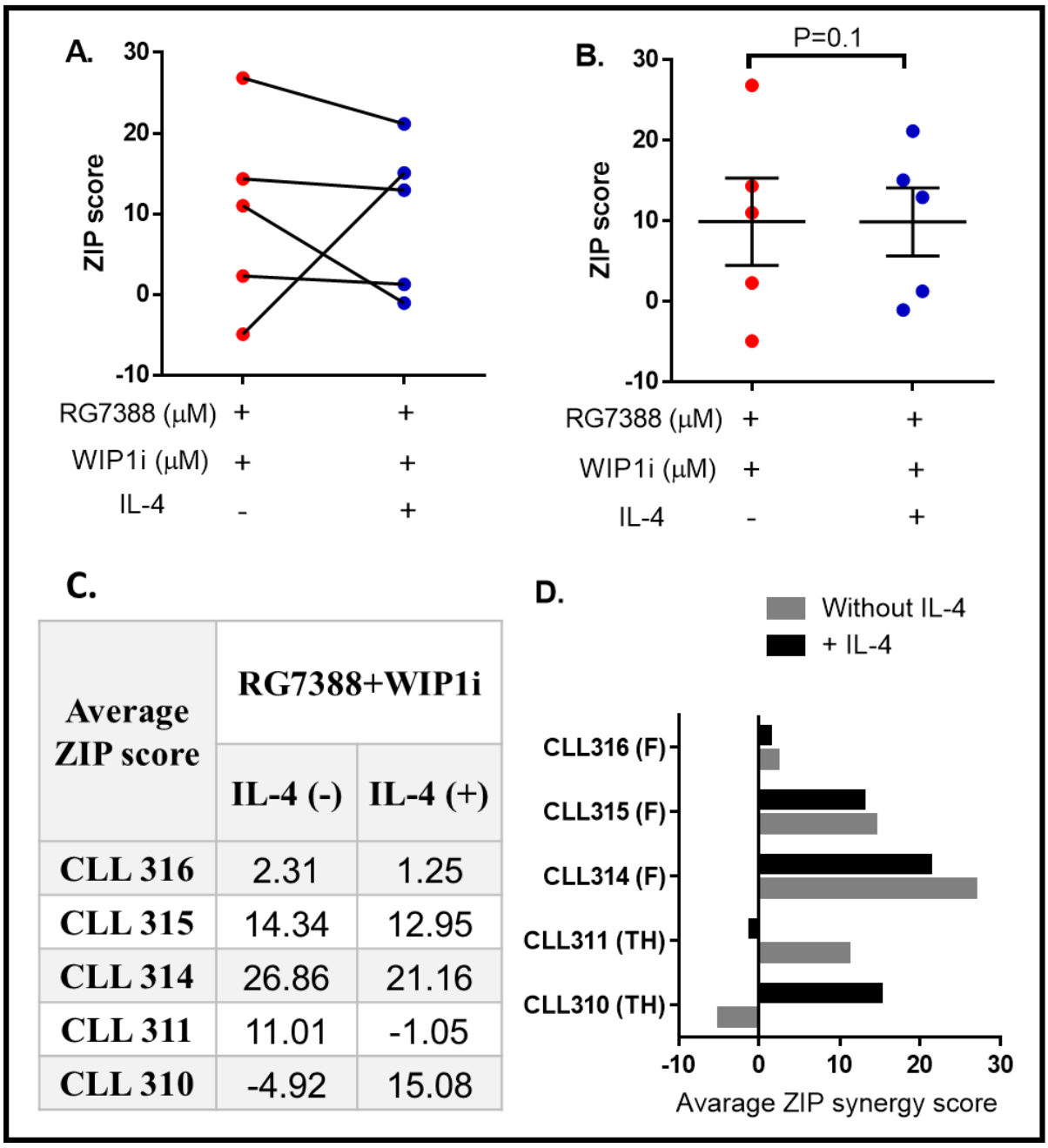

Average ZIP score	RG7388+WIP1i	
	IL-4 (-)	IL-4 (+)
CLL 316	2.31	1.25
CLL 315	14.34	12.95
CLL 314	26.86	21.16
CLL 311	11.01	-1.05
CLL 310	-4.92	15.08

Figure 6.20 Summary displaying the synergy score of WIP1 inhibitor and RG7388 on CLL samples in the presence of IL-4 determined by zero interaction potency (ZIP) model. Different primary CLL samples (n=4) treated with range of RG7388 in combination with GSK2830371 with and without IL-4 for 48hrs followed by XTT assay to determine cell viability. The red dots represents the synergy score without IL-4 and blue dots shows the presence of IL-4. (A) ZIP synergy score for individual CLL sample in response to combination treatment with and without IL-4. (B) Difference between the mean ZIP scores of combination treatment ± IL-4. The error bars show ± SEM of total CLL samples (n=4). (C) Value of the mean ZIP score for each individual CLL sample. (D) The induction of mean ZIP scores with the presences of IL-4 compared to the absence of IL-4. Each CLL sample was normalized to independent DMSO treatment for individual sample. The ZIP score analysed using Synergyfinder.com. Statistical significance was determined by one tail t-test.

6.3.5.2 The peak synergy ZIP score for RG7388 and WIP1 inhibitor-treated CLL samples mostly decreases with the effect of IL-4

(Figure 6.21 A) shows the peak ZIP synergy score for each CLL sample in response to the combination effect of RG7388 and WIP1 inhibitor with and without the effect of IL-4. The majority of the CLL samples showed a reduced peak synergy response to the RG7388 and WIP1 inhibitor combination in the presence of IL-4 (Figure 6.21 B). Overall, IL-4 reduces the degree of synergy, as well as having a protective effect against RG7388 alone or in combination with WIP1 inhibitor.

A.

Peak ZIP synergy score	RG7388+WIP1i	
	IL-4 (-)	IL-4 (+)
CLL 316	11.51	8.56
CLL 315	34.04	21.35
CLL 314	97.54	42.65
CLL 311	29.07	8.44
CLL 310	15.05	47.52

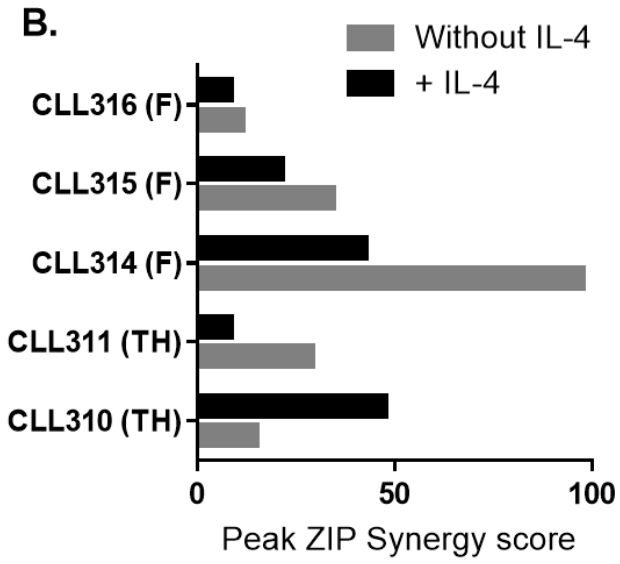

Figure 6.21 The peak synergy score of CLL samples in response to WIP1 inhibitor and RG7388 of IL-4. (A) The value of the peak ZIP score for each individual CLL sample (n=5). (B) The difference in the peak ZIP score for each individual CLL sample with and without the presence of IL-4 in grey and black column respectively. In 4 out of 5 CLL samples, the CLL cells express less synergistic effect of WIP1 inhibitor and RG7388 in the presence of IL-4 compared to the absence of IL-4. Fresh isolated CLL (F), Thawed sample (TH).

6.3.5.3 Freshly isolated CLL cells have a significantly reduced peak ZIP synergy score for combination treatment with RG7388 and WIP1 inhibitor in the presence of IL-4

The peak synergy score for freshly isolated CLL cells treated with WIP1 inhibitor and RG7388 was reduced in the presence IL-4 relative to the absence of IL-4 (Figure 6.22 A). CLL cells also become less responsive to the WIP1 and MDM2 inhibitor combination in the presence of IL-4. IL-4 appears to induce a protective mechanism against the effect of WIP1 inhibitor and RG7388 (Figure 6.22 B). There was a significant difference in the normalised inhibition peak ZIP synergy scores for CLL cells treated with the combination in the presence of IL-4 activity compared to the effect of the combination treatment in the absence of IL-4 ($p=0.04$).

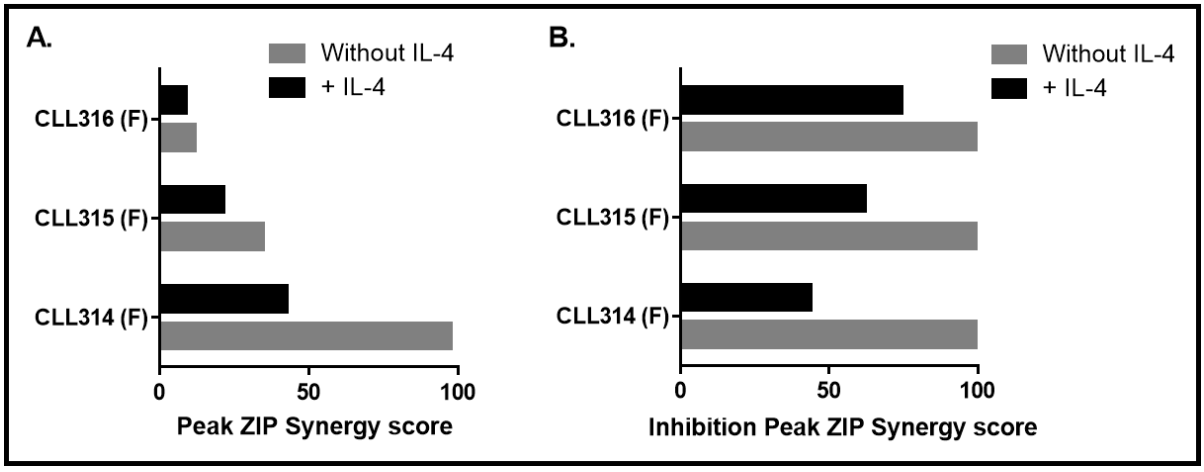

Figure 6.22 Summary effect of IL-4 on the synergistic response of freshly isolated CLL samples to RG7388 and WIP1 inhibitor combination. (A) The peak ZIP synergy score of individual freshly isolated CLL cells in the presence of IL-4. (B) When the ZIP score is normalised (to the absence of IL-4) there is a significant difference in the inhibition peak ZIP synergy score of the CLL sample in the response to RG7388 and WIP1 inhibitor between the presence and the absence of IL-4 ($p=0.02$). Statistical significance was determined by one tail t-test. Fresh isolated CLL (F).

6.3.6 IL-4 induces the transcription level of anti-apoptotic genes following treatment with the WIP1 inhibitor

In this section, these mechanistic investigations are extended to the gene transcriptional level. The changes in transcriptional messages of *TP53* target genes and that of the anti-apoptotic genes *MCL1* and *BCL2* were measured, to determine the effect of the WIP1 and MDM2 inhibitors on CLL cells. In these experiments, the CLL cells were treated with a range of RG7388 and WIP1 inhibitor concentrations in the presence of IL-4 for 6 and 24 hours. The genes included *TP53* negative regulator target genes (*TP53*, *MDM2*, *PPM1D* and *CDKN1A*), the pro apoptotic genes (*PUMA*, *NOXA*, *BAX* and *FAS*), the *CDKN1A* gene to identify cell growth arrest signalling, and the anti-apoptotic genes, *MCL1* and *BCL2*.

Four different CLL samples were treated with the WIP1 inhibitor (2.5μM) in the presence of IL-4 for 6 and 24 hours (Figure 6.23). The mRNA expression of the chosen gene set was measured by qRT-PCR following 6 and 24 hour treatment times, *TP53* and *TP53INP1* are expressed following the WIP1 inhibitor (2.5μM) alone (Figure 6.23 A), however, *FAS* and *TP53INP1* are expressed upon the addition of IL-4 (Figure 6.23 B). Following the 24-hour treatment, *PUMA* and *PPM1D* show an induction following treatment with the WIP1 inhibitor (2.5μM) alone (Figure 6.23 C). Addition of IL-4 increases expression of *PUMA*, *TP53INP1*, *NOXA* and *BAX* (Figure 6.23 D). The statistical fold change differences between the mRNA expression in presences and absence of IL-4 were identified in different figures.

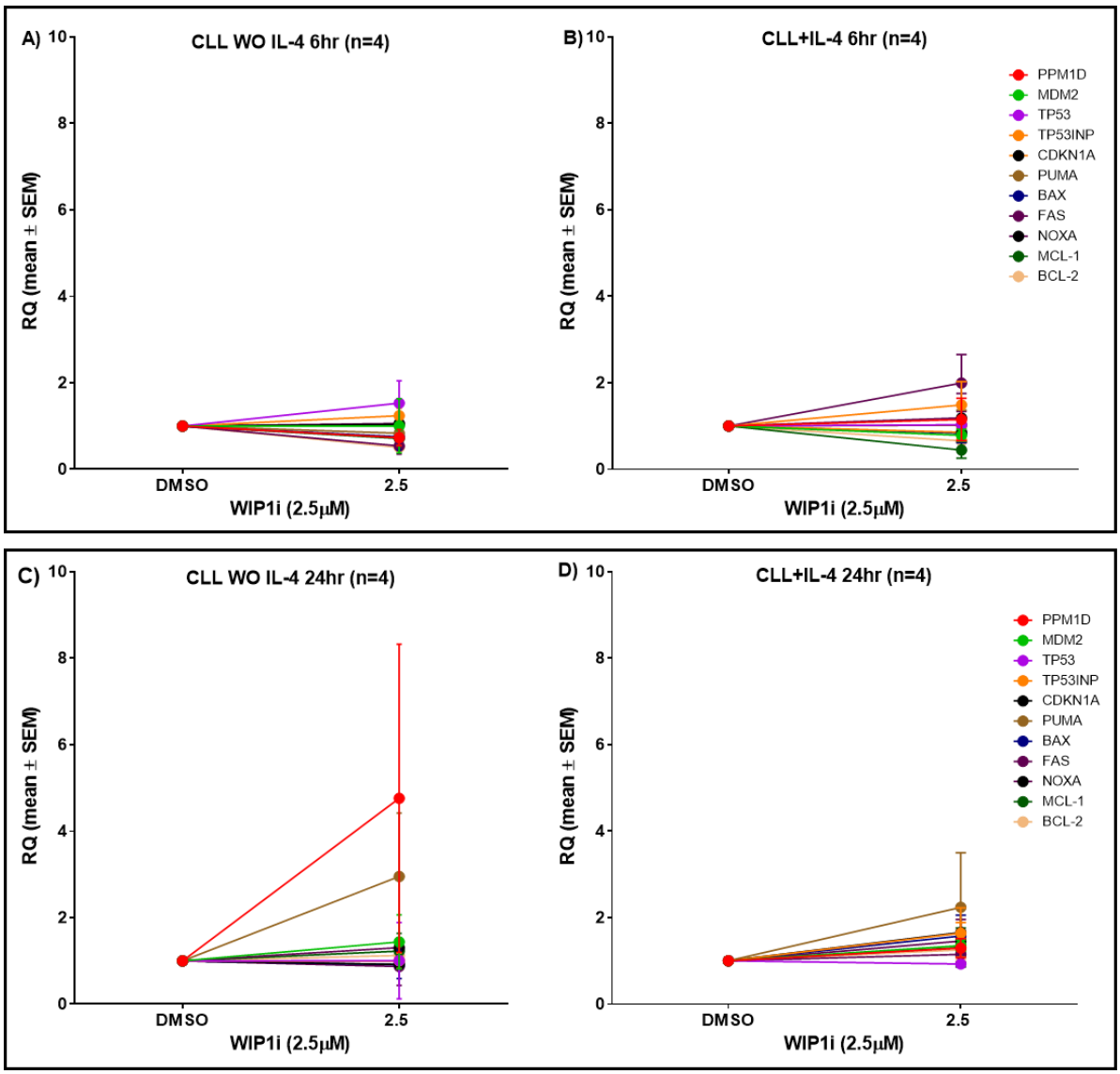

Figure 6.23 Fold changes in mRNA expression of selected genes in response to WIP1 inhibitor (2.5µM) in the presence and absence of IL-4 by qRT-PCR. Primary CLL samples (n=4) treated with GSK2830371 (2.5µM) with and without IL-4 for (A&B) 6hrs and (C&D) 24hrs. *β-ACTIN* used as the endogenous control and DMSO-treated cells were used as the calibrator between three intra-replicate wells of treatment concentration. Error bars represent the mean ± SEM of different CLL samples. The experiment performed in (n=1) repeat on each primary CLL sample. RQ values were calculated using the formula 2ΔΔCt.

6.3.6.1 Summary of the mRNA expression for certain TP53 target genes with WIP1 inhibitor in the presence of IL-4 at (6hr)

The following section is showing the differences in the mRNA expression of certain genes after treated the CLL cells with WIP1 inhibitor at (2.5µM) in the presence and absence of IL-4 for 6 and 24 hours. The genes were chosen based on the fold change increase in their mRNA expression between the presence and absence of IL-4. It is clear there was no significance differences in fold change expression of any of the gene panel with WIP1 inhibitor at 6 hours with the presence of IL-4 (Figure 6.24). Although, there was an increase in the expression of

pro-apoptotic genes *NOXA* and *FAS* in the presence of IL-4 however, it is non-significant (p=0.4, p=0.08).

At 24 hours, the mRNA expression of *PPM1D* showed more than 4-fold increase in response to WIP1 inhibitor in the absence of IL-4 which is lost in the presence of IL-4. In addition, *PUMA* showed 3-fold increases in response to WIP1 inhibitor in the absence of IL-4 compared to presence of IL-4 (Figure 6.25).

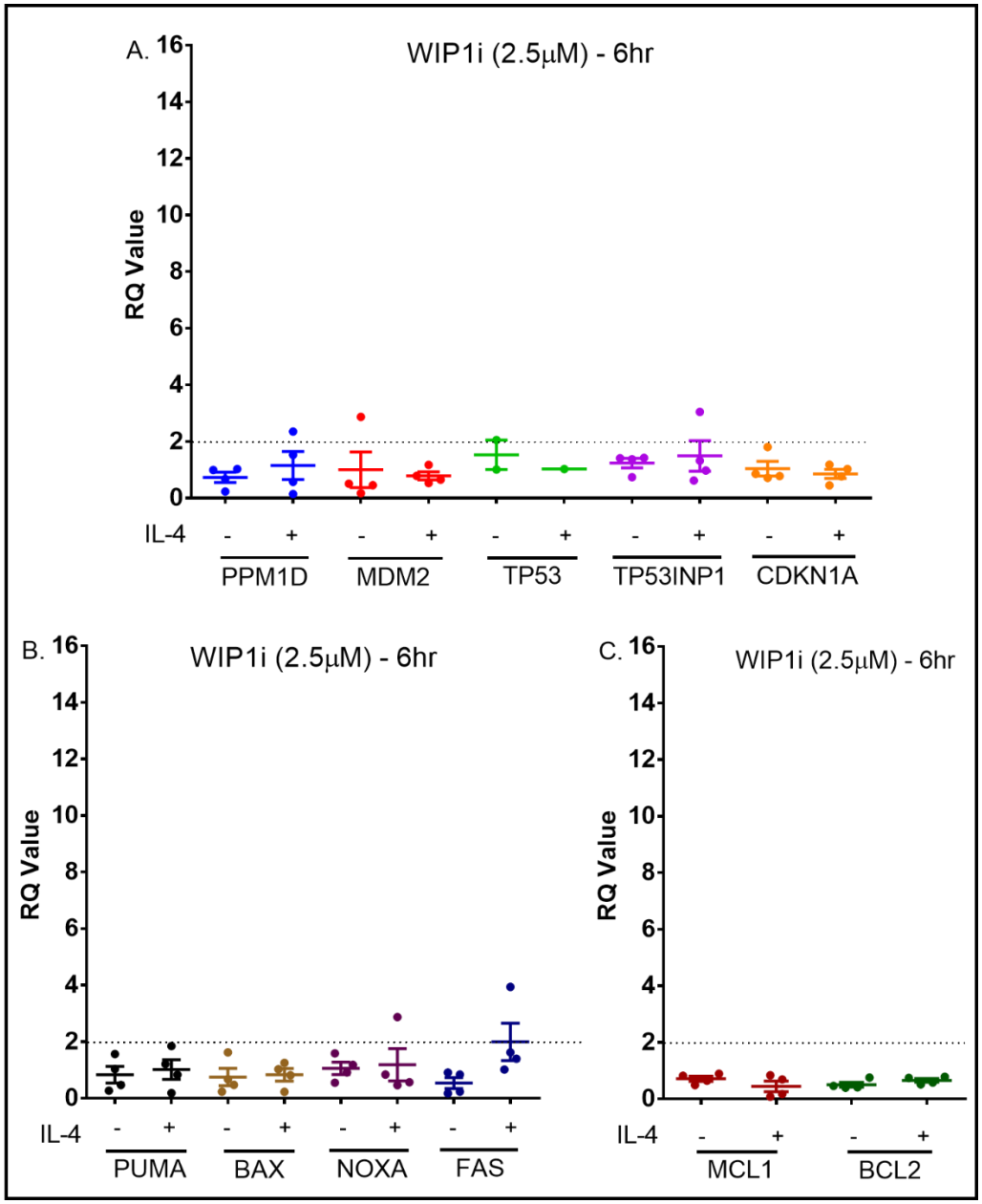

Figure 6.24 Summary comparing the fold change of TP53 target gene expression in response to WIP1 inhibitor (2.5μM) in the presence of IL-4 for 6hrs. (A) negative regulator p53 genes. (B) pro-apoptotic genes (C) Anti-apoptotic genes. Each point represents the mean value for an individual patient. Each colour showed mRNA expression of certain gene in response to GSK2830371 (2.5μM) with and without IL-4. The error bar represent mean ± SEM of different CLL samples (n=4). Statistical significance was determined by paired t-test one tail between the presence and absence of IL-4 in response to WIP1i ($p < 0.05$).

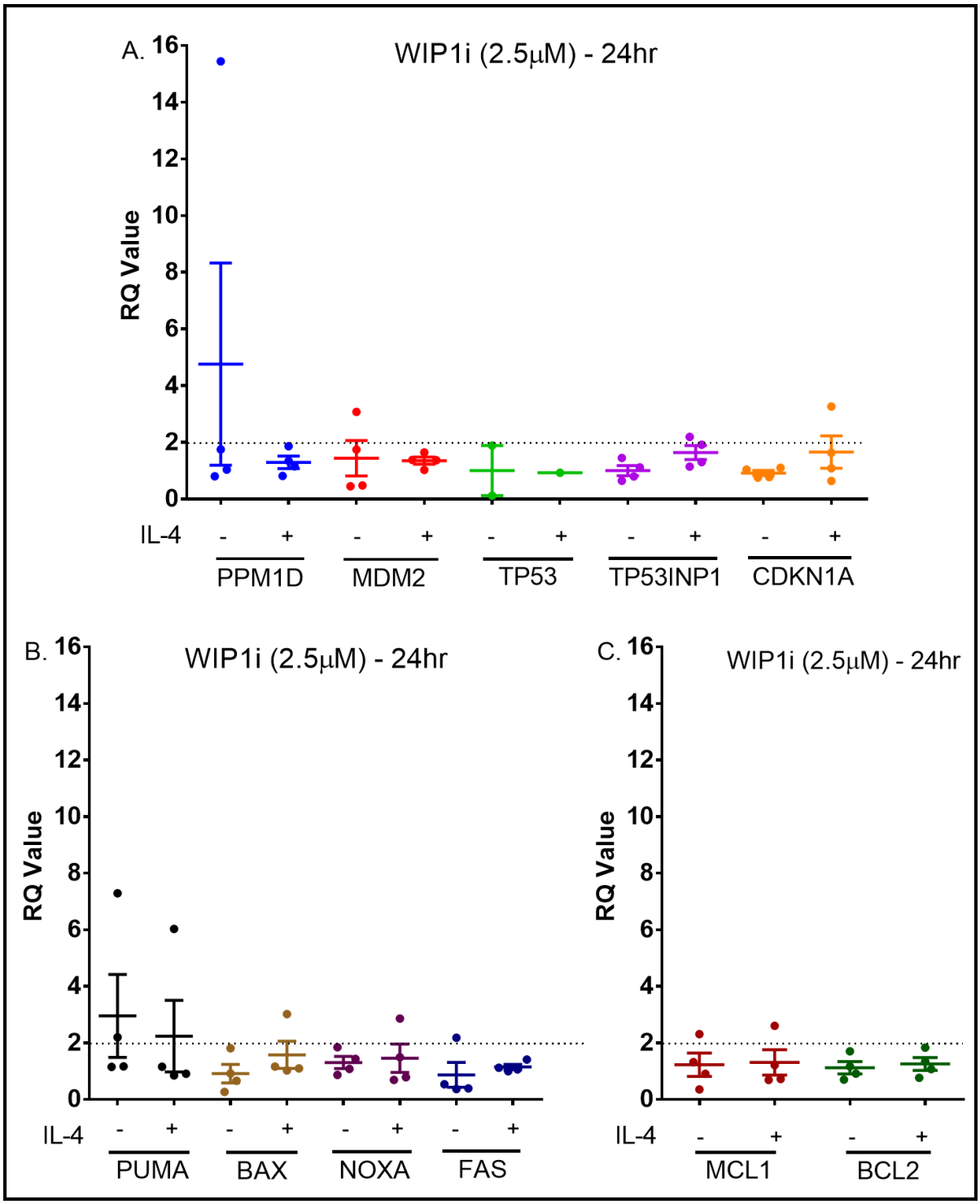

Figure 6.25 Summary comparing the fold change of the TP53 target gene expression in response to WIP1 inhibitor (2.5μM) in the presence of IL-4 for 24 hrs. (A) negtive regulator p53 genes. (B) pro-apoptotic genes (C) Anti-apoptotic genes. Each point represents the mean value for an individual patient. Each colour showed mRNA expression of certain gene in response to GSK2830371 (2.5μM) with and without IL-4. The error bar represent mean ± SEM of different CLL samples (n=4). Statistical significance was determined by paired t-test one tail between the presence and absence of IL-4 in response to WIP1i ($p < 0.05$).

6.3.7 RG7388 induces the mRNA upregulation of TP53 target genes in CLL cells with and without the presence IL-4

A wide range of RG7388 concentrations were used to determine the response of four primary CLL samples in the presence of IL-4 at 6 and 24 hours (Figure 6.26). After 6 hours treatment with RG7388, the mRNA expression of the majority of the gene set is induced at 0.3µM concentration especially *PPM1D*, *MDM2* and *PUMA*. Following with the next 1µM concentration, *PPM1D* showed the highest fold change expression relative to DMSO control. In addition, most of the gene set, *TP53*, *TP53INP1*, *CDKN1A*, *NOXA* and *BAX* showed fold change induction with a concentration dependent of RG7388 apart from *MDM2* and *PUMA* which showed a decrease in their fold changes. In contrast, the anti-apoptotic genes, *MCL1* and *BCL2* showed a decrease in their fold change expression relative to DMSO. (Figure 6.26 A). In the presence of the IL-4, *MDM2*, *PUMA*, *PPM1D* and *CDKN1A* show high fold changes for 6 hours treatment of RG7388 in the presence of IL-4 across other gene set (Figure 6.26 B).

Following 24 hours with RG7388 alone, *PUMA* is only gene that is increased (5-fold) following RG7388 (0.3µM) compared to the other genes. Higher concentration of RG7388 (1µM) is decreased crashed and no increased fold changes in expression were detected (Figure 6.26). Addition of IL-4 with the RG7388 (0.3µM) for 24 hours increased the fold change expression of *MDM2*, *TP53INP*, *CDKN1A*, *FAS* and *NOXA* (Figure 6.26 C). Moreover, expression of *CDKN1A* and *NOXA* was higher following treatment with RG7388 (1µM) in the presence of IL-4 compared to *MDM2* and *FAS* which show a small reduction in their mRNA expression (Figure 6.26 D). The statistical t-test will be provided in the following summary section at which the fold change of mRNA expression was compared between the presence and absence of IL-4.

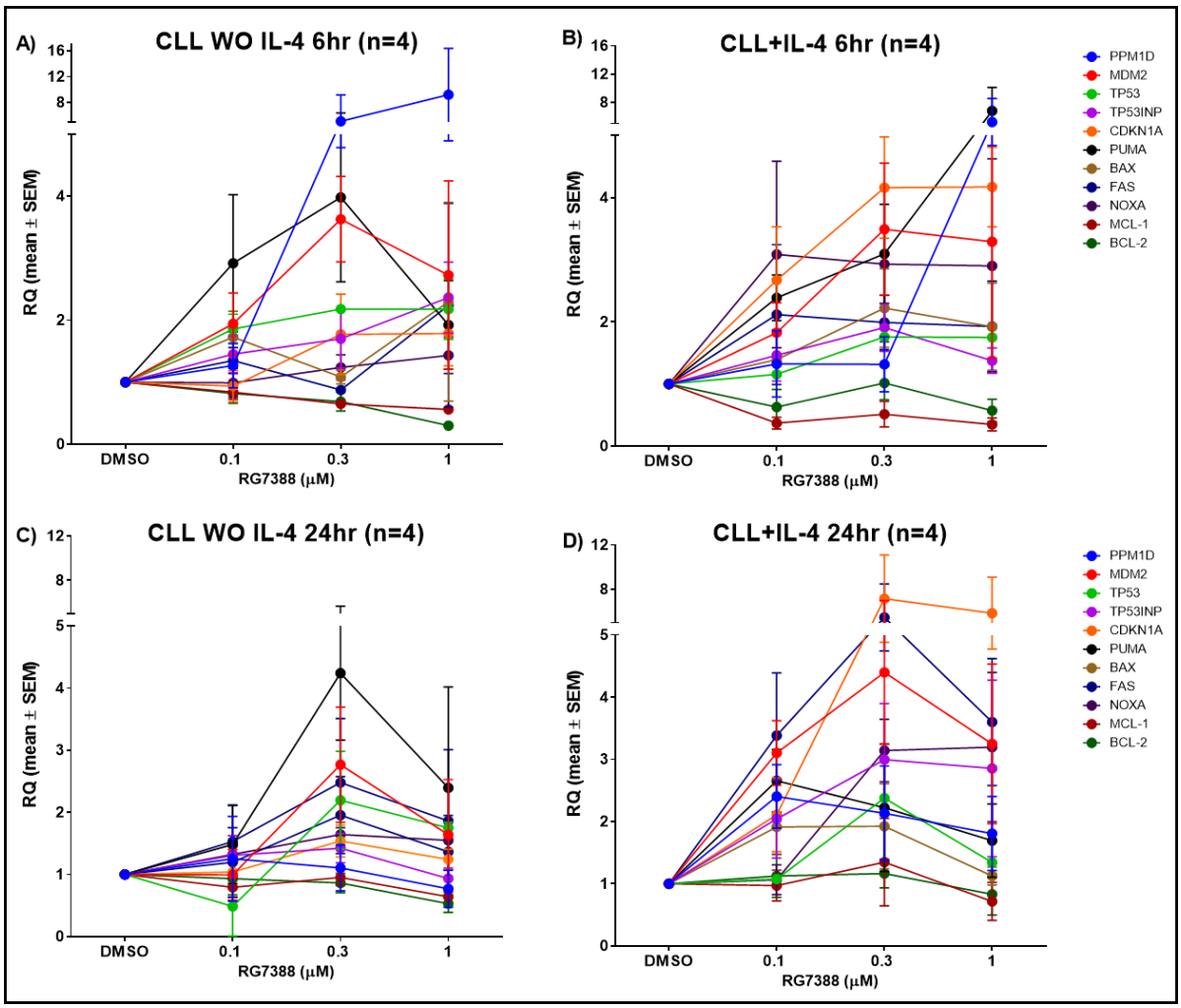

Figure 6.26 Fold changes in the mRNA expression of gene set with RG7388 treatment in the presence and absence of IL-4 qRT-PCR. Primary CLL cells (n=4) treated with RG7388 (0.1-0.3-1μM) (A&B) 6hrs (C&D) 24hrs with and without IL-4. mRNA expression normalised to untreated control DMSO solvent and *β-ACTIN* by acting as the calibrator between three intra-replicated wells of each concentration for each independent sample. The experiment performed in (n=1) repeat on each independent CLL sample. Each colour represents certain gene and the error bars represent the mean ± SEM of CLL samples. RQ values were calculated using the formula $2\Delta\Delta Ct$.

6.3.7.1 IL-4 induces mRNA upregulation of pro-apoptotic TP53 target genes in CLL cells following treatment with RG7388 for (6hr)

RG7388 (0.1µM) alone induced the mRNA expression of *PUMA* at 6 hours following treatment. The addition of IL-4 induced the expression of *CDKN1A, FAS* and *NOXA* at 6 hours treatment (Figure 6.27 A&B).

Furthermore, the effect of RG7388 (0.3µM) in the absence of IL-4 was to increase the fold change expression of the *MDM2* gene. There is one primary CLL sample that showing an induction in the *PPM1D, TP53INP1, CDKN1A* and *PUMA* genes expression (Figure 6.27 C).

The presence of IL-4 following treatment with RG7388 (0.3µM) induced an increase in the fold change expression of *MDM2*, *TP53INP1*, *CDKN1A*, *PUMA*, *BAX* and *NOXA* after 6 hours of treatment (Figure 6.27 D).

Treatment with RG7388 (1µM) as a single agent induced the mRNA expression of *PPM1D*, *TP53INP1*, *CDKN1A* and *PUMA*. There is one primary CLL sample that was an outlier-expressing high fold changes (7-folds) in the expression of *PPM1D*, *MDM2*, *BAX* and *FAS* (Figure 6.27 E). This sample had a high basal mRNA expression compared to the other CLL cells in the cohort. Regarding to the basal mRNA expression of *PPM1D* in (n=11) CLL samples in my study, I found the mRNA expression of the *PPM1D* is varies between CLL samples.

The presence of IL-4 induced the expression of *PPM1D*, *MDM2*, *CDKN1A* and *PUMA* genes expression following RG7388 (1µM). Moreover, only one primary CLL sample had a high fold change expression in *BAX*, *FAS* and *NOXA* (Figure 6.27 F).

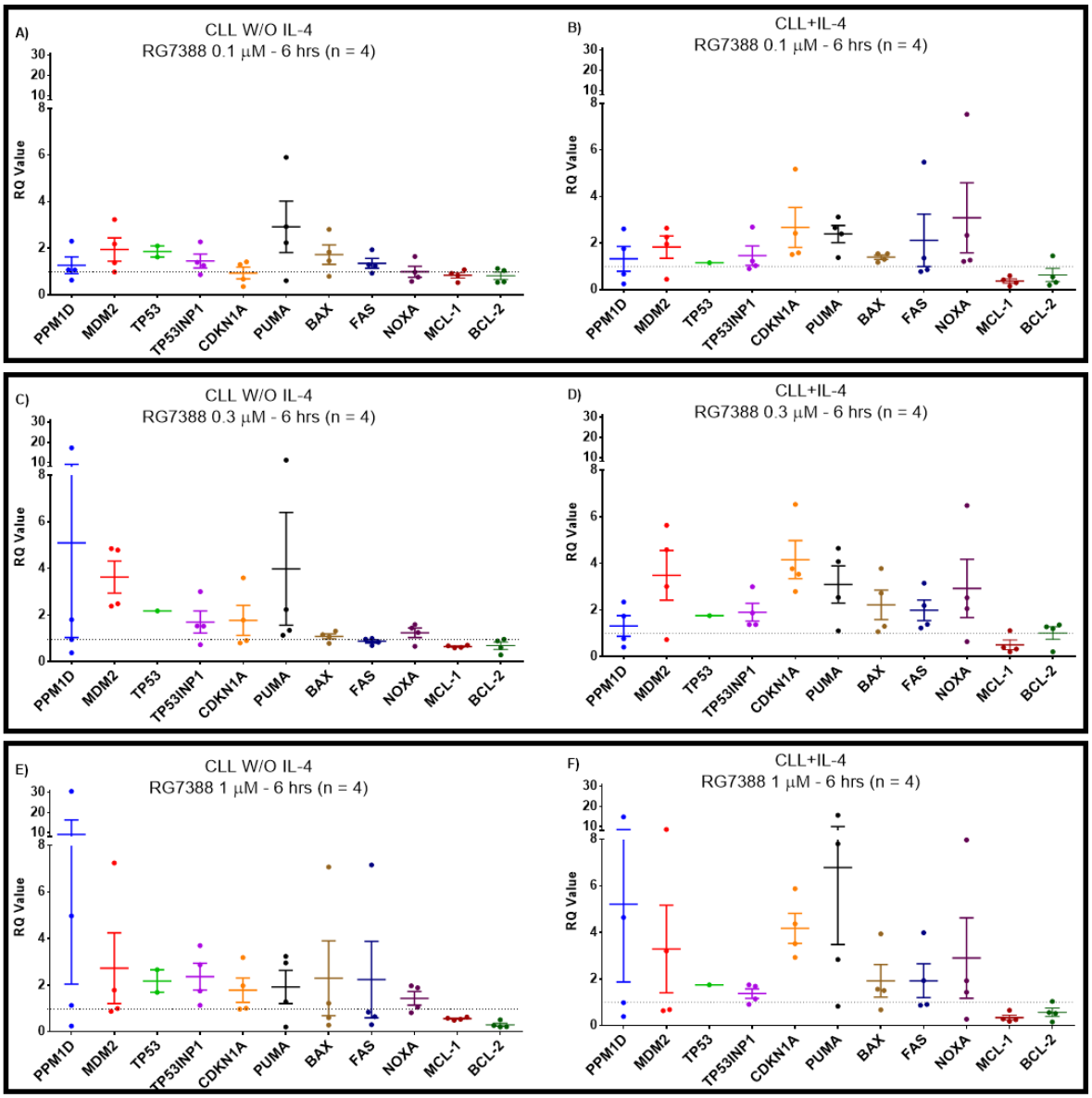

Figure 6.27 Summary of fold change in gene expression of CLL cells treated with RG7388 for 6 hrs in the presence and absence of IL-4. (A&B) RG7388 (0.1µM), (C&D) RG7388 (0.3µM), (E-F) RG7388 (1µM). The experiment performed one time on individual primary CLL samples (n=4). Each point represents the mean value for an individual patient and the error bars in each case represent the average mean ± SEM for the patient samples. Each colour represents mRNA expression of certain gene in response to the treatment. *β-ACTIN* and DMSO treated cells normalized the three intra-replicate wells of each concentration. RQ values were calculated using the formula 2ΔΔCt.

6.3.7.2 RG7388, in the presence of IL-4 significantly induces the mRNA expression of *CDKN1A* and *FAS* gene

The following is a summary of the previous data with statistical analyses. The fold changes in the mRNA expression of certain genes that showed an increase in response to RG7388 in the presence and absence of IL-4.

A comparison between the effect of RG7388 concentrations (0.1, 0.3 and 1μM) in the presence and the absence of IL-4 at 6 hours on selected genes is shown in Figure 6.28. There is no significant change in the expression of *MDM2* across the different concentrations of RG7388 with and without the effect of IL-4. Moreover, *PPM1D* has no obvious changes in the expression of mRNA in response to RG7388 concentrations with and without IL-4 except for one CLL sample that has high expression with RG7388 (0.3 and 1μM) in the absence of IL-4.

For *CDKN1A*, there is a trend for an increase in the mRNA expression in the response to RG7388 with the effect of IL-4. RG7388 (0.1 and 0.3μM) does not alter *PUMA* expression either with or without the presence of IL-4. However, RG7388 (1μM) in the presence of IL-4 induces the expression of *PUMA* in comparison to its expression following RG7388 alone ($p=0.014$). Furthermore, there is a trend towards an increase in *FAS* expression in response to the RG7388 in the presence of IL-4.

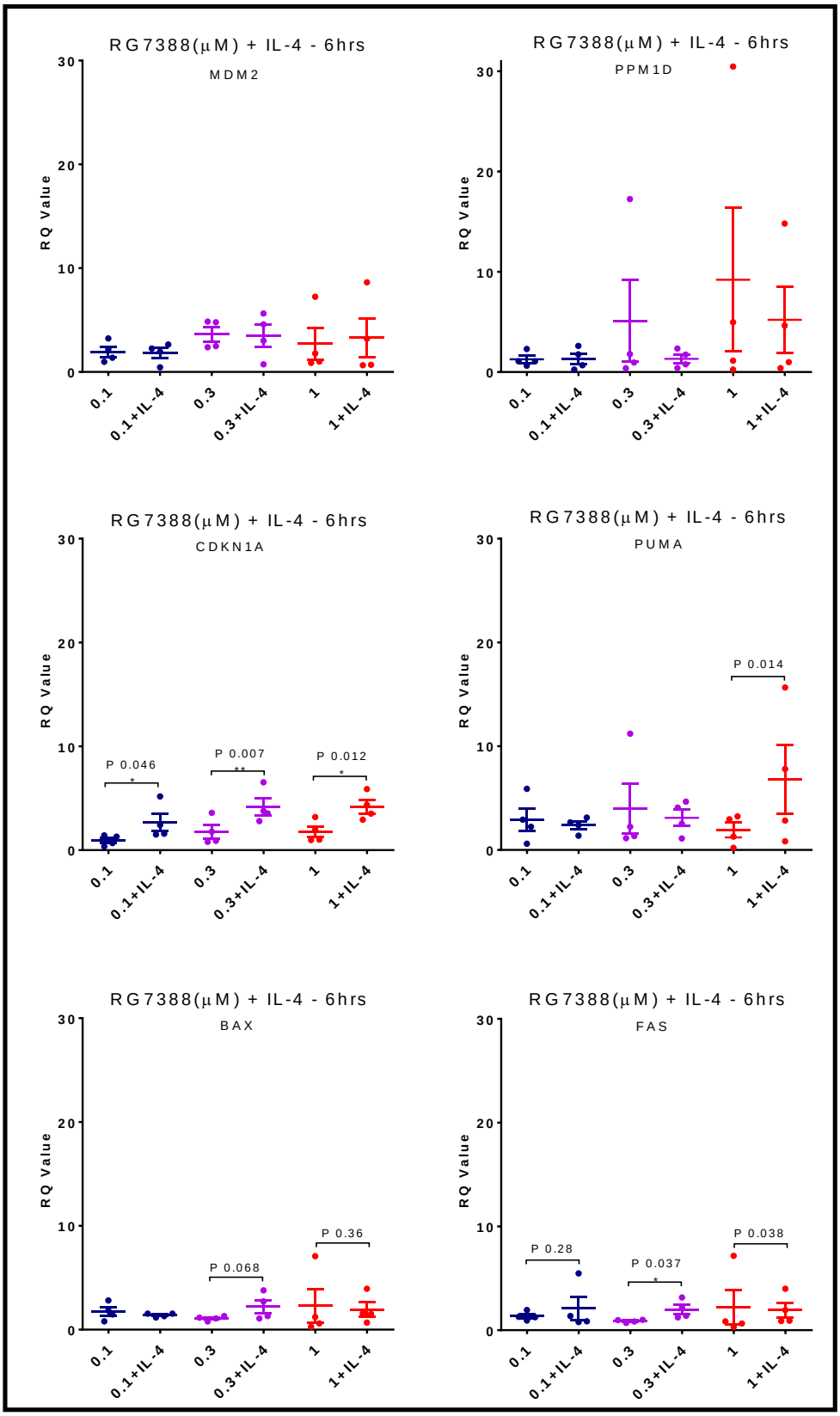

Figure 6.28 Summary plot comparing the differences in mRNA expression of TP53 target gene in response to RG7388 with and without IL-4 for 6 hrs. Primary different CLL samples (n=4) treated with RG7388 (0.1, 0.3, 1µM) in the presence of IL-4. Selected genes showed an increase in response to the treatment, *MDM2*, *PPM1D*, *CDKN1A*, *PUMA*, *BAX*, *FAS*. The experiment performed one time on individual primary CLL samples (n=4). Each point represents the mean value for an individual patient and the error bars in each case represent the average mean ± SEM for the patient samples. Each colour represents mRNA expression of certain gene in response to the treatment. Statistical significance of differences is shown for each treatment compared the presence and absence of IL-4 using paired t-test one tailed.

6.3.7.3 IL-4 upregulates the expression of *CDKN1A* and pro-apoptotic TP53 target genes (*FAS*, *NOXA*) following RG7388 treatment for (24hr)

this section is showing the fold changes in mRNA expression for a panel of gene in response to RG7388 for 24 hours. The statistical test for the genes that showed an increase in their mRNA expression will be displayed in the summary section.

In (Figure 6.29 A), primary CLL cells were treated with RG7388 (0.1µM) for 24 hours. The CLL cells do not show significant changes in the translation level of *TP53* target gene expressions. There is only one individual CLL sample that shows an increase in the expression of *PPM1D*, *PUMA*, *BAX* and *FAS* genes. However, with the presence of IL-4, treatment with RG7388 (0.1µM) increased the expression of *PPM1D*, *MDM2*, *TP53INP1*, *CDKN1A*, *PUMA*, *BAX* and especially *FAS*, which showed the highest fold change expression (2-fold increase) (Figure 6.29 B).

Furthermore, with RG7388 (0.3µM) treatment at 24 hours, the CLL cells show an induction in the mRNA expression of *MDM2*, *PUMA*, *BAX* and *FAS* (Figure 6.29 C). Addition of IL-4 with RG7388 (0.3µM) at 24 hours induces the expression of *TP53INP1*, *CDKN1A*, *PUMA*, *BAX*, *NOXA* and *FAS*. CLL311 showed high expression mRNA level of *MDM2* compared to the rest of the CLL samples in the cohort (Figure 6.29 D).

The fold change expression in response to RG7388 (1µM) at 24 hours is increased only with CLL316 for the mRNA expression of *MDM2*, *PUMA*, *BAX* and *FAS* genes (Figure 6.29 E). In response to RG7388 (1µM) in the presence of IL-4 at 24 hours, *MDM2*, *CDKN1A*, *FAS* and *NOXA* show an increase in the fold change expression (Figure 6.29 F).

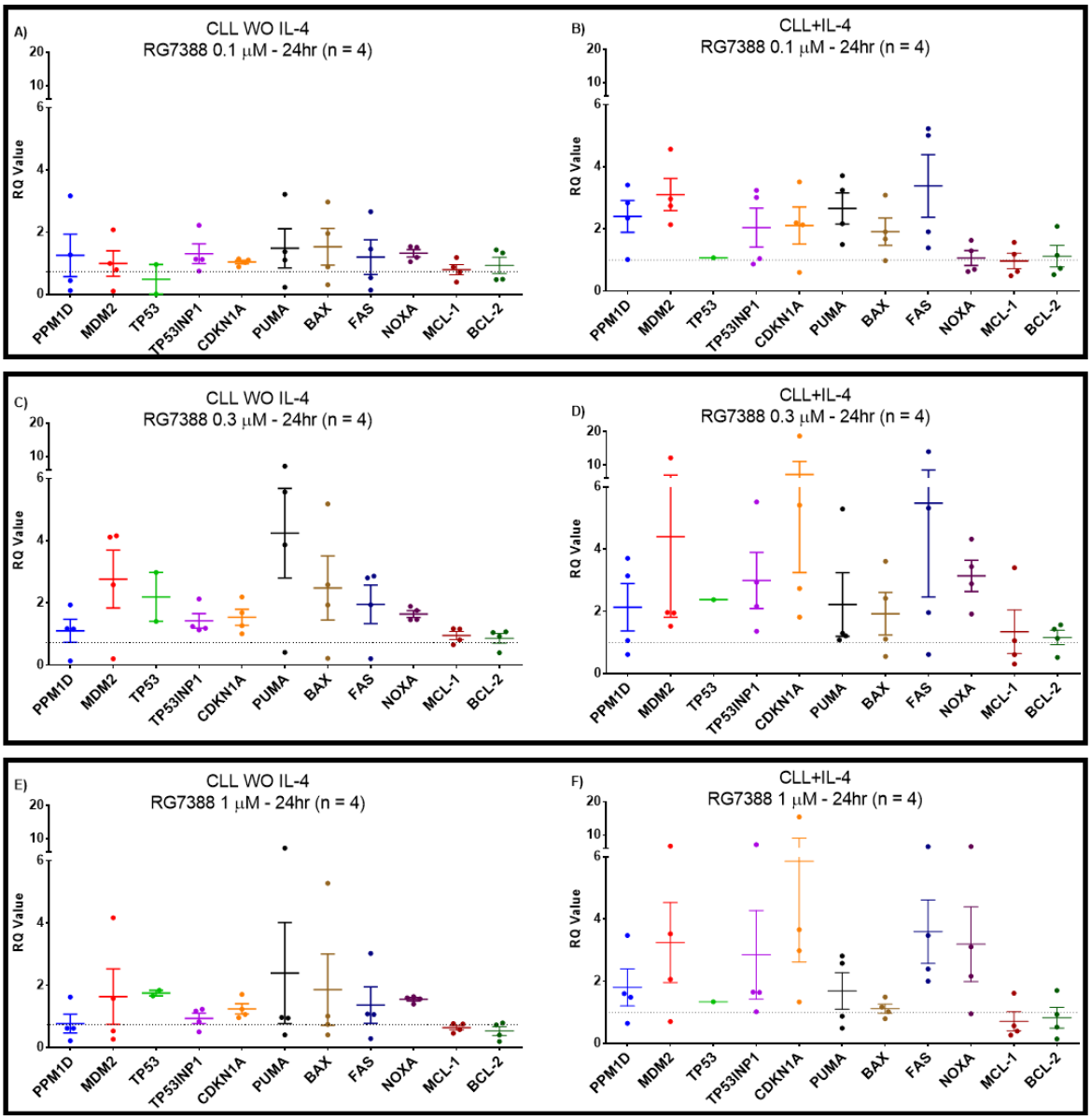

Figure 6.29 Summary plot of differences in mRNA expression of CLL cells treated with RG7388 in the presence and absence of IL-4 for 24hrs. (A&B) RG7388 (0.1μM), (C&D) With RG7388 (0.3μM), (E&F) RG7388 (1μM). Each point represents the mean value for an individual patient (n=4) and the error bars in each case represent the average mean ± SEM of all samples. Each colour represents mRNA expression of certain gene in response to the treatment. *β-ACTIN* and DMSO-treated cells normalized the three intra-replicate wells of each concentration. RQ values were calculated using the formula $2^{-\Delta\Delta Ct}$.

6.3.7.4 The mRNA expression of *FAS* and *CDKN1A* and *MDM2* mRNA are induced with RG7388 treatment in the presence of IL-4 at (24hr)

Selected genes showing changes in their mRNA expression were chosen from the set panel to compare the effect of IL-4 in response to RG7388 (Figure 6.30). There is a trend in response to RG7388 either in the presence or in absence of IL-4. *MDM2*, *PPM1D*, *CDKN1A* and *FAS* show an increase in their mRNA expression level whenever the IL-4 was added. *PUMA* shows an induction in mRNA fold change expression with RG7388 at concentrations (0.1 and 0.3μM). Moreover, the presence of IL-4 reduces the fold change expression relative to the effect of RG7388 (0.3 and 1μM) in the absence of IL-4. The mRNA fold change expression in *CDKN1A* is induced with the additional of IL-4. CLL samples were treated with RG7388 (0.1μM) and with IL-4 ($p=0.77$).

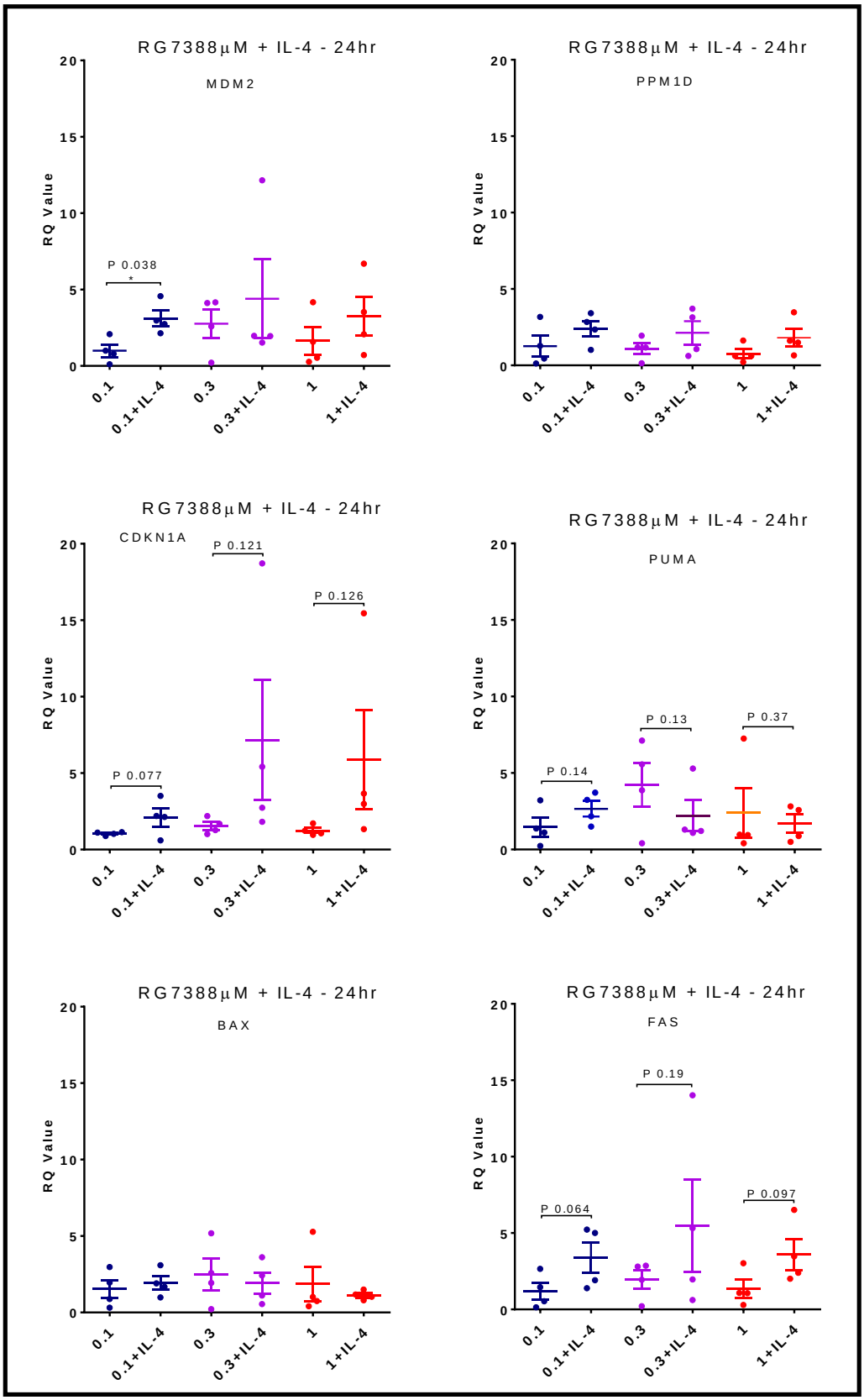

Figure 6.30 Summary plot comparing the fold change of the TP53 target gene expression in response to RG7388 with and without the effect of IL-4 for 24hr. Primary different CLL samples (n=4) treated with RG7388 (0.1, 0.3, 1µM) in the presence of IL-4. Selected genes, *MDM2*, *PPM1D*, *CDKN1A*, *PUMA*, *BAX*, *FAS* showed an increase in response to the treatment. Each point represents the mean value for an individual patient and the error bars in each case represent the average mean ± SEM for the patient samples (n=4). Each colour represents mRNA expression of certain gene in response to the treatment. Statistical significance of differences is shown for each treatment compared the presence and absence of IL-4 using paired t-test one tailed.

6.3.8 The mRNA expression of CDKN1A is induced by the combination effect of WIP1 inhibitor and RG7388 in the presence of IL-4

Four primary CLL cells were treated with wide ranges of RG7388 concentrations (in combination with WIP1 inhibitor at (2.5μM) in the presence or absence of IL-4 for 6 and 24 hours. The mRNA levels were measured on the gene panel (Figure 6.31). Following with 6 hours of RG7388 and WIP1 (2.5μM) combination treatment, *MDM2*, *TP53INP1* and *PPM1D* genes were induced with RG7388 (0.3μM). In comparison, all other genes in the panel were decreased with a combination of RG7388 (1μM) with WIP1 inhibitor (2.5μM) (Figure 6.31 A). The presence of IL-4 in RG7388 and WIP1 inhibitor treated cells at 6 hours induces the expression of the most genes in the panel. *MDM2*, *CDKN1A*, *PPM1D* and *PUMA* are the genes that express the highest fold change expression (Figure 6.31 B).

Next, treating the CLL cells with RG7388 concentrations (0.1, 0.3 and 1μM) in a combination to WIP1 inhibitor at (2.5μM) for 24 hours (Figure 6.31 C&D) was compared with 6 hours. The peak mRNA expression of *MDM2*, *PUMA*, *BAX* and *FAS* were obtained with RG7388 (0.1μM) and WIP1 inhibitor (2.5μM) in the absence of IL-4. Moreover, treating the CLL cells with further high concentrations of RG7388 (0.3 and 1μM) with WIP1 inhibitor (2.5μM) show a reduction in the expression of all genes in the panel (Figure 6.31 C). In contrast, the presence of the IL-4 with a combination treatment of RG7388 and WIP1 inhibitor at (2.5μM) induces the fold change expression of most genes in the panel in particular, *MDM2*, *CDKN1A*, *PPM1D*, *PUMA*, *FAS* and *NOXA* (Figure 6.31 D).

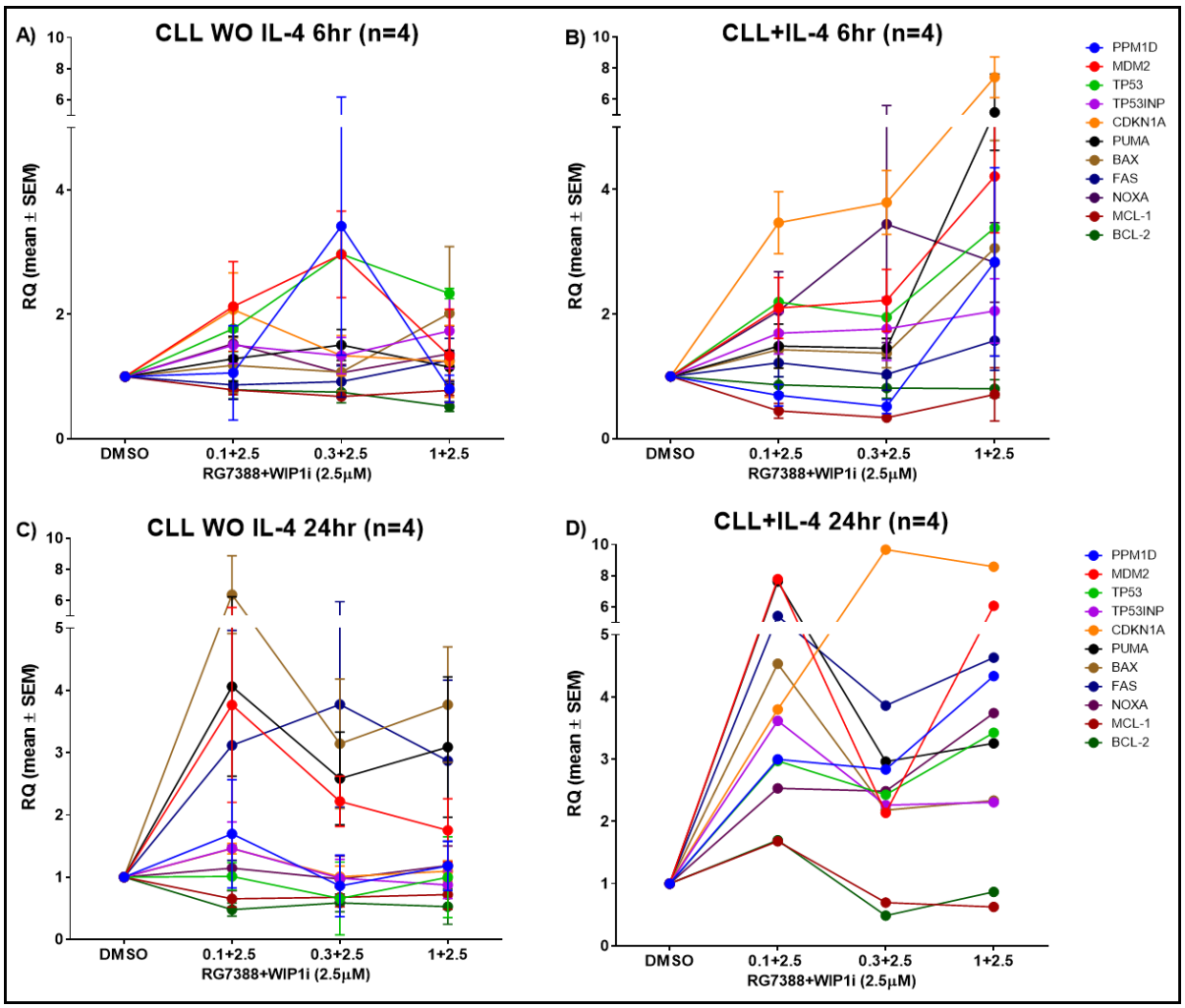

Figure 6.31 Fold change in the mRNA expression of selected TP53 transcriptional target genes of primary CLL cells in response to RG7388 in combination with WIP1 inhibitor (2.5μM) in presence of IL-4 by qRT-PCR. (A&B) 6hrs (C&D) 24hrs. Primary CLL cells (n=4) treated with RG7388 (0.1, 0.3, 1μM) in combination with GSK2830371 (2.5μM) with and without IL-4**.** The experiment performed in (n=1) repeat on each independent CLL sample. Each colour represents certain gene and the error bars represent the mean ± SEM of CLL samples. *β-ACTIN* used as the endogenous control and DMSO-treated cells used as the calibrator between three replicated intra-experimental of each concentration. RQ values were calculated using the formula 2ΔΔCt

6.3.8.1 IL-4 upregulates the mRNA expression of TP53 target genes following treatment with the WIP1 inhibitor in combination with RG7388 for (6hr)

Four primary CLL samples were treated with a combination of WIP1 inhibitor (2.5μM) and range of RG7388 concentrations (0.1, 0.3 and 1μM) for 6 hours in the presence and absence of IL-4 (Figure 6.32). The mRNA transcriptional level for specific set of genes were determined by qRT-PCR.

Treatment of the CLL cells with a combination of WIP1 inhibitor (2.5μM) and RG7388 (0.1μM) for 6 hours induces the mRNA transcriptional level of *MDM2* and *CDKN1A* (Figure 6.32 A). Moreover, the presence of IL-4 further induces the mRNA expression of *MDM2*, *CDKN1A* and *NOXA* (Figure 6.32 B).

(Figure 6.32 D shows the fold change in genes expression with the effect of WIP1 inhibitor (2.5μM) and RG7388 (0.3μM) in the presence of IL-4. *MDM2*, *TP53INP1*, *CDKN1A* and *NOXA* are the genes that highly expressed in the presence of IL-4. In contrast with the effect of WIP1 inhibitor (2.5μM) and RG7388 (0.3μM), only one CLL sample shows high mRNA expression of *PPM1D* gene. This might be an outlier (Figure 6.32 C).

Looking at the effect of WIP1 inhibitor (2.5μM) with RG7388 (1μM) (Figure 6.32 E), there is a variation between the CLL samples in the expression of *MDM2*, *CDKN1A* and *BAX*. With each gene, different CLL samples show increases in the transcriptional level. In contrast, the presence of IL-4 induces the mRNA expression level of *PPM1D*, *MDM2*, *CDKN1A*, *PUMA*, *BAX* and *NOXA* (Figure 6.32 F).

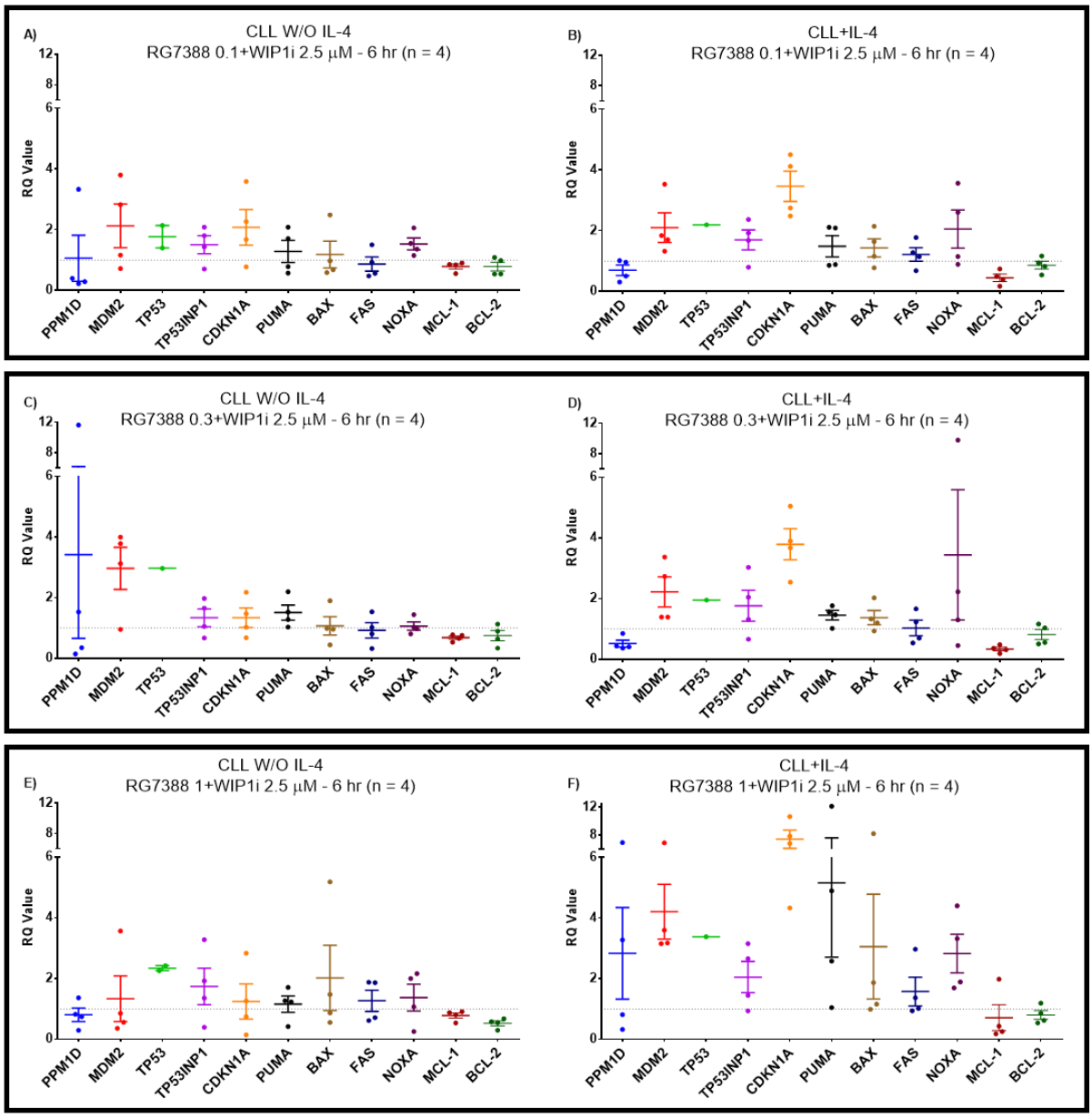

Figure 6.32 Summary plot of mRNA transcriptional change in CLL samples treated with WIP1 inhibitor (2.5µM) in combination with RG7388 in the presence of IL-4 for 6 hrs.(A&B) RG7388 (0.1µM) WIP1i, (C&D) RG7388 (0.3µM) WIP1i, (E&F) RG7388 (1µM) WIP1i. Each point represents the mean value for an individual patient (n=4) and the error bars represent the average mean ± SEM for the patient samples. Each colour represents mRNA expression of certain gene in response to the treatment. In each independent experimennt, *β-ACTIN* used as the endogenous control and DMSO-treated cells used as the calibrator between three intra-replicate wells of the concentrations.

6.3.8.2 The expression of *MDM2, CDKN1A* and *PUMA* are increased with the combination effect of WIP1 inhibitor and RG7388 in the presence of IL-4

Certain genes were selected, and their mRNA expression was compared following treatment with RG7388 concentrations (0.1, 0.3 and 1μM) and WIP1 inhibitor (2.5μM) in the presence of IL-4 for 6 hours (Figure 6.33). The expression of *MDM2* does not show fold change difference with combination treatment of RG7388 (0.1 and 0.3μM) and WIP1 inhibitor (2.5μM) wither with or without IL-4. However, there is a significant difference in the expression of *MDM2* with combination treatment of RG7388 (1μM) and WIP1 inhibitor (2.5μM) in the presence of IL-4 compared to the absence of IL-4 (p=0.0007).

Looking to the fold change expression of *PPM1D*, apart from the one CLL sample with high expression, there is no significant difference in the expression of *PPM1D* gene level either in the presence or absence of IL-4 up to RG7388 (0.3μM) and WIP1 inhibitor (2.5μM). However, the presence of IL-4 with combination effect of RG7388 (1μM) and WIP1 inhibitor (2.5μM) does show a trend of increased expression of *PPM1D* (p=0.126).

There is a concentration dependent increase in the mRNA fold change expression of *CDKN1A* whenever IL-4 is added to the combination treatment of RG7388 and WIP1 inhibitor (2.5μM). The presence of IL-4 significantly induces the mRNA expression of *CDKN1A* following treatment withRG7388 (0.1μM) and WIP1 inhibitor (2.5μM) by 2-fold (p=0.082), and with RG7388 (0.3μM) and WIP1 inhibitor (2.5μM) is 2-fold (p=0.002), RG7388 (1μM) and WIP1 inhibitor (2.5μM) is (8-fold) (p=0.00002).

Following treatment with RG7388 (0.1-0.3μM) and WIP1 inhibitor (2.5μM), there is no significant difference in the mRNA expression of *PUMA* gene either in the presence or absence of IL-4. However, the combination effect of RG7388 (1μM) and WIP1 inhibitor (2.5μM) show significant increases in the expression of *PUMA* gene with the presence of IL-4 relative to the absence (p=0.097).

BAX and *FAS* genes show no significant difference in their expression against the combination effect of RG7388 and WIP1 inhibitor (2.5μM) in either the presence or absence of IL-4.

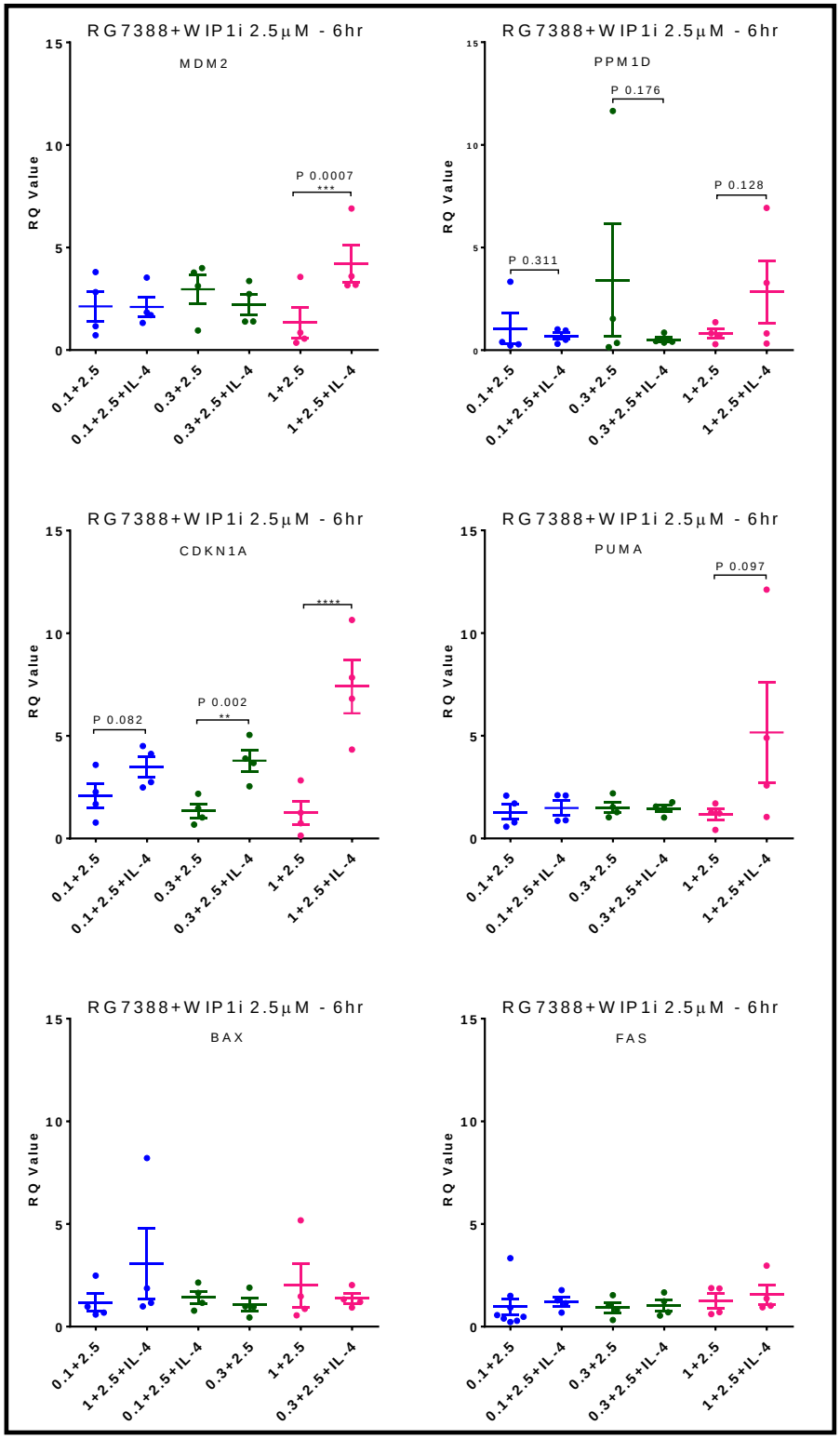

Figure 6.33 Summary plot comparing the mRNA fold change of selected TP53 target genes of CLL cells in response to WIP1 inhibitor in combination with RG7388 in the presence of IL-4 for 6 hrs qRT-PCR
Different primary CLL samples (n=4) treated with GSK2830371 (2.5µM) in combination with RG7388 (0.1, 0.3, 1µM) with and without IL-4. Selected genes, *MDM2*, *PPM1D*, *CDKN1A*, *PUMA*, *BAX*, *FAS* showed change in response to the treatment. qRT-PCR experiment performed in (n=1) repeat on each primary CLL sample. Each colour showed mRNA expression in response to different RG7388 concentration with WIP1i combination with and without IL-4. Each point represents the mean mRNA expression for an individual patient and the error bars in each condition represent the average mean ± SEM for patient samples (n=4). One tailed paired t-test p-values are shown for the significance of differences between the mean values for combination treatment with or without IL-4. Only statistical significance of differences is displayed above the horizontal bars for mean change in response to the treatment with and without IL-4, significance taken at $p < 0.05$.

6.3.8.3 The expression of pro-apoptotic TP53 target genes are upregulated with combination of WIP1 inhibitor and RG7388 in the presence of IL-4

A cohort of four different primary CLL samples were treated with ranges of RG7388 concentrations (0.1, 0.3 and 1μM) and WIP1 inhibitor (2.5μM) in combination for 24 hours in the presence and absence of IL-4 (Figure 6.34). The fold change in the mRNA expression for a set of genes were determined by qRT-PCR technique.

The combination treatment of RG7388 (0.1μM) with WIP1 inhibitor (2.5μM) for 24 hours induced the fold change expression of *MDM2*, *PUMA*, *BAX* and *FAS* (Figure 6.34 A). The additional of IL-4 with a combination treatment of RG7388 (0.1μM) with WIP1 inhibitor (2.5μM) further induced the expression of *MDM2*, *TP53INP1*, *CDKN1A*, *PUMA*, *BAX*, *FAS* and *NOXA* (Figure 6.34 B).

Treating the CLL samples with RG7388 (0.3μM) with WIP1 inhibitor (2.5μM) for 24 hours increased the mRNA expression of *PUMA*, *BAX* and *FAS* (Figure 6.34 C). However, in the presence of IL-4, *PPM1D*, *CDKN1A*, *PUMA*, *BAX*, *FAS* and *NOXA* are the genes that were highly expressed following the combination treatment (Figure 6.34 D).

(Figure 6.34 E) shows the effect of RG7388 (1μM) and WIP1 inhibitor (2.5μM) on CLL cells for 24 hours, with *PUMA*, *BAX* and *FAS* showing an increase in their mRNA expression level. Addition of IL-4 induces the fold change in the expression of *PPM1D*, *MDM2*, *CDKN1A*, *PUMA*, *FAS* and *NOXA* genes (Figure 6.34 F).

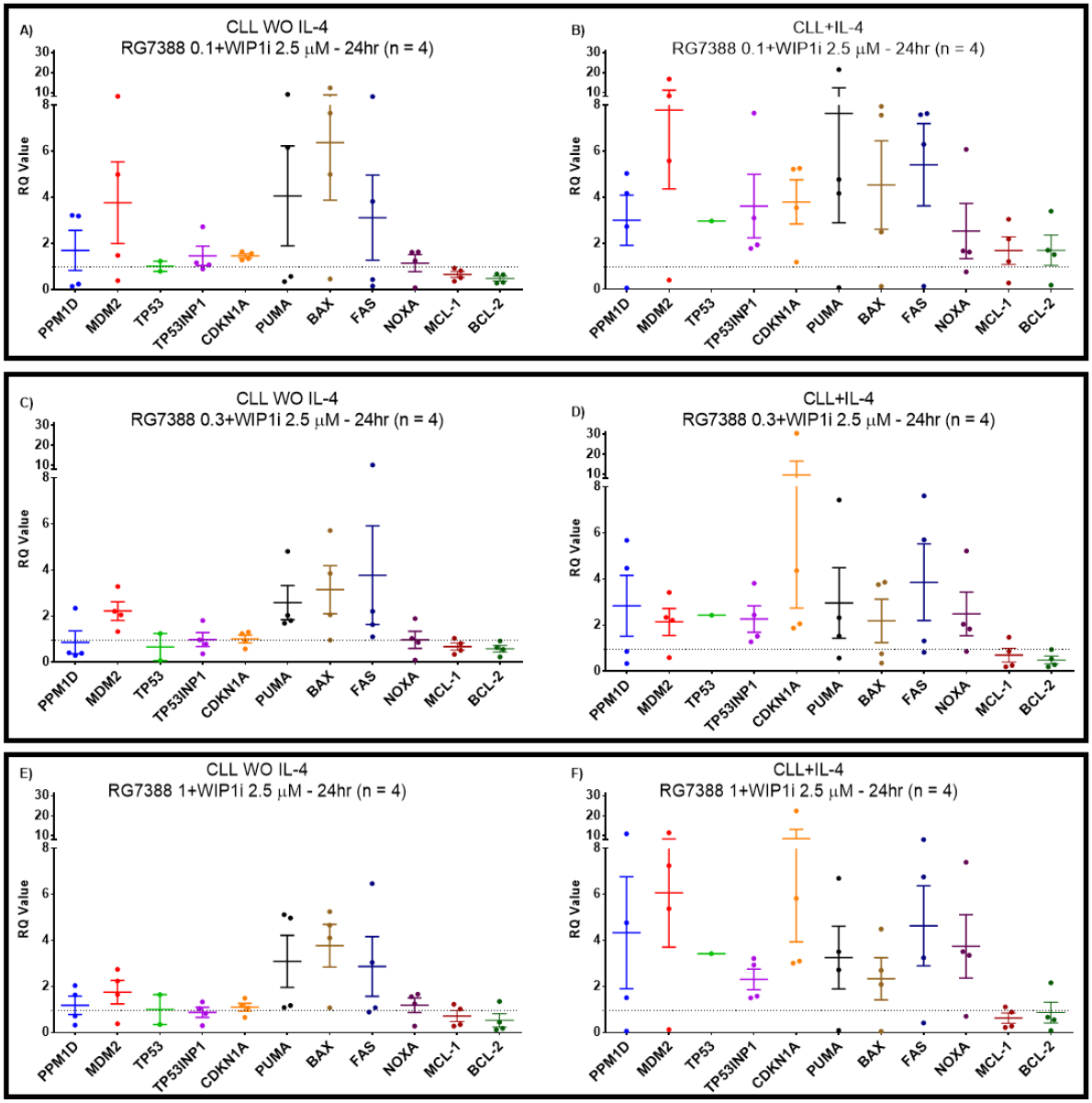

Figure 6.34 The mRNA transcriptional fold change of CLL cells in response to WIP1 inhibitor (2.5μM) in combination with RG7388 in the presence or absence of IL-4 for 24 hrs. Primary CLL cells treated with GSK2830371 (2.5μM) and RG7388 (A&B) 0.1μM, (C&D) 0.3μM, (E&F) 1μM. Each point represents the mean value for an individual patient (n=4) and the error bars represent the average mean ± SEM for the patient samples. Each colour represents mRNA expression of certain gene in response to the treatment. qRT-PCR experiment performed in (n=1) repeat on each primary CLL sample. In each independent experiment, *β-ACTIN* used as the endogenous control and DMSO-treated cells used as the calibrator between three intra-replicate wells of the concentrations.

6.3.8.4 The combination effect of WIP1 inhibitor and RG7388 on the expression of selected TP53 target genes with the presence of IL-4 at (24hr)

The *MDM2* gene is expressed with the combination effect of RG7388 (0.1 and 1µM) and WIP1 inhibitor (2.5µM) in the presence of IL-4 compared to the absence of IL-4 (Figure 6.35). Furthermore, the presence of IL-4 does not have much increasing effect in the fold change expression of *MDM2* gene with a combination treatment of RG7388 (0.3µM) and WIP1 inhibitor (2.5µM).

Both *PPM1D* and *CDKN1A* genes show a trend of concentration dependent increase in their mRNA expression following treatment with the combination of WIP1 inhibitor (2.5µM) with RG7388 in the presence and absence of IL-4.

There are no differences in the expression of *PUMA, BAX and FAS* genes in response to WIP1 inhibitor (2.5µM) in a combination with RG7388 wither in the presence or absence of IL-4.

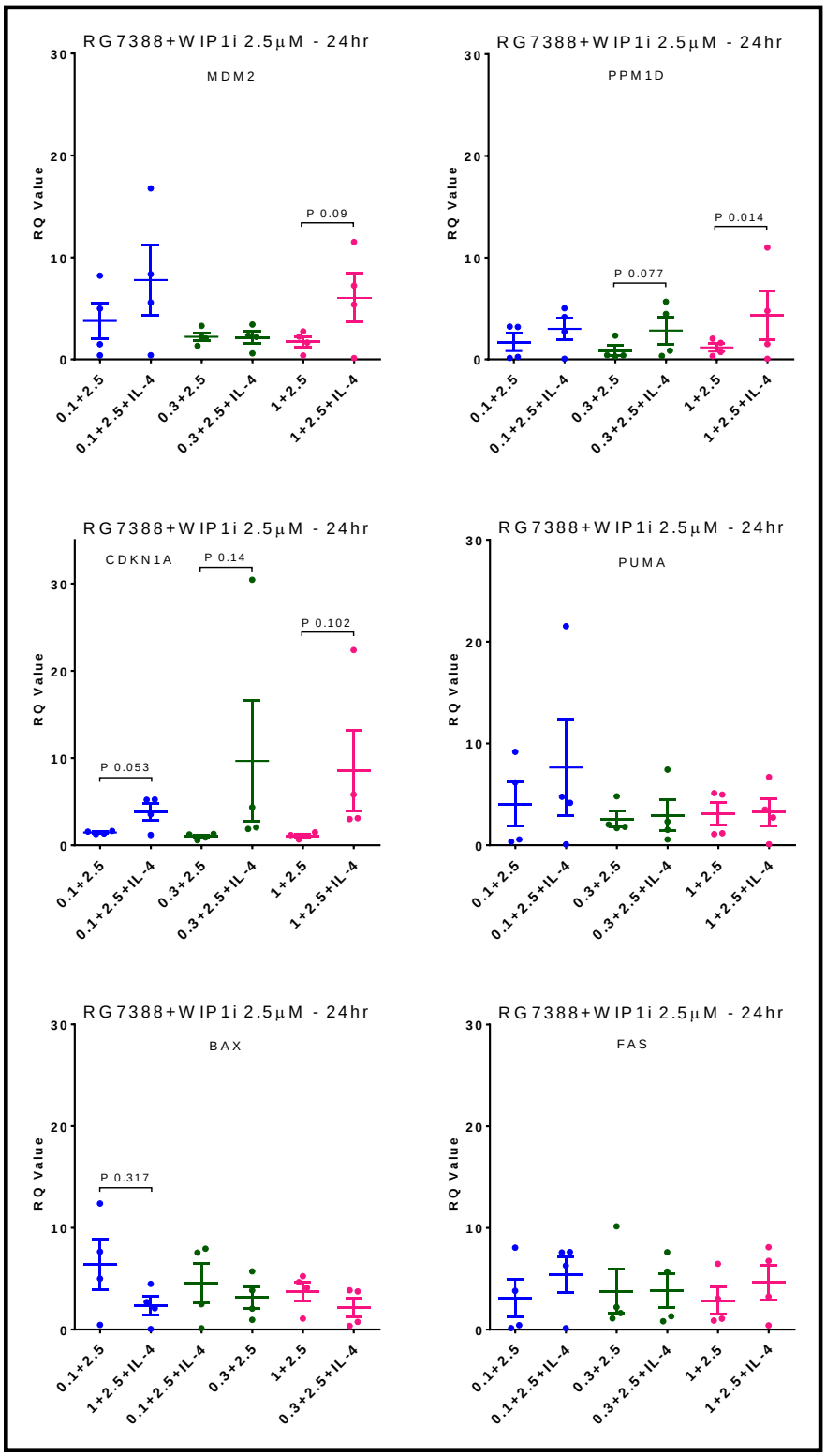

Figure 6.35 Summary plot comparing the mRNA transcription of selected TP53 target genes of CLL cells in response to WIP1 inhibitor in combination with RG7388 in the presence of IL-4 for 24hrs. Different primary CLL samples (n=4) treated with GSK2830371 (2.5µM) in combination with RG7388 (0.1, 0.3, 1µM) with and without IL-4. Selected genes, *MDM2*, *PPM1D*, *CDKN1A*, *PUMA*, *BAX*, *FAS* showed change in response to the treatment. qRT-PCR experiment performed in (n=1) repeat on each primary CLL sample. Each colour showed mRNA expression in response to different RG7388 concentration with WIP1i combination with and without IL-4. Each point represents the mean mRNA expression for an individual patient and the error bars in each condition represent the average mean ± SEM for patient samples (n=4). One tailed paired t-test p-values are shown for the significance of differences between the mean values for combination treatment with or without IL-4. Only statistical significance of differences is displayed above the horizontal bars for mean change in response to the treatment with and without IL-4, significance taken at $p<0.05$.

6.4 Discussion

In our study, we mimic the *ex-vivo* micro-environmental for CLL cells by stimulating the CLL cells through the IL-4 receptor signalling pathway. The study was conducted on cryopreserved and freshly isolated CLL cells. It was observed that the freshly isolated CLL samples have higher metabolic activity than the cryopreserved CLL cells (Figure 6.4), however; the responses to the treatment still can be evaluated and showing a concentration dependent inhibition effect (Figure 6.8 and Figure 6.13). The novel of our study is to evaluate the CLL viability in response to RG7388 and WIP1 inhibitor in the presence of IL-4 in *ex-vivo* microenvironments. There is no study, which evaluates the effect of RG7388 with WIP1 inhibitors in the presence of IL-4 on CLL cells.

It has been discovered in mice model, IL-4 signals play a crucial role in B-cell proliferation, differentiation, and formation of the germinal centres (King & Mohrs, 2009; Vajdy et al., 1995). On the other hand, in B-cells *ex-vivo* experiments, the binding of IL-4 molecules to the IL-4 receptor activates JAK1/3-mediated phosphorylation of STAT6 (pSTAT6) (Murata et al., 1998) which is induces the expression of the anti-apoptotic genes.

In the absence of IL-4, the WIP1 inhibitor as a single agent shows a little inhibition of the metabolic activity (viability) (Figure 6.5 B). By contrast, treatment with RG7388 shows a concentration dependent inhibition in the viability of CLL samples (Figure 6.9). Furthermore, the combination of WIP1 inhibitor (2.5µM) with RG7388 also shows a concentration dependent inhibition of the CLL cells metabolic activity (Figure 6.14).

We can see CLL309 cells (Figure 6.11 A&B) showed a very low metabolic activity absorbance at 450nm but still showing a concentration dependent inhibition effect with both treatment RG7388 and in a combination with WIP1 inhibitor in the absence of IL-4. However, in the presence of IL-4 the metabolic activity of the CLL309 was increased (Figure 6.11). In fact, there is no significant differences in the responses to the compound whether on the CLL which were freshly isolated or cryopreserved (Figure 6.14). Further to that, the additional of IL-4 increases the metabolic activity of both freshly isolated and cryopreserved CLL cells (Figure 6.4).

Interestingly, Byrd J, found in the presences of IL-4 treatment the naïve mutated CLL (M-CLL) cells by ibrutinib express low responses and CLL cells produce less complete remissions than unmutated V-gene CLL (U-CLL). Frequently, poor prognosis of the CLL patients appeared with U-CLL cells, expressing high level of sIgM receptors which

subsequently produce more signals compared to M-CLL in response to anti-IgM stimulation (Byrd et al., 2015).

Looking at the effect of the treatment in the presence of IL-4, CLL cells treated with WIP1 inhibitor in the presence of IL-4 have significantly high absorbance activity compared to parallel CLL cells treated in the absence of IL-4 ($p=0.021$) (Figure 6.5 A). The basal absorbance value of untreated CLL cells (controlled) in the presence of IL-4 is significantly increased compared to absences of IL-4 ($p=0.016$) (Figure 6.5 A). However, WIP1 inhibitor as a single agent has no significant inhibitory effect on CLL cells viability in neither in the presence nor absence of IL-4 (Figure 6.5 B).
On the RG7388 treatment, freshly isolated CLL cells become less sensitive to the RG7388 treatment in the presence of IL-4 compared to cryopreserved ones (Figure 6.9). IL-4 has less protective activity on cryopreserved CLL cells treated with RG7388 compared to freshly isolated CLL cells (Figure 6.6 and Figure 6.7). There is a concentration dependent inhibition in the metabolic activity of CLL cells whether they are freshly isolated or cryopreserved. The absorbance and metabolic activity of the CLL are significantly increased in response to RG7388 treatment in the presence of IL-4 (Figure 6.9). The LC_{70} of RG7388 for CLL cells is significantly increased in the presence of IL-4 compared to the absence of IL-4 ($p=0.042$) (Figure 6.10).

For the combination treatment of WIP1 inhibitor with RG7388, CLL cells become less sensitive to the combination treatment in the presence of IL-4 compared to the absence of IL-4. There is a significantly different increase in the effect of the WIP1 inhibitor (2.5µM) and RG7388 in the presence of IL-4 compared to the absence of IL-4 (Figure 6.14). The CLL metabolic activity (absorbance) was increased with the presence of IL-4 whether with or without the combination treatment. The LC_{70} of the combination treatment of WIP1 inhibitor with RG7388 was significantly increased with IL-4 compared to the effect without IL-4 ($p=0.05$) (Figure 6.15).

Andrew Steele and his group suggested IL-4 signalling pathway augments BCR signalling and promote B-cell proliferation and survival, especially within the U-CLL subset. In his study, they found IL-4 decreases the inhibitory effects of idelalisib or ibrutinib on anti-IgM–induced signalling and protects the CLL cells against BCR kinase inhibitor induced apoptosis (Aguilar-Hernandez et al., 2016). Chen, L. also, reported the CLL cells with more responsive signalling through sIgM engagement may be more sensitive to IL-4 thus, U-CLL showed the greater effect with IL-4 signals (L. Chen et al., 2002, 2005).

IL-4 acts as a micro-environmental signalling factor that can influence the BCR signals to promote sIgM-mediated signalling in CLL cells (Cui et al., 2014). IL-4 appears to promote the sIgM signalling through direct upregulation of IgM expression at the CLL cell surface.

Gene set enrichment analysis (GSEA) clearly revealed that IL-4 mediated transcription in the LN of the CLL patients were comparable matched to the blood and BM samples. This indicated that IL-4 might act on the malignant cells in the LN tissue.

In this study, we looked to the downstream expression of MDM2 target proteins, p53, $p21^{WAF1}$ and WIP1. Phosphorylation of p53 is indicates the stabilization activity of p53. cPARP protein expression was used to evaluate the endpoint for apoptosis.

The IL-4 regulated the downstream cascade expression and function of CXCR4 in CLL cell by reflecting the effect of BCR stimulation on IL-4 receptor (Quiroga et al., 2009; Vlad et al., 2009). Regarding to the time limitation, it is interesting to look to the phosphorylation of STAT6 protein and determine the association of the MDM2 inhibitor on both PI3Kδ and JAK1/2 pathways. In addition, looking to the change on CXCR4.

Considering the protein expression, WIP1 inhibitor (2.5μM) as a single agent is capable of degrading the WIP1 protein in both with and without the presence of IL-4 (Figure 6.17). Furthermore, the WIP1 inhibitor (2.5μM) can potentiate the activity of RG7388 by increasing the stability of p53. Moreover, RG7388 alone stabilises the activity of p53 in a concentration dependent manner whether in the presence or absence of IL-4. Phosphorylated p53 activity is varies to detected in primary CLL cells. This might be because the CLL cells are not proliferative cells *in-vivo* condition without any micro-environmental stimulation factors. However, phosphorylation p53 was detected with wild type TP53(+/+) NALM-6 cell line (Figure 3.13). The $p21^{WAF1}$ is varies across the CLL samples and it is hard to be detected (Figure 6.17). In addition, full-length PARP is reduced with the treatment and cPARP is induced in a concentration- dependent manner with the absence of IL-4 condition. In contrast, in the presence of IL-4, the full-length PARP expression is increased with the treatment and cPARP is not expressed at 6 hours. However, at 24 hours treatment with IL-4, cPARP is detected as an indication of apoptosis or dead CLL cells. The densitometry analysis showed RG7388 stabilises the activity of total p53 of CLL cells in the presence and absence of IL-4 and the combination of WIP1 inhibitor induces the stabilization further more (Figure 6.17) In addition, cPARP was induced with combination treatment of RG7388 with WIP1 inhibitor in the presence of IL-4 at 24 hours (Figure 6.17 H).

Using a wide range of RG7388 and WIP1 inhibitor concentration to determine the synergy score, CLL cells become less responsive to the treatment in the presence of IL-4 compared to the absence (Figure 6.20 D). The peak ZIP synergy score of individual freshly isolated CLL cells in the presences of IL-4 is significantly lower than the peak of parallel CLL cells in the absence of IL-4 (p=0.13) (Figure 6.21).

The changes in the transcriptional level due to the effect of WIP1 inhibitor (2.5μM) alone does not have fundamental differences in the mRNA expression levels across the gene set whether with or without IL-4 (Figure 6.24). On the other hand, Figure 6.28 illustrates the 6 hours treatment with RG7388 significantly increases the mRNA expression of *CDKN1A* in the presences of IL-4. Moreover, *MDM*2 and *FAS* show a trend of increased gene expression with IL-4 activity. *PPM1D* and *BAX* genes show no significant differences in their mRNA expression following 6 hours treatment of RG7388 either with or without IL-4. *PUMA* shows non-significant changes of the mRNA expression in response to RG7388 (0.1 and 0.3μM) with and without IL-4 activity however, RG7388 (1μM) significantly increases the *PUMA* gene expression with IL-4. In comparison, following 24 hours treatment with RG7388 shows a trend of increasing mRNA expression of *CDKN1A, PPM1D, MDM2* and *FAS* in the presence of IL-4 (Figure 6.30).

In other several *ex-vivo* environments, IL-4 signals suppress the basal and chemotherapy-induced apoptotic levels of the CLL cells (Ghia et al., 2005; Panayiotidis et al., 1993; Steele et al., 2010). by increasing the expression of anti-apoptotic proteins (Steele et al., 2010). However, in my study, I find the combination treatment of RG7388 with WIP1 inhibitor induces the expression of *CDKN1A*, which causes cell cycle arrest. Furthermore, the combination of RG7388 at (1μM) with WIP1 inhibitor (2.5μM) significantly induces the fold changes expression of *PUMA*, pro-apoptotic gene, which indicates the CLL cells drive to apoptosis.

The combination of WIP1 inhibitor (2.5μM) with RG7388 results in a significant increase in the *CDKN1A* gene expression with the presence of IL-4 after 6 hours of treatment (Figure 6.33). Furthermore, *MDM2*, *PPM1D* and *PUMA* genes did not show a significant change in the mRNA gene expression with a combination treatment of WIP1 inhibitor (2.5μM) and RG7388 (0.1 and 0.3μM) in the presence of IL-4 activity. However, IL-4 significantly increases the mRNA expression of *MDM*2 with a combination of WIP1 inhibitor (2.5μM) and RG7388 (1μM), although, the expression of *PPM1D* and *PUMA* genes are also increased. *FAS* and *BAX* did not show significant changes on their gene expression in response to WIP1 inhibitor (2.5μM) and RG7388 in the presence of IL-4.

For CLL cells with WIP1 inhibitor (2.5µM) in a combination with RG7388 for 24 hours, *PPM1D* and *CDKN1A* genes show a concentration dependent increase in their mRNA expression in the presence of IL-4. *PUMA* also showed a slightly increase in a concentration dependent manner following incubation with IL-4 activity. *MDM2* shows an increase in the expression with the combination treatment of WIP1 inhibitor (2.5µM) and RG7388 (0.1 and 1µM) in the presence of IL-4. By contrast, gene expression of *BAX* is reduced in a concentration-dependent manner with the combination treatment in the presence of IL-4. By contrast, the *FAS* gene has no significant changes in the mRNA expression in the presence of IL-4 against the combination treatment (Figure 6.35).

In terms of effects of IL-4 on CLL cells, Andrew Steele in his study found that sIgM increased by following of IL-4 treatment *in-vitro* (Aguilar-Hernandez et al., 2016). Because there was no detectable increase in total cellular IgM after IL-4 treatment, however the increase in surface expression may be due to "shunting" of IgM from the ER to the cell surface. Their data in CLL cells are similar to Guo. B and his group described in mouse splenocytes where IL-4 promoted sIgM expression, leading to (Guo et al., 2007; Guo & Rothstein, 2005, 2013)07; Guo & Rothstein, 2005, 2013). Moreover, IL-4 also stimulates IgM expression following by increasing the antigen engagement and subsequent downstream signalling pathway (Quiroga et al., 2009; Vlad et al., 2009).

In conclusion, the presence of IL-4 signal increases the metabolic activity of the primary CLL cells and reduces the sensitivity of the CLL cells in response to both WIP1 and MDM2 inhibitors. WIP1 inhibitors had less potentiation effect on RG7388 activity in the presence of IL-4 signals relative to the potentiation activity in the absence of IL-4 signals. In addition, CLL cells was less sensitive to RG7388 alone in the presence of IL-4 compared to absence of IL-4 signals. The gene expression of *CDKN1A* and *NOXA*, pro-apoptotic, were induced with WIP1 inhibitor in a combination with RG7388 compared to RG7388 alone.

Chapter 7: The Effect of Anti-IgM Stimulation on CLL Cell

7.1 Introduction

Despite the chromosomal changes, *in-vivo* engagement of CLL cells with the surrounding microenvironment is similar to the normal B-cells. The interaction between antigens and the sIg is one of the *in-vivo* microenvironmental factors that could have an impact on B-cell proliferation, activation and differentiation. *In-vivo* engagement between the antigen and the sIgM occurs in *IGHV* mutant (M-CLL) and un-mutated *IGHV* (U-CLL). In both M-CLL and U-CLL cells, antigen engagement with BCR occurs, presumably leading to cell proliferation, survival, influencing tumour growth and response to therapy. However, M-CLL express less sIgM signalling than U-CLL. Thus, M-CLL cases show low therapeutic responses and are described as “anergic.” U-CLL cells have the capability to maintain antigen-induced modulation of sIgM signals, which leads to an increase the proliferation and survival levels in aggressive disease. In contrast, M-CLL is associated with indolent disease.

An *in-vivo* study was performed on CLL cases to confirm the fact that peripheral blood CLL cells can recover the expression of antigen binding to sIgM consistently with down-regulation of signalling. It is likely that antigen mediates the BCR signalling for constitutive activation of kinases and of nuclear factor-κB (NF-κB) in CLL cells. Interestingly, surface immunoglobulin-G (sIgG) is another type of surface antigen that behaves differently from sIgM with no evidence for down-modulation signalling cascade.

7.2 Hypothesis

The interaction of CLL cells with B cell receptor (BCR) signalling through antigen binding, such as anti-IgM antibody, is another stimulation signals that known to promote CLL cell survival, proliferation, and resistance to therapy.

The magnetic beads coated with immobilized anti-IgM antibody used to mimic the *ex-vivo* microenvironment of migrated CLL cells in lymph node and provide a spontaneous suitable signalling to activate and proliferate CLL cells.

In this chapter, our hypothesis proposes that by immobilizing beads coated with anti-IgM antibody, we would like to investigate the effect of the combination of WIP1 inhibitor with MDM2 inhibition on *ex-vivo* microenvironment that mimics the BCR signalling detected in lymphoid tissues migration.

7.3 Aims

Stimulation of CLL cells using the immobilised beads coated with Anti-IgM antibody (to stimulate BCR) will alter to the cellular response to the MDM2 inhibitor as a single agent and in a combination with WIP1 inhibitor.

1. To identify the effectiveness of RG7388 on stimulated CLL cells through immobilized beads coated with anti-IgM antibody.
2. To assess the effectiveness GSK2830371 to potentiate the activity of RG7388 on stimulated CLL cells through immobilized beads coated with anti-IgM antibody.
3. To investigate the downstream signalling pathway of activated CLL cells upon stimulation with immobilized beads coated with anti-IgM antibody.
4. To compare the cellular responses of CLL cells stimulated with immobilized beads coated with anti-IgM antibody to those in control groups that either coated with anti-IgG antibody or with non-stimulation.
5. To examine the impact of immobilized bead-mediated stimulation on the gene expression profile of CLL cells in response to the GSK2830371 and RG7388 inhibitors.

7.4 Results

7.4.1 Increase in Phosphorylation activity of ERK protein after stimulation of the CLL cells with immobilised beads coated with Anti-IgM antibodies

In Figure 7.1, we would like to optimize the appropriate concentration of the immobilized either IgM or IgG antibody that can stimulate the CLL cells. Two different concentrations (2µg/ml and 10µg/ml) of magnetic beads coated with immobilized either Anti-IgM or Anti-IgG antibodies were used to stimulate the CLL307 at a concentration of $1x10^6$ cells/ml for 1 hour. Following the stimulation, the CLL cells were collected and the cell pellet was harvest for a western blotting analysis. The CLL cell lysates were probed with specific antibodies that can detect downstream target proteins. Phosphorylated S6K antibody was used to determine CLL cell growth activity and proliferation. In addition, phosphorylated ERK antibody was used to identify the MAPK kinase signals pathway which play a role in regulation of meiosis, mitosis, and post mitotic functions in differentiated cells.

The phosphorylation of ERK protein is expressed following stimulation with immobilised beads coated with Anti-IgM compared to control and Anti-IgG beads. Furthermore, a concentration of 2µg/ml of immobilised Anti-IgM induces the phosphorylation activity of ERK than 10µg of immobilised Anti-IgM. Phosphorylated ERK protein is one of the downstream targets of the LYN and SYK pathway, which facilitates cell survival and proliferation activity.

Parallel to Phospho-ERK activity, the total ERK protein activity remains stable with immobilised Anti-IgG and Anti-IgM antibody stimulation at 2µg/ml. However, total ERK activity is reduced with 10µg/ml of magnetic beads stimulation on both Anti-IgG and Anti-IgM antibodies relative to control.

On the other hand, the phosphorylation activity of ribosomal S6 kinase (S6K) is increased with immobilised Anti-IgM antibody compared to the control non-stimulated cells and Anti-IgG immobilised antibody stimulation. In addition, 10µg/ml of Anti-IgM immobilised antibody stimulation expresses more phosphorylation activity of S6K than 2µg/ml of Anti-IgM stimulation.

Total p70 S6K activity shows slightly higher levels of the protein expression at 2µg/ml stimulation with both Anti-IgG and Anti-IgM antibody relative to the non-stimulation CLL cells. However, with a concentration of 10µg/ml stimulation the total p70 S6K protein is lower compared to the non-stimulated CLL cells as well as 2µg/ml immobilised antibody stimulation of relative condition. The role of ribosomal protein S6K phosphorylation and the total p70 S6K is acting as a signalling pathway in the regulation of cell growth and proliferation. Looking to the Ponceau stain result, it shows that the samples were loaded equally in all wells (Figure 7.1 B).

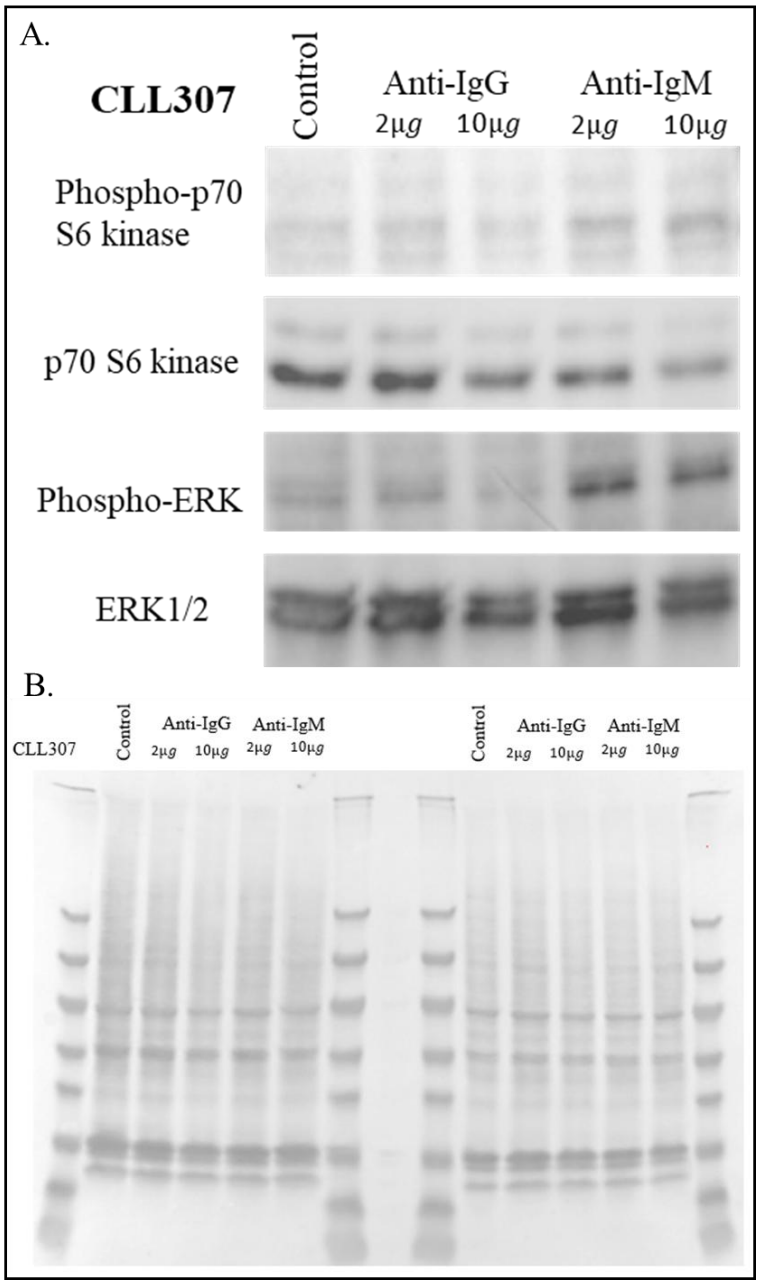

Figure 7.1 Immobilised Anti-IgM stimulate phospho-ERK pathway in CLL cells. (A) CLL307 was stimulated with the immobilised beads coated with Anti-IgM and Anti-IgG (2µg/ml and 10µg/ml) to activate downstream signalling pathway of CLL proliferation and survival. (B) Ponceau stain showing the equal loading of protein across the wells.

7.4.2 Immobilised anti-IgG and IgM antibody stimulation induced the basal metabolic activity of the CLL cells

The aim of this experiment is to identify the basal stimulation signals of immobilised both Anti-IgM and Anti-IgG antibody on the primary CLL cells. The majority of CLL samples become metabolically active with both immobilised Anti-IgG and Anti-IgM antibody stimulation compared to non-stimulation CLL cells. There is a significant increase in the metabolic activity of CLL cells stimulated with Anti-IgG and Anti-IgM antibody (p=0.0003).

There is a heterogeneity between CLL cases in the responses to the Anti-IgG and Anti-IgM stimulation. The response varies depending on the surface Ig receptors on the CLL cells and the signalling capacity. Beads immobilised with Anti-IgG antibody were used as a negative control for non-specific binding to BCR because they do not activate the downstream pathways for SYN and LYN cascade. In contrast, beads immobilised with Anti-IgM antibody were able to activate the downstream pathway for SYN and LYN and phosphorylation of ERK1/2, which is a signal of proliferation.

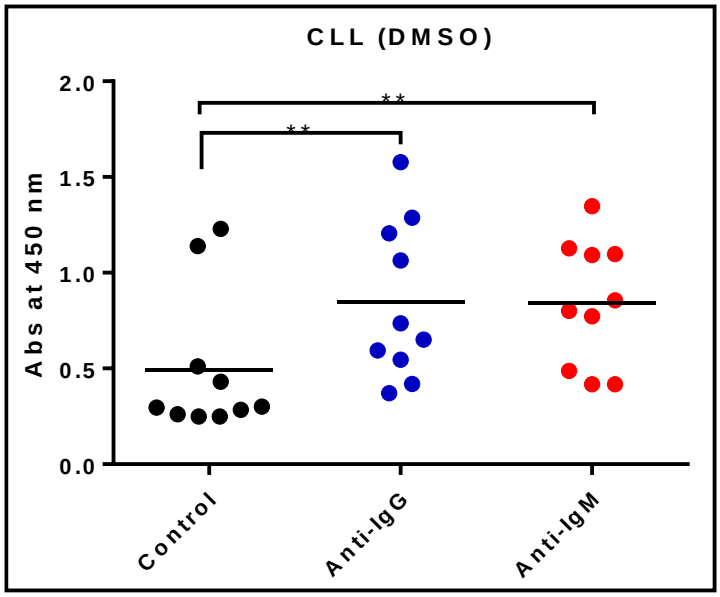

Figure 7.2 Basal absorbance of CLL cells increased by immobilised Anti-IgG and Anti-IgM stimulation relative to the absence of stimulation. CLL samples (n=9) were stimulated with 2µg/ml of beads immobilised beads coated either with Anti-IgG or Anti-IgM antibody for 1 hour prior the treatment with DMSO (0.5%) for 48 hours**.** The primary CLL cells viability was determined by XTT assay. Each independent experiment was performed once on the primary CLL cells and averaged within itself of intra-replicate concentrations. The mean show ± SEM. Statistical significance was determined by RM 1-way ANOVA test for multiple comparisons, significance taken at $p < 0.005$.

7.4.3 WIP1 inhibitor has small inhibition effect on the viability of the primary CLL cells stimulated with either immobilised Anti-IgM or Anti-IgG antibody

Different primary CLL samples (n=9) were stimulated either with immobilised Anti-IgM or IgG antibody for 1 hour prior exposure to the treatment of WIP1 inhibitor at (2.5µM). The aim of this experiment was to determine whether WIP1 inhibitor as a single agent had an effect on the metabolic activity of the CLL cells (Figure 7.3). Due to the heterogeneity of between the CLL samples, some of the primary CLL samples showed more inhibition in the cell viability in response to WIP1 inhibitor compared to others.

Figure 7.5 showed the absorbance of the CLL samples in response to WIP1inhibitor relative to untreated control (DMSO) in the presence of immobilised Anti-IgM or IgG antibody signals. There was no significant difference between the absorbance of the CLL samples in response to WIP1 inhibitor relative to DMSO whether in the presence nor in the absence of antibody stimulation signals. Interestingly, the *ex-vivo* microenvironment of BCR stimulation via Anti-IgM and Anti-IgG antibody significantly induces the absorbance and the metabolic activity of CLL samples compared to non-stimulated (Figure 7.4).

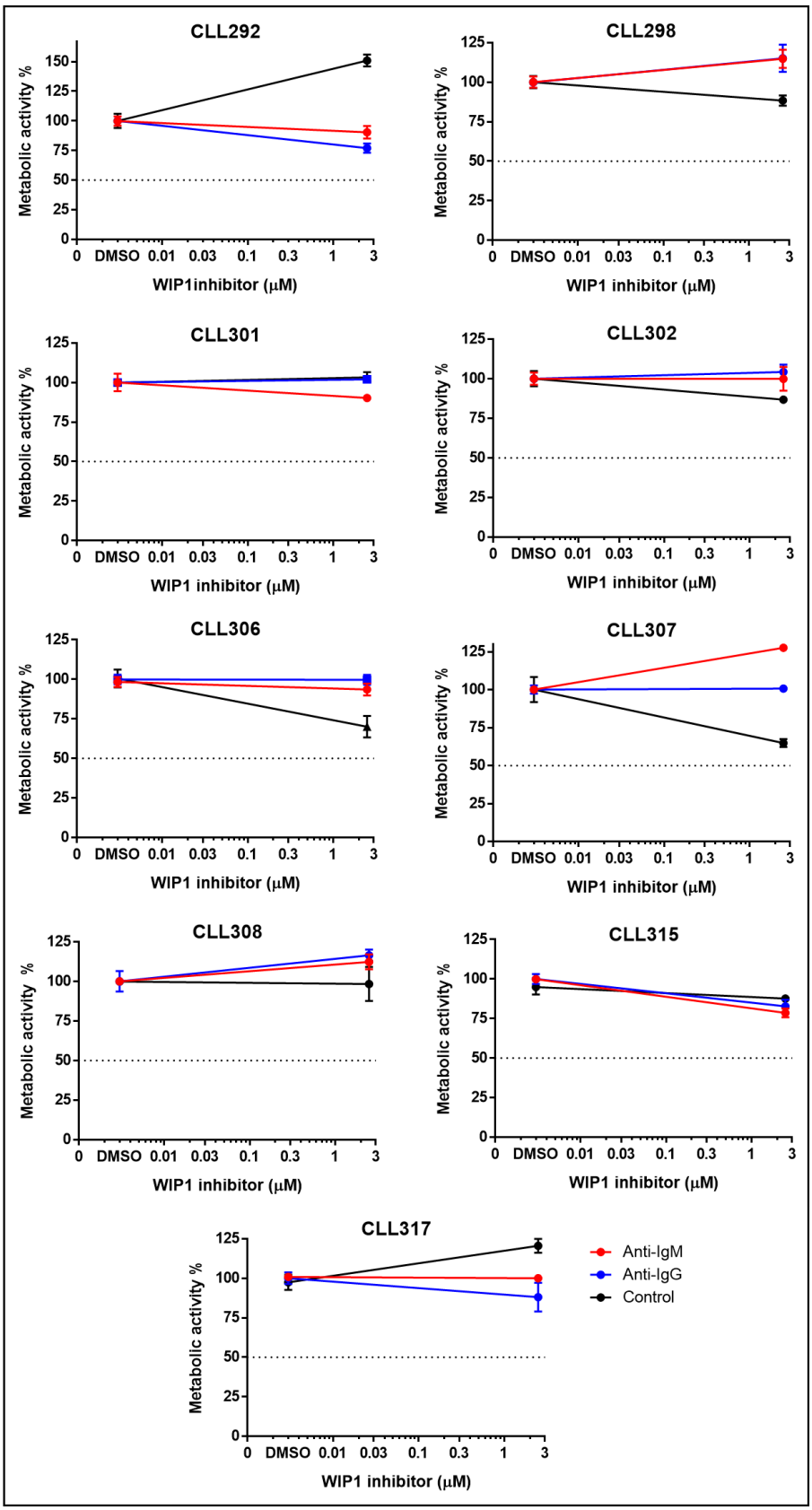

Figure 7.3 The *ex-vivo* effect of WIP1 inhibitor on CLL cells in the presence of Anti-IgM antibody. Panel of primary CLL samples (n=9) stimulated by immobilised either Anti-IgG or Anti-IgM antibodies for 1hr prior treatment of GSK2830371 (2.5μM) for 48hrs. CLL cells seeded in ratio (1:2) cells to antibody. XTT assay determined cell metabolic activity %, which was normalized to DMSO treatment for individual experiment. Each experiment was performed once on the primary CLL cells with three intra-replicates for each concentration and error bar shows the mean ± SEM of intra-replicates. Each line shows an independent cell effect in response to the treatment in the presence of stimulation.

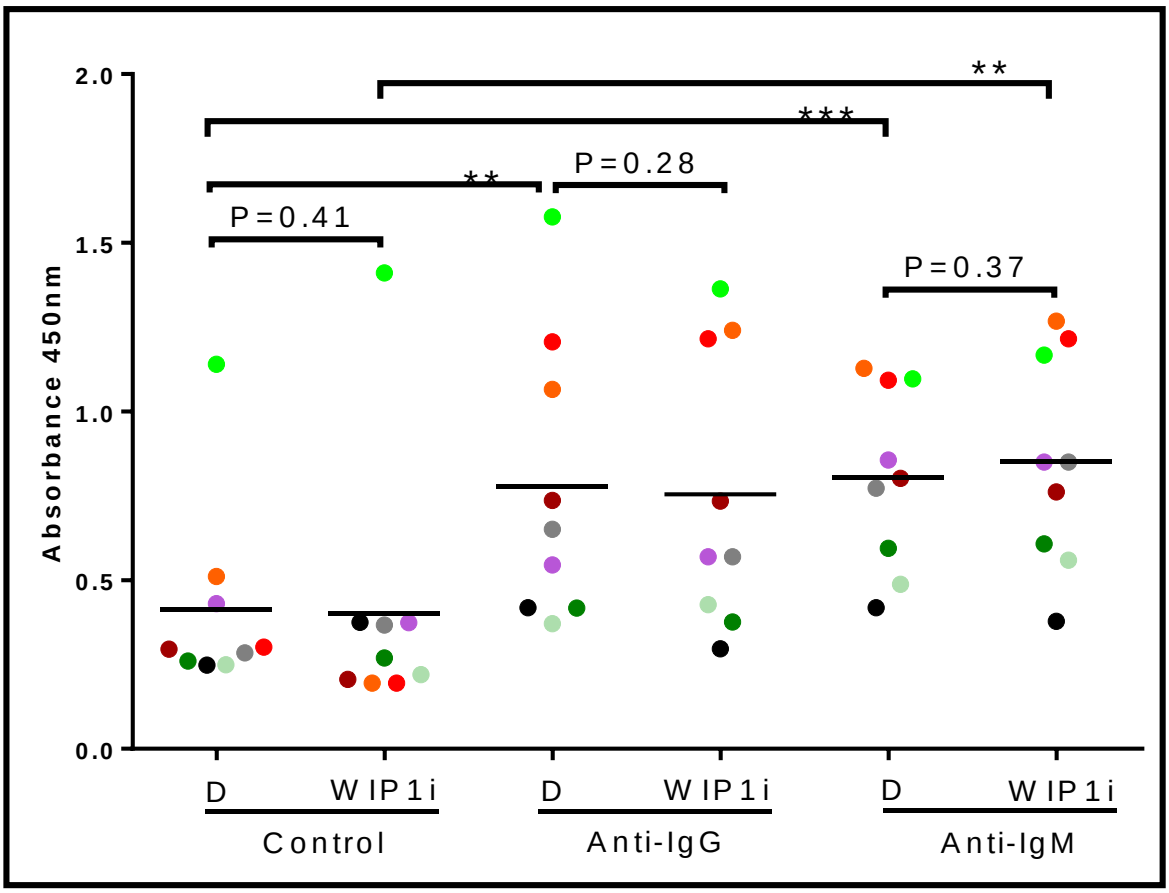

Figure 7.4 Summary absorbance of primary CLL cells treated with WIP1 inhibitor in the presence of immobilised Anti-IgM and Anti-IgG antibody stimulation. Raw data absorbance at 450nm of cohort set of CLL samples (n=9) exposed to GSK2830371 (2.5μM) with immobilised Anti-IgM and Anti-IgG antibody for 1hr prior the treatment of 48hrs by XTT analysis. DMSO (D), show the basal absorbance of CLL cells in the presence or absence of stimulation only without the effect of WIP1i. Each colour represents the mean value for an individual CLL patient sample in response to the treatment and the error bars in each case represent the average mean ± SEM of all patient samples. Each experiment was performed once on individual CLL sample with three intra-replicates of concentration within the experiment. Statistical significance of differences (** $p < 0.005$, ***, $p < 0.0005$) is determined by paired t-test one tail.

7.4.4 RG7388 had concentration dependent inhibition on CLL cells viability in the presence of immobilised Anti-IgG and Anti-IgM antibody

Here we would like to determine the effect of Anti-IgM or Anti-IgG antibody stimulation on sensitivity of CLL cells to RG7388 treatment. The majority of the primary CLL samples, which were conducted in this experiment, were cryopreserved CLL samples stored in -80ºC and one freshly isolated CLL317 sample.

7.4.4.1 Cohort of CLL samples sensitive to MDM2 inhibitor (RG7388) in the presence of immobilised Anti-IgG and Anti-IgM antibody

The following Figure 7.5 showed the cohort of the primary CLL cells that reached the LC_{50} inhibition of RG7388 with the stimulation of Anti-IgM antibody stimulation signals. The primary CLL samples were divided into two groups regarding to the LC_{50} inhibition in response to the RG7388 treatment with *ex-vivo* microenvironment of Anti-IgM antibody stimulation.

CLL cells show a concentration dependent inhibition effect following RG7388 treatment (Figure 7.5). CLL cells with immobilised Anti-IgM antibody stimulation become less sensitive to RG7388 relative to the absence of Anti-IgM stimulation. The response to the stimulation is depends on the sIg receptors and signalling capacity. On the other hand, immobilised Anti-IgG antibody stimulation could increase the metabolic activity of CLL cells in certain samples, however the signals might just improve the metabolic activity of the CLL cell but not the downstream pathway signals of cell proliferation or survival (Liu et al., 2019).

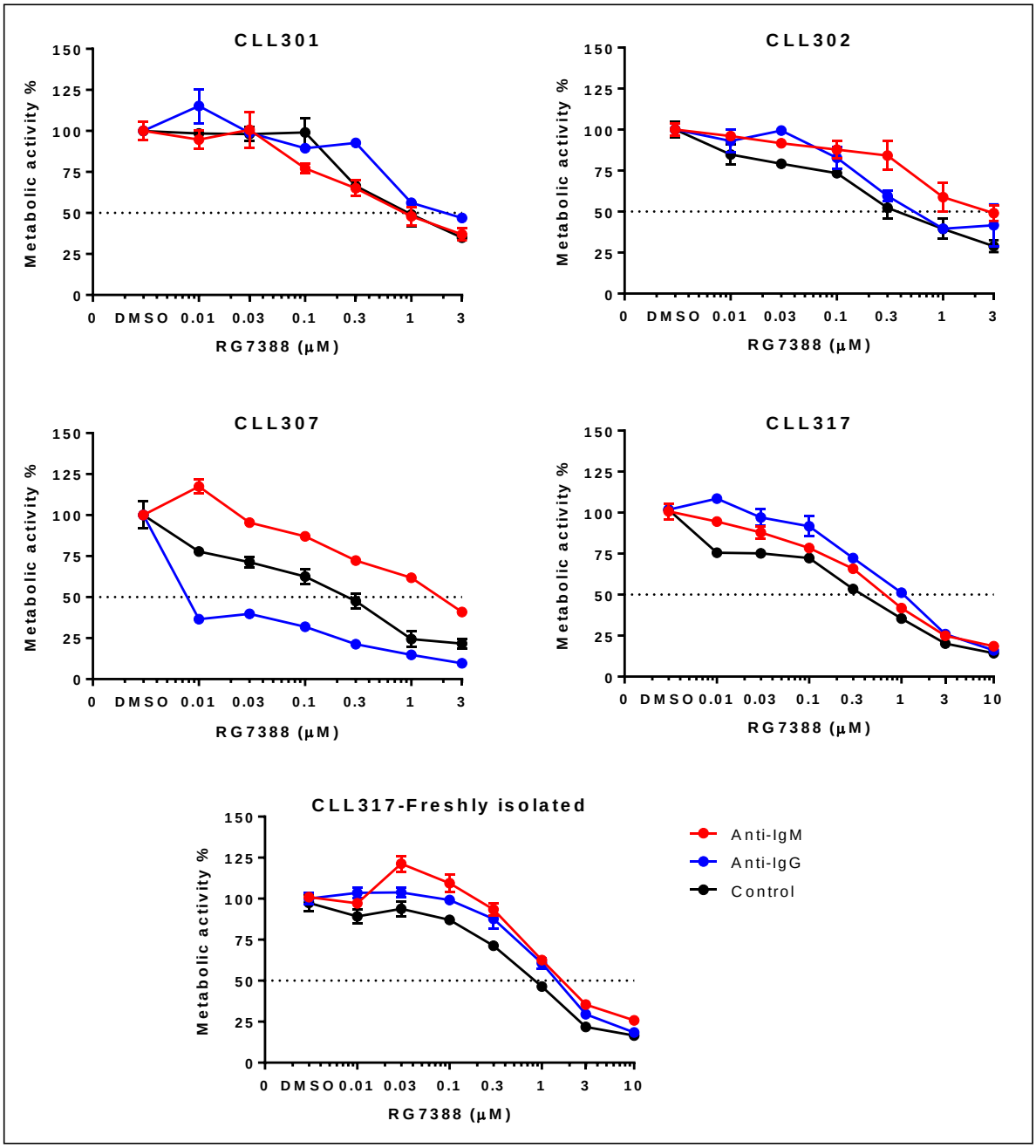

Figure 7.5 The effect of RG7388 on CLL samples stimulated with Anti-IgM and Anti-IgG antibody. Panel of primary CLL samples (n=4) stimulated by immobilised either Anti-IgG or Anti-IgM antibodies for 1hr prior treatment with range of RG7388 concentrations for 48hrs. The effect of RG7388 was investigated on stimulated freshly isolated CLL317 and thawed CLL samples. CLL cells seeded in ratio (1:2) cells to antibody. XTT assay determined cell metabolic activity %, which was normalized to DMSO treatment for individual experiment. The CLL samples in this cohort reached to the RG7388 LC_{50} in response to Anti-IgM stimulation. Each experiment was performed once on the primary CLL cells with three intra-replicates for each concentration and error bar shows the mean ± SEM of intra-replicates. Each line shows an independent cell effect in response to the treatment in the presence of stimulation.

7.4.4.2 Cohort of CLL samples showing resistance to MDM2 inhibitor (RG7388) with immobilised Anti-IgG and Anti-IgM antibody

The following (Figure 7.6) representing the cohort of primary CLL samples that could not reach the LC_{50} of RG7388 with *ex-vivo* microenvironment of anti-IgM antibody signalling. The LC_{50} values of RG7388 treatment were illustrated below in a (Table 7.1). Different cryopreserved CLL samples (n=5) were stimulated with immobilised Anti-IgG and Anti-IgM antibody prior to treatment with RG7388. These CLL cell samples show resistance to RG7388 up to (3µM), with an increased mitochondrial metabolic activity level compared to the samples examined in (Figure 7.5). Despite immobilised Anti-IgM antibody stimulation, none of this cohort of CLL samples reached the LC_{50} concentrations lower to (3µM) of RG7388, except CLL308, which achieved an RG7388 LC_{50} concentration with immobilised Anti-IgG stimulation and with un-stimulation CLL cells. Interestingly, RG7388 shows a concentration-dependent effect of RG7388 treatment with low cell metabolic inhibition level. CLL cells in this cohort are still expressing a reduction in their metabolic activity even in low inhibitory manner behaving with increasing in RG7388 concentrations.

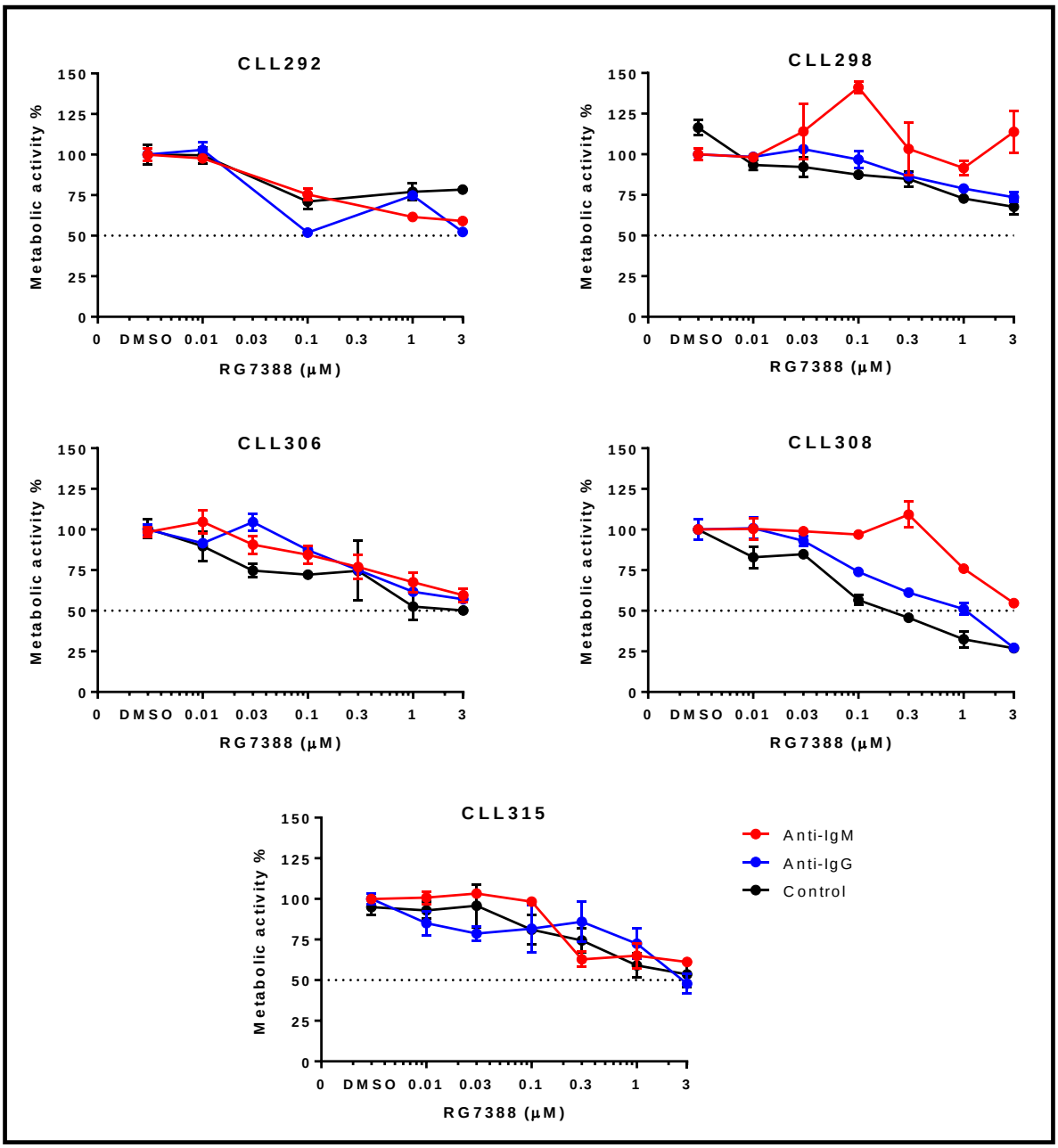

Figure 7.6 CLL samples less sensitive to RG7388 treatment in the presence of Anti-IgM and Anti-IgG antibody. Panel of cryopreserved CLL samples (n=5) stimulated by immobilised either Anti-IgG or Anti-IgM antibodies for 1hr prior treatment with range of RG7388 concentrations up to 3µM for 48hrs. CLL cells seeded in ratio (1:2) cells to antibody. XTT assay determined cell metabolic activity %, which was normalized to DMSO treatment for individual experiment. The CLL samples in this cohort could not achieve the RG7388 LC_{50} in response to Anti-IgM stimulation. Each experiment was performed once on the CLL cells with three intra-replicates for each concentration and error bar shows the mean ± SEM of intra-replicates. Each line shows an independent cell effect in response to the treatment in the presence of stimulation.

7.4.5 Combination of WIP1 inhibitor with RG7388 adverse the antagonistic effect of immobilised anti-IgG and anti-IgM antibody in CLL cells

In this section WIP1 inhibitor was investigated to potentiate the activity of RG7388 on CLL in the presence of the *ex-vivo* microenvironment of BCR stimulation through Anti-IgM antibody signalling.

7.4.5.1 CLL samples showing a potentiation activity of WIP1 inhibitor with RG7388 in the presence of immobilised anti-IgG and anti-IgM antibody

The following (Figure 7.7) represented the combination effect of GSK2830371 with RG7388 on the primary CLL samples that reached the LC_{50} inhibition of RG7388 in its own in the presences of BCR signalling. The solid line represented the combination effect of GSK2830371 with RG7388 and the dash line represented the single effect of RG7388. It is obviously seen that GSK2830371 potentiated the effect of RG7388 to stabilise the wild type *TP53* CLL cells.

Three cryopreserved CLL samples and one freshly isolated CLL sample were stimulated with immobilised Anti-IgG and Anti-IgM prior to treatment with RG7388 on a combination with WIP1 inhibitor (Figure 7.8). The LC_{50} concentration of RG7388 with WIP1 inhibitor (2.5μM) combination treatment increased in some CLL cells in the presence of Anti-IgG and Anti-IgM stimulations compared to non-stimulated CLL cells. Generally, there is a concentration-dependent inhibition effect of the combination treatment with the presence and absence of the stimulations. However, there is no significant change in the effect of RG7388 in the presence or absences of WIP1 inhibitor (2.5μM) under any different conditions.

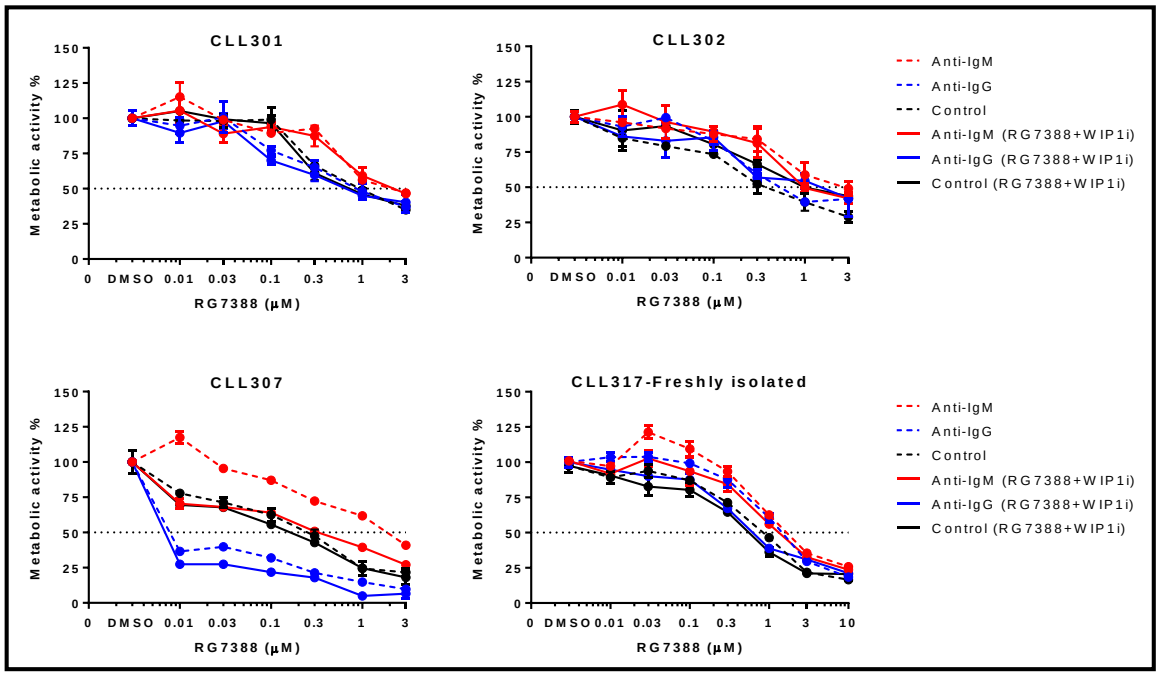

Figure 7.7 WIP1 inhibitor potentiated the inhibitory effect of MDM2 antagonist in CLL samples stimulated with Anti-IgM and Anti-IgG antibody in dependent manner. Panel of primary CLL samples (n=4) stimulated by immobilised either Anti-IgG or Anti-IgM antibodies for 1hr prior treatment of GSK2830371 (2.5µM) in combination with range of RG7388 concentrations up to (3µM) for 48hrs. The combination treatment effect of RG7388 and WIP1i was investigated on freshly isolated CLL317 and thawed CLL samples upon stimulation. CLL cells seeded in ratio (1:2) cells to antibody. XTT assay determined cell metabolic activity %, which was normalized to DMSO treatment for individual experiment. Each experiment was performed once on the primary CLL cells with three intra-replicates for each concentration and error bar shows the mean ± SEM of intra-replicates. Each line shows an independent cell effect in response to the treatment in the presence of stimulation. Dash line shows the effect of RG7388 alone and solid line show the combination effect with WIP1i. In this cohort CLL samples, the combination of WIP1i potentiates the effect of RG7388 to achieve the LC_{50} concentration in response to Anti-IgM stimulation.

7.4.5.2 CLL samples become less sensitive to RG7388 in combination of WIP1 inhibitor in the presence of immobilised Anti-IgG and Anti-IgM antibody

The following (Figure 7.8) showing the effect of WIP1 inhibitor in a combination with RG7388 on primary CLL sample cohort that could not reach the LC_{50} of RG7388 with *ex-vivo* microenvironment of anti-IgM antibody signalling. The purpose of this experiment was to determine whether the combination of GSK2830371 potentiated the activity of RG7388 and increases the inhibition of CLL cells.

As previously mentioned, the behaviour response of CLL cells to the treatment varies from sample to sample regarding to the number of sIg receptors and signalling capacity. In this cohort of CLL cells, the combination of WIP1 inhibitor (2.5µM) showed no or little potentiation on RG7388 activity (Figure 7.8). However, CLL cells become less sensitive to the combination treatment in the presence of Anti-IgM stimulation compared to non-

stimulation. Combination of RG7388 with WIP1 inhibitor (2.5µM) expressed a concentration-dependent manner effect on cell metabolic mitochondrial activity. In this cohort, CLL cells did not reach to the LC_{50} concentration even with a combination treatment up to 3µM of RG7338.

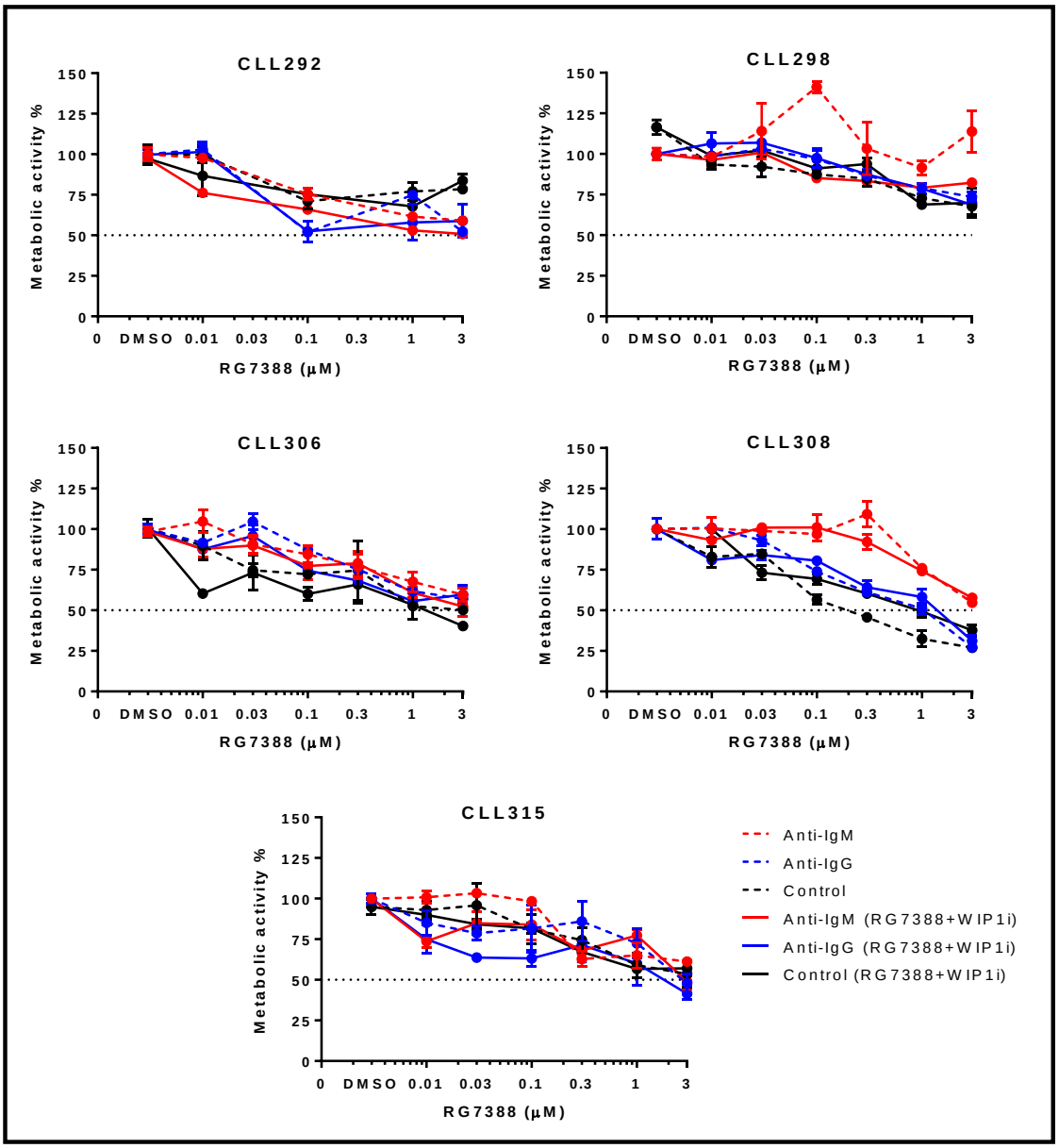

Figure 7.8 The combination effect of WIP1 inhibitor and MDM2 antagonist in CLL samples stimulated with Anti-IgM and Anti-IgG antibody. Panel of cryopreserve CLL samples (n=5) stimulated by immobilised either Anti-IgG or Anti-IgM antibodies for 1hr prior the combination treatment of GSK2830371 (2.5µM) with range of RG7388 concentrations up to (3µM) for 48hrs. CLL cells seeded in ratio (1:2) cells to antibody. XTT assay determined cell metabolic activity %, which was normalized to DMSO treatment for individual experiment. Each experiment was performed once on the primary CLL cells with three intra-replicates for each concentration and error bar shows the mean ± SEM of intra-replicates. Each line shows an independent cell effect in response to the treatment in the presence of stimulation. Dash line shows the effect of RG7388 alone and solid line show the combination effect with WIP1i. In this cohort CLL samples, the combination of WIP1i with RG7388 could not achieve the LC_{50} value in response to Anti-IgM stimulation.

7.4.5.3 WIP1 inhibitor had no or little potentiation on RG7388 in the presence of immobilised Anti-IgM antibody stimulation.

The following figures summarizes the effect of RG7388 as a single agent and in combination with GSK2830371 on CLL cells stimulated through Anti-IgM and Anti-IgG antibody. The aim of this section is to illustrate the statistical differences between the combination and a single treatment across different *ex-vivo* microenvironment stimulation signals. In addition, to determine whether GSK2830371 significantly potentiated the effect of RG7388 in the presence of Anti-IgM antibody stimulation.

Anti-IgM antibody stimulation had a protective effect on CLL cells against the response of RG7388 and in combination with WIP1 inhibitor treatment in comparison to the absence of the stimulation. CLL cells become significantly less sensitive to the RG7388 treatment alone in the presence of Anti-IgM antibody stimulation. However, the combination of WIP1 inhibitor had little or no significant potentiation effect on the activity of RG7388in any condition. Thus, Anti-IgM antibody stimulation protects the CLL cells from apoptotic mechanism in response to RG7388 and in combination with WIP1 inhibitor treatment.

Anti-IgM stimulation significantly protects the CLL cells in response to RG7388 (1µM) alone ($p=0.006$) and in combination of WIP1 inhibitor ($p=0.017$) compared to non- stimulation (Figure 7.9 A).

(Figure 7.9 B) showed CLL cells become significantly less sensitive to RG7388 (3µM) as a single treatment in the presence of Anti-IgM stimulation ($p=0.03$). In addition, in combination of WIP1inhibitor with RG7388 (3µM) CLL cell become less sensitive to treatment in the presences of Anti-IgM antibody stimulation relative to the non-stimulated cells ($p=0.25$). Furthermore, WIP1 inhibitor significantly potentiates the activity of RG7388 in the presences of Anti-IgM stimulation ($p=0.01$).

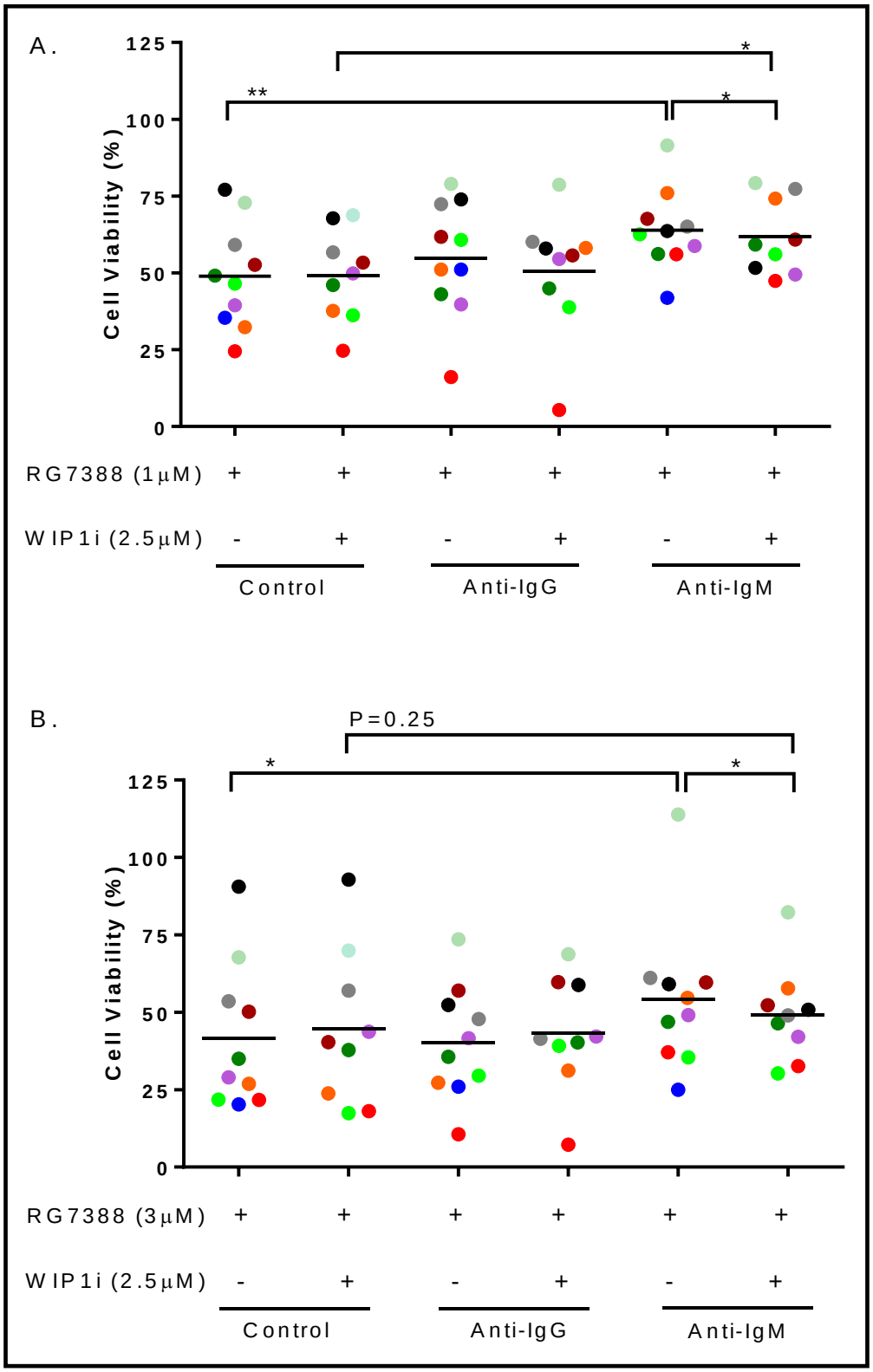

Figure 7.9 Summary plot comparing the *ex-vivo* combination effect of WIP1 inhibitor with RG7388 on primary CLL cells in the presence of immobilised Anti-IgG and Anti-IgM antibody stimulation. (A) RG7388 (1µM) (B) RG7388 (3µM). A cohort of CLL samples (n=10) stimulated with immobilised Anti-IgG and Anti-IgM antibody for 1hr followed by treatment of RG7388 (1, 3µM) in combination with GSK2830371 (2.5µM) for 48hrs. CLL cell viability was determined by XTT assay. Each CLL sample was normalized with DMSO treatment of corresponding sample. Each colour represents individual CLL sample in response to the treatment with Anti-IgG and Anti-IgM stimulation. The median line in each condition represents average mean ± SEM of all patient samples. Each experiment was performed once on individual CLL sample with three intra-replicates of each concentration within the experiment. Statistical significance of differences (** $p < 0.005$, ***, $p < 0.0005$) is determined by paired t-test one tail.

7.4.5.4 LC_{50} values for RG7388 alone and in combination with WIP1 inhibitor on CLL samples stimulated with immobilised beads coated with anti-IgG and anti-IgM antibody

The following Figure 7.10 showed the LC_{50} values of the RG7388 as a single agent and in a combination with GSK2830371 on the cohort of the primary CLL samples (n=9) stimulated by immobilised Anti-IgM and Anti-IgG antibody signals. Since some of the CLL cells could not reach the LC_{50} values, the CLL cohort was divided into two groups regarding to the LC_{50} achievement with RG7388 (3μM) as the highest concentration were used in the study.

Figure 7.10, nine cryopreserved and one freshly isolated CLL cell from nine different patients were stimulated with Anti-IgG or Anti-IgM antibody prior treatment with RG7388 and WIP1 inhibitor. In terms of the LC_{50} values, most of the CLL samples become less sensitive to RG7388 when they are stimulated with immobilised Anti-IgM or Anti-IgG antibody. It is clear that immobilised Anti-IgG and Anti-IgM antibody stimulation reduces the CLL cell sensitivity to MDM2 and WIP1 inhibitors. Five out of ten CLL samples did not reach to the LC_{50} values of RG7388 alone and in combination with WIP1 inhibitor when they were stimulated with immobilised Anti-IgM antibody. CLL cells become less sensitive to RG7388 in the presence to Anti-IgG stimulation and even less sensitive with Anti-IgM antibody stimulation ($p=0.006$). However, following the combination treatment of RG7388 with WIP1 inhibitor at (2.5μM), the majority of CLL samples become less sensitive to the treatment in the presence of the immobilised Anti-IgG or Anti-IgM antibody stimulation in comparison to the absence of the stimulation (Figure 7.10 B). There is difference in CLL cell response to RG7388 in combination with the WIP1 inhibitor at (2.5μM). The LC_{50} values of combination treatment of RG7388 with WIP inhibitor 2.5μM are increased in the presence of immobilised Anti-IgM ($p=0.05$) or Anti-IgG antibody compared with the non-stimulated condition. There is a protective effect of RG7388 on the CLL cells in the presence of either immobilised Anti-IgM or Anti-IgG antibody stimulation compared to the absence of the Anti-Ig stimulation.

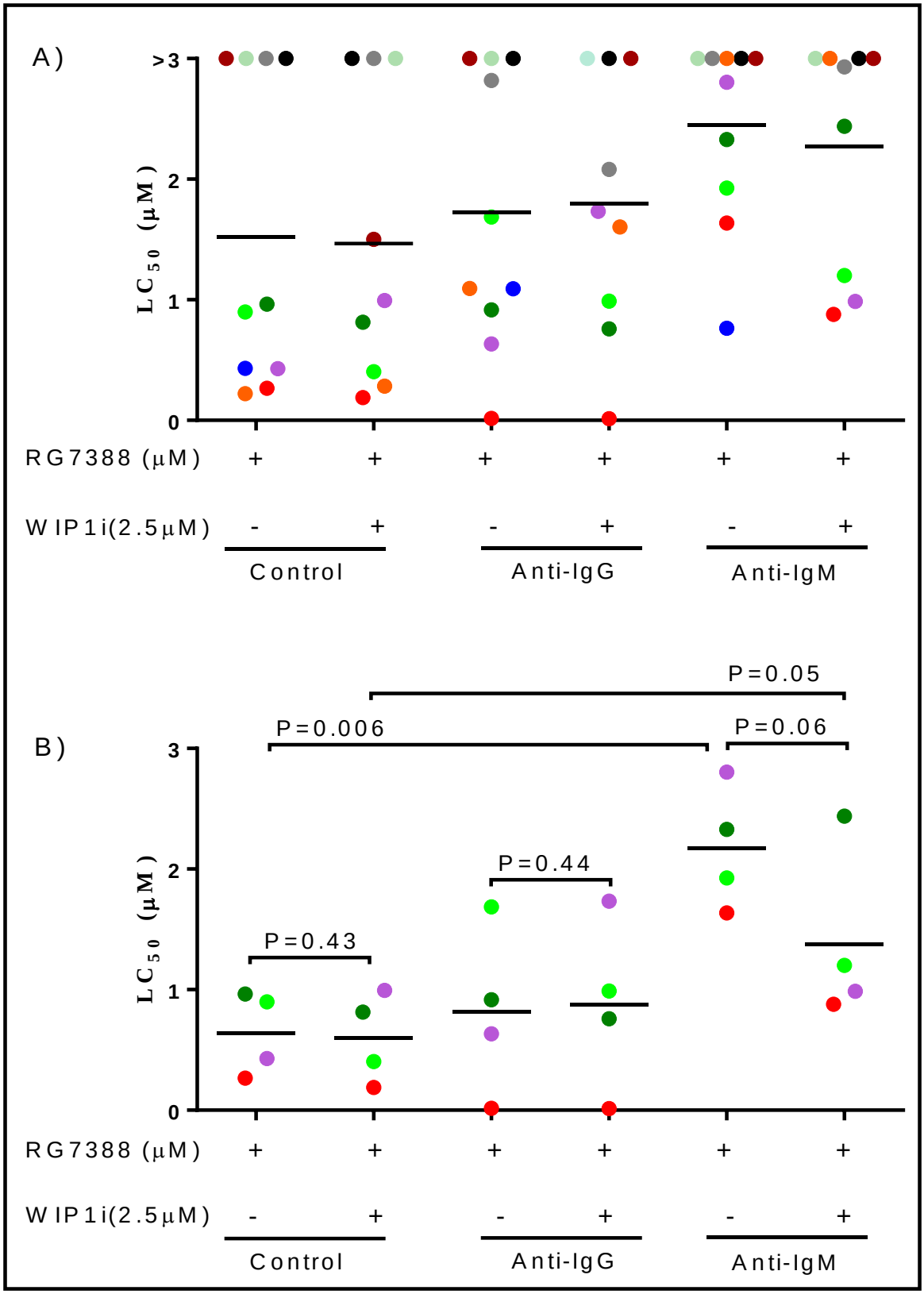

Figure 7.10 Summary plot comparing the LC_{50} values of WIP1 inhibitor in combination with RG7388 for primary CLL cells stimulated by immobilised Anti-IgG and IgM antibody. (A) A cohort set of stimulated CLL samples (n=9) including the ones that could not achieve the LC_{50} values with combination treatment up to (3µM) of RG7388. (B) CLL samples (n=4) achieved the LC_{50} values with combination treatment in the presence of stimulation. Each colour represents the effect of individual primary CLL sample (n=9) in response to the GSK2830371 (2.5µM) and RG7388 treatment in the presence of Anti-IgG and IgM for 48hrs by XTT assay. The median represents average mean ± SEM of all CLL samples. Statistical significance was determined by paired t-test one tail ($p < 0.05$).

LC_{50} (µM)	RG7388			RG7388+WIP1i		
	Control	IgG	IgM	Control	IgG	IgM
CLL 292	>3	>3	>3	>3	>3	>3
CLL 298	>3	>3	>3	>3	>3	>3
CLL 301	0.963	0.917	2.330	0.815	0.76	2.439
CLL 302	0.428	0.634	2.804	0.994	1.733	0.987
CLL 306	>3	>3	>3	1.5	>3	>3
CLL 307	0.267	0.016	1.636	0.188	0.014	0.880
CLL 308	0.222	1.093	>3	0.285	1.604	>3
CLL 315	>3	2.82	>3	>3	2.081	2.93
CLL 317 (F)	0.9	1.687	1.927	0.404	0.988	1.202
CLL 317	0.432	1.09	0.763			

Table 7.1 The LC_{50} of RG7388 in combination with WIP1 inhibitor in the presence of immobilised Anti-IgG and IgM antibody stimulation. Cryopreserve CLL samples (n=9) and CLL317(F) freshly isolated sample treated with GSK2830371 (2.5uM) in combination with range of RG7388 concentrations in the presence of immobilised Anti-IgM and Anti-IgG antibody stimulation.

7.4.6 WIP1 inhibitor induces PUMA mRNA expression in CLL cells with or without the presence of Anti-IgG or Anti-IgM stimulation

In this section, I would like to investigate the transcriptional changes in the negative regulator of *TP53* target genes in CLL cells stimulated through BCR. A cohort of different cryopreserved primary CLL samples were stimulated with immobilised Anti-IgG and Anti-IgM antibody prior treatment either with WIP1 inhibitor or RG7388 as a single agent and in combination for 6 hours.

The expression of different genes measured the intrinsic apoptosis (*BAX*, *PUMA*, *TP53INP1*), extrinsic apoptosis (*FAS*, *NOXA*), cell cycle arrest (*CDKN1A*), and p53 negative autoregulation (*MDM2*, *WIP1*) to determine effect of WIP1 inhibitor and RG7388 relative to DMSO. In RQ calculation, the basal level of all conditions is equal 1 which means no change in the gene expression relative to DMSO untreated and normalized to β-actin. The cut off expression is considered to be 2-fold change.

Looking to non-stimulated (control) CLL cell treated with WIP1 inhibitor, *PUMA* showed the highest gene expression level over the panel of genes (Figure 7.11 A). In contrast, with Anti-IgG stimulation, *PUMA*, and *FAS* were showed the highest fold change expression (Figure 7.11 B). However, the increase in the *PPM1D*, *MDM2*, *TP53INP1* and *BAX* were occurred because of one CLL sample, CLL309 which were expressed on (Figure 7.12 B). It is clearly seen through the expression of each individual CLL sample through the set of genes, that CLL309 in particular expressed high fold changes over the other CLL samples either with non-stimulated and Anti-IgG antibody stimulation (Figure 7.12 A and B).

Looking to the Anti-IgM stimulation, *PUMA* was expressed more with WIP1 inhibitor relative DMSO un-treated condition relative to the other genes in the panel (Figure 7.11 C). Interestingly, Anti-IgM antibody stimulation decreases the expression of *PPM1D*, *MDM2*, *TP53INP1* and *FAS* for CLL in response to WIP1 inhibitor in particularly for CLL309. In addition, Anti-IgM antibody stimulation reduces the expression of *MCL1* and *BCL2* in CLL309 (Figure 7.12 C).

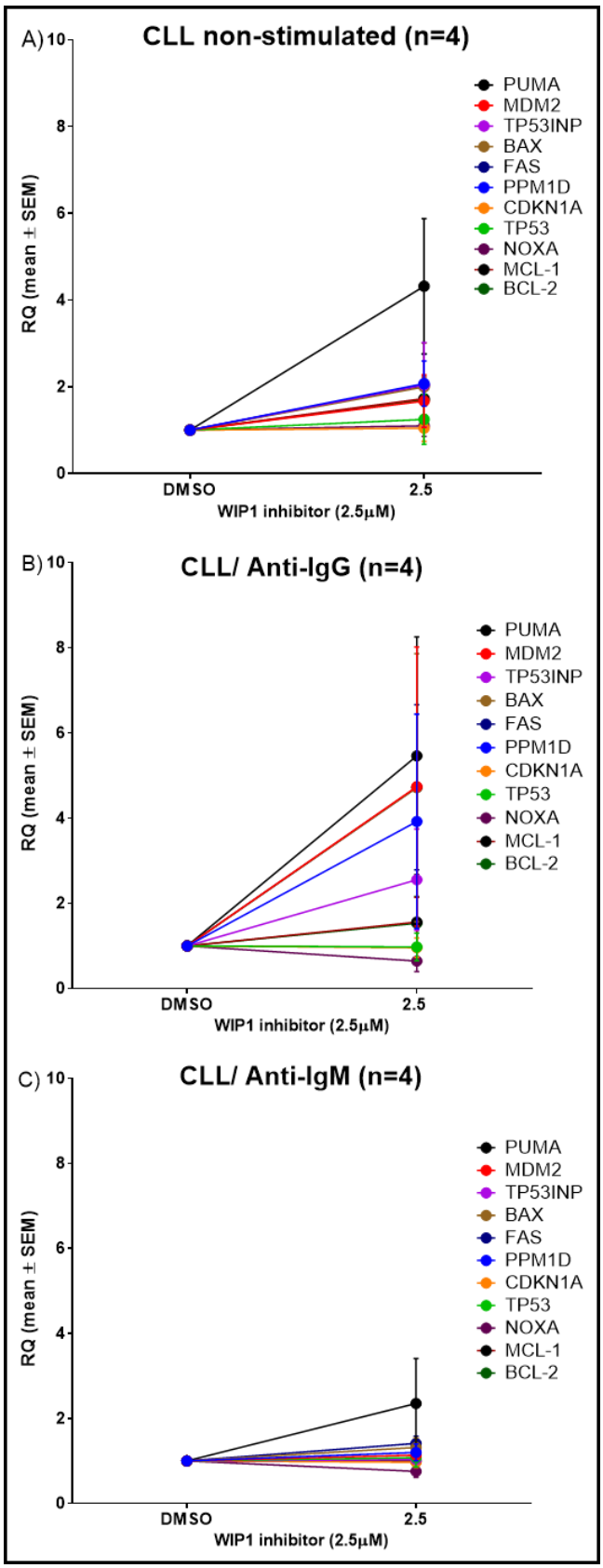

Figure 7.11 mRNA expression of selected p53 transcriptional target genes of primary CLL sample exposed to WIP1 inhibitor in the presence of immobolised coated antidbodies. (A) non-stimulated (control), (B) Anti-IgG, (C) Anti-IgM. Different primary CLL samples (n=4) stimulated with antidbodies for 1hr prior treatment of GSK2830371 (2.5μM) for 6hrs. qRT-PCR performed in (n=1) repeat on each primary CLL sample extraction. The gene expression was normalized to *β-ACTIN* and DMSO treatment of three intra-replicate wells. Error bars represent the mean ± SEM of different CLL samples. RQ values were calculated using the formula $2^{-\Delta\Delta Ct}$.

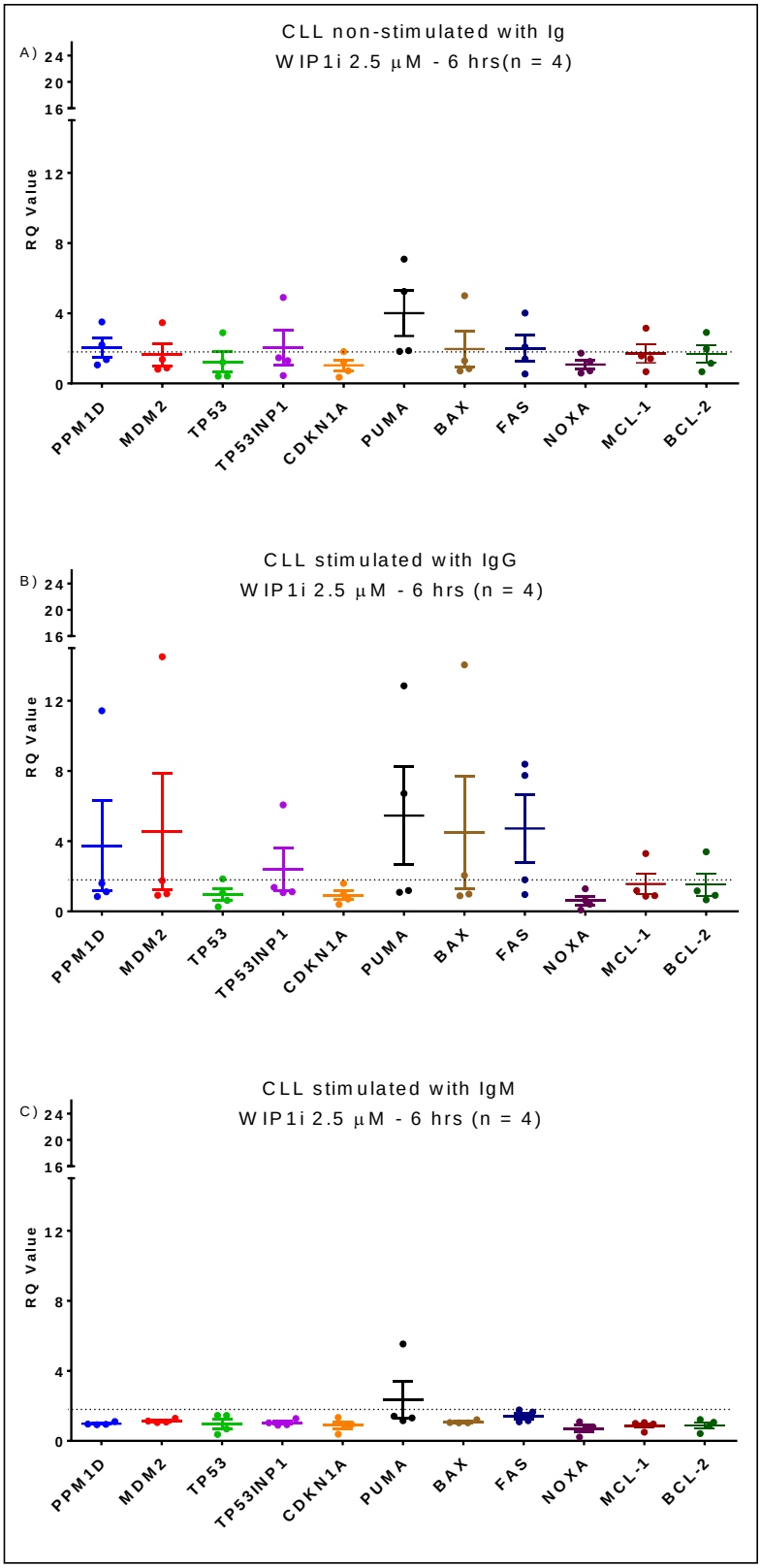

Figure 7.12 Summary of fold change in p53 target gene expression of CLL cells treated with WIP1 inhibitor in the presence of immobolised coated antidbodies. (A) non-stimulated (control), (B) Anti-IgG, (C) Anti-IgM. Different primary CLL samples (n=4) stimulated with antidbodies for 1hr prior treatment of GSK2830371 (2.5µM) for 6hrs. qRT-PCR measures genes expression from (n=1) cell extract of each CLL sample. Each point represents the mean value for an individual patient and the error bars represent the average mean ± SEM for the total patient samples. Each colour represents mRNA expression of certain gene in response to the treatment**.** The gene expression was normalized to *β-ACTIN*, endogenous control and DMSO-treated cells, the calibrator between three intra-replicate wells of each concentration.

7.4.7 RG7388 induces upregulation of pro-apoptotic p53 target genes of CLL cells stimulated with immobilised Anti-IgM antibody

Figure 7.13 showed the change in selected genes expression of CLL cells in response to RG7388 in the presence of either Anti-IgG or Anti-IgM antibody stimulation. It is obviously seen that few genes were increased in response to RG7388 with non-stimulated CLL cells and Anti-IgG stimulation, *MDM2* and *PUMA* (Figure 7.14 A&B). In contrast, the expression of *MDM2*, *PUMA* and *FAS* were increased in response to RG7388 in the presence of Anti-IgM stimulation. Obviously, the extrinsic pro-apoptotic gene, *FAS* was highly expressed with Anti-IgM antibody stimulation in response to RG7388 in a concentration dependent manner. However, the pro-apoptotic gene, *PUMA* was highly expressed with non-stimulation control and Anti-IgG antibody stimulation CLL cells in response to RG7388.

Furthermore, the expression of *TP53*, *CDKN1A* and *NOXA* genes did not express significant fold changes following RG7388 in the presence and the absence of immobilised Anti-Ig antibody stimulation. The anti-apoptotic genes, *MCL1* and *BCL2* show similar pattern following RG7388 with both conditions (Figure 7.14).

In conclusion, following treatment with RG7388, *MDM2*, *PUMA* and *BAX* were expressed in the absence of Anti-Ig stimulation. However, with Anti-IgG stimulation, *MDM2*, *PUMA*, *BAX* and *FAS* gene expression was induced in response to RG7388. Certainly, with Anti-IgG stimulation *MDM2*, *PUMA* and *BAX* were highly expressed relative to non-stimulated condition in response to RG7388.

Following the Anti-IgM stimulation, RG7388 increases the fold change expression of *MDM2*, *TP53INP1*, *PUMA*, *BAX* and *FAS* relative to DMSO. Indeed, *MDM2* and *FAS* showed the highest fold change expression compared to their expression in the absence of the Anti-IgM stimulation.

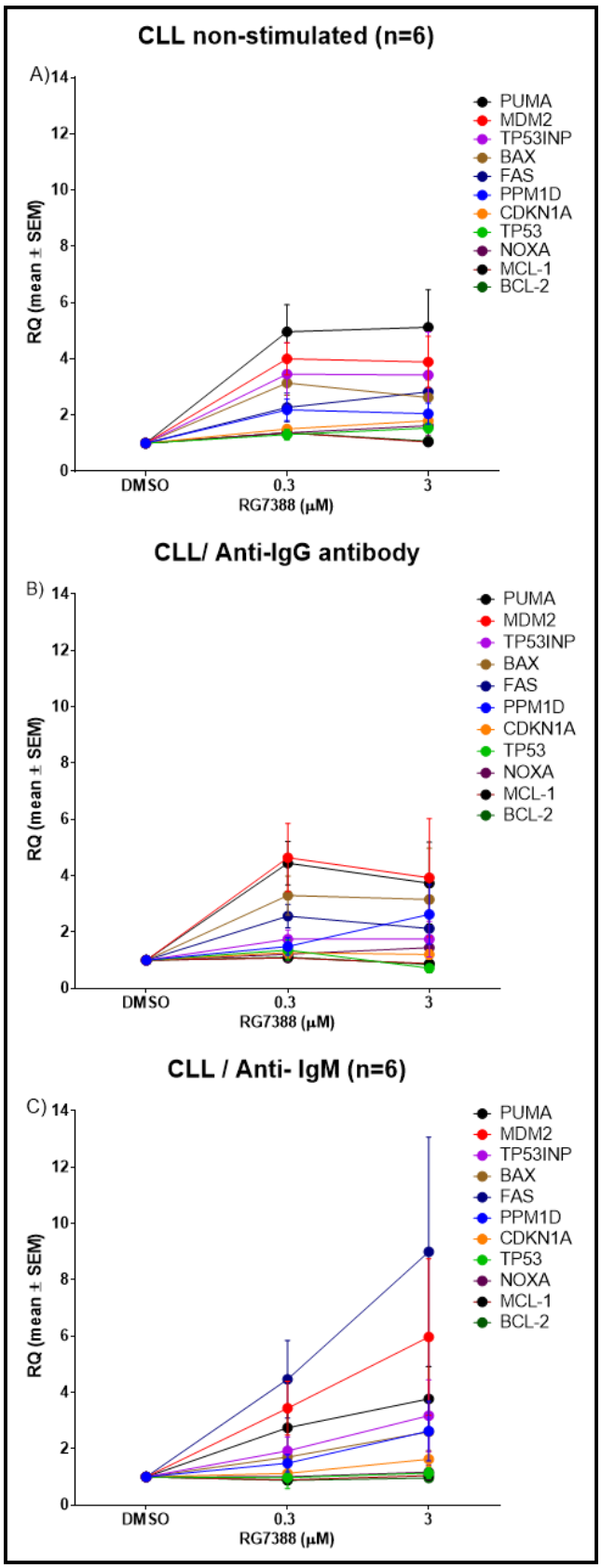

Figure 7.13 mRNA expression of selected p53 transcriptional target genes of primary CLL sample exposed to RG7388 in the presence of immobolised coated antidbodies. (A) non-stimulated (control), (B) Anti-IgG, (C) Anti-IgM. Different primary CLL samples (n=6) stimulated with antidbodies for 1hr prior treatment of RG7388 (0.3, 3µM) for 6hrs. qRT-PCR performed in (n=1) repeat on each primary CLL sample extraction. The gene expression was normalized relative to *β-ACTIN*, endogenous control and DMSO treatment of three intra-replicate wells. Error bars represent the mean ± SEM of different CLL samples. RQ values were calculated using the formula 2ΔΔCt.

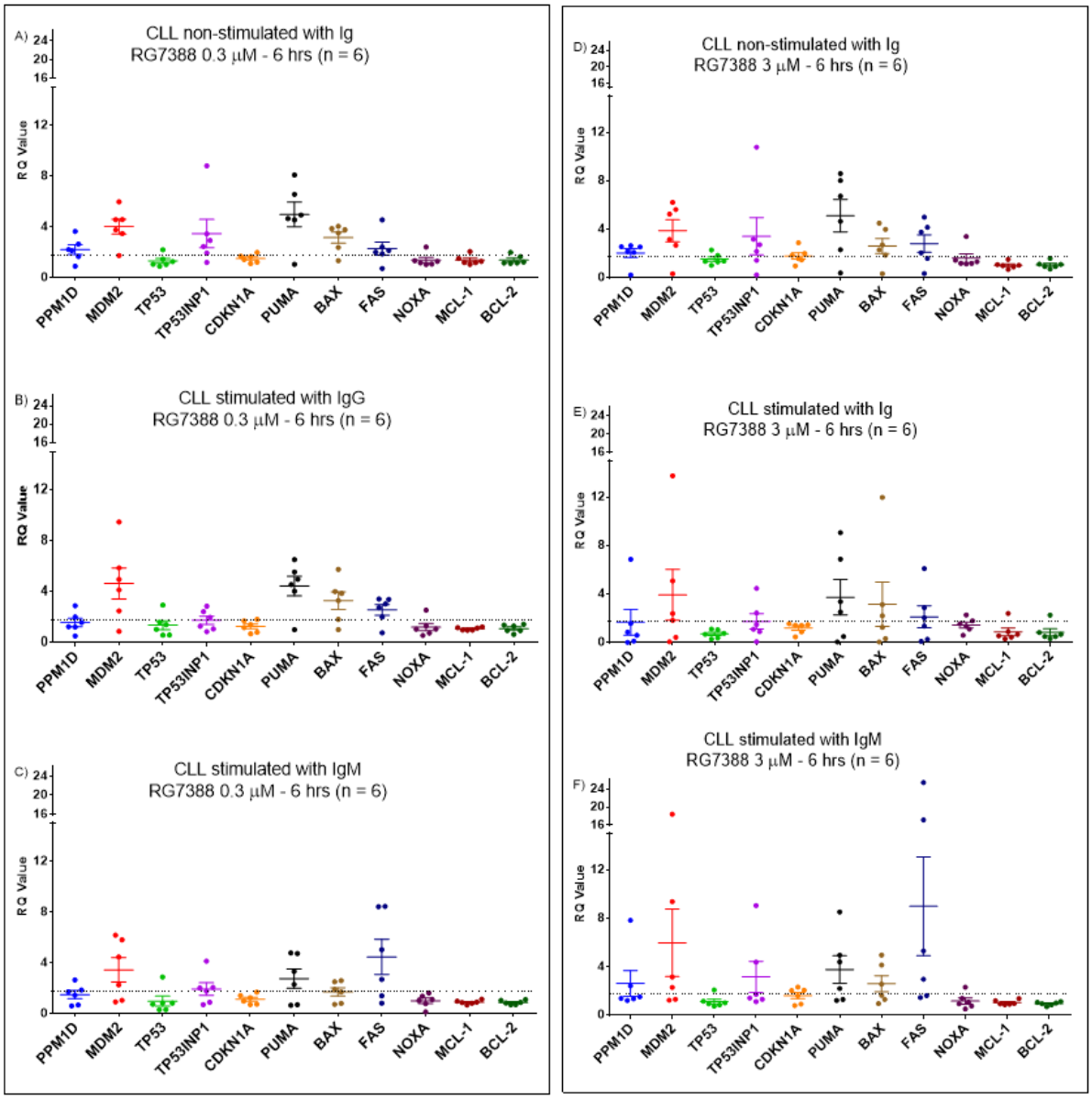

Figure 7.14 Summary of fold change in p53 target genes expression of CLL cells treated with RG7388 in the presence of immobolised coated antidbodies. (A-D) non-stimulated CLL cells, (B-E) Anti-IgG stimulation and (C-D) Anti-IgM. The left graphs show the RG7388 (0.3µM) and the right graphs show the RG7388 (3µM). Different primary CLL samples (n=6) stimulated with antidbodies for 1hr prior treatment of RG7388 (0.3, 3µM) for 6hrs. qRT-PCR measures genes expression from (n=1) cell extracts of each CLL sample. Each point represents the mean value for an individual patient and the error bars represent the average mean ± SEM for the total patient samples. Each colour represents mRNA expression of certain gene in response to the treatment. The gene expression was normalized to *β-ACTIN*, endogenous control and DMSO-treated cells, the calibrator between three intra-replicate wells of each concentration.

7.4.8 Combination of WIP1 inhibitor with RG7388 induces the mRNA upregulation of pro-apoptotic p53 target genes in CLL cells in the presence of Immobilised Anti-IgM antibody

In this experiment, four CLL samples were treated with a WIP1 inhibitor in combination with RG7388 in the presence of Anti-IgG and Anti-IgM stimulations. The aim of this section is to investigate the transcriptional change of negative regulator *TP53* target genes in CLL cells stimulated through BCR in response to the combination treatment. Thus, the expression of the same set of genes was evaluated to determine any potentiation effects WIP1 inhibitor and RG7388 on the primary CLL cells. The experiment was conducted on the four different cryopreserved primary CLL cell samples which were exposed to the single agent. The dashed line represents the effect of RG7388 alone while the sold line represents the effect of a combination treatment.

In non-stimulated CLL cells, the expression of *MDM2*, *TP53INP1*, *PUMA*, *BAX* and *FAS* showed fold change expression in response to RG7388 (0.3μM) and in a combination with WIP1 inhibitor (Figure 7.16). Furthermore, with RG7388 (3μM), *MDM2*, *PUMA*, *BAX* and *FAS* expression increased with single agent and in combination of WIP1 inhibitor (Figure 7.17). However, the fold change expression of the selected genes in response to RG7388 (3μM) is decreased compared to (0.3μM) (Figure 7.15 A).

In terms of the Anti-IgG stimulation, *MDM2, PUMA*, *BAX* and *FAS* genes showed the highest mRNA expression across in the gene panel in response to RG7388 and in combination with WIP1 inhibitor (Figure 7.16 and Figure 7.17 C&D).

With Anti-IgM stimulation, *MDM2, PUMA* and *FAS* genes showed the highest fold change expression across in the gene panel in response to RG7388 and in combination with WIP1 inhibitor (Figure 7.16 and Figure 7.17 E&F). Moreover*, FAS* was the highest gene expressed with the treatment in the presence of Anti-IgM.

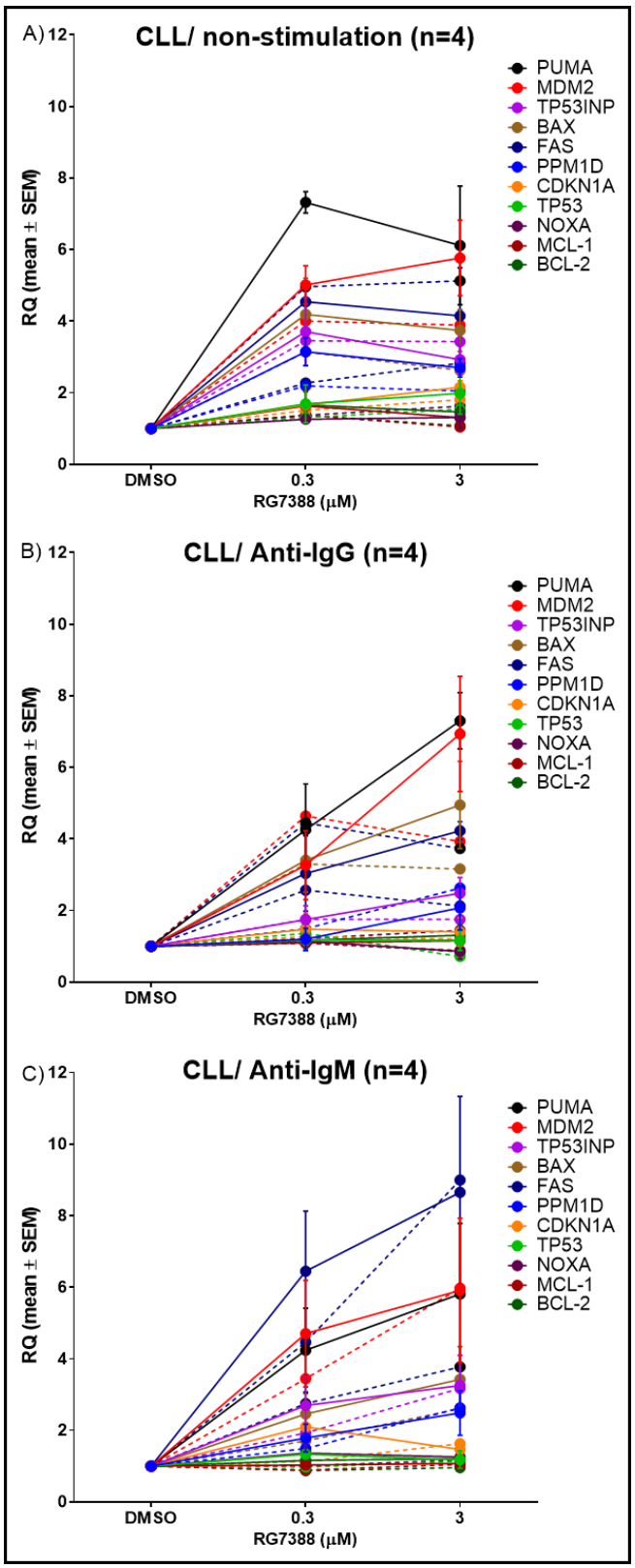

Figure 7.15 mRNA expression of selected p53 transcriptional target genes of primary CLL sample exposed to RG7388 in the presence of immobolised coated antidbodies. (A) non-stimulated (control), (B) Anti-IgG, (C) Anti-IgM. Different primary CLL samples (n=4) stimulated with antidbodies for 1hr followed by treatment of GSK2830371 (2.5μM) in combination with RG7388 (0.3, 3μM) for additional 6hrs. The effect of RG7388 alone represents in dash line, and the combination with WIP1i (2.5μM) is solid line. The gene expression was normalized relative to *β-ACTIN*, endogenous control and DMSO treatment of three intra-replicate wells of each concentration for individual sample. qRT-PCR performed in (n=1) repeat on each primary CLL sample extraction. Error bars represent the average mean ± SEM of different CLL samples. RQ values were calculated using the formula 2ΔΔCt.

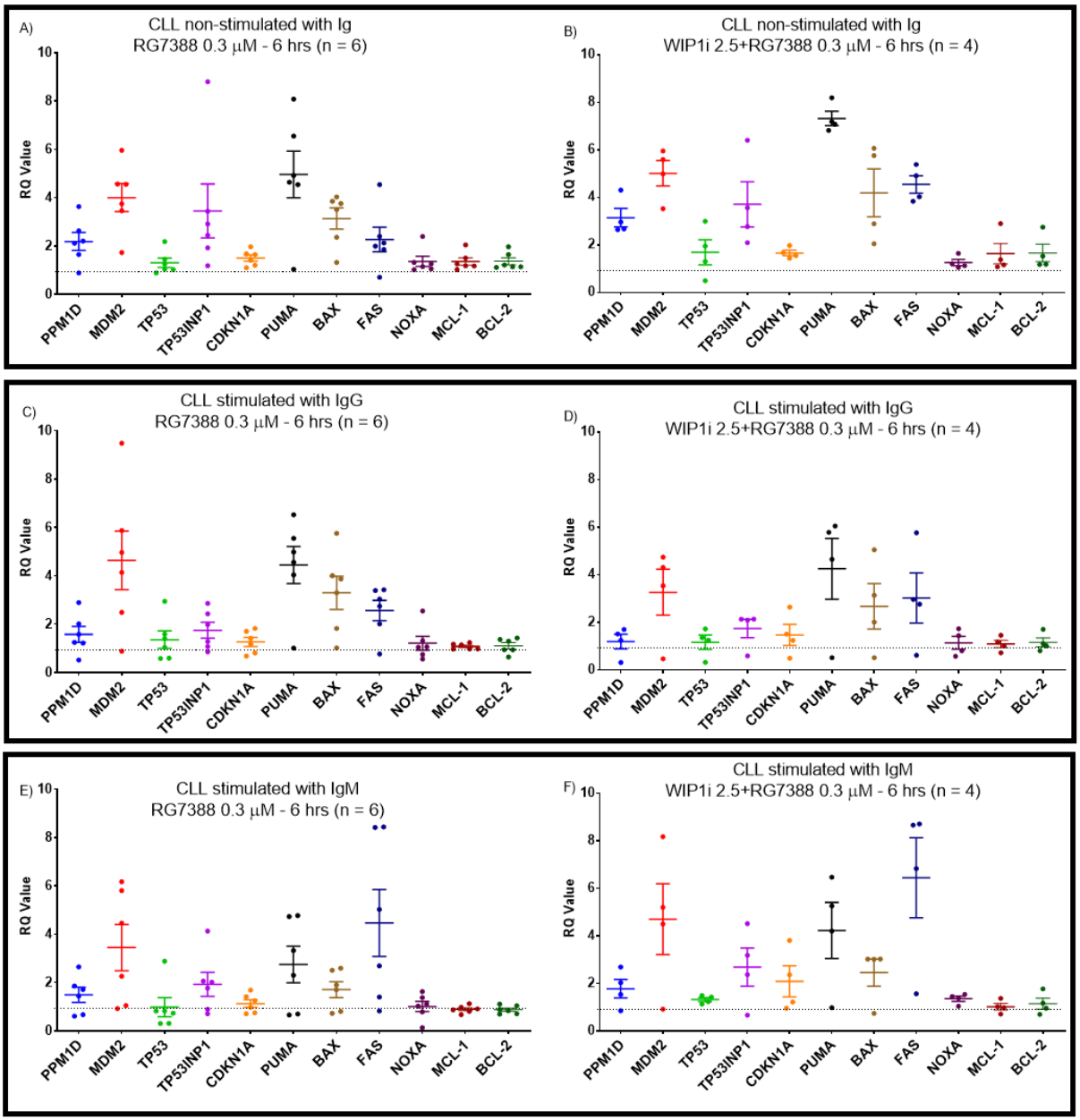

Figure 7.16 Summary plot of mRNA transcriptional change in CLL cells treated with WIP1 inhibitor in combination with RG7388 (0.3μM) in the presence of immobilised coated antibodies for 6hrs. (A-B) non-stimulated CLL cell (C-D) Anti-IgG and (E-F) Anti-IgM. The left graphs show the RG7388 (0.3μM) and the right graphs show the combination of GSK2830371 (2.5μM) with RG7388 (0.3μM). Different primary CLL samples stimulated with antibodies for 1hr prior treatment of either RG7388 alone (n=6) or in combination with WIP1i (n=4). Each point represents the mean value for an individual patient and the error bars represent the average mean ± SEM for the total patient samples. Each colour represents mRNA expression of certain gene in response to the treatment normalized to *β-ACTIN*, endogenous control and DMSO-treated cells, the calibrator between three intra-replicate wells of each concentration. qRT-PCR measures genes expression from (n=1) cell extracts of each CLL sample.

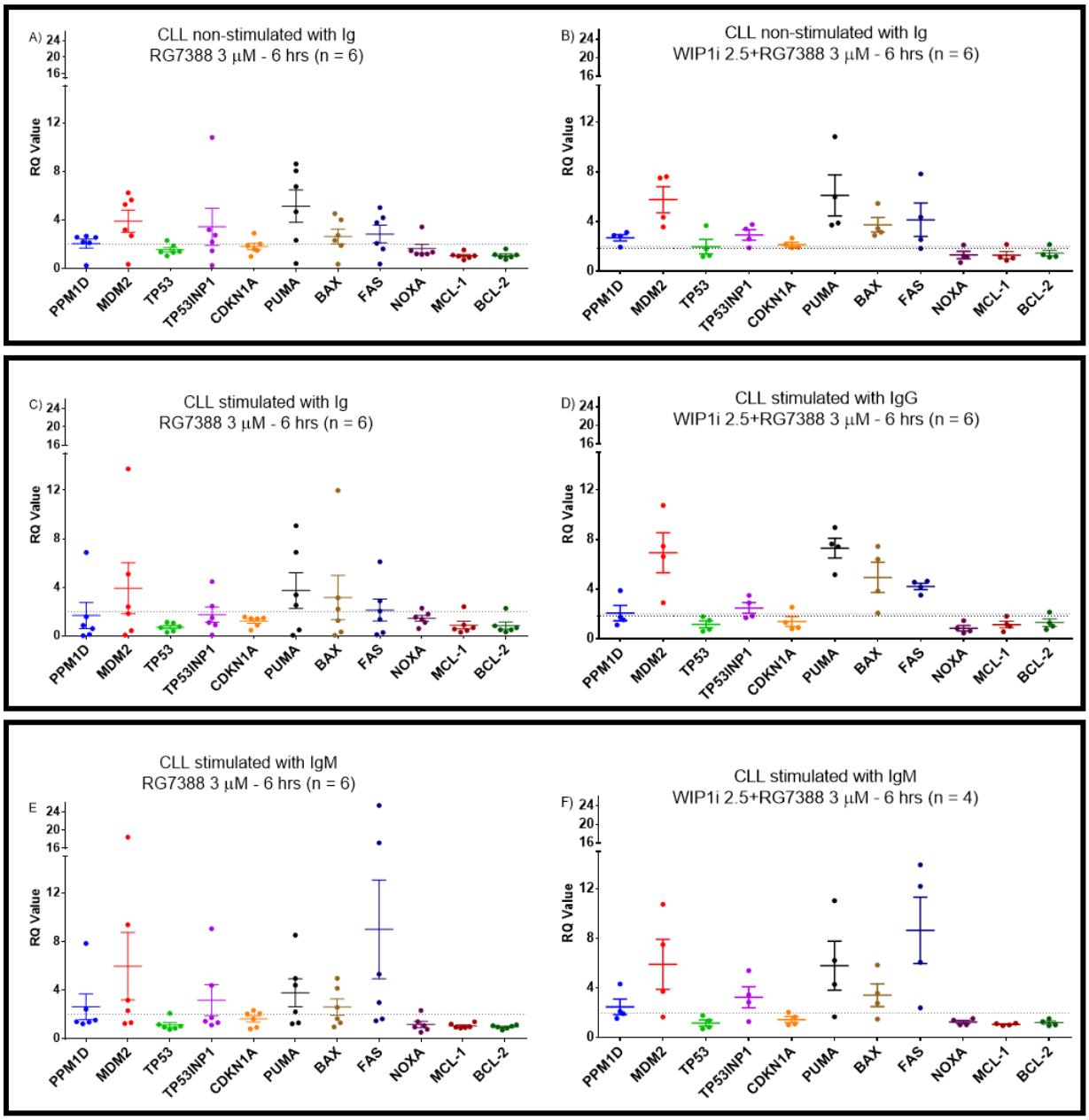

Figure 7.17 Summary plot of mRNA transcriptional change in CLL cells treated with WIP1 inhibitor in combination with RG7388 (3µM) in the presence of immobilised coated antibodies for 6hrs. (A-B) non-stimulated CLL cell (C-D) Anti-IgG and (E-F) Anti-IgM. The left graphs show the RG7388 (3µM) and the right graphs show the combination of GSK2830371 (2.5µM) with RG7388 (3µM). Different primary CLL samples stimulated with antibodies for 1hr prior treatment of either RG7388 alone (n=6) or in combination with WIP1i (n=4). Each point represents the mean value for an individual patient and the error bars represent the average mean ± SEM for the total patient samples. Each colour represents mRNA expression of certain gene in response to the treatment normalized to *β-ACTIN*, endogenous control and DMSO-treated cells, the calibrator between three intra-replicate wells of each concentration. qRT-PCR measures genes expression from (n=1) cell extracts of each CLL sample.

7.4.9 Combination of WIP1 inhibitor with RG7388 induce the mRNA expression of FAS gene in the presences of immobilised Anti-IgM antibody stimulation

In this section, we summarize the changes in transcription level of gene panel in response to MDM2 and WIP1 inhibitor in the presence of Anti-IgG and Anti-IgM stimulations.

With Anti-IgM stimulation, the expression of TP53 negative regulator (*MDM2*, *TP53INP1*, *CDKN1A*) and pro-apoptotic genes (*PUMA BAX*, *FAS*) were increased following the combination treatment of WIP1 inhibitor with RG7388 (0.3µM) compared to RG7388 (0.3µM) alone. In contrast, with non-stimulated CLL cells, the expression of TP53 negative regulator (*MDM2*) and pro-apoptotic genes (*PUMA BAX*, *FAS*) were increased following the combination treatment of WIP1 inhibitor with RG7388 (0.3µM) compared to RG7388 (0.3µM) alone (Figure 7.18).

Moreover, *FAS* expression was increased with the effect of RG7388 (0.3µM) in combination with WIP1 inhibitor in the presence of Anti-IgM stimulation compared to non-stimulated CLL cells (p=0.19). In comparison, single treatment of RG7388 increases the *FAS* expression with Anti-IgM stimulation compared to non-stimulation CLL cells (P=0.006) (Figure 7.18 E) and (p=0.18) (Figure 7.19 E).

PUMA and *BAX* expressions were reduced with Anti-IgM stimulation relative to non-stimulated conditions following RG7388 treatment. Furthermore, the combination of WIP1 inhibitor increase the expression of *PUMA* and *BAX* compared to RG7388. In contrast, with Anti-IgG stimulation, *PUMA* expression showed no much changes either with RG7388 (0.3µM) or in combination of WIP1 inhibitor (Figure 7.18 C&D). However, with RG7388 (3µM), *PUMA* was expressed more in a combination of WIP1 inhibitor relative to RG7388 alone (Figure 7.19 C&D).

The expression of *TP53INP* was reduced with Anti-IgM stimulation relative to non-stimulated conditions following RG7388 (0.3µM) treatment even though, RG7388 (3µM) did not show a large change. However, the combination of WIP1 inhibitor increase the expression of *TP53INP* compared to RG7388 alone (Figure 7.18 & Figure 7.19 B).

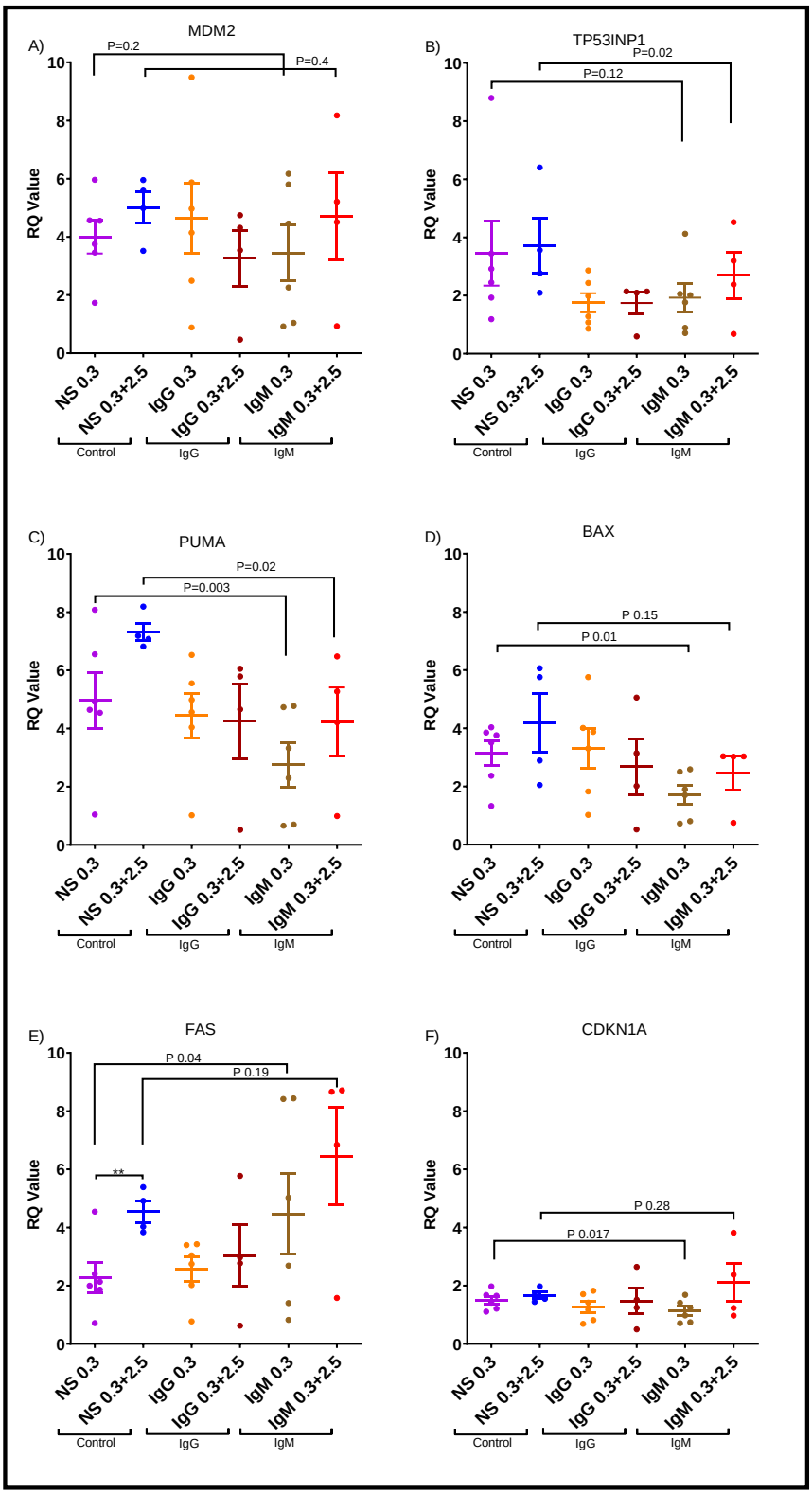

Figure 7.18 Summary comparing the fold change of p53 target genes expression of CLL cells treated with WIP1 inhibitor in combination with RG7388 (0.3μM) in the presence of immobolised coated antidbodies by qRT-PCR. (A) *MDM2* (B) *TP53INP1* (C) *PUMA* (D) *BAX* (E) *FAS* (F) *CDKN1A*. Primary CLL samples stimulated with antibodies either Anti-IgG or Anti-IgM for 1hr prior treatment of either RG7388 alone (n=6) or in combination with GSK2830371 (2.5μM) (n=4) for 6 hrs. Each colour showed mRNA expression of certain gene in response to different treatment condition. The experiment performed on (n=1) cell extracts of each CLL sample. Each point represents the mean value for an individual patient and the error bars represent the average mean ± SEM for the total patient samples. One tailed paired t-test p-values are shown for the significance of differences between the mean values of treatment with or without Anti-IgM is displayed above the horizontal bars, significance taken at $p < 0.05$.

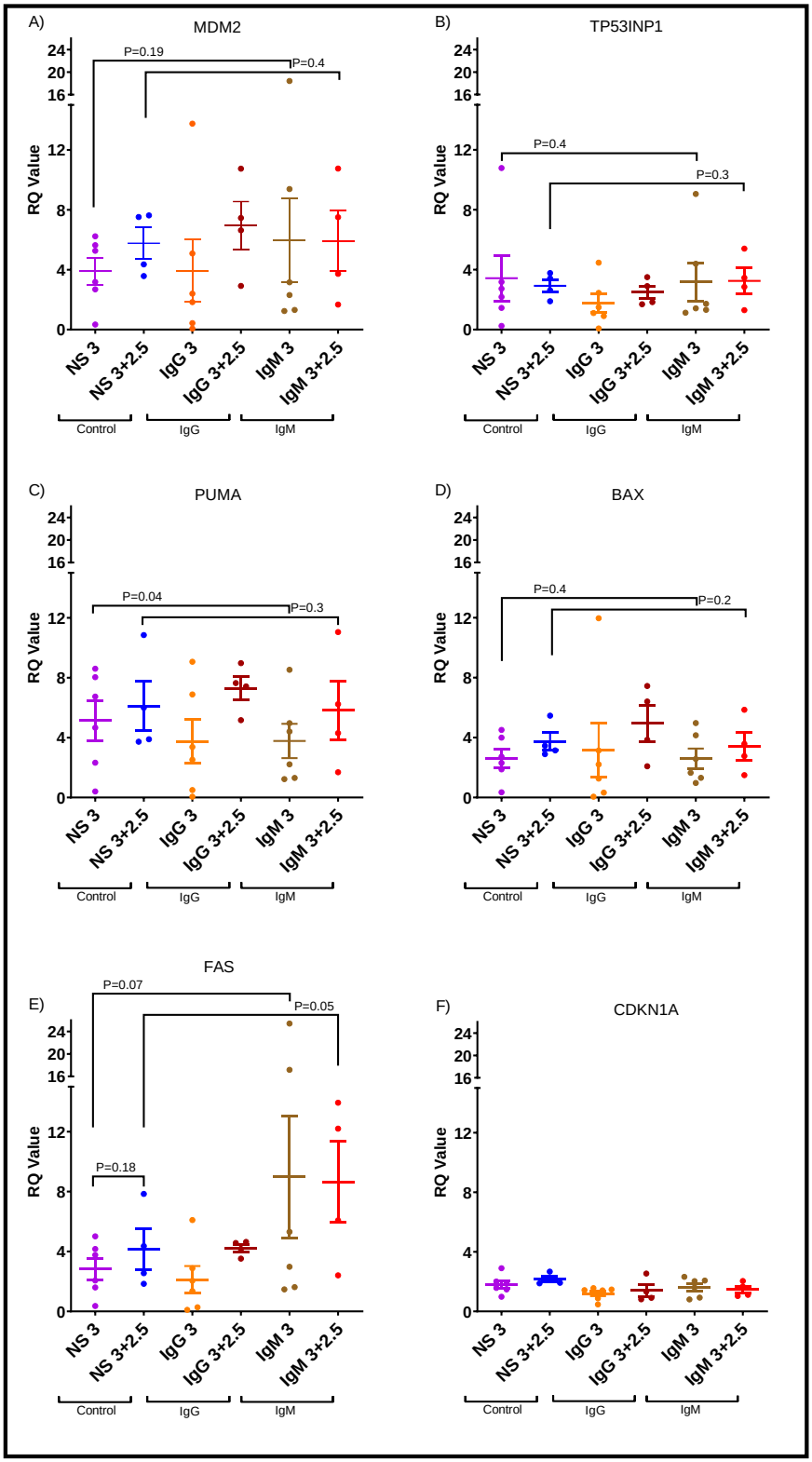

Figure 7.19 Summary plot comparing the fold change in the mRNA expression of p53 target genes expression for CLL cells treated with WIP1 inhibitor in combination with RG7388 (3µM) in the presence of immobolised coated antidbodies by qRT-PCR. (A) *MDM2* (B) *TP53INP1* (C) *PUMA* (D) *BAX* (E) *FAS* (F) *CDKN1A*. Primary CLL samples stimulated with antibodies either Anti-IgG or Anti-IgM for 1hr prior treatment of either RG7388 alone (n=6) or in combination with GSK2830371 (2.5µM) (n=4) for 6 hrs. Each colour showed mRNA expression of certain gene in response to different treatment condition. Each point represents the mean value for an individual patient and the error bars represent the average mean ± SEM for the total patient samples. The experiment performed on (n=1) cell extracts of each CLL sample. One tailed paired t-test p-values are shown for the significance of differences between the mean values of treatment with or without Anti-IgM is displayed above the horizontal bars, significance taken at $p < 0.05$.

7.5 Discussion

In this chapter, beads coated with immobilised Anti-IgM antibody were used to mimic aspects of the *in-vivo* environmental conditions of progressive CLL cells. An *ex-vivo* microenvironment experimental model was designed based on the interaction between the BCR of CLL cells with immobilised Anti-IgM antibody. It was clearly and notably observed that both immobilised Anti-IgG and Anti-IgM antibodies significantly increased the metabolic activity of CLL cells compared to non-stimulated CLL cells (Figure 7.2). Moreover, the detection of phosphorylated ERK protein confirmed the activation of downstream BCR signalling by contact with immobilised Anti-IgM antibody, which in association with FcμR can promote the BCR signalling (Figure 7.1). However, binding of immobilised Anti-IgG antibody is associated with FcγRIIB, which inhibits the BCR signals (Liu et al., 2019).

These results are in line with several studies which have identified that immobilised Anti-IgM antibody triggers BCR signalling and induces more powerful growth and survival stimulation signals in B CLL cells, regardless of *IGHV* mutation status (Quiroga et al., 2009; Vlad et al., 2009). The anti-apoptotic effect initiated by BCR stimulation was detected in both *IGHV* M-CLL and unmutated U-CLL cells. However, with M-CLL a rapid and strong protective response against apoptosis was observed compared to U-CLL cells, which are more resistant to spontaneous apoptosis (Rombout et al., 2016). Using immobilised Anti-IgM antibody to stimulate BCR signalling provides understanding of the *in-vivo* response of CLL cells to microenvironmental factors including potential differences in gene expression of CLL cells located in lymph nodes (Herishanu, Pérez-Galán, et al., 2011).

Looking to the effect of WIP1 inhibitor, GSK2830371 at (2.5μM), as a single agent this had minimum or no effect on the viability of the CLL cells whether in the presence or absence of both immobilised Anti-IgG and Anti-IgM antibodies compared to non-stimulated CLL cells (**Figure** 7.3). Although, both BCR stimulation and unstimulated CLL cells showed no inhibition effect in response to WIP1 inhibitor however, Anti-IgG and Anti-IgM stimulated CLL cells showed higher cell viability than non-stimulated (control) CLL cells.

Looking to the mRNA changes in a panel of genes in response to WIP1 inhibitor, the expression of *PUMA* was increased whether in the presence or absence of the BCR stimulation signals (Figure 7.12). there was not much difference in the mRNA expression of the genes in the panel relative to the DMSO treatment level, apart from sample CLL309.

Unlike other CLL samples in the cohort, CLL309 showed high fold changes expression in response to WIP1 inhibitor compared to the other CLL samples in the cohort. Taking that in accounts, WIP1 inhibition increased the expression of *PPM1D*, *MDM2*, *PUMA*, *BAX* and *FAS* of CLL309 in the presence of immobilised Anti-IgG antibody stimulation compared to non-stimulation control. However, with immobilised Anti-IgM antibody stimulation, *PUMA* was the only gene particularly in CLL309 whose expression was increased compared to the other genes in the panel (Figure 7.12).

Looking to the effect of MDM2 inhibitor, immobilised Anti-IgM antibody stimulated CLL cells become less responsive to RG7388 compared to non-stimulated CLL cells. CLL cell become more viable and metabolically active when exposed to and stimulated by Anti-IgM and the CLL cells also become less sensitive to the RG7388 treatment (1μM p= 0.01, 3μM p=0.04) (Figure 7.9).

The combination of WIP1 inhibitor with RG7388 potentiated the activity of RG7388 on Anti-IgM antibody stimulated CLL cells. The viability of immobilised Anti-IgM antibody stimulated CLL cells was reduced by the combination of WIP1 inhibitor with RG7388 compared to the effect of RG7388 alone (1μM P=0.03, 3μM p=0.3) (Figure 7.9).

Since some of the CLL samples in the cohort could not achieve the LC_{50} of RG7388 at (3μM) concentration, a statistical test for LC_{50} difference could only be applied to the group of samples for which an LC_{50} was reached. It was found that in the presence of immobilised Anti-IgM antibody stimulation CLL cells become less sensitive to RG7388 alone or in combination with WIP1 inhibitor compared to in the absence of BCR stimulation signals (Figure 7.10 A).

WIP1 inhibitor was not able to potentate the activity of RG7388 on CLL cells in the absence of immobilised Anti-IgM antibody stimulation signals through BCR although, in the presence of immobilised Anti-IgM antibody stimulation signals, CLL cells become more sensitive to RG7388 in combination with WIP1 inhibitor compared to RG7388 alone (Figure 7.10 B). In contrast, another study reported that dasatinib produces potential effect on pro-survival activity of CLL cells mediated by BCR signalling (Mccaig et al., 2011).

Regarding to the changes in expression of the gene panel, *MDM2* and *PUMA* were the only two genes that consistently showed an increase in response to RG7388 alone whether in the presence or absence of the BCR stimulation signals (Figure 7.14). However, on addition of the WIP1 inhibitor, *MDM2* and the pro-apoptotic *FAS*, *BAX* and *PUMA*, were increased with

combination treatment of WIP1 inhibitor with RG7388, either in the presence or absence of the BCR stimulation signals (Figure 7.16)

In non-stimulated CLL cells, RG7388 induce the expression of *MDM2*, *TP53INP1* and *PUMA* genes. The increase in *PUMA* indicated that RG7388 as a single agent drives the CLL cells towards apoptosis. The increases in the regulators of TP53 signalling, *MDM2* and *TP53INP1*, potentially have opposing effects (Figure 7.14). *MDM2* is a negative regulator of *TP53*, whereas *TP53INP1* is reported to be a positive anti-proliferative and proapoptotic protein. Furthermore, the combination of WIP1 inhibitor with RG7388 increased the expression of *MDM2* and *TP53INP1* which indicated increased activation of TP53 in CLL cells. In addition, the pro-apoptotic genes, *PUMA*, *BAX* and *FAS* were further induced with WIP1 inhibitor in combination of RG7388. It was evident that CLL cells were increasingly pushed toward apoptosis with WIP1 inhibitor in a combination with RG7388 in the absence of BCR stimulation signals (Figure 7.17 A&B).

In immobilised Anti-IgG antibody stimulation, the fold changes in expression of *MDM2*, *BAX* and *PUMA* were increased with RG7388 treatment alone and the combination of WIP1 inhibitor further increased the expression of these genes, as well as resulting in a significant induction of *FAS* (Figure 7.18).

With immobilised Anti-IgM antibody stimulation, *MDM2*, *FAS* and *PUMA* showed an increase in expression in response to RG7388 treatment relative to the DMSO control and the addition of WIP1 inhibitor further increased their expression, and *BAX* additionally became further induced (Figure 7.19).

Our results supported the data of Bernal *et al*, who showed apoptosis inhibition and induction of *BCL2* and *MCL1* by blocking PI3-K pathway, a critical mediator of signals through the engagement of antigen surface IgM receptor (Bernal et al., 2001). In addition, Deglesne et al. showed that immobilized antibody stimulation signals promoted resistance against spontaneous apoptosis cascade in *ex-vivo* microenvironmental modelling experiments with B-CLL cells over a period of 3 days (Deglesne et al., 2006).

Guarini et al. found that upon the Anti-IgM ligation with BCR, a limited set of genes were involved in upregulation of the apoptosis pathway in U-CLL cells. These genes are *EGR3*, *NR4A1*, *DUSP4*, *LRMP* and *CD39*. Thus, apoptosis may occur in a small population upon IgM stimulation (Guarini et al., 2008).

Further studies identified increases in anti-apoptotic gene expression levels upon IgM stimulation, associated with the TNF (tumour necrosis factor) and NFKB signalling pathways. The upregulation of specific genes including, CD40, TRAF (TNF receptor-associated factor), and TNFAIP3 (a gene involved in the negative regulation of the NFKB pathway), indicates that these genes play a role in inhibiting apoptosis (Chung et al., 2002; E. G. Lee et al., 2000). These findings suggested that IgM stimulation plays a role in promoting the survival of U-CLL cells. On the other hand, in M-CLL, no induction in anti-apoptotic signals was triggered by IgM stimulation.

Other studies have reported that IgM stimulation increases the apoptotic pathway in CLL samples compared to normal healthy B-cells. In addition, unexpected upregulation of pro-apoptotic genes in CLL samples from patients with aggressive disease compared with normal B-cells were also reported. This might be due to the heterogeneity of CLL samples or short time periods of CLL stimulation with IgM antibody (Chung et al., 2002; Aggarwal, 2003).

In summary, Anti-IgM stimulation through BCR had a protective effect on CLL cells in the absence of RG7388 and made them more resistance to RG7388 treatment. However, WIP1 inhibition had no significant effect under any of these conditions, apart from a small potentiation effect on RG7388 responses at 3μM in the presence of IgM stimulation.

Chapter 8: Conclusions and future directions

8.1 Conclusions

Despite the advances made in the treatment of CLL over the last fifteen years, it remains an incurable disease for the majority of patients. With the discovery of novel targeted treatments, such as ibrutinib and venetoclax, treatment is becoming more personalised however, there is still a need to unravel the molecular mechanisms behind the disease in order to develop more effective targeted treatment options. Therefore, the aims of this thesis were to determine the response of haematological cell lines and primary CLL patient derived samples to small molecule MDM2 inhibitors as single agents and in combination with a WIP1 inhibitor GSK2830371, and to investigate the potential effect of *in-vivo* microenvironmental factors on these responses by modelling these factors *ex-vivo*.

Microenvironment signals play a critical role in promoting CLL disease progression, survival, proliferation, and resistance to therapies. In this study, different microenvironment factors were modelled *ex-vivo* to mimic some of the potential surrounding interaction factors that can influence CLL cell proliferation and survival once they have migrated to the lymph nodes.

These microenvironment signals can be mediated through cell adhesion molecules, such as CD40L (Chapter 5), cytokines IL-4 (Chapter 6), BCR (immobilised IgM antibodies) (Chapter 7), and other factors produced by other cellular components within the microenvironment including, but not limited to, T cells.

Interaction between CLL cells and T cells in the microenvironment can trigger signalling pathways that activate survival and proliferation signals, including the BCR pathway, NF-κB, and PI3K pathway. These pathways promote CLL cell survival and proliferation which contributes to disease progression and inhibition of apoptosis.

Furthermore, the microenvironment signals can also influence CLL cell viability and response to therapies. The interactions between the microenvironment and CLL cells activate survival cascades, leading to treatment resistance (Crassini et al., 2017; Pedersen & Reed, 2004).

Understanding the *ex-vivo* microenvironment signalling in CLL is necessary to improve the development of targeted therapies that can disrupt these interactions and enhance the effectiveness of treatments. Targeting specific signalling pathways or disrupting the interactions between CLL cells and the microenvironment, may offer new therapeutic strategies to overcome treatment resistance and improve patient outcomes in CLL.

One such targetable signalling pathway of interest is the MDM2/TP53/PPM1D signalling network. Throughout this thesis, the response of both haematological B-cell lines (Chapter 3) and primary CLL patient samples (Chapter 4) to small molecule MDM2 inhibition, alone and in combination with a WIP1 inhibitor, were investigated.

8.1.1 WIP1 inhibitor potentiated the stabilization of functional TP53 in response to MDM2 inhibitor in B-cell lines and primary CLL cells

Consistent with the findings reported by Gilmartin et al. in 2014, this study revealed that the WIP1 inhibitor, GSK2830371, exhibited a dual impact on WIP1 protein inhibition. This compound not only suppressed the enzymatic activity of WIP1, as demonstrated by an increase in phosphorylated p53 (Ser15) levels, which serves as a substrate for WIP1 phosphatase, following WIP1 inhibitor treatment, but also facilitated the degradation of WIP1 protein, as evidenced by a decrease in WIP1 protein expression subsequent to WIP1 inhibitor treatment. The dual effects of the WIP1 inhibitor are of particular significance in preventing the reactivation of WIP1 through p53 stabilization following treatment with an MDM2 inhibitor.

It was clearly identified that the WIP1 inhibitor potentiated p53 stabilisation observed with MDM2 inhibitors (RG7388 and HDM201) in wild type *TP53* leukaemia B-cell lines (Nalm-6 and OCI-Ly3) and heterozygous NALM-6$^{(-/+)}$ with one functional allele of *TP53* to sub-micromolar concentrations of the clinically relevant MDM2 inhibitors (Chapter 3). Potentiation of RG7388 induced cytotoxicity by WIP1 inhibition was also shown for the *ex-vivo* primary non-proliferative CLL cells at sub-micromolar concentrations. Several studies from our group and by others have confirmed that the combination of WIP1 inhibitor (GSK2830371) potentiates the growth inhibitory and cytotoxic activity of RG7388 across a wide range of cancer cell types in a p53 dependent manner by increasing the phosphorylation of p53(Esfandiari et al., 2016). Our group have gone on to show this leads to the increased growth inhibition of liver adenocarcinoma cells (Wu et al., 2021), uterine Leiomyosarcoma (uLMS) (Chamberlain et al., 2021), and cutaneous and uveal melanoma (Wu et al., 2018).

In the current study, the viability of the cells was determined using the XTT assay and supporting evidence of on-target mechanism was provided by the prominent stabilisation of p53 and the increase in *TP53* downstream transcriptional targets by western blot analysis.

Addition, mechanistic evidence was provided by measuring the difference in mRNA levels for a panel of *TP53* transcriptional target genes.

MDM2 inhibitor (RG7388) as a single agent induces stabilisation of TP53 and increases in downstream target gene protein levels, including MDM2. Furthermore, combination with WIP1 inhibitor enhanced the induction of TP53 target gene protein levels. Moreover, cPARP protein was induced to a greater extent with WIP1 inhibitor combination compared to RG7388 alone, showing that the combination treatment drove both haematological functional TP53 cell lines and the non-proliferative primary CLL cells into apoptosis (Chapter 3 and Chapter 4).

Furthermore, the GSK2830371 in a combination with RG7388 was associated with increased upregulation of pro-apoptotic genes (*PUMA*, *BAX, NOXA* and *FAS*) in functional *TP53* NALM-6 cells and *ex-vivo* non-proliferative CLL cells. In addition, the p53-dependent genes, *MDM2*, *TP53INP1* and *CDKN1A* were induced to a greater extent with GSK2830371 and RG7388 in combination compared with the response to RG7388 alone. Similar findings were reported by Wu et al. for the combination treatment of cutaneous melanoma cell lines with RG7388 and GSK2830371 (Wu et al., 2018). Chamberlain et al also reported in her study of $p53^{WT}$ uLMS cells that the mRNA expression of coupled pro-apoptotic genes, *PUMA*, *FAS* and *NOXA* were increased, consistent with the increased p53 transcriptional activity pushing the cells into apoptosis (Chamberlain et al., 2021). All the results in the current study on B-cells and CLL supported further evaluation of the therapeutic use of WIP1inhibitor in combination with MDM2 inhibitors for patients with wild type *TP53* CLL.

Conversely, for the $TP53^{MUT}$ NALM-6 cell line there was a no detectable change in the level of p53 stabilisation activity in response to treatment with MDM2 inhibitor (RG7388 and HDM201) up to (10μM) and the cells were resistant to the antiproliferative and cytotoxic effect of the MDM2 inhibitors, showing these effects to be mediated by wild-type functional TP53 (Drummond et al., 2016). Similar observations were reported through our group by Aptullahoglu for $p53^{MUT}$ Ramos and Raji cell lines that showed no detectable change in the p53 protein levels nor any increase in the transcriptional target gene products of *MDM2* and $p21^{WAF1}$, in response to treatment with RG7388, HDM201 and Nutlin-3a (Aptullahoglu, 2018).

However, the combination of GSK2830371 with RG7388 significantly potentiated the stabilisation activity of functional wild type p53 in response to RG7388 and HDM201 with concentration dependent inhibition manner. In addition, increases the mRNA expression of

genes regulated by p53 transcription in functional p53 ($p53^{WT}$) cell lines as reported in (Wu et al., 2018; Chamberlain et al., 2021).

The results obtained from the B-cell lines (Chapter 3) provided evidence of the specificity and efficacy of the WIP1 inhibitor to potentiate the stabilisation and activation of TP53 in response to second generation MDM2 inhibitors currently in clinical trial for a range of malignancies.

The novel finding of the current study is that this is the first investigation of a WIP1 inhibitor used in combination with a second generation RG7388 on primary CLL patient samples. XTT cytotoxicity assay and western blot results indicated that the combination of WIP1 inhibitor significantly potentiated the response to RG7388 of functional *TP53* CLL cells at sub-micromolar and hence clinically achievable concentrations. This is an exciting observation as it has the potential to provide an alternative treatment for relapsed CLL. However, it would be important to establish whether there is a therapeutic advantage of the combination treatment without increasing any dose limiting cytotoxicity associated with MDM2 inhibitors.

8.1.2 The effect of ex-vivo modelling of microenvironment signals on the response to MDM2 and WIP1 inhibition

The microenvironment plays a crucial role in CLL cell progression and therapeutic responses. This study investigated the *ex-vivo* effect of GSK2830371 in combination with the MDM2 inhibitor RG7388 on CLL cells, and how this response might be affected by microenvironmental factors signals for CLL cells. The main types of microenvironment signals which impact on CLL cell survival and proliferation within the lymph node, that were modelled *ex-vivo* in this study, included CD40L, IL-4 and BCR signalling.

8.1.2.1 The effect of co-culture with CDL40/IL-4 on primary CLL cells

Mouse fibroblast cells expressing CD40L on their surface were used to support the survival and proliferation of CLL cells. In addition, IL-4 was included to enhance the survival and proliferation signals.

The result showed that CD40L/CD40 interaction stimulated the proliferation of CLL cells although, the CLL cells co-cultured with CD40L/IL-4 become more sensitive to RG7388 with GI_{50} doses of (0.03μM ± 0.01) compared to NTL/IL-4 co-cultured (0.064μM ± 0.015) (Table 5.3). CLL cells co-cultured with CD40L could not proliferate under the effect of RG7388 exposure. RG7388 prevent the CLL cell number to get increased under the influence of CD40L/IL-4 co-culture relative to the DMSO untreated condition. RG7388 inhibited the proliferation activity of wild type *TP53* CLL cells co-cultured with CD40L and IL-4 signals (Figure 5.12 and Figure 5.13). In contrast, CLL cells co-cultured with NTL, parental mouse cells not expressing CD40, in the presence of IL-4 produced a protective effect and increased survival in response to RG7388 treatment. Thus, the effect of IL-4 signals on CLL cells was investigated. Consistent with the results reported by Ciardullo et al that co-culturing CLL cells with moused fibroblast expressing CD40L, with the addition of IL-4 significantly reduced the spontaneous apoptosis of CLL cells and induces their proliferation, and also that RG7388 inhibited the proliferation of CD40L/IL4 stimulated CLL cells (Ciardullo et al., 2019).

In my study, further investigation was performed on the mRNA expression of *TP53* target genes in response to a combination of WIP1 and MDM2 inhibitors. *TP53* negative regulator genes (*MDM2*, *CDKN1A*) were induced with the combination of GSK2830371 with RG7388 compared to the effect of RG7388 alone in the presence of CD40L/IL-4 stimulation. Moreover, along with the combination treatment in the presences of CD40L/IL-4 stimulation, the expression of the pro-apoptotic genes, *PUMA*, *BAX* and *NOXA* were induced indication the CLL cells undergo for apoptosis (Figure 5.26 and Figure 5.27).

It was previously identified that CD40 signalling has a role in regulating the expression of multiple genes encoding antiapoptotic proteins, such as BCL-xL, cIAP2, and A20 (Craxton et al., 1998; Z. Wan et al., 1995). Several studies have shown that, in CLL cells activated by CD40L, multiple genes associated with increased antiapoptotic activity, including *CFLAR* (*FLIP*), *TRAF1*, *BIRC3* (*cIAP2*), and *TNFAIP3* (*A20*), exhibit significantly higher expression levels compared to activated healthy B-cells. Notably, *CFLAR* (*FLIP*) functions by suppressing Fas-mediated apoptosis through interference with the activation of pro-caspase 8 at the level of the death-inducing signalling complex (DISC) (Thome & Tschopp, 2001). Moreover, it was reported by Eldering et al, that *NOXA* expression was reduced in *ex-vivo* CD40L stimulation of CLL cells (Smit et al., 2007).

In my results, it was demonstrated that RG7388 decreases the expression of pro-apoptotic genes, *PUMA*, *BAX* and *NOXA* for CLL stimulated by CD40L/IL-4 however, the combination

of WIP1 inhibitor induces those genes expression leading the CLL cells to undergo apoptosis. Interestingly, MDM2 inhibitor (RG7388) could overcome and inhibit the proliferation and survival signals (anti-apoptotic) of CD40L/IL-4 in stimulated CLL cells (Figure 5.26 and Figure 5.27).

In contrast, looking to the mRNA expression of *MDM2*, *CDKN1A* with NTL/IL-4, it obviously seen that the combination treatment of WIP1 and MDM2 induced compared to RG7388 alone. In addition, the pro-apoptotic genes were also induced with combination treatment of WIP1 and MDM2 inhibitors in the presence of NTL/IL-4 stimulation. This means the WIP1 inhibitor has the ability to potentiate wild-type TP53 stabilization in the presence of both CD40L and IL-4 microenvironment signals, despite the protective effect of these microenvironmental factors.

8.1.2.2 The effect of IL-4 on primary CLL cells

To determine its individual contribution, experiments were also conducted to investigate the effect of IL-4 alone on the response to MDM2 and WIP1 inhibitor treatment. IL-4 can provide signalling that supports *ex-vivo* survival of B-cells by itself but without increasing their cell division or proliferation (Seda et al., 2021; Dancescu et al., 1992). However, for CLL cell proliferation to occur, pre-activation of the CD40 pathway or simultaneous stimulation is required (Granziero et al., 2001; Néron et al., 2011). It is worth noting that IL-4 also stimulates the production of anti-apoptotic proteins, including MCL1, in CLL cells (Dancescu et al., 1992). Additionally, IL4 plays a role in enhancing the expression of surface IgM (Aguilar-Hernandez et al., 2016; Guo et al., 2016) and CD20 both of which are relevant to BCR signalling (Sandova et al., 2021).

8.1.2.3 The effect of Anti-IgM induced BCR signalling on primary CLL cells

In CLL cells, both IL-4 and stimulation of BCR signalling initiate the activation of pathways that promote cell survival and resistance to spontaneous cell apoptosis. Stimulation of the CLL cells through the BCR or IL-4 signalling pathways can have synergistic effects on the survival and progression of CLL cells and resistance to therapy.

Several studies identified that BCR and IL-4 signalling increased CLL cell survival and resistance to apoptosis. This suggests cooperative involvement of signalling activation pathways or the modulation of downstream targets by both BCR and IL-4 signalling (Parada et al., 1984; Burger & Chiorazzi, 2013; ten Hacken et al., 2019).

The impact of IL-4 signalling on the survival of CLL cells is significant. Binding of IL-4 cytokine with its receptors on CLL cells, IL-4 activates downstream signalling pathways that promote cell survival. IL-4 upregulates the expression of *MCL1*, anti-apoptotic gene that enhance CLL cells survival (Herishanu, Gibellini, et al., 2011).

In the current study both IL-4 (Figure 6.4) and immobilised anti-IgM antibody (Figure 7.2) signals significantly increase the viability of the primary CLL cells relative to the non-stimulated, leading to induce the survival and proliferation of the CLL cells, which was determined by XTT sassy. In addition, both IL-4 (Figure 6.14) and immobilised anti-IgM antibody (Figure 7.9) stimulated CLL cells to become less sensitive to treatment with RG7388 alone and in combination with WIP1 inhibitor compared to non-stimulated CLL cells.

For the majority of wild type *TP53* CLL cell samples the IC_{50} inhibition was not reached in response to either RG7388 alone or in combination with GSK2830371in the presence of IL-4 (Figure 6.15) and anti-IgM antibody (Figure 7.10) stimulation in comparison to the non-stimulated CLL cells (control). Nevertheless, WIP1 inhibitor potentiated the effect of RG7388 on the CLL sample cohort despite not achieve the LC_{50} in the presence of IL-4 or anti-IgM antibody signals. Thus, the potentiation of WIP1 inhibitor with RG7388 treatment were measured by identifying the LC_{70} inhibition effect on CLL with IL-4 signalling and the ratio of effect for a given dose with anti-IgM antibody stimulation.

In the presence of IL-4, the downstream increase of TP53 target proteins was induced with RG7388 and further increased with WIP1 inhibitor combination. In addition, the cPARP protein level was reduced in the presence of IL-4 in response to both RG7388 alone and in combination with WIP1 inhibitor. In contrast, in the absence of IL-4 the expression of cPARP protein apoptotic marker was detected with RG7388 and further increased with the combination of WIP1 inhibitor (Figure 6.16).

Consistent with our finding results, Murata reported that in *ex-vivo* experiments with B-cells, the binding of IL-4 molecules to the IL-4 receptor activates JAK1/3-mediated phosphorylation of STAT6 (pSTAT6) which induces the expression of genes involved in tumour cell survival, metastasis and proliferation (Murata et al., 1998).

In along with this, the *TP53* negative regulator genes expression of *MDM2*, *PPM1D* and *CDKN1A* were induced with IL-4 signals in response to the combination treatment of RG7388 and GSK2830371 (Figure 6.34). In comparison, with immobilised anti-IgM antibody stimulation, *MDM2* showed fold changes increases as a *TP53* dependent negative regulator gene (Figure 7.17).

Looking to the fold changes in mRNA expression level, the pro-apoptotic genes, *PUMA* and *FAS* were highly increased in the CLL samples stimulated with immobilised anti-IgM antibody in response to RG7388 and WIP1 inhibitor combination compared to control (Figure 7.18 and Figure 7.19).

In contrast, in the presence of IL-4, *CDKN1A*, *MDM2*, *PPM1D* and the pro-apoptotic genes (*PUMA*, *BAX*, *NOXA*) genes expression were increased in CLL samples in response to combination treatment with RG7388 and GSK2830371 (Figure 6.32).

In this study the anti-apoptotic gene expression of BCL family either *MCL1* or *BCL2* did express fold change differences in their mRNA expression level neither with any of the microenvironment stimulations (CD40L, IL-4 and Anti-IgM) in response to RG7388 and in combination with WIP1 inhibitor. Our finding is similar to the Ciardullo reported in our group previous study (Ciardullo et al., 2019).

Andrew Steele and his group suggested that the IL-4 signalling pathway augments BCR signalling and promote B-cell proliferation and survival, especially within the U-CLL patient sample subset. In their study, they found IL-4 decreases the inhibitory effects of idelalisib or ibrutinib on anti-IgM–induced signalling and protects the CLL cells against BCR kinase inhibitor induced apoptosis (Aguilar-Hernandez et al., 2016). These protective effects are similar to what was observed in the current study for responses to MDM2 and WIP1 inhibitor treatment.

To sum up all the investigations, WIP1 inhibitor, GSK2830371, potentiated the activity of RG7388 and further stabilises protein and gene expressions of functional p53 for *in-vivo* primary CLL cell. GSK2830371 prevent the dephosphorylation mechanisms which keeps TP53 continue phosphorylated and active for CLL cells stabilisation. In addition, RG7388 prevents MDM2 from targeting p53 for degradation which keeps p53 levels high to regulate genes involved in the CLL cell cycle arrest and apoptosis.

In contrast, with *ex-vivo* microenvironment stimulation, CD40L, IL-4 and Anti-IgM, the primary CLL cells become more metabolically active and less sensitive in responses to the

RG7388 and WIP1 inhibitor. Although, WIP1 inhibitor had lower potentiation effect on RG7388 activity in the presence of stimulation, however, CLL cells was showing concentration dependent inhibition manner in response to the treatment.

In *ex-vivo* experiment, the combination of GSK2830371 with RG7388 enhances p53 stabilization and transcriptional activity in TP53 wild-type B-cell lines and primary CLL cells. This effect promotes apoptosis in CLL cells through the upregulation of pro-apoptotic genes such as *PUMA*, *BAX*, *NOXA*, and *FAS*.

With CD40L/IL-4 co-culture, CLL cells become more sensitive to RG7388 compared to the absence of CD40L/IL-4 mouse fibroblast cells. The IC_{50} of RG7388 in CLL cells co-culture with CD40L/IL-4 is (0.03μM ± 0.01), while the IC50 of RG7388 in non-stimulated *ex-vivo* CLL cells is (0.71μM ± 0.23). The combination of GSK2830371 further potentiates the effect of RG7388, reducing the IC_{50} to (0.28μM ± 0.02). In contrast, IL-4 and immobilised Anti-IgM antibody stimulation increase the basal metabolic activity of the CLL cells making the CLL cells more viable compared to non-stimulated CLL cells. Thus, CLL cells become less sensitive to RG7388 and the CLL cells could not achieve the IC_{50}. The combination of GSK2830371 enhances the activity of RG7388 and producing adverse negative effect against the mechanism of IL-4 and immobilised Anti-IgM antibody stimulations.

Looking at mRNA expression, the combination of GSK2830371 with RG7388 further induces the expression of *TP53* negative regulator genes (*MDM2*, *CDKN1A*) and pro-apoptotic genes (*PUMA*, *BAX*, *NOXA*) relative to the effect of RG7388 alone in response to the CLL cells co-cultured with CD40L/IL-4. Conversely, the presence of IL-4 increases the expression of *TP53* negative regulator genes (*MDM2*, *CDKN1A, PPM1D*) and pro-apoptotic genes (*PUMA*, *BAX*, *NOXA*) in response to the combination of GSK2830371 with RG7388. However, the expression of *PUMA* and *BAX* is reduced, while *FAS* is induced in response to the combination of GSK2830371 with RG7388 for CLL cells in the presence of immobilised Anti-IgM antibody stimulation.

Over all, the combination of GSK2830371 with RG7388 generate significant promise in targeting the p53 pathway in CLL, potentially leading to more effective treatment options for patients, particularly those with resistant forms of the disease due to longer remission times or TP53 mutations. By enhancing TP53 pathway activity, the treatment could lead to longer remission times and improved patient outcomes. Furthermore, CLL cells co-cultured with CD40L/IL-4 increased the sensitivity to RG7388. This will give chance that the combination

of GSK2830371 with RG7388 could have more potentiation effect on CLL cell which were migrated to lymph node or T cells.

8.1.3 Future works

1. CLL patients often develop resistance to targeted therapies over time. Therefore, it is important to use the *ex-vivo* model system to test the effect of microenvironmental factors on the response to MDM2 and WIP1i combination on CLL samples from patients who have become resistant to prior treatments, as well as those who experience relapse or remain in remission following previous therapies.
2. Use the *ex-vivo* response model to identify CLL patients that are more likely to show greater potentiation of MDM2-p53 binding antagonists by WIP1 inhibitors in the presence of protective microenvironment factors. Investigate the relationship of these responses to clinical and pathology variables.
3. Next-generation sequencing and single-cell RNA sequencing could be used to identify genetic profiles and mutations as potential biomarkers of treatment response. This will give better understanding of the heterogeneity of CLL cell populations and how it relates to the response to combination treatment.
4. Investigate the potential synergistic effects of MDM2 inhibitor treatment with other established and evolving CLL therapies such as the use of BTK inhibitors to inhibit B cell receptor signalling
5. Target p53-independent pathways simultaneously, such as PI3K and BCL-2 inhibitors, to target *TP53* mutant subpopulations which would be resistant to MDM2 and WIP1 inhibitor combinations.
6. Investigate apoptotic end points in CLL cells in response to WIP1 and MDM2 inhibitor treatment using Caspase-glo 3/7 assay and FACS-based AnnexinV and propidium iodide staining assays.
7. Determine the effect of MDM2 inhibitor and GSK2830371 combination treatment on normal dose limiting tissues, including CD34+ stem cells to establish whether there is a therapeutic advantage in the treatment combinations.
8. Currently there are no WIP1 inhibitors suitable for clinical evaluation. Until recently this has been held back by the lack of an atomic resolution X-ray crystal structure of WIP1. This is an active area of drug development research in the Newcastle.

References

Abdel-Ghafar, A.A.A., El Telbany, M.A.S.E.D., Mahmoud, H.M. & El-Sakhawy, Y.N. (2012) 'Immunophenotyping of chronic B-cell neoplasms: flow cytometry versus immunohistochemistry', *Hematology reports*, 4(1), pp. 6–11.

Aggarwal, B.B. (2003) 'Signalling pathways of the TNF superfamily: a double-edged sword', *Nature reviews. Immunology*, 3(9), pp. 745–756.

Aguilar-Hernandez, M.M., Blunt, M.D., Dobson, R., Yeomans, A., Thirdborough, S., Larrayoz, M., Smith, L.D., Linley, A., Strefford, J.C., Davies, A., Johnson, P.M.W., Savelyeva, N., Cragg, M.S., Forconi, F., Packham, G., Stevenson, F.K. & Steele, A.J. (2016) 'IL-4 enhances expression and function of surface IgM in CLL cells', *Blood*, 127(24), pp. 3015–3025.

Almasri, N.M., Duque, R.E., Iturraspe, J., Everett, E. & Braylan, R.C. (1992) 'Reduced expression of CD20 antigen as a characteristic marker for chronic lymphocytic leukemia', *American journal of hematology*, 40(4), pp. 259–263.

Amin, R.H. & Schlissel, M.S. (2008) 'Foxo1 directly regulates the transcription of recombination-activating genes during B cell development', *Nature immunology*, 9(6), pp. 613–622.

Anderson, M.A., Deng, J., Seymour, J.F., Tam, C., Kim, S.Y., Fein, J., Yu, L., Brown, J.R., Westerman, D., Si, E.G., Majewski, I.J., Segal, D., Heitner Enschede, S.L., Huang, D.C.S., Davids, M.S., Letai, A. & Roberts, A.W. (2016) 'The BCL2 selective inhibitor venetoclax induces rapid onset apoptosis of CLL cells in patients via a TP53-independent mechanism', *Blood*, 127(25), pp. 3215–3224.

Andreeff, M., Kelly, K.R., Yee, K., Assouline, S., Strair, R., Popplewell, L., Bowen, D., Martinelli, G., Drummond, M.W., Vyas, P., Kirschbaum, M., Padmanabhan Iyer, S., Ruvolo, V., Nogueras Gonz Alez, G.M., Huang, X., Graves, B., Blotner, S., Bridge, P., Jukofsky, L., et al. (2016) 'Cancer Therapy: Clinical Results of the Phase I Trial of RG7112, a Small-Molecule MDM2 Antagonist in Leukemia', *Clinical cancer research : an official journal of the American Association for Cancer Research*, 22(4), pp. 868–76.

Ang, H.C., Joerger, A.C., Mayer, S. & Fersht, A.R. (2006) 'Effects of common cancer mutations on stability and DNA binding of full-length p53 compared with isolated core domains', *The Journal of biological chemistry*, 281(31), pp. 21934–21941.

Apollonio, B., Scielzo, C., Bertilaccio, M.T.S., Ten Hacken, E., Scarfò, L., Ranghetti, P., Stevenson, F., Packham, G., Ghia, P., Muzio, M. & Caligaris-Cappio, F. (2013) 'Targeting B-cell anergy in chronic lymphocytic leukemia', *Blood*, 121(19), pp. 3879–3888.

Aptullahoglu, E., Ciardullo, C., Wallis, J.P., Marr, H., Marshall, S., Bown, N., Willmore, E. & Lunec, J. (2023) 'Splicing Modulation Results in Aberrant Isoforms and Protein Products of p53 Pathway Genes and the Sensitization of B Cells to Non-Genotoxic MDM2 Inhibition', *International journal of molecular sciences*, 24(3), .

Aptullahoglu, E., Wallis, J.P., Marr, H., Marshall, S., Bown, N., Willmore, E. & Lunec, J. (2023) 'SF3B1 Mutations Are Associated with Resistance to Non-Genotoxic MDM2

Inhibition in Chronic Lymphocytic Leukemia', *International Journal of Molecular Sciences*, 24(14), p. 11335.

Araki, S., Eitel, J.A., Batuello, C.N., Bijangi-Vishehsaraei, K., Xie, X.J., Danielpour, D., Pollok, K.E., Boothman, D.A. & Mayo, L.D. (2010) 'TGF-beta1-induced expression of human Mdm2 correlates with late-stage metastatic breast cancer', *The Journal of clinical investigation*, 120(1), pp. 290–302.

Arana, E., Vehlow, A., Harwood, N.E., Vigorito, E., Henderson, R., Turner, M., Tybulewicz, V.L.L.J. & Batista, F.D. (2008) 'Activation of the small GTPase Rac2 via the B cell receptor regulates B cell adhesion and immunological-synapse formation', *Immunity*, 28(1), pp. 88–99.

Austen, B., Powell, J.E., Alvi, A., Edwards, I., Hooper, L., Starczynski, J., Taylor, A.M.R., Fegan, C., Moss, P. & Stankovic, T. (2005) 'Mutations in the ATM gene lead to impaired overall and treatment-free survival that is independent of IGVH mutation status in patients with B-CLL', *Blood*, 106(9), pp. 3175–3182.

Aziz, M.H., Shen, H. & Maki, C.G. (2011) 'Acquisition of p53 mutations in response to the non-genotoxic p53 activator Nutlin-3', *Oncogene*, 30(46), pp. 4678–4686.

Bagnara, D., Kaufman, M.S., Calissano, C., Marsilio, S., Patten, P.E.M., Simone, R., Chum, P., Yan, X.J., Allen, S.L., Kolitz, J.E., Baskar, S., Rader, C., Mellstedt, H., Rabbani, H., Lee, A., Gregersen, P.K., Rai, K.R. & Chiorazzi, N. (2011) 'A novel adoptive transfer model of chronic lymphocytic leukemia suggests a key role for T lymphocytes in the disease', *Blood*, 117(20), pp. 5463–5472.

Baker, S.J., Fearon, E.R., Nigro, J.M., Hamilton, S.R., Preisinger, A.C., Jessup, J.M., Vantuinen, P., Ledbetter, D.H., Barker, D.F., Nakamura, Y., White, R. & Vogelstein, B. (1989) 'Chromosome 17 deletions and p53 gene mutations in colorectal carcinomas', *Science (New York, N.Y.)*, 244(4901), pp. 217–221.

Banchereau, J., Bazan'·, F., Blanchard, D., Briere, F., Galizzi, J.P., Van Kooten, C., Liu, Y.L., Rousset, F. & Saeland, S. (1994) *THE CD40 ANTIGEN AND ITS LIGAND*,

Banchereau, J., Blanchard, D., Brière, F., Galizzi, J.P., Garrone, P., Hermann, P., Lebecque, S. & Rousset, F. (1993) 'Role of cytokines in human B lymphocyte growth and differentiation.', *Nouvelle revue francaise d'hematologie*, 35(1), pp. 61–6.

Banin, S., Moyal, L., Shieh, S.Y., Taya, Y., Anderson, C.W., Chessa, L., Smorodinsky, N.I., Prives, C., Reiss, Y., Shiloh, Y. & Ziv, Y. (1998) 'Enhanced phosphorylation of p53 by ATM in response to DNA damage', *Science (New York, N.Y.)*, 281(5383), pp. 1674–1677.

Bargonetti, J., Friedman, P.N., Kern, S.E., Vogelstein, B. & Prives, C. (1991) 'Wild-type but not mutant p53 immunopurified proteins bind to sequences adjacent to the SV40 origin of replication', *Cell*, 65(6), pp. 1083–1091.

Bartel, F., Taubert, H. & Harris, L.C. (2002) 'Alternative and aberrant splicing of MDM2 mRNA in human cancer', *Cancer Cell*, 2(1), pp. 9–15.

Bazargan, A., Tam, C.S. & Keating, M.J. (2012) 'Predicting survival in chronic lymphocytic leukemia', *Expert review of anticancer therapy*, 12(3), pp. 393–403.

Begleiter, A., Mowat, M., Israels, L.G. & Johnston, J.B. (1996) 'Chlorambucil in chronic lymphocytic leukemia: mechanism of action', *Leukemia & lymphoma*, 23(3–4), pp. 187–201.

Bernal, A., Pastore, R.D., Asgary, Z., Keller, S.A., Cesarman, E., Liou, H.C. & Schattner, E.J. (2001) 'Survival of leukemic B cells promoted by engagement of the antigen receptor', *Blood*, 98(10), pp. 3050–3057.

Berndt, S.I., Skibola, C.F., Joseph, V., Camp, N.J., Nieters, A., Wang, Z., Cozen, W., Monnereau, A., Wang, S.S., Kelly, R.S., Lan, Q., Teras, L.R., Chatterjee, N., Chung, C.C., Yeager, M., Brooks-Wilson, A.R., Hartge, P., Purdue, M.P., Birmann, B.M., et al. (2013) 'Genome-wide association study identifies multiple risk loci for chronic lymphocytic leukemia', *Nature genetics*, 45(8), pp. 868–876.

Berridge, M. V., Herst, P.M. & Tan, A.S. (2005) 'Tetrazolium dyes as tools in cell biology: New insights into their cellular reduction', *Biotechnology Annual Review*, 11(SUPPL.), pp. 127–152.

Bhattacharya, N., Reichenzeller, M., Caudron-Herger, M., Haebe, S., Brady, N., Diener, S., Nothing, M., Döhner, H., Stilgenbauer, S., Rippe, K. & Mertens, D. (2015) 'Loss of cooperativity of secreted CD40L and increased dose-response to IL4 on CLL cell viability correlates with enhanced activation of NF-kB and STAT6.', *International journal of cancer*, 136(1), pp. 65–73.

Binet, J.L., Auquier, A., Dighiero, G., Chastang, C., Piguet, H., Goasguen, J., Vaugier, G., Potron, G., Colona, P., Oberling, F., Thomas, M., Tchernia, G., Jacquillat, C., Boivin, P., Lesty, C., Duault, M.T., Monconduit, M., Belabbes, S. & Gremy, F. (1981) 'A new prognostic classification of chronic lymphocytic leukemia derived from a multivariate survival analysis.', *Cancer*, 48(1), pp. 198–206.

Bond, G.L., Hirshfield, K.M., Kirchhoff, T., Alexe, G., Bond, E.E., Robins, H., Bartel, F., Taubert, H., Wuerl, P., Hait, W., Toppmeyer, D., Offit, K. & Levine, A.J. (2006) 'MDM2 SNP309 accelerates tumor formation in a gender-specific and hormone-dependent manner', *Cancer research*, 66(10), pp. 5104–5110.

Brown, C.J., Lain, S., Verma, C.S., Fersht, A.R. & Lane, D.P. (2009) 'Awakening guardian angels: drugging the p53 pathway', *Nature reviews. Cancer*, 9(12), pp. 862–873.

Brown, J.R., Byrd, J.C., Coutre, S.E., Benson, D.M., Flinn, I.W., Wagner-Johnston, N.D., Spurgeon, S.E., Kahl, B.S., Bello, C., Webb, H.K., Johnson, D.M., Peterman, S., Li, D., Jahn, T.M., Lannutti, B.J., Ulrich, R.G., Yu, A.S., Miller, L.L. & Furman, R.R. (2014) 'Idelalisib, an inhibitor of phosphatidylinositol 3-kinase p110δ, for relapsed/refractory chronic lymphocytic leukemia', *Blood*, 123(22), pp. 3390–3397.

Brown, J.R., Eichhorst, B., Hillmen, P., Jurczak, W., Kaźmierczak, M., Lamanna, N., O'Brien, S.M., Tam, C.S., Qiu, L., Zhou, K., Simkovic, M., Mayer, J., Gillespie-Twardy, A., Ferrajoli, A., Ganly, P.S., Weinkove, R., Grosicki, S., Mital, A., Robak, T., et al. (2023) 'Zanubrutinib or Ibrutinib in Relapsed or Refractory Chronic Lymphocytic Leukemia', *The New England journal of medicine*, 388(4), pp. 319–332.

Brown, J.R., Harb, W.A., Hill, B.T., Gabrilove, J., Sharman, J.P., Schreeder, M.T., Barr, P.M., Foran, J.M., Miller, T.P., Burger, J.A., Kelly, K.R., Mahadevan, D., Ma, S., Li, Y., Pierce, D.W., Barnett, E., Marine, J., Miranda, M., Azaryan, A., et al. (2016) 'Phase I study of

single-agent CC-292, a highly selective Bruton's tyrosine kinase inhibitor, in relapsed/refractory chronic lymphocytic leukemia', *Haematologica*, 101(7), pp. e295–e298.

Brugarolas, J., Chandrasekaran, C., Gordon, J.I., Beach, D., Jacks, T. & Hannon, G.J. (1995) 'Radiation-induced cell cycle arrest compromised by p21 deficiency', *Nature*, 377(6549), pp. 552–557.

Buccheri, V., Barreto, W.G., Fogliatto, L.M., Capra, M., Marchiani, M. & Rocha, V. (2018) 'Prognostic and therapeutic stratification in CLL: focus on 17p deletion and p53 mutation', *Annals of hematology*, 97(12), pp. 2269–2278.

Buggins, A.G.S., Pepper, C., Patten, P.E.M., Hewamana, S., Gohil, S., Moorhead, J., Folarin, N., Yallop, D., Thomas, N.S.B., Mufti, G.J., Fegan, C. & Devereux, S. (2010) 'Interaction with vascular endothelium enhances survival in primary chronic lymphocytic leukemia cells via NF-κB activation and de novo gene transcription', *Cancer Research*, 70(19), pp. 7523–7533.

Buhmann, R., Nolte, A., Westhaus, D., Emmerich, B. & Hallek, M. (1999) 'CD40-Activated B-Cell Chronic Lymphocytic Leukemia Cells for Tumor Immunotherapy: Stimulation of Allogeneic Versus Autologous T Cells Generates Different Types of Effector Cells', *Blood*, 93(6), pp. 1992–2002.

Bulavin, D. V., Demidov, O.N., Saito, S., Kauraniemi, P., Phillips, C., Amundson, S.A., Ambrosino, C., Sauter, G., Nebreda, A.R., Anderson, C.W., Kallioniemi, A., Fornace, A.J. & Appella, E. (2002) 'Amplification of PPM1D in human tumors abrogates p53 tumor-suppressor activity', *Nature Genetics 2002 31:2*, 31(2), pp. 210–215.

Bunz, F., Dutriaux, A., Lengauer, C., Waldman, T., Zhou, S., Brown, J.P., Sedivy, J.M., Kinzler, K.W. & Vogelstein, B. (1998) 'Requirement for p53 and p21 to sustain G2 arrest after DNA damage', *Science (New York, N.Y.)*, 282(5393), pp. 1497–1501.

Burger, J.A. (2011) 'Nurture versus nature: the microenvironment in chronic lymphocytic leukemia.', *Hematology. American Society of Hematology. Education Program*, 2011pp. 96–103.

Burger, J.A. & Chiorazzi, N. (2013) 'B cell receptor signaling in chronic lymphocytic leukemia', *Trends in immunology*, 34(12), pp. 592–601.

Burger, J.A. & Gandhi, V. (2009) 'The lymphatic tissue microenvironments in chronic lymphocytic leukemia: in vitro models and the significance of CD40-CD154 interactions.', *Blood*, 114(12), pp. 2560–1; author reply 2561-2.

Burger, J.A., Tedeschi, A., Barr, P.M., Robak, T., Owen, C., Ghia, P., Bairey, O., Hillmen, P., Bartlett, N.L., Li, J., Simpson, D., Grosicki, S., Devereux, S., McCarthy, H., Coutre, S., Quach, H., Gaidano, G., Maslyak, Z., Stevens, D.A., et al. (2015) 'Ibrutinib as Initial Therapy for Patients with Chronic Lymphocytic Leukemia', *New England Journal of Medicine*, 373(25), pp. 2425–2437.

Burger, J.A. & Wiestner, A. (2018) 'Targeting B cell receptor signalling in cancer: preclinical and clinical advances', *Nature reviews. Cancer*, 18(3), pp. 148–167.

Burgess, A., Chia, K.M., Haupt, S., Thomas, D., Haupt, Y. & Lim, E. (2016) 'Clinical overview of MDM2/X-targeted therapies', *Frontiers in Oncology*, 6(JAN), p. 7.

Burley, T.A., Kennedy, E., Broad, G., Boyd, M., Li, D., Woo, T., West, C., Ladikou, E.E., Ashworth, I., Fegan, C., Johnston, R., Mitchell, S., Mackay, S.P., Pepper, A.G.S. & Pepper, C. (2022) 'Targeting the Non-Canonical NF-κB Pathway in Chronic Lymphocytic Leukemia and Multiple Myeloma', *Cancers*, 14(6), .

Burnette, W.N. (1981) '"Western Blotting": Electrophoretic transfer of proteins from sodium dodecyl sulfate-polyacrylamide gels to unmodified nitrocellulose and radiographic detection with antibody and radioiodinated protein A', *Analytical Biochemistry*, 112(2), pp. 195–203.

Byrd, J.C., Brown, J.R., O'Brien, S., Barrientos, J.C., Kay, N.E., Reddy, N.M., Coutre, S., Tam, C.S., Mulligan, S.P., Jaeger, U., Devereux, S., Barr, P.M., Furman, R.R., Kipps, T.J., Cymbalista, F., Pocock, C., Thornton, P., Caligaris-Cappio, F., Robak, T., et al. (2014) 'Ibrutinib versus ofatumumab in previously treated chronic lymphoid leukemia', *The New England journal of medicine*, 371(3), pp. 213–223.

Byrd, J.C., Furman, R.R., Coutre, S.E., Burger, J.A., Blum, K.A., Coleman, M., Wierda, W.G., Jones, J.A., Zhao, W., Heerema, N.A., Johnson, A.J., Shaw, Y., Bilotti, E., Zhou, C., James, D.F. & O'Brien, S. (2015) 'Three-year follow-up of treatment-naïve and previously treated patients with CLL and SLL receiving single-agent ibrutinib', *Blood*, 125(16), pp. 2497–2506.

Byrd, J.C., Furman, R.R., Coutre, S.E., Flinn, I.W., Burger, J.A., Blum, K.A., Grant, B., Sharman, J.P., Coleman, M., Wierda, W.G., Jones, J.A., Zhao, W., Heerema, N.A., Johnson, A.J., Sukbuntherng, J., Chang, B.Y., Clow, F., Hedrick, E., Buggy, J.J., et al. (2013) 'Targeting BTK with ibrutinib in relapsed chronic lymphocytic leukemia', *The New England journal of medicine*, 369(1), pp. 32–42.

Byrd, J.C., Hillmen, P., Ghia, P., Kater, A.P., Chanan-Khan, A., Furman, R.R., O'Brien, S., Nuri Yenerel, M., Illés, A., Kay, N., Garcia-Marco, J.A., Mato, A., Pinilla-Ibarz, J., Seymour, J.F., Lepretre, S., Stilgenbauer, S., Robak, T., Rothbaum, W., Izumi, R., et al. (2021) 'Acalabrutinib Versus Ibrutinib in Previously Treated Chronic Lymphocytic Leukemia: Results of the First Randomized Phase III Trial', *Journal of clinical oncology : official journal of the American Society of Clinical Oncology*, 39(31), pp. 3441–3452.

Byrd, J.C., Hillmen, P., O'Brien, S., Barrientos, J.C., Reddy, N.M., Coutre, S., Tam, C.S., Mulligan, S.P., Jaeger, U., Barr, P.M., Furman, R.R., Kipps, T.J., Thornton, P., Moreno, C., Montillo, M., Pagel, J.M., Burger, J.A., Woyach, J.A., Dai, S., et al. (2019) 'Long-term follow-up of the RESONATE phase 3 trial of ibrutinib vs ofatumumab', *Blood*, 133(19), pp. 2031–2042.

Byrd, J.C., Woyach, J.A., Furman, R.R., Martin, P., O'Brien, S., Brown, J.R., Stephens, D.M., Barrientos, J.C., Devereux, S., Hillmen, P., Pagel, J.M., Hamdy, A., Izumi, R., Patel, P., Wang, M.H., Jain, N. & Wierda, W.G. (2021) 'Acalabrutinib in treatment-naive chronic lymphocytic leukemia', *Blood*, 137(24), pp. 3327–3338.

Caligaris-Cappio, F. (2003) 'Role of the microenvironment in chronic lymphocytic leukaemia', *British Journal of Haematology*, 123(3), pp. 380–388.

Caligaris-Cappio, F. & Ghia, P. (2008) 'Novel insights in chronic lymphocytic leukemia: are we getting closer to understanding the pathogenesis of the disease?', *Journal of clinical*

oncology : official journal of the American Society of Clinical Oncology, 26(27), pp. 4497–4503.

Calissano, C., Damle, R.N., Marsilio, S., Yan, X.J., Yancopoulos, S., Hayes, G., Emson, C., Murphy, E.J., Hellerstein, M.K., Sison, C., Kaufman, M.S., Kolitz, J.E., Allen, S.L., Rai, K.R., Ivanovic, I., Dozmorov, I.M., Roa, S., Scharff, M.D., Li, W., et al. (2011) 'Intraclonal complexity in chronic lymphocytic leukemia: fractions enriched in recently born/divided and older/quiescent cells', *Molecular medicine (Cambridge, Mass.)*, 17(11–12), pp. 1374–1382.

Cambier, J.C., Gauld, S.B., Merrell, K.T. & Vilen, B.J. (2007) 'B-cell anergy: from transgenic models to naturally occurring anergic B cells?', *Nature reviews. Immunology*, 7(8), pp. 633–643.

Campo, E., Cymbalista, F., Ghia, P., Jäger, U., Pospisilova, S., Rosenquist, R., Schuh, A. & Stilgenbauer, S. (2018) 'TP53 aberrations in chronic lymphocytic leukemia: an overview of the clinical implications of improved diagnostics', *Haematologica*, 103(12), pp. 1956–1968.

Cantwell, M., Hua, T., Pappas, J. & Kipps, T.J. (1997) 'Acquired CD40-ligand deficiency in chronic lymphocytic leukemia', *Nature Medicine 1997 3:9*, 3(9), pp. 984–989.

Cantwell, M.J., Sharma, S., Friedmann, T. & Kipps, T.J. (1996) 'Adenovirus vector infection of chronic lymphocytic leukemia B cells', *Blood*, 88(12), pp. 4676–4683.

Carlsson, M., Söderberg, O. & Nilsson, K. (1993) 'Interleukin-4 (IL-4) enhances homotypic adhesion of activated B-chronic lymphocytic leukaemia (B-CLL) cells via a selective up-regulation of CD54.', *Scandinavian journal of immunology*, 37(4), pp. 515–22.

Carr, C., Aykent, S., Kimack, N.M. & Levine, A.D. (1991) 'Disulfide assignments in recombinant mouse and human interleukin 4.', *Biochemistry*, 30(6), pp. 1515–23.

Castello, A., Gaya, M., Tucholski, J., Oellerich, T., Lu, K.H., Tafuri, A., Pawson, T., Wienands, J., Engelke, M. & Batista, F.D. (2013) 'Nck-mediated recruitment of BCAP to the BCR regulates the PI(3)K-Akt pathway in B cells', *Nature immunology*, 14(9), pp. 966–975.

Cato, M.H., Chintalapati, S.K., Yau, I.W., Omori, S.A. & Rickert, R.C. (2011) 'Cyclin D3 Is Selectively Required for Proliferative Expansion of Germinal Center B Cells', *Molecular and Cellular Biology*, 31(1), p. 127.

Catovsky, D., Richards, S., Matutes, E., Oscier, D., Dyer, M., Bezares, R., Pettitt, A., Hamblin, T., Milligan, D., Child, J., Hamilton, M., Dearden, C., Smith, A., Bosanquet, A., Davis, Z., Brito-Babapulle, V., Else, M., Wade, R. & Hillmen, P. (2007) 'Assessment of fludarabine plus cyclophosphamide for patients with chronic lymphocytic leukaemia (the LRF CLL4 Trial): a randomised controlled trial', *Lancet (London, England)*, 370(9583), pp. 230–239.

Chamberlain, V., Drew, Y. & Lunec, J. (2021) 'Tipping Growth Inhibition into Apoptosis by Combining Treatment with MDM2 and WIP1 Inhibitors in p53WT Uterine Leiomyosarcoma', *Cancers*, 14(1), .

Chan, T.A., Hwang, P.M., Hermeking, H., Kinzler, K.W. & Vogelstein, B. (2000) 'Cooperative effects of genes controlling the G(2)/M checkpoint', *Genes & development*, 14(13), pp. 1584–1588.

Chang-Liu, C.M. & Woloschak, G.E. (1997) 'Effect of passage number on cellular response to DNA-damaging agents: cell survival and gene expression', *Cancer letters*, 113(1–2), pp. 77–86.

Chao, C.C.K. (2015) 'Mechanisms of p53 degradation', *Clinica chimica acta; international journal of clinical chemistry*, 438pp. 139–147.

Chapeau, E.A., Gembarska, A., Durand, E.Y., Mandon, E., Estadieu, C., Romanet, V., Wiesmann, M., Tiedt, R., Lehar, J., Weck, A. De, Rad, R., Barysb, L., Jeay, S., Ferretti, S., Kauffmann, A., Sutter, E., Grevot, A., Moulin, P., Murakami, M., et al. (2017) 'Resistance mechanisms to TP53-MDM2 inhibition identified by in vivo piggyBac transposon mutagenesis screen in an Arf-/- mouse model', *Proceedings of the National Academy of Sciences of the United States of America*, 114(12), pp. 3151–3156.

Chen, C.-H., Martin, V.A., Gorenstein, N.M., Geahlen, R.L. & Post, C.B. (2011) 'Two closely spaced tyrosines regulate NFAT signaling in B cells via Syk association with Vav', *Molecular and cellular biology*, 31(14), pp. 2984–2996.

Chen, L., Apgar, J., Huynh, L., Dicker, F., Giago-McGahan, T., Rassenti, L., Weiss, A. & Kipps, T.J. (2005) 'ZAP-70 directly enhances IgM signaling in chronic lymphocytic leukemia.', *Blood*, 105(5), pp. 2036–41.

Chen, L., Rousseau, R.F., Middleton, S.A., Nichols, G.L., Newell, D.R., Lunec, J. & Tweddle, D.A. (2015) 'Pre-clinical evaluation of the MDM2-p53 antagonist RG7388 alone and in combination with chemotherapy in neuroblastoma', *Oncotarget*, 6(12), pp. 10207–10221.

Chen, L., Widhopf, G., Huynh, L., Rassenti, L., Rai, K.R., Weiss, A. & Kipps, T.J. (2002) 'Expression of ZAP-70 is associated with increased B-cell receptor signaling in chronic lymphocytic leukemia.', *Blood*, 100(13), pp. 4609–14.

Chène, P. (2003) 'Inhibiting the p53-MDM2 interaction: an important target for cancer therapy', *Nature reviews. Cancer*, 3(2), pp. 102–109.

Cheng, G. & Baltimore, D. (1996) 'TANK, a co-inducer with TRAF2 of TNF- and CD 40L-mediated NF-kappaB activation.', *Genes & development*, 10(8), pp. 963–73.

Chi, S.W., Lee, S.H., Kim, D.H., Ahn, M.J., Kim, J.S., Woo, J.Y., Torizawa, T., Kainosho, M. & Han, K.H. (2005) 'Structural details on mdm2-p53 interaction', *Journal of Biological Chemistry*, 280(46), pp. 38795–38802.

Chini, E.N., Chini, C.C.S., Kato, I., Takasawa, S. & Okamoto, H. (2002) 'CD38 is the major enzyme responsible for synthesis of nicotinic acid-adenine dinucleotide phosphate in mammalian tissues', *The Biochemical journal*, 362(Pt 1), pp. 125–130.

Chiorazzi, N., Rai, K.R. & Ferrarini, M. (2005) 'Chronic lymphocytic leukemia.', *The New England journal of medicine*, 352(8), pp. 804–15.

Choi, J., Nannenga, B., Demidov, O.N., Bulavin, D. V., Cooney, A., Brayton, C., Zhang, Y., Mbawuike, I.N., Bradley, A., Appella, E. & Donehower, L.A. (2002) 'Mice deficient for

the wild-type p53-induced phosphatase gene (Wip1) exhibit defects in reproductive organs, immune function, and cell cycle control', *Molecular and cellular biology*, 22(4), pp. 1094–1105.

Choi, P. & Reiser, H. (1998) 'IL-4: role in disease and regulation of production.', *Clinical and experimental immunology*, 113(3), pp. 317–9.

Chomarat, P. & Banchereau, J. (1998) 'Interleukin-4 and interleukin-13: their similarities and discrepancies.', *International reviews of immunology*, 17(1–4), pp. 1–52.

Chuman, Y., Kurihashi, W., Mizukami, Y., Nashimoto, T., Yagi, H. & Sakaguchi, K. (2009) 'PPM1D430, a novel alternative splicing variant of the human PPM1D, can dephosphorylate p53 and exhibits specific tissue expression', *Journal of biochemistry*, 145(1), pp. 1–12.

Chung, J.Y., Park, Y.C., Ye, H. & Wu, H. (2002) 'All TRAFs are not created equal: common and distinct molecular mechanisms of TRAF-mediated signal transduction', *Journal of cell science*, 115(Pt 4), pp. 679–688.

Ciardullo, C., Aptullahoglu, E., Woodhouse, L., Lin, W.Y., Wallis, J.P., Marr, H., Marshall, S., Bown, N., Willmore, E. & Lunec, J. (2019) 'Non-genotoxic MDM2 inhibition selectively induces a pro-apoptotic p53 gene signature in chronic lymphocytic leukemia cells', *Haematologica*, 104(12), p. 2429.

Cimmino, A., Calin, G.A., Fabbri, M., Iorio, M. V., Ferracin, M., Shimizu, M., Wojcik, S.E., Aqeilan, R.I., Zupo, S., Dono, M., Rassenti, L., Alder, H., Volinia, S., Liu, C.G., Kipps, T.J., Negrini, M. & Croce, C.M. (2005) 'miR-15 and miR-16 induce apoptosis by targeting BCL2', *Proceedings of the National Academy of Sciences of the United States of America*, 102(39), pp. 13944–13949.

Clague, M.J., Urbé, S. & Komander, D. (2019) 'Breaking the chains: deubiquitylating enzyme specificity begets function', *Nature Reviews Molecular Cell Biology 2019 20:6*, 20(6), pp. 338–352.

Clark, E.A. & Ledbetter, J.A. (1994) 'How B and T cells talk to each other', *Nature 1994 367:6462*, 367(6462), pp. 425–428.

Coelho, V., Krysov, S., Steele, A., Hidalgo, M.S., Johnson, P.W., Chana, P.S., Packham, G., Stevenson, F.K. & Forconi, F. (2013) 'Identification in CLL of circulating intraclonal subgroups with varying B-cell receptor expression and function', *Blood*, 122(15), pp. 2664–2672.

Colombo, E., Marine, J.C., Danovi, D., Falini, B. & Pelicci, P.G. (2002) 'Nucleophosmin regulates the stability and transcriptional activity of p53', *Nature cell biology*, 4(7), pp. 529–533.

Corbali, M.O. & Eskazan, A.E. (2020) 'Idasanutlin as a new treatment option in improving the therapeutic odyssey of relapsed/refractory AML', *Future oncology (London, England)*, 16(14), pp. 887–889.

Corneth, O.B.J., Klein Wolterink, R.G.J. & Hendriks, R.W. (2016) 'BTK Signaling in B Cell Differentiation and Autoimmunity', *Current topics in microbiology and immunology*, 393pp. 67–105.

Cortese, D., Sutton, L.A., Cahill, N., Smedby, K.E., Geisler, C., Gunnarsson, R., Juliusson, G., Mansouri, L. & Rosenquist, R. (2013) 'On the way towards a "CLL prognostic index": focus on TP53, BIRC3, SF3B1, NOTCH1 and MYD88 in a population-based cohort', *Leukemia 2014 28:3*, 28(3), pp. 710–713.

Cory, S. & Adams, J.M. (2002) 'The Bcl2 family: regulators of the cellular life-or-death switch', *Nature reviews. Cancer*, 2(9), pp. 647–656.

Coscia, M., Pantaleoni, F., Riganti, C., Vitale, C., Rigoni, M., Peola, S., Castella, B., Foglietta, M., Griggio, V., Drandi, D., Ladetto, M., Bosia, A., Boccadoro, M. & Massaia, M. (2011) 'IGHV unmutated CLL B cells are more prone to spontaneous apoptosis and subject to environmental prosurvival signals than mutated CLL B cells', *Leukemia 2011 25:5*, 25(5), pp. 828–837.

Cosimo, E., McCaig, A.M., Carter-Brzezinski, L.J.M., Wheadon, H., Leach, M.T., Le Ster, K., Berthou, C., Durieu, E., Oumata, N., Galons, H., Meijer, L. & Michie, A.M. (2013) 'Inhibition of NF-κB-mediated signaling by the cyclin-dependent kinase inhibitor CR8 overcomes prosurvival stimuli to induce apoptosis in chronic lymphocytic leukemia cells', *Clinical Cancer Research*, 19(9), pp. 2393–2405.

Coughlin, J.J., Stang, S.L., Dower, N.A. & Stone, J.C. (2005) 'RasGRP1 and RasGRP3 regulate B cell proliferation by facilitating B cell receptor-Ras signaling.', *Journal of immunology (Baltimore, Md. : 1950)*, 175(11), pp. 7179–84.

Coutré, S.E., Barrientos, J.C., Brown, J.R., De Vos, S., Furman, R.R., Keating, M.J., Li, D., Obrien, S.M., Pagel, J.M., Poleski, M.H., Sharman, J.P., Yao, N.S. & Zelenetz, A.D. (2015) 'Management of adverse events associated with idelalisib treatment: expert panel opinion', *Leukemia & lymphoma*, 56(10), pp. 2779–2786.

Coutre, S.E., Flinn, I.W., De Vos, S., Barrientos, J.C., Schreeder, M.T., Wagner-Johnson, N.D., Sharman, J.P., Boyd, T.E., Fowler, N., Dreiling, L., Kim, Y., Mitra, S., Rai, K., Leonard, J.P. & Furman, R.R. (2018) 'Idelalisib in Combination With Rituximab or Bendamustine or Both in Patients With Relapsed/Refractory Chronic Lymphocytic Leukemia', *HemaSphere*, 2(3), p. 3.

Cramer, P., Fürstenau, M., Robrecht, S., Giza, A., Zhang, C., Fink, A.M., Fischer, K., Langerbeins, P., Al-Sawaf, O., Tausch, E., Schneider, C., Schetelig, J., Dreger, P., Böttcher, S., Kreuzer, K.A., Schilhabel, A., Ritgen, M., Brüggemann, M., Kneba, M., et al. (2022) 'Obinutuzumab, acalabrutinib, and venetoclax, after an optional debulking with bendamustine in relapsed or refractory chronic lymphocytic leukaemia (CLL2-BAAG): a multicentre, open-label, phase 2 trial', *The Lancet Haematology*, 9(10), pp. e745–e755.

Cramer, P. & Hallek, M. (2011) 'Prognostic factors in chronic lymphocytic leukemia-what do we need to know?', *Nature reviews. Clinical oncology*, 8(1), pp. 38–47.

Crassini, K., Shen, Y., Mulligan, S. & Giles Best, O. (2017) 'Modeling the chronic lymphocytic leukemia microenvironment in vitro', *Leukemia and Lymphoma*, 58(2), pp. 266–279.

Craxton, A., Jiang, A., Kurosaki, T. & Clark, E.A. (1999) 'Syk and Bruton's tyrosine kinase are required for B cell antigen receptor-mediated activation of the kinase Akt', *The Journal of biological chemistry*, 274(43), pp. 30644–30650.

Craxton, A., Shu, G., Graves, J.D., Saklatvala, J., Krebs, E.G. & Clark, E.A. (1998) 'p38 MAPK Is Required for CD40-Induced Gene Expression and Proliferation in B Lymphocytes', *The Journal of Immunology*, 161(7), pp. 3225–3236.

Crombie, J. & Davids, M.S. (2017) 'IGHV mutational status testing in chronic lymphocytic leukemia', *American journal of hematology*, 92(12), pp. 1393–1397.

Crotty, S. (2014) 'T follicular helper cell differentiation, function, and roles in disease.', *Immunity*, 41(4), pp. 529–42.

Cui, B., Chen, L., Zhang, S., Mraz, M., Fecteau, J.-F., Yu, J., Ghia, E.M., Zhang, L., Bao, L., Rassenti, L.Z., Messer, K., Calin, G.A., Croce, C.M. & Kipps, T.J. (2014) 'MicroRNA-155 influences B-cell receptor signaling and associates with aggressive disease in chronic lymphocytic leukemia.', *Blood*, 124(4), pp. 546–54.

Damgaard, R.B. (2021) 'The ubiquitin system: from cell signalling to disease biology and new therapeutic opportunities', *Cell Death & Differentiation*, 28pp. 423–426.

Damle, R.N., Wasil, T., Fais, F., Ghiotto, F., Valetto, A., Allen, S.L., Buchbinder, A., Budman, D., Dittmar, K., Kolitz, J., Lichtman, S.M., Schulman, P., Vinciguerra, V.P., Rai, K.R., Ferrarini, M. & Chiorazzi, N. (1999) 'Ig V Gene Mutation Status and CD38 Expression As Novel Prognostic Indicators in Chronic Lymphocytic Leukemia', *Blood*, 94(6), pp. 1840–1847.

Dancescu, M., Rubio-Trujillo, M., Biron, G., Bron, D., Delespesse, G. & Sarfati, M. (1992) 'Interleukin 4 protects chronic lymphocytic leukemic B cells from death by apoptosis and upregulates Bcl-2 expression.', *The Journal of experimental medicine*, 176(5), pp. 1319–26.

Daver, N.G., Dail, M., Garcia, J.S., Jonas, B.A., Yee, K.W.L., Kelly, K.R., Vey, N., Assouline, S., Roboz, G.J., Paolini, S., Pollyea, D.A., Tafuri, A., Brandwein, J.M., Pigneux, A., Powell, B.L., Fenaux, P., Olin, R.L., Visani, G., Martinelli, G., et al. (2023) 'Venetoclax and idasanutlin in relapsed/refractory AML: a nonrandomized, open-label phase 1b trial', *Blood*, 141(11), pp. 1265–1276.

Davies, A., Kater, A.P., Sharman, J.P., Stilgenbauer, S., Vitolo, U., Klein, C., Parreira, J. & Salles, G. (2022) 'Obinutuzumab in the treatment of B-cell malignancies: a comprehensive review', *Future Oncology*, 18(26), pp. 2943–2966.

Deaglio, S., Vaisitti, T., Bergui, L., Bonello, L., Horenstein, A.L., Tamagnone, L., Boumsell, L. & Malavasi, F. (2005) 'CD38 and CD100 lead a network of surface receptors relaying positive signals for B-CLL growth and survival', *Blood*, 105(8), pp. 3042–3050.

Deglesne, P.A., Chevallier, N., Letestu, R., Baran-Marszak, F., Beitar, T., Salanoubat, C., Sanhes, L., Nataf, J., Roger, C., Varin-Blank, N. & Ajchenbaum-Cymbalista, F. (2006) 'Survival response to B-cell receptor ligation is restricted to progressive chronic lymphocytic leukemia cells irrespective of Zap70 expression', *Cancer research*, 66(14), pp. 7158–7166.

Delavaine, L. & La Thangue, N.B. (1999) 'Control of E2F activity by p21Waf1/Cip1', *Oncogene*, 18(39), pp. 5381–5392.

Delgado, J., Espinet, B., Oliveira, A.C., Abrisqueta, P., de la Serna, J., Collado, R., Loscertales, J., Lopez, M., Hernandez-Rivas, J.A., Ferra, C., Ramirez, A., Roncero, J.M.,

Lopez, C., Aventin, A., Puiggros, A., Abella, E., Carbonell, F., Costa, D., Carrio, A., et al. (2012) 'Chronic lymphocytic leukaemia with 17p deletion: a retrospective analysis of prognostic factors and therapy results', *British journal of haematology*, 157(1), pp. 67–74.

Deng, W., Li, J., Dorrah, K., Jimenez-Tapia, D., Arriaga, B., Hao, Q., Cao, W., Gao, Z., Vadgama, J. & Wu, Y. (2020) *The role of PPM1D in cancer and advances in studies of its inhibitors*,

Dengler, H.S., Baracho, G. V, Omori, S.A., Bruckner, S., Arden, K.C., Castrillon, D.H., DePinho, R.A. & Rickert, R.C. (2008) 'Distinct functions for the transcription factor Foxo1 at various stages of B cell differentiation', *Nature immunology*, 9(12), pp. 1388–1398.

Ding, Q., Zhang, Z., Liu, J.J., Jiang, N., Zhang, J., Ross, T.M., Chu, X.J., Bartkovitz, D., Podlaski, F., Janson, C., Tovar, C., Filipovic, Z.M., Higgins, B., Glenn, K., Packman, K., Vassilev, L.T. & Graves, B. (2013) 'Discovery of RG7388, a potent and selective p53-MDM2 inhibitor in clinical development', *Journal of Medicinal Chemistry*, 56(14), pp. 5979–5983.

Döhner, H., Stilgenbauer, S., Benner, A., Leupolt, E., Kröber, A., Bullinger, L., Döhner, K., Bentz, M. & Lichter, P. (2000) 'Genomic aberrations and survival in chronic lymphocytic leukemia', *The New England journal of medicine*, 343(26), pp. 1910–1916.

Dominguez-Sola, D., Kung, J., Holmes, A.B., Wells, V.A., Mo, T., Basso, K. & Dalla-Favera, R. (2015) 'The FOXO1 Transcription Factor Instructs the Germinal Center Dark Zone Program', *Immunity*, 43(6), pp. 1064–1074.

Donehower, L.A., Harvey, M., Slagle, B.L., McArthur, M.J., Montgomery, C.A., Butel, J.S. & Bradley, A. (1992) 'Mice deficient for p53 are developmentally normal but susceptible to spontaneous tumours.', *Nature*, 356(6366), pp. 215–21.

Dong, C., Davis, R.J. & Flavell, R.A. (2002) 'MAP kinases in the immune response', *Annual review of immunology*, 20pp. 55–72.

Dotto, G.P. (2000) 'p21(WAF1/Cip1): more than a break to the cell cycle?', *Biochimica et biophysica acta*, 1471(1), .

Douglas, R.S., Capocasale, R.J., Lamb, R.J., Nowell, P.C. & Moore, J.S. (1997) 'Chronic lymphocytic leukemia B cells are resistant to the apoptotic effects of transforming growth factor-beta.', *Blood*, 89(3), pp. 941–7.

Drakos, E., Singh, R.R., Rassidakis, G.Z., Schlette, E., Li, J., Claret, F.X., Ford, R.J., Vega, F. & Medeiros, L.J. (2011) 'Activation of the p53 pathway by the MDM2 inhibitor nutlin-3a overcomes BCL2 overexpression in a preclinical model of diffuse large B-cell lymphoma associated with t(14;18)(q32;q21)', *Leukemia*, 25pp. 856–867.

Drummond, C.J., Esfandiari, A., Liu, J., Lu, X., Hutton, C., Jackson, J., Bennaceur, K., Xu, Q., Makimanejavali, A.R., Del Bello, F., Piergentili, A., Newell, D.R., Hardcastle, I.R., Griffin, R.J. & Lunec, J. (2016) 'TP53 mutant MDM2-amplified cell lines selected for resistance to MDM2-p53 binding antagonists retain sensitivity to ionizing radiation', *Oncotarget*, 7(29), pp. 46203–46218.

Du, Z. & Lovly, C.M. (2018) ‘Mechanisms of receptor tyrosine kinase activation in cancer’, *Molecular cancer*, 17(1), .

Durie, F.H., Foy, T.M., Masters, S.R., Laman, J.D. & Noelle, R.J. (1994) ‘The role of CD40 in the regulation of humoral and cell-mediated immunity’, *Immunology Today*, 15(9), pp. 406–411.

Dürig, J., Naschar, M., Schmücker, U., Renzing-Köhler, K., Hölter, T., Hŧttman, A. & Dührsen, U. (2002) ‘CD38 expression is an important prognostic marker in chronic lymphocytic leukaemia’, *Leukemia*, 16(1), pp. 30–35.

Dürig, J., Nückel, H., Cremer, M., Führer, A., Halfmeyer, K., Fandrey, J., Möröy, T., Klein-Hitpass, L. & Dührsen, U. (2003) ‘ZAP-70 expression is a prognostic factor in chronic lymphocytic leukemia’, *Leukemia*, 17(12), pp. 2426–2434.

Edelmann, J., Klein-Hitpass, L., Carpinteiro, A., Führer, A., Sellmann, L., Stilgenbauer, S., Dührsen, U. & Dürig, J. (2008) ‘Bone marrow fibroblasts induce expression of PI3K/NF-kappaB pathway genes and a pro-angiogenic phenotype in CLL cells’, *Leukemia research*, 32(10), pp. 1565–1572.

Efremov, D.G., Turkalj, S. & Laurenti, L. (2020) ‘Mechanisms of B Cell Receptor Activation and Responses to B Cell Receptor Inhibitors in B Cell Malignancies.’, *Cancers*, 12(6), .

Eichhorst, B., Goede, V. & Hallek, M. (2009) ‘Treatment of elderly patients with chronic lymphocytic leukemia’, *Leukemia & lymphoma*, 50(2), pp. 171–178.

Eichhorst, B., Robak, T., Montserrat, E., Ghia, P., Hillmen, P., Hallek, M. & Buske, C. (2015) ‘Chronic lymphocytic leukaemia: ESMO Clinical Practice Guidelines for diagnosis, treatment and follow-up’, *Annals of oncology : official journal of the European Society for Medical Oncology*, 26 Suppl 5pp. vi50–vi54.

El-Deiry, W.S., Kern, S.E., Pietenpol, J.A., Kinzler, K.W. & Vogelstein, B. (1992) ‘Definition of a consensus binding site for p53’, *Nature genetics*, 1(1), pp. 45–49.

El-Deiry, W.S., Tokino, T., Velculescu, V.E., Levy, D.B., Parsons, R., Trent, J.M., Lin, D., Mercer, W.E., Kinzler, K.W. & Vogelstein, B. (1993) ‘WAF1, a potential mediator of p53 tumor suppression’, *Cell*, 75(4), pp. 817–825.

Eliyahu, D., Raz, A., Gruss, P., Givol, D. & Oren, M. (1984) ‘Participation of p53 cellular tumour antigen in transformation of normal embryonic cells’, *Nature*, 312(5995), pp. 646–649.

Elter, T., Gercheva-Kyuchukova, L., Pylylpenko, H., Robak, T., Jaksic, B., Rekhtman, G., Kyrcz-Krzemień, S., Vatutin, M., Wu, J., Sirard, C., Hallek, M. & Engert, A. (2011) ‘Fludarabine plus alemtuzumab versus fludarabine alone in patients with previously treated chronic lymphocytic leukaemia: a randomised phase 3 trial’, *The Lancet. Oncology*, 12(13), pp. 1204–1213.

Endo, S., Yamato, K., Hirai, S., Moriwaki, T., Fukuda, K., Suzuki, H., Abei, M., Nakagawa, I. & Hyodo, I. (2011) ‘Potent in vitro and in vivo antitumor effects of MDM2 inhibitor nutlin-3 in gastric cancer cells’, *Cancer science*, 102(3), pp. 605–613.

Endo, T., Nishio, M., Enzler, T., Cottam, H.B., Fukuda, T., James, D.F., Karin, M. & Kipps, T.J. (2007) 'BAFF and APRIL support chronic lymphocytic leukemia B-cell survival through activation of the canonical NF-kappaB pathway', *Blood*, 109(2), pp. 703–710.

Engels, N., König, L.M., Heemann, C., Lutz, J., Tsubata, T., Griep, S., Schrader, V. & Wienands, J. (2009) 'Recruitment of the cytoplasmic adaptor Grb2 to surface IgG and IgE provides antigen receptor-intrinsic costimulation to class-switched B cells', *Nature immunology*, 10(9), pp. 1018–1025.

Esfandiari, A., Hawthorne, T.A., Nakjang, S. & Lunec, J. (2016) 'Chemical inhibition of wild-type p53-induced phosphatase 1 (WIP1/PPM1D) by GSK2830371 potentiates the sensitivity to MDM2 inhibitors in a p53-dependent manner', *Molecular Cancer Therapeutics*, 15(3), pp. 379–391.

Fakharzadeh, S.S., Trusko, S.P. & George, D.L. (1991) 'Tumorigenic potential associated with enhanced expression of a gene that is amplified in a mouse tumor cell line.', *The EMBO Journal*, 10(6), pp. 1565–1569.

Ferretti, E., Bertolotto, M., Deaglio, S., Tripodo, C., Ribatti, D., Audrito, V., Blengio, F., Matis, S., Zupo, S., Rossi, D., Ottonello, L., Gaidano, G., Malavasi, F., Pistoia, V. & Corcione, A. (2011) 'A novel role of the CX3CR1/CX3CL1 system in the cross-talk between chronic lymphocytic leukemia cells and tumor microenvironment', *Leukemia 2011 25:8*, 25(8), pp. 1268–1277.

Fields, S. & Jang, S.K. (1990) 'Presence of a potent transcription activating sequence in the p53 protein', *Science (New York, N.Y.)*, 249(4972), pp. 1046–1049.

Finlay, C.A., Hinds, P.W. & Levine, A.J. (1989) 'The p53 proto-oncogene can act as a suppressor of transformation', *Cell*, 57(7), pp. 1083–1093.

Finlay, C.A., Hinds, P.W., Tan, T.-H., Eliyahu, D., Oren, M. & Levine, A.J. (2023) 'Activating Mutations for Transformation by p53 Produce a Gene Product That Forms an hsc70-p53 Complex with an Altered Half-Life', *https://doi.org/10.1128/mcb.8.2.531-539.1988*, 8(2), pp. 531–539.

Fischer, K., Al-Sawaf, O., Bahlo, J., Fink, A.-M., Tandon, M., Dixon, M., Robrecht, S., Warburton, S., Humphrey, K., Samoylova, O., Liberati, A.M., Pinilla-Ibarz, J., Opat, S., Sivcheva, L., Le Dû, K., Fogliatto, L.M., Niemann, C.U., Weinkove, R., Robinson, S., et al. (2019) 'Venetoclax and Obinutuzumab in Patients with CLL and Coexisting Conditions', *The New England journal of medicine*, 380(23), pp. 2225–2236.

Fischer, K., Bahlo, J., Fink, A.M., Goede, V., Herling, C.D., Cramer, P., Langerbeins, P., Von Tresckow, J., Engelke, A., Maurer, C., Kovacs, G., Herling, M., Tausch, E., Kreuzer, K.A., Eichhorst, B., Böttcher, S., Seymour, J.F., Ghia, P., Marlton, P., et al. (2016) 'Long-term remissions after FCR chemoimmunotherapy in previously untreated patients with CLL: updated results of the CLL8 trial', *Blood*, 127(2), pp. 208–215.

Flaswinkel, H. & Reth, M. (1994) 'Dual role of the tyrosine activation motif of the Ig-alpha protein during signal transduction via the B cell antigen receptor', *The EMBO journal*, 13(1), pp. 83–89.

Flinn, I.W., O'Brien, S., Kahl, B., Patel, M., Oki, Y., Foss, F.F., Porcu, P., Jones, J., Burger, J.A., Jain, N., Kelly, V.M., Allen, K., Douglas, M., Sweeney, J., Kelly, P. & Horwitz, S.

(2018) ‘Duvelisib, a novel oral dual inhibitor of PI3K-δ,γ, is clinically active in advanced hematologic malignancies’, *Blood*, 131(8), pp. 877–887.

Flørenes, V.A., Mælandsmo, G.M., Forus, A., Andreassen, Å., Myklebost, O. & Fodstad, Ø. (1994) ‘MDM2 gene amplification and transcript levels in human sarcomas: relationship to TP53 gene status’, *Journal of the National Cancer Institute*, 86(17), pp. 1297–1302.

Forconi, F., Potter, K.N., Wheatley, I., Darzentas, N., Sozzi, E., Stamatopoulos, K., Mockridge, C.I., Packham, G. & Stevenson, F.K. (2010) ‘The normal IGHV1-69-derived B-cell repertoire contains stereotypic patterns characteristic of unmutated CLL’, *Blood*, 115(1), pp. 71–77.

Fujimoto, M., Fujimoto, Y., Poe, J.C., Jansen, P.J., Lowell, C.A., DeFranco, A.L. & Tedder, T.F. (2000) ‘CD19 regulates Src family protein tyrosine kinase activation in B lymphocytes through processive amplification’, *Immunity*, 13(1), pp. 47–57.

Furet, P., Masuya, K., Kallen, J., Stachyra-Valat, T., Ruetz, S., Guagnano, V., Holzer, P., Mah, R., Stutz, S., Vaupel, A., Chène, P., Jeay, S. & Schlapbach, A. (2016) ‘Discovery of a novel class of highly potent inhibitors of the p53-MDM2 interaction by structure-based design starting from a conformational argument’, *Bioorganic & Medicinal Chemistry Letters*, 26pp. 4837–4841.

Furman, R.R., Asgary, Z., Mascarenhas, J.O., Liou, H.C. & Schattner, E.J. (2000) ‘Modulation of NF-kappa B activity and apoptosis in chronic lymphocytic leukemia B cells.’, *Journal of immunology (Baltimore, Md. : 1950)*, 164(4), pp. 2200–6.

Furman, R.R., Sharman, J.P., Coutre, S.E., Cheson, B.D., Pagel, J.M., Hillmen, P., Barrientos, J.C., Zelenetz, A.D., Kipps, T.J., Flinn, I., Ghia, P., Eradat, H., Ervin, T., Lamanna, N., Coiffier, B., Pettitt, A.R., Ma, S., Stilgenbauer, S., Cramer, P., et al. (2014) ‘Idelalisib and rituximab in relapsed chronic lymphocytic leukemia’, *The New England journal of medicine*, 370(11), pp. 997–1007.

Gagez, A.L. & Cartron, G. (2014) ‘Obinutuzumab: A new class of anti-CD20 monoclonal antibody’, *Current Opinion in Oncology*, 26(5), pp. 484–491.

Gazumyan, A., Reichlin, A. & Nussenzweig, M.C. (2006) ‘Igβ tyrosine residues contribute to the control of B cell receptor signaling by regulating receptor internalization’, *Journal of Experimental Medicine*, 203(7), pp. 1785–1794.

Geha, R.S., Jabara, H.H. & Brodeur, S.R. (2003) ‘The regulation of immunoglobulin E class-switch recombination.’, *Nature reviews. Immunology*, 3(9), pp. 721–32.

Gessner, A., Mohrs, K. & Mohrs, M. (2005) ‘Mast cells, basophils, and eosinophils acquire constitutive IL-4 and IL-13 transcripts during lineage differentiation that are sufficient for rapid cytokine production.’, *Journal of immunology (Baltimore, Md. : 1950)*, 174(2), pp. 1063–72.

Ghia, P., Circosta, P., Scielzo, C., Vallario, A., Camporeale, A., Granziero, L. & Caligaris-Cappio, F. (2005) ‘Differential effects on CLL cell survival exerted by different microenvironmental elements.’, *Current topics in microbiology and immunology*, 294pp. 135–45.

Ghia, P., Strola, G., Granziero, L., Geuna, M., Guida, G., Sallusto, F., Ruffing, N., Montagna, L., Piccoli, P., Chilosi, M. & Caligaris-Cappio, F. (2002) ‘Chronic lymphocytic leukemia

B cells are endowed with the capacity to attract CD4+, CD40L+ T cells by producing CCL22.', *European journal of immunology*, 32(5), pp. 1403–13.

Gianna Hoffman-Luca, C., Ziazadeh, D., McEachern, D., Zhao, Y., Sun, W., Debussche, L. & Wang, S. (2015) 'Elucidation of Acquired Resistance to Bcl-2 and MDM2 Inhibitors in Acute Leukemia In Vitro and In Vivo', *Clinical cancer research : an official journal of the American Association for Cancer Research*, 21(11), pp. 2558–2568.

Gilleece, M. & Dexter, T. (1993) 'Effect of Campath-1H Antibody on Human Hematopoietic Progenitors In Vitro', *Blood*, 82(3), pp. 807–812.

Gilmartin, A.G., Faitg, T.H., Richter, M., Groy, A., Seefeld, M.A., Darcy, M.G., Peng, X., Federowicz, K., Yang, J., Zhang, S.Y., Minthorn, E., Jaworski, J.P., Schaber, M., Martens, S., McNulty, D.E., Sinnamon, R.H., Zhang, H., Kirkpatrick, R.B., Nevins, N., et al. (2014) 'Allosteric Wip1 phosphatase inhibition through flap-subdomain interaction', *Nature chemical biology*, 10(3), pp. 181–187.

Glickman, M.H. & Ciechanover, A. (2002) 'The ubiquitin-proteasome proteolytic pathway: Destruction for the sake of construction', *Physiological Reviews*, 82(2), pp. 373–428.

Goede, V., Fischer, K., Busch, R., Engelke, A., Eichhorst, B., Wendtner, C.M., Chagorova, T., de la Serna, J., Dilhuydy, M.-S., Illmer, T., Opat, S., Owen, C.J., Samoylova, O., Kreuzer, K.-A., Stilgenbauer, S., Döhner, H., Langerak, A.W., Ritgen, M., Kneba, M., et al. (2014) 'Obinutuzumab plus chlorambucil in patients with CLL and coexisting conditions', *The New England journal of medicine*, 370(12), pp. 1101–1110.

Goede, V., Klein, C. & Stilgenbauer, S. (2015) 'Obinutuzumab (GA101) for the treatment of chronic lymphocytic leukemia and other B-cell non-hodgkin's lymphomas: a glycoengineered type II CD20 antibody', *Oncology research and treatment*, 38(4), pp. 185–192.

Goenka, S. & Kaplan, M.H. (2011) 'Transcriptional regulation by STAT6.', *Immunologic research*, 50(1), pp. 87–96.

Grammer, A.C. & Lipsky, P.E. (2000) 'CD40-mediated regulation of immune responses by TRAF-dependent and TRAF-independent signaling mechanisms', *Advances in immunology*, 76pp. 61–178.

Granziero, L., Ghia, P., Circosta, P., Gottardi, D., Strola, G., Geuna, M., Montagna, L., Piccoli, P., Chilosi, M. & Caligaris-Cappio, F. (2001) 'Survivin is expressed on CD40 stimulation and interfaces proliferation and apoptosis in B-cell chronic lymphocytic leukemia', *Blood*, 97(9), pp. 2777–2783.

Grdisa, M. (2003) 'Influence of CD40 ligation on survival and apoptosis of B-CLL cells in vitro', *Leukemia Research*, 27(10), pp. 951–956.

Green, D.R. & Kroemer, G. (2009) 'Cytoplasmic functions of the tumour suppressor p53', *Nature*, 458(7242), pp. 1127–1130.

Gregory, M.A., Qi, Y. & Hann, S.R. (2003) 'Phosphorylation by glycogen synthase kinase-3 controls c-myc proteolysis and subnuclear localization', *The Journal of biological chemistry*, 278(51), pp. 51606–51612.

Greipp, P.T., Smoley, S.A., Viswanatha, D.S., Frederick, L.S., Rabe, K.G., Sharma, R.G., Slager, S.L., Van Dyke, D.L., Shanafelt, T.D., Tschumper, R.C. & Zent, C.S. (2013) 'Patients with chronic lymphocytic leukaemia and clonal deletion of both 17p13.1 and 11q22.3 have a very poor prognosis', *British journal of haematology*, 163(3), pp. 326–333.

Grever, M.R., Lucas, D.M., Dewald, G.W., Neuberg, D.S., Reed, J.C., Kitada, S., Flinn, I.W., Tallman, M.S., Appelbaum, F.R., Larson, R.A., Paietta, E., Jelinek, D.F., Gribben, J.G. & Byrd, J.C. (2007) 'Comprehensive assessment of genetic and molecular features predicting outcome in patients with chronic lymphocytic leukemia: results from the US Intergroup Phase III Trial E2997', *Journal of clinical oncology : official journal of the American Society of Clinical Oncology*, 25(7), pp. 799–804.

Gribben, J.G. (2009) 'Stem cell transplantation in chronic lymphocytic leukemia', *Biology of blood and marrow transplantation : journal of the American Society for Blood and Marrow Transplantation*, 15(1 Suppl), pp. 53–58.

Gross, J.A., Dillon, S.R., Mudri, S., Johnston, J., Littau, A., Roque, R., Rixon, M., Schou, O., Foley, K.P., Haugen, H., McMillen, S., Waggie, K., Schreckhise, R.W., Shoemaker, K., Vu, T., Moore, M., Grossman, A. & Clegg, C.H. (2001) 'TACI-Ig Neutralizes Molecules Critical for B Cell Development and Autoimmune Disease: Impaired B Cell Maturation in Mice Lacking BLyS', *Immunity*, 15(2), pp. 289–302.

Grumont, R.J., Rourke, I.J. & Gerondakis, S. (1999) 'Rel-dependent induction of A1 transcription is required to protect B cells from antigen receptor ligation-induced apoptosis.', *Genes & development*, 13(4), pp. 400–11.

Guarini, A., Chiaretti, S., Tavolaro, S., Maggio, R., Peragine, N., Citarella, F., Ricciardi, M.R., Santangelo, S., Mahnelli, M., De Propris, M.S., Messina, M., Mauro, F.R., Del Giudice, I. & Foà, R. (2008) 'BCR ligation induced by IgM stimulation results in gene expression and functional changes only in IgV H unmutated chronic lymphocytic leukemia (CLL) cells', *Blood*, 112(3), pp. 782–792.

Guo, B., Blair, D., Chiles, T.C., Lowell, C.A. & Rothstein, T.L. (2007) 'Cutting Edge: B cell receptor (BCR) cross-talk: the IL-4-induced alternate pathway for BCR signaling operates in parallel with the classical pathway, is sensitive to Rottlerin, and depends on Lyn.', *Journal of immunology (Baltimore, Md. : 1950)*, 178(8), pp. 4726–30.

Guo, B. & Rothstein, T.L. (2005) 'B cell receptor (BCR) cross-talk: IL-4 creates an alternate pathway for BCR-induced ERK activation that is phosphatidylinositol 3-kinase independent.', *Journal of immunology (Baltimore, Md. : 1950)*, 174(9), pp. 5375–81.

Guo, B. & Rothstein, T.L. (2013) 'IL-4 upregulates Igα and Igβ protein, resulting in augmented IgM maturation and B cell receptor-triggered B cell activation.', *Journal of immunology (Baltimore, Md. : 1950)*, 191(2), pp. 670–7.

Guo, B., Zhang, L., Chiorazzi, N. & Rothstein, T.L. (2016) 'IL-4 rescues surface IgM expression in chronic lymphocytic leukemia', *Blood*, 128(4), pp. 553–562.

ten Hacken, E., Gounari, M., Ghia, P. & Burger, J.A. (2019) 'The importance of B cell receptor isotypes and stereotypes in chronic lymphocytic leukemia', *Leukemia*, 33(2), pp. 287–298.

Haines, D.S., Landers, J.E., Engle, L.J. & George, D.L. (1994) 'Physical and functional interaction between wild-type p53 and mdm2 proteins', *Molecular and cellular biology*, 14(2), pp. 1171–1178.

Hallek, M. (2019) 'Chronic lymphocytic leukemia: 2020 update on diagnosis, risk stratification and treatment', *American journal of hematology*, 94(11), pp. 1266–1287.

Hallek, M. & Al-Sawaf, O. (2021) 'Chronic lymphocytic leukemia: 2022 update on diagnostic and therapeutic procedures', *American Journal of Hematology*, 96(12), pp. 1679–1705.

Hallek, M., Cheson, B.D., Catovsky, D., Caligaris-Cappio, F., Dighiero, G., Döhner, H., Hillmen, P., Keating, M., Montserrat, E., Chiorazzi, N., Stilgenbauer, S., Rai, K.R., Byrd, J.C., Eichhorst, B., O'Brien, S., Robak, T., Seymour, J.F. & Kipps, T.J. (2018) 'iwCLL guidelines for diagnosis, indications for treatment, response assessment, and supportive management of CLL', *Blood*, 131(25), pp. 2745–2760.

Hallek, M., Cheson, B.D., Catovsky, D., Caligaris-Cappio, F., Dighiero, G., Döhner, H., Hillmen, P., Keating, M.J., Montserrat, E., Rai, K.R. & Kipps, T.J. (2008) 'Guidelines for the diagnosis and treatment of chronic lymphocytic leukemia: a report from the International Workshop on Chronic Lymphocytic Leukemia updating the National Cancer Institute–Working Group 1996 guidelines', *Blood*, 111(12), pp. 5446–5456.

Hallek, M., Fischer, K., Fingerle-Rowson, G., Fink, A.M., Busch, R., Mayer, J., Hensel, M., Hopfinger, G., Hess, G., Von Grünhagen, U., Bergmann, M., Catalano, J., Zinzani, P.L., Caligaris-Cappio, F., Seymour, J.F., Berrebi, A., Jäger, U., Cazin, B., Trneny, M., et al. (2010) 'Addition of rituximab to fludarabine and cyclophosphamide in patients with chronic lymphocytic leukaemia: a randomised, open-label, phase 3 trial', *Lancet (London, England)*, 376(9747), pp. 1164–1174.

Hallek, M., Shanafelt, T.D. & Eichhorst, B. (2018) 'Chronic lymphocytic leukaemia', *Lancet (London, England)*, 391(10129), pp. 1524–1537.

Hamblin, T.J. (2003) 'CD38: what is it there for?', *Blood*, 102(6), pp. 1939–1940.

Hamblin, T.J., Davis, Z., Gardiner, A., Oscier, D.G. & Stevenson, F.K. (1999) 'Unmutated Ig VH Genes Are Associated With a More Aggressive Form of Chronic Lymphocytic Leukemia', *Blood*, 94(6), pp. 1848–1854.

Hamilton, E., Pearce, L., Morgan, L., Robinson, S., Ware, V., Brennan, P., Thomas, N.S.B., Yallop, D., Devereux, S., Fegan, C., Buggins, A.G.S. & Pepper, C. (2012) 'Mimicking the tumour microenvironment: three different co-culture systems induce a similar phenotype but distinct proliferative signals in primary chronic lymphocytic leukaemia cells', *British Journal of Haematology*, 158(5), pp. 589–599.

Hanissian, S.H. & Geha, R.S. (1997) 'Jak3 is associated with CD40 and is critical for CD40 induction of gene expression in B cells', *Immunity*, 6(4), pp. 379–387.

Harrington, B.K., Gulrajani, M., Covey, T., Kaptein, A., Van Lith, B., Izumi, R., Hamdy, A., Ulrich, R.G., Byrd, J.C., Lannutti, B.J. & Johnson, A.J. (2015) 'ACP-196 Is a Second Generation Inhibitor of Bruton Tyrosine Kinase (BTK) with Enhanced Target Specificity', *Blood*, 126(23), p. 2908.

Harris, S.L. & Levine, A.J. (2005) 'The p53 pathway: positive and negative feedback loops', *Oncogene*, 24(17), pp. 2899–2908.

Haselager, M., Thijssen, R., West, C., Young, L., Van Kampen, R., Willmore, E., Mackay, S., Kater, A. & Eldering, E. (2021) 'Regulation of Bcl-XL by non-canonical NF-κB in the context of CD40-induced drug resistance in CLL.', *Cell death and differentiation*, 28(5), pp. 1658–1668.

Hashimoto, A., Okada, H., Jiang, A., Kurosaki, M., Greenberg, S., Clark, E.A. & Kurosaki, T. (1998) 'Involvement of Guanosine Triphosphatases and Phospholipase C-2 in Extracellular Signal-regulated Kinase, c-Jun NH 2-terminal Kinase, and p38 Mitogen-activated Protein Kinase Activation by the B Cell Antigen Receptor', *J. Exp. Med*, 188(7), pp. 1287–1295.

Haupt, Y., Maya, R., Kazaz, A. & Oren, M. (1997) 'Mdm2 promotes the rapid degradation of p53', *Nature*, 387(6630), pp. 296–299.

Herishanu, Y., Gibellini, F., Njuguna, N., Hazan-Halevy, I., Farooqui, M., Bern, S., Keyvanfar, K., Lee, E., Wilson, W. & Wiestner, A. (2011) 'Activation of CD44, a receptor for extracellular matrix components, protects chronic lymphocytic leukemia cells from spontaneous and drug induced apoptosis through MCL-1', *Leukemia & lymphoma*, 52(9), pp. 1758–1769.

Herishanu, Y., Pérez-Galán, P., Liu, D., Biancotto, A., Pittaluga, S., Vire, B., Gibellini, F., Njuguna, N., Lee, E., Stennett, L., Raghavachari, N., Liu, P., McCoy, J.P., Raffeld, M., Stetler-Stevenson, M., Yuan, C., Sherry, R., Arthur, D.C., Maric, I., et al. (2011) 'The lymph node microenvironment promotes B-cell receptor signaling, NF-κB activation, and tumor proliferation in chronic lymphocytic leukemia', *Blood*, 117(2), pp. 563–574.

Herman, S.E.M., Gordon, A.L., Hertlein, E., Ramanunni, A., Zhang, X., Jaglowski, S., Flynn, J., Jones, J., Blum, K.A., Buggy, J.J., Hamdy, A., Johnson, A.J. & Byrd, J.C. (2011) 'Bruton tyrosine kinase represents a promising therapeutic target for treatment of chronic lymphocytic leukemia and is effectively targeted by PCI-32765', *Blood*, 117(23), pp. 6287–6296.

Herman, S.E.M., Montraveta, A., Niemann, C.U., Mora-Jensen, H., Gulrajani, M., Krantz, F., Mantel, R., Smith, L.L., McClanahan, F., Harrington, B.K., Colomer, D., Covey, T., Byrd, J.C., Izumi, R., Kaptein, A., Ulrich, R., Johnson, A.J., Lannutti, B.J., Wiestner, A., et al. (2017) 'The Bruton Tyrosine Kinase (BTK) Inhibitor Acalabrutinib Demonstrates Potent On-Target Effects and Efficacy in Two Mouse Models of Chronic Lymphocytic Leukemia.', *Clinical cancer research : an official journal of the American Association for Cancer Research*, 23(11), pp. 2831–2841.

Hernández, J.A., Land, K.J. & McKenna, R.W. (1995) 'Leukemias, myeloma, and other lymphoreticular neoplasms', *Cancer*, 75(1 Suppl), pp. 381–394.

Hess, R.A., Bunick, D., Lee, K.H., Bahr, J., Taylor, J.A., Korach, K.S. & Lubahn, D.B. (1997) 'A role for oestrogens in the male reproductive system', *Nature*, 390(6659), pp. 509–512.

Hewamana, S., Lin, T.T., Jenkins, C., Burnett, A.K., Jordan, C.T., Fegan, C., Brennan, P., Rowntree, C. & Pepper, C. (2008) 'The Novel Nuclear Factor-κB Inhibitor LC-1 Is Equipotent in Poor Prognostic Subsets of Chronic Lymphocytic Leukemia and Shows Strong Synergy with Fludarabine', *Clinical Cancer Research*, 14(24), pp. 8102–8111.

Hikida, M. & Kurosaki, T. (2005) 'Regulation of phospholipase C-gamma2 networks in B lymphocytes', *Advances in immunology*, 88pp. 73–96.

Hillmen, P., Robak, T., Janssens, A., Babu, K.G., Kloczko, J., Grosicki, S., Doubek, M., Panagiotidis, P., Kimby, E., Schuh, A., Pettitt, A.R., Boyd, T., Montillo, M., Gupta, I. V., Wright, O., Dixon, I., Carey, J.L., Chang, C.N., Lisby, S., et al. (2015) 'Chlorambucil plus ofatumumab versus chlorambucil alone in previously untreated patients with chronic lymphocytic leukaemia (COMPLEMENT 1): a randomised, multicentre, open-label phase 3 trial', *Lancet (London, England)*, 385(9980), pp. 1873–1883.

Hiromura, K., Pippin, J.W., Fero, M.L., Roberts, J.M. & Shankland, S.J. (1999) 'Modulation of apoptosis by the cyclin-dependent kinase inhibitor p27(Kip1)', *Journal of Clinical Investigation*, 103(5), pp. 597–604.

HK, M.-H. (2008) 'Chronic lymphocytic leukaemia/small lymphocytic lymphoma', *WHO Classification of Tumours of Haematopoietic and Lymphoid Tissues*, pp. 180–182.

Hoellenriegel, J., Meadows, S.A., Sivina, M., Wierda, W.G., Kantarjian, H., Keating, M.J., Giese, N., O'Brien, S., Yu, A., Miller, L.L., Lannutti, B.J. & Burger, J.A. (2011) 'The phosphoinositide 3'-kinase delta inhibitor, CAL-101, inhibits B-cell receptor signaling and chemokine networks in chronic lymphocytic leukemia', *Blood*, 118(13), pp. 3603–3612.

Hollenhorst, P.C. (2012) 'RAS/ERK pathway transcriptional regulation through ETS/AP-1 binding sites', *Small GTPases*, 3(3), pp. 154–158.

Hollstein, M., Sidransky, D., Vogelstein, B. & Harris, C.C. (1991) 'p53 mutations in human cancers', *Science (New York, N.Y.)*, 253(5015), pp. 49–53.

Holroyd, A.K. & Michie, A.M. (2018) 'The role of mTOR-mediated signaling in the regulation of cellular migration', *Immunology letters*, 196pp. 74–79.

Hömig-Hölzel, C., Hojer, C., Rastelli, J., Casola, S., Strobl, L.J., Müller, W., Quintanilla-Martinez, L., Gewies, A., Ruland, J., Rajewsky, K. & Zimber-Strobl, U. (2008) 'Constitutive CD40 signaling in B cells selectively activates the noncanonical NF-kappaB pathway and promotes lymphomagenesis', *The Journal of experimental medicine*, 205(6), pp. 1317–1329.

Hostager, B.S., Catlett, I.M. & Bishop, G.A. (2000) 'Recruitment of CD40 and tumor necrosis factor receptor-associated factors 2 and 3 to membrane microdomains during CD40 signaling', *The Journal of biological chemistry*, 275(20), pp. 15392–15398.

Hou, P., Araujo, E., Zhao, T., Zhang, M., Massenburg, D., Veselits, M., Doyle, C., Dinner, A.R. & Clark, M.R. (2006) 'B cell antigen receptor signaling and internalization are mutually exclusive events', *PLoS biology*, 4(7), pp. 1147–1158.

Van Den Hove, L.E., Van Gool, S.W., Vandenberghe, P., Bakkus, M., Thielemans, K., Boogaerts, M.A. & Ceuppens, J.L. (1997) 'CD40 triggering of chronic lymphocytic leukemia B cells results in efficient alloantigen presentation and cytotoxic T lymphocyte induction by up-regulation of CD80 and CD86 costimulatory molecules', *Leukemia 1997 11:4*, 11(4), pp. 572–580.

Huang, B., Deo, D., Xia, M. & Vassilev, L.T. (2009) 'Pharmacologic p53 activation blocks cell cycle progression but fails to induce senescence in epithelial cancer cells', *Molecular cancer research : MCR*, 7(9), pp. 1497–1509.

Hyman, D., Chatterjee, M., Langenberg, M.H.G., Lin, C.C., Suárez, C., Tai, D., Cassier, P., Yamamoto, N., Weger, V.A. De, Jeay, S., Meille, C., Halilovic, E., Mariconti, L., Guerreiro, N., Kumar, A., Wuerthner, J.U. & Bauer, S. (2016) 'Wednesday 29 November 2016: Poster Sessions: Molecular targeted agents II: Poster/Poster in the spotlight (Board P070)', *European Journal of Cancer*, S1(69), pp. S128–S129.

Ianevski, A., He, L., Aittokallio, T. & Tang, J. (2017) 'SynergyFinder: a web application for analyzing drug combination dose-response matrix data.', *Bioinformatics (Oxford, England)*, 33(15), pp. 2413–2415.

Ibrahim, S., Keating, M., Do, K.A., O'Brien, S., Huh, Y.O., Jilani, I., Lerner, S., Kantarjian, H.M. & Albitar, M. (2001) 'CD38 expression as an important prognostic factor in B-cell chronic lymphocytic leukemia', *Blood*, 98(1), pp. 181–186.

Inoki, K., Li, Y., Zhu, T., Wu, J. & Guan, K.L. (2002) 'TSC2 is phosphorylated and inhibited by Akt and suppresses mTOR signalling', *Nature cell biology*, 4(9), pp. 648–657.

Ishiai, M., Kurosaki, M., Pappu, R., Okawa, K., Ronko, I., Fu, C., Shibata, M., Iwamatsu, A., Chan, A.C. & Kurosaki, T. (1999) 'BLNK required for coupling Syk to PLC gamma 2 and Rac1-JNK in B cells.', *Immunity*, 10(1), pp. 117–25.

Ishizawa, J., Nakamaru, K., Seki, T., Tazaki, K., Kojima, K., Chachad, D., Zhao, R., Heese, L., Ma, W., Ma, M.C.J., DiNardo, C., Pierce, S., Patel, K.P., Tse, A., Eric Davis, R., Rao, A. & Andreeff, M. (2018) 'Predictive Gene Signatures Determine Tumor Sensitivity to MDM2 Inhibition', *Cancer research*, 78(10), pp. 2721–2731.

Italiano, A., Miller, W.H., Blay, J.Y., Gietema, J.A., Bang, Y.J., Mileshkin, L.R., Hirte, H.W., Higgins, B., Blotner, S., Nichols, G.L., Chen, L.C., Petry, C., Yang, Q.J., Schmitt, C., Jamois, C. & Siu, L.L. (2021) 'Phase I study of daily and weekly regimens of the orally administered MDM2 antagonist idasanutlin in patients with advanced tumors', *Investigational new drugs*, 39(6), pp. 1587–1597.

Iwabuchi, K., Li, B., Bartel, P. & Fields, S. (1993) 'Use of the two-hybrid system to identify the domain of p53 involved in oligomerization.', *Oncogene*, 8(6), pp. 1693–1696.

Jacob, A., Pound, J.D., Challa, A. & Gordon, J. (1998) 'Release of clonal block in B cell chronic lymphocytic leukaemia by engagement of co-operative epitopes on CD40.', *Leukemia research*, 22(4), pp. 379–82.

Jain, N., Keating, M., Thompson, P., Ferrajoli, A., Burger, J., Borthakur, G., Takahashi, K., Estrov, Z., Fowler, N., Kadia, T., Konopleva, M., Alvarado, Y., Yilmaz, M., DiNardo, C., Bose, P., Ohanian, M., Pemmaraju, N., Jabbour, E., Sasaki, K., et al. (2019) 'Ibrutinib and Venetoclax for First-Line Treatment of CLL', *The New England journal of medicine*, 380(22), pp. 2095–2103.

Jaksic, B., Brugiatelli, M., Krc, I., Losonczi, H., Holowiecki, J., Planinc-Peraica, A., Kusec, R., Morabito, F., Iacopino, P. & Lutz, D. (1997) 'High dose chlorambucil versus Binet's modified cyclophosphamide, doxorubicin, vincristine, and prednisone regimen in the treatment of patients with advanced B-cell chronic lymphocytic leukemia. Results of an international multicenter randomized trial. International Society for Chemo-Immunotherapy, Vienna.', *Cancer*, 79(11), pp. 2107–14.

Jänicke, R.U. (2009) ‘MCF-7 breast carcinoma cells do not express caspase-3’, *Breast cancer research and treatment*, 117(1), pp. 219–221.

Jänicke, R.U., Sprengart, M.L., Wati, M.R. & Porter, A.G. (1998) ‘Caspase-3 is required for DNA fragmentation and morphological changes associated with apoptosis’, *The Journal of biological chemistry*, 273(16), pp. 9357–9360.

Jayappa, K.D., Portell, C.A., Gordon, V.L., Capaldo, B.J., Bekiranov, S., Axelrod, M.J., Brett, L.K., Wulfkuhle, J.D., Gallagher, R.I., Petricoin, E.F., Bender, T.P., Williams, M.E. & Weber, M.J. (2017) ‘Microenvironmental agonists generate de novo phenotypic resistance to combined ibrutinib plus venetoclax in CLL and MCL’, *Blood advances*, 1(14), pp. 933–946.

Jeay, S., Gaulis, S., Ferretti, S., Bitter, H., Ito, M., Valat, T., Murakami, M., Ruetz, S., Guthy, D.A., Rynn, C., Jensen, M.R., Wiesmann, M., Kallen, J., Furet, P., Gessier, F., Holzer, P., Masuya, K., Würthner, J., Halilovic, E., et al. (2015) ‘A distinct p53 target gene set predicts for response to the selective p53-HDM2 inhibitor NVP-CGM097’, *eLife*, 4(MAY), .

Jenkins, J.R., Rudge, K. & Currie, G.A. (1984) ‘Cellular immortalization by a cDNA clone encoding the transformation-associated phosphoprotein p53’, *Nature*, 312(5995), pp. 651–654.

Joerger, A.C. & Fersht, A.R. (2008) ‘Structural biology of the tumor suppressor p53’, *Annual review of biochemistry*, 77pp. 557–582.

Joerger, A.C. & Fersht, A.R. (2007) ‘Structure-function-rescue: the diverse nature of common p53 cancer mutants’, *Oncogene*, 26(15), pp. 2226–2242.

Johnson-Farley, N., Veliz, J., Bhagavathi, S. & Bertino, J.R. (2015) ‘ABT-199, a BH3 mimetic that specifically targets Bcl-2, enhances the antitumor activity of chemotherapy, bortezomib and JQ1 in “double hit” lymphoma cells.’, *Leukemia & lymphoma*, 56(7), pp. 2146–52.

Johnston, R.J., Poholek, A.C., DiToro, D., Yusuf, I., Eto, D., Barnett, B., Dent, A.L., Craft, J. & Crotty, S. (2009) ‘Bcl6 and Blimp-1 are reciprocal and antagonistic regulators of T follicular helper cell differentiation.’, *Science (New York, N.Y.)*, 325(5943), pp. 1006–10.

Jones, J.A., Robak, T., Brown, J.R., Awan, F.T., Badoux, X., Coutre, S., Loscertales, J., Taylor, K., Vandenberghe, E., Wach, M., Wagner-Johnston, N., Ysebaert, L., Dreiling, L., Dubowy, R., Xing, G., Flinn, I.W. & Owen, C. (2017) ‘Efficacy and safety of idelalisib in combination with ofatumumab for previously treated chronic lymphocytic leukaemia: an open-label, randomised phase 3 trial’, *The Lancet. Haematology*, 4(3), pp. e114–e126.

Jones, J.A., Ruppert, A.S., Zhao, W., Lin, T.S., Rai, K., Peterson, B., Larson, R.A., Marcucci, G., Heerema, N.A. & Byrd, J.C. (2013) ‘Patients with chronic lymphocytic leukemia with high-risk genomic features have inferior outcome on successive Cancer and Leukemia Group B trials with alemtuzumab consolidation: subgroup analysis from CALGB 19901 and CALGB 10101’, *Leukemia & lymphoma*, 54(12), pp. 2654–2659.

Juliusson, G., Oscier, D.G., Fitchett, M., Ross, F.M., Stockdill, G., Mackie, M.J., Parker, A.C., Castoldi, G.L., Cuneo, A., Knuutila, S., Elonen, E. & Gahrton, G. (1990) ‘Prognostic

subgroups in B-cell chronic lymphocytic leukemia defined by specific chromosomal abnormalities', *The New England journal of medicine*, 323(11), pp. 720–724.

Jung, J., Lee, J.S., Dickson, M.A., Schwartz, G.K., Le Cesne, A., Varga, A., Bahleda, R., Wagner, A.J., Choy, E., De Jonge, M.J., Light, M., Rowley, S., Macé, S. & Watters, J. (2016) 'TP53 mutations emerge with HDM2 inhibitor SAR405838 treatment in de-differentiated liposarcoma', *Nature communications*, 7.

Junttila, I.S., Mizukami, K., Dickensheets, H., Meier-Schellersheim, M., Yamane, H., Donnelly, R.P. & Paul, W.E. (2008) 'Tuning sensitivity to IL-4 and IL-13: differential expression of IL-4Ralpha, IL-13Ralpha1, and gammac regulates relative cytokine sensitivity.', *The Journal of experimental medicine*, 205(11), pp. 2595–608.

Kater, A.P., Evers, L.M., Remmerswaal, E.B.M., Jaspers, A., Oosterwijk, M.F., Van Lier, R.A.W., Van Oers, M.H.J. & Eldering, E. (2004) 'CD40 stimulation of B-cell chronic lymphocytic leukaemia cells enhances the anti-apoptotic profile, but also Bid expression and cells remain susceptible to autologous cytotoxic T-lymphocyte attack', *British Journal of Haematology*, 127(4), pp. 404–415.

Kawano, Y., Moschetta, M., Manier, S., Glavey, S., Görgün, G.T., Roccaro, A.M., Anderson, K.C. & Ghobrial, I.M. (2015) 'Targeting the bone marrow microenvironment in multiple myeloma', *Immunological Reviews*, 263(1), pp. 160–172.

Kay, N.E. & Pittner, B.T. (2003) 'IL-4 biology: impact on normal and leukemic CLL B cells.', *Leukemia & lymphoma*, 44(6), pp. 897–903.

Kay, N.E., Shanafelt, T.D., Strege, A.K., Lee, Y.K., Bone, N.D. & Raza, A. (2007) 'Bone biopsy derived marrow stromal elements rescue chronic lymphocytic leukemia B-cells from spontaneous and drug induced cell death and facilitates an "angiogenic switch"', *Leukemia research*, 31(7), pp. 899–906.

Kelly-Welch, A., Hanson, E.M. & Keegan, A.D. (2005) 'Interleukin-4 (IL-4) pathway.', *Science's STKE : signal transduction knowledge environment*, 2005(293), p. cm9.

Khan, W.N., Alt, F.W., Gerstein, R.M., Malynn, B.A., Larsson, I., Rathbun, G., Davidson, L., Müller, S., Kantor, A.B., Herzenberg, L.A., Rosen, F.S. & Sideras, P. (1995) 'Defective B cell development and function in Btk-deficient mice', *Immunity*, 3(3), pp. 283–299.

Khanna, K.K., Keating, K.E., Kozlov, S., Scott, S., Gatei, M., Hobson, K., Taya, Y., Gabrielli, B., Chan, D., Lees-Miller, S.P. & Lavin, M.F. (1998) 'ATM associates with and phosphorylates p53: mapping the region of interaction', *Nature genetics*, 20(4), pp. 398–400.

King, I.L. & Mohrs, M. (2009) 'IL-4-producing CD4+ T cells in reactive lymph nodes during helminth infection are T follicular helper cells.', *The Journal of experimental medicine*, 206(5), pp. 1001–7.

Kitada, S., Zapata, J.M., Andreeff, M. & Reed, J.C. (1999) 'Bryostatin and CD40-ligand enhance apoptosis resistance and induce expression of cell survival genes in B-cell chronic lymphocytic leukaemia.', *British journal of haematology*, 106(4), pp. 995–1004.

Kitayner, M., Rozenberg, H., Kessler, N., Rabinovich, D., Shaulov, L., Haran, T.E. & Shakked, Z. (2006) 'Structural basis of DNA recognition by p53 tetramers', *Molecular cell*, 22(6), pp. 741–753.

Klein, A., Miera, O., Bauer, O., Golfier, S. & Schriever, F. (2000) 'Chemosensitivity of B cell chronic lymphocytic leukemia and correlated expression of proteins regulating apoptosis, cell cycle and DNA repair.', *Leukemia*, 14(1), pp. 40–6.

Klein, U., Lia, M., Crespo, M., Siegel, R., Shen, Q., Mo, T., Ambesi-Impiombato, A., Califano, A., Migliazza, A., Bhagat, G. & Dalla-Favera, R. (2010) 'The DLEU2/miR-15a/16-1 Cluster Controls B Cell Proliferation and Its Deletion Leads to Chronic Lymphocytic Leukemia', *Cancer Cell*, 17(1), pp. 28–40.

Kojima, K., Konopleva, M., McQueen, T., O'Brien, S., Plunkett, W. & Andreeff, M. (2006) 'Mdm2 inhibitor Nutlin-3a induces p53-mediated apoptosis by transcription-dependent and transcription-independent mechanisms and may overcome Atm-mediated resistance to fludarabine in chronic lymphocytic leukemia', *Blood*, 108(3), pp. 993–1000.

Kojima, K., Konopleva, M., Samudio, I.J., Shikami, M., Cabreira-Hansen, M., McQueen, T., Ruvolo, V., Tsao, T., Zeng, Z., Vassilev, L.T. & Andreeff, M. (2005) 'MDM2 antagonists induce p53-dependent apoptosis in AML: implications for leukemia therapy', *Blood*, 106(9), pp. 3150–3159.

Konopleva, M., Martinelli, G., Daver, N., Papayannidis, C., Wei, A., Higgins, B., Ott, M., Mascarenhas, J. & Andreeff, M. (2020) 'Molecular targets for therapy MDM2 inhibition: an important step forward in cancer therapy', *Leukemia*, 34pp. 2858–2874.

Konopleva, M.Y., Röllig, C., Cavenagh, J., Deeren, D., Girshova, L., Krauter, J., Martinelli, G., Montesinos, P., Schäfer, J.A., Ottmann, O., Petrini, M., Pigneux, A., Rambaldi, A., Recher, C., Rodriguez-Veiga, R., Taussig, D., Vey, N., Yoon, S.S., Ott, M., et al. (2022) 'Idasanutlin plus cytarabine in relapsed or refractory acute myeloid leukemia: results of the MIRROS trial', *Blood advances*, 6(14), pp. 4147–4156.

Van Kooten, G. & Banchereau, J. (2000) 'CD40-CD40 ligand', *Journal of Leukocyte Biology*, 67(1), pp. 2–17.

Krysov, S., Dias, S., Paterson, A., Mockridge, C.I., Potter, K.N., Smith, K.A., Ashton-Key, M., Stevenson, F.K. & Packham, G. (2012) 'Surface IgM stimulation induces MEK1/2-dependent MYC expression in chronic lymphocytic leukemia cells', *Blood*, 119(1), pp. 170–179.

Kubbutat, M.H.G., Jones, S.N. & Vousden, K.H. (1997) 'Regulation of p53 stability by Mdm2', *Nature*, 387(6630), pp. 299–303.

Kurosaki, T., Shinohara, H. & Baba, Y. (2010) 'B cell signaling and fate decision', *Annual review of immunology*, 28pp. 21–55.

Kussie, P.H., Gorina, S., Marechal, V., Elenbaas, B., Moreau, J., Levine, A.J. & Pavletich, N.P. (1996) 'Structure of the MDM2 oncoprotein bound to the p53 tumor suppressor transactivation domain', *Science (New York, N.Y.)*, 274(5289), pp. 948–953.

Lam, K.P., Kühn, R. & Rajewsky, K. (1997) 'In vivo ablation of surface immunoglobulin on mature B cells by inducible gene targeting results in rapid cell death', *Cell*, 90(6), pp. 1073–1083.

Lambros, M.B., Natrajan, R., Geyer, F.C., Lopez-Garcia, M.A., Dedes, K.J., Savage, K., Lacroix-Triki, M., Jones, R.L., Lord, C.J., Linardopoulos, S., Ashworth, A. & Reis-Filho, J.S. (2010) 'PPM1D gene amplification and overexpression in breast cancer: a qRT-PCR

and chromogenic in situ hybridization study.', *Modern pathology : an official journal of the United States and Canadian Academy of Pathology, Inc*, 23(10), pp. 1334–45.

Lampson, B.L., Kim, H.T., Davids, M.S., Abramson, J.S., Freedman, A.S., Jacobson, C.A., Armand, P.A., Joyce, R.M., Arnason, J.E., Rassenti, L.Z., Kipps, T.J., Fein, J., Fernandes, S.M., Hanna, J.R., Fisher, D.C. & Brown, J.R. (2019) 'Efficacy results of a phase 2 trial of first-line idelalisib plus ofatumumab in chronic lymphocytic leukemia', *Blood advances*, 3(7), pp. 1167–1174.

Landau, D.A., Carter, S.L., Stojanov, P., McKenna, A., Stevenson, K., Lawrence, M.S., Sougnez, C., Stewart, C., Sivachenko, A., Wang, L., Wan, Y., Zhang, W., Shukla, S.A., Vartanov, A., Fernandes, S.M., Saksena, G., Cibulskis, K., Tesar, B., Gabriel, S., et al. (2013) 'Evolution and impact of subclonal mutations in chronic lymphocytic leukemia', *Cell*, 152(4), pp. 714–726.

Landau, D.A., Tausch, E., Taylor-Weiner, A.N., Stewart, C., Reiter, J.G., Bahlo, J., Kluth, S., Bozic, I., Lawrence, M., Böttcher, S., Carter, S.L., Cibulskis, K., Mertens, D., Sougnez, C.L., Rosenberg, M., Hess, J.M., Edelmann, J., Kless, S., Kneba, M., et al. (2015) 'Mutations driving CLL and their evolution in progression and relapse', *Nature*, 526(7574), pp. 525–530.

Lane, D.P. & Crawford, L. V. (1979) 'T antigen is bound to a host protein in SV40-transformed cells', *Nature*, 278(5701), pp. 261–263.

Lavin, M.F. (2008) 'Ataxia-telangiectasia: from a rare disorder to a paradigm for cell signalling and cancer', *Nature reviews. Molecular cell biology*, 9(10), pp. 759–769.

LeBlanc, R., Catley, L.P., Hideshima, T., Lentzsch, S., Mitsiades, C.S., Mitsiades, N., Neuberg, D., Goloubeva, O., Pien, C.S., Adams, J., Gupta, D., Richardson, P.G., Munshi, N.C. & Anderson, K.C. (2002) 'Proteasome inhibitor PS-341 inhibits human myeloma cell growth in vivo and prolongs survival in a murine model.', *Cancer research*, 62(17), pp. 4996–5000.

Lee, E.G., Boone, D.L., Chai, S., Libby, S.L., Chien, M., Lodolce, J.P. & Ma, A. (2000) 'Failure to regulate TNF-induced NF-kappaB and cell death responses in A20-deficient mice', *Science (New York, N.Y.)*, 289(5488), pp. 2350–2354.

Lee, F., Yokota, T., Otsuka, T., Meyerson, P., Villaret, D., Coffman, R., Mosmann, T., Rennick, D., Roehm, N. & Smith, C. (1986) 'Isolation and characterization of a mouse interleukin cDNA clone that expresses B-cell stimulatory factor 1 activities and T-cell- and mast-cell-stimulating activities.', *Proceedings of the National Academy of Sciences of the United States of America*, 83(7), pp. 2061–5.

Lee, H.H., Dadgostar, H., Cheng, Q., Shu, J. & Cheng, G. (1999) 'NF-kappaB-mediated up-regulation of Bcl-x and Bfl-1/A1 is required for CD40 survival signaling in B lymphocytes.', *Proceedings of the National Academy of Sciences of the United States of America*, 96(16), pp. 9136–41.

Lee, J., Kim, J., Kim, E.M., Kim, U., Kang, A.R., Park, J.K. & Um, H.D. (2021) 'p21WAF1/CIP1 promotes p53 protein degradation by facilitating p53-Wip1 and p53-Mdm2 interaction', *Biochemical and biophysical research communications*, 543pp. 23–28.

Lee, J.T. & Gu, W. (2010) ‘The multiple levels of regulation by p53 ubiquitination’, *Cell death and differentiation*, 17(1), pp. 86–92.

Leemans, C.R., Braakhuis, B.J.M. & Brakenhoff, R.H. (2011) ‘Chemoradiation The molecular biology of head and neck cancer’, *Nature Publishing Group*, 11(9), .

Leroy, B., Anderson, M. & Soussi, T. (2014) ‘TP53 mutations in human cancer: database reassessment and prospects for the next decade’, *Human mutation*, 35(6), pp. 672–688.

Letai, A.G. (2008) ‘Diagnosing and exploiting cancer’s addiction to blocks in apoptosis’, *Nature reviews. Cancer*, 8(2), pp. 121–132.

Levine, A.J. & Oren, M. (2009) ‘The first 30 years of p53: growing ever more complex’, *Nature reviews. Cancer*, 9(10), pp. 749–758.

Li, J., Yang, Y., Peng, Y., Austin, R.J., van Eyndhoven, W.G., Nguyen, K.C.Q., Gabriele, T., McCurrach, M.E., Marks, J.R., Hoey, T., Lowe, S.W. & Powers, S. (2002) ‘Oncogenic properties of PPM1D located within a breast cancer amplification epicenter at 17q23.’, *Nature genetics*, 31(2), pp. 133–4.

Liao, G., Yang, D., Ma, L., Li, W., Hu, L., Zeng, L., Wu, P., Duan, L. & Liu, Z. (2018) ‘The development of piperidinones as potent MDM2-P53 protein-protein interaction inhibitors for cancer therapy’, *European Journal of Medicinal Chemistry*, 159pp. 1–9.

Limon, J.J. & Fruman, D.A. (2012) ‘Akt and mTOR in B Cell Activation and Differentiation’, *Frontiers in Immunology*, 3(AUG), .

Lin, Y.C., Jhunjhunwala, S., Benner, C., Heinz, S., Welinder, E., Mansson, R., Sigvardsson, M., Hagman, J., Espinoza, C.A., Dutkowski, J., Ideker, T., Glass, C.K. & Murre, C. (2010) ‘A global network of transcription factors, involving E2A, EBF1 and Foxo1, that orchestrates B cell fate’, *Nature immunology*, 11(7), pp. 635–643.

Linares, L.K., Hengstermann, A., Ciechanover, A., Müller, S. & Scheffner, M. (2003) ‘HdmX stimulates Hdm2-mediated ubiquitination and degradation of p53’, *Proceedings of the National Academy of Sciences of the United States of America*, 100(21), pp. 12009–12014.

Linzer, D.I.H. & Levine, A.J. (1979) ‘Characterization of a 54K dalton cellular SV40 tumor antigen present in SV40-transformed cells and uninfected embryonal carcinoma cells’, *Cell*, 17(1), pp. 43–52.

Liu, J., Wang, Y., Xiong, E., Hong, R., Lu, Q., Ohno, H. & Wang, J.Y. (2019) ‘Role of the IgM Fc Receptor in Immunity and Tolerance’, *Frontiers in immunology*, 10(MAR), .

Loughery, J. & Meek, D. (2013) ‘Switching on p53: an essential role for protein phosphorylation?’, *Biodiscovery*, (7), .

Lowe, J., Cha, H., Lee, M.O., Mazur, S.J., Appella, E. & Fornace, A.J. (2012) ‘Regulation of the Wip1 phosphatase and its effects on the stress response’, *Frontiers in bioscience : a journal and virtual library*, 17(4), p. 1480.

Lu, X., Ma, O., Nguyen, T.A., Jones, S.N., Oren, M. & Donehower, L.A. (2007) ‘The Wip1 Phosphatase Acts as a Gatekeeper in the p53-Mdm2 Autoregulatory Loop’, *Cancer Cell*, 12(4), pp. 342–354.

Lu, X., Nguyen, T.A., Moon, S.H., Darlington, Y., Sommer, M. & Donehower, L.A. (2008) 'The type 2C phosphatase Wip1: an oncogenic regulator of tumor suppressor and DNA damage response pathways', *Cancer metastasis reviews*, 27(2), pp. 123–135.

Luna, R.M.D.O., Wagner, D.S. & Lozano, G. (1995) 'Rescue of early embryonic lethality in mdm2-deficient mice by deletion of p53', *Nature*, 378(6553), pp. 203–206.

M, K., E, M., R, C. & P, M. (1979) 'Simian virus 40-transformed cells express new species of proteins precipitable by anti-simian virus 40 tumor serum', *Journal of virology*, 31(2), pp. 472–483.

MacKay, F., Figgett, W.A., Saulep, D., Lepage, M. & Hibbs, M.L. (2010) 'B-cell stage and context-dependent requirements for survival signals from BAFF and the B-cell receptor', *Immunological reviews*, 237(1), pp. 205–225.

Mainou-Fowler, T., Copplestone, J.A. & Prentice, A.G. (1995) 'Effect of interleukins on the proliferation and survival of B cell chronic lymphocytic leukaemia cells.', *Journal of clinical pathology*, 48(5), pp. 482–7.

Mainou-Fowler, T., Proctor, S.J., Miller, S. & Dickinson, A.M. (2001) 'Expression and production of interleukin 4 in B-cell chronic lymphocytic leukaemia.', *Leukemia & lymphoma*, 42(4), pp. 689–98.

Majid, A., Lin, T.T., Best, G., Fishlock, K., Hewamana, S., Pratt, G., Yallop, D., Buggins, A.G.S., Wagner, S., Kennedy, B.J., Miall, F., Hills, R., Devereux, S., Oscier, D.G., Dyer, M.J.S., Fegan, C. & Pepper, C. (2011) 'CD49d is an independent prognostic marker that is associated with CXCR4 expression in CLL', *Leukemia Research*, 35(6), pp. 750–756.

Malcikova, J., Tausch, • E, Rossi, • D, Sutton, • L A, Soussi, • T, Zenz, • T, Kater, • A P, Niemann, • C U, Gonzalez, • D, Davi, • F, Gonzalez Diaz, • M, Moreno, • C, Gaidano, • G, Stamatopoulos, • K, Rosenquist, • R, Stilgenbauer, • S, Ghia, • P & Pospisilova, • S (2018) 'Chronic lymphocytic leukemia ERIC recommendations for TP53 mutation analysis in chronic lymphocytic leukemia-update on methodological approaches and results interpretation on behalf of the European Research Initiative on Chronic Lymphocytic Leukemia (ERIC)-TP53 network', *Leukemia*, 32pp. 1070–1080.

Malkin, D., Li, F.P., Strong, L.C., Fraumeni, J.F., Nelson, C.E., Kim, D.H., Kassel, J., Gryka, M.A., Bischoff, F.Z., Tainsky, M.A. & Friend, S.H. (1990) 'Germ line p53 mutations in a familial syndrome of breast cancer, sarcomas, and other neoplasms', *Science (New York, N.Y.)*, 250(4985), pp. 1233–1238.

Malumbres, M. & Barbacid, M. (2001) 'To cycle or not to cycle: a critical decision in cancer', *Nature reviews. Cancer*, 1(3), pp. 222–231.

Mansson, R., Welinder, E., Åhsberg, J., Lin, Y.C., Benner, C., Glass, C.K., Lucas, J.S., Sigvardsson, M. & Murre, C. (2012) 'Positive intergenic feedback circuitry, involving EBF1 and FOXO1, orchestrates B-cell fate', *Proceedings of the National Academy of Sciences of the United States of America*, 109(51), pp. 21028–21033.

Marasca, R., Maffei, R., Martinelli, Silvia, Fiorcari, S., Bulgarelli, J., Debbia, G., Rossi, D., Rossi, F.M., Rigolin, G.M., Martinelli, Sara, Gattei, V., Del Poeta, G., Laurenti, L., Forconi, F., Montillo, M., Gaidano, G. & Luppi, M. (2013) 'Clinical heterogeneity of de

novo 11q deletion chronic lymphocytic leukaemia: prognostic relevance of extent of 11q deleted nuclei inside leukemic clone', *Hematological oncology*, 31(2), pp. 348–355.

Marine, J.C., Francoz, S., Maetens, M., Wahl, G., Toledo, F. & Lozano, G. (2006) 'Keeping p53 in check: essential and synergistic functions of Mdm2 and Mdm4', *Cell death and differentiation*, 13(6), pp. 927–934.

Martín-Caballero, J., Flores, J.M., García-Palencia, P. & Serrano, M. (2001) 'Tumor susceptibility of p21(Waf1/Cip1)-deficient mice.', *Cancer research*, 61(16), pp. 6234–8.

Mascarenhas, J., Passamonti, F., Burbury, K., El-Galaly, T.C., Gerds, A., Gupta, V., Higgins, B., Wonde, K., Jamois, C., Kovic, B., Huw, L.-Y., Katakam, S., Maffioli, M., Mesa, R., Palmer, J., Bellini, M., Ross, D.M., Vannucchi, A.M. & Yacoub, A. (2022) 'The MDM2 antagonist idasanutlin in patients with polycythemia vera: results from a single-arm phase 2 study.', *Blood advances*, 6(4), pp. 1162–1174.

Mato, A., Nabhan, C., Kay, N.E., Weiss, M.A., Lamanna, N., Kipps, T.J., Grinblatt, D.L., Flinn, I.W., Kozloff, M.F., Flowers, C.R., Farber, C.M., Kiselev, P., Swern, A.S., Sullivan, K., Flick, E.D. & Sharman, J.P. (2016) 'Real-world clinical experience in the Connect® chronic lymphocytic leukaemia registry: a prospective cohort study of 1494 patients across 199 US centres', *British Journal of Haematology*, 175(5), p. 892.

Matrai, Z. (2013) 'CD38 as a prognostic marker in CLL', *https://doi.org/10.1080/10245330400020470*, 10(1), pp. 39–46.

Mauro, F.R., Molica, S., Laurenti, L., Cortelezzi, A., Carella, A.M., Zaja, F., Chiarenza, A., Angrilli, F., Nobile, F., Marasca, R., Musolino, C., Brugiatelli, M., Piciocchi, A., Vignetti, M., Fazi, P., Gentile, G., De Propris, M.S., Starza, I. Della, Marinelli, M., et al. (2014) 'Fludarabine plus alemtuzumab (FA) front-line treatment in young patients with chronic lymphocytic leukemia (CLL) and an adverse biologic profile', *Leukemia research*, 38(2), pp. 198–203.

Mccaig, A.M., Cosimo, E., Leach, M.T. & Michie, A.M. (2011) 'Dasatinib inhibits B cell receptor signalling in chronic lymphocytic leukaemia but novel combination approaches are required to overcome additional pro-survival microenvironmental signals', *British Journal of Haematology*, 153(2), pp. 199–211.

McDonald, C., Xanthopoulos, C. & Kostareli, E. (2021) 'The role of Bruton's tyrosine kinase in the immune system and disease', *Immunology*, 164(4), pp. 722–736.

Mehra, S., Messner, H., Minden, M. & Chaganti, R.S.K. (2002) 'Molecular cytogenetic characterization of non-Hodgkin lymphoma cell lines', *Genes Chromosomes and Cancer*, 33(3), pp. 225–234.

Messmer, B.T., Messmer, D., Allen, S.L., Kolitz, J.E., Kudalkar, P., Cesar, D., Murphy, E.J., Koduru, P., Ferrarini, M., Zupo, S., Cutrona, G., Damle, R.N., Wasil, T., Rai, K.R., Hellerstein, M.K. & Chiorazzi, N. (2005) 'In vivo measurements document the dynamic cellular kinetics of chronic lymphocytic leukemia B cells', *The Journal of Clinical Investigation*, 115(3), pp. 755–764.

Michaelis, M., Rothweiler, F., Barth, S., Cinat, J., Van Rikxoort, M., Löschmann, N., Voges, Y., Breitling, R., Von Deimling, A., Rödel, F., Weber, K., Fehse, B., MacK, E., Stiewe, T., Doerr, H.W., Speidel, D. & Cinatl, J. (2011) 'Adaptation of cancer cells from different

entities to the MDM2 inhibitor nutlin-3 results in the emergence of p53-mutated multi-drug-resistant cancer cells', *Cell death & disease*, 2(12), .

Miller, D.J. & Hayes, C.E. (1991) 'Phenotypic and genetic characterization of a unique B lymphocyte deficiency in strain A/WySnJ mice', *European journal of immunology*, 21(5), pp. 1123–1130.

Mockridge, C.I., Potter, K.N., Wheatley, I., Neville, L.A., Packham, G. & Stevenson, F.K. (2007) 'Reversible anergy of sIgM-mediated signaling in the two subsets of CLL defined by VH-gene mutational status', *Blood*, 109(10), pp. 4424–4431.

Moll, U.M. & Petrenko, O. (2003) 'The MDM2-p53 interaction.', *Molecular cancer research : MCR*, 1(14), pp. 1001–8.

Momand, J., Zambetti, G.P., Olson, D.C., George, D. & Levine, A.J. (1992) 'The mdm-2 oncogene product forms a complex with the p53 protein and inhibits p53-mediated transactivation', *Cell*, 69(7), pp. 1237–1245.

Monserrat, J., Sánchez, M.Á., de Paz, R., Díaz, D., Mur, S., Reyes, E., Prieto, A., de la Hera, A., Martínez-A, C. & Alvarez-Mon, M. (2014) 'Distinctive patterns of naïve/memory subset distribution and cytokine expression in CD4 T lymphocytes in ZAP-70 B-chronic lymphocytic patients.', *Cytometry. Part B, Clinical cytometry*, 86(1), pp. 32–43.

Moore, V.D.G., Brown, J.R., Certo, M., Love, T.M., Novina, C.D. & Letai, A. (2007) 'Chronic lymphocytic leukemia requires BCL2 to sequester prodeath BIM, explaining sensitivity to BCL2 antagonist ABT-737', *The Journal of clinical investigation*, 117(1), pp. 112–121.

Moreno, C., Greil, R., Demirkan, F., Tedeschi, A., Anz, B., Larratt, L., Simkovic, M., Samoilova, O., Novak, J., Ben-Yehuda, D., Strugov, V., Gill, D., Gribben, J.G., Hsu, E., Lih, C.J., Zhou, C., Clow, F., James, D.F., Styles, L., et al. (2019) 'Ibrutinib plus obinutuzumab versus chlorambucil plus obinutuzumab in first-line treatment of chronic lymphocytic leukaemia (iLLUMINATE): a multicentre, randomised, open-label, phase 3 trial', *The Lancet. Oncology*, 20(1), pp. 43–56.

Muller, P.A.J. & Vousden, K.H. (2013) 'p53 mutations in cancer', *Nature cell biology*, 15(1), pp. 2–8.

Mullis, K.B. (1990) *The Unusual Origin of the Polymerase Chain Reaction*, 262(4), pp. 56–65.

Murata, T., Obiri, N.I. & Puri, R.K. (1998) 'Structure of and signal transduction through interleukin-4 and interleukin-13 receptors (review).', *International journal of molecular medicine*, 1(3), pp. 551–7.

Nadeu, F., Delgado, J., Royo, C., Baumann, T., Stankovic, T., Pinyol, M., Jares, P., Navarro, A., Martín-García, D., Beà, S., Salaverria, I., Oldreive, C., Aymerich, M., Suárez-Cisneros, H., Rozman, M., Villamor, N., Colomer, D., López-Guillermo, A., González, M., et al. (2016) 'Clinical impact of clonal and subclonal TP53, SF3B1, BIRC3, NOTCH1, and ATM mutations in chronic lymphocytic leukemia', *Blood*, 127(17), pp. 2122–2130.

Nagaoka, H., Takahashi, Y., Hayashi, R., Nakamura, T., Ishii, K., Matsuda, J., Ogura, A., Shirakata, Y., Karasuyama, H., Sudo, T., Nishikawa, S.I., Tsubata, T., Mizuochi, T.,

Asano, T., Sakano, H. & Takemori, T. (2000) 'Ras Mediates Effector Pathways Responsible for Pre-B Cell Survival, Which Is Essential for the Developmental Progression to the Late Pre-B Cell Stage', *Journal of Experimental Medicine*, 192(2), pp. 171–182.

Negrini, S., Gorgoulis, V.G. & Halazonetis, T.D. (2010) 'Genomic instability--an evolving hallmark of cancer', *Nature reviews. Molecular cell biology*, 11(3), pp. 220–228.

Néron, S., Nadeau, P.J., Darveau, A. & Leblanc, J.F. (2011) 'Tuning of CD40-CD154 interactions in human B-lymphocyte activation: a broad array of in vitro models for a complex in vivo situation', *Archivum immunologiae et therapiae experimentalis*, 59(1), pp. 25–40.

Nims, R.W., Sykes, G., Cottrill, K., Ikonomi, P. & Elmore, E. (2010) 'Short tandem repeat profiling: part of an overall strategy for reducing the frequency of cell misidentification', *In vitro cellular & developmental biology. Animal*, 46(10), pp. 811–819.

Nishio, M., Endo, T., Tsukada, N., Ohata, J., Kitada, S., Reed, J.C., Zvaifler, N.J. & Kipps, T.J. (2005) 'Nurselike cells express BAFF and APRIL, which can promote survival of chronic lymphocytic leukemia cells via a paracrine pathway distinct from that of SDF-1α', *Blood*, 106(3), pp. 1012–1020.

Noma, Y., Sideras, P., Naito, T., Bergstedt-Lindquist, S., Azuma, C., Severinson, E., Tanabe, T., Kinashi, T., Matsuda, F., Yaoita, Y. & Honjo, T. (1986) 'Cloning of cDNA encoding the murine IgG1 induction factor by a novel strategy using SP6 promoter', *Nature 1986 319:6055*, 319(6055), pp. 640–646.

Nowakowski, G.S., Hoyer, J.D., Shanafelt, T.D., Geyer, S.M., LaPlant, B.R., Call, T.G., Jelinek, D.F., Zent, C.S. & Kay, N.E. (2007) 'Using smudge cells on routine blood smears to predict clinical outcome in chronic lymphocytic leukemia: a universally available prognostic test', *Mayo Clinic proceedings*, 82(4), pp. 449–453.

Nurieva, R.I., Chung, Y., Martinez, G.J., Yang, X.O., Tanaka, S., Matskevitch, T.D., Wang, Y.-H. & Dong, C. (2009) 'Bcl6 mediates the development of T follicular helper cells.', *Science (New York, N.Y.)*, 325(5943), pp. 1001–5.

O'Brien, S., Jones, J.A., Coutre, S.E., Mato, A.R., Hillmen, P., Tam, C., Österborg, A., Siddiqi, T., Thirman, M.J., Furman, R.R., Ilhan, O., Keating, M.J., Call, T.G., Brown, J.R., Stevens-Brogan, M., Li, Y., Clow, F., James, D.F., Chu, A.D., et al. (2016) 'Ibrutinib for patients with relapsed or refractory chronic lymphocytic leukaemia with 17p deletion (RESONATE-17): a phase 2, open-label, multicentre study', *The Lancet. Oncology*, 17(10), pp. 1409–1418.

O'Brien, S.M., Kantarjian, H., Thomas, D.A., Giles, F.J., Freireich, E.J., Cortes, J., Lerner, S. & Keating, M.J. (2001) 'Rituximab dose-escalation trial in chronic lymphocytic leukemia', *Journal of Clinical Oncology*, 19(8), pp. 2165–2170.

O'Brien, S.M., Lamanna, N., Kipps, T.J., Flinn, I., Zelenetz, A.D., Burger, J.A., Holes, L., Johnson, D.M., Gu, J., Dansey, R.D., Dubowy, R.L. & Coutre, S.E. (2013) 'A phase II study of the selective phosphatidylinositol 3-kinase delta (PI3Kδ) inhibitor idelalisib (GS-1101) in combination with rituximab (R) in treatment-naive patients (pts) ≥65 years with chronic lymphocytic leukemia (CLL) or small lymphocytic lymphoma (SLL).', *https://doi.org/10.1200/jco.2013.31.15_suppl.7005*, 31(15_suppl), pp. 7005–7005.

O'Brien, S.M., Lamanna, N., Kipps, T.J., Flinn, I., Zelenetz, A.D., Burger, J.A., Keating, M., Mitra, S., Holes, L., Yu, A.S., Johnson, D.M., Miller, L.L., Kim, Y., Dansey, R.D., Dubowy, R.L. & Coutre, S.E. (2015) 'A phase 2 study of idelalisib plus rituximab in treatment-naïve older patients with chronic lymphocytic leukemia', *Blood*, 126(25), pp. 2686–2694.

Oh-Hora, M., Johmura, S., Hashimoto, A., Hikida, M. & Kurosaki, T. (2003) 'Requirement for Ras guanine nucleotide releasing protein 3 in coupling phospholipase C-gamma2 to Ras in B cell receptor signaling', *The Journal of experimental medicine*, 198(12), pp. 1841–1851.

Okkenhaug, K. & Vanhaesebroeck, B. (2003) 'PI3K in lymphocyte development, differentiation and activation', *Nature reviews. Immunology*, 3(4), pp. 317–330.

Oliner, J.D., Pietenpol, J.A., Thiagalingam, S., Gyuris, J., Kinzler, K.W. & Vogelstein, B. (1993) 'Oncoprotein MDM2 conceals the activation domain of tumour suppressor p53', *Nature*, 362(6423), pp. 857–860.

Olivier, M., Eeles, R., Hollstein, M., Khan, M.A., Harris, C.C. & Hainaut, P. (2002) 'The IARC TP53 database: new online mutation analysis and recommendations to users', *Human mutation*, 19(6), pp. 607–614.

Olivier, M., Hollstein, M. & Hainaut, P. (2010) 'TP53 mutations in human cancers: origins, consequences, and clinical use', *Cold Spring Harbor perspectives in biology*, 2(1), .

O'Rourke, L.M., Tooze, R., Turner, M., Sandoval, D.M., Carter, R.H., Tybulewicz, V.L.J. & Fearon, D.T. (1998) 'CD19 as a membrane-anchored adaptor protein of B lymphocytes: costimulation of lipid and protein kinases by recruitment of Vav', *Immunity*, 8(5), pp. 635–645.

Otto, T. & Sicinski, P. (2017) 'Cell cycle proteins as promising targets in cancer therapy', *Nature reviews. Cancer*, 17(2), pp. 93–115.

Ouillette, P., Collins, R., Shakhan, S., Li, J., Li, C., Shedden, K. & Malek, S.N. (2011) 'The prognostic significance of various 13q14 deletions in chronic lymphocytic leukemia', *Clinical cancer research : an official journal of the American Association for Cancer Research*, 17(21), pp. 6778–6790.

Ouillette, P., Erba, H., Kujawski, L., Kaminski, M., Shedden, K. & Malek, S.N. (2008) 'Integrated genomic profiling of chronic lymphocytic leukemia identifies subtypes of deletion 13q14', *Cancer research*, 68(4), pp. 1012–1021.

Pan, R., Ruvolo, V., Mu, H., Leverson, J.D., Nichols, G., Reed, J.C., Konopleva, M. & Andreeff, M. (2017) 'Synthetic Lethality of Combined Bcl-2 Inhibition and p53 Activation in AML: Mechanisms and Superior Antileukemic Efficacy', *Cancer cell*, 32(6), pp. 748-760.e6.

Pan, Z., Scheerens, H., Li, S.J., Schultz, B.E., Sprengeler, P.A., Burrill, L.C., Mendonca, R. V., Sweeney, M.D., Scott, K.C.K., Grothaus, P.G., Jeffery, D.A., Spoerke, J.M., Honigberg, L.A., Young, P.R., Dalrymple, S.A. & Palmer, J.T. (2007) 'Discovery of selective irreversible inhibitors for Bruton's tyrosine kinase', *ChemMedChem*, 2(1), pp. 58–61.

Panayiotidis, P., Ganeshaguru, K., Jabbar, S.A. & Hoffbrand, A. V (1993) 'Interleukin-4 inhibits apoptotic cell death and loss of the bcl-2 protein in B-chronic lymphocytic leukaemia cells in vitro.', *British journal of haematology*, 85(3), pp. 439–45.

Parada, L.F., Land, H., Weinberg, R.A., Wolf, D. & Rotter, V. (1984) 'Cooperation between gene encoding p53 tumour antigen and ras in cellular transformation', *Nature*, 312(5995), pp. 649–651.

París, R., Henry, R.E., Stephens, S.J., McBryde, M. & Espinosa, J.M. (2008) 'Multiple p53-independent gene silencing mechanisms define the cellular response to p53 activation', *http://dx.doi.org/10.4161/cc.6420*, 7(15), pp. 2427–2433.

Parker, H., Rose-Zerilli, M.J.J., Parker, A., Chaplin, T., Wade, R., Gardiner, A., Griffiths, M., Collins, A., Young, B.D., Oscier, D.G. & Strefford, J.C. (2011) '13q deletion anatomy and disease progression in patients with chronic lymphocytic leukemia', *Leukemia*, 25(3), pp. 489–497.

Patten, P.E.M., Buggins, A.G.S., Richards, J., Wotherspoon, A., Salisbury, J., Mufti, G.J., Hamblin, T.J. & Devereux, S. (2008) 'CD38 expression in chronic lymphocytic leukemia is regulated by the tumor microenvironment', *Blood*, 111(10), pp. 5173–5181.

Pechackova, S., Burdova, K., Benada, J., Kleiblova, P., Jenikova, G. & Macurek, L. (2016) 'Inhibition of WIP1 phosphatase sensitizes breast cancer cells to genotoxic stress and to MDM2 antagonist nutlin-3', *Oncotarget*, 7(12), pp. 14458–14475.

Pecháčková, S., Burdová, K. & Macurek, L. (2017) 'WIP1 phosphatase as pharmacological target in cancer therapy', *Journal of Molecular Medicine 2017 95:6*, 95(6), pp. 589–599.

Pedersen, I.M. & Reed, J.C. (2004) 'Microenvironmental interactions and survival of CLL B-cells', *Leukemia & lymphoma*, 45(12), pp. 2365–2372.

Pepper, C., Hoy, T. & Bentley, D.P. (1997) 'Bcl-2/Bax ratios in chronic lymphocytic leukaemia and their correlation with in vitro apoptosis and clinical resistance', *British journal of cancer*, 76(7), pp. 935–938.

Pepper, C., Lin, T.T., Pratt, G., Hewamana, S., Brennan, P., Hiller, L., Hills, R., Ward, R., Starczynski, J., Austen, B., Hooper, L., Stankovic, T. & Fegan, C. (2008) 'Mcl-1 expression has in vitro and in vivo significance in chronic lymphocytic leukemia and is associated with other poor prognostic markers', *Blood*, 112(9), pp. 3807–3817.

Pepper, C., Mahdi, J.G., Buggins, A.G.S., Hewamana, S., Walsby, E., Mahdi, E., Al-Haza'a, A., Mahdi, A.J., Lin, T.T., Pearce, L., Morgan, L., Bowen, I.D., Brennan, P. & Fegan, C. (2011) 'Two novel aspirin analogues show selective cytotoxicity in primary chronic lymphocytic leukaemia cells that is associated with dual inhibition of Rel A and COX-2', *Cell Proliferation*, 44(4), pp. 380–390.

Pernis, A.B. & Rothman, P.B. (2002) 'JAK-STAT signaling in asthma.', *The Journal of clinical investigation*, 109(10), pp. 1279–83.

Petlickovski, A., Laurenti, L., Li, X., Marietti, S., Chiusolo, P., Sica, S., Leone, G. & Efremov, D.G. (2005) 'Sustained signaling through the B-cell receptor induces Mcl-1 and promotes survival of chronic lymphocytic leukemia B cells', *Blood*, 105(12), pp. 4820–4827.

Pettitt, A.R. (2003) ‘Mechanism of action of purine analogues in chronic lymphocytic leukaemia’, *British Journal of Haematology*, 121(5), pp. 692–702.

Pettitt, A.R., Sherrington, P.D., Stewart, G., Cawley, J.C., Malcolm R Taylor, A. & Stankovic, T. (2001) ‘p53 dysfunction in B-cell chronic lymphocytic leukemia: inactivation of ATM as an alternative to TP53 mutation’, *Blood*, 98(3), pp. 814–822.

Pflug, N., Bahlo, J., Shanafelt, T.D., Eichhorst, B.F., Bergmann, M.A., Elter, T., Bauer, K., Malchau, G., Rabe, K.G., Stilgenbauer, S., Döhner, H., Jäger, U., Eckart, M.J., Hopfinger, G., Busch, R., Fink, A.M., Wendtner, C.M., Fischer, K., Kay, N.E., et al. (2014) ‘Development of a comprehensive prognostic index for patients with chronic lymphocytic leukemia’, *Blood*, 124(1), pp. 49–62.

Phelan, J.D., Young, R.M., Webster, D.E., Roulland, S., Wright, G.W., Kasbekar, M., Shaffer, A.L., Ceribelli, M., Wang, J.Q., Schmitz, R., Nakagawa, M., Bachy, E., Huang, D.W., Ji, Y., Chen, L., Yang, Y., Zhao, H., Yu, X., Xu, W., et al. (2018) ‘A multiprotein supercomplex controlling oncogenic signalling in lymphoma’, *Nature*, 560(7718), pp. 387–391.

Picksley, S.M. & Lane, D.P. (1993) ‘The p53-mdm2 autoregulatory feedback loop: a paradigm for the regulation of growth control by p53?’, *BioEssays : news and reviews in molecular, cellular and developmental biology*, 15(10), pp. 689–90.

Pierce, S.K. & Liu, W. (2010) ‘The tipping points in the initiation of B cell signalling: how small changes make big differences’, *Nature Reviews. Immunology*, 10(11), p. 767.

Pizzolo, G., Chilosi, M., Ambrosetti, A., Semenzato, G., Fiore-Donati, L. & Perona, G. (1983) ‘Immunohistologic Study of Bone Marrow Involvement in B-Chronic Lymphocytic Leukemia’, *Blood*, 62(6), pp. 1289–1296.

Podar, K., Chauhan, D. & Anderson, K.C. (2009) ‘Bone marrow microenvironment and the identification of new targets for myeloma therapy’, *Leukemia : official journal of the Leukemia Society of America, Leukemia Research Fund, U.K*, 23(1), p. 10.

Polański, R., Noon, A.P., Blaydes, J., Phillips, A., Rubbi, C.P., Parsons, K., Vlatković, N. & Boyd, M.T. (2014) ‘Senescence induction in renal carcinoma cells by Nutlin-3: a potential therapeutic strategy based on MDM2 antagonism’, *Cancer Letters*, 353(2), pp. 211–219.

Ponader, S., Chen, S.S., Buggy, J.J., Balakrishnan, K., Gandhi, V., Wierda, W.G., Keating, M.J., O’Brien, S., Chiorazzi, N. & Burger, J.A. (2012) ‘The Bruton tyrosine kinase inhibitor PCI-32765 thwarts chronic lymphocytic leukemia cell survival and tissue homing in vitro and in vivo’, *Blood*, 119(5), pp. 1182–1189.

Puente, X.S., Beà, S., Valdés-Mas, R., Villamor, N., Gutiérrez-Abril, J., Martín-Subero, J.I., Munar, M., Rubio-Pérez, C., Jares, P., Aymerich, M., Baumann, T., Beekman, R., Belver, L., Carrio, A., Castellano, G., Clot, G., Colado, E., Colomer, D., Costa, D., et al. (2015) ‘Non-coding recurrent mutations in chronic lymphocytic leukaemia’, *Nature*, 526(7574), pp. 519–524.

Puente, X.S., Pinyol, M., Quesada, V., Conde, L., Ordóñez, G.R., Villamor, N., Escaramis, G., Jares, P., Beá, S., González-Díaz, M., Bassaganyas, L., Baumann, T., Juan, M., López-Guerra, M., Colomer, D., Tubío, J.M.C., López, C., Navarro, A., Tornador, C., et al.

(2011) ‘Whole-genome sequencing identifies recurrent mutations in chronic lymphocytic leukaemia’, *Nature*, 475(7354), pp. 101–105.

Quiroga, M.P., Balakrishnan, K., Kurtova, A. V, Sivina, M., Keating, M.J., Wierda, W.G., Gandhi, V. & Burger, J.A. (2009) ‘B-cell antigen receptor signaling enhances chronic lymphocytic leukemia cell migration and survival: specific targeting with a novel spleen tyrosine kinase inhibitor, R406.’, *Blood*, 114(5), pp. 1029–37.

Rai, K.R., Döhner, H., Keating, M.J. & Montserrat, E. (2001) ‘Chronic Lymphocytic Leukemia: Case-Based Session’, *Hematology*, 2001(1), pp. 140–156.

Rai, K.R., Peterson, B.L., Appelbaum, F.R., Kolitz, J., Elias, L., Shepherd, L., Hines, J., Threatte, G.A., Larson, R.A., Cheson, B.D. & Schiffer, C.A. (2000) ‘Fludarabine compared with chlorambucil as primary therapy for chronic lymphocytic leukemia’, *The New England journal of medicine*, 343(24), pp. 1750–1757.

Rai, K.R., Sawitsky, A., Cronkite, E.P., Chanana, A.D., Levy, R.N. & Pasternack, B.S. (1975) ‘Clinical staging of chronic lymphocytic leukemia’, *Blood*, 46(2), pp. 219–234.

Ranheim, E.A., Cantwell, M.J. & Kipps, T.J. (1995) ‘Expression of CD27 and its ligand, CD70, on chronic lymphocytic leukemia B cells.’, *Blood*, 85(12), pp. 3556–65.

Ranheim, E.A. & Kipps, T.J. (1995) ‘Tumor necrosis factor-α facilitates induction of CD80 (B7-1) and CD54 on human B cells by activated T cells: Complex regulation by IL-4, IL-10, and CD40L’, *Cellular Immunology*, 161(2), pp. 226–235.

Rathmell, J.C., Cooke, M.P., Ho, W.Y., Grein, J., Townsend, S.E., Davis, M.M. & Goodnow, C.C. (1995) ‘CD95 (Fas)-dependent elimination of self-reactive B cells upon interaction with CD4+ T cells.’, *Nature*, 376(6536), pp. 181–4.

Rauta, J., Alarmo, E.-L., Kauraniemi, P., Karhu, R., Kuukasjärvi, T. & Kallioniemi, A. (2006) ‘The serine-threonine protein phosphatase PPM1D is frequently activated through amplification in aggressive primary breast tumours.’, *Breast cancer research and treatment*, 95(3), pp. 257–63.

Rawstron, A.C., Bennett, F.L., O’Connor, S.J.M., Kwok, M., Fenton, J.A.L., Plummer, M., de Tute, R., Owen, R.G., Richards, S.J., Jack, A.S. & Hillmen, P. (2008) ‘Monoclonal B-Cell Lymphocytosis and Chronic Lymphocytic Leukemia’, *New England Journal of Medicine*, 359(6), pp. 575–583.

Ray-Coquard, I., Blay, J.Y., Italiano, A., Le Cesne, A., Penel, N., Zhi, J., Heil, F., Rueger, R., Graves, B., Ding, M., Geho, D., Middleton, S.A., Vassilev, L.T., Nichols, G.L. & Bui, B.N. (2012) ‘Effect of the MDM2 antagonist RG7112 on the P53 pathway in patients with MDM2-amplified, well-differentiated or dedifferentiated liposarcoma: an exploratory proof-of-mechanism study’, *The Lancet Oncology*, 13(11), pp. 1133–1140.

Reid, Y., Storts, D., Riss, T. & Minor, L. (2023) ‘Authentication of Human and Mouse Cell Lines by Short Tandem Repeat (STR) DNA Genotype Analysis’, *Assay Guidance Manual*,

Roberts, A.W., Davids, M.S., Pagel, J.M., Kahl, B.S., Puvvada, S.D., Gerecitano, J.F., Kipps, T.J., Anderson, M.A., Brown, J.R., Gressick, L., Wong, S., Dunbar, M., Zhu, M., Desai, M.B., Cerri, E., Heitner Enschede, S., Humerickhouse, R.A., Wierda, W.G. & Seymour,

J.F. (2016) ‘Targeting BCL2 with Venetoclax in Relapsed Chronic Lymphocytic Leukemia’, *The New England journal of medicine*, 374(4), pp. 311–322.

Roberts, A.W., Seymour, J.F., Brown, J.R., Wierda, W.G., Kipps, T.J., Khaw, S.L., Carney, D.A., He, S.Z., Huang, D.C.S., Xiong, H., Cui, Y., Busman, T.A., McKeegan, E.M., Krivoshik, A.P., Enschede, S.H. & Humerickhouse, R. (2012) ‘Substantial susceptibility of chronic lymphocytic leukemia to BCL2 inhibition: results of a phase I study of navitoclax in patients with relapsed or refractory disease’, *Journal of clinical oncology : official journal of the American Society of Clinical Oncology*, 30(5), pp. 488–496.

Robertson, K.D. & Jones, P.A. (1998) ‘The human ARF cell cycle regulatory gene promoter is a CpG island which can be silenced by DNA methylation and down-regulated by wild-type p53’, *Molecular and cellular biology*, 18(11), pp. 6457–6473.

Robertson, L.E., Chubb, S., Meyn, R.E., Story, M., Ford, R., Hittelman, W.N. & Plunkett, W. (1993) ‘Induction of apoptotic cell death in chronic lymphocytic leukemia by 2- chloro-2’-deoxyadenosine and 9-beta-D-arabinosyl-2-fluoroadenine’, *Blood*, 81(1), pp. 143–150.

Robertson, L.E., Plunkett, W., McConnell, K., Keating, M.J. & McDonnell, T.J. (1996) ‘Bcl-2 expression in chronic lymphocytic leukemia and its correlation with the induction of apoptosis and clinical outcome.’, *Leukemia*, 10(3), pp. 456–459.

Rodrigues, C.A., Gonçalves, M.V., Ikoma, M.R.V., Lorand-Metze, I., Pereira, A.D., Farias, D.L.C. de, Chauffaille, M. de L.L.F., Schaffel, R., Ribeiro, E.F.O., Rocha, T.S. da, Buccheri, V., Vasconcelos, Y., Figueiredo, V.L. de P., Chiattone, C.S. & Yamamoto, M. (2016) ‘Diagnosis and treatment of chronic lymphocytic leukemia: recommendations from the Brazilian Group of Chronic Lymphocytic Leukemia’, *Revista brasileira de hematologia e hemoterapia*, 38(4), pp. 346–357.

Rodrigues, D.A., Sagrillo, F.S. & Fraga, C.A.M. (2018) *Duvelisib: A 2018 Novel FDA-Approved Small Molecule Inhibiting Phosphoinositide 3-Kinases*,

Romano, M.F., Lamberti, A., Tassone, P., Alfinito, F., Costantini, S., Chiurazzi, F., Defrance, T., Bonelli, P., Tuccillo, F., Turco, M.C. & Venuta, S. (1998) ‘Triggering of CD40 antigen inhibits fludarabine-induced apoptosis in B chronic lymphocytic leukemia cells.’, *Blood*, 92(3), pp. 990–5.

Rombout, A., Lust, S., Offner, F., Naessens, E., Verhasselt, B. & Philippé, J. (2016) ‘Mimicking the tumour microenvironment of chronic lymphocytic leukaemia in vitro critically depends on the type of B-cell receptor stimulation’, *British journal of cancer*, 114(6), pp. 704–712.

Rossi, D., Cerri, M., Deambrogi, C., Sozzi, E., Cresta, S., Rasi, S., De Paoli, L., Spina, V., Gattei, V., Capello, D., Forconi, F., Lauria, F. & Gaidano, G. (2009) ‘The prognostic value of TP53 mutations in chronic lymphocytic leukemia is independent of Del17p13: implications for overall survival and chemorefractoriness’, *Clinical cancer research : an official journal of the American Association for Cancer Research*, 15(3), pp. 995–1004.

Rossi, D., Khiabanian, H., Spina, V., Ciardullo, C., Bruscaggin, A., Famà, R., Rasi, S., Monti, S., Deambrogi, C., De Paoli, L., Wang, J., Gattei, V., Guarini, A., Foà, R., Rabadan, R. & Gaidano, G. (2014) ‘Clinical impact of small TP53 mutated subclones in chronic lymphocytic leukemia’, *Blood*, 123(14), pp. 2139–2147.

Rossi, D., Rasi, S., Fabbri, G., Spina, V., Fangazio, M., Forconi, F., Marasca, R., Laurenti, L., Bruscaggin, A., Cerri, M., Monti, S., Cresta, S., Famà, R., De Paoli, L., Bulian, P., Gattei, V., Guarini, A., Deaglio, S., Capello, D., et al. (2012) 'Mutations of NOTCH1 are an independent predictor of survival in chronic lymphocytic leukemia', *Blood*, 119(2), pp. 521–529.

Rossi, D., Rasi, S., Spina, V., Bruscaggin, A., Monti, S., Ciardullo, C., Deambrogi, C., Khiabanian, H., Serra, R., Bertoni, F., Forconi, F., Laurenti, L., Marasca, R., Dal-Bo, M., Rossi, F.M., Bulian, P., Nomdedeu, J., Del Poeta, G., Gattei, V., et al. (2013) 'Integrated mutational and cytogenetic analysis identifies new prognostic subgroups in chronic lymphocytic leukemia', *Blood*, 121(8), pp. 1403–1412.

Rothstein, T.L., Wang, J.K., Panka, D.J., Foote, L.C., Wang, Z., Stanger, B., Cui, H., Ju, S.T. & Marshak-Rothstein, A. (1995) 'Protection against Fas-dependent Th1-mediated apoptosis by antigen receptor engagement in B cells.', *Nature*, 374(6518), pp. 163–5.

Rowland, S.L., DePersis, C.L., Torres, R.M. & Pelanda, R. (2010) 'Ras activation of Erk restores impaired tonic BCR signaling and rescues immature B cell differentiation', *The Journal of experimental medicine*, 207(3), pp. 607–621.

Saha, M.N., Jiang, H. & Chang, H. (2010) 'Molecular mechanisms of nutlin-induced apoptosis in multiple myeloma: evidence for p53-transcription-dependent and -independent pathways', *Cancer biology & therapy*, 10(6), pp. 567–578.

Saijo, K., Schmedt, C., Su, I. hsin, Karasuyama, H., Lowell, C.A., Reth, M., Adachi, T., Patke, A., Santana, A. & Tarakhovsky, A. (2003) 'Essential role of Src-family protein tyrosine kinases in NF-kappaB activation during B cell development', *Nature immunology*, 4(3), pp. 274–279.

Saiki, R.K., Gelfand, D.H., Stoffel, S., Scharf, S.J., Higuchi, R., Horn, G.T., Mullis, K.B. & Erlich, H.A. (1988) 'Primer-directed enzymatic amplification of DNA with a thermostable DNA polymerase', *Science*, 239(4839), pp. 487–491.

Sancar, A., Lindsey-Boltz, L.A., Ünsal-Kaçmaz, K. & Linn, S. (2004) 'Molecular mechanisms of mammalian DNA repair and the DNA damage checkpoints', *Annual review of biochemistry*, 73pp. 39–85.

Sanchez, M., Misulovin, Z., Burkhardt, A.L., Mahajan, S., Costa, T., Franke, R., Bolen, J.B. & Nussenzweig, M. (1993) 'Signal transduction by immunoglobulin is mediated through Ig alpha and Ig beta.', *The Journal of experimental medicine*, 178(3), pp. 1049–55.

Sander, S., Chu, V.T., Yasuda, T., Franklin, A., Graf, R., Calado, D.P., Li, S., Imami, K., Selbach, M., Di Virgilio, M., Bullinger, L. & Rajewsky, K. (2015) 'PI3 Kinase and FOXO1 Transcription Factor Activity Differentially Control B Cells in the Germinal Center Light and Dark Zones', *Immunity*, 43(6), pp. 1075–1086.

Sandova, V., Pavlasova, G.M., Seda, V., Cerna, K.A., Sharma, S., Palusova, V., Brychtova, Y., Pospisilova, S., Fernandes, S.M., Panovska, A., Doubek, M., Davids, M.S., Brown, J.R., Mayer, J. & Mraz, M. (2021) 'IL4-STAT6 signaling induces CD20 in chronic lymphocytic leukemia and this axis is repressed by PI3Kδ inhibitor idelalisib', *Haematologica*, 106(11), pp. 2995–2999.

Satterthwaite, A.B. & Witte, O.N. (2000) 'The role of Bruton's tyrosine kinase in B-cell development and function: a genetic perspective', *Immunological Reviews*, 175(1), pp. 120–127.

Saucedo, L.J., Myers, C.D. & Perry, M.E. (1999) 'Multiple murine double minute gene 2 (MDM2) proteins are induced by ultraviolet light', *The Journal of biological chemistry*, 274(12), pp. 8161–8168.

Sawai, H. & Domae, N. (2011) 'Discrimination between primary necrosis and apoptosis by necrostatin-1 in Annexin V-positive/propidium iodide-negative cells', *Biochemical and biophysical research communications*, 411(3), pp. 569–573.

Schattner, E.J. (2000) 'CD40 ligand in CLL pathogenesis and therapy', *Leukemia and Lymphoma*, 37(5–6), pp. 461–472.

Scheffold, A., Jebaraj, B.M.C. & Stilgenbauer, S. (2018) 'Venetoclax: Targeting BCL2 in hematological cancers', *Recent Results in Cancer Research*, 212pp. 215–242.

Schmitt, N. & Ueno, H. (2015) 'Regulation of human helper T cell subset differentiation by cytokines.', *Current opinion in immunology*, 34pp. 130–6.

Schulz, H., Klein, S.K., Rehwald, U., Reiser, M., Hinke, A., Knauf, W.U., Aulitzky, W.E., Hensel, M., Herold, M., Huhn, D., Hallek, M., Diehl, V. & Engert, A. (2002) 'Phase 2 study of a combined immunochemotherapy using rituximab and fludarabine in patients with chronic lymphocytic leukemia', *Blood*, 100(9), pp. 3115–3120.

Schweighoffer, E., Vanes, L., Nys, J., Cantrell, D., McCleary, S., Smithers, N. & Tybulewicz, V.L.J. (2013) 'The BAFF receptor transduces survival signals by co-opting the B cell receptor signaling pathway', *Immunity*, 38(3), pp. 475–488.

Scielzo, C., Apollonio, B., Scarfò, L., Janus, A., Muzio, M., Ten Hacken, E., Ghia, P. & Caligaris-Cappio, F. (2011) 'The functional in vitro response to CD40 ligation reflects a different clinical outcome in patients with chronic lymphocytic leukemia', *Leukemia 2011 25:11*, 25(11), pp. 1760–1767.

Scudiere, D.A., Shoemaker, R.H., Paul, K.D., Monks, A., Tierney, S., Nofziger, T.H., Currens, M.J., Seniff, D. & Boyd, M.R. (1988) 'Evaluation of a Soluble Tetrazolium/Formazan Assay for Cell Growth and Drug Sensitivity in Culture Using Human and Other Tumor Cell Lines1', *CANCER RESEARCH*, 48pp. 4827–4833.

Seda, V., Vojackova, E., Ondrisova, L., Kostalova, L., Sharma, S., Loja, T., Mladonicka Pavlasova, G., Zicha, D., Kudlickova Peskova, M., Krivanek, J., Liskova, K., Kren, L., Benes, V., Musilova Litzmanova, K., Borsky, M., Oppelt, J., Verner, J., Pospisilova, S., Brychtova, Y., et al. (2021) 'FoxO1-GAB1 axis regulates homing capacity and tonic AKT activity in chronic lymphocytic leukemia', *Blood*, 138(9), pp. 758–772.

Seifert, M., Sellmann, L., Bloehdorn, J., Wein, F., Stilgenbauer, S., Dürig, J. & Küppers, R. (2012) 'Cellular origin and pathophysiology of chronic lymphocytic leukemia', *The Journal of experimental medicine*, 209(12), pp. 2183–2198.

Sellick, G.S., Goldin, L.R., Wild, R.W., Slager, S.L., Ressenti, L., Strom, S.S., Dyer, M.J.S., Mauro, F.R., Marti, G.E., Fuller, S., Lyttelton, M., Kipps, T.J., Keating, M.J., Call, T.G., Catovsky, D., Caporaso, N. & Houlston, R.S. (2007) 'A high-density SNP genome-wide

linkage search of 206 families identifies susceptibility loci for chronic lymphocytic leukemia', *Blood*, 110(9), pp. 3326–3333.

Sellner, L., Dietrich, S., Dreger, P., Glimm, H. & Zenz, T. (2012) 'Can prognostic factors be used to direct therapy in chronic lymphocytic leukemia?', *Current hematologic malignancy reports*, 7(1), pp. 3–12.

Seymour, J.F., Kipps, T.J., Eichhorst, B., Hillmen, P., D'Rozario, J., Assouline, S., Owen, C., Gerecitano, J., Robak, T., De la Serna, J., Jaeger, U., Cartron, G., Montillo, M., Humerickhouse, R., Punnoose, E.A., Li, Y., Boyer, M., Humphrey, K., Mobasher, M., et al. (2018) 'Venetoclax-Rituximab in Relapsed or Refractory Chronic Lymphocytic Leukemia', *The New England journal of medicine*, 378(12), pp. 1107–1120.

Shanafelt, T.D., Geyer, S.M., Bone, N.D., Tschumper, R.C., Witzig, T.E., Nowakowski, G.S., Zent, C.S., Call, T.G., LaPlant, B., Dewald, G.W., Jelinek, D.F. & Kay, N.E. (2008) 'CD49d expression is an independent predictor of overall survival in patients with chronic lymphocytic leukaemia: a prognostic parameter with therapeutic potential', *British Journal of Haematology*, 140(5), pp. 537–546.

Shanafelt, T.D., Hanson, C., Dewald, G.W., Witzig, T.E., LaPlant, B., Abrahamzon, J., Jelinek, D.F. & Kay, N.E. (2008) 'Karyotype Evolution on Fluorescent In Situ Hybridization Analysis Is Associated With Short Survival in Patients With Chronic Lymphocytic Leukemia and Is Related to CD49d Expression', *Journal of clinical oncology : official journal of the American Society of Clinical Oncology*, 26(14), p. e5.

Shangary, S. & Wang, S. (2009) 'Small-molecule inhibitors of the MDM2-p53 protein-protein interaction to reactivate p53 function: a novel approach for cancer therapy', *Annual review of pharmacology and toxicology*, 49pp. 223–241.

Sharman, J.P., Egyed, M., Jurczak, W., Skarbnik, A., Pagel, J.M., Flinn, I.W., Kamdar, M., Munir, T., Walewska, R., Corbett, G., Fogliatto, L.M., Herishanu, Y., Banerji, V., Coutre, S., Follows, G., Walker, P., Karlsson, K., Ghia, P., Janssens, A., et al. (2020) 'Acalabrutinib with or without obinutuzumab versus chlorambucil and obinutuzmab for treatment-naive chronic lymphocytic leukaemia (ELEVATE TN): a randomised, controlled, phase 3 trial', *Lancet (London, England)*, 395(10232), pp. 1278–1291.

Sherr, C.J. & Roberts, J.M. (1995) 'Inhibitors of mammalian G1 cyclin-dependent kinases.', *Genes & Development*, 9(10), pp. 1149–1163.

Shiloh, Y. (2003) 'ATM and related protein kinases: safeguarding genome integrity', *Nature reviews. Cancer*, 3(3), pp. 155–168.

Shinohara, H., Maeda, S., Watarai, H. & Kurosaki, T. (2007) 'IkappaB kinase beta-induced phosphorylation of CARMA1 contributes to CARMA1 Bcl10 MALT1 complex formation in B cells.', *The Journal of experimental medicine*, 204(13), pp. 3285–93.

Shinohara, H., Yasuda, T., Aiba, Y., Sanjo, H., Hamadate, M., Watarai, H., Sakurai, H. & Kurosaki, T. (2005) 'PKC beta regulates BCR-mediated IKK activation by facilitating the interaction between TAK1 and CARMA1', *The Journal of experimental medicine*, 202(10), pp. 1423–1431.

Shvarts, A., Steegenga, W.T., Riteco, N., Van Laar, T., Dekker, P., Bazuine, M., Van Ham, R.C.A., Van Der Houven Van Oordt, W., Hateboer, G., Van Der Eb, A.J. & Jochemsen,

A.G. (1996) ‘MDMX: a novel p53-binding protein with some functional properties of MDM2.’, *The EMBO Journal*, 15(19), pp. 5349–5357.

Siegel, R.L., Miller, K.D., Wagle, N.S. & Jemal, A. (2023) ‘Cancer statistics, 2023’, *CA: A Cancer Journal for Clinicians*, 73(1), pp. 17–48.

Skalniak, L., Kocik, J., Polak, J., Skalniak, A., Rak, M., Wolnicka-Glubisz, A. & Holak, T.A. (2018) ‘Prolonged Idasanutlin (RG7388) Treatment Leads to the Generation of p53-Mutated Cells’, *Cancers*, 10(11), .

Skehan, P., Storeng, R., Scudiero, D., Monks, A., Mcmahon, J., Vistica, D., Warren, J.T., Bokesch, H., Kenney, S. & Boyd, M.R. (1990) ‘New Colorimetric Cytotoxicity Assay for Anticancer-Drug Screening’, *JNCI: Journal of the National Cancer Institute*, 82(13), pp. 1107–1112.

Smit, L.A., Hallaert, D.Y.H., Spijker, R., De Goeij, B., Jaspers, A., Kater, A.P., Van Oers, M.H.J., Van Noesel, C.J.M. & Eldering, E. (2007) ‘Differential Noxa/Mcl-1 balance in peripheral versus lymph node chronic lymphocytic leukemia cells correlates with survival capacity’, *Blood*, 109(4), pp. 1660–1668.

Smith, A., Howell, D., Patmore, R., Jack, A. & Roman, E. (2011) ‘Incidence of haematological malignancy by sub-type: a report from the Haematological Malignancy Research Network’, *British journal of cancer*, 105(11), pp. 1684–1692.

Smith, A.E., Smith, R. & Paucha, E. (1979) ‘Characterization of different tumor antigens present in cells transformed by simian virus 40’, *Cell*, 18(2), pp. 335–346.

Souers, A.J., Leverson, J.D., Boghaert, E.R., Ackler, S.L., Catron, N.D., Chen, J., Dayton, B.D., Ding, H., Enschede, S.H., Fairbrother, W.J., Huang, D.C.S., Hymowitz, S.G., Jin, S., Khaw, S.L., Kovar, P.J., Lam, L.T., Lee, J., Maecker, H.L., Marsh, K.C., et al. (2013) ‘ABT-199, a potent and selective BCL-2 inhibitor, achieves antitumor activity while sparing platelets’, *Nature medicine*, 19(2), pp. 202–208.

Soussi, T., Ishioka, C., Claustres, M. & Béroud, C. (2006) ‘Locus-specific mutation databases: pitfalls and good practice based on the p53 experience’, *Nature reviews. Cancer*, 6(1), pp. 83–90.

Srinivasan, L., Sasaki, Y., Calado, D.P., Zhang, B., Paik, J.H., DePinho, R.A., Kutok, J.L., Kearney, J.F., Otipoby, K.L. & Rajewsky, K. (2009) ‘PI3 kinase signals BCR-dependent mature B cell survival’, *Cell*, 139(3), pp. 573–586.

Srivastava, S., Zou, Z., Pirollo, K., Blattner, W. & Chang, E.H. (1990) ‘Germ-line transmission of a mutated p53 gene in a cancer-prone family with Li-Fraumeni syndrome’, *Nature*, 348(6303), pp. 747–749.

Stamatopoulos, B., Timbs, A., Bruce, D., Smith, T., Clifford, R., Robbe, P., Burns, A., Vavoulis, D. V., Lopez, L., Antoniou, P., Mason, J., Dreau, H. & Schuh, A. (2017) ‘Targeted deep sequencing reveals clinically relevant subclonal IgHV rearrangements in chronic lymphocytic leukemia’, *Leukemia*, 31(4), pp. 837–845.

Steele, A.J., Prentice, A.G., Cwynarski, K., Hoffbrand, A.V., Hart, S.M., Lowdell, M.W., Samuel, E.R. & Wickremasinghe, R.G. (2010) ‘The JAK3-selective inhibitor PF-956980 reverses the resistance to cytotoxic agents induced by interleukin-4 treatment of chronic

lymphocytic leukemia cells: potential for reversal of cytoprotection by the microenvironment', *Blood*, 116(22), pp. 4569–4577.

Stevenson, F.K. & Caligaris-Cappio, F. (2004) 'Chronic lymphocytic leukemia: revelations from the B-cell receptor', *Blood*, 103(12), pp. 4389–4395.

Stevenson, F.K., Krysov, S., Davies, A.J., Steele, A.J. & Packham, G. (2011) 'B-cell receptor signaling in chronic lymphocytic leukemia', *Blood*, 118(16), pp. 4313–4320.

Stilgenbauer, S., Eichhorst, B., Schetelig, J., Coutre, S., Seymour, J.F., Munir, T., Puvvada, S.D., Wendtner, C.M., Roberts, A.W., Jurczak, W., Mulligan, S.P., Böttcher, S., Mobasher, M., Zhu, M., Desai, M., Chyla, B., Verdugo, M., Enschede, S.H., Cerri, E., et al. (2016) 'Venetoclax in relapsed or refractory chronic lymphocytic leukaemia with 17p deletion: a multicentre, open-label, phase 2 study', *The Lancet. Oncology*, 17(6), pp. 768–778.

Stilgenbauer, S., Schnaiter, A., Paschka, P., Zenz, T., Rossi, M., Döhner, K., Bühler, A., Böttcher, S., Ritgen, M., Kneba, M., Winkler, D., Tausch, E., Hoth, P., Edelmann, J., Mertens, D., Bullinger, L., Bergmann, M., Kless, S., Mack, S., et al. (2014) 'Gene mutations and treatment outcome in chronic lymphocytic leukemia: results from the CLL8 trial', *Blood*, 123(21), pp. 3247–3254.

Stilgenbauer, S. & Zenz, T. (2010) 'Understanding and managing ultra high-risk chronic lymphocytic leukemia', *Hematology. American Society of Hematology. Education Program*, 2010pp. 481–488.

Stilgenbauer, S., Zenz, T., Winkler, D., Bühler, A., Schlenk, R.F., Groner, S., Busch, R., Hensel, M., Dührsen, U., Finke, J., Dreger, P., Jäger, U., Lengfelder, E., Hohloch, K., Söling, U., Schlag, R., Kneba, M., Hallek, M. & Döhner, H. (2009) 'Subcutaneous alemtuzumab in fludarabine-refractory chronic lymphocytic leukemia: clinical results and prognostic marker analyses from the CLL2H study of the German Chronic Lymphocytic Leukemia Study Group', *Journal of clinical oncology : official journal of the American Society of Clinical Oncology*, 27(24), pp. 3994–4001.

Sun, D., Li, Z., Rew, Y., Gribble, M., Bartberger, M.D., Beck, H.P., Canon, J., Chen, A., Chen, X., Chow, D., Deignan, J., Duquette, J., Eksterowicz, J., Fisher, B., Fox, B.M., Fu, J., Gonzalez, A.Z., Gonzalez-Lopez De Turiso, F., Houze, J.B., et al. (2014) 'Discovery of AMG 232, a potent, selective, and orally bioavailable MDM2-p53 inhibitor in clinical development', *Journal of medicinal chemistry*, 57(4), pp. 1454–1472.

Sutherland, C.L., Heath, A.W., Pelech, S.L., Young, P.R. & Gold, M.R. (1996) 'Differential activation of the ERK, JNK, and p38 mitogen-activated protein kinases by CD40 and the B cell antigen receptor.', *The Journal of Immunology*, 157(8), pp. 3381–3390.

Takeda, A.J., Maher, T.J., Zhang, Y., Lanahan, S.M., Bucklin, M.L., Compton, S.R., Tyler, P.M., Comrie, W.A., Matsuda, M., Olivier, K.N., Pittaluga, S., McElwee, J.J., Long Priel, D.A., Kuhns, D.B., Williams, R.L., Mustillo, P.J., Wymann, M.P., Koneti Rao, V. & Lucas, C.L. (2019) 'Human PI3Kγ deficiency and its microbiota-dependent mouse model reveal immunodeficiency and tissue immunopathology', *Nature communications*, 10(1), .

Tam, C., Grigg, A.P., Opat, S., Ku, M., Gilbertson, M., Anderson, M.A., Seymour, J.F., Ritchie, D.S., Dicorleto, C., Dimovski, B., Hedrick, E., Yang, J., Wang, L., Luo, L., Xue,

L. & Roberts, A.W. (2015) 'The BTK Inhibitor, Bgb-3111, Is Safe, Tolerable, and Highly Active in Patients with Relapsed/ Refractory B-Cell Malignancies: Initial Report of a Phase 1 First-in-Human Trial', *Blood*, 126(23), p. 832.

Tam, C.S., O'Brien, S., Wierda, W., Kantarjian, H., Wen, S., Do, K.A., Thomas, D.A., Cortes, J., Lerner, S. & Keating, M.J. (2008) 'Long-term results of the fludarabine, cyclophosphamide, and rituximab regimen as initial therapy of chronic lymphocytic leukemia', *Blood*, 112(4), pp. 975–980.

Tan, D.S.P., Lambros, M.B.K., Rayter, S., Natrajan, R., Vatcheva, R., Gao, Q., Marchiò, C., Geyer, F.C., Savage, K., Parry, S., Fenwick, K., Tamber, N., Mackay, A., Dexter, T., Jameson, C., McCluggage, W.G., Williams, A., Graham, A., Faratian, D., et al. (2009) 'PPM1D is a potential therapeutic target in ovarian clear cell carcinomas.', *Clinical cancer research : an official journal of the American Association for Cancer Research*, 15(7), pp. 2269–80.

Tanaka, S. & Baba, Y. (2020) 'B Cell Receptor Signaling.', *Advances in experimental medicine and biology*, 1254pp. 23–36.

Tangudu, N.K., Buth, N., Strnad, P., Cirstea, I.C. & Spasić, M.V. (2019) 'Duvelisib: A 2018 Novel FDA-Approved Small Molecule Inhibiting Phosphoinositide 3-Kinases', *Pharmaceuticals (Basel, Switzerland)*, 12(2), .

Tausch, E., Schneider, C., Robrecht, S., Zhang, C., Dolnik, A., Bloehdorn, J., Bahlo, J., Al-Sawaf, O., Ritgen, M., Fink, A.M., Eichhorst, B., Kreuzer, K.A., Tandon, M., Humphrey, K., Jiang, Y., Schary, W., Bullinger, L., Mertens, D., Lurà, M.P., et al. (2020) 'Prognostic and predictive impact of genetic markers in patients with CLL treated with obinutuzumab and venetoclax', *Blood*, 135(26), pp. 2402–2412.

Tedder, T.F. & Engel, P. (1994) 'CD20: a regulator of cell-cycle progression of B lymphocytes', *Immunology today*, 15(9), pp. 450–454.

Teeling, J.L., Mackus, W.J.M., Wiegman, L.J.J.M., van den Brakel, J.H.N., Beers, S.A., French, R.R., van Meerten, T., Ebeling, S., Vink, T., Slootstra, J.W., Parren, P.W.H.I., Glennie, M.J. & van de Winkel, J.G.J. (2006) 'The biological activity of human CD20 monoclonal antibodies is linked to unique epitopes on CD20', *Journal of immunology (Baltimore, Md. : 1950)*, 177(1), pp. 362–371.

Tembhare, P.R., Marti, G., Wiestner, A., Degheidy, H., Farooqui, M., Kreitman, R.J., Jasper, G.A., Yuan, C.M., Liewehr, D., Venzon, D. & Stetler-Stevenson, M. (2013) 'Quantification of expression of antigens targeted by antibody-based therapy in chronic lymphocytic leukemia', *American journal of clinical pathology*, 140(6), pp. 813–818.

Thian, M., Hoeger, B., Kamnev, A., Poyer, F., Bal, S.K., Caldera, M., Jiménez-Heredia, R., Huemer, J., Pickl, W.F., Groß, M., Ehl, S., Lucas, C.L., Menche, J., Hutter, C., Attarbaschi, A., Dupré, L. & Boztug, K. (2020) 'Germline biallelic PIK3CG mutations in a multifaceted immunodeficiency with immune dysregulation', *Haematologica*, 105(10), .

Thome, M. & Tschopp, J. (2001) 'Regulation of lymphocyte proliferation and death by FLIP', *Nature reviews. Immunology*, 1(1), pp. 50–58.

Thompson, J.S., Bixler, S.A., Qian, F., Vora, K., Scott, M.L., Cachero, T.G., Hession, C., Schneider, P., Sizing, I.D., Mullen, C., Strauch, K., Zafari, M., Benjamin, C.D., Tschopp, J., Browning, J.L. & Ambrose, C. (2001) 'BAFF-R, a newly identified TNF receptor that specifically interacts with BAFF', *Science*, 293(5537), pp. 2108–2111.

Thorsélius, M., Kröber, A., Murray, F., Thunberg, U., Tobin, G., Bühler, A., Kienle, D., Albesiano, E., Maffei, R., Dao-Ung, L.P., Wiley, J., Vilpo, J., Laurell, A., Merup, M., Roos, G., Karlsson, K., Chiorazzi, N., Marasca, R., Döhner, H., et al. (2006) 'Strikingly homologous immunoglobulin gene rearrangements and poor outcome in VH3-21-using chronic lymphocytic leukemia patients independent of geographic origin and mutational status', *Blood*, 107(7), pp. 2889–2894.

Tony, H.P., Lehrnbecher, T., Merz, H., Sebald, W. & Wilhelm, M. (1991) 'Regulation of IL-4 responsiveness in lymphoma B cells.', *Leukemia research*, 15(10), pp. 911–9.

Toshiyuki, M. & Reed, J.C. (1995) 'Tumor suppressor p53 is a direct transcriptional activator of the human bax gene', *Cell*, 80(2), pp. 293–299.

de Totero, D., Reato, G., Mauro, F., Cignetti, A., Ferrini, S., Guarini, A., Gobbi, M., Grossi, C.E. & Foa, R. (1999) 'IL4 production and increased CD30 expression by a unique CD8+ T-cell subset in B-cell chronic lymphocytic leukaemia.', *British journal of haematology*, 104(3), pp. 589–99.

Tovar, C., Rosinski, J., Filipovic, Z., Higgins, B., Kolinsky, K., Hilton, H., Zhao, X., Vu, B.T., Qing, W., Packman, K., Myklebost, O., Heimbrook, D.C. & Vassilev, L.T. (2006) 'Small-molecule MDM2 antagonists reveal aberrant p53 signaling in cancer: implications for therapy', *Proceedings of the National Academy of Sciences of the United States of America*, 103(6), pp. 1888–1893.

Tromp, J.M., Tonino, S.H., Elias, J.A., Jaspers, A., Luijks, D.M., Kater, A.P., Van Lier, R.A.W., Van Oers, M.H.J. & Eldering, E. (2010) 'Dichotomy in NF-kappaB signaling and chemoresistance in immunoglobulin variable heavy-chain-mutated versus unmutated CLL cells upon CD40/TLR9 triggering', *Oncogene*, 29(36), pp. 5071–5082.

Tsukada, S., Saffran, D.C., Rawlings, D.J., Parolini, O., Allen, R.C., Klisak, I., Sparkes, R.S., Kubagawa, H., Mohandas, T., Quan, S., Belmont, J.W., Cooper, M.D., Conley, M.E. & Witte, O.N. (1993) 'Deficient expression of a B cell cytoplasmic tyrosine kinase in human X-linked agammaglobulinemia', *Cell*, 72(2), pp. 279–290.

Uyanik, B., Goloudina, A.R., Akbarali, A., Grigorash, B.B., Petukhov, A. V., Singhal, S., Eruslanov, E., Chaloyard, J., Lagorgette, L., Hadi, T., Baidyuk, E. V., Sakai, H., Tessarollo, L., Ryffel, B., Mazur, S.J., Lirussi, F., Garrido, C., Appella, E. & Demidov, O.N. (2021) 'Inhibition of the DNA damage response phosphatase PPM1D reprograms neutrophils to enhance anti-tumor immune responses', *Nature Communications*, 12(1), .

Vajdy, M., Kosco-Vilbois, M.H., Kopf, M., Köhler, G. & Lycke, N. (1995) 'Impaired mucosal immune responses in interleukin 4-targeted mice.', *The Journal of experimental medicine*, 181(1), pp. 41–53.

Vaseva, A. V. & Moll, U.M. (2009) 'The mitochondrial p53 pathway', *Biochimica et biophysica acta*, 1787(5), pp. 414–420.

Vassilev, L.T., Vu, B.T., Graves, B., Carvajal, D., Podlaski, F., Filipovic, Z., Kong, N., Kammlott, U., Lukacs, C., Klein, C., Fotouhi, N. & Liu, E.A. (2004) 'In vivo activation of the p53 pathway by small-molecule antagonists of MDM2', *Science (New York, N.Y.)*, 303(5659), pp. 844–848.

Verghese, A., Brady, E., Kapur, C.C. & Horwitz, R.I. (2011) 'The bedside evaluation: ritual and reason', *Annals of internal medicine*, 155(8), pp. 550–553.

Vermeulen, K., Van Bockstaele, D.R. & Berneman, Z.N. (2003) 'The cell cycle: a review of regulation, deregulation and therapeutic targets in cancer', *Cell proliferation*, 36(3), pp. 131–149.

Vitale, C., Falchi, L., Ciccone, M., Burger, J., Pemmaraju, N., Borthakur, G., Wierda, W.G., Keating, M.J. & Ferrajoli, A. (2020) 'Ofatumumab is safe and effective as front-line treatment in older patients with chronic lymphocytic leukemia and severe co-morbidities, including other malignancies', *Journal of geriatric oncology*, 11(1), pp. 19–23.

Vlad, A., Deglesne, P.-A., Letestu, R., Saint-Georges, S., Chevallier, N., Baran-Marszak, F., Varin-Blank, N., Ajchenbaum-Cymbalista, F. & Ledoux, D. (2009) 'Down-regulation of CXCR4 and CD62L in chronic lymphocytic leukemia cells is triggered by B-cell receptor ligation and associated with progressive disease.', *Cancer research*, 69(16), pp. 6387–95.

Vogelstein, B. (1990) 'Cancer. A deadly inheritance', *Nature*, 348(6303), pp. 681–682.

Vogelstein, B., Lane, D. & Levine, A.J. (2000) 'Surfing the p53 network', *Nature*, 408(6810), pp. 307–310.

Vu, B., Wovkulich, P., Pizzolato, G., Lovey, A., Ding, Q., Jiang, N., Liu, J.J., Zhao, C., Glenn, K., Wen, Y., Tovar, C., Packman, K., Vassilev, L. & Graves, B. (2013) 'Discovery of RG7112: A Small-Molecule MDM2 Inhibitor in Clinical Development', *ACS medicinal chemistry letters*, 4(5), pp. 466–469.

Wade, M., Li, Y.C. & Wahl, G.M. (2013) 'MDM2, MDMX and p53 in oncogenesis and cancer therapy', *Nature reviews. Cancer*, 13(2), pp. 83–96.

Wade, M., Wang, Y. V. & Wahl, G.M. (2010) 'The p53 orchestra: Mdm2 and Mdmx set the tone', *Trends in cell biology*, 20(5), pp. 299–309.

Wagner, E.F., Hleb, M., Hanna, N. & Sharma, S. (1998) 'A Pivotal Role of Cyclin D3 and Cyclin-Dependent Kinase Inhibitor p27 in the Regulation of IL-2-, IL-4-, or IL-10-Mediated Human B Cell Proliferation', *The Journal of Immunology*, 161(3), pp. 1123–1131.

Waldman, T., Lengauer, C., Kinzler, K.W. & Vogelstein, B. (1996) 'Uncoupling of S phase and mitosis induced by anticancer agents in cells lacking p21', *Nature*, 381(6584), pp. 713–716.

Wan, Y. & Wu, C.J. (2013) 'SF3B1 mutations in chronic lymphocytic leukemia', *Blood*, 121(23), pp. 4627–4634.

Wan, Z., Karras, J.G., Howard, R.G. & Rothstein2, T.L. (1995) 'Induction of bcl-x by CD40 engagement rescues sIg-induced apoptosis in murine B cells.', *The Journal of Immunology*, 155(8), pp. 3722–3725.

Wang, B., Xiao, Z. & Ren, E.C. (2009) 'Redefining the p53 response element', *Proceedings of the National Academy of Sciences of the United States of America*, 106(34), pp. 14373–14378.

Wang, Y., Zhang, L.L., Champlin, R.E. & Wang, M.L. (2015) 'Targeting Bruton's tyrosine kinase with ibrutinib in B-cell malignancies.', *Clinical pharmacology and therapeutics*, 97(5), pp. 455–68.

Wang, Y.H., Fan, L., Xu, W. & Li, J.Y. (2012) 'Detection methods of ZAP-70 in chronic lymphocytic leukemia', *Clinical and experimental medicine*, 12(2), pp. 69–77.

Wei, S.J., Joseph, T., Sim, A.Y.L., Yurlova, L., Zolghadr, K., Lane, D., Verma, C. & Ghadessy, F. (2013) 'In vitro selection of mutant HDM2 resistant to Nutlin inhibition', *PloS one*, 8(4), .

Wendtner, C.M. (2019) 'Ibrutinib: the home run for cure in CLL?', *Blood*, 133(19), pp. 2003–2004.

Wierda, W.G., Kipps, T.J., Mayer, J., Stilgenbauer, S., Williams, C.D., Hellmann, A., Robak, T., Furman, R.R., Hillmen, P., Trneny, M., Dyer, M.J.S., Padmanabhan, S., Piotrowska, M., Kozak, T., Chan, G., Davis, R., Losic, N., Wilms, J., Russell, C.A., et al. (2010) 'Ofatumumab as single-agent CD20 immunotherapy in fludarabine-refractory chronic lymphocytic leukemia', *Journal of clinical oncology : official journal of the American Society of Clinical Oncology*, 28(10), pp. 1749–1755.

Wierda, W.G., O'Brien, S., Wang, X., Faderl, S., Ferrajoli, A., Do, K.A., Cortes, J., Thomas, D., Garcia-Manero, G., Koller, C., Beran, M., Giles, F., Ravandi, F., Lerner, S., Kantarjian, H. & Keating, M. (2007) 'Prognostic nomogram and index for overall survival in previously untreated patients with chronic lymphocytic leukemia', *Blood*, 109(11), pp. 4679–4685.

Wiestner, A., Rosenwald, A., Barry, T.S., Wright, G., Davis, R.E., Henrickson, S.E., Zhao, H., Ibbotson, R.E., Orchard, J.A., Davis, Z., Stetler-Stevenson, M., Raffeld, M., Arthur, D.C., Marti, G.E., Wilson, W.H., Hamblin, T.J., Oscier, D.G. & Staudt, L.M. (2003) 'ZAP-70 expression identifies a chronic lymphocytic leukemia subtype with unmutated immunoglobulin genes, inferior clinical outcome, and distinct gene expression profile', *Blood*, 101(12), pp. 4944–4951.

Willmore, E.A., Aptullahoğlu, E.A., Zhao, Y.A., Kyle, S.A., Thomas, H.A., Ahn, M.A., Fazal, L.A., Noble, M.A., Hardcastle, I.A., Howard, S.A., Chessari, G.A., Lunec, J.A. & Wedge, S.P. (2020) 'Targeting the MDM2-p53 interaction: evaluation of a novel, potent MDM2-p53 antagonist in patient-derived CLL cells', *Leukemia & lymphoma.*, 61p. 81.

Woyach, J.A., Furman, R.R., Liu, T.-M., Ozer, H.G., Zapatka, M., Ruppert, A.S., Xue, L., Li, D.H.-H., Steggerda, S.M., Versele, M., Dave, S.S., Zhang, J., Yilmaz, A.S., Jaglowski, S.M., Blum, K.A., Lozanski, A., Lozanski, G., James, D.F., Barrientos, J.C., et al. (2014) 'Resistance Mechanisms for the Bruton's Tyrosine Kinase Inhibitor Ibrutinib', *The New England journal of medicine*, 370(24), p. 2286.

Wu, C.-E., Chen, C.-P., Pan, Y.-R., Jung, S.-M., Chang, J.W.-C., Chen, J.-S., Yeh, C.-N. & Lunec, J. (2022) 'In vitro and in vivo study of GSK2830371 and RG7388 combination in liver adenocarcinoma', *American Journal of Cancer Research*, 12(9), p. 4399.

Wu, C.E., Esfandiari, A., Ho, Y.H., Wang, N., Mahdi, A.K., Aptullahoglu, E., Lovat, P. & Lunec, J. (2018) 'Targeting negative regulation of p53 by MDM2 and WIP1 as a therapeutic strategy in cutaneous melanoma', *British journal of cancer*, 118(4), pp. 495–508.

Wu, C.E., Huang, C.Y., Chen, C.P., Pan, Y.R., Chang, J.W.C., Chen, J.S., Yeh, C.N. & Lunec, J. (2021) 'WIP1 Inhibition by GSK2830371 Potentiates HDM201 through Enhanced p53 Phosphorylation and Activation in Liver Adenocarcinoma Cells', *Cancers*, 13(15), .

Wu, J., Zhang, M. & Liu, D. (2017) 'Oncotarget 7201 www.impactjournals.com/oncotarget Bruton tyrosine kinase inhibitor ONO/GS-4059: from bench to bedside', *Oncotarget*, 8(4), pp. 7201–7207.

Wu, X., Bayle, J.H., Olson, D. & Levine, A.J. (1993) 'The p53-mdm-2 autoregulatory feedback loop', *Genes & development*, 7(7A), pp. 1126–1132.

Yasuda, T., Sanjo, H., Pagès, G., Kawano, Y., Karasuyama, H., Pouysségur, J., Ogata, M. & Kurosaki, T. (2008) 'Erk Kinases Link Pre-B Cell Receptor Signaling to Transcriptional Events Required for Early B Cell Expansion', *Immunity*, 28(4), pp. 499–508.

Yee, K., Martinelli, G., Assouline, S., Kasner, M., Vey, N., Kelly, K.R., Drummond, M.W., Dennis, M., Seiter, K., Blotner, S., Jukofsky, L., Middleton, S., Zhi, J., Chen, G., Zhong, H. & Nichols, G. (2013) 'Phase 1b Study Of The MDM2 Antagonist RG7112 In Combination With 2 Doses/Schedules Of Cytarabine', *Blood*, 122(21), pp. 498–498.

Yee, K., Papayannidis, C., Vey, N., Dickinson, M.J., Kelly, K.R., Assouline, S., Kasner, M., Seiter, K., Drummond, M.W., Yoon, S.S., Lee, J.H., Blotner, S., Jukofsky, L., Pierceall, W.E., Zhi, J., Simon, S., Higgins, B., Nichols, G., Monnet, A., et al. (2021) 'Murine double minute 2 inhibition alone or with cytarabine in acute myeloid leukemia: Results from an idasanutlin phase 1/1b study⋆', *Leukemia research*, 100.

Yoshimura, M., Ishizawa, J., Ruvolo, V., Dilip, A., Quintás-Cardama, A., Mcdonnell, T.J., Neelapu, S.S., Kwak, L.W., Shacham, S., Kauffman, M., Tabe, Y., Yokoo, M., Kimura, S., Andreeff, M. & Kojima, K. (2014) 'Induction of p53-mediated transcription and apoptosis by exportin-1 (XPO1) inhibition in mantle cell lymphoma', *Cancer science*, 105(7), pp. 795–801.

Zanjirband, M., Edmondson, R.J. & Lunec, J. (2016) 'Pre-clinical efficacy and synergistic potential of the MDM2-p53 antagonists, Nutlin-3 and RG7388, as single agents and in combined treatment with cisplatin in ovarian cancer', *Oncotarget*, 7(26), pp. 40115–40115.

Zelenetz, A.D., Barrientos, J.C., Brown, J.R., Coiffier, B., Delgado, J., Egyed, M., Ghia, P., Illés, Á., Jurczak, W., Marlton, P., Montillo, M., Morschhauser, F., Pristupa, A.S., Robak, T., Sharman, J.P., Simpson, D., Smolej, L., Tausch, E., Adewoye, A.H., et al. (2017) 'Idelalisib or placebo in combination with bendamustine and rituximab in patients with relapsed or refractory chronic lymphocytic leukaemia: interim results from a phase 3, randomised, double-blind, placebo-controlled trial', *The Lancet Oncology*, 18(3), pp. 297–311.

Zenz, T., Eichhorst, B., Busch, R., Denzel, T., Häbe, S., Winkler, D., Bühler, A., Edelmann, J., Bergmann, M., Hopfinger, G., Hensel, M., Hallek, M., Döhner, H. & Stilgenbauer, S.

(2010) ‘TP53 Mutation and Survival in Chronic Lymphocytic Leukemia’, *J Clin Oncol*, 28pp. 4473–4479.

Zenz, T., Kröber, A., Scherer, K., Häbe, S., Bühler, A., Benner, A., Denzel, T., Winkler, D., Edelmann, J., Schwänen, C., Döhner, H. & Stilgenbauer, S. (2008) ‘Monoallelic TP53 inactivation is associated with poor prognosis in chronic lymphocytic leukemia: results from a detailed genetic characterization with long-term follow-up’, *Blood*, 112(8), pp. 3322–3329.

Zhang, H., Hannon, G.J. & Beach, D. (1994) ‘p21-containing cyclin kinases exist in both active and inactive states’, *Genes & development*, 8(15), pp. 1750–1758.

Zhang, W., Kater, A.P., Widhopf, G.F., Chuang, H.Y., Enzler, T., James, D.F., Poustovoitov, M., Tseng, P.H., Janz, S., Hoh, C., Herschman, H., Karin, M. & Kipps, T.J. (2010) ‘B-cell activating factor and v-Myc myelocytomatosis viral oncogene homolog (c-Myc) influence progression of chronic lymphocytic leukemia’, *Proceedings of the National Academy of Sciences of the United States of America*, 107(44), pp. 18956–18960.

Zhang, Y. & Xiong, Y. (2001) ‘Control of p53 ubiquitination and nuclear export by MDM2 and ARF.’, *Cell growth & differentiation : the molecular biology journal of the American Association for Cancer Research*, 12(4), pp. 175–86.

Zhang, Y.W., Hunter, T. & Abraham, R.T. (2006) ‘Turning the replication checkpoint on and off’, *Cell cycle (Georgetown, Tex.)*, 5(2), pp. 125–128.

Zhao, Y., Aguilar, A., Bernard, D. & Wang, S. (2015) ‘Small-molecule inhibitors of the MDM2-p53 protein-protein interaction (MDM2 Inhibitors) in clinical trials for cancer treatment’, *Journal of medicinal chemistry*, 58(3), pp. 1038–1052.

Zheng, Z., Venkatapathy, S., Rao, G. & Harrington, C.A. (2002) ‘Expression profiling of B cell chronic lymphocytic leukemia suggests deficient CD1-mediated immunity, polarized cytokine response, altered adhesion and increased intracellular protein transport and processing of leukemic cells.’, *Leukemia*, 16(12), pp. 2429–37.

Appendix

cancers

MDPI

Article

Targeting the MDM2-p53 Interaction with Siremadlin: A Promising Therapeutic Strategy for Treating *TP53* Wild-Type Chronic Lymphocytic Leukemia

Erhan Aptullahoglu [1,2], Mohammed Howladar [1], Jonathan P. Wallis [3], Helen Marr [3], Scott Marshall [4], Julie Irving [1], Elaine Willmore [1] and John Lunec [1,*]

[1] Biosciences Institute & Newcastle University Cancer Centre, Medical Faculty, Newcastle University, Newcastle upon Tyne NE2 4HH, UK; erhan.aptullahoglu@bilecik.edu.tr (E.A.); m.howladar2@newcastle.ac.uk (M.H.); julie.irving@ncl.ac.uk (J.I.); elaine.willmore@ncl.ac.uk (E.W.)
[2] Department of Molecular Biology and Genetics, Faculty of Science, Bilecik Şeyh Edebali University, 11100 Bilecik, Türkiye
[3] Department of Haematology, Freeman Hospital, Newcastle upon Tyne NHS Foundation Trust, Newcastle upon Tyne NE7 7DN, UK
[4] Department of Haematology, City Hospitals Sunderland NHS Trust, Sunderland SR4 7TP, UK
* Correspondence: john.lunec@ncl.ac.uk

Simple Summary: This study explores HDM201, a second-generation MDM2-p53 binding antagonist, as a potential novel treatment for chronic lymphocytic leukemia (CLL). Using a range of B cell lines and primary CLL samples with different *TP53* statuses, we found that HDM201 effectively targets *TP53* wild-type and heterozygous *TP53*-KO cells but shows limited efficacy in *TP53* mutant and homozygous *TP53*-KO cells. HDM201 stabilizes p53 and induces apoptosis in sensitive cells, demonstrating its potential as a targeted therapy for *TP53* wild-type CLL cases. This study highlights the importance of *TP53* status in predicting treatment response and suggests further research on resistance mechanisms and combination therapies.

Abstract: Background: Chronic lymphocytic leukemia (CLL) treatment has transitioned from traditional chemotherapy to more targeted therapies, but challenges such as resistance and suboptimal responses persist. This study aimed to evaluate HDM201, a second-generation MDM2-p53 binding antagonist, as a novel therapeutic strategy for CLL, with a focus on its effectiveness across different *TP53* genetic contexts. **Methods:** We utilized a panel of B cell leukemia-derived cell lines with varying *TP53* statuses, including *TP53*-knockout (KO) derivatives of the human B cell line Nalm-6, and assessed the impact of HDM201 on primary CLL samples with both *TP53* wild-type and mutant backgrounds. **Results:** Our results revealed that *TP53* wild-type and heterozygous *TP53*-KO Nalm-6 cells were sensitive to HDM201, whereas homozygous *TP53*-KO cells and B cells with *TP53* mutations exhibited significant resistance. Resistance was also noted in primary CLL samples with *TP53* mutations. HDM201 effectively stabilized p53 and induced apoptosis in *TP53* wild-type cells but had limited efficacy in *TP53* mutant cells. **Conclusions:** These findings indicate that HDM201 holds promise as an additional targeted therapy option for wild-type *TP53* CLL. The results underline the importance of *TP53* status in predicting treatment efficacy and highlight the potential of HDM201 as a valuable addition to explore in CLL therapy. Future research should focus on identifying additional biomarkers of response and exploring the optimal way to include HDM201 in combination therapies to improve treatment outcomes in CLL.

check for updates

Received: 12 November 2024
Revised: 9 January 2025
Accepted: 9 January 2025
Published: 16 January 2025

Citation: Aptullahoglu, E.; Howladar, M.; Wallis, J.P.; Marr, H.; Marshall, S.; Irving, J.; Willmore, E.; Lunec, J. Targeting the MDM2-p53 Interaction with Siremadlin: A Promising Therapeutic Strategy for Treating *TP53* Wild-Type Chronic Lymphocytic Leukemia. *Cancers* **2025**, *17*, 274. https://doi.org/10.3390/cancers17020274

Keywords: MDM2-p53 antagonists; siremadlin (HDM201); chronic lymphocytic leukemia (CLL); p53; p53-dependent apoptosis

1. Introduction

Chronic lymphocytic leukemia (CLL) is one of the most common types of leukemia in adults [1], characterized by the accumulation of dysfunctional B lymphocytes in the blood, bone marrow, and lymphoid tissues [2,3]. Over the past 25 years, significant advancements have reshaped our understanding and management of CLL. Landmark studies published in 1999 [4,5] highlighted the critical role of somatic hypermutation of the *IGHV* genes in prognosis, driving extensive research into the biology, genetic factors, and diagnostic technologies relevant to the clinical management of CLL. These advances have not only propelled research within CLL but have also influenced the broader field of B cell malignancies. Despite significant progress, challenges remain due to the unique biological and clinical features of CLL.

Recent decades have witnessed a paradigm shift in CLL treatment, moving from traditional purine analog-based chemotherapy to novel therapeutic approaches, including the use of chemo-immunotherapy and B cell receptor (BCR) antagonists [6–8]. While chemo-immunotherapy historically provided durable disease control, its limitations in managing relapsed and high-risk cases [9–11] have highlighted the need for new strategies. The introduction of targeted therapies, including Bruton's tyrosine kinase (BTK) inhibitors and BCL-2 (B cell lymphoma 2) inhibitors, has markedly improved treatment efficacy and tolerability, particularly for older patients with complex conditions. These therapies have largely replaced older treatments in both frontline and relapsed settings. Looking ahead, novel approaches such as bi-specific antibody therapies [12,13] and third-generation BTK inhibitors hold promise for tackling difficult cases like Richter's transformation and heavily pre-treated CLL [14,15]. Nevertheless, in CLL patients, the predominant resistance mechanism to the BTK inhibitor ibrutinib is mutations in the *BTK* gene [16–18], and similar resistance mechanisms are also observed with next-generation inhibitors such as acalabrutinib [19]. There is, therefore, a need for novel therapeutic strategies to overcome these resistance challenges, improve treatment efficacy, and address a broader range of patient needs.

Given the crucial role of p53 in preventing abnormal cell proliferation and maintaining genomic integrity, there is a strong interest in developing non-genotoxic pharmacological strategies to modulate p53, aiming to enhance the selectivity and effectiveness of cancer cell elimination [20,21]. Importantly, compared to other cancers, *TP53* deletions and/or mutations are relatively infrequent in CLL at diagnosis, occurring in approximately only 10% of cases [22,23]. It is worth noting that, more generally, approximately 50% of human cancers harbor mutations in the *TP53* gene [24–26]. Furthermore, over 17% of tumors exhibit amplification and overexpression of the *MDM2* gene, which encodes the primary negative regulator of p53. These alterations, whether occurring individually or together, are associated with poor prognosis and treatment resistance [27–29]. Emerging therapies targeting the non-genotoxic activation of functional p53 protein offer promising avenues for enhancing treatment outcomes in CLL. The activity and levels of p53 are primarily regulated by its interaction with MDM2, a human homolog of the murine double-minute 2 protein [30]. MDM2 acts as an E3 ubiquitin ligase, controlling p53's stability through ubiquitin-dependent proteasomal degradation [30]. Cellular stress induces the post-translational modifications of p53, resulting in disruption of the p53-MDM2 interaction, resulting in the release and accumulation of p53 to activate its target genes involved in

cell cycle arrest, apoptosis, or senescence [30,31]. Nutlin-3 was the first selective MDM2-p53 binding antagonist (MDM2 inhibitor) shown to activate p53 and downstream signaling in preclinical models. Several new-generation MDM2 inhibitors have been developed, including RG7388 [32], HDM201 [33], AMG232 [34], DS-3032 [35], ASTX295 [36], and MI-77301 [37], which have been shown to reduce cancer cell viability and proliferation in preclinical models, including leukemia and lymphoma cells [38–44]. Most of these compounds are also currently being evaluated in clinical trials, both as monotherapies [45,46] and in combination therapies [47–50]. These non-genotoxic compounds bind specifically to the p53-binding pocket of MDM2 [51], stabilizing p53 and activating the p53 pathway.

A number of second-generation MDM2 inhibitors, including Siremadlin (HDM201), have progressed to evaluation in several recent and ongoing clinical trials for their efficacy in treating cancers with wild-type p53. Results from a first-in-human phase I study of HDM201 in patients with advanced wild-type *TP53* solid tumors and acute leukemia indicated a consistent safety profile and noted preliminary activity, particularly in acute myeloid leukemia (AML). This study also established recommended dosing regimens for subsequent combination studies [45]. HDM201 monotherapy in relapsed AML patients following allogeneic stem cell transplantation (allo-SCT) demonstrated consistent safety with no excessive graft vs. host disease (GvHD) and allowed continuation at full or reduced doses. Preliminary data suggest it has anti-leukemic activity, supporting further investigation as a potential maintenance or pre-emptive treatment to enhance graft-versus-leukemia effects [52]. Furthermore, a phase Ib proof-of-concept study investigating the co-targeting of MDM2 and CDK4/6 with HDM201 and ribociclib for patients with well-differentiated or dedifferentiated liposarcoma (WDLPS/DDLPS) demonstrated manageable toxicity and early signs of antitumor activity [49]. Current data and multiple ongoing clinical trials suggest that HDM201 is a promising candidate for the treatment of cancers with activatable functional p53. In this study, we assessed the effects of HDM201 on B cell lines and ex vivo patient-derived primary CLL cells and compared these effects with those observed in *TP53* mutant cells as well as on normal hematopoietic cells.

2. Materials and Methods

2.1. Cell Lines and Compound

Human B cell lines, including Nalm-6, OCI-Ly3, and HAL-01 (wild-type *TP53*), as well as Ramos, Raji, and Pfeiffer (*TP53* mutant), were acquired from authenticated cell line repositories (ATCC or DSMZ). Nalm-6 *TP53* monoallelic (+/−) and biallelic (−/−) isogenic knockout cell lines were purchased from Horizon Discovery (Cambridge, UK) and were generated using gene targeting by homologous recombination with an exon-2 deleted *TP53* DNA construct [53].

All these cell lines were cultured in RPMI-1640 medium (Sigma-Aldrich, St. Louis, MO, USA), supplemented with 10% fetal calf serum and 100 U/mL penicillin/streptomycin (Sigma-Aldrich, St. Louis, MO, USA). HDM201 (>99% purity) was obtained by a custom synthesis through the CRUK Drug Discovery Programme at the Newcastle University Cancer Centre and from Selleck Chem. The compound was accurately weighed and dissolved in dimethyl sulfoxide (DMSO; Sigma-Aldrich, St. Louis, MO, USA) to achieve a final concentration of 20 mM. From this stock solution, aliquots of lower concentrations were prepared and stored at −20 °C.

2.2. Cell Viability Assay for the Cell Lines

Cells were plated at a density of 0.2×10^6 cells/mL in 100 µL of culture medium per well in a 96-well plate (Corning) and incubated for 24 h prior to treatment with HDM201 at concentrations ranging from 0 to 10 µM for a duration of 72 h at 37 °C. Growth inhibition

was assessed using the XTT Assay Kit (Cayman Chemical Company, Ann Arbor, MI, USA) relative to a DMSO control. The optimal incubation time with the XTT reagents was determined to be 4 h for the cell lines through pre-optimization procedures. Data were normalized to the DMSO control and expressed as a percentage of relative growth. The mean ± standard error of the mean (SEM) for IC_{50} values from at least three independent experiments was calculated.

2.3. Patient Samples

Peripheral blood samples from patients with CLL were collected following informed consent and in accordance with institutional guidelines and the Declaration of Helsinki. This study was approved by the UK NHS Research Ethics Service, and research has been conducted using samples obtained through the Newcastle Biobank (Study ID: 17/NE/0361, Date of Approval: 29 April 2014). The diagnosis of CLL was confirmed based on the IWCLL-164 NCI 2008 criteria [54]. Peripheral blood samples were obtained from CLL patients with total white blood cell counts of at least 30×10^9 cells/L, supporting the high proportion of malignant CD5+/CD19+ B cells. Mononuclear cells were purified by density gradient centrifugation (Lymphoprep, Axis-Shield Ltd., Dundee, UK) following the manufacturer's protocol. Sensitivity to MDM2 inhibitors was always assessed on fresh samples just after collecting from the patients. The cells were cultured in RPMI-1640 medium (Sigma-Aldrich, St. Louis, MO, USA), supplemented with 10% fetal calf serum and 100 U/mL penicillin/streptomycin (Sigma-Aldrich, St. Louis, MO, USA). HDM201 was dissolved in DMSO (Sigma-Aldrich) and used at a final concentration of 0.5% (v/v) DMSO in the medium. This concentration of DMSO was previously demonstrated to have minimal cytotoxic effects on the cells [55].

Normal peripheral blood mononuclear cells (PBMCs) were isolated from three healthy donors. Normal PBMCs and CLL cells were isolated by density gradient centrifugation (Lymphoprep, Axis-Shield Ltd., Dundee, UK) following the manufacturer's protocol.

2.4. Patient Sample Information

The details of Sanger sequencing of *SF3B1* in primary CLL samples have been described in a previous study [39]. The *TP53* mutational status of CLL samples was assessed by next-generation sequencing (using Roche 454 GS FLX and Illumina MiSeq platforms) in all samples. The functional status of p53 in CLL samples was determined by observing the stabilization of p53 and activation of downstream proteins, $p21^{WAF1}$ and MDM2, following exposure to the MDM2 inhibitor HDM201. Viability was routinely assessed by trypan blue exclusion assay and was >95% in fresh and thawed samples after 24 h culture.

2.5. Cell Viability Assay for the Primary Cells

An amount of 5×10^6 cells/mL in 100 µL of medium per well in a 96-well plate was exposed to a range of concentrations (from 0 to 3000 nM) of HDM201 at 37 °C for 48 h. Ex vivo cytotoxicity was assessed by the XTT Assay Kit (Cayman Chemical Company, Ann Arbor, MI, USA). The optimal incubation time with the XTT reagents was determined to be 8 h through pre-optimization procedures. Results were normalized to DMSO controls and expressed as % viability.

2.6. Immunoblotting

An amount of 5×10^6 cells/mL primary CLL cells were seeded in 2 mL per well of a 6-well plate (Corning) and subjected to treatment with HDM201. Protein lysates were harvested using 2% SDS lysis buffer at 24 h, heated at 95 °C for 10 min, and sonicated. Protein concentration was measured using a Pierce™ BCA Protein Assay Kit (Thermo Fisher Scientific, Rugby, UK). Primary antibodies against p53 (DO-7) (#M7001, Dako, Santa

Clara, CA, USA), MDM2 (Ab-1) (#OP46, Merck Millipore, Jaffrey, NH, USA), $p21^{WAF1}$ (Calbiochem, San Diego, CA, USA), PARP (Trevigen, Gaithersburg, ML, USA), Actin (Sigma, Livonia, MI, USA), and secondary goat anti-mouse/rabbit horseradish peroxidase-conjugated antibodies (Dako, Santa Clara, CA, USA) were used. All antibodies were diluted in 5% (w/v) nonfat milk or BSA in TBS-tween20. Protein bands were visualized using enhanced chemiluminescence reagents (GE Healthcare, Alger, OH, USA).

2.7. Annexin V-FITC/PI Analysis

Peripheral blood mononuclear cells (PBMCs) from CLL patients were resuspended in pre-warmed medium and seeded at 5×10^6 cells/mL in a 24-well plate. After a 1-h equilibration period, cells were treated with various drug concentrations for 48 h. Following treatment, cells were harvested, washed with cold PBS, and resuspended in 1× binding buffer (10 mM Hepes/NaOH (pH 7.4), 0.14 M NaCl, 2.5 mM $CaCl_2$) at 1×10^6 cells/mL. Cells (100 µL of 1×10^5 cells) were transferred to round-bottom tubes and stained with 5 µL of annexin V-FITC (BD Pharmingen™, Hong Kong) and 5 µL of propidium iodide (PI, BD Pharmingen™, Hong Kong). Controls included unstained cells and cells stained with either annexin V-FITC or PI alone. After a 15-min incubation in the dark, 400 µL of 1× binding buffer was added for analysis within 1 h. Flow cytometry was conducted using an Attune™ NxT Acoustic Focusing Flow Cytometer. Data were acquired for 25,000 events per sample, with detection of annexin V-FITC on the FL1 channel (max emission wavelength = 519 nm; max excitation wavelength = 495 nm) and PI on the FL2 channel (max emission wavelength = 617 nm; max excitation wavelength = 536 nm). FCS files were analyzed with FCS Express 6 software.

2.8. Statistical Analysis

The data from the repeated experiments were presented as mean ± standard error of the mean (SEM) unless otherwise stated. Statistical tests were carried out using GraphPad Prism 6 software, and all p-values represent paired or unpaired t-tests of at least three independent repeats unless otherwise stated.

3. Results

3.1. TP53 Wild-Type B Cell Lines Demonstrate Sensitivity to MDM2 Inhibition Using HDM201

Six different B cell lines were exposed to increasing concentrations of the MDM2 inhibitor HDM201. An XTT assay was used to measure the relative growth of the cells. Figure 1 displays growth inhibition curves for the cell lines treated with HDM201 for 72 h. Three out of the six B cell lines were sensitive to the MDM2 inhibitor, with IC_{50} values $\leq$ 146 nM (Figure 1A–C). In contrast, HDM201 had no significant effect on *TP53* mutant cell lines Ramos and Raji, nor on *TP53*-null Pfeiffer, even at concentrations up to 10 µM (Figure 1D–F). Figure 1I and Table 1 summarize the IC_{50} values of HDM201 and the *TP53* gene status for all cell lines used in this study.

To directly evaluate the effect of *TP53* status alone on the response of B cells to HDM201 while minimizing the impact of additional genomic variations, we utilized otherwise isogenic *TP53*-knockout (*TP53*-KO) derivatives of the human B cell line Nalm-6. These cells were treated with HDM201, and their responses were assessed and compared. Both *TP53*+/+ and heterozygous KO (*TP53*+/−) Nalm-6 cells exhibited sensitivity to the compound at low concentrations (mean ± SEM IC_{50}s are 146 ± 20 nM and 123 ± 22 nM, respectively) (Figure 1I and Table 1; *TP53*+/+ vs. *TP53*+/− paired t-test $p = 0.27$). In contrast, homozygous KO (*TP53*−/−) cells showed markedly increased resistance to HDM201, with an IC_{50} exceeding 3 µM, the highest concentration tested (Figure 1H,I and Table 1).

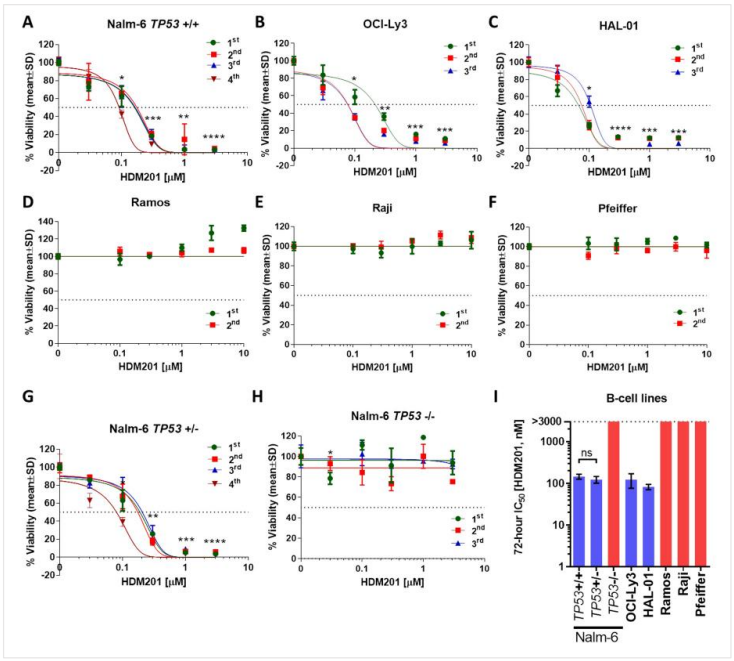

Figure 1. The concentration-dependent effect of HDM201 on the proliferation of a panel of B cell lines: (**A**) Nalm-6 *TP53* (+/+), (**B**) OCI-Ly3, (**C**) HAL-01, (**D**) Ramos, (**E**) Raji, and (**F**) Pfeiffer. Isogenic NALM-6 cell lines with (**G**) *TP53* (+/−) and (**H**) *TP53* (−/−) genotypes were also incorporated into the growth inhibition assays. Each cell line shows independent repeats (e.g., 1st: green, 2nd: red, 3rd: blue, and 4th: brown). Bars show the mean IC_{50} ± SD. The asterisks show how significantly the drug induces cell death for each concentration compared to DMSO control. Each independent repeat of the experiment was averaged within itself, and then a paired *t*-test was applied to compare paired measurements (*, $p < 0.05$; **, $p < 0.01$; ***, $p < 0.001$; ****, $p < 0.0001$). (**I**) Summary IC50 values of HDM201 for the panel of B cell lines. The results for *TP53* wild-type and *TP53* mutant cell lines are shown in blue and red bars, respectively. Bars show the mean ± SEM. A standard parametric paired *t*-test was applied to compare *TP53*+/+ with *TP53*+/− Nalm-6 cells. ns, not significant.

Table 1. Mean IC_{50} concentrations of HDM201 for the panel of B cell lines.

Cell Line	*TP53* Gene Status	HDM201 IC_{50} (nM)
OCI-Ly3	Wild-type	123 ± 47
HAL-01	Wild-type	83 ± 12
Nalm-6	+/+	146 ± 20
	+/−	123 ± 22
	−/−	>3000
Ramos	Mutant (Homozygous) c.761T > A; p.I254N	>10,000
Raji	Mutant (Heterozygous) c.638G > A; p.R213Q c.700T > C; p.Y234H	>10,000
Pfeiffer	Null c.(del)	>10,000

The IC_{50} values shown represent the mean of at least $n = 3$ independent repeats ± SEM.

3.2. TP53 Wild-Type Primary CLL Samples Are Sensitive to MDM2 Inhibition Using HDM201

Ex vivo cytotoxicity of HDM201 was evaluated using an XTT assay after 48 h of treatment compared with untreated DMSO vehicle controls. HDM201 significantly and potently reduced the viability of *TP53* wild-type CLL cells but had minimal or no effect on cells with mutant *TP53* (Figure 2A,C). The LC_{50} values (concentration required for 50% loss of viability) for each primary CLL sample, as summarized in Figure 2C, indicate that *TP53* wild-type CLL cells overall were sensitive to HDM201-induced cytotoxicity (median LC_{50} = 0.253 μM), whereas CLL samples with mutated *TP53* were substantially more resistant (median LC_{50} = 2.63 μM; Figure 2C). Since the LC_{50} values did not follow a normal distribution (D'Agostino–Pearson omnibus test, $p < 0.05$), row median and mean values with the range bars are presented in Figure 2C. Detailed information on *TP53* mutations and LC_{50} values for each *TP53* mutant CLL sample is provided in Table 2. The LC_{50} data for all CLL primary samples utilized in this study are also provided in Supplementary Material Table S1.

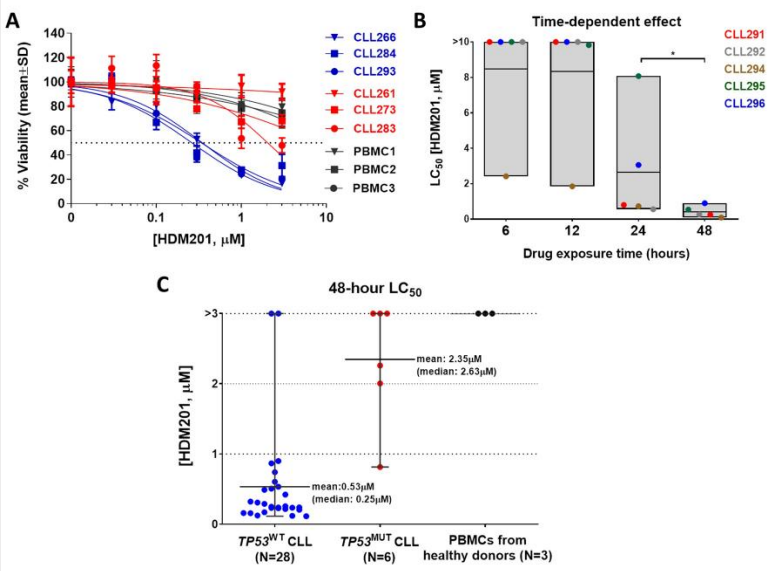

Figure 2. Time- and concentration-dependent effects of HDM201 on primary CLL samples: (**A**) Representative cytotoxicity curves for *TP53* wild-type (blue) and mutant (red) CLL samples. The samples were treated with increasing concentrations of HDM201 (ranging from 0 to 3 μM) for a duration of 48 h. To compare with the response of normal cells to HDM201, three PBMC samples (black) sourced from individual healthy donors were tested using the XTT assay. (**B**) LC50 values of HDM201 for each individual CLL sample across increasing exposure durations (6, 12, 24, and 48 h) are plotted. The time-dependent effects of HDM201 exposure were analyzed for the five CLL samples. Each CLL sample is a different color. A statistically significant difference in LC50 was observed between 24 h and 48 h exposure (paired *t*-test, denoted as * $p < 0.05$). (C) A summary of the LC50 values for the MDM2-p53 binding antagonist HDM201, tested on primary CLL samples with *TP53* wild-type (N = 28) and mutant (N = 6) profiles. The samples were subjected to increasing concentrations of HDM201 (ranging from 0 to 3 μM) for a 48-h exposure period. The three PBMC samples (indicated in black), derived from healthy donors, exhibited LC50 values exceeding 3 μM. Horizontal bars show mean values.

Table 2. Detailed information on *TP53* mutations and LC_{50} values for each *TP53* mutant CLL sample.

Tumor ID	[1] VAF (%)	[2] CDS Mutation	Amino Acid Mutation	HDM201 LC_{50} (μM)
CLL258	35	c.626_627delGA	p.R209fs*6 (Deletion—Frameshift)	0.82
CLL261	97	c.626_627delGA	p.R209fs*6 (Deletion—Frameshift)	>3
CLL273	20	c.1067G > C	p.G356A	>3
	20	c.1069A > C	p.K357Q	
CLL281	28	c.623A > T	p.D208V	>3
	66	c.659A > G	p.Y220C	
CLL283	48	c.745A > G	p.R249G	2.26
CLL287	50	c.524G > A	p.R175H	2.01

[1] VAF: variant allele frequency; [2] CDS: coding sequence.

To assess the effect of HDM201 on normal cells, PBMC samples from healthy donors were exposed to HDM201 for 48 h. In contrast to *TP53* wild-type CLL cells, normal PBMCs were resistant to HDM201 and exhibited LC_{50} values consistently greater than 3 μM (Figure 2A,C).

For evaluating the time-dependent effects of HDM201, five CLL patient samples with functional p53 were treated with various concentrations of HDM201 or left untreated. At different time points (6, 12, 24, or 48 h), the compound was washed out, and the cells were resuspended in complete medium without the drug. The cells were then plated in a 96-well format, and viability was assessed at 48 h using the XTT assay. These wash-out experiments showed that HDM201 decreased CLL viability in both a concentration-dependent and time-dependent manner (paired *t*-test, 24 h vs. 48 h, $p = 0.02$). Median LC_{50} values across CLL samples decreased over time, with LC_{50} values exceeding 10 μM for 6- and 12-h exposures (except for CLL294) but decreasing significantly with longer exposure periods (Figure 2B).

3.3. HDM201 Induces p53 Stabilization and Functional Activation in TP53 Wild-Type CLL Cells

The functional integrity of the p53 signaling pathway was evaluated by treating CLL cells with the MDM2-p53 antagonist HDM201 for 24 h and assessing the protein expression of p53 transcriptional target genes. Inhibition of MDM2 led to the prevention of ubiquitin-mediated degradation of p53, resulting in p53 stabilization. In *TP53* wild-type CLL cells, HDM201 induced a concentration-dependent stabilization of p53, which was accompanied by the activation of p53 target genes, *CDKN1A* (encoding the $p21^{WAF1}$ protein) and *MDM2* (Figure 3A). The concentration-dependent accumulation of p53 was consistently observed in all *TP53* wild-type CLL samples within 24 h of treatment (Figure 3A). To monitor apoptosis, PARP-1 cleavage was analyzed, revealing a concentration-dependent decrease in the levels of full-length PARP accompanied by an increase in the 85 kDa cleavage product (cPARP) in p53-functional CLL cells treated with HDM201 for 24 h. Densitometric analysis of p53, MDM2, and cPARP bands, normalized to actin, showed a significant concentration-dependent increase in these proteins when analyzed across five samples using paired *t*-tests (Figure 3B–D).

In contrast, CLL samples with *TP53* mutations exhibited no induction of $p21^{WAF1}$ following treatment with HDM201, even at concentrations up to 3 μM (Figure 3E). The absence of $p21^{WAF1}$ induction was noted in *TP53* mutant CLL cells from patients CLL281, CLL283, and CLL287. Additionally, there was no significant change in the levels of full-length PARP-1 or cPARP following 24 h of exposure of *TP53* mutant CLL cells to HDM201. Although some degree of p53 stabilization was observed in CLL283 and CLL287 samples after 24 h of HDM201 exposure, it did not result in downstream activation of $p21^{WAF1}$. The

markedly intense p53 band observed in sample CLL281, including the untreated control sample and the absence of both MDM2 and p21^{WAF1} signals, indicates the accumulation of mutant non-functional p53 (Figure 3E). It is important to note that the *TP53* mutant CLL samples analyzed include a mixed clonal population of *TP53* mutant and wild-type cells with varying variant allele frequencies (Table 2).

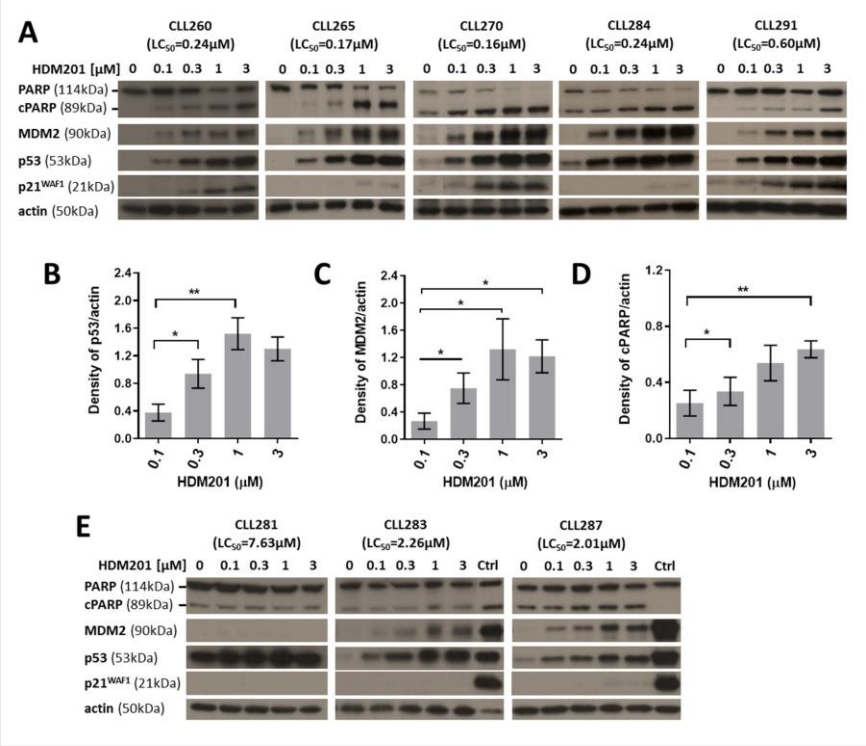

Figure 3. Western immunoblot analyses illustrating the response to HDM201 of both functional and non-functional p53 CLL samples: (**A**) Western immunoblots depicting *TP53* wild-type CLL cells, either untreated (DMSO control) or exposed to increasing concentrations of HDM201 (0.1, 0.3, 1, and 3 μM) for 24 h. Actin served as a loading control. Densitometry was performed for p53 (**B**), MDM2 (**C**), and cPARP (**D**) bands and normalized to actin. Statistical comparisons of different HDM201 concentrations were carried out using a paired *t*-test (*, $p < 0.05$; **, $p < 0.01$). Data are presented as mean ± SEM. (**E**) Representative Western immunoblots for *TP53* mutant CLL samples. In contrast to functional samples, there was no discernible increase in either the p21^{WAF1} or the cleaved PARP-1 (cPARP) marker of apoptotic signaling. Ctrl: Control lysate from OCI-Ly3 cells treated with 0.3 μM RG7388 (idasanutlin) for 24 h. Control lysates were run on the same gel with the sample shown beside the controls.

3.4. HDM201 Treatment Increases the Proportions of Early and Late Apoptotic CLL Cells

Western blot analysis revealed a concentration-dependent increase in cPARP levels in p53-functional CLL cells following 24 h of HDM201 treatment. To further characterize the apoptotic effects of HDM201, flow cytometry was employed using annexin V and propidium iodide (PI) staining. The intensity of PI staining was plotted against annexin V staining to distinguish between viable (annexin V-negative/PI-negative), early apoptotic

(annexin V-positive/PI-negative), and late apoptotic or necrotic (annexin V-positive/PI-positive) cells. Cell debris was excluded from the analysis, and the cell population of interest was identified based on forward and side scatter intensity (Figure 4). Figure 4A–C illustrate concentration-dependent changes in the proportion of cells staining positively for annexin V and/or PI, reflecting apoptosis induction in three freshly isolated CLL primary samples: CLL289, CLL295, and CLL293.

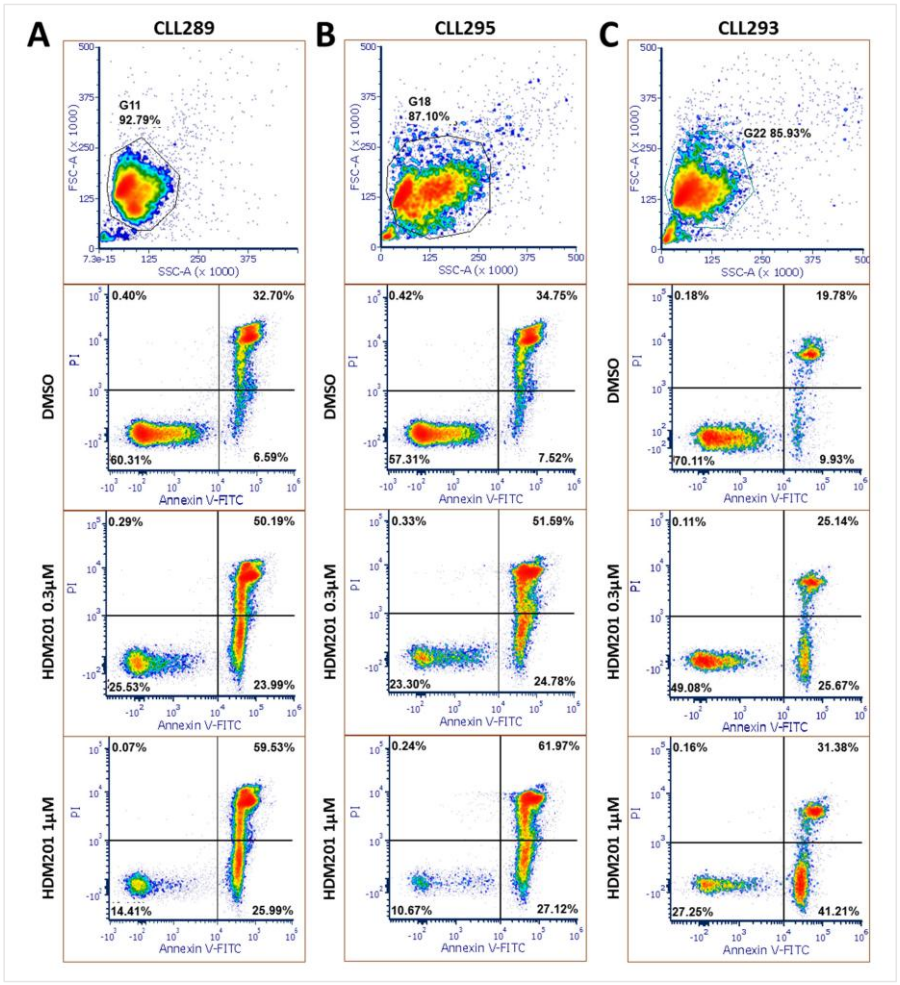

Figure 4. Induction of apoptosis in freshly isolated CLL samples CLL289 (**A**), CLL295 (**B**), and CLL293 (**C**) following treatment with HDM201. CLL cells were exposed to two distinct concentrations of HDM201 (0.3 µM and 1 µM) or a vehicle control (DMSO) for 48 h. Apoptosis was assessed by flow cytometry after staining with annexin V-FITC and PI. The lower left quadrants indicate viable cells (annexin V-negative/PI-negative), the lower right quadrants represent cells in the early stage of apoptosis (annexin V-positive/PI-negative), and the upper right quadrants denote cells in the late stage of apoptosis or necrosis (annexin V-positive/PI-positive). The percentages of the cell populations within each quadrant are presented.

After 48 h of HDM201 treatment, a significant decrease in the proportion of viable cells was observed. The normalized percentages of viable cells decreased to 51 ± 10% (mean ± SEM) at 0.3 µM of HDM201 and to 27 ± 6% (mean ± SEM) at 1 µM of HDM201 (Figure 5A; 0.3 µM vs. 1 µM paired *t*-test, $p = 0.02$). Conversely, early apoptotic cell proportions (Figure 5B) and late apoptotic cell proportions (Figure 5C) relative to DMSO control increased following 48 h of HDM201 treatment.

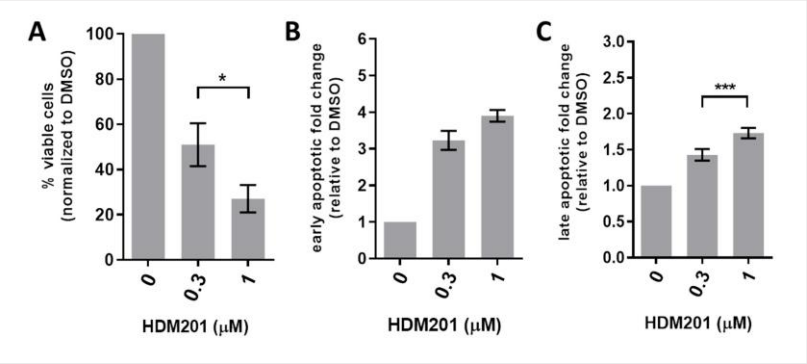

Figure 5. HDM201 induces apoptosis in CLL cells in a concentration-dependent manner. Freshly isolated CLL samples ($n = 3$) were treated with either 0.3 µM or 1 µM HDM201, or with a vehicle control (DMSO), for 48 h. Apoptosis was assessed using FACS analysis of annexin V/PI staining. (**A**) The percentage of viable cells remaining was calculated relative to untreated control samples. The fold change in the percentage of early (**B**) and late (**C**) apoptotic cells relative to the DMSO control is presented for the two different concentrations. Data are expressed as mean ± SEM. Statistically significant differences between concentrations were determined using a paired sample *t*-test (*, $p < 0.05$; ***, $p < 0.001$).

A total of 73 ± 11% (mean ± SEM) of CLL cells lost viability at 1 µM HDM201 compared to the DMSO control (Figure 5A). The reduction in viability observed in these CLL samples, as measured by FACS analysis of annexin V/PI staining, showed a strong positive correlation with the results from the XTT cell viability assay (mean ± SD: 69 ± 6% viability decrease at 1 µM HDM201). This correlation was statistically significant (Pearson's test: r = 0.99; $p = 0.01$; $n = 3$).

4. Discussion

The landscape of CLL treatment has undergone substantial evolution over the past decades, marked by a transition from traditional chemotherapy to more sophisticated targeted therapies. Despite significant advancements, challenges persist, particularly concerning resistance mechanisms and suboptimal responses in high-risk cases. Our study has focused on exploring the potential of HDM201, a second-generation MDM2-p53 binding antagonist, as a novel therapeutic strategy to include for CLL. The promise of HDM201 stems from its ability to specifically target the MDM2-p53 interaction, thereby stabilizing p53 and activating its tumor-suppressive functions in a non-genotoxic manner. This approach contrasts with traditional treatments that largely rely on direct cytotoxicity or modulation of immune responses. The rationale behind targeting the p53 pathway in CLL is grounded in the relatively low frequency of *TP53* alterations at diagnosis (approximately 10%), which suggests that a significant portion of CLL cases could benefit from therapies aimed at activating p53 function.

The safety profile of HDM201 observed in clinical trials appears promising, showing manageable toxicity and no severe adverse effects. This is crucial for CLL patients, who are often older and may have multiple comorbidities. The ability of HDM201 to be administered without excessive toxicity could make it a viable option for long-term or combination therapy, particularly in settings where current treatments have failed or have become less effective.

One of the initial aims of this study was to directly evaluate the effects of HDM201 on various B cell lines with differing *TP53* status, employing otherwise isogenic *TP53*-knockout (*TP53*-KO) derivatives of the human B cell line Nalm-6 to minimize the impact of other genomic variations. Our results demonstrated that both parental (*TP53* wild-type) and heterozygous KO (*TP53*+/−) Nalm-6 cells were sensitive to HDM201. In contrast, B cells with *TP53* mutations or deletions, including homozygous *TP53*-KO (*TP53*−/−) cells, showed a lack of response to HDM201. These findings underscore the crucial role of *TP53* in mediating the response to HDM201 and emphasize the specificity of the compound. Our results reinforce the notion that *TP53* status is a critical factor in determining the therapeutic efficacy of MDM2 inhibitors, highlighting the importance of assessing *TP53* status as a patient selection biomarker to predict the responsiveness of B cell malignancies to HDM201.

We also evaluated HDM201 in malignant B cells isolated from the peripheral blood of patients with CLL. Almost all *TP53* wild-type samples exhibited a response to the compound within clinically acceptable limits [45]. In contrast, *TP53* mutant samples demonstrated varying responses based on the specific mutation type and mutant allele frequency, with drug resistance being generally predominant. The clinical applicability of such treatments hinges on their selective toxicity toward malignant cells while sparing healthy cells. Previous studies have shown that MDM2 inhibitors effectively target malignant cells while sparing normal B cells and stem cells [38,56,57]. Although MDM2 inhibitors activate p53 in both normal and tumor cells with functional p53, the resulting gene expression and cytotoxic effects differ significantly between these cell types [38]. We have previously shown that MDM2 inhibition selectively induces a pro-apoptotic p53 gene signature in CLL cells [38]. This difference leads to distinct cell fates and provides a therapeutic window that has important implications for the use of MDM2 inhibitors as potential cancer treatments. This mechanism is supported by the reversible growth arrest in normal cells as the primary response to MDM2 inhibition, observed with both first-generation and second-generation MDM2 antagonists [38,43,58]. To further investigate this, we isolated peripheral B cells from three different healthy donors and treated them with HDM201 to assess its effects on normal healthy B cells. Remarkably, all isolated B cells displayed resistance to the drug. These findings are significant as they underline the selective toxicity and clinical relevance of targeted therapies, supporting prior research on MDM2 inhibitors.

One notable challenge revealed by our preclinical study is the potential for resistance mechanisms, a common issue across various targeted therapies. In our analysis of 28 primary CLL samples with wild-type *TP53*, we identified two samples exhibiting notable resistance to HDM201 (Figure 2C). Previous research has demonstrated that *SF3B1* mutations, alongside *TP53* status, are an important determinant of response to MDM2 inhibitors [59]. To further explore this, we checked the *SF3B1* gene status of these two resistant samples from our previous comprehensive sequencing data. Notably, one of these two samples, CLL290, was found to carry the *SF3B1* c.2110A > T (p.I704F) point mutation [59]. Despite being *TP53* wild-type, this sample showed significant resistance not only to HDM201 but also to another MDM2 inhibitor, RG7388 (idasanutlin), with an LC_{50} exceeding 10 μM [59]. These results further emphasize the substantial impact of

SF3B1 mutations on the effectiveness of MDM2 inhibitors and underscore the importance of identifying and considering additional biomarkers of treatment response.

The role of HDM201 as an MDM2-p53 binding antagonist is to stabilize p53 in *TP53* wild-type CLL cells by preventing its ubiquitin-mediated degradation. This stabilization was demonstrated in our study and promoted the increased expression of key downstream TP53 transcriptional targets CDKN1A ($p21^{WAF1}$) essential for inhibition of cell cycle progression and the futile increased expression of the negative feedback autoregulator MDM2. PARP-1 is one of several known cellular substrates of caspases. Cleavage of PARP-1 by caspases is considered to be a hallmark of apoptosis [60]. As a marker of caspase-dependent apoptosis, we evaluated PARP-1 cleavage in Western blot experiments. The increased levels of cPARP in *TP53* wild-type CLL cells provided mechanistic evidence of the pro-apoptotic effect of HDM201. These findings were corroborated by flow cytometry, Western blot, and XTT assay results, demonstrating the capacity of HDM201 to induce apoptosis through the activation of the p53 pathway. Conversely, *TP53* mutant CLL cells exhibited resistance to HDM201, consistent with the lack of $p21^{WAF1}$ induction and minimal apoptosis (Figure 3). *TP53* mutations result in dysfunctional p53, impairing its ability to trigger downstream apoptotic pathways. The intense p53 bands in our *TP53* mutant samples, especially in sample CLL281, indicate the accumulation of non-functional and conformationally altered p53, which is no longer recognized by MDM2 and, therefore, not able to be targeted for normal turnover degradation. This is consistent with the known behavior of some mutant forms of TP53 and associated resistance mechanisms. The clonal heterogeneity observed in *TP53* mutant CLL samples (Table 2) complicates the overall effect of treatment, as subclones will differ in their response to HDM201. This complexity underlines the need for tailored therapeutic strategies to address clonal resistance and optimize treatment efficacy by choosing appropriate targeted drug combinations in genetically diverse CLL populations.

In a recently published study, we conducted a detailed transcriptome analysis of a small subpopulation of CLL samples resistant to the MDM2 inhibitor RG7388 and identified several candidate genes [61]. Although these genes are also potential candidates for HDM201, which operates through the same mechanism as RG7388, further research is needed to thoroughly characterize their roles and validate their relevance to the efficacy of HDM201. Further evaluation of apoptotic and DNA damage response pathways could be highly beneficial, particularly for elucidating resistance mechanisms in the limited number of samples and for a more mechanistic understanding of drug response. Future research should focus on delineating the precise mechanisms through which resistance to HDM201 and other MDM2 inhibitors may develop and seek to identify biomarkers that predict response or resistance. This could involve evaluating the impact of co-occurring mutations or the role of the microenvironment in influencing drug efficacy. Furthermore, combination strategies involving HDM201 and other targeted agents, such as BTK inhibitors or novel immunotherapies, could potentially enhance therapeutic outcomes and overcome resistance barriers.

5. Conclusions

Here, we present a rationale for the further evaluation of the new-generation MDM2 inhibitor HDM201 in CLL therapy. Our observations indicate that CLL cells are particularly primed for p53-dependent apoptosis compared to normal PBMCs. Given the promising results observed in B cell lines and primary patient samples, HDM201 could become a valuable addition to the therapeutic arsenal for CLL. Integrating HDM201 into treatment regimens may offer a new strategy for managing relapsed or refractory cases. These results support the investigation of MDM2 inhibitors in CLL clinical trials, which will determine their optimal use in clinical treatment strategies.

Supplementary Materials: The following supporting information can be downloaded at https://www.mdpi.com/article/10.3390/cancers17020274/s1: Figure S1: Densitometry readings; Table S1: Detailed information on *TP53* mutations and LC_{50} values for each CLL sample.

Author Contributions: Conceptualization, E.A., E.W. and J.L.; data curation, E.A. and M.H.; formal analysis, E.A. and M.H.; funding acquisition, E.W. and J.L.; investigation, E.A. and M.H.; methodology, E.A.; resources, J.L., E.W., J.I., J.P.W., H.M. and S.M.; supervision, E.W. and J.L.; writing—original draft, E.A. and M.H.; writing—review and editing, E.A., E.W. and J.L. All authors have read and agreed to the published version of the manuscript.

Funding: This study was supported by Cancer Research UK (Awards #C2215/A21421), Blood Cancer UK (formerly Bloodwise; grant #13034), the JGW Paterson Foundation (grant #BH152495) and the Newcastle Healthcare Charity (grant #BH152694). The Turkish Ministry of National Education funded the first author's Ph.D. study.

Institutional Review Board Statement: This study was conducted in accordance with the Declaration of Helsinki and approved by the Institutional Review Board (or Ethics Committee) of the Newcastle Academic Health Partners Biobank (https://www.ncl.ac.uk/biobank/collections/nbrtb/ (accessed on 11 January 2025)). Samples were collected and stored for research under the auspices of the Newcastle Biobank, with Research Ethics Committee (REC) reference 17/NE/0361 (Date of Approval: 29 April 2014).

Informed Consent Statement: Informed consent was obtained from all subjects involved in this study. Written informed consent has been obtained from the CLL patients.

Data Availability Statement: The data presented in this study and released under a CC-BY 4.0 license are available upon request from the corresponding authors.

Acknowledgments: The authors gratefully acknowledge Newcastle University and Cancer Research UK for infrastructure funding at the Newcastle University Cancer Centre. We would also like to thank CLL patients for their generous consent and supply of blood samples for research, collected following approved ethical guidelines.

Conflicts of Interest: The authors declare no conflicts of interest.

References

1. Chiorazzi, N.; Rai, K.R.; Ferrarini, M. Chronic lymphocytic leukemia. *N. Engl. J. Med.* **2005**, *352*, 804–815. [CrossRef] [PubMed]
2. Ponzoni, M.; Doglioni, C.; Caligaris-Cappio, F. Chronic lymphocytic leukemia: The pathologist's view of lymph node microenvironment. *Semin. Diagn. Pathol.* **2011**, *28*, 161–166. [CrossRef] [PubMed]
3. Burger, J.A.; Ghia, P.; Rosenwald, A.; Caligaris-Cappio, F. The microenvironment in mature B-cell malignancies: A target for new treatment strategies. *Blood* **2009**, *114*, 3367–3375. [CrossRef]
4. Damle, R.N.; Wasil, T.; Fais, F.; Ghiotto, F.; Valetto, A.; Allen, S.L.; Buchbinder, A.; Budman, D.; Dittmar, K.; Kolitz, J.; et al. Ig V gene mutation status and CD38 expression as novel prognostic indicators in chronic lymphocytic leukemia. *Blood* **1999**, *94*, 1840–1847. [CrossRef]
5. Hamblin, T.J.; Davis, Z.; Gardiner, A.; Oscier, D.G.; Stevenson, F.K. Unmutated Ig V(H) genes are associated with a more aggressive form of chronic lymphocytic leukemia. *Blood* **1999**, *94*, 1848–1854. [CrossRef]
6. Iyer, P.; Wang, L. Emerging Therapies in CLL in the Era of Precision Medicine. *Cancers* **2023**, *15*, 1583. [CrossRef] [PubMed]
7. Herman, S.E.; Mustafa, R.Z.; Gyamfi, J.A.; Pittaluga, S.; Chang, S.; Chang, B.; Farooqui, M.; Wiestner, A. Ibrutinib inhibits BCR and NF-kappaB signaling and reduces tumor proliferation in tissue-resident cells of patients with CLL. *Blood* **2014**, *123*, 3286–3295. [CrossRef]
8. Parmar, S.; Patel, K.; Pinilla-Ibarz, J. Ibrutinib (imbruvica): A novel targeted therapy for chronic lymphocytic leukemia. *Pharm. Ther.* **2014**, *39*, 483–519.
9. Seiler, T.; Dohner, H.; Stilgenbauer, S. Risk stratification in chronic lymphocytic leukemia. *Semin. Oncol.* **2006**, *33*, 186–194. [CrossRef]
10. Takahashi, K.; Hu, B.; Wang, F.; Yan, Y.; Kim, E.; Vitale, C.; Patel, K.P.; Strati, P.; Gumbs, C.; Little, L.; et al. Clinical implications of cancer gene mutations in patients with chronic lymphocytic leukemia treated with lenalidomide. *Blood* **2018**, *131*, 1820–1832. [CrossRef]

11. Schlette, E.J.; Admirand, J.; Wierda, W.; Abruzzo, L.; Lin, K.I.; O'Brien, S.; Lerner, S.; Keating, M.J.; Tam, C. p53 expression by immunohistochemistry is an important determinant of survival in patients with chronic lymphocytic leukemia receiving frontline chemo-immunotherapy. *Leuk. Lymphoma* **2009**, *50*, 1597–1605. [CrossRef]
12. Mhibik, M.; Gaglione, E.M.; Eik, D.; Herrick, J.; Le, J.E.; Ahn, I.E.; Chiu, C.; Wielgos-Bonvallet, M.; Hiemstra, I.H.; Breij, E.C.W.; et al. Cytotoxicity of the CD3xCD20 bispecific antibody epcoritamab in CLL is increased by concurrent BTK or BCL-2 targeting. *Blood Adv.* **2023**, *7*, 4089–4101. [CrossRef]
13. Liu, L.; Lam, C.K.; Long, V.; Widjaja, L.; Yang, Y.; Li, H.; Jin, L.; Burke, S.; Gorlatov, S.; Brown, J.; et al. MGD011, A CD19 x CD3 Dual-Affinity Retargeting Bi-specific Molecule Incorporating Extended Circulating Half-life for the Treatment of B-Cell Malignancies. *Clin. Cancer Res.* **2017**, *23*, 1506–1518. [CrossRef]
14. Mato, A.R.; Woyach, J.A.; Brown, J.R.; Ghia, P.; Patel, K.; Eyre, T.A.; Munir, T.; Lech-Maranda, E.; Lamanna, N.; Tam, C.S.; et al. Pirtobrutinib after a Covalent BTK Inhibitor in Chronic Lymphocytic Leukemia. *N. Engl. J. Med.* **2023**, *389*, 33–44. [CrossRef]
15. Guo, Y.; Liu, Y.; Hu, N.; Yu, D.; Zhou, C.; Shi, G.; Zhang, B.; Wei, M.; Liu, J.; Luo, L.; et al. Discovery of Zanubrutinib (BGB-3111), a Novel, Potent, and Selective Covalent Inhibitor of Bruton's Tyrosine Kinase. *J. Med. Chem.* **2019**, *62*, 7923–7940. [CrossRef]
16. Woyach, J.A.; Furman, R.R.; Liu, T.M.; Ozer, H.G.; Zapatka, M.; Ruppert, A.S.; Xue, L.; Li, D.H.; Steggerda, S.M.; Versele, M.; et al. Resistance mechanisms for the Bruton's tyrosine kinase inhibitor ibrutinib. *N. Engl. J. Med.* **2014**, *370*, 2286–2294. [CrossRef]
17. Kanagal-Shamanna, R.; Jain, P.; Patel, K.P.; Routbort, M.; Bueso-Ramos, C.; Alhalouli, T.; Khoury, J.D.; Luthra, R.; Ferrajoli, A.; Keating, M.; et al. Targeted multigene deep sequencing of Bruton tyrosine kinase inhibitor-resistant chronic lymphocytic leukemia with disease progression and Richter transformation. *Cancer* **2019**, *125*, 559–574. [CrossRef]
18. Ahn, I.E.; Underbayev, C.; Albitar, A.; Herman, S.E.; Tian, X.; Maric, I.; Arthur, D.C.; Wake, L.; Pittaluga, S.; Yuan, C.M.; et al. Clonal evolution leading to ibrutinib resistance in chronic lymphocytic leukemia. *Blood* **2017**, *129*, 1469–1479. [CrossRef]
19. Nakhoda, S.; Vistarop, A.; Wang, Y.L. Resistance to Bruton tyrosine kinase inhibition in chronic lymphocytic leukaemia and non-Hodgkin lymphoma. *Br. J. Haematol.* **2023**, *200*, 137–149. [CrossRef] [PubMed]
20. Chene, P. Inhibiting the p53-MDM2 interaction: An important target for cancer therapy. *Nat. Rev. Cancer* **2003**, *3*, 102–109. [CrossRef] [PubMed]
21. Brown, C.J.; Lain, S.; Verma, C.S.; Fersht, A.R.; Lane, D.P. Awakening guardian angels: Drugging the p53 pathway. *Nat. Rev. Cancer* **2009**, *9*, 862–873. [CrossRef]
22. Zenz, T.; Eichhorst, B.; Busch, R.; Denzel, T.; Habe, S.; Winkler, D.; Buhler, A.; Edelmann, J.; Bergmann, M.; Hopfinger, G.; et al. TP53 mutation and survival in chronic lymphocytic leukemia. *J. Clin. Oncol.* **2010**, *28*, 4473–4479. [CrossRef] [PubMed]
23. Dicker, F.; Herholz, H.; Schnittger, S.; Nakao, A.; Patten, N.; Wu, L.; Kern, W.; Haferlach, T.; Haferlach, C. The detection of TP53 mutations in chronic lymphocytic leukemia independently predicts rapid disease progression and is highly correlated with a complex aberrant karyotype. *Leukemia* **2009**, *23*, 117–124. [CrossRef]
24. Chen, X.; Zhang, T.; Su, W.; Dou, Z.; Zhao, D.; Jin, X.; Lei, H.; Wang, J.; Xie, X.; Cheng, B.; et al. Mutant p53 in cancer: From molecular mechanism to therapeutic modulation. *Cell Death Dis.* **2022**, *13*, 974. [CrossRef] [PubMed]
25. Hollstein, M.; Sidransky, D.; Vogelstein, B.; Harris, C.C. p53 mutations in human cancers. *Science* **1991**, *253*, 49–53. [CrossRef]
26. Wu, C.E.; Chen, C.P.; Huang, W.K.; Pan, Y.R.; Aptullahoglu, E.; Yeh, C.N.; Lunec, J. p53 as a biomarker and potential target in gastrointestinal stromal tumors. *Front. Oncol.* **2022**, *12*, 872202. [CrossRef] [PubMed]
27. Levine, A.J.; Oren, M. The first 30 years of p53: Growing ever more complex. *Nat. Rev. Cancer* **2009**, *9*, 749–758. [CrossRef]
28. Momand, J.; Jung, D.; Wilczynski, S.; Niland, J. The MDM2 gene amplification database. *Nucleic Acids Res.* **1998**, *26*, 3453–3459. [CrossRef]
29. Zhang, R.; Wang, H. MDM2 oncogene as a novel target for human cancer therapy. *Curr. Pharm. Des.* **2000**, *6*, 393–416. [CrossRef]
30. Moll, U.M.; Petrenko, O. The MDM2-p53 interaction. *Mol. Cancer Res.* **2003**, *1*, 1001–1008.
31. Chen, J.D. The Cell-Cycle Arrest and Apoptotic Functions of p53 in Tumor Initiation and Progression. *Cold Spring Harb. Perspect. Med.* **2016**, *6*, a026104. [CrossRef] [PubMed]
32. Ding, Q.; Zhang, Z.; Liu, J.J.; Jiang, N.; Zhang, J.; Ross, T.M.; Chu, X.J.; Bartkovitz, D.; Podlaski, F.; Janson, C.; et al. Discovery of RG7388, a potent and selective p53-MDM2 inhibitor in clinical development. *J. Med. Chem.* **2013**, *56*, 5979–5983. [CrossRef]
33. Furet, P.; Masuya, K.; Kallen, J.; Stachyra-Valat, T.; Ruetz, S.; Guagnano, V.; Holzer, P.; Mah, R.; Stutz, S.; Vaupel, A.; et al. Discovery of a novel class of highly potent inhibitors of the p53-MDM2 interaction by structure-based design starting from a conformational argument. *Bioorganic Med. Chem. Lett.* **2016**, *26*, 4837–4841. [CrossRef]
34. Rew, Y.; Sun, D. Discovery of a small molecule MDM2 inhibitor (AMG 232) for treating cancer. *J. Med. Chem.* **2014**, *57*, 6332–6341. [CrossRef]
35. Arnhold, V.; Schmelz, K.; Proba, J.; Winkler, A.; Wunschel, J.; Toedling, J.; Deubzer, H.E.; Kunkele, A.; Eggert, A.; Schulte, J.H.; et al. Reactivating TP53 signaling by the novel MDM2 inhibitor DS-3032b as a therapeutic option for high-risk neuroblastoma. *Oncotarget* **2018**, *9*, 2304–2319. [CrossRef]

36. Willmore, E.; Ahn, M.; Kyle, S.; Zhao, Y.; Thomas, H.; Rankin, K.S.; Bevan, L.; Fazal, L.; Hearn, K.; Wilsher, N.; et al. Targeting the MDM2-p53 interaction: Time- and concentration-dependent studies in tumor and normal human bone marrow cells reveal strategies for an enhanced therapeutic index. *Cancer Res.* **2024**, *84*, 3333. [CrossRef]
37. Wang, S.M.; Sun, W.; Zhao, Y.J.; McEachern, D.; Meaux, I.; Barrière, C.; Stuckey, J.A.; Meagher, J.L.; Bai, L.C.; Liu, L.; et al. SAR405838: An Optimized Inhibitor of MDM2-p53 Interaction That Induces Complete and Durable Tumor Regression. *Cancer Res.* **2014**, *74*, 5855–5865. [CrossRef]
38. Ciardullo, C.; Aptullahoglu, E.; Woodhouse, L.; Lin, W.Y.; Wallis, J.P.; Marr, H.; Marshall, S.; Bown, N.; Willmore, E.; Lunec, J. Non-genotoxic MDM2 inhibition selectively induces a pro-apoptotic p53 gene signature in chronic lymphocytic leukemia cells. *Haematologica* **2019**, *104*, 2429–2442. [CrossRef] [PubMed]
39. Aptullahoglu, E.; Ciardullo, C.; Wallis, J.P.; Marr, H.; Marshall, S.; Bown, N.; Willmore, E.; Lunec, J. Splicing Modulation Results in Aberrant Isoforms and Protein Products of p53 Pathway Genes and the Sensitization of B Cells to Non-Genotoxic MDM2 Inhibition. *Int. J. Mol. Sci.* **2023**, *24*, 2410. [CrossRef] [PubMed]
40. Johansson, K.B.; Zimmerman, M.S.; Dmytrenko, I.V.; Gao, F.; Link, D.C. Idasanutlin and navitoclax induce synergistic apoptotic cell death in T-cell acute lymphoblastic leukemia. *Leukemia* **2023**, *37*, 2356–2366. [CrossRef]
41. Seipel, K.; Schmitter, K.; Bacher, U.; Pabst, T. Rationale for a Combination Therapy Consisting of MCL1- and MEK-Inhibitors in Acute Myeloid Leukemia. *Cancers* **2019**, *11*, 1779. [CrossRef] [PubMed]
42. Ghotaslou, A.; Samii, A.; Boustani, H.; Kiani Ghalesardi, O.; Shahidi, M. AMG-232, a New Inhibitor of MDM-2, Enhance Doxorubicin Efficiency in Pre-B Acute Lymphoblastic Leukemia Cells. *Rep. Biochem. Mol. Biol.* **2022**, *11*, 111–124. [CrossRef]
43. Bell, H.L.; Blair, H.J.; Jepson Gosling, S.J.; Galler, M.; Astley, D.; Moorman, A.V.; Heidenreich, O.; Veal, G.J.; van Delft, F.W.; Lunec, J.; et al. Combination p53 activation and BCL-x(L)/BCL-2 inhibition as a therapeutic strategy in high-risk and relapsed acute lymphoblastic leukemia. *Leukemia* **2024**, *38*, 1223–1235. [CrossRef] [PubMed]
44. Gungordu, S.; Aptullahoglu, E. Targeting MDM2-mediated suppression of p53 with idasanutlin: A promising therapeutic approach for acute lymphoblastic leukemia. *Investig. New Drugs* **2024**, *42*, 603–611. [CrossRef] [PubMed]
45. Stein, E.M.; DeAngelo, D.J.; Chromik, J.; Chatterjee, M.; Bauer, S.; Lin, C.C.; Suarez, C.; de Vos, F.; Steeghs, N.; Cassier, P.A.; et al. Results from a First-in-Human Phase I Study of Siremadlin (HDM201) in Patients with Advanced Wild-Type TP53 Solid Tumors and Acute Leukemia. *Clin. Cancer Res.* **2022**, *28*, 870–881. [CrossRef]
46. Koyama, T.; Shimizu, T.; Kojima, Y.; Sudo, K.; Okuma, H.S.; Shimoi, T.; Ichikawa, H.; Kohsaka, S.; Sadachi, R.; Hirakawa, A.; et al. Clinical Activity and Exploratory Resistance Mechanism of Milademetan, an MDM2 Inhibitor, in Intimal Sarcoma with MDM2 Amplification: An Open-Label Phase Ib/II Study. *Cancer Discov.* **2023**, *13*, 1814–1825. [CrossRef]
47. Daver, N.G.; Dail, M.; Garcia, J.S.; Jonas, B.A.; Yee, K.W.L.; Kelly, K.R.; Vey, N.; Assouline, S.; Roboz, G.J.; Paolini, S.; et al. Venetoclax and idasanutlin in relapsed/refractory AML: A non-randomized, open-label phase 1b trial. *Blood* **2022**, *141*, 1265–1276. [CrossRef] [PubMed]
48. Konopleva, M.Y.; Rollig, C.; Cavenagh, J.; Deeren, D.; Girshova, L.; Krauter, J.; Martinelli, G.; Montesinos, P.; Schafer, J.A.; Ottmann, O.; et al. Idasanutlin plus cytarabine in relapsed or refractory acute myeloid leukemia: Results of the MIRROS trial. *Blood Adv.* **2022**, *6*, 4147–4156. [CrossRef]
49. Abdul Razak, A.R.; Bauer, S.; Suarez, C.; Lin, C.C.; Quek, R.; Hutter-Kronke, M.L.; Cubedo, R.; Ferretti, S.; Guerreiro, N.; Jullion, A.; et al. Co-Targeting of MDM2 and CDK4/6 with Siremadlin and Ribociclib for the Treatment of Patients with Well-Differentiated or Dedifferentiated Liposarcoma: Results from a Proof-of-Concept, Phase Ib Study. *Clin. Cancer Res.* **2022**, *28*, 1087–1097. [CrossRef]
50. Senapati, J.; Muftuoglu, M.; Ishizawa, J.; Abbas, H.A.; Loghavi, S.; Borthakur, G.; Yilmaz, M.; Issa, G.C.; Dara, S.I.; Basyal, M.; et al. A Phase I study of Milademetan (DS3032b) in combination with low dose cytarabine with or without venetoclax in acute myeloid leukemia: Clinical safety, efficacy, and correlative analysis. *Blood Cancer J.* **2023**, *13*, 101. [CrossRef]
51. Chen, J.; Marechal, V.; Levine, A.J. Mapping of the p53 and mdm-2 interaction domains. *Mol. Cell. Biol.* **1993**, *13*, 4107–4114.
52. Stein, E.M.; Chromik, J.; Carpio, C.; Mous, R.; Kiladjian, J.J.; Alatrash, G.; Curti, A.; Craddock, C.; Schmid, C.; Zeiser, R.; et al. Siremadlin (HDM201) Is Well Tolerated and Demonstrates Clinical Activity in Patients with Acute Myeloid Leukemia Who Have Relapsed after Allogeneic Stem Cell Transplantation: A Subset Analysis of Safety and Preliminary Efficacy. *Blood* **2021**, *138*, 3417. [CrossRef]
53. Adachi, N.; So, S.; Iiizumi, S.; Nomura, Y.; Murai, K.; Yamakawa, C.; Miyagawa, K.; Koyama, H. The human pre-B cell line Nalm-6 is highly proficient in gene targeting by homologous recombination. *DNA Cell Biol.* **2006**, *25*, 19–24. [CrossRef]
54. Hallek, M.; Cheson, B.D.; Catovsky, D.; Caligaris-Cappio, F.; Dighiero, G.; Dohner, H.; Hillmen, P.; Keating, M.J.; Montserrat, E.; Rai, K.R.; et al. Guidelines for the diagnosis and treatment of chronic lymphocytic leukemia: A report from the International Workshop on Chronic Lymphocytic Leukemia updating the National Cancer Institute-Working Group 1996 guidelines. *Blood* **2008**, *111*, 5446–5456. [CrossRef] [PubMed]
55. Shen, M.; Zhang, Y.; Saba, N.; Austin, C.P.; Wiestner, A.; Auld, D.S. Identification of therapeutic candidates for chronic lymphocytic leukemia from a library of approved drugs. *PLoS ONE* **2013**, *8*, e75252. [CrossRef]

56. Shangary, S.; Qin, D.; McEachern, D.; Liu, M.; Miller, R.S.; Qiu, S.; Nikolovska-Coleska, Z.; Ding, K.; Wang, G.; Chen, J.; et al. Temporal activation of p53 by a specific MDM2 inhibitor is selectively toxic to tumors and leads to complete tumor growth inhibition. *Proc. Natl. Acad. Sci. USA* **2008**, *105*, 3933–3938. [CrossRef] [PubMed]
57. Shangary, S.; Ding, K.; Qiu, S.; Nikolovska-Coleska, Z.; Bauer, J.A.; Liu, M.; Wang, G.; Lu, Y.; McEachern, D.; Bernard, D.; et al. Reactivation of p53 by a specific MDM2 antagonist (MI-43) leads to p21-mediated cell cycle arrest and selective cell death in colon cancer. *Mol. Cancer Ther.* **2008**, *7*, 1533–1542. [CrossRef] [PubMed]
58. Stühmer, T.; Chatterjee, M.; Hildebrandt, M.; Herrmann, P.; Gollasch, H.; Gerecke, C.; Theurich, S.; Cigliano, L.; Manz, R.A.; Daniel, P.T.; et al. Nongenotoxic activation of the p53 pathway as a therapeutic strategy for multiple myeloma. *Blood* **2005**, *106*, 3609–3617. [CrossRef]
59. Aptullahoglu, E.; Wallis, J.P.; Marr, H.; Marshall, S.; Bown, N.; Willmore, E.; Lunec, J. SF3B1 Mutations Are Associated with Resistance to Non-Genotoxic MDM2 Inhibition in Chronic Lymphocytic Leukemia. *Int. J. Mol. Sci.* **2023**, *24*, 11335. [CrossRef] [PubMed]
60. Kaufmann, S.H.; Desnoyers, S.; Ottaviano, Y.; Davidson, N.E.; Poirier, G.G. Specific proteolytic cleavage of poly(ADP-ribose) polymerase: An early marker of chemotherapy-induced apoptosis. *Cancer Res.* **1993**, *53*, 3976–3985. [PubMed]
61. Aptullahoglu, E.; Nakjang, S.; Wallis, J.P.; Marr, H.; Marshall, S.; Willmore, E.; Lunec, J. RNA Sequencing Reveals Candidate Genes and Pathways Associated with Resistance to MDM2 Antagonist Idasanutlin in TP53 Wild-Type Chronic Lymphocytic Leukemia. *Biomedicines* **2024**, *12*, 1388. [CrossRef] [PubMed]